frontiers | Research Topics

Reproductive biotechnologies and challenges in their application

Edited by
Stefan Gregore Ciornei, Mihai Cenariu and Graça Lopes

Published in
Frontiers in Veterinary Science

ISSN 1664-8714
ISBN 978-2-8325-6013-6
DOI 10.3389/978-2-8325-6013-6

About Frontiers

Frontiers is more than just an open access publisher of scholarly articles: it is a pioneering approach to the world of academia, radically improving the way scholarly research is managed. The grand vision of Frontiers is a world where all people have an equal opportunity to seek, share and generate knowledge. Frontiers provides immediate and permanent online open access to all its publications, but this alone is not enough to realize our grand goals.

Frontiers journal series

The Frontiers journal series is a multi-tier and interdisciplinary set of open-access, online journals, promising a paradigm shift from the current review, selection and dissemination processes in academic publishing. All Frontiers journals are driven by researchers for researchers; therefore, they constitute a service to the scholarly community. At the same time, the *Frontiers journal series* operates on a revolutionary invention, the tiered publishing system, initially addressing specific communities of scholars, and gradually climbing up to broader public understanding, thus serving the interests of the lay society, too.

Dedication to quality

Each Frontiers article is a landmark of the highest quality, thanks to genuinely collaborative interactions between authors and review editors, who include some of the world's best academicians. Research must be certified by peers before entering a stream of knowledge that may eventually reach the public - and shape society; therefore, Frontiers only applies the most rigorous and unbiased reviews. Frontiers revolutionizes research publishing by freely delivering the most outstanding research, evaluated with no bias from both the academic and social point of view. By applying the most advanced information technologies, Frontiers is catapulting scholarly publishing into a new generation.

What are Frontiers Research Topics?

Frontiers Research Topics are very popular trademarks of the *Frontiers journals series*: they are collections of at least ten articles, all centered on a particular subject. With their unique mix of varied contributions from Original Research to Review Articles, Frontiers Research Topics unify the most influential researchers, the latest key findings and historical advances in a hot research area.

Find out more on how to host your own Frontiers Research Topic or contribute to one as an author by contacting the Frontiers editorial office: frontiersin.org/about/contact

Reproductive biotechnologies and challenges in their application

Topic editors

Stefan Gregore Ciornei — Iasi, University of Life Science (IULS), Romania
Mihai Cenariu — University of Agricultural Sciences and Veterinary Medicine of Cluj-Napoca, Romania
Graça Lopes — University of Porto, Portugal

Citation

Ciornei, S. G., Cenariu, M., Lopes, G., eds. (2025). *Reproductive biotechnologies and challenges in their application*. Lausanne: Frontiers Media SA.
doi: 10.3389/978-2-8325-6013-6

Table of contents

frontiers | Frontiers in Veterinary Science

TYPE Editorial
PUBLISHED 04 February 2025
DOI 10.3389/fvets.2025.1558641

OPEN ACCESS

EDITED AND REVIEWED BY
Regiane R. Santos,
Schothorst Feed Research, Netherlands

*CORRESPONDENCE
Mihai Cenariu
✉ mihai.cenariu@usamvcluj.ro

RECEIVED 10 January 2025
ACCEPTED 27 January 2025
PUBLISHED 04 February 2025

CITATION
Ciornei SG, Lopes G and Cenariu M (2025) Editorial: Reproductive biotechnologies and challenges in their application.
Front. Vet. Sci. 12:1558641.
doi: 10.3389/fvets.2025.1558641

Editorial: Reproductive biotechnologies and challenges in their application

Stefan G. Ciornei[1], Graça Lopes[2] and Mihai Cenariu[3]*

[1]Faculty of Veterinary Medicine, Ion Ionescu de la Brad University of Life Sciences Iasi, Iasi, Romania, [2]School of Medicine and Biomedical Sciences (ICBAS), University of Porto, Porto, Portugal, [3]Faculty of Veterinary Medicine, University of Agricultural Sciences and Veterinary Medicine of Cluj-Napoca, Cluj-Napoca, Romania

KEYWORDS

reproductive biotechnologies, embryo, semen cryopreservation, reproductive endocrinology, postpartum management

Editorial on the Research Topic
Reproductive biotechnologies and challenges in their application

Reproductive biotechnologies and challenges in their application, a Research Topic hosted by Frontiers in Veterinary Science (Animal Reproduction—Theriogenology) was launched in February 2024. The aim was to explore the advancements made by researchers in the field of reproductive biotechnologies, assess their potential for improving reproductive health and efficiency, and address the challenges associated with their ethical, technical, and practical applications. This research is fundamental for the progress of animal reproductive health and productivity, by addressing infertility challenges, and ensuring the ethical and sustainable application of state-of-the-art biotechnological solutions in this field. Thus, 17 original research papers, as well as a brief research report were published.

Several papers focused on embryology across various species, including bovines, equines, swine, and monkeys.

Jung et al. evaluated the efficiency of slow freezing bovine blastocysts with sucrose added prior to freezing, to overcome ice crystal formation caused by insufficient dehydration (1). The study revealed that treating bovine embryos with 0.25 M sucrose before slow freezing improved their post freeze-thawing viability.

Antral follicle count (AFC) is a crucial factor in bovine embryo production and donor selection (2). Gawai et al. assessed the effect of AFC on follicular and luteal development during the estrous cycle and superovulatory period, as well as on superovulatory response and *in vivo* embryo quality in Sahiwal cows. Their research confirmed that an AFC exceeding 30 is a reliable phenotypic marker for predicting the reproductive potential of Sahiwal donors, making it significant for commercial *in vivo* embryo production programs.

Lipids play a key role in embryo-maternal signaling and early embryo development (3). Lawson et al. conducted lipidomic profiling of early equine embryos *in vitro*, revealing that triglycerides were consistently released into the culture environment, while diglycerides were depleted. This highlights the importance of a well-defined embryo culture medium.

Myo-inositol is known for its protective role against oxidative stress via the NRF2/KEAP1 signaling pathway (4). Jawad et al. investigated its effect on porcine embryonic development after parthenogenetic activation. Findings demonstrated that 20 mM Myo-inositol supplementation of culture media enhanced blastocyst development and improved mitochondrial function by regulating apoptosis, reducing oxidative stress, and activating the NRF2 pathway.

Nonhuman primates are critical for generating gene-edited models for human disease research (5). Lee et al. investigated the efficacy of superovulated and uterine-embryo synchronized recipients of embryo transfer in cynomolgus monkeys. Outcomes confirmed that superovulated recipients were as effective as synchronized ones, facilitating efficient gene-edited model generation.

Various papers focused on spermology, providing insights into semen cryopreservation in several species.

Avdatek et al. assessed the impact of baicalein, previously studied for its anti-inflammatory, antioxidant, and anticancer potential (6), on ram semen parameters post freeze-thawing. The addition of 0.5 mM baicalein to semen extenders improved progressive motility and chromatin integrity of ram spermatozoa.

Boar semen doses are typically stored at 16–18°C, which is challenging to maintain during transport (7). Hallberg et al. comparatively evaluated boar sperm quality and fertility after storage in AndroStar Premium extender at 4°C and 16–18°C for 1 week. They found better membrane integrity in semen stored at 16–18°C, while DNA fragmentation was lower at 4°C. There was no significant difference in the number of blastocysts developed post *in vitro* fertilization between the two storage temperatures.

Dog semen cryopreservation allows preservation of gametes from individuals with significant genetic value, while also overcoming the constraints associated with traditional breeding methods (8). Domain et al. provided a comprehensive analysis of the use and popularity of frozen sperm among dog breeders in Belgium and the Netherlands, while also characterizing the individuals presented for sperm cryopreservation. The study revealed a growing trend in semen cryopreservation, with annual growth rates between 8.4 and 41.9%. Most dogs presented for cryopreservation were aged 1–9 years, and the frozen sperm was primarily intended for international shipment, although a significant portion remained unused.

Rooster semen quality declines after storage at 2–5°C for more than 24 h, likely due to oxidative stress (9). Koedkanmark et al. investigated the impact of adding *Eurycoma longifolia* (EL) extract as an antioxidant in semen extender on Thai chicken semen quality and fertility. Data indicated that supplementing the sperm cooling medium with 15 mg/ml of EL extract improved semen quality during 5°C storage for up to 48 h, by reducing lipid peroxidation, and significantly enhanced the fertility of Thai rooster semen stored for up to 24 h.

Endocrinological challenges were also approached by several authors, and their research explored various hormonal implications in the reproductive processes.

The anti-Müllerian hormone (AMH) is recognized as a valuable marker for evaluating testicular function (10). Posastiuc et al. found that higher serum levels and tissue expression of AMH are linked to smaller seminiferous tubules and poorer Johnsen scores, suggesting AMH as a marker of testicular degeneration in dogs.

Scopolamine has emerged as a viable alternative to traditional ecbolic substances in managing the postpartum period in dairy cows (11). Carbonari et al. compared the effect of oxytocin, prostaglandin F2α (PGF2α) and scopolamine on uterine involution and resumption of ovarian activity in dairy cows and concluded that treatment with scopolamine and PGF2α resulted in faster uterine involution and ovarian recovery.

Gonadotropin-releasing hormone (GnRH) is commonly used in fixed time artificial insemination protocols for sheep, although its effect on pregnancy rates continues to be a subject of debate (12). Zhang et al. evaluated its influence on pregnancy rates and pre-implantation metabolites in Huyang ewes, synchronized using a progestogen-eCG protocol. Evidence showed a significant decrease in hydroxyproline and an increase in corticosterone and prostaglandin D2 levels, correlating with lower pregnancy rates.

GnRH administration significantly decreases the pregnancy rate of recipient ewes after embryo transfer, possibly because it affects endometrial epithelial cell function (13). Jiao, Chu, et al. investigated the effect of GnRH on endometrial epithelial cells by screening the S100A4 gene transcription. Results revealed that GnRH suppresses S100A4 expression in the endometrium, consequently inhibiting endometrial cell proliferation via the S100A4/GNAI2/MAPK signaling pathway, potentially explaining decreased embryo implantation rate. Another study by Jiao, Jiao, et al. highlighted the role of GnRH in endometrial cell senescence, identifying interactions between S100A4 and PPP1CA, and its involvement in cellular senescence regulation through the S100A4/PPP1CA/IL-17 pathway.

Peripartal and postpartum management in dairy cows was also approached, thus Rafa et al. characterized the metabolic and hormonal profiles of Romanian Spotted cows during the peripartum period, exploring possible correlations with retained fetal membranes (RFM), a pathology frequently associated with economic loss, due to decreased milk production and high costs of medical treatment (14). Their findings confirmed that significant metabolic and physiological changes due to RFM occur postpartum, emphasizing the need for targeted management strategies.

Chinese herbal medicine (CHM) has shown beneficial effects on cow health and production (15). Abulaiti et al. evaluated the effects of a CHM preparation on the growth, milk yield, and reproductive efficiency of dairy cows in early postpartum period. The study found no adverse effects on biochemical indicators for immunity, digestibility, and metabolism, while improving estrus, ovulation, and pregnancy rates.

A novel method using micro-computed tomography to explore swine oviduct anatomy was developed by Belda-Perez et al. This approach provided detailed parameters like shape factor, fractal dimension, and lacunarity, enabling more precise embryo production and epigenetic reprogramming.

Finally, Nechifor et al. published a brief report on the uterine bacteriological load in Holstein Friesian cows, based on parturition type (eutocia/dystocia). They found a significant increase in germ count during the first 14 days postpartum, with higher levels in cows experiencing dystocic calving.

In conclusion, these studies collectively provide a comprehensive resource for researchers, scholars, and practitioners in veterinary reproduction and reproductive biotechnologies.

Author contributions

SC: Validation, Writing – original draft. GL: Validation, Writing – review & editing. MC: Conceptualization, Supervision, Validation, Writing – original draft, Writing – review & editing.

Conflict of interest

The authors declare that the research was conducted in the absence of any commercial or financial relationships that could be construed as a potential conflict of interest.

Publisher's note

References

1. Mucci N, Aller J, Kaiser GG, Hozbor F, Cabodevila J, Alberio RH. Effect of estrous cow serum during bovine embryo culture on blastocyst development and cryotolerance after slow freezing or vitrification. *Theriogenology.* (2006) 65:1551–62. doi: 10.1016/j.theriogenology.2005.08.020

2. Lollato JPM, Souza ACC, Silva RCP, Marques MO, Crozara AS, Gonçalves RL, et al. *In vivo* embryo production in bovine donors with low and high antral follicle counts superovulated with low and high FSH doses. *Livest Sci.* (2022) 262:104985. doi: 10.1016/j.livsci.2022.104985

3. Salamonsen LA, Evans J, Nguyen HP, Edgell TA. The microenvironment of human implantation: determinant of reproductive success. *Am J Reprod Immunol.* (2016) 75:218–25. doi: 10.1111/aji.12450

4. Jiang WD, Hu K, Liu Y, Jiang J, Wu P, Zhao J, et al. Dietary myo-inositol modulates immunity through antioxidant activity and the Nrf2 and E2F4/cyclin signaling factors in the head kidney and spleen following infection of juvenile fish with Aeromonas hydrophila. *Fish Shellfish Immunol.* (2016) 49:374–86. doi: 10.1016/j.fsi.2015.12.017

5. Niu Y, Shen B, Cui Y, Chen Y, Wang J, Wang L, et al. Generation of gene-modified cynomolgus monkey via Cas9/RNA-mediated gene targeting in one-cell embryos. *Cell.* (2014) 156:836–43. doi: 10.1016/j.cell.2014.01.027

6. Chen Y, Zhao Z, Li Y, Yang Y, Li L, Jiang Y, et al. Baicalein alleviates hyperuricemia by promoting uric acid excretion and inhibiting xanthine oxidase. *Phytomedicine.* (2021) 80:153374. doi: 10.1016/j.phymed.2020.153374

7. Ciornei S, Drugociu D, Ciornei LM, Mareş M, Roşca P. Total aseptization of boar semen, to increase the biosecurity of reproduction in swine. *Molecules.* (2021) 26:6183. doi: 10.3390/molecules26206183

8. Suzuki H, Watanabe H, Abe Y. Assisted reproductive techniques for canines: preservation of genetic material in domestic dogs. *J Reprod Dev.* (2022) 68:1–11. doi: 10.1262/jrd.2021-111

9. Kheawkanha T, Chankitisakul V, Thananurak P, Pimprasert M, Boonkum W, Vongpralub T. Solid storage supplemented with serine of rooster semen enhances higher sperm quality and fertility potential during storage at 5°C for up to 120 h. *Poult Sci.* (2023) 102:102648. doi: 10.1016/j.psj.2023.102648

10. Walter B, Fischer S, Otzdorff C. Anti-Mullerian hormone concentrations in dogs with testicular atrophy. In: *1st European Symposium on Animal Reproduction*. Nantes: Reproduction in Domestic Animals (2023), p. 191.

11. Rizzo A, Gazza C, Silvestre A, Maresca L, Sciorsci RL. Scopolamine for uterine involution of dairy cows. *Theriogenology.* (2018) 122:35–40. doi: 10.1016/j.theriogenology.2018.08.025

12. Hameed N, Khan MI, Zubair M, Andrabi SMH. Approaches of estrous synchronization in sheep: developments during the last two decades: a review. *Trop Anim Health Prod.* (2021) 53:485. doi: 10.1007/s11250-021-02932-8

13. Ciornei Ş, Drugociu D, Ciornei LM, Roşca P. Ovarian response to P4-PGF-FSH treatment in Suffolk sheep and P4-PGF-PMSG synchronization in cross-bred ewes, for IVD and ET protocol. *Vet Med Sci.* (2022) 8:726–34. doi: 10.1002/vms3.705

14. Bicalho MLS, Lima FS, Ganda EK, Foditsch C, Meira EBS Jr, Machado VS, et al. Effect of trace mineral supplementation on selected minerals, energy metabolites, oxidative stress, and immune parameters and its association with uterine diseases in dairy cattle. *J Dairy Sci.* (2014) 97:4281–95. doi: 10.3168/jds.2013-7832

15. Wang X, Xie H, Liu F, Wang Y. Production performance, immunity, and heat stress resistance in Jersey cattle fed a concentrate fermented with probiotics in the presence of a Chinese herbal combination. *Anim Feed Sci Technol.* (2017) 228:59–65. doi: 10.1016/j.anifeedsci.2017.03.015

frontiers | Frontiers in Veterinary Science

TYPE Original Research
PUBLISHED 05 April 2024
DOI 10.3389/fvets.2024.1394273

OPEN ACCESS

EDITED BY
Stefan Gregore Ciornei,
Iasi University of Life Science (IULS),
Romania

REVIEWED BY
Gaffari Türk,
Firat University, Türkiye
Barış Atalay Uslu,
Cumhuriyet University, Türkiye

*CORRESPONDENCE
Umut Taşdemir
✉ tasdemiru@gmail.com

RECEIVED 01 March 2024
ACCEPTED 15 March 2024
PUBLISHED 05 April 2024

CITATION
Avdatek F, Güngör Ş, Gülhan MF, İnanç ME, Olğaç KT, Denk B, Yeni D and Taşdemir U (2024) Cryopreservation of ram semen: baicalein efficiency on oxidative stress, chromatin integrity, viability and motility post thaw.
Front. Vet. Sci. 11:1394273.
doi: 10.3389/fvets.2024.1394273

Cryopreservation of ram semen: baicalein efficiency on oxidative stress, chromatin integrity, viability and motility post thaw

Fatih Avdatek[1], Şükrü Güngör[2], Mehmet Fuat Gülhan[3], Muhammed Enes İnanç[2], Kemal Tuna Olğaç[4], Barış Denk[5], Deniz Yeni[1] and Umut Taşdemir[6]*

[1]Faculty of Veterinary Medicine, Department of Reproduction and Artificial Insemination, Afyon Kocatepe University, Afyonkarahisar, Türkiye, [2]Faculty of Veterinary Medicine, Department of Reproduction and Artificial Insemination, Mehmet Akif Ersoy University, Burdur, Türkiye, [3]Technical Sciences Vocational School, Department of Aromatic Plants, Aksaray University, Aksaray, Türkiye, [4]Faculty of Veterinary Medicine, Department of Reproduction and Artificial Insemination, Ankara University, Ankara, Türkiye, [5]Faculty of Veterinary Medicine, Department of Biochemistry, Afyon Kocatepe University, Afyonkarahisar, Türkiye, [6]Faculty of Veterinary Medicine, Department of Reproduction and Artificial Insemination, Aksaray University, Aksaray, Türkiye

Baicalein (B) has potential antioxidant properties, but it has not been tested as a ram semen extender. This study aimed to assess the impact of B on various sperm parameters and determine its potential influence on semen quality after the freeze-thawing process. During the breeding season, ejaculates were obtained from four rams with the aid of an artificial vagina. The collected mixed semen samples were divided into four groups: control (C; 0), B0.5 (0.5 mM), B1 (1 mM), and B2 (2 mM). After semen extension, the samples were loaded into 0.25 mL straws and stored for 2 h at 4°C prior to freezing in liquid nitrogen vapor and thawed in a water bath at 37°C. Among the groups, B0.5 demonstrated the highest progressive motility results, while B1 and B2 exhibited reduced motility ($p < 0.05$). In terms of high mitochondrial membrane potential, plasma membrane and acrosome integrity, and viability, B0.5 showed significantly superior outcomes to the other B groups ($p < 0.05$), although it was not significantly better than C. B1 displayed the highest plasma membrane integrity levels ($p < 0.05$). Notably, B2 displayed the lowest total antioxidant status levels among the groups ($p < 0.05$). The findings of this study suggested that the *in vitro* spermatological characteristics of ram spermatozoa such as progressive motility and chromatin integrity can be protected from the freeze-thawing process by using the 0.5 mM dose of baicalein as a semen extender. The treatment of sperm freezing might benefit from further in-depth research on the role of B in the improvement of cryoinjury and its underlying processes.

KEYWORDS

ram semen, cryopreservation, baicalein, chromatin damage, antioxidant, oxidative stress

1 Introduction

Semen freezing is a technique that is employed to preserve sperm cells for future utilization in assisted reproductive technologies (1, 2). However, different freezing techniques can impact sperm cell viability and motility, and proper handling and storage conditions are essential to preserving the quality of sperm cells over time (3–5). The addition of antioxidants in extenders is a potential approach to reducing cryo-damage (6, 7).

Reactive oxygen species (ROS) are chemicals that can degrade DNA, proteins, and cell membranes. Antioxidants are molecules that can counteract the effects of ROS (8). Several studies have examined the use of antioxidants, including vitamin E, vitamin C, and melatonin, in semen cryopreservation (9–11). It has been reported that adding antioxidant supplements increases post-thaw sperm cell viability, motility, and DNA integrity.

As a natural flavonoid and aglycone, Baicalein (B) can be found in the roots of the Chinese plant *Scutellaria baicalensis* (12). B has the chemical formula $C_{15}H_{10}O_5$ and a relative molecular mass of 270.24 g/moL. Researchers have studied B for its anti-inflammatory, antioxidant, and anticancer potential (12). Additionally, it has been demonstrated that B has antimicrobial activity against a variety of pathogens, such as bacteria and viruses. The possibility of using it to treat neurological illnesses, including Alzheimer's and Parkinson's, has also been explored (13–15).

Furthermore, B can block the production of ROS by inhibiting xanthine oxidase activity (16). Hydrogen peroxide and other peroxides can damage neurons. B has a greater antioxidant activity and considerable protective benefits against H_2O_2-induced oxidative damage in human neural cells (17). A significant improvement in cell viability and mitochondrial protection through a redox-dependent mechanism has been demonstrated in studies on cellular toxicity. Authors have suggested that B plays an important role in mitochondrial functioning, it reduces apoptosis and the mitochondrial membrane potential, inhibits caspase activation, improves the production of ATP, and triggers the consumption of ADP (13, 14, 18, 19).

Several studies have investigated the impact of B on cell signaling pathways involved in mitochondrial functions in the context of maintaining mitochondrial physiology and determining the fate of cells (14, 20–22). B may have antioxidant properties that can be beneficial for reproductive health, but further research is required to fully appreciate its potential advantages in this regard. Cryopreservation of ram's semen using B as a semen extender has not been studied. Given this information, this study aims to evaluate the effects of B on ram semen by measuring sperm motility, chromatin damage, oxidative stress, and other antioxidant parameters to reduce the likelihood of cryo-damage caused by freeze-thawing.

2 Materials and methods

2.1 Study design

The Animal Research Ethics Committee of Afyon Kocatepe University (Approval No. 49533702/333) approved the protocol of this study. Four Sönmez (25% Chios and 75% Tahirova) breed rams, aged 2–3 years, were included in the experiment. During the reproductive season, 28 ejaculate samples were collected from four males, twice a week, with the aid of an artificial vagina. The ejaculates which had >80% motility, ≥1.5 mL volume, and ≥ 1×10^9 spermatozoa/mL were used for the study. The ejaculate samples were mixed for the procedures and analyses. Four distinct groups were created to study the effects of B (item no. 70610, 95%, Cayman Chemical Company, Michigan, United States). The groups included the experimental groups in which 0.5 mM, 1 mM, and 2 mM doses of B were added as semen extenders (B0.5, B1, and B2, respectively) and a control group (C). The mixed ejaculates that were separated into four aliquots and extended using a Tris-based extender (3.63 g Tris [T1503], 0.5 g fructose [F0127], 1.82 g citric acid [C0759]/100 mL double-distilled water) to dilute them, as well as 15% egg yolk and 6% glycerol. To produce the groups, 2 mM of B was dissolved in 1 mL of ethanol (Merck, 99%). Extended semen equilibrated at 4°C for 2 h, after equilibration held in liquid nitrogen vapor (11 cm above the liquid nitrogen, −110 to 120°C) for 12 min. Then the samples were frozen in a flow of liquid nitrogen vapor and placed in a container of liquid nitrogen for long-term storage. Following the cryopreservation process, the frozen semen samples were subjected to thawing in a water bath set at 37°C for a duration of 30 s, after which they were considered ready for analysis. Progressive motility, total motility, and kinetic spermatozoon parameters were evaluated with a computer-assisted sperm analyzer (CASA; MICROPTIC S.L., Sperm Class Analyzer software, SCA® v.4.2; Spain) system. Mitochondrial membrane potential (MMP), plasma membrane acrosome integrity (PMAI), and viability were evaluated by flow cytometry (Beckman Coulter, United States). DNA fragmentation was evaluated by the alkaline single-cell gel electrophoresis method (COMET assay). Biochemical analyses were carried out by spectrophotometric methods.

2.2 Motility and kinetic characteristics

The analysis was performed using a CASA system (Nikon Eclipse 50i; Japan) and a heating plate. The curvilinear velocity (VCL) parameter was classified five categories: static (<10 μm/s), slow (10–45 μm/s), medium (45–75 μm/s), fast (>75 μm/s), and progressive (>75% straightness). Before analysis the samples were thawed, an amount of 5 μL was then put on a slide, covered with a cover slide, and heated on the microscope's heating plate to 37°C. At least 200 spermatozoa were counted and examined in five different microscopic zones for each sample (23). Frozen–thawed semen samples were analyzed in terms of total motility (TMOT, %), progressive motility (PMOT, %), straightness (STR, %), curvilinear velocity (VCL, μm/s), linearity (LIN, %), straight-line velocity (VSL, μm/s), average path velocity (VAP, μm/s), wobble (WOB, %), beat-cross frequency (BCF, Hz), and amplitude of lateral head displacement (ALH, μm/s).

2.3 Flow cytometric analyses

Tests were performed using a CytoFLEX flow cytometer (Beckman Coulter, CA, United States) equipped with emission filters at 610 ± 20 nm, 585 ± 42 nm, and 525 ± 40 nm, as well as a 50 mW (488 nm) laser output. An average of 10,000 spermatozoa were analyzed for each test. Pseudo-color plots were used to compare the side scatter area (SSC-A) to the forward scatter area (FSC-A) of the

sperm cells to facilitate the selection process. Forward scatter height (FSC-H) and forward scatter area (FSC-A) were used to exclude doublets from the analysis (24). All aliquots of 50 µL were made from the stain stock solutions prepared using DMSO and kept at −20°C.

A FITC/PNA-PI staining protocol was used to detect spermatozoon parameters using the method described by İnanç et al. (25), 100 µg/mL of FITC-PNA (Sigma, L7381), and 2.99 mM propidium iodide (PI, L7011 Molecular Probes, Invitrogen). The sperm cell concentration was adjusted to 5×10^6 by diluting the semen samples with 492 µL of PBS. Then, 5 µL of FITC and 3 µL of PI were added to the mixture, and the mixture was incubated at 37°C for 15 min in a dark environment. After the analysis, the FITC- and PI-populations were recorded as PMAI (%). The MMP of the sperm was determined using 5,5′,6,6′ tetrachloro-1,1′,3,3′-tetramethyl benzimidazolyl-carbocyanine iodide (JC-1) (25). The concentration of JC-1 (T3198 molecular probes, Invitrogen) was 0.153 mM. The sperm cell concentration was adjusted to 5×10^6 by diluting the semen samples with 495 µL of PBS. 5 µL of JC-1 was added to the mixture, which was then incubated at 37°C for 15 min in the dark. Spermatozoa were evaluated based on their HMMP status after the analysis. The viability of sperm cells was determined using the SYBR and PI protocols (5). We used 1:10 SYBR and 2.99 mM PI from among Invitrogen's L7011 Molecular Probes. The sperm cell concentration was adjusted to 5×10^6 by diluting the semen samples with 492 µL of PBS. 5 µL of SYBR-14 and 3 µL of PI were introduced into the mixture, which was then subjected to incubation at 37°C for a duration of 15 min in the dark. After the analysis, the SYBR+ and PI-populations were recorded as viable (plasma membrane integrity, %).

2.4 Evaluations of chromatin fragmentation

The method reported by Gündoğan et al. (26) was used to conduct a COMET assay to test sperm chromatin integrity. The samples that were stained and processed were examined using a microscope (Olympus CX31) equipped with a fluorescence attachment. The Comet Score software (TriTek, V. 1.5) was utilized to evaluate the sperm cells. A total of 200 sperm cells were examined and evaluated across six distinct microscopic zones.

2.5 Biochemical analyses

Malondialdehyde (MDA) was used in to quantify the degree of lipid peroxidation (LPO), in accordance with the procedure described by Draper and Hadley (27). The MDA concentration was assessed based on the reaction between lipid peroxides and thiobarbituric acid, followed by the measurement of absorbance at 532 nm. The concentration of MDA was determined in units of nanomoles per milliliter (nmol/mL). Ellman's method was employed to determine the quantity of reduced glutathione (GSH), and the resulting concentration was computed as mg/dL with the methodology reported by Hissin and Hilf (28). Total antioxidant status (TAS) measurements were made using a colorimetric test kit (REL Assay Diagnostics, Gaziantep, TR). The experiment entailed a reduction of the oxidized radical 2,2-azino-bis-3-ethylbenzothiazoline-6-sulfonic acid (ABTS) through the action of the antioxidant compounds present in the samples, leading to visible alterations in color. A spectrophotometer was utilized to measure color intensity at a wavelength of 660 nm, and the outcomes are expressed in units of mmol/L. Total oxidant status (TOS) measurements were made using a colorimetric test kit (REL Assay Diagnostics, Gaziantep, TR). The methodology employed in this study involved the assessment of the oxidation of Fe^{+2} to Fe^{+3} by the usage of oxidizing agents. The concentration of the solution was determined in µmol/L and measured via the spectrophotometric analysis method at a wavelength of 660 nm. Finally, the oxidative stress index (OSI) was calculated using the formula OSI = [(TOS)/ (TAS × 100)] (29).

2.6 Statistical analyses

Prior to conducting the significance tests, the data were assessed for normality using the Shapiro-Wilks test. Levene's test was used to determine the homogeneity of the variances. ANOVA was used to statistically test the differences between groups of data. The Duncan test was applied to evaluate differences between groups. Descriptive statistics are presented as "mean ± standard error of the mean" (Mean ± SE). Using the SPSS 13.0 package program, the results of all statistical analyses were evaluated with a maximum error margin of 5%. A p-value of 0.05 was accepted as the threshold of statistical significance.

3 Results

The progressive motility rate showed statistically significant differences among the groups ($p < 0.05$). In comparison to C, B1 and B2 had contrasting effects on both total and progressive motility (Table 1; $p < 0.05$). B0.5 achieved numerically better results compared to C in terms of VSL and hyperactivity. The results for VAP, VSL, VCL, BCF, and WOB in B2 were found to be significantly lower compared to those in C and B0.5 ($p < 0.05$). It was determined that the higher doses of treatment (1 and 2 mM) did not have positive effects on kinetic parameters. B0.5 produced significantly better HMMP and viability outcomes than the other B groups ($p < 0.05$), but C had the highest HMMP results ($p < 0.05$). The highest PMAI value was found in B1 ($p < 0.05$). The results on the PMAI, HMMP, and viability parameters showed that the highest concentration of B (2 mM) did not prevent damage to the ram semen caused by the cryopreservation process ($p > 0.05$; Table 2). B0.5 and B1 had significantly lower levels of chromatin damage compared to C ($p < 0.05$). Except for B2, chromatin integrity was preserved in all B groups compared to C ($p < 0.05$; Table 3). As seen in Table 4, there were no significant changes in GSH, MDA, TOS, and OSI levels among the groups ($p > 0.05$). While the highest GSH activity and OSI and the lowest MDA and TAS levels were in B2 among all groups, ($p < 0.05$).

4 Discussion

Successful cryopreservation of sperm cells requires an understanding of the changes that occur throughout the process, and there have been several studies on this topic (30–32). Research

10.3389/fvets.2024.1394273

TABLE 1 Sperm motility and kinetic parameters of frozen–thawed ram semen.

Parameters	C	B0.5	B1	B2	*p*
Progressive motility (%)	12.47 ± 1.48^{b}	17.50 ± 1.99^{a}	8.21 ± 1.01^{c}	2.85 ± 0.46^{d}	*
Total motility (%)	59.52 ± 2.87^{a}	66.80 ± 1.96^{a}	38.48 ± 4.27^{b}	16.16 ± 1.31^{c}	*
VAP (μm/s)	35.94 ± 1.43^{a}	35.38 ± 2.66^{a}	33.05 ± 1.50^{a}	27.19 ± 2.20^{b}	*
VSL (μm/s)	21.83 ± 1.01^{a}	21.92 ± 1.80^{a}	21.23 ± 1.27^{a}	16.65 ± 1.85^{b}	*
VCL (μm/s)	57.26 ± 1.66^{a}	56.50 ± 3.14^{a}	54.52 ± 1.95^{ab}	48.35 ± 2.00^{b}	*
ALH (μm/s)	2.38 ± 0.07	2.43 ± 0.09	2.40 ± 0.11	2.36 ± 0.07	–
BCF (Hz)	8.42 ± 0.35^{a}	7.64 ± 0.33^{ab}	6.81 ± 0.31^{b}	5.26 ± 0.51^{c}	*
LIN (%)	38.19 ± 1.21	37.52 ± 1.78	38.64 ± 2.52	32.83 ± 2.37	–
STR (%)	58.76 ± 0.95^{ab}	58.38 ± 0.79^{ab}	59.87 ± 2.22^{a}	53.96 ± 2.26^{b}	*
WOB (μm/s)	61.72 ± 1.12^{a}	60.97 ± 2.24^{a}	59.05 ± 1.91^{ab}	54.12 ± 2.23^{b}	*
Hyperactivity	0.98 ± 0.21^{ab}	1.19 ± 0.28^{ab}	1.71 ± 0.37^{a}	0.53 ± 0.19^{b}	*

[a,b,c,d] Different superscripts on the same row demonstrate significant differences ($*p < 0.05$). No significant difference ($p > 0.05$). Straight line velocity (VSL), curvilinear velocity (VCL), straight line linearity (LIN) [(VSL/VCL) × 100], average path velocity (VAP), straightness (STR) [(VSL/VAP) × 100], amplitude of lateral head displacement (ALH), cross beat frequency (BCF), wobble (WOB) [(VAP/VCL) × 100]. Mean (±SE).

TABLE 2 PMAI, HMMP and SYBR14+ activities in frozen–thawed ram semen.

Parameters	C	B0.5	B1	B2	*p*
PMAI (%)	17.87 ± 2.39^{b}	20.89 ± 1.19^{b}	30.00 ± 2.14^{a}	11.31 ± 0.80^{c}	*
HMMP (%)	15.51 ± 0.42^{a}	13.26 ± 0.47^{b}	11.66 ± 0.49^{c}	5.69 ± 0.29^{d}	*
Viability (%)	68.79 ± 1.09^{ab}	72.46 ± 1.03^{a}	67.76 ± 1.29^{b}	59.66 ± 2.00^{c}	*

[a,b,c,d] Different superscripts on the same row demonstrate significant differences ($*p < 0.05$). High mitochondrial membrane potential (HMMP), plasma membrane and acrosome integrity (PMAI), viability (plasma membrane integrity). Mean (±SE).

efforts have concentrated on diverse attributes, including but not limited to the motility and viability of sperm, the integrity of sperm cell membranes, and chromatin integrity. One of the primary challenges in establishing uniform protocols for the cryopreservation of sperm is inter-individual variability in the response of sperm cells to identical freezing procedures. Studies in the relevant field aim to gain an insight into the anticipated reaction of sperm cells to cryopreservation. Secondly, they strive to create customized cryopreservation protocols tailored to optimize the effectiveness of their technique. The primary goal is to enhance spermatological characteristics during freeze–thaw cycles (31). Previous studies have attempted to explain the processes that regulate B. These are the blockage of the Fas/FasL pathway (reducing cell apoptosis), the activation of the nuclear factor erythroid 2-related factor 2 (Nrf2) (promoting anti-oxidative stress effects), the inhibition of the Nrf2/HO-1 (heme oxygenase 1) signaling pathway, and the regulation of the mTOR pathway (cell regulator) (33–36). This study aimed to determine whether the addition of B at three different doses improves the resistance of sperm cells to cryodamage during cryopreservation. It was found that the 0.5 mM dose of B (B0.5) prevented damage to progressive motility, in agreement with increased doses of B also caused toxicity (35). This might be due to the use of low doses of B compared to high doses shows its effect by blocking the Fas/FasL pathway. This result confirmed the results of previous studies, indicating that B shows dose-dependent effects, as demonstrated by Fan et al. (37). B has not been used in sperm extenders, and thus, we are unable to discuss these results along with the results of similar studies. On the other hand, the data in our study were in accordance with prior information that antioxidant agents that are added to semen extenders could promote progressive motility in a dose-dependent manner (5, 38, 39). B has different effects on cell-induced apoptosis, whereas it inhibits metastasis, on the other hand, and protects the viability of mitochondria and cells (40–42).

Comparable outcomes were obtained in B1 group with regard to plasma membrane integrity. This could have been caused by B's effect in the activation of the signaling pathway Nrf2 and regulation of the mTOR pathway. Sperm cells, unlike other cells, have a unique structure in terms of their sensitivity to damage by LPO and defense reactions (43). According to Kovalski et al. (44), sperm cells cannot repair themselves following damage resulting out of LPO. The absence of cytoplasmic enzymes within these cells creates an imbalance favoring the production of ROS, leading to the heightened susceptibility of semen to oxidative stress. In our study, while B0.5 positive outcomes in terms of progressive motility, it did not have positive results regarding oxidative stress parameters. Although B did not have a positive effect on oxidative stress parameters, B0.5 had a positive effect on motility, suggesting that B may provide an intrinsic antioxidant property by donating electrons to the spermatozoon plasma membrane. Among other studies in which contradictory results have been presented, a correlation was observed between elevated levels of ROS and reduced motility (45). Alahmar (46) argued that the correlation

TABLE 3 DNA damage values in frozen–thawed ram semen.

Parameters	C	B0.5	B1	B2	*p*
Tail length (μm/s)	25.23 ± 0.92^{a}	14.00 ± 0.99^{c}	14.07 ± 0.83^{c}	18.46 ± 1.29^{b}	*
Tail DNA (%)	36.67 ± 3.13^{a}	23.75 ± 2.17^{b}	22.72 ± 2.40^{b}	34.70 ± 0.96^{a}	*
Tail moment (μm/s)	20.66 ± 1.86^{a}	15.51 ± 1.78^{bc}	12.36 ± 1.05^{c}	18.91 ± 0.75^{ab}	*

^{a,b,c} Different superscripts on the same row demonstrate significant differences ($*p < 0.05$). Mean (±SE).

TABLE 4 GSH and MDA activities, TAS, TOS, and OSI values in frozen–thawed ram semen.

Parameters	C	B0.5	B1	B2	*p*
GSH (mg/dL)	45.30 ± 2.64	40.51 ± 1.26	40.42 ± 0.87	46.15 ± 2.49	–
MDA (nmol/mL)	5.90 ± 0.08	5.96 ± 0.05	5.81 ± 0.15	4.15 ± 0.06	–
TAS (mmol/L)	3.42 ± 0.14^{ab}	3.53 ± 0.11^{ab}	3.55 ± 0.02^{a}	3.22 ± 0.07^{b}	*
TOS (μmol/L)	8.33 ± 0.48	7.84 ± 0.27	7.94 ± 0.20	8.02 ± 0.42	–
OSI (TOS/TASx100)	24.37 ± 1.15	22.31 ± 1.02	22.37 ± 0.55	24.81 ± 0.89	–

^{a,b} Different superscripts on the same row demonstrate significant differences ($*p < 0.05$). $^{-}$ No significant difference ($p > 0.05$). Malondialdehyde (MDA), glutathione (GSH), total antioxidant status (TAS), and total oxidant status (TOS), oxidative stress index (OSI). Mean (±SE).

between ROS and reduced motility can be attributed to a sequence of events that culminate in a decline in the phosphorylation of axonemal proteins and the subsequent immobilization of sperm. The primary function of antioxidants in the human body is to mitigate the impact of oxidative processes (47). This can be achieved either through direct means, such as the catalysis of enzymatic reactions, or indirectly, by acting as compounds that neutralize free radicals and interrupt chain reactions. B could effectively inhibit the generation of ROS by reducing hydrogen peroxide (37). Moreover, similar studies have added different antioxidants to sperm extenders before freezing (5, 38, 48–50). B could also reduce the expression of caspase 9 and caspase 3 (41). Beside these effects, B promotes the viability of neuroblastoma cells and prevents the apoptosis-inducing effects of hydrogen peroxide on neurocytes. This effect is probably related to the upregulation of deacetylase sirtuin 1 (SIRT1), which is responsible for cellular functions that are favorable for the lifespan of organisms and is often considered an "anti-aging" enzyme, and the downregulation of caspase 3 (12, 41). In this study, B0.5 did not show significant improvements in viability. This result contradicted the results found by Pan et al. (41) and Wang et al. (15). Oxidative damage to mitochondrial DNA is a well-documented phenomenon occurring in aerobic cells, including sperm cells, due to their abundance of mitochondria. Prior research has indicated that the application of B at minimal concentrations can effectively lower the rate of apoptosis in bovine mammary epithelial cells (51). These results were in accordance with our results. The B doses in B0.5 and B1 protected the sperm from chromatin damage, while the dose in B2 did not. It is thought that B could block H_2O_2-induced DNA damage by inhibition of DNA tail formation and γH2AX phosphorylation. Thereby protect it from oxidative damage. Fan et al. (37) suggested that an excessive B dose beyond the physiological concentration may induce cellular stress, leading to cellular toxicity. Similar findings have been reported in the flow cytometric assessments of plasma membrane acrosome integrity, viability, and mitochondrial membrane status.

5 Conclusion

The results of this study suggested that the 0.5 mM dosage of B could preserve the progressive motility and chromatin integrity of ram sperm cells after the freeze-thawing process. Additional comprehensive studies on the function of B in the progression of cryoinjury and its underlying mechanisms are expected to yield novel insights and approaches for the improvement of the semen cryopreservation process.

Data availability statement

The original contributions presented in the study are included in the article/supplementary material, further inquiries can be directed to the corresponding author/s.

Ethics statement

The animal studies were approved by the Animal Research Ethics Committee of Afyon Kocatepe University (Approval No. 49533702/333). The studies were conducted in accordance with the local legislation and institutional requirements. Written informed consent was obtained from the owners for the participation of their animals in this study.

Author contributions

FA: Investigation, Resources, Writing – original draft. ŞG: Data curation, Investigation, Resources, Writing – original draft. MG: Investigation, Resources, Writing – original draft. Mİ: Investigation, Resources, Writing – original draft. KO: Investigation, Writing – original draft. BD: Investigation, Writing – original draft. DY: Investigation, Resources, Writing – original draft. UT: Investigation, Methodology, Project administration, Resources, Writing – review & editing.

Funding

The author(s) declare financial support was received for the research, authorship, and/or publication of this article. This study was supported by the Aksaray University Scientific Research Fund (BAP2021/008). The funders had no role in the study's design, data collection, or analysis.

Acknowledgments

The authors would like to thank Kapucuoğlu Sheep Farm for allowing the use of their facilities and herd.

Conflict of interest

The authors declare that the research was conducted in the absence of any commercial or financial relationships that could be construed as a potential conflict of interest.

Publisher's note

All claims expressed in this article are solely those of the authors and do not necessarily represent those of their affiliated organizations, or those of the publisher, the editors and the reviewers. Any product that may be evaluated in this article, or claim that may be made by its manufacturer, is not guaranteed or endorsed by the publisher.

References

1. Peris-Frau P, Soler AJ, Iniesta-Cuerda M, Martín-Maestro A, Sánchez-Ajofrín I, Medina-Chávez DA, et al. Sperm Cryodamage in ruminants: understanding the molecular changes induced by the cryopreservation process to optimize sperm quality. *Int J Mol Sci*. (2020) 21:2781. doi: 10.3390/ijms21082781

2. Şengül E, Dayanikli C, Alpcan Künyeli B, Çoban İ, Bülbül B, Üstüner B, et al. Effect of Equex on ram semen in different freezing extenders. *Kafkas Univ Vet Fak Derg*. (2024) 30:207–14. doi: 10.9775/kvfd.2023.30789

3. Benson JD, Woods EJ, Walters EM, Critser JK. The cryobiology of spermatozoa. *Theriogenology*. (2012) 78:1682–99. doi: 10.1016/j.theriogenology.2012.06.007

4. Lusignan MF, Li X, Herrero B, Delbes G, Chan PTK. Effects of different cryopreservation methods on DNA integrity and sperm chromatin quality in men. *Andrology*. (2018) 6:829–35. doi: 10.1111/andr.12529

5. Yeni D, Güngör Ş, Avdatek F, Gülhan MF, Olğaç KT, İnanç ME, et al. Investigation of changes in spermatozoon characteristics, chromatin structure, and antioxidant/oxidant parameters after freeze-thawing of hesperidin (vitamin P) doses added to ram semen. *Life (Basel)*. (2022) 12:1780. doi: 10.3390/life12111780

6. Agarwal A, Majzoub A. Role of antioxidants in assisted reproductive techniques. *World J Mens Health*. (2017) 35:77–93. doi: 10.5534/wjmh.2017.35.2.77

7. Önder NT, Gökdemır T, Kılıç MC, Şahın O, Yıldız S, Kaçar C, et al. Insulin and bull sperm interactions during cryopreservation. *Kafkas Univ Vet Fak Derg*. (2023) 29:401–5. doi: 10.9775/kvfd.2023.29623

8. Salamon S, Maxwell WM. Storage of ram semen. *Anim Reprod Sci*. (2000) 62:77–111. doi: 10.1016/s0378-4320(00)00155-x

9. Domínguez-Rebolledo AE, Fernández-Santos MR, Bisbal A, Ros-Santaella JL, Ramón M, Carmona M, et al. Improving the effect of incubation and oxidative stress on thawed spermatozoa from red deer by using different antioxidant treatments. *Reprod Fertil Dev*. (2010) 22:856–70. doi: 10.1071/RD09197

10. Martín-Ramírez R, González-Fernández R, Hernández J, Martín-Vasallo P, Palumbo A, Ávila J. Celastrol and melatonin modify SIRT1, SIRT6 and SIRT7 gene expression and improve the response of human granulosa-lutein cells to oxidative stress. *Antioxidants (Basel)*. (2021) 10:1871. doi: 10.3390/antiox10121871

11. Peña FJ, Saravia F, García-Herreros M, Núñez-martínez I, Tapia JA, Johannisson A, et al. Identification of sperm morphometric subpopulations in two different portions of the boar ejaculate and its relation to postthaw quality. *J Androl*. (2005) 26:716–23. doi: 10.2164/jandrol.05030

12. Chen Y, Zhao Z, Li Y, Yang Y, Li L, Jiang Y, et al. Baicalein alleviates hyperuricemia by promoting uric acid excretion and inhibiting xanthine oxidase. *Phytomedicine*. (2021) 80:153374. doi: 10.1016/j.phymed.2020.153374

13. Li J, Huang Q, Chen J, Qi H, Liu J, Chen Z, et al. Neuroprotective potentials of Panax Ginseng against Alzheimer's disease: a review of preclinical and clinical evidences. *Front Pharmacol*. (2021) 12:688490. doi: 10.3389/fphar.2021.688490

14. Liu H, Zhong L, Dai Q, Yang J, Zhang Y, Zhang B, et al. Zuoguiwan ameliorates cognitive deficits and neuro-inflammation in Streptozotocin-induced Alzheimer's disease rats. *Neuroimmunomodulation*. (2022) 29:63–9. doi: 10.1159/000516396

15. Wang M, Dong Y, Wu J, Li H, Zhang Y, Fan S, et al. Baicalein ameliorates ionizing radiation-induced injuries by rebalancing gut microbiota and inhibiting apoptosis. *Life Sci*. (2020) 261:118463. doi: 10.1016/j.lfs.2020.118463

16. Zhao T, Tang H, Xie L, Zheng Y, Ma Z, Sun Q, et al. (Lamiaceae): a review of its traditional uses, botany, phytochemistry, pharmacology and toxicology. *J Pharm Pharmacol*. (2019) 71:1353–69. doi: 10.1111/jphp.13129

17. Gao Z, Huang K, Xu H. Protective effects of flavonoids in the roots of Scutellaria baicalensis Georgi against hydrogen peroxide-induced oxidative stress in HS-SY5Y cells. *Pharmacol Res*. (2001) 43:173–8. doi: 10.1006/phrs.2000.0761

18. Lee HZ, Leung HW, Lai MY, Wu CH. Baicalein induced cell cycle arrest and apoptosis in human lung squamous carcinoma CH27 cells. *Anticancer Res*. (2005) 25:959–64.

19. Zhang S, Ye J, Dong G. Neuroprotective effect of baicalein on hydrogen peroxide-mediated oxidative stress and mitochondrial dysfunction in PC12 cells. *J Mol Neurosci*. (2010) 40:311–20. doi: 10.1007/s12031-009-9285-5

20. de Oliveira MR, Nabavi SF, Habtemariam S, Erdogan Orhan I, Daglia M, Nabavi SM. The effects of baicalein and baicalin on mitochondrial function and dynamics: a review. *Pharmacol Res*. (2015) 100:296–308. doi: 10.1016/j.phrs.2015.08.021

21. Liang W, Huang X. Chen W the effects of Baicalin and Baicalein on cerebral ischemia: a review. *Aging Dis*. (2017) 8:850–67. doi: 10.14336/AD.2017.0829

22. Qi X, Li H, Cong X, Wang X, Jiang Z, Cao R, et al. Baicalin increases developmental competence of mouse embryos in vitro by inhibiting cellular apoptosis and modulating HSP70 and DNMT expression. *J Reprod Dev*. (2016) 62:561–9. doi: 10.1262/jrd.2016-047

23. Olğaç KT, Akçay E. Effects of Spermine and spermidine supplemented extenders on post-thaw Spermatological parameters in stallion semen cryopreservation. *Cryobiology*. (2021) 100:72–6. doi: 10.1016/j.cryobiol.2021.03.008

24. Bucher K, Malama E, Siuda M, Janett F, Bollwein H. Multicolor flow cytometric analysis of cryopreserved bovine sperm: a tool for the evaluation of bull fertility. *J Dairy Sci*. (2019) 102:11652–69. doi: 10.3168/jds.2019-16572

25. İnanç ME, Güngör Ş, Öztürk C, Korkmaz F, Baştan İ, Çil B. Cholesterol-loaded cyclodextrin plus trehalose improves quality of frozen-thawed ram sperm. *Vet Med*. (2019) 64:118–24. doi: 10.17221/146/2018-VETMED

26. Gündoğan M, Yeni D, Avdatek F, Fidan AF. Influence of sperm concentration on the motility, morphology, membrane and DNA integrity along with oxidative stress parameters of ram sperm during liquid storage. *Anim Reprod Sci*. (2010) 122:200–7. doi: 10.1016/j.anireprosci.2010.08.012

27. Draper HH, Hadley M. Malondialdehyde determination as index of lipid peroxidation. *Methods Enzymol*. (1990) 186:421–31. doi: 10.1016/0076-6879(90)86135-i

28. Hissin PJ, Hilf R. A fluorometric method for determination of oxidized and reduced glutathione in tissues. *Anal Biochem*. (1976) 74:214–26. doi: 10.1016/0003-2697(76)90326-2

29. Esen C, Alkan BA, Kırnap M, Akgül O, Işıkoğlu S, Erel O. The effects of chronic periodontitis and rheumatoid arthritis on serum and gingival crevicular fluid total antioxidant/oxidant status and oxidative stress index. *J Periodontol*. (2012) 83:773–9. doi: 10.1902/jop.2011.110420

30. Holt WV. Basic aspects of frozen storage of semen. *Anim Reprod Sci*. (2000) 62:3–22. doi: 10.1016/s0378-4320(00)00152-4

31. Ramón M, Pérez-Guzmán MD, Jiménez-Rabadán P, Esteso MC, García-Álvarez O, Maroto-Morales A, et al. Sperm cell population dynamics in ram semen during the cryopreservation process. *PLoS One*. (2013) 8:e59189. doi: 10.1371/journal.pone.0059189

32. Thurston LM, Watson PF, Holt WV. Semen cryopreservation: a genetic explanation for species and individual variation? *Cryo Letters*. (2002) 23:255–62.

33. Lin M, Li L, Zhang Y, Zheng L, Xu M, Rong R, et al. Baicalin ameliorates H_2O_2 induced cytotoxicity in HK-2 cells through the inhibition of ER stress and the activation of Nrf2 signaling. *Int J Mol Sci*. (2014) 15:12507–22. doi: 10.3390/ijms150712507

34. Meng X, Hu L, Li W. Baicalin ameliorates lipopolysaccharide-induced acute lung injury in mice by suppressing oxidative stress and inflammation via the activation of the Nrf2-mediated HO-1 signaling pathway. *Naunyn Schmiedeberg's Arch Pharmacol*. (2019) 392:1421–33. doi: 10.1007/s00210-019-01680-9

35. Sui J, Feng Y, Li H, Cao R, Tian W, Jiang Z. Baicalin protects mouse testis from injury induced by heat stress. *J Therm Biol*. (2019) 82:63–9. doi: 10.1016/j.jtherbio.2019.03.009

36. Yu H, Chen B, Ren Q. Baicalin relieves hypoxia-aroused H9c2 cell apoptosis by activating Nrf2/HO-1-mediated HIF1α/BNIP3 pathway. *Artif Cells Nanomed Biotechnol*. (2019) 47:3657–63. doi: 10.1080/21691401.2019.1657879

37. Fan H, He J, Bai Y, He Q, Zhang T, Zhang J, et al. Baicalin improves the functions of granulosa cells and the ovary in aged mice through the mTOR signaling pathway. *J Ovarian Res*. (2022) 15:34. doi: 10.1186/s13048-022-00965-7

38. İnanç ME, Güngör Ş, Avdatek F, Yeni D, Gülhan MF, Olğaç KT, et al. Thymoquinone improves motility, plasma membrane integrity and DNA integrity of frozen-thawed ram semen. *Andrologia*. (2022) 54:e14547. doi: 10.1111/and.14547

39. Taşdemir U, Yeni D, İnanç ME, Avdatek F, Çil B, Türkmen R, et al. Red pine (*Pinus brutia* ten) bark tree extract preserves sperm quality by reducing oxidative stress and preventing chromatin damage. *Andrologia*. (2020) 52:e13603. doi: 10.1111/and.13603

40. Kang KA, Zhang R, Piao MJ, Chae S, Kim HS, Park JH, et al. Hyun JW Baicalein inhibits oxidative stress-induced cellular damage via antioxidant effects. *Toxicol Ind Health*. (2012) 28:412–21. doi: 10.1177/0748233711413799

41. Pan Y, Song D, Zhou W, Lu X, Wang H, Li Z. Baicalin inhibits C2C12 myoblast apoptosis and prevents against skeletal muscle injury. *Mol Med Rep*. (2019) 20:709–18. doi: 10.3892/mmr.2019.10298

42. Sahu BD, Kumar JM, Kuncha M, Borkar RM, Srinivas R, Sistla R. Baicalein alleviates doxorubicin-induced cardiotoxicity via suppression of myocardial oxidative stress and apoptosis in mice. *Life Sci*. (2016) 144:8–18. doi: 10.1016/j.lfs.2015.11.018

43. Maneesh M, Jayalekshmi H. Role of reactive oxygen species and antioxidants on pathophysiology of male reproduction. *Indian J Clin Biochem*. (2006) 21:80–9. doi: 10.1007/BF02912918

44. Kovalski NN, de Lamirande E, Gagnon C. Reactive oxygen species generated by human neutrophils inhibit sperm motility: protective effect of seminal plasma and scavengers. *Fertil Steril*. (1992) 58:809–16. doi: 10.1016/S0015-0282(16)55332-1

45. Aitken RJ, Baker MA. Oxidative stress and male reproductive biology. *Reprod Fertil Dev*. (2004) 16:581–8. doi: 10.10371/RD03089

46. Alahmar AT. Role of oxidative stress in male infertility: an updated review. *J Hum Reprod Sci*. (2019) 12:4–18. doi: 10.4103/jhrs.JHRS_150_18

47. Wagner H, Cheng JW, Ko EY. Role of reactive oxygen species in male infertility: an updated review of literature. *Arab J Urol*. (2018) 16:35–43. doi: 10.1016/j.aju.2017.11.001

48. Fernández-Santos MR, Domínguez-Rebolledo AE, Esteso MC, Garde JJ, Martínez-Pastor F. Catalase supplementation on thawed bull spermatozoa abolishes the detrimental effect of oxidative stress on motility and DNA integrity. *Int J Androl*. (2009) 32:353–9. doi: 10.1111/j.1365-2605.2008.00871.x

49. Gadea J, García-Vazquez F, Matás C, Gardón JC, Cánovas S, Gumbao D. Cooling and freezing of boar spermatozoa: supplementation of the freezing media with reduced glutathione preserves sperm function. *J Androl*. (2005) 26:396–404. doi: 10.2164/jandrol.04155

50. Güngör S, İnanç ME, Yeni D, Avdatek F, Türkmen R, Taşdemir U. The effect of gallic acid addition to tris-based extender on frozen bull semen. *Kafkas Univ Vet Fak Derg*. (2021) 27:633–9. doi: 10.9775/kvfd.2021.26023

51. Perruchot MH, Gondret F, Robert F, Dupuis E, Quesnel H, Dessauge F. Effect of the flavonoid baicalin on the proliferative capacity of bovine mammary cells and their ability to regulate oxidative stress. *PeerJ*. (2019) 7:e6565. doi: 10.7717/peerj.6565

frontiers | Frontiers in Veterinary Science

TYPE Original Research
PUBLISHED 10 April 2024
DOI 10.3389/fvets.2024.1400899

OPEN ACCESS

EDITED BY
Omer Ucar,
Muğla Sıtkı Koçman University, Türkiye

REVIEWED BY
Umut Cagin Ari,
Kafkas University, Türkiye
Silviu-Ionuț Borș,
Research and Development Station for Cattle Breeding Dancu, Romania

*CORRESPONDENCE
Joohyeong Lee
✉ durubit@gmail.com
Sang-Hwan Hyun
✉ shhyun@cbu.ac.kr

RECEIVED 14 March 2024
ACCEPTED 29 March 2024
PUBLISHED 10 April 2024

CITATION
Jung S, Sul H, Oh D, Jung Y-G, Lee J and Hyun S-H (2024) Slow freezing cryopreservation of Korean bovine blastocysts with an additional sucrose pre-equilibration step.
Front. Vet. Sci. 11:1400899.
doi: 10.3389/fvets.2024.1400899

Slow freezing cryopreservation of Korean bovine blastocysts with an additional sucrose pre-equilibration step

Seungki Jung[1,2], Hyeonseok Sul[2], Dongjin Oh[1,3], Yeon-Gil Jung[2], Joohyeong Lee[4]* and Sang-Hwan Hyun[1,3,5]*

[1]Veterinary Medical Center and College of Veterinary Medicine, Laboratory of Veterinary Embryology and Biotechnology (VETEMBIO), Chungbuk National University, Cheongju, Republic of Korea, [2]ET Biotech Co. Ltd., Jangsu, Republic of Korea, [3]Institute of Stem Cell and Regenerative Medicine (ISCRM), Chungbuk National University, Cheongju, Republic of Korea, [4]Department of Companion Animal Industry, Semyung University, Jecheon, Republic of Korea, [5]Graduate School of Veterinary Biosecurity and Protection, Chungbuk National University, Cheongju, Republic of Korea

Introduction: Embryo cryopreservation is a valuable technique used for preserving genetic resources for long periods. However, the survival rate of embryos is dependent on the method used. Therefore, in this study, we evaluated the efficiency of slow freezing method but with an additional dehydration step prior to freezing to overcome the formation of ice crystals.

Methods: Oocytes collected from the ovaries of native Korean cattle subjected to *in vitro* fertilization were cultured for 7 days until the formation of expanded blastocysts. Before freezing, the blastocysts were placed in four pre-equilibration media: a control medium with no addition of sucrose, and three experimental media with the addition of 0.1, 0.25, and 0.5 M sucrose, respectively. Then, the pre-equilibrated embryos were frozen. Embryo survival and hatching rates were evaluated morphologically at 24, 48, and 72 h after thawing. Immunofluorescence staining, terminal deoxynucleotidyl transferase-mediated dUTP nick end labeling (TUNEL) assay, and gene expression analysis of the re-expanded blastocytes were examined 24 h after freeze–thawing.

Results: The survival rate was significantly higher in the 0.1 M group than in the control group ($p < 0.05$), and the hatching rate at 72 h was significantly higher in the 0.25 and 0.5 M groups than in the control group ($p < 0.05$). TUNEL-positive cells were significantly lower in the 0.25 M group than in the control group (12.5 ± 0.9 vs. 8.3 ± 0.8; $p < 0.05$). The gene expression of *BCL2* associated X, heat shock protein 70 kDa, and aquaporin 3 in the 0.25 M group was significantly lower than that in the control group ($p < 0.05$).

Conclusion: Our study revealed that treatment with 0.25 M sucrose before slow freezing improved the viability of bovine embryos after freeze–thawing.

KEYWORDS

sucrose, blastocyst, slow freezing, *in vitro* production, bovine

1 Introduction

Currently, *in vitro* production (IVP) of embryos is a commercially successful approach for cattle breeding; the number of embryo transfers following IVP has increased since the establishment of the ovum pick-up-*in vitro* fertilization (IVF) system (1). In addition, the number of transplanted embryos produced *in vitro* is higher than that *in vivo* (1). The pregnancy rate of embryos produced after freeze-thawing is lower for embryos produced *in vitro* than for embryos produced *in vivo* (2, 3). Therefore, improvements in freezing methods are needed to increase the productivity of *in vitro* embryos after embryo transfer.

Cryopreservation methods, such as slow freezing, vitrification (4, 5), and low-temperature storage, are used to preserve cattle embryos (6). The slow freezing and vitrification methods can preserve genetic resources for long periods and have the advantage of embryos being transferred 7 days after the natural estrus cycle without synchronization. Vitrification has a faster cooling rate and does not form ice crystals, resulting in higher embryo survival and conception rates after embryo transfer (4, 5). However, vitrification involves the use of cryoprotectants at high concentrations, requiring their removal during the embryo thawing process (4, 7, 8). Therefore, this method is difficult to apply in field settings, because it requires skilled technicians, separate sterile facilities, and specific laboratory equipment at the embryo transfer site. In slow freezing, although relatively lower concentrations of cryoprotectants are used and in straw dilution and direct embryo transfer are practically applicable, the survival and conception rates of embryos in this method are relatively low (9), because of ice crystal formation within the embryos from the remaining water due to insufficient dehydration (10). Nevertheless, this process can be used at embryo transfer sites because the thawed embryos in the straws can be directly transferred into the recipients' uterus (11). As intracellular ice formation has been identified as an important factor in slow frozen embryo survival, the possibility that improvements in embryo dehydration before slow freezing could improve the conception rate requires investigation. This aspect becomes particularly important as expanded bovine blastocysts produced *in vitro* with higher water content offer better conception rates (12).

Sucrose is a non-penetrating cryoprotectant used for removing intracellular water and protecting cells from osmotic shock in freezing media (7, 13). Bovine embryos were reportedly pre-equilibrated with sucrose before slow freezing; however, pretreatment did not improve embryo re-expansion and apoptosis rates (14). Bui-Xuan-Nguyen (15) pretreated bovine embryos with sucrose before slow freezing in a medium containing glycerol; however, viability did not improve. Usually, ethylene glycol (EG) is used as a freezing medium for direct embryo transfer owing to its low molecular weight and high permeability compared to glycerol. In addition, Voelkel and Hu (16) reported that embryos were slow freeze-thawed using EG, propylene giycol, dimethyl sulfoxide, and glycerol as cryoprotectants, and that embryos frozen in EG showed high viability.

The use of slow-freezing media supplemented with sucrose to freeze embryos is a well-known technique (17–19). However, there are limited reports on sucrose pre-equilibration using bovine embryos (14, 15). In this study, we aimed to evaluate embryo viability after slow freezing and thawing by inducing artificial shrinkage of the blastocoel cavity using different concentrations of sucrose medium before equilibration in a freezing medium containing EG. In addition, we investigated any differences in immunofluorescence staining, terminal deoxynucleotidyl transferase-mediated dUTP nick end labeling (TUNEL) assay results, and mRNA expression in blastocysts pretreated with sucrose at the optimal concentration compared with those in the control group.

2 Materials and methods

2.1 Oocyte collection and *in vitro* maturation

Ovaries from Korean native cattle (*Bos taurus coreanae*) were collected immediately after slaughter and transported to the laboratory in a physiological saline solution (0.9% NaCl) at 32°C. Cumulus–oocyte complexes (COCs) were collected via the aspiration of 2–8-mm follicles using an 18 G needle connected to a 10 mL syringe. The aspirated COCs with a homogeneous cytoplasm and at least three layers of cumulus cells were washed three times in OCM (IFP9611; Research Institute for the Functional Peptides, Yamagata, Japan). The selected COCs were then washed three times in HP-M199 (IFP971; Research Institute for the Functional Peptides) supplemented with 0.5 μg/mL follicle-stimulating hormone (Folltropin V; Bioniche Animal Health, Belleville, ON, Canada) and 5% fetal bovine serum (FBS; Access Biologicals, Vista, CA, United States) used as *in vitro* maturation (IVM) medium. The COCs were randomly cultured in 5-well dishes with 50 COCs per well (1 mL IVM medium per well) for 22 h at 38.9°C under 5% CO_2 and 100% humidity.

2.2 *In vitro* fertilization and *in vitro* culture of embryos

In vitro fertilization was performed as reported by Kim et al. (6) with minor modifications. Frozen semen from Korean cattle were stored at −196°C in 0.5-mL straws until required. The straws were thawed in a 38°C water bath for 40 s. The thawed sperm were transferred into a 15-mL conical tube containing 1 mL of SPF45 and 1 mL of 80 SpermFilter® (Gynotec, Malden, Netherlands) and centrifuged at 600 *g* for 15 min. The precipitate was then transferred to a new centrifuge tube with 4 mL of IVF100 (IFP9630; Research Institute for the Functional Peptides) and centrifuged at 600 *g* for 10 min. 3.7 mL of supernatant was removed and 15 μL of sperm suspension (1×10^7 cells/mL) was added to 50 μL of IVF100 drops, resulting in a final sperm concentration of 2×10^6 cells/mL. Approximately 10–15 cumulus cell expanded oocytes were placed per drop and incubated at 38.9°C under 5% CO_2 and 100% humidity for 6 h. The day of fertilization was labeled as day 0. At the end of IVF,

Abbreviations: *AQP3*, Aquaporin 3; *BAX*, *BCL2* associated X; cDNA, Complementary DNA; COC, Cumulus–oocyte complex; DPBS, Dulbecco's phosphate buffered saline; EG, Ethylene glycol; *GAPDH*, Glyceraldehyde 3-phosphate dehydrogenase; *HSPA1A*, Heat shock protein 70 kDa; IVC, *In vitro* culture; IVF, *In vitro* fertilization; IVM, *In vitro* maturation; IVP, *In vitro* production; *PLAC8*, Placenta-specific 8; qRT-PCR, Quantitative reverse transcription-PCR; TUNEL, Terminal deoxynucleotidyl transferase-mediated dUTP nick end labeling; Ct, Threshold cycle.

the presumptive zygote was removed from the cumulus cells and sperm by pipetting. For *in vitro* culture (IVC), 10–15 presumptive zygotes were placed in a 50 mL drop of potassium simplex optimized medium and incubated for 7 days at 38.9°C under 5% CO_2, 5% O_2, and 100% humidity.

2.3 Experimental design

2.3.1 Experiment 1: survival and hatching rates of expanded bovine blastocysts exposed to various concentrations of sucrose prior to slow freeze–thawing

Expanded blastocysts developed 7 days after IVF were divided into four groups treated with 0 (control), 0.1, 0.25, and 0.5 M sucrose media. To investigate the effect of artificial shrinkage of the blastocoel cavity on embryos treated with sucrose before slow freezing, the survival rate was morphologically evaluated by the number of re-expanded blastocysts 24 h after thawing and the hatching rate at 24, 48, and 72 h.

2.3.2 Experiment 2: influence of pre-exposure of bovine blastocysts to 0.25 M sucrose on different post-thaw viability measurements

Based on the total number of embryos hatched and embryo hatching/survival rates in Experiment 1, Experiment 2 was conducted using control and 0.25 M sucrose pretreatment groups. The total and apoptotic cell numbers of embryos thawed using each freezing method were confirmed using the TUNEL assay, and the total inner cell mass (ICM) number was determined using SOX2 antibody immunofluorescence. Finally, the effects of sucrose pretreatment before slow freezing on the gene expression levels of *BCL2* associated X (*BAX*), heat shock protein 70 kDa (*HSPA1A*), aquaporin 3 (*AQP3*), and placenta-specific 8 (*PLAC8*) in embryos after thawing were investigated.

2.4 Slow freezing

All experiments were performed using good-quality expanded blastocysts developed 7 days after IVF and were scored according to the International Embryo Technology Society guidelines (20). As shown in Figure 1, the expanded blastocysts were exposed to control, and 0.1, 0.25, and 0.5 M sucrose solution in Dulbecco's phosphate buffered saline (DPBS; Gibco, Waltham, MA, United States) containing 20% FBS for 3 min at 20–25°C. The expanded blastocysts were washed three times in freezing medium without sucrose, containing 1.8 M EG (IFP9620; Research Institute for the Functional Peptides) to completely remove the sucrose pretreatment medium; the blastocysts were then equilibrated in the same freezing medium for 12 min at 20–25°C. During EG exposure, 5–10 expanded blastocysts per group were inserted in 0.25-mL straws (IMV Technologies, L'Aigle, France). Following exposure, the straws were placed in a freezer (FREEZE CONTROL®; Cryologic, Victoria, Australia) at −6°C. After 2 min, seeding was induced using a pair of tweezers to avoid supercooling. After another 10 min, the straws were frozen to −35°C at a rate of −0.3°C per min. After freezing, the straws were stored in liquid nitrogen for at least 1 week. The frozen straws containing the expanded blastocysts were thawed for 10 s in air and 30 s in 35°C water. The recovered expanded blastocysts were then washed three times in DPBS containing 10% FBS, diluted in IVC medium for 10 min, and cultured in the same medium for 72 h at 38.9°C under 5%CO_2, 5%O_2, and 100% humidity. Survival and hatching rates were determined based on the number of re-expanded and hatched blastocysts 24, 48, and 72 h after thawing.

2.5 Immunofluorescence analysis for surviving embryos after slow freeze–thawing

Immunofluorescence analysis was performed as reported by Lee et al. (21). Re-expanded or hatched blastocysts in 24-h culture after freeze–thawing were fixed with 4% (v/v) paraformaldehyde, washed with DPBS, and permeabilized with 0.5% (v/v) Triton X-100 for 30 min. The blastocysts were then co-incubated with a blocking solution and SOX2 primary antibody (sc-365823, 1:100; Santa Cruz Biotechnology, Santa Cruz, CA, United States) overnight at 4°C. After rinsing with washing medium (Tween20, Triton X-100, and DPBS), the expanded blastocysts were incubated with the secondary antibodies: goat anti-mouse IgG (H + L) Alexa FluorTM 488 (A11029, 1:200; Invitrogen Corporation, Carlsbad, CA, United States), donkey anti-rabbit IgG (H + L) Alexa FluorTM 594 (A21207, 1:400; Invitrogen) for 1 h at 20°C–25°C. The nuclei were stained with

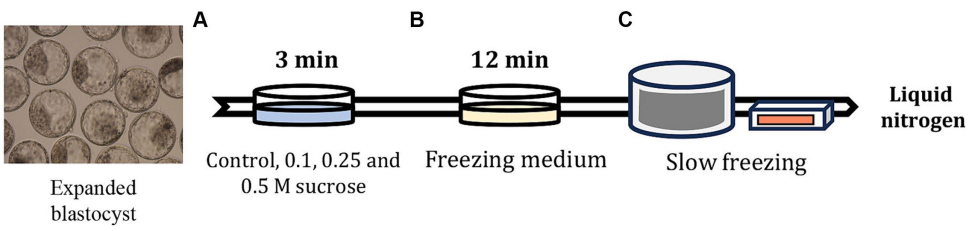

FIGURE 1
Slow freezing process after artificially shrinking the embryo blastocoel cavity using sucrose medium. **(A)** After 7 days of IVF, the expanded blastocysts were pre-equilibrated in Dulbecco's phosphate buffered saline (DPBS) containing sucrose and 20% FBS for 3 min. **(B)** After confirming blastocoel cavity shrinkage, the embryos were equilibrated in DPBS containing 1.8 M EG for 12 min, and then the embryos were inserted in 0.25-mL straws and sealed. **(C)** The straws containing embryos were placed in a freezer maintained at −6°C and seeded after equilibration for 2 min. After 10 min, the straws were gradually frozen to −35°C at −0.3°C/min and stored in liquid nitrogen.

Hoechst-33342 and examined under an epifluorescence microscope using the ZEN 3.5 Blue Edition software (Zeiss, Germany).

2.6 TUNEL assay for surviving embryos after slow freeze–thawing

The TUNEL assay was performed as described by Lee et al. (21). To analyze apoptosis in the re-expanded and hatched blastocysts 24 h after freeze–thawing, the blastocysts were fixed with 4% paraformaldehyde for 1 h at 20–25°C and washed with DPBS. Permeabilization was performed using 0.1% Triton X-100 in 0.1% (w/v) sodium citrate for 1 h at 20–25°C. After washing with DPBS, the expanded blastocysts were stained with 45 mL of TUNEL-Label solution (Roche, Germany) containing 5 mL of TUNEL-Enzyme solution (Roche) for 1 h at 39°C in a dark, humidified atmosphere. Subsequently, the nuclei were stained with 5 μg/mL Hoechst-33342 for 10 min and the blastocysts were analyzed under an epifluorescence microscope.

2.7 Quantitative reverse transcription-PCR analysis for surviving embryos after slow freeze–thawing

mRNA was isolated from three replicates, each replicate containing five embryos. Quantitative reverse transcription-PCR (qRT-PCR) was performed as reported by Oh et al. (22). mRNA expression of four genes, *BAX*, *HSPA1A*, *AQP3*, and *PLAC8*, was analyzed using qRT-PCR with the primer sequences listed in Table 1. After recovery from freeze–thawing for 24 h, the re-expanded or hatched blastocysts were washed with DPBS and snap frozen sampled at −80°C prior to experimentation. The total RNA was extracted using TRIzol reagent (TaKaRa Bio, Inc., Otsu, Shiga, Japan) according to the manufacturer's protocol and quantified by measuring the absorbance at 260/280 nm. The purity of the extracted RNA was 1.9; the RNA was stored at −80°C until use. Total RNA (1 μg) was converted to complementary DNA (cDNA) using the SuperScript IV VILO Master Mix (Thermo Fisher Scientific, Waltham, MA, United States). The synthesized cDNA, SYBR Premix Ex Taq (TaKaRa Bio, Inc.), and specific primers (Macrogen, Inc., Seoul, Republic of Korea) were used for qRT-PCR. mRNA expression was analyzed using the CFX96 Touch Real-Time PCR Detection System (Bio-Rad, Hercules, CA, United States). The cycling parameters were as follows: 40 cycles for 5 min at 95°C, 15 s at 95°C, 15 s at 56°C, and 30 s at 72°C. Relative quantification was performed by comparing threshold cycles (Ct) at a constant fluorescence intensity. Relative mRNA expression (*R*) was calculated using the equation $R = 2^{-[1\text{Ctsample}-1\text{Ctcontrol}]}$ (23). The *R*-values were normalized to those of glyceraldehyde 3-phosphate dehydrogenase (*GAPDH*) in each blastocyst group (24).

2.8 Statistical analysis

Statistical analyses were performed using the Statistical Analysis System software (version 9.4; SAS Institute, Cary, NC, United States). Data were analyzed using the general linear model approach, followed by the mean separation method, with the least significant difference ($p < 0.05$) when there was a difference between treatments. Percentage data were arcsine-transformed prior to analysis to maintain the homogeneity of variance. Results are expressed as mean ± standard error of the mean.

3 Results

3.1 Effect of sucrose pretreatment on blastocyst survival after slow freezing and thawing

In Experiment 1, the embryos were freeze-thawed using sucrose of various concentrations to determine the optimal sucrose concentration for treatment before slow freezing. The blastocyst survival rate after slow freeze–thawing is shown in Table 2. The survival rate was higher in the 0.1 M group than in the control group ($p < 0.05$); however, no significant differences were observed between the 0.25 and 0.5 M groups. There were no significant differences in the hatching rates among the groups at 24 and 48 h. However, the hatching rate at 72 h was significantly higher

TABLE 1 Primer sequences for quantitative reverse transcription PCR analysis.

Gene	Primer sequence	Product size (bp)	GenBank accession number
BAX	F: 5′-TGTCGCCCTTTTCTACTTTG-3′	204	NM_173894.1
	R: 5′-GCCACAAAGATGGTCACTGT-3′		
HSPA1A	F: 5′-GAGTCGTACGCCTTCAACAT-3′	194	NM_203322.3
	R: 5′-ATGATGGGGTTACACACCTG-3′		
PLAC8A	F: 5′-GACTGGCATCTTTGACTGCT-3′	195	NM_001025325.2
	R: 5′-GTCAGACACAGGCAATCCTT-3′		
AQP3	F: 5′-TTGGTCATCGGTACCTCAAT-3′	196	NM_001079794.1
	R: 5′-TCATGAGCTGGTACACGAAG-3′		
GAPDH	F: 5′-CTGGAGAAACCTGCCAAGTA-3′	186	NM_001034034.2
	R: 5′-GAGCTTGACAAAGTGGTCGT-3′		

TABLE 2 Effect of sucrose on survival rate at 24 h and hatching rate of bovine blastocysts at 72 h after slow freezing and thawing.

Sucrose (M)	Survived (re-expanded) embryos/No. of Blastocysts (%)	No. of hatched blastocysts (%)			Embryo hatched/ Survived (%)
		24 h	48 h	72 h	
0 (Control)	59/65 (90.1 ± 4.5)[a]	5 (6.5 ± 2.6)	30 (43.6 ± 5.9)	38 (58.0 ± 6.4)[a]	38 (65.3 ± 7.2)[a]
0.1	64/65 (99.2 ± 0.8)[b]	13 (18.6 ± 8.1)	37 (53.8 ± 10.5)	48 (76.6 ± 6.1)[ab]	48 (77.1 ± 5.9)[ab]
0.25	62/65 (97.5 ± 2.5)[ab]	12 (17.1 ± 6.7)	34 (55.1 ± 8.2)	54 (87.6 ± 6.0)[b]	54 (89.6 ± 5.0)[b]
0.5	61/66 (95.4 ± 3.0)[ab]	16 (24.6 ± 9.7)	38 (59.4 ± 4.6)	50 (80.1 ± 5.6)[b]	50 (83.5 ± 3.9)[ab]

Seven replicates; data are presented as mean ± standard error. [a,b]Values in the same column with different superscript letters are significantly different ($p < 0.05$).

TABLE 3 Effect of sucrose on bovine blastocyst cells as determined using immunofluorescence analysis and TUNEL assay after slow freezing and thawing.

Sucrose (M)	Immunofluorescence analysis					TUNEL assay			
	No. of Blastocysts (No. of replicates)	Total cells	ICM	TE	ICM/ TE cells (%)	No. of blastocysts (No. of replicates)	Total cells	Apoptotic cells	Apoptotic/ total cells (%)
		Mean	Mean	Mean			Mean	Mean	
0 (Control)	13 (3)	171.0 ± 9.2	52.2 ± 7.1	118.8 ± 7.6	30.5 ± 3.3	24 (3)	171.1 ± 6.5	12.5 ± 0.9[a]	7.5 ± 0.6[a]
0.25	13 (3)	183.2 ± 7.1	55.3 ± 7.2	127.8 ± 5.2	30.2 ± 3.3	19 (3)	184.4 ± 8.7	8.3 ± 0.8[b]	4.6 ± 0.5[b]

Data are presented as mean ± standard error. [a,b]Values in the same column with different superscript letters are significantly different ($p < 0.05$).

($p < 0.05$) in the 0.25 and 0.5 M groups than in the control group. The hatching rate at 72 h was not significantly different among the 0.1, 0.25, and 0.5 M groups. The proportion of hatched blastocysts among those that survived slow freezing and thawing was higher ($p < 0.05$) in the 0.25 M group than in the control group, and the proportion in the 0.1 and 0.5 M groups was not significantly different from that in the control and 0.25 M groups. Hence, we performed Experiment 2 using 0.25 M sucrose. The results suggested that pretreatment with 0.25 M sucrose could affect embryo recovery after thawing.

3.2 Effects of sucrose pretreatment on ICM and trophectoderm of blastocysts after slow freezing and thawing

For Experiment 2 (0 and 0.25 M sucrose treatments), 24 h after thawing the embryos, we examined the ICM and TE using immunofluorescence analysis. No significant differences were observed in the total cell, ICM, or TE numbers between the groups. In addition, the ICM ratio of the total cell number showed no significant differences between the control and 0.25 M groups ($p > 0.05$, Table 3).

3.3 Effect of sucrose pretreatment on the apoptosis of blastocysts after slow freezing and thawing

To analyze apoptosis, the embryos were subjected to TUNEL assay 24 h after thawing. The total cell and apoptotic cell numbers in the blastocysts are shown in Table 3. No significant differences were observed in the total cell number between the control and 0.25 M groups. However, the number of apoptotic cells was significantly higher in the control group than in the 0.25 M group ($p < 0.05$).

3.4 Effect of sucrose pretreatment on gene expression levels in blastocysts after slow freezing and thawing

To analyze the effect of sucrose pretreatment on gene expression in embryos after freeze–thawing, qRT-PCR was performed. In the 0.25 M group, the relative mRNA expression of *BAX*, *HSP1A1*, and *AQP3* was significantly lower ($p < 0.05$) than that in the control group (Figure 2). However, the control and 0.25 M groups showed no significant differences in *PLAC8* expression (Figure 2).

4 Discussion

In this study, we investigated the effect of sucrose treatment on bovine embryos before freezing on the viability of the embryos after thawing. We demonstrated that embryos treated with sucrose before freezing had improved hatching rate after thawing. In addition, we demonstrated that sucrose treatment of bovine embryos prior to freezing decreased the transcript levels of apoptosis and cell stress related genes after thawing.

A slow freezing method for shrinking cattle embryos by adding sucrose to the freezing medium has been designed (9, 11, 17, 25). However, data on slow freezing methods using sucrose pretreatment prior to freezing are insufficient. Hence, in this study, we investigated blastocyst apoptosis and hatching rates upon pretreatment with

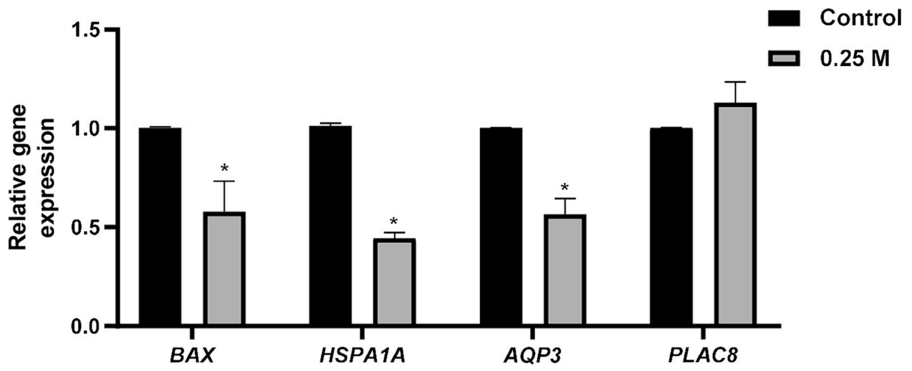

FIGURE 2
Effect of sucrose medium treatment before slow freezing of bovine blastocysts on the relative mRNA expression after thawing. *BAX*, BCL2 associated X; *HSPA1A*, Heat shock protein 70 kDa; *AQP3*, Aquaporin 3; *PLAC8*, Placenta specific 8. *Different superscripts indicate significant differences for each gene ($p < 0.05$).

various concentrations of sucrose before slow freezing. Iwayama et al. (26) reported no differences in the overall implantation rate when vitrification was performed after artificial shrinkage using a sucrose medium. However, high implantation rates were confirmed in embryos that recovered quickly after vitrification warming via sucrose medium pretreatment (26). In addition, Dang-Nguyen et al. (27) evaluated porcine oocyte quality using 0.2 M sucrose medium and Van Soom et al. (28) induced contraction of bovine morulae using 0.3 M sucrose medium; however, these treatments did not have a negative effect on viability. In this study, artificial shrinkage of the blastocoel cavity and blastomeres was induced using control, and 0.1, 0.25, and 0.5 M sucrose medium before slow freezing. We were unable to examine the effect of using sucrose medium on embryos without subsequent freezing; however, no adverse effects on embryos were identified after freeze–thawing. Additionally, we found that pretreating bovine embryos with 0.25 M sucrose resulted in higher hatching and hatching/survival rates at 72 h than in the control group after freeze–thawing. Thus, using the osmotic agent medium dehydrates the embryos and blastomeres. When the embryos are exposed to the freezing medium, a higher amount of the cryoprotectant penetrates them, possibly improving the viability of the embryos after slow freeze–thawing. Moreover, the blastocoel cavity could be artificially shrunk using a sucrose medium; it does not require special equipment or techniques and is easy to prepare sucrose medium.

The embryo does not fully recover within 24 h after thawing. We examined the hatching rate at 72 h after thawing to determine the possibility of implantation. However, in Experiment 2, the embryos were used 24 h after thawing to evaluate the quality of surviving embryos. Apoptosis maintains embryonic development and homeostasis, producing normal cells or removing abnormal cells; increased apoptosis is an important indicator for evaluating embryo quality. Apoptosis has been used to evaluate the quality of bovine (25), mouse (29), goat (30), equine (31), and human (29) embryos produced using the IVP system and that of *in vivo* and *in vitro* embryos. Additionally, vitrification and slow freezing methods damage embryonic cells by physical, chemical, and thermal factors during the freezing process; therefore, cell death is an important indicator of the effect of each freezing method on embryos (32, 33). In our study, only the control and 0.25 M groups were used to evaluate apoptosis, because the 0.25 M group showed the highest viability after freezing among the 0.1, 0.25, and 0.5 M groups. In addition, TUNEL staining showed no difference in the total number of cells between the groups evaluated 24 h after thawing, but the number of apoptotic cells was significantly lower in the 0.25 M group than in the control group. Compared to the control group, the 0.25 M group was confirmed to artificially shrink embryonic cells. The damage to blastomeres was assumed to be reduced by reducing ice crystal formation along with the dehydration of embryos. In future studies, the conception rate of frozen blastocysts after artificial shrinkage using 0.25 M sucrose before freezing should be examined.

The first lineage specification event during mammalian embryogenesis is the differentiation of the TE and ICM. The ICM develops into the hypodermis and ectoderm, and the TE develops outward from the fetal portion of the placenta. In human embryos, differences in cell numbers between the ICM and TE have been reported to reduce early embryo loss and improve implantation and birth rates (34). In cattle, the ICM and TE cell numbers are vary significantly depending on the culture system (35, 36). The ratio and distribution of these cells are a potential indicator of embryo quality and are considered crucial for implantation (37). However, in this study, no differences were observed in the number of ICM and TE cells between the control and 0.25 M groups. In the additional experiments, no differences were observed in TE cell numbers; however, confirming the embryo quality through the analysis of *INFT2*, which affects the conception rate, is necessary.

The relative mRNA expression in embryos after freeze–thawing has been widely reported. The relative mRNA expression levels in embryos vary according to culture conditions and time after freeze–thawing. *BAX* is a pro-apoptotic gene associated with apoptosis and a factor in determining embryo quality (38, 39). In this study, a significant difference was confirmed in *BAX* expression level between the control and 0.25 M groups. Together with TUNEL staining, this finding demonstrated that the number of positive cells in the 0.25 M group was smaller than that in the control group at the gene expression level. HSPs belong to a class of proteins called chaperones, whose expression is induced as a defense mechanism under all types of cellular stress; they are important cellular stress markers (40, 41). In addition, a previous study has observed an increase in *HSPA1A* level along with DNA fragmentation and apoptosis (42). Mori et al. (40) reported an increase in *HSPA1A* level in embryos under heat

stress, indicating a decrease in embryo quality and viability. Park et al. (42) reported an increase in *HSP70* expression in embryos and a decrease in their viability based on the freezing method. In this study, *HSPA1A* expression was higher in the control group than in the 0.25 M group, suggesting that pretreatment with 0.25 M sucrose reduced expanded blastocyst stress. This result implies the possibility that pretreatment with sucrose before slow freezing can prevent damage to embryonic cells and reduce stress by dehydrating blastomeres and embryos. *AQP3* is a water molecule channel protein that allows water to flow across the membrane in the osmotic gradient direction, primarily expressed in epithelial tissues (43). *AQP3* expression levels in different culture conditions for bovine embryos (43, 44), mouse oocytes (45), and mouse embryos (46) have been investigated. Wang et al. (43) have reported that adding melatonin to the IVC medium significantly lowered the relative mRNA expression of *AQP3* compared with the control and increased survival after freeze–thawing. Similar results were obtained in this study; however, a previous study indicated that a decrease in the relative expression of *AQP3* adversely affected viability after freeze–thawing (47, 48). Hence, the difference in the culture system and increased *AQP3* expression are speculated indicators of rapid water influx after freeze–thawing and osmotic stress in embryos; further studies are needed in this field. Although *PLAC8* expression is not well established in cattle, its expression is related to placental development (49). High *PLAC8* expression in bovine embryos results in increased conception rates after embryo transfer (50); *PLAC8* expression is higher in the endometrium of pregnant cows than in that of non-pregnant cows (51). However, in this study, no difference was observed in *PLAC8* expression between the control and 0.25 M groups, because cell death and stress are reduced by *BAX* and *HSPA1A* expression, which has a beneficial effect on embryo survival and quality. However, embryo survival rates may not affect the conception rate, requiring additional embryo transfer experiments.

This study is limited in that it only demonstrated viability after freeze-thawing without embryo transfer using *in vitro* embryos. In addition, it did not quantify changes in embryos after treatment with sucrose medium. To overcome these limitations, further studies on conception rates in farmer's fields by freeze-thawing bovine embryos pretreated with sucrose and direct embryo transfer are needed, and this study will help inform future frozen embryo transfer studies because embryo survival and conception rates are closely related (14, 52).

Our results indicate that artificially shrinking the blastocoel cavity using 0.25 M sucrose prior to slow freezing affects blastocyst viability and apoptosis after freezing–thawing. In addition, the relative mRNA expression of *BAX, HSPA1A*, and *AQP3* significantly decreased up on 0.25 M sucrose treatment. These results imply that the quality of bovine blastocysts can be improved using the slow freezing method aided by dehydration with a sucrose medium.

Data availability statement

The datasets presented in this study can be found in online repositories. The names of the repository/repositories and accession number(s) can be found in the article/supplementary material.

Ethics statement

Ethical approval was not required for the studies on animals in accordance with the local legislation and institutional requirements because only commercially available established cell lines were used.

Author contributions

SJ: Conceptualization, Formal analysis, Investigation, Methodology, Validation, Writing – original draft, Writing – review & editing. HS: Formal analysis, Investigation, Methodology, Writing – original draft. DO: Formal analysis, Investigation, Methodology, Writing – original draft. Y-GJ: Formal analysis, Investigation, Methodology, Writing – original draft. JL: Conceptualization, Funding acquisition, Validation, Writing – original draft, Writing – review & editing. S-HH: Conceptualization, Funding acquisition, Validation, Writing – original draft, Writing – review & editing.

Funding

The author(s) declare that financial support was received for the research, authorship, and/or publication of this article. This work was partially supported by the National Research Foundation of Korea Grant funded by the Korean Government (2020R1A2C2008276 and 2021R1C1C2013954), and Technology Innovation Program (20023068), funded by the Ministry of Trade, Industry & Energy (MOTIE, Republic of Korea), Republic of Korea.

Acknowledgments

The authors are grateful to ET biotech Co., Ltd. for providing bovine ovaries.

Conflict of interest

SJ, HS, and Y-GJ were employed by ET Biotech Co. Ltd.

The remaining authors declare that the research was conducted in the absence of any commercial or financial relationships that could be construed as a potential conflict of interest.

Publisher's note

References

1. Seneda MM, Zangirolamo AF, Bergamo LZ, Morotti F. Follicular wave synchronization prior to ovum pick-up. *Theriogenology*. (2020) 150:180–5. doi: 10.1016/j.theriogenology.2020.01.024

2. Hasler JF, Henderson WB, Hurtgen PJ, Jin ZQ, McCauley AD, Mower SA, et al. Production, freezing and transfer of bovine Ivf embryos and subsequent calving results. *Theriogenology*. (1995) 43:141–52. doi: 10.1016/0093-691X(94)00020-U

3. Pontes JH, Nonato-Junior I, Sanches BV, Ereno-Junior JC, Uvo S, Barreiros TR, et al. Comparison of embryo yield and pregnancy rate between in vivo and in vitro methods in the same Nelore (*Bos Indicus*) donor cows. *Theriogenology*. (2009) 71:690–7. doi: 10.1016/j.theriogenology.2008.09.031

4. Caamano JN, Gomez E, Trigal B, Munoz M, Carrocera S, Martin D, et al. Survival of vitrified in vitro-produced bovine embryos after a one-step warming in-straw Cryoprotectant dilution procedure. *Theriogenology*. (2015) 83:881–90. doi: 10.1016/j.theriogenology.2014.11.021

5. Do VH, Catt S, Amaya G, Batsiokis M, Walton S, Taylor-Robinson AW. Comparison of pregnancy in cattle when non-vitrified and vitrified in vitro-derived embryos are transferred into recipients. *Theriogenology*. (2018) 120:105–10. doi: 10.1016/j.theriogenology.2018.07.027

6. Kim D, Sul H, Jung YG, Roh S. Holding of bovine blastocysts at Suprazero temperatures using small molecules. *Sci Rep*. (2017) 7:9490. doi: 10.1038/s41598-017-10014-9

7. Kuwayama M. Highly efficient Vitrification for cryopreservation of human oocytes and embryos: the Cryotop method. *Theriogenology*. (2007) 67:73–80. doi: 10.1016/j.theriogenology.2006.09.014

8. Vieira AD, Forell F, Feltrin C, Rodrigues JL. In-straw Cryoprotectant dilution of Ivp bovine blastocysts vitrified in hand-pulled glass micropipettes. *Anim Reprod Sci*. (2007) 99:377–83. doi: 10.1016/j.anireprosci.2006.06.010

9. Min SH, Kim JW, Lee YH, Park SY, Jeong PS, Yeon JY, et al. Forced collapse of the blastocoel cavity improves developmental potential in cryopreserved bovine blastocysts by slow-rate freezing and Vitrification. *Reprod Domest Anim*. (2014) 49:684–92. doi: 10.1111/rda.12354

10. Mucci N, Aller J, Kaiser GG, Hozbor F, Cabodevila J, Alberio RH. Effect of estrous cow serum during bovine embryo culture on blastocyst development and Cryotolerance after slow freezing or Vitrification. *Theriogenology*. (2006) 65:1551–62. doi: 10.1016/j.theriogenology.2005.08.020

11. Dochi O. Direct transfer of frozen-thawed bovine embryos and its application in cattle reproduction management. *J Reprod Dev*. (2019) 65:389–96. doi: 10.1262/jrd.2019-025

12. Kubisch HM, Sirisathien S, Bosch P, Hernandez-Fonseca HJ, Clements G, Liukkonen JR, et al. Effects of developmental stage, embryonic interferon-tau secretion and recipient synchrony on pregnancy rate after transfer of in vitro produced bovine blastocysts. *Reprod Domest Anim*. (2004) 39:120–4. doi: 10.1111/j.1439-0531.2004.00491.x

13. Gomez E, Rodriguez A, Munoz M, Caamano JN, Hidalgo CO, Moran E, et al. Serum free embryo culture medium improves in vitro survival of bovine blastocysts to Vitrification. *Theriogenology*. (2008) 69:1013–21. doi: 10.1016/j.theriogenology.2007.12.015

14. Owen CM, Johnson MA, Rhodes-Long KA, Gumber DJ, Barcelo-Fimbres M, Altermatt JL, et al. Novel synthetic Oviductal fluid for conventional freezing 1 (Scf1) culture medium improves development and Cryotolerance of in vitro produced Holstein embryos. *J Anim Sci*. (2022) 100. doi: 10.1093/jas/skac043

15. Bui-Xuan-Nguyen N, Heyman Y, Renard JP. Direct freezing of cattle embryos after partial dehydration at room temperature. *Theriogenology*. (1984) 22:389–99. doi: 10.1016/0093-691x(84)90459-x

16. Voelkel SA, Hu YX. Use of ethylene glycol as a Cryoprotectant for bovine embryos allowing direct transfer of frozen-thawed embryos to recipient females. *Theriogenology*. (1992) 37:687–97. doi: 10.1016/0093-691x(92)90148-k

17. Hasler JF, Hurtgen PJ, Jin ZQ, Stokes JE. Survival of Ivf-derived bovine embryos frozen in glycerol or ethylene glycol. *Theriogenology*. (1997) 48:563–79. doi: 10.1016/s0093-691x(97)00274-4

18. Martinez AG, Brogliatti GM, Valcarcel A, de Las Heras A. Pregnancy rates after transfer of frozen bovine embryos: a field trial. *Theriogenology*. (2002) 58:963–72. doi: 10.1016/s0093-691x(02)00936-6

19. Dochi O, Imai K, Takakura H. Birth of calves after direct transfer of thawed bovine embryos stored frozen in ethylene glycol. *Anim Reprod Sci*. (1995) 38:179–85. doi: 10.1016/0378-4320(94)01362-P

20. Bo G, Mapletoft R. Evaluation and classification of bovine embryos. *Anim Reprod*. (2013) 10:344–8.

21. Lee J, Cai L, Kim M, Choi H, Oh D, Jawad A, et al. Blastomere aggregation using Phytohemagglutinin-L improves the establishment efficiency of porcine parthenogenesis-derived embryonic stem-like cell lines. *Front Cell Dev Biol*. (2022) 10:948778. doi: 10.3389/fcell.2022.948778

22. Oh D, Choi H, Kim M, Cai L, Lee J, Jawad A, et al. Interleukin-7 enhances in vitro development and blastocyst quality in porcine parthenogenetic embryos. *Front Vet Sci*. (2022) 9:1052856. doi: 10.3389/fvets.2022.1052856

23. Livak KJ, Schmittgen TD. Analysis of relative gene expression data using real-time quantitative Pcr and the 2(-Delta Delta C (T)) method. *Methods*. (2001) 25:402–8. doi: 10.1006/meth.2001.1262

24. Pfaffl MW. A new mathematical model for relative quantification in real-time Rt-Pcr. *Nucleic Acids Res*. (2001) 29:e45. doi: 10.1093/nar/29.9.e45

25. Inaba Y, Miyashita S, Somfai T, Geshi M, Matoba S, Dochi O, et al. Cryopreservation method affects DNA fragmentation in Trophectoderm and the speed of re-expansion in bovine blastocysts. *Cryobiology*. (2016) 72:86–92. doi: 10.1016/j.cryobiol.2016.03.006

26. Iwayama H, Hochi S, Yamashita M. In vitro and in vivo viability of human blastocysts collapsed by laser pulse or osmotic shock prior to Vitrification. *J Assist Reprod Genet*. (2011) 28:355–61. doi: 10.1007/s10815-010-9522-4

27. Dang-Nguyen TQ, Nguyen HT, Somfai T, Wells D, Men NT, Viet-Linh N, et al. Sucrose assists selection of high-quality oocytes in pigs. *Anim Sci J*. (2018) 89:880–7. doi: 10.1111/asj.13015

28. Van Soom A, Ysebaert MT, Vanhoucke-De Medts A, Van de Velde A, Merton S, Delval A, et al. Sucrose-induced shrinkage of in vitro produced bovine morulae: effect on viability. *Morphol Ease Eval Theriogenol*. (1996) 46:1131–47. doi: 10.1016/s0093-691x(96)00285-3

29. Li L, Zhang X, Zhao L, Xia X, Wang W. Comparison of DNA apoptosis in mouse and human blastocysts after Vitrification and slow freezing. *Mol Reprod Dev*. (2012) 79:229–36. doi: 10.1002/mrd.22018

30. Batista AM, Gomes WA, Carvalho CC, Monteiro PL Jr, Silva FL, Almeida FC, et al. Effect of leptin on in vivo goat embryo production. *Reprod Domest Anim*. (2014) 49:476–80. doi: 10.1111/rda.12314

31. Canesin HS, Ortiz I, Rocha Filho AN, Salgado RM, Brom-de-Luna JG, Hinrichs K. Effect of warming method on embryo quality in a simplified equine embryo Vitrification system. *Theriogenology*. (2020) 151:151–8. doi: 10.1016/j.theriogenology.2020.03.012

32. Moreira da Silva F, Metelo R. Relation between physical properties of the zona Pellucida and viability of bovine embryos after slow-freezing and Vitrification. *Reprod Domest Anim*. (2005) 40:205–9. doi: 10.1111/j.1439-0531.2005.00575.x

33. Nedambale TL, Dinnyes A, Groen W, Dobrinsky JR, Tian XC, Yang X. Comparison on in vitro fertilized bovine embryos cultured in Ksom or Sof and cryopreserved by slow freezing or Vitrification. *Theriogenology*. (2004) 62:437–49. doi: 10.1016/j.theriogenology.2003.10.020

34. Van den Abbeel E, Balaban B, Ziebe S, Lundin K, Cuesta MJ, Klein BM, et al. Association between blastocyst morphology and outcome of single-blastocyst transfer. *Reprod Biomed Online*. (2013) 27:353–61. doi: 10.1016/j.rbmo.2013.07.006

35. Wooldridge LK, Ealy AD. Interleukin-6 increases inner cell mass numbers in bovine embryos. *BMC Dev Biol*. (2019) 19:2. doi: 10.1186/s12861-019-0182-z

36. Kocyigit A, Cevik M. Effects of leukemia inhibitory factor and insulin-like growth factor-I on the cell allocation and Cryotolerance of bovine blastocysts. *Cryobiology*. (2015) 71:64–9. doi: 10.1016/j.cryobiol.2015.05.068

37. Vejlsted M, Avery B, Gjorret JO, Maddox-Hyttel P. Effect of leukemia inhibitory factor (Lif) on in vitro produced bovine embryos and their outgrowth colonies. *Mol Reprod Dev*. (2005) 70:445–54. doi: 10.1002/mrd.20221

38. Pang YW, Sun YQ, Jiang XL, Huang ZQ, Zhao SJ, Du WH, et al. Protective effects of melatonin on bovine sperm characteristics and subsequent in vitro embryo development. *Mol Reprod Dev*. (2016) 83:993–1002. doi: 10.1002/mrd.22742

39. Vining LM, Zak LJ, Harvey SC, Harvey KE. The role of apoptosis in cryopreserved animal oocytes and embryos. *Theriogenology*. (2021) 173:93–101. doi: 10.1016/j.theriogenology.2021.07.017

40. Mori M, Hayashi T, Isozaki Y, Takenouchi N, Sakatani M. Heat shock decreases the embryonic quality of frozen-thawed bovine blastocysts produced in vitro. *J Reprod Dev*. (2015) 61:423–9. doi: 10.1262/jrd.2015-003

41. Amaral CS, Koch J, Correa Junior EE, Bertolin K, Mujica LKS, Fiorenza MF, et al. Heat stress on oocyte or zygote compromises embryo development, impairs interferon tau production and increases reactive oxygen species and oxidative stress in bovine embryos produced in vitro. *Mol Reprod Dev*. (2020) 87:899–909. doi: 10.1002/mrd.23407

42. Park SY, Kim EY, Cui XS, Tae JC, Lee WD, Kim NH, et al. Increase in DNA fragmentation and apoptosis-related gene expression in frozen-thawed bovine blastocysts. *Zygote*. (2006) 14:125–31. doi: 10.1017/S0967199406003649

43. Wang F, Tian X, Zhou Y, Tan D, Zhu S, Dai Y, et al. Melatonin improves the quality of in vitro produced (Ivp) bovine embryos: implications for blastocyst development, Cryotolerance, and modifications of relevant gene expression. *PLoS One*. (2014) 9:e93641. doi: 10.1371/journal.pone.0093641

44. Kuzmany A, Havlicek V, Wrenzycki C, Wilkening S, Brem G, Besenfelder U. Expression of Mrna, before and after freezing, in bovine blastocysts cultured under

different conditions. *Theriogenology*. (2011) 75:482–94. doi: 10.1016/j.theriogenology.2010.09.016

45. Jo JW, Jee BC, Suh CS, Kim SH, Choi YM, Kim JG, et al. Effect of maturation on the expression of aquaporin 3 in mouse oocyte. *Zygote*. (2011) 19:9–14. doi: 10.1017/S0967199410000171

46. Nong YQ, Liu FH, Chen Y, Wang F. The expression and distribution of aquaporin 3 in mouse embryos before and after Vitrification. *J Assist Reprod Genet*. (2013) 30:601–6. doi: 10.1007/s10815-013-9965-5

47. Asaadi A, Kafi M, Atashi H, Azari M, Hostens M. Frozen-thawed Ampullary cell monolayer improves bovine embryo in vitro development and quality. *Zygote*. (2019) 27:337–46. doi: 10.1017/S0967199419000388

48. Lopera-Vasquez R, Hamdi M, Maillo V, Gutierrez-Adan A, Bermejo-Alvarez P, Ramirez MA, et al. Effect of bovine Oviductal extracellular vesicles on embryo development and quality in vitro. *Reproduction*. (2017) 153:461–70. doi: 10.1530/REP-16-0384

49. Galaviz-Hernandez C, Stagg C, de Ridder G, Tanaka TS, Ko MS, Schlessinger D, et al. Plac 8 and Plac 9, novel placental-enriched genes identified through microarray analysis. *Gene*. (2003) 309:81–9. doi: 10.1016/s0378-1119(03)00508-0

50. El-Sayed A, Hoelker M, Rings F, Salilew D, Jennen D, Tholen E, et al. Large-scale transcriptional analysis of bovine embryo biopsies in relation to pregnancy success after transfer to recipients. *Physiol Genomics*. (2006) 28:84–96. doi: 10.1152/physiolgenomics.00111.2006

51. Klein C, Bauersachs S, Ulbrich SE, Einspanier R, Meyer HH, Schmidt SE, et al. Monozygotic twin model reveals novel embryo-induced transcriptome changes of bovine endometrium in the Preattachment period. *Biol Reprod*. (2006) 74:253–64. doi: 10.1095/biolreprod.105.046748

52. Lim KT, Jang G, Ko KH, Lee WW, Park HJ, Kim JJ, et al. Improved cryopreservation of bovine preimplantation embryos cultured in chemically defined medium. *Anim Reprod Sci*. (2008) 103:239–48. doi: 10.1016/j.anireprosci.2006.12.020

frontiers | Frontiers in Veterinary Science

TYPE Original Research
PUBLISHED 02 May 2024
DOI 10.3389/fvets.2024.1405746

OPEN ACCESS

EDITED BY
Stefan Gregore Ciornei,
Iasi University of Life Science (IULS), Romania

REVIEWED BY
Andra-Sabina Neculai-Valeanu,
Research & Development Station for Cattle Breeding, Dancu, Romania
Şükrü Güngör,
Mehmet Akif Ersoy University, Türkiye

*CORRESPONDENCE
Vincenzo Cicirelli
✉ vincenzo.cicirelli@uniba.it

RECEIVED 23 March 2024
ACCEPTED 19 April 2024
PUBLISHED 02 May 2024

CITATION
Carbonari A, Burgio M, Frattina L, Ceci E, Sciannamblo M, Ricci P, Cicirelli V and Rizzo A (2024) Oxytocin, prostaglandin F2$_\alpha$, and scopolamine for uterine involution of dairy cows.
Front. Vet. Sci. 11:1405746.
doi: 10.3389/fvets.2024.1405746

Oxytocin, prostaglandin F2$_\alpha$, and scopolamine for uterine involution of dairy cows

Alice Carbonari, Matteo Burgio, Lorenza Frattina, Edmondo Ceci, Maurizio Sciannamblo, Pasquale Ricci, Vincenzo Cicirelli* and Annalisa Rizzo

Department of Veterinary Medicine, University of Bari Aldo Moro, Valenzano, Italy

The aim of the study was to compare the effect of three substances with ecbolic activity, Oxytocin, Prostaglandin F2α (PGF2α) and Scopolamine, on the uterine involution process in dairy cows and on the resumption of ovarian activity. Eighty bovine were randomly divided in four groups: GROUP C: 20 cows treated, within 24h of calving, with 5mL/head of saline solution; GROUP PG: 20 cows treated, within 24h of calving, with 150μg/head of d-cloprostenol; GROUP OX: 20 cows treated, within 24h of calving, with 50IU/head of oxytocin acetate; GROUP S: 20 cows treated, within 24h of calving, with 40mg/q Scopolamine Butylbromide. Each cow was subjected to blood samples to evaluate the Hydroxyproline (HYP) levels, at T0, within 24h after calving, and T7, T14, T28, 7, 14, and 28days after calving, respectively. At T14 and T28, an ultrasound examination was performed to measure the diameter of ex-pregnant horn. In all cows, the reproductive indices (days to first service and number of artificial insemination for conception) were evaluated. In all groups, the HYP concentrations have been rising from T0 to T28, with the maximum levels obtained at T28 in the groups PG and S. As regard the diameter of uterine horn, the comparison among the groups showed significant differences only at T28, with lower values in the group PG and S. In group S and PG, the days to first service were less than other groups. Treatment with Scopolamine and PGF2α resulted in better outcomes, evidenced clinically by more efficient uterine involution and faster ovarian recovery.

KEYWORDS

bovine, oxytocin, prostaglandin F2$_\alpha$, scopolamine, uterine involution

Introduction

Post-partum (PP) in dairy cows is the period that most influences the productive and reproductive efficiency of the animal (1). To allow a new pregnancy occurs the female genital apparatus undergoes physiological changes, such as uterine involution, epithelial regeneration, elimination of bacteria and resumption of ovarian cyclicity (2).Uterine involution is characterized by a series of macroscopic, microscopic and molecular events. The macroscopic ones affect the volume and weight of the uterus, while the microscopic ones concern regeneration. These changes are characterized by the phenomena of necrosis and desquamation of the caruncles and regeneration of the endometrium, which lead to a decrease in the weight of the organ, from an average weight of 13 kg before delivery to 1 kg 30 days later (3). These events are intended to ensure that the uterus regains suitable

conditions for a new gestation (2). Furthermore, the molecular changes characterized by the reconstitution of Ca^{2+} and glucose reserves are crucial for the proper resumption of uterine contractility. The latter, after an initial increase, undergoes a reduction in the frequency and number of contractions to about 14 per hour in the next few hours after delivery; in the next 42 h, contractile events must further reduce to 1 per hour to ensure that placental retention does not occur (4). Complete uterine involution is reached around 40–50 days PP (2).The number of days required for proper involution increases in cows that have experienced complications during parturition (e.g., dystocias) or retention of fetal membranes; in these cows the risk of developing a uterine infection increases, as the possibility of bacterial colonization is greater (5). Failure of the uterus and cervix to return to normal size, in particular a cervical diameter of 7.5 cm, between 20 and 33 days PP, is associated with a reduced rate of conception as reported by LeBlanc et al. (6). Several pharmacological approaches are used to condition PP, all of which focus on modulating the contractile activity of the uterus. Currently, ecbolic drugs such as oxytocin (OX) and natural or synthetic Prostaglandin F2α (PGF2α) analogs are widely used in cattle breeding (7–9). There are conflicting opinions on the use of such ecbolics. Treatment with OX has a positive effect on uterine contractility up to day 2 PP, given its low half-life (7). The administration of PGF2α has a positive effect on uterine involution (8, 9), promoting a rapid completion of the process and a rapid recovery of ovarian activity (10). Stephen et al. (11), on the other hand, compared the two ecbolics administered for 1 week postpartum and found no positive effects on uterine involution, incidence of endometritis and reproductive performance. The parasympathetic nervous system also regulates the contractile activity of the uterus, promotes its vascularization and stimulates secretion from the cervical glands (12, 13). These activities are mediated by acetylcholine, which binds to muscarinic receptors, M2 and M3. Binding to the M2 receptor prevents relaxation of the uterus, while binding to the M3 receptor promotes its contraction (14). The distribution of the receptors is regulated by the hormone most present: estrogens stimulate the synthesis of the M2 receptor, while reducing that of the M3 receptor. In the 24 h after delivery, estrogens are still present in high concentrations and, therefore, M2 receptors are the most prevalent muscarinic receptor subtypes (15). Rizzo et al. (16) evaluated the effect of an antimuscarinic (parasympatholytic) drug, scopolamine, administered within 24 h after calving, to regularize uterine contractions and, thus, improve uterine involution in dairy cows. Scopolamine has proved to be a valid alternative to traditional ecbolic substances in the management of PP in dairy cows, regularizing uterine contractility by blocking, for the duration of its half-life (2–3 h), uterine contractions in PP, which are then more efficient and regular when they resume (16). The aim of the present study was to compare the effect of three substances with ecbolic activity, Oxytocin, PGF2α and Scopolamine, administered within 24 h of calving, on the uterine involution process in dairy cows and on the resumption of ovarian activity. To compare the efficacy of these drugs, hydroxyproline (HYP) levels, an important marker of uterine involution (16), ultrasound examination, for the measurement of the diameter of the uterine horns and reproductive indices (days to first service and number of artificial insemination for conception) were evaluated.

Materials and methods

All procedures were conducted in accordance with animal welfare and use guidelines, with the informed consent of the owner and approval of the ethics committee (protocol no. 10/2023).

Animals

The study involved 80 Friesan dairy cows located on a farm in the province of Benevento, from 4 to 6 year old, with 550 kg mean weight (range: 520–600 kg), free from non-infectious and infectious diseases. The free-housed animals were fed by unifeed, composed of corn silage, oat hay, medical hay, corn flour, soybean meal, cotton, crushed barley, beet pulp, and vitamin and oligomineral supplements. All cows, prior to any experimental procedure, underwent a general and particular objective examination of the reproductive apparatus, by means of rectal exploration, to diagnose any pathologies. All the subjects examined had eutocic calving and had no retention of fetal membranes.

The cows were randomly divided into four groups:

- GROUP C: 20 cows treated, within 24 h of calving, with 5 mL/head of saline solution (NaCl 0.9%), in one I.M. administration;
- GROUP PG: 20 cows treated, within 24 h of calving, with 150 µg/head of d-cloprostenol (Dalmazin®- Fatro-Italy), equivalent to 2 mL/head, in one I.M. administration;
- GROUP OX: 20 cows treated, within 24 h of calving, with 50 IU/head of oxytocin acetate (Neurofisin®- Fatro-Italy), equivalent to 5 mL/head, in one I.M. administration;
- GROUP S: 20 cows treated, within 24 h of calving, with 40 mg/q Scopolamine Butylbromide (Spasmolax®- Fatro-Italy), equivalent to 2 mL/q, in one I.M. administration.

Blood withdrawals

Each cow was subjected to blood samples to evaluate the HYP levels, at the following time points, in according to Rizzo et al. (16):

- T0: within 24 h after calving.
- T7: 7 days after calving.
- T14: 14 days after calving.
- T28: 28 days after calving.

Blood samples were taken from the coccygeal vein in serum vacutainer tubes and transferred to the laboratory (20 ± 10 min). The samples were centrifuged at 1,620 × g for 10 min at +4°C. The serum was stored in 1.5-mL Eppendorf tubes at −20°C until further analyses. ELISA kit (Bovine Hydroxyproline ELISA Kit MyBio Source Inc., California) was used to measure the serum HYP levels, by using the following manufacter's instructions. The kit has a detection range of 2,000 to 31.2 ng/mL; a sensitivity such that the minimum detectable is greater than 12 ng/mL; a specificity such that no cross-reaction with other substances occurred; an intra-assay accuracy of ≤8%; and an inter-assay precision of ≤12%.

Ultrasound examination

At each check-up, all cows underwent a particular objective examination of the reproductive apparatus, by means of rectal exploration, to assess the possible occurrence of metritis and ovarian function; during the checks carried out at T14 and T28, an ultrasound examination was also carried out to measure the diameter of the uterine horn that had received the previous pregnancy, to monitor the degree of uterine involution. Ultrasound examination was performed using a multifrequency linear probe (5–10 MHz, set at 7.5 MHz) (SonoSite MicroMaxx Bothell, WA, United States) and filter set to 100 Hz. Ultrasound was always carried out by the same expert technician. To reduce the interposition of air, cause of artifacts, the probe was placed in the finger of an examination glove with ultrasound gel, before the examination. Feces were removed from the rectum and the diameter of the ex-pregnant uterine horn was measured in the B-mode. At least three images of uterine horn were stored and on this each one a cross-sectional diameter (from serosa to serosa) was detected. The mean of three transverse diameters was calculated, for each bovine.

Reproductive indices

In all the enrolled cows, the reproductive indices in the postpartum were evaluated: days to first service and number of artificial insemination (AI) for conception. Around the 40th day of the postpartum, a clinical visit, to evaluate the condition of the genital system, was performed. Estrus detection, oedema of the vulva, clear mucosal vaginal discharge, standing to be mounted were observed. Estrus was confirmed by the detection of a preovulatory follicle on transrectal palpation. At healthy heat, all the cows were inseminated with frozen semen of proven bulls, obtained from specialized centers and referenced for preparation. Artificial insemination was always carried out by the same operator. The cows that did not return to heat, 40 days after the AI, underwent a clinical examination, during which the diagnosis of pregnancy was confirmed by means of a trans-rectal ultrasound with a multifrequency linear probe (5–10 MHz, set at 7.5 MHz) (SonoSite, MicroMaxx Bothell, WA, United States). The number of AI for conception was determined based on the number of AIs to obtain a pregnancy, so at each return to heat the cows were reinseminated until pregnancy was diagnosed.

Statistical analysis

The results were analyzed using the statistical program SPSS 19 (IBM, NY). The ANOVA test was used for comparison between groups, while the GLM test for repeated measures with LSD post-hoc test was used for comparison within groups. For all tests, statistically significant differences were considered for $p < 0.05$.

Results

The administration of all drugs did not produce any side effects. In the group C, two cows reported an acute metritis; in the group PG one cow showed subacute metritis; in the group OX one cow reported the left abomasal displacement and two cows follicular cyst; in the group S, one cow showed follicular cysts. These cows were not included in the experimental study.

Hydroxyproline level

The levels of the HYP in four groups are shown in Figure 1. The serum concentration are in agreement with reported in literature (16–18). The comparison among the four groups highlighted significant differences at T7, T14 and T28 among group C and the other experimental groups. In all groups, the HYP concentrations have been rising from T0 to T28, with the maximum levels obtained at T28 in the groups PG and S.

Ultrasound examination

In the B-mode mode, the diameter of the ex-pregnant horn in the four groups are shown in Table 1. Representative ultrasound images of a cow of the S group, at T14 and T28 is showed in Figure 2. The mean diameter of the uterine horn decreased from T14 to T28, in all groups, in a statistically significant way. The comparison among the groups showed significant differences only at T28, with lower values in the group PG and S.

Reproductive indices

The days to first service and number of artificial insemination are reported in Table 2.

Discussion

The aim of the present study was to compare the effect of three substances with ecbolic activity, Oxytocin, PGF2α and Scopolamine, administered within 24 h of calving, on the uterine involution process in dairy cows and on the resumption of ovarian activity. The first two are conventional ecbolic drugs, commonly used, while scopolamine is an parasympatholytic drug that it was demonstrated to have ecbolic activity, regularizing uterine contractility (16). In present study, the efficacy of these drugs has been demonstrated by assaying HYP concentration, marker of uterine involution (16, 19). It increased from T0 to T28 in all groups, with concentrations lower in control group than the other groups. This confirm that the treatments with PGF2α, oxytocin and scopolamine, administrated within 24 h after calving, induced an improvement of uterine involution. They may have acted through their tonic effect on uterus, increasing the myometrial contractions and, consequently, improving the reduction of the organ and the clearance of intrauterine fluid (20, 21). HYP, in fact, is produced following to the uterine collagen fiber degradation, during the involution process (19). Among experimental groups, the higher HYP concentrations, at T28, are shown in groups PG and S. These results are also confirmed by those obtained with ultrasonography: in fact, the diameters of ex-pregnant uterine horn were reduced from T14 to T28, with values lower in groups PG and S than C and OX groups. It was hypothesizable that uterine involution was improved with PGF2α

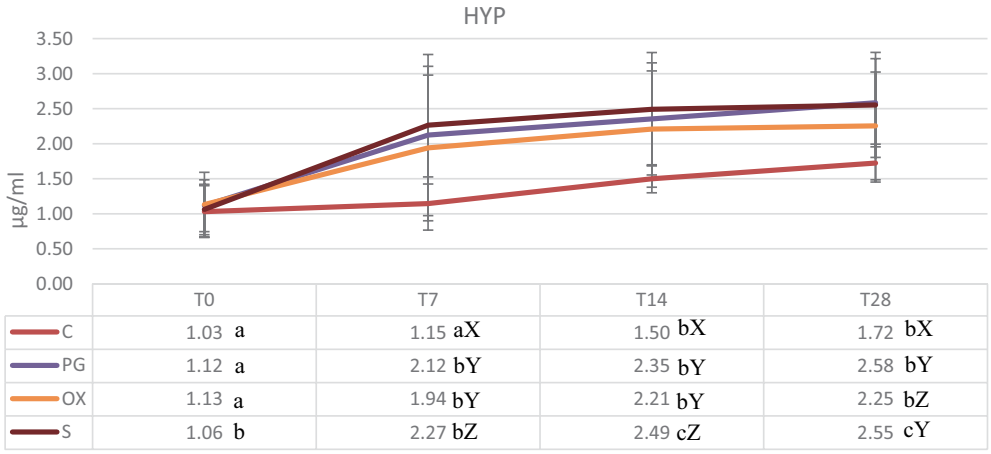

FIGURE 1
Concentrations (mean ± SD) (µg/mL) of serum hydroxyproline in groups C (control), PG (treated with d-cloprostenol), OX (treated with oxytocin acetate), S (treated with Scopolamine Butylbromide), at time T0 (within 24 h of delivery), T7, T14, and T28, at 7, 14, and 28 from delivery, respectively. Different letters in the same row show significant differences between means: $^{a,b}p < 0.01$. Different letters in the same column show significant differences between means $^{X,Y,Z}p < 0.05$.

TABLE 1 Diameter (mean ± SD) (mm) of the ex-pregnant uterine horn in groups C (control), PG (treated with d-cloprostenol), OX (treated with oxytocin acetate), S (treated with Scopolamine Butylbromide), at time T14 and T28, 14 and 28 from delivery, respectively.

Groups	T14	T28
C	48.81 ± 5.41^{a}	35.95 ± 4.20^{Xb}
PG	44.78 ± 7.04^{a}	28.36 ± 6.33^{Yb}
OX	47.86 ± 9.14^{a}	33.45 ± 5.96^{Zb}
S	46.86 ± 2.24^{a}	28.97 ± 2.86^{Yb}

Different letters in the same row show significant differences between means: $^{a,b}p < 0.001$. Different letters in the same column show significant differences between means $^{X,Y,Z}p < 0.05$.

administration, as prostaglandins act not only on contractile activity but also on activation of the immune response and triggering of phagocytosis (9, 17). Moreover, prostaglandins act on contraction of cervical smooth muscle, promoting remodeling of the structure (22). Then, these activities can explain the higher HYP levels showed in group PG. In the S group, also, higher HYP concentrations were obtained. It is hypothesizable that, in this group, rebound effect was exploited, with positive influences on the involution of the organ, in agreement with Rizzo et al. (16). In other word, scopolamine temporarily has blocked the uterus contractions, for a period of time corresponding to its half-life (2–3 h). Following the disappearance of its pharmacological effect, the uterus has resumed contracting more effectively and increased glandular secretions, useful for self-cleansing activity. Moreover, it was demonstrated that the activation of muscarinic receptors M3 in muscle cells stimulates glucose uptake, essential element for the contractility (23). The activity on uterine involution by scopolamine could thus be attributed to both a regularization of contractility and an increase in contractile force due to increased glucose up-take. The efficacy of scopolamine on uterine involution was then demonstrated by both the high HYP levels and the reduction of the uterine horn diameters. In OX-treated subjects, on the other hand, there is an increase in the frequency of uterine contractions that promote the reduction of uterine volume, but immune stimulation is lacking. This would explain the lower HYP concentrations recorded in the OX group cows compared with the groups. Oxytocin, therefore, acting only on uterine contractility, was not as effective, in reducing diameters, as the other two drugs tested. In literature, Oxytocin and prostaglandin were used to influence the evolution of postpartum. However, there are conflicting opinions. Stephen et al. (11) compared the effect of oxytocin and dinoprost, administered for the first 7 days postpartum, on uterine involution, postpartum endometritis, and reproductive performance. The Authors concluded that these ecbolic drugs, as used in this study, were not recommended for use in clinical practice to improve involution or reproductive tract health in normal cows (11). On the other hand, Abdel-Khalek et al. (21) demonstrated that cows, treated with oxytocin or PGF2α within 6–12 h postpartum, showed similar results in terms of diameters of uterine horns (gravid and non-gravid), cervical and vaginal length than that occurred in the control cows. Moreover, the authors concluded that PGF2α and oxytocin treatment showed similar beneficial effects on uterine involution, meanwhile prostaglandin treatment obtained the best results on conception rate and number of services per conception within 90 days-post-partum (21).

As reproductive indices in present study, group S achieved the best results, in terms of days to first service that were less than other groups. It is known that the ovarian recovery is closely correlated with good uterine involution. Therefore, in this group, the improvement of the reproductive efficacy may be due to the scopolamine activity that regularize the uterine contractility but it also acts on vascularization (13) and on cervical glandular secretion (12). These activities are important for improving uterine clearance and, thus, allowing earlier resumption of reproductive function.

Conclusion

The results of this study support the use of ecbolics in the immediate postpartum period to accelerate uterine involution and improve the reproductive efficiency of the dairy cow. Treatment with Scopolamine

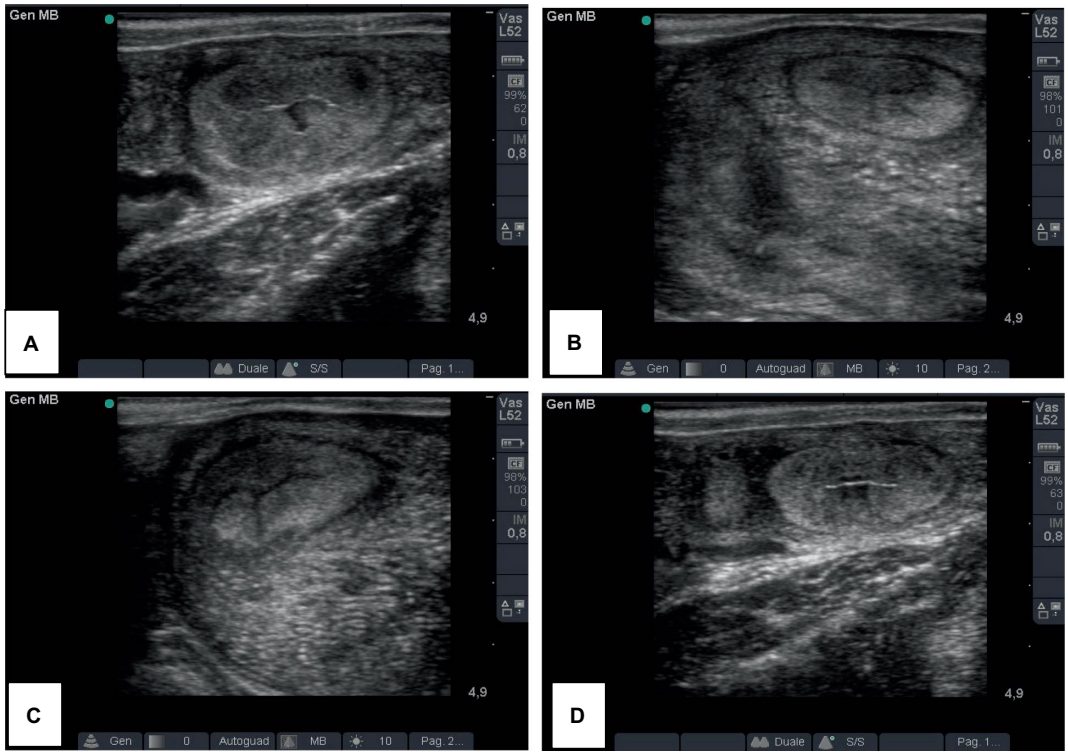

FIGURE 2
Representative ultrasound images of the ex-pregnant uterine horn of a cow of the S group **(A,B)** and a cow of the C group **(C,D)**, at T14 and T28, 14 and 28 days after delivery, respectively.

TABLE 2 **Reproductive indices (days to first service and number of artificial insemination -AI) in groups C (control), PG (treated with d-cloprostenol), OX (treated with oxytocin acetate) and S (treated with Scopolamine Butylbromide).**

Groups	Days to first service	N° AI
C	49.9 ± 4.63^{X}	3.2 ± 0.92^{X}
PG	48.3 ± 3.95^{X}	1.7 ± 0.67^{Y}
OX	53.1 ± 4.75^{Y}	2.7 ± 0.82^{Z}
S	45.4 ± 2.95^{Z}	1.8 ± 0.79^{Y}

Different letters in the same column show significant differences between means $^{X,Y,Z}P < 0.05$.

and PGF2α resulted in better outcomes, evidenced clinically by more efficient uterine involution and faster ovarian recovery.

Data availability statement

The raw data supporting the conclusions of this article will be made available by the authors, without undue reservation.

Ethics statement

All procedures were conducted in accordance with animal welfare and use guidelines, with the informed consent of the owner and approval of the ethics committee (protocol no. 10/2023). The studies were conducted in accordance with the local legislation and institutional requirements. Written informed consent was obtained from the owners for the participation of their animals in this study.

Author contributions

AC: Conceptualization, Investigation, Methodology, Writing – original draft. MB: Data curation, Methodology, Writing – original draft. LF: Investigation, Methodology, Writing – original draft. EC: Investigation, Methodology, Writing – original draft. MS: Data curation, Writing – original draft. PR: Investigation, Writing – original draft. VC: Data curation, Methodology, Writing – original draft. AR: Conceptualization, Data curation, Methodology, Project administration, Supervision, Writing – original draft.

Funding

The author(s) declare financial support was received for the research, authorship, and/or publication of this article. The authors stated that they received the financial support for the publication of this article from Fatro SpA, Ozzano Emilia, (BO) Italy. The authors declare that the funder was not involved in the study design, collection, analysis, interpretation of data, the writing of this article or the decision to submit it for publication.

Conflict of interest

The authors declare that the research was conducted in the absence of any commercial or financial relationships that could be construed as a potential conflict of interest.

Publisher's note

References

1. Noakes DE, Parkinson TJ, England GCW. *Veterinary reproduction and obstetrics. 10th edn*. Elsevier, editor. Philadelphia, USA: Saunders Ltd (2018). p. 1–837.

2. Sheldon IM. The postpartum uterus. *Vet Clin North Am*. (2004) 20:569–91. doi: 10.1016/j.cvfa.2004.06.008

3. Kaidi R, Brown PJ, David JSE. Uterine involution in cattle In: CSG Grunsell and ME Raw, editors. *The veterinary annual*. Oxford: Blackwell Scientific Publications (1991). 38–50.

4. Gunay A, Gunay U, Orman A. Effects of retained placenta on the fertility in treated dairy cows. *Bulg J Agric Sci*. (2011) 17:126–31.

5. Sheldon IM, Lewis GS, LeBlanc S, Gilbert RO. Defining postpartum uterine disease in cattle. *Theriogenology*. (2006) 65:1516–30. doi: 10.1016/j.theriogenology.2005.08.021

6. LeBlanc SJ, Duffield TF, Leslie KE, Bateman KG, Keefe GP, Walton JS, et al. Defining and diagnosing postpartum clinical endometritis and its impact on reproductive performance in dairy cows. *J Dairy Sci*. (2002) 85:2223–36. doi: 10.3168/jds.S0022-0302(02)74302-6

7. Giama I, Elze K, Eulenberger K. Studies into postpartal uterus motility of cattle. II. Uterus motility in early puerperium of cow following oxytocin application. *Monatsh Veterinarmed*. (1976) 31:940–2.

8. Lindell JO, Kindahl H. Exogenous prostaglandin F2 alpha promotes uterine involution in the cow. *Acta Vet Scand*. (1983) 24:269–74. doi: 10.1186/BF03546730

9. Vigo D, Munari E, Faustini M, Russo V, Pace M, Granata A, et al. Attività funzionale degli analoghi di sintesi delle Prostaglandine F2a nell'involuzione uterina della vacca da latte. *Atti SIB*. (2001) 33:67–74.

10. Madej A, Kindahl H, Woyno W, Edqvist LE, Stupnicki R. Blood levels of 15- keto-13, 14-dihydroprostaglandin F(2alpha) during the postpartum period in primiparous cows. *Theriogenology*. (1984) 21:279–87. doi: 10.1016/0093-691X(84)90413-8

11. Stephen CP, Johnson WH, Leblanc SJ, Foster RA, Chenier TS. The impact of ecbolic therapy in the early postpartum period on uterine involution and reproductive health in dairy cows. *J Vet Med Sci*. (2019) 81:491–8. doi: 10.1292/jvms.18-0617

12. Hammarström M. Autonomic nervous control of cervical secretion in the guinea-pig. *Acta Physiol Scand*. (1989) 135:367–71. doi: 10.1111/j.1748-1716.1989.tb08589.x

13. Sato Y, Hotta H, Nakayama H, Suzuki H. Sympathetic and parasympathetic regulation of the uterine blood flow and contraction in the rat. *J Auton Nerv Syst*. (1996) 59:151–8. doi: 10.1016/0165-1838(96)00019-7

14. Kitazawa T, Hirama R, Masunaga K, Nakamura T, Asakawa K, Cao J, et al. Muscarinic receptor subtypes involved in carbachol-induced contraction of mouse uterine smooth muscle. *Naunyn Schmiedeberg's Arch Pharmacol*. (2008) 377:503–13. doi: 10.1007/s00210-007-0223-1

15. Katsuhiko Y, Genichiro S, Chiharu K, Tatsuya N, Tomoko T, Hiayuu C, et al. Effects of ovarian hormone treatment on the gene expression of muscarinic acetylcholine receptors in the ovariectomized rat myometrium. *J Steroid Biochem Mol Biol*. (2014) 143:81–9. doi: 10.1016/j.jsbmb.2014.02.012

16. Rizzo A, Gazza C, Silvestre A, Maresca L, Sciorsci RL. Scopolamine for uterine involution of dairy cows. *Theriogenology*. (2018) 122:35–40. doi: 10.1016/j.theriogenology.2018.08.025

17. Maffeo G, Russo V, Faustini M, Vigo D. Somministrazione di PGF2a dopo il parto nella bovina da latte: effetti sulla concentrazione ematica di idrossiprolina. *Atti Soc It Buiatria* (1996) XXVIII:351–63.

18. Bytyçi X. The effectiveness of antagonist opioid e naltrexone in cow involution after calving period. *Anim Welfare Etol Tartástechnol*. (2009) 5:44, 54.

19. Dai T, Ma Z, Guo X, Wei S, Ding B, Ma Y, et al. Study on the pattern of postpartum uterine involution in dairy cows. *Animals*. (2023) 13:3693. doi: 10.3390/ani13233693

20. Bajcsy ÁC, Szenci O, Der Weijden GCV, Doornenbal A, Maassen F, Bartyik J, et al. The effect of a single oxytocin or carbetocin treatment on uterine contractility in early postpartum dairy cows. *Theriogenology*. (2006) 65:400–14. doi: 10.1016/j.theriogenology.2005.05.040

21. Abdel-Khalek A, El-Harairy M, Mehrez A, Fouad W. Uterine involution and reproductive performance of lactating Friesian cows treated with oxytocin and prostaglandin (Pgf2A) at calving. *J Anim Poult Prod*. (2013) 4:349–62. doi: 10.21608/jappmu.2013.71346

22. van Engelen E, Taverne MAM, Everts ME, van der Weijden GC, Doornenbal A, Breeveld Dwarkasing VNA. Cervical diameter in relation to uterine and cervical EMG activity in early postpartum dairy cows with retained placentas after PGF2alpha induced calving. *Theriogenology*. (2007) 68:213–22. doi: 10.1016/j.theriogenology.2007.04.054

23. Merlin J, Evans BA, Csikasz RI, Bengtsson T, Summers RJ, Hutchinson DS. The M3-muscarinic acetylcholine receptor stimulates glucose uptake in L6 skeletal muscle cells by a CaMKK-AMPK-dependent mechanism. *Cell Signal*. (2010) 22:1104–13. doi: 10.1016/j.cellsig.2010.03.004

frontiers | Frontiers in Veterinary Science

TYPE Original Research
PUBLISHED 23 May 2024
DOI 10.3389/fvets.2024.1409666

OPEN ACCESS

EDITED BY
Stefan Gregore Ciornei,
Iasi University of Life Sciences (IULS), Romania

REVIEWED BY
Şükrü Güngör,
Mehmet Akif Ersoy University, Türkiye
Camelia Tulcan,
University of Life Sciences King Mihai I Timişoara, Romania

*CORRESPONDENCE
Sanda Andrei
✉ sandrei@usamvcluj.ro

RECEIVED 30 March 2024
ACCEPTED 10 May 2024
PUBLISHED 23 May 2024

CITATION
Rafa H, Oroian I, Cozma OM, Morohoschi AG, Dumitraș DA, Ștefănuț CL, Neagu D, Borzan A and Andrei S (2024) Peripartal changes of metabolic and hormonal parameters in Romanian spotted cows and their relation with retained fetal membranes. *Front. Vet. Sci.* 11:1409666. doi: 10.3389/fvets.2024.1409666

Peripartal changes of metabolic and hormonal parameters in Romanian spotted cows and their relation with retained fetal membranes

Horatiu Rafa[1], Ioan Oroian[2], Oana Maria Cozma[3], Andreea Georgiana Morohoschi[1], Daria Antonia Dumitraș[1], Cristina Laura Ștefănuț[1], Daniela Neagu[3], Alex Borzan[3] and Sanda Andrei[1]*

[1]Department of Preclinical Sciences, Faculty of Veterinary Medicine, University of Agricultural Sciences and Veterinary Medicine Cluj-Napoca, Cluj-Napoca, Romania, [2]Cattle Breeding Research and Development Station, Sângeorgiu de Mureș, Romania, [3]Department of Clinical Sciences, Faculty of Veterinary Medicine, University of Agricultural Sciences and Veterinary Medicine Cluj-Napoca, Cluj-Napoca, Romania

This clinical study investigates various metabolic and physiological parameters in dairy cows during puerperium. Retained fetal membranes (RFM) is a significant postpartum complication that can affect the overall health, fertility and productivity of dairy cattle. The research focuses on changes in total proteins, albumin, glucose, triglycerides, total cholesterol, aspartate aminotransferase (AST) and alanine aminotransferase (ALT), cortisol, insulin, and insulin-like growth factor 1 (IGF-1) levels among cows experiencing normal post-partum period (NP) and those with RFM. A significant increase in protein levels was noted during the post-partum period in the RFM group, indicating physiological impacts of RFM at this stage. Albumin levels showed significant differences, highlighting a significant biological effect of RFM in the post-partum period. Glucose levels varied significantly in the weeks leading to parturition, suggesting altered metabolic states in cows that suffered RFM. Triglyceride and cholesterol levels were significantly higher during the antepartum period in the group that experienced reproductive failure, indicating substantial alterations in lipid metabolism which could herald the apparition of RFM. AST and ALT levels provided insights into cellular stress and liver function, with significant increases noted around parturition which could be attributed to the substantial physiological strain of parturition itself. Cortisol levels were higher in RFM cows 2 weeks before parturition, which could indicate an increasing stress response or a physiological preparation for the upcoming labor, and may be more pronounced in cows predisposed to RFM. Insulin levels decreased significantly before and at parturition in RFM cows, indicating a strong energy deficit. IGF-1 levels decreased significantly in RFM cows after parturition. Significant changes in metabolic parameters, such as glucose, triglycerides, and cholesterol levels, delineate the pronounced metabolic challenges faced by cows with RFM. The study elucidates that while some variations are noted as parturition approaches, the most substantial impacts attributable to RFM on metabolic and physiological parameters occur after parturition. These changes may have implications for the health, recovery, and productivity of cows postpartum, suggesting the need for targeted management strategies to mitigate the effects of RFM.

KEYWORDS

cows, parturition, placenta, metabolic profile, hormones

1 Introduction

The study of postpartum uterine diseases occupies a crucial position in veterinary medical research, impacting not only the welfare of animals but also their reproductive efficiency. These conditions lead to a decline in reproductive function, which is associated with increased financial burdens, manifested through decreased milk production and higher costs of medical treatment (1). Among such conditions, retained fetal membranes (RFM) is particularly significant, as it prevents the normal process of uterine involution and contributes to the development of chronic endometritis, both during and after the puerperal period, culminating in diminished fertility (2, 3).

Endocrinologically, the period of parturition is characterized by the intricate interplay of a variety of biologically active substances, including steroidal and non-steroidal hormones, along with prostaglandins (4). The transitional phase, which spans from the end of gestation to the commencement of lactation, represents the most metabolically challenging period for dairy cows, necessitating a complex metabolic adaptation that involves the activation and coordination of metabolic pathways. This adaptation is influenced by endocrine and neuroendocrine systems in response to environmental and physiological changes, thereby affecting the metabolism of proteins, lipids, and carbohydrates across various tissues (5).

To satisfy the increased endogenous demands for energy and nutrients, there is an enhancement in hepatic gluconeogenesis and the mobilization of proteins and lipids within the body (5). A deficiency in prepartum diet can lead to reduced serum glucose and insulin levels, instigating adipose tissue lipolysis, an increase in serum unsaturated free fatty acids, accumulation of hepatic triglycerides, and consequently, the onset of steatosis and ketosis. Addressing the negative energy balance is deemed crucial for the prevention of fatty liver conditions (6, 7). Consequently, there is a significant correlation between fatty liver syndrome and ketosis. Typically, fatty liver syndrome is concomitantly linked with liver function irregularities. These irregularities manifest as a diminished oxidation of non-esterified fatty acids within the tricarboxylic acids cycle and an impaired synthesis of lipoproteins. As a result, there is a rapid and sustained elevation in the plasma concentrations of ketone bodies (8).

Biochemical markers such as total protein (TP) and albumin (ALB) are indicators of liver synthetic function, as they are produced solely by hepatocytes. Decreases in these markers suggest reduced hepatic synthesis. Additionally, enzymes like aspartate aminotransferase (AST) and alanine aminotransferase (ALT), serve as biomarkers for hepatocyte damage; elevated levels in the blood indicate hepatocellular injury or necrosis. Thus, analyzing these enzyme activities provides insight into liver health (8).

The maternal immune system's recognition of class I proteins of the major histocompatibility complex within a mature placenta initiates immune and inflammatory responses that are crucial for the expulsion of the allantochorion at parturition. This underscores the immune system's broader role beyond mere pathogen recognition. The ensuing maternal immune response, which is characterized by the production of leukocyte activation factors, plays a key role in the immunological detachment of the allantochorion. A decrease in the activity of peripheral leukocytes is linked to an increased incidence of placental retention and related complications (9).

Moreover, Insulin-like growth factor 1 (IGF-I) significantly influences the immune response across different animal species, including cattle (10), by affecting the population of T helper 1 lymphocytes (11). These lymphocytes are essential to the immune mechanism responsible for the elimination of the placenta in the postpartum period (12). Cortisol, an immunosuppressive hormone, inhibits the proliferation and vital functions of leukocytes, thereby disrupting the normal immunological processes for identifying and eliminating fetal tissues (7, 13). Insulin contributes to the regulation of glucose supply to various tissues, including the uterine smooth muscles, thus playing a crucial role in regulating uterine motility and the strength of contraction (7, 14).

The incidence of RFM can be influenced by various factors, including metabolic and hormonal changes around parturition. Understanding these changes in Romanian Spotted cows, a breed significant to the Romanian dairy industry, is crucial for developing better management and intervention strategies to minimize the incidence of RFM and improve animal health and productivity.

The goals of this study are to characterize the metabolic (cholesterol, triglycerides, glucose, protein, albumin) enzymatic (ASAT, ALAT) and hormonal (insulin, cortisol, IGF-1) profiles of Romanian Spotted cows during the peripartum period, and to explore the dynamics of these metabolic and hormonal changes before, during, and after parturition and their possible correlations with RFM.

This study is among the first to focus on the Romanian Spotted breed, offering valuable breed-specific data that can inform targeted interventions and management practices.

By examining a wide range of metabolic and hormonal parameters over a nine-week period encompassing pre-parturition, parturition, and post-parturition, this study provides a detailed temporal understanding of the physiological changes occurring around calving.

The comparison of metabolic and hormonal profiles between cows with and without RFM may identify novel predictors or biomarkers for RFM, contributing to early detection and prevention strategies. Insights from this study could lead to the development of nutritional or management interventions tailored to the specific needs of Romanian Spotted cows during the peripartum period, ultimately enhancing animal welfare and productivity.

2 Materials and methods

2.1 Chemicals and reagents

The kits utilized in the current study were procured from Elabscience Biotechnology Inc., located in Texas, HT, USA. The additional chemicals were acquired from Sigma Aldrich and Merck, both located in Darmstadt, Germany.

2.2 Experimental animals

The clinical study involved a collaboration with a Romanian Spotted cattle farm located in Mureș County, Romania. At that time, the farm housed a total of 240 cattle, including both adults and young stock. The study was conducted between February 2021 and October 2021, during which a group of 50 cows was identified for which the breeding date and approximate calving date were verified.

The Bălțată Românească (Romanian Spotted, RS) breed, classified under the Simmental group, serves a bi-functional purpose and is currently documented with a population of 376,000 cows, comprising 36% of Romania's cattle breed demographic (15, 16). Originating in the 18th century, the RS breed was developed through the non-methodical interbreeding of Simmental bulls, imported from Austria and Switzerland, with domestically undeveloped Podolic Grey cattle (16, 17). The lactational milk yield of the RS breed is quantified between 5,000 and 5,700 kg, with the adult female's body mass ranging from 600 to 620 kg and the fattening young bulls experiencing an average daily weight gain of 1,000 to 1,200 g (16, 18). The breeding selection index for the RS is strategically concentrated on enhancing milk production (50%), with additional emphasis on the improvement of growth rates and carcass quality (20%), as well as the augmentation of fitness-associated characteristics (30%) (16, 19).

With regards to the shelter infrastructure, it features walls enclosing three sides, leaving one elongated side completely open. The construction material for these walls consists of reinforced concrete elements. The roofing design incorporates a single-sloped configuration, with the lowest point situated at 1.6 meters in the rear section of the structure, while the highest point reaches 3.2 meters toward the front. The flooring substrate is composed of concrete, providing an optimal foundation for the application of a continuous bedding system. This bedding is replenished with straw biweekly and replaced every 6–7 weeks or as dictated by specific circumstances. The shelter facility is equipped with two calving enclosures, each boasting a 20-square meter area, facilitating the segregation of cattle approaching the calving phase. Post-calving, cows are housed within these enclosures alongside their calves, effectively mitigating potential conflicts and injuries.

2.3 Experimental model

The study conducted on a total of 50 cows involved multiple samplings, both during the ante and post-partum periods, following the protocol below:

- Antepartum period: at 4, 3, 2, 1 week(s) before parturition (AP-W4; AP-W3; AP-W2; AP-W1)
- At the moment of parturition ±12 h after parturition (P)
- Postpartum period: 1, 2, 3, 4 weeks after parturition (PP-W1; PP-W2; PP-W3; PP-W4)

Blood samples were collected at the same period of time, between 6 and 8 am, all through the course of the experiment, from the coccygeal vein using vacutainers with a coagulant. After collection, they were left at room temperature to allow serum expression. The respective serum was separated and placed in Eppendorf tubes, each tube containing 0.5 mL of serum. The samples were stored at −80°C.

From the initial group of 50 cows, only 22 met the criteria for inclusion in the study by providing the necessary nine samples for evaluation. Throughout the experiment, situations of abortion, misdiagnosed pregnancies, or premature births before the calculated term were encountered. At the end of the experiment, it was observed that out of the 22 cows, only 7 presented placental retention, while the remaining cattle had no postpartum complications.

All applicable international, national and institutional guidelines for the care and use of animals were followed. The animal study protocol was ethically approved by the university local Bioethics Committee (no.417/13.12.2023) and followed the guidelines of the European Law Directive 63/2010, materialized by Romanian National Law no. 43/2014.

2.4 Biochemical analysis

Various parameters including albumin (ALB), glucose (GLU), triglycerides (TRG), cholesterol (COL), aspartate aminotransferase (AST)/glutamic oxaloacetic transaminase (GOT) and alanine aminotransferase (ALT)/glutamic-pyruvic transaminase (GPT) and total protein were quantified in the serum samples employing specific assay kits (Elabscience Biotechnology Inc., Texas, HT, USA). All biochemical analyses underwent rigorous validation and were performed through spectrophotometry using the SPECTROstar® Nano microplate spectrophotometer, BMG Labtech in Germany.

2.5 Determination of hormone concentrations in blood

The specific quantitative ELISA assay kits (Elabscience Biotechnology Inc., Houston, TX, USA) were used to measure the blood cortisol, insulin, and IGF-1 concentrations. All the measurements were assessed in line with the instructions provided in the kit, using the SPECTROstar® Nano microplate spectrophotometer, BMG Labtech in Germany.

2.6 Statistical analysis

Statistical analysis was conducted using the GraphPad Prism 9 software program (San Diego, CA, USA). Data were statistically evaluated through Unpaired t test with Welch correction. Significance levels were set at $p < 0.05$, $p < 0.01$, $p < 0.001$, and $p < 0.0001$ to assess differences between the cows with retained fetal membranes and the ones with normal parturition. All determinations were carried out using the two-stage step-up method (Benjamini, Krieger, and Yekutieli), and the results were presented as the mean values ± standard deviations.

3 Results and discussion

3.1 Blood metabolic profile

The findings of the study regarding total proteins and albumins during the prepartum, parturition, and postpartum periods are displayed in Figure 1. In the prepartum phase, from AP-W4 to AP-W1, no statistically significant differences were observed

between the RFM and normal parturition (NP) groups. This suggests that any alterations in protein levels in cows that later developed RFM are either not present or not detectable until parturition.

During parturition (P), we observed a statistically significant elevation in protein levels in the RFM group compared to the NP group, surpassing the threshold for strong significance ($p < 0.01$). This period appears to be a critical point; physiological parameters are significantly modified in cows with RFM.

The immediate postpartum period presented a dynamic shift in protein levels. At PP-W1, the protein levels in cows with RFM were significantly lower than those in the NP group ($p < 0.01$), indicating a continuation of the significant physiological differences noted at parturition. However, by PP-W2, the significance of these differences decreased ($p < 0.05$), hinting at a possible transitional recovery phase. A notable spike in protein levels was observed in the RFM group at PP-W3 which not only re-established the strong significance seen during parturition but also reached a very high level of significance ($p < 0.001$). This could imply a delayed or sustained response to the physiological stress of RFM, with potential implications for the cow's metabolic state and recovery. By PP-W4, the differences in protein levels between the two groups were no longer statistically significant ($p > 0.05$), suggesting a return to homeostatic levels or an adaptation to postpartum conditions. The lack of significant difference at this stage may indicate that the initial postpartum disturbances have resolved or that compensatory mechanisms have effectively mitigated the metabolic discrepancies associated with RFM.

During the prepartum phase, the albumin levels show statistically significant differences at 1 week before parturition ($p < 0.05$) indicating that changes in albumin levels associated with RFM become more pronounced as parturition approaches. Interestingly, the albumin levels at 4 weeks before parturition also demonstrate significant differences ($p < 0.05$), albeit the effect is less pronounced than at AP-W1. This suggests that while albumin levels begin to diverge between RFM and NP groups several weeks before parturition, the most substantial alterations occur closer to parturition.

The point of parturition (P) itself marks a highly significant decrease in albumin levels in RFM cows compared to NP cows ($p < 0.0001$), reflecting a major physiological impact during this critical time. This acute change likely represents a combination of stress responses and the metabolic demands placed on the liver, which is the primary site of albumin synthesis.

Postpartum albumin levels indicate a return toward normalcy but with some fluctuations. Immediately after parturition (PP-W1), the difference in albumin levels is not statistically significant ($p > 0.05$). However, by the second week postpartum (PP-W2), there is a significant increase in albumin levels in the RFM group ($p < 0.01$), suggesting a rebound effect or a delayed response to the physiological events of parturition. By the third week postpartum (PP-W3), albumin levels in RFM cows are again significantly higher than in NP cows ($p < 0.001$), indicating ongoing physiological adjustments or the continued effects of RFM. Finally, by the fourth week postpartum (PP-W4), the albumin levels are not significantly different between the two groups ($p > 0.05$), which may indicate a stabilization of albumin levels as cows recover from RFM.

Data on the variations in glucose, triglyceride, and total cholesterol concentrations during parturition and the antepartum and postpartum periods are presented in Figure 2.

In the weeks leading up to parturition, there were remarkable differences in glucose levels between the two groups. Starting at 4 weeks prior to parturition (AP-W4), cows with RFM exhibited significantly higher glucose levels than NP cows ($p < 0.001$), which persisted into the second week (AP-W2) before parturition. These findings may suggest an altered metabolic state or an increased stress response in RFM cows, which ultimately contribute to the development of such pathology. However, 3 weeks before parturition (AP-W3), RFM cows had extraordinarily high glucose levels ($p < 0.01$), which could imply an acute stress response or a compensatory mechanism against metabolic demands. Intriguingly, 1 week before parturition (AP-W1), RFM cows showed significantly lower glucose levels than NP cows ($p < 0.001$), indicating a possible metabolic shift or the onset of energy depletion as parturition approached. At the

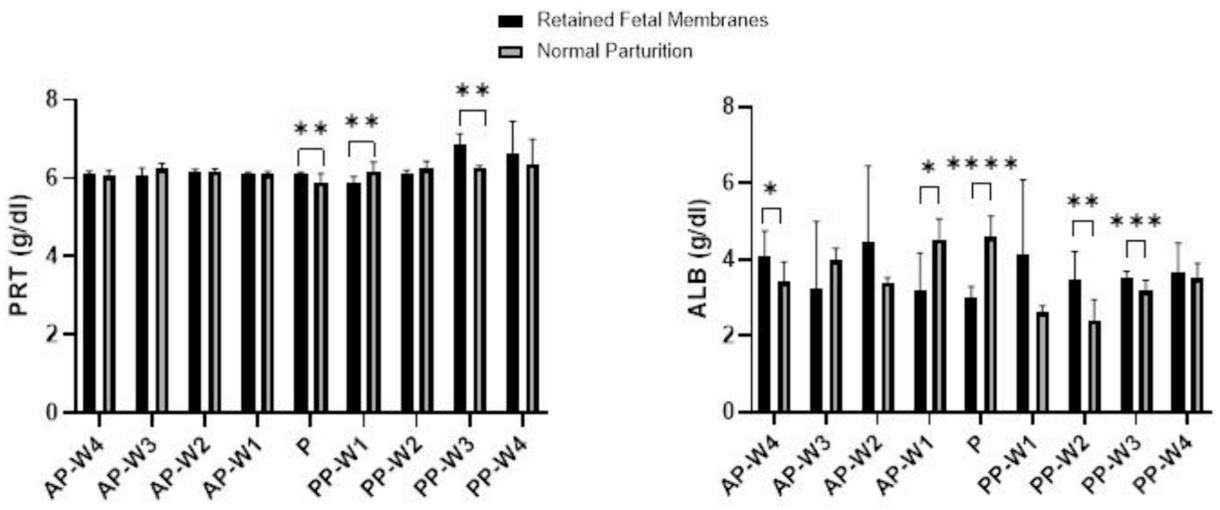

FIGURE 1
Total protein and albumin levels. Statistical significance *$p < 0.05$, **$p < 0.01$, ***$p < 0.001$, ****$p < 0.001$. The outcomes represent mean ± SD of three replicate analyses.

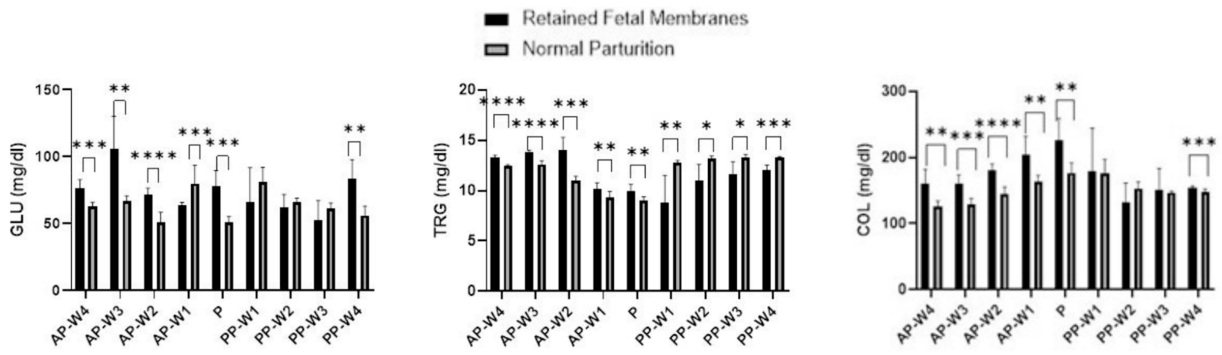

FIGURE 2
Glucose, triglycerides and total cholesterol levels. Statistical significance *$p < 0.05$, **$p < 0.01$, ***$p < 0.001$, ****$p < 0.001$. The outcomes represent mean ± SD of three replicate analyses.

point of parturition (P), glucose levels in RFM cows were significantly higher ($p < 0.001$) compared to NP cows. The marked elevation in glucose could reflect the intense energy requirements and stress associated with RFM cows. This is a critical finding as it underscores the metabolic challenge faced by cows with RFM during labor, which may have implications for their health and recovery postpartum.

Immediately after parturition (PP-W1), the difference in glucose levels was not statistically significant ($p > 0.05$), which may suggest an initial period of recovery where glucose levels begin to stabilize. However, the subsequent weeks (PP-W2 and PP-W3) continued to show no significant differences ($p > 0.05$), indicating that the metabolic disturbance observed prepartum may resolve or diminish in the early postpartum period. Notably, by the fourth week postpartum (PP-W4), RFM cows demonstrated a significant increase in glucose levels ($p < 0.01$), which might indicate a delayed response to the metabolic demands or a secondary stress event.

In the antepartum period, the data indicate a statistically significant elevation in triglyceride levels in cows with RFM when compared to NP cows. This elevation is evident from 4 weeks before parturition (AP-W4) with a p-value <0.0001 and becomes more pronounced 3 weeks before parturition (AP-W3) with a p-value <0.0001. This suggests a substantial alteration in the lipid metabolism of RFM cows well before parturition, potentially due to increased mobilization of fat reserves or a stress-related increase in lipolysis. By 2 weeks prior to parturition (AP-W2), the difference peaks significantly ($p < 0.001$), indicating the highest disparity in triglyceride levels between the two groups during the prepartum period. Interestingly, 1 week before parturition (AP-W1), while the levels remain significantly higher in RFM cows ($p < 0.01$), the difference diminishes somewhat, which could suggest the beginning of a metabolic adjustment as parturition approaches. At the time of parturition (P), RFM cows continue to exhibit significantly higher triglyceride levels ($p < 0.01$) compared to NP cows. This persistent hypertriglyceridemia may reflect the ongoing metabolic stress or an inflammatory state associated with RFM, which could have implications for the cow's energy status and the health of the neonate. Following parturition, the pattern reverses; the RFM group shows significantly lower triglyceride levels than the NP group from the first week postpartum (PP-W1, $p < 0.01$) through to the fourth week postpartum (PP-W4, $p < 0.001$). This decline could be indicative of a higher postpartum energy deficit in RFM cows, possibly due to a more extensive use of fat reserves for energy production or due to a reduced feed intake. The significant drop in triglycerides during the postpartum period may also signal a risk for the development of metabolic disorders, such as fatty liver syndrome, which is a concern in dairy cattle management.

Significant elevations in cholesterol were observed in RFM cows as early as 4 weeks before parturition (AP-W4), with a p-value <0.01, which may suggest an altered lipid metabolism or an increase in mobilization of fat reserves as part of the body's preparation for the energy demands of parturition. This elevation persisted through the third week (AP-W3, $p < 0.001$) and peaked at the second week (AP-W2, $p < 0.0001$) before parturition, indicating the highest level of dyslipidemia in the prepartum period. The continued significant difference 1 week before parturition (AP-W1, $p < 0.01$) adds to the evidence that RFM is associated with marked changes in cholesterol metabolism leading up to parturition. At the point of parturition (P), there was a notable peak in cholesterol levels in RFM cows ($p < 0.01$), suggesting that the physiological stress of parturition may exacerbate the hypercholesterolemia. This could reflect the acute metabolic demands placed on the liver for cholesterol, which is vital for hormone synthesis and cellular functions that are critical during parturition. Immediately after parturition (PP-W1), the difference in cholesterol levels between RFM and NP cows was not statistically significant ($p > 0.05$), which may indicate a transient return to baseline levels or effective management of cholesterol following parturition. However, by the fourth week postpartum (PP-W4), a significant difference re-emerged ($p < 0.001$), suggesting a possible delayed response in the cholesterol metabolism of RFM cows or a secondary stress response as the cows continue to recover. The non-significant findings at PP-W2 ($p > 0.05$) and PP-W3 ($p > 0.05$) indicate no substantial differences in cholesterol levels between the two groups during this period. It is possible that the lipid metabolism is stabilizing during this time, or the cows may have adapted to the postpartum state regardless of the complications associated with RFM.

Figure 3 displays the results of the blood transaminase activity (ALT and AST) assays. Leading up to parturition, we observe no statistically significant differences in AST levels at 4 weeks (AP-W4, $p > 0.05$) and 2 weeks (AP-W2, $p > 0.05$) before parturition. However, a significant spike in AST activity is noted at 3 weeks before parturition (AP-W3, $p < 0.0001$), suggesting an early onset of cellular stress or damage in cows that would later exhibit RFM. The reason for this

elevation is not immediately apparent but could be indicative of the metabolic and physiological changes preparing the cows for the upcoming parturition. At 1 week before parturition (AP-W1), the increase in AST activity approaches significance ($p < 0.05$), possibly heralding the impending stress of labor. At the time of parturition (P), there is a highly significant elevation in AST levels in RFM cows ($p < 0.0001$), which could be attributed to the substantial physiological strain of parturition itself. The elevated AST levels could reflect increased cellular turnover or damage, potentially as a result of hypoxia or inflammation related to RFM.

Interestingly, the postpartum period shows no significant differences immediately after parturition (PP-W1 PP-W2, PP-W3, $p > 0.05$). This lack of significant difference might indicate that the acute stress on tissues typically resolves or diminishes after delivery. However, by the fourth week postpartum (PP-W4), there is a profound and highly significant decrease in AST levels in RFM cows ($p < 0.0001$). This decrease could suggest a resolution of the cellular stress or a possible compensatory mechanism after the initial postpartum period. The significant decrease in AST at PP-W4, especially considering the high levels during parturition, may also point to a substantial recovery or normalization process that extends into the postpartum period. This could be reflective of the liver and muscle tissues' repair and regeneration capabilities.

The data indicate no significant difference in ALT levels between RFM and NP cows during the majority of the prepartum period, with non-significant p-values at AP-W4, AP-W2 and AP-W1 ($p > 0.05$). However, there is a notable exception at 3 weeks before parturition (AP-W3), where a significant increase in ALT levels in RFM cows ($p < 0.05$) suggests an early onset of hepatic stress or subclinical liver injury that may be related to the metabolic changes preceding parturition. At the time of parturition (P), a modest increase in ALT levels is observed ($p < 0.05$). While not highly significant, this increase aligns with the physiological strain of labor and could be indicative of mild liver stress or increased muscular activity associated with parturition efforts. In the immediate postpartum period (PP-W1), ALT levels show no significant difference ($p > 0.05$), suggesting no sustained hepatic insult following parturition. However, by the second week postpartum (PP-W2), there is a significant elevation in ALT levels in RFM cows ($p < 0.0001$), which could be indicative of ongoing liver stress or a delayed response to the metabolic challenges posed by RFM. By the third week postpartum (PP-W3), ALT levels are not significantly different ($p > 0.05$), potentially signaling a trend toward normalization. Yet, by the fourth week postpartum (PP-W4), there is a highly significant decrease in ALT levels in RFM cows ($p < 0.0001$), which is a somewhat unexpected finding. This decrease may reflect a resolution of earlier hepatic strain or a compensatory adaptation after the initial postpartum period. However, the lower levels of ALT could also raise concerns about the liver's functional capacity, considering that such a significant decrease might also imply a reduction in hepatocellular mass or function.

3.2 Blood hormonal profiles

The data suggest that cortisol levels in cows with RFM are not significantly higher than those with NP at 4 weeks before parturition (AP-W4, $p > 0.05$), suggesting that at this stage, stress levels do not differ markedly between the two groups. However, a trend begins to emerge 3 weeks' prior (AP-W3, $p < 0.05$) and becomes significant 2 weeks before parturition (AP-W2, $p < 0.01$), with RFM cows exhibiting higher cortisol levels. This could indicate an increasing stress response or a physiological preparation for the upcoming labor, which may be more pronounced in cows predisposed to RFM. One week prior to parturition (AP-W1), the difference in cortisol levels is not significant ($p > 0.05$), which might suggest a complex interplay of factors as the cow's approach labor. Interestingly, at the time of parturition (P), the data do not show a significant difference in cortisol levels between the two groups ($p > 0.05$). This could be due to the high variability of cortisol responses during labor or a possible equalization of stress levels between RFM and NP cows induced by the parturition process itself. In the postpartum period, the cortisol levels do not show significant differences between RFM and NP cows at any week (PP-W1 to PP-W4), with p-values >0.05. This lack of significant variation postpartum suggests that the stress associated with RFM may not extend beyond parturition in a way that is reflected in systemic cortisol levels, or that both groups of cows experience a

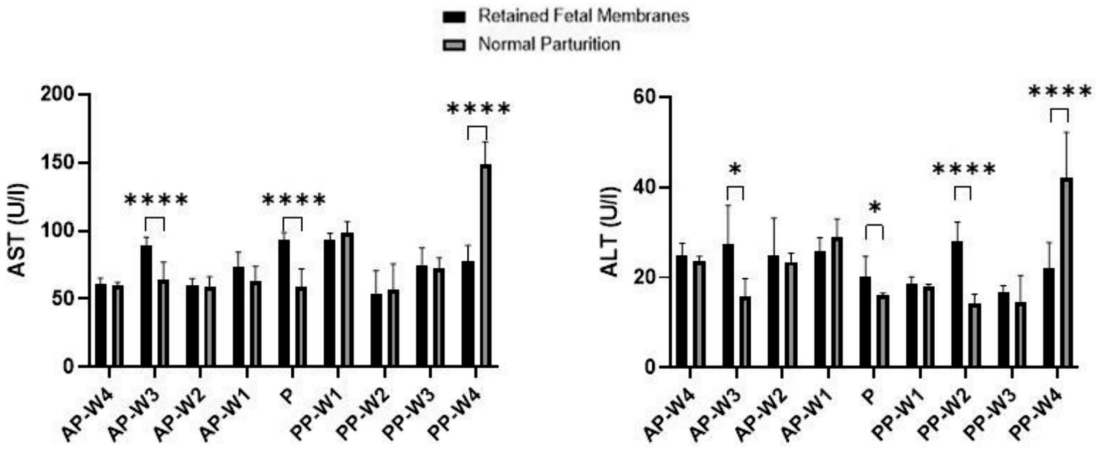

FIGURE 3
AST and ALT activity. Statistical significance *$p < 0.05$, ****$p < 0.001$. The outcomes represent mean ± SD of three replicate analyses.

normalization of cortisol levels as they recover from parturition. However, it is noteworthy that the cortisol levels in RFM cows significantly decrease by the fourth week after parturition (PP-W4, $p > 0.05$), approaching significance. This decrease may reflect a return to baseline stress levels or successful adaptation to postpartum life. Figure 4 shows a detailed replication of these outcomes.

Figure 5 displays the data obtained following the evaluation of blood insulin and IGF-1 concentrations during antepartum period, parturition and postpartum period.

During the prepartum phase, there were no significant differences in insulin levels between RFM and NP cows 4 weeks before parturition (AP-W4, $p > 0.05$) and 2 weeks before parturition (AP-W2, $p > 0.05$). However, a significant decrease in insulin levels was observed 3 weeks before parturition (AP-W3, $p < 0.0001$) in cows with RFM. This suggests an early metabolic alteration in these cows, potentially indicative of a stress response or altered glucose metabolism. Additionally, 1 week before parturition (AP-W1), a significant difference is noted again ($p < 0.01$), which could signify the continuation or amplification of these metabolic changes as parturition approaches. At the time of parturition (P), a significant reduction in insulin levels is observed in cows with RFM ($p < 0.001$). This notable decrease may reflect a strong stress response or an energy deficit due to the increased demands of labor, which could be exacerbated in cows that go on to develop RFM. Immediately following parturition (PP-W1), insulin levels do not differ significantly between the two groups ($p > 0.05$), suggesting a return to baseline or a resolution of the acute parturition-related metabolic disturbances. However, the second week postpartum (PP-W2) shows a significant increase in insulin levels in RFM cows ($p < 0.05$). This might reflect a postpartum metabolic adaptation or a rebound from the energy deficits incurred during parturition. By the third week postpartum (PP-W3) and the fourth week postpartum (PP-W4), although the differences in insulin levels are not statistically significant ($p > 0.05$), there is a trend toward higher insulin levels in RFM cows. This could indicate a persistent alteration in glucose metabolism or insulin sensitivity in these cows, which may have long-term implications for their health and productivity.

Significant decreases in IGF-1 levels were observed in cows with RFM compared to NP cows as early as 4 weeks before parturition (AP-W4, $p < 0.01$), and these persisted through to 3 weeks (AP-W3, $p < 0.01$) and 2 weeks (AP-W2, $p < 0.05$) before parturition. This trend suggests a possible alteration in the metabolic state of RFM cows, which could be due to a higher energy demand or a stress response related to the impending parturition. Intriguingly, 1 week before parturition (AP-W1), RFM cows showed an increase in IGF-1 levels compared to NP cows ($p < 0.05$), which could indicate a compensatory mechanism or a distinct shift in metabolic focus as parturition approaches. At the time of parturition (P), no significant difference was found in IGF-1 levels between RFM and NP cows ($p > 0.05$). This could be due to the acute and possibly equal physiological stress of parturition on all animals, overshadowing the subtler chronic stressors that may differentiate RFM from NP cows. Immediately following parturition (PP-W1), a significant decrease in IGF-1 levels was detected in RFM cows ($p < 0.0001$). This suggests a continuation of the energy deficit or a more pronounced response to the metabolic and physiological stresses of RFM. The significant differences continue into the second and third weeks postpartum ($p < 0.001$). By the fourth week postpartum (PP-W4), IGF-1 levels in RFM cows were still significantly lower than NP cows ($p < 0.01$), which could reflect a longer-term impact of RFM on the metabolic health of the cows, possibly influencing recovery and subsequent productivity.

4 Discussion

There is a notable increment in serum total protein levels in bovines commencing 2 months prior to the expected parturition date, reaching a zenith 1 month before parturition, followed by a swift decrement approaching the parturition period (20). This pattern underscores the translocation of immunoglobulins from the serum to the mammary gland, initiating several weeks before parturition and attaining maximum concentrations between 1 to 3 days before the (20, 21).

The typical plasma concentration range of albumin in bovines is established to be 3.03 to 3.55 g/dL (22). Albumin is classified as a negative acute-phase protein, characterized by a gradual decrement in its concentration, with more significant reductions observed in the context of chronic inflammatory disorders. Negative acute-phase proteins are delineated as serum proteins that exhibit a decrease in concentration of 25% or greater during the acute phase in response to

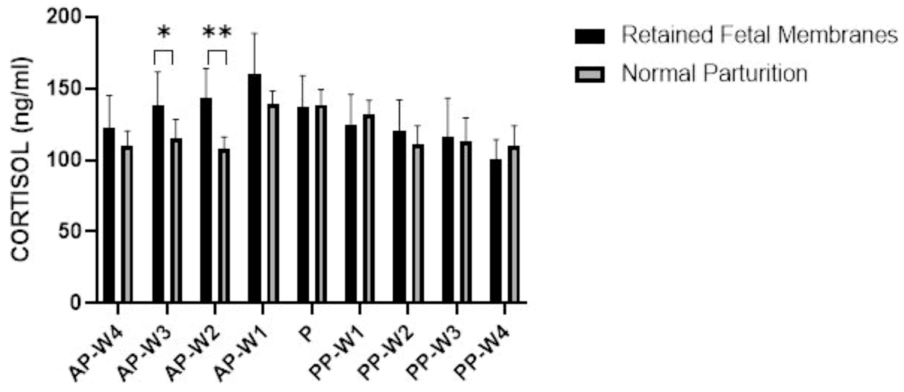

FIGURE 4
Blood cortisol concentrations. Statistical significance *$p < 0.05$, **$p < 0.01$. The outcomes represent mean ± SD of three replicate analyses.

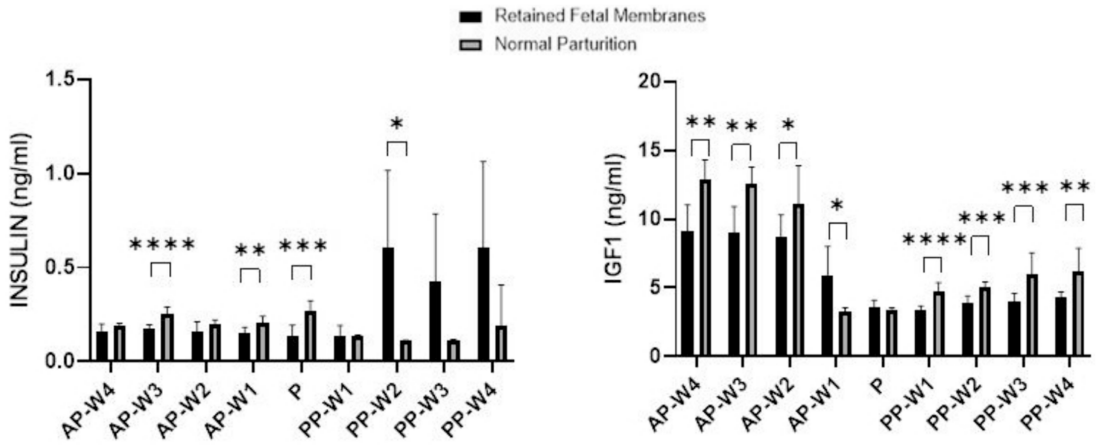

FIGURE 5
Blood Insulin and IGF-1 concentrations. Statistical significance *$p < 0.05$, **$p < 0.01$, ***$p < 0.001$, ****$p < 0.001$. The outcomes represent mean ± SD of three replicate analyses.

infection, inflammation, or trauma (20). Trevisi et al. (23) documented the inflammatory alterations following a retained placenta, indicating that cows exhibit diminished albumin levels during the postpartum period (Day 1–28.3 g/L; Day 7–28.3 g/L; Day 14–28.6 g/L; Day 21–29.4 g/L; Day 28–30.3 g/L) in comparison to their healthy counterparts (Day 1–34.2 g/L; Day 7–32.1 g/L; Day 14–32.1 g/L; Day 21–32.8 g/L; Day 28–33.4 g/L). This reduction is attributed to compromised hepatic function and a deteriorated energy balance. Corresponding observations were presented in the research by Semacan and Seminc (24), where bovines with a retained placenta demonstrated lower albumin levels (2.93 ± 0.07 g/100 mL) relative to those in a healthy condition (3.32 ± 0.07 g/100 mL). A typical decline in albumin levels immediately post-calving is noted (25, 26), which is also observed in cows undergoing normal calving, indicating an improved protein status at the organismal level.

The basal plasma concentration of total proteins in bovines is delineated within a range of 6.74 to 7.46 g/dL, as documented by Farver et al. (22). Investigations by Hashem and Amer (27) reveal an elevation in total protein concentrations in bovines afflicted with retained placenta (8.70 ± 0.44 mg/1 dL) in comparison to those undergoing uneventful parturition (8.41 ± 1.58 mg/1 dL). Conversely, research by Civelek et al. (28) indicates a reduction in total protein levels during parturition in cows with retained placenta (6.62 ± 0.13 mg/dL) relative to those with normal parturition processes (8.15 ± 0.36 mg/dL). Kumari et al. (29) corroborate these findings, noting significantly diminished total protein concentrations in bovines with retained placenta across multiple time points: 14 days, 7 days, and 5 days preceding parturition, during the parturition event itself, and on the first and second days postpartum, when compared to bovines experiencing normal parturition. In our studies, during parturition, we observed a significant elevation in protein levels in the RFM group compared to the NP group, this period appears to be a critical point; physiological parameters are significantly modified in cows with RFM. Three weeks after parturition, there was a noticeable increase in protein levels in the RFM group. This may indicate a prolonged or delayed reaction to the stress of RFM, which could have consequences for the cow's recovery and metabolic state. The protein levels in the RFM group were not significantly different from the NP group by week 4 postpartum, indicating a return to physiologic values or an adaptation to postpartum conditions.

The normative plasma glucose concentration in bovines is quantified as ranging between 45 and 75 mg/dL, according to Farver et al. (22). Empirical data elucidate that bovines suffering from retained placenta manifest diminished glucose levels during the immediate aftermath of parturition compared to those experiencing normal delivery. Semacan and Sevinc (24) reported a significant disparity in blood glucose levels, with cows afflicted by retained placenta showing lower levels (61.6 ± 6 mg/dL) versus those in healthy conditions (88.9 ± 7.3 mg/dL). This trend of reduced glucose levels in cows with retained placenta relative to those undergoing normal calving is consistently observed across various studies (27, 28). Kumari et al. (29) established that bovines with retained placenta exhibited lower glucose concentrations on days 14, 7, 5, 3, 1 preceding calving, during the calving process, and on the first postpartum day in comparison to cows with uneventful deliveries. These findings are in accordance with the data that was obtained during our investigations. Compared to NP cows, RFM cows had significantly higher glucose levels at parturition (P). The high energy requirements and stress that RFM cows experience may be the cause of the significant increase in glucose.

The occurrence of hypoglycemia in bovines with retained placenta underpins the hypothesis that glucose concentrations toward the culmination of pregnancy act as an indicator of elevated risk for retained placenta. An alternative explanation posits that the decreased glucose levels may be attributed to augmented nutritional demands of the fetus and the formation of colostrum (27). Furthermore, hypoglycemia might be associated with elevated cortisol levels related to retained placenta and postpartum metritis, either in a direct or indirect manner (27, 30). The presence of hypoglycemia during the final month of gestation is identified as a risk factor for the development of retained placenta and postpartum metritis (27, 31).

Additionally, the increased susceptibility to retained placenta is linked to hypotonia or atonia within the musculature of the reproductive and digestive tracts, a condition precipitated by diminished concentrations of glucose and calcium within the smooth muscle cells (7, 32).

The typical plasma concentration range for triglycerides in bovines is reported to be 0 to 14 mg/dL (22). Kaczmarowski et al. (30) posited that diminished lipid and triglyceride levels might result from altered lipid metabolism, augmented activity of tissue lipolytic enzymes, or ketosis in afflicted animals, with ketone bodies measured at 765 ± 427 μmol/L in cows with retained placenta versus 754 ± 296 μmol/L in their healthy counterparts. A lower amount of triglycerides was observed throughout our research, which may indicate that RFM cows have a greater postpartum energy deficit. In addition, the significant decrease in triglycerides during the postpartum phase may also indicate a risk for the development of metabolic disorders (such fatty liver syndrome).

Deviations in triglyceride concentrations are frequently linked to hepatic disorders, as illustrated by Semacan and Sevinc (24), where bovines with retained placenta exhibited lower triglyceride levels (15.57 ± 1.4 mg/100 mL) in comparison to healthy bovines (21.5 ± 1.6 mg/100 mL). Fatty liver infiltration or hepatic steatosis, which can significantly impair hepatic function, is one such disorder. A notable effect of hepatic steatosis includes a reduction in serum albumin levels, indicative of compromised liver synthetic capacity, and an increase in plasma enzyme activity such as AST, aligning with observations made in this discourse.

The normative plasma cholesterol range in bovines is delineated as 80 to 120 mg/dL, according to Farver et al. (22). It has been observed that cows with retained placenta demonstrate significantly elevated plasma cholesterol levels compared to those that efficiently expel fetal membranes. Moreover, decreased circulating cholesterol levels during the antepartum period have been associated with a heightened risk of retained placenta. This trend is corroborated by Semacan and Sevinc (24), where cows with retained placenta had cholesterol levels of 96.1 ± 6.8 mg/100 mL, whereas healthy cows had 141.3 ± 9.8 mg/100 mL. Similar findings were echoed in additional studies comparing healthy cows to those with retained placenta (25, 27, 28). In our study, significant increases in cholesterol have been observed in RFM cows antepartum. The RFM cows' cholesterol levels peaked at parturition (P), indicating that the physiological stress associated with parturition might exacerbate the hypercholesterolemia.

On the other hand, Kaczmarowski et al. (30) found no statistically significant differences in cholesterol levels between cows with retained placenta and healthy ones (2.08 ± 0.83 mmol/L vs. 2.17 ± 0.83 mmol/L). Kumari et al. (29) reported lower cholesterol levels in cows with retained placenta on day 1 antepartum, during parturition, and on day 1 postpartum. Blood cholesterol concentration serves as a vital marker for hepatic lipoprotein synthesis and the availability of exogenous energy. Despite cholesterol levels surpassing physiological norms in both groups, cows with retained placenta exhibited higher cholesterol levels compared to those without postpartum pathologies. Blood cholesterol content thus acts as a crucial indicator of hepatic lipoprotein synthesis and external energy availability (29), which in turn reflects on liver health.

The standard enzymatic activity range for Aspartate Aminotransferase (ASAT) in bovines is identified as 78 to 132 U/L, as established by Farver et al. (22). Elevated ASAT levels observed in this study correlate with the known association between hepatic steatosis (fatty liver) and cows experiencing retained placenta, as highlighted by Semacan and Sevinc (24). The infiltration of fat within the liver is associated with an escalation in hepatic enzyme activities alongside a decrease in blood glucose, total lipids, cholesterol, and triglycerides. The spectrum of liver fat accumulation, from mild to severe, can precipitate liver dysfunction without leading to hepatocyte death, albeit with an increase in hepatic enzyme activity (24, 27). Semacan and Sevinc (24) attribute the accumulation of lipids within hepatocytes of cows with retained placenta to the presence of endotoxins stemming from infectious diseases such as endometritis, which can induce hepatic lesions and necrosis, thereby causing varying degrees of liver dysfunction.

AST activity, which is inherently high in the liver of all domestic species, typically surges in serum levels during both acute and chronic liver damages. Given that AST is also abundant in muscles, kidneys, pancreas, and erythrocytes, damage to these tissues can likewise result in elevated serum AST levels (33), as observed in cows with normal calving during the fourth postpartum week.

The normative range for ALAT activity in bovines is set at 11–40 U/L (22). Significant increases in ALT activity are typically indicative of hepatocellular inflammation. In such scenarios, a progressive reduction in ALT activity might signal recovery, with a decrease of 50% or more in serum ALT activity over several days being viewed as a positive prognostic indicator. However, some animals with severe liver disease may present with normal serum ALT levels, and a reduction in serum ALT activity could signify a substantial loss of viable hepatocytes or a diminished synthesis of transaminases (33).

The induction of corticotropin and adrenocorticotropic hormone production serves as a pivotal mechanism activating the hypothalamic–pituitary axis, which in turn elevates plasma cortisol levels significantly from a normative baseline of approximately 5 ng/mL to a range of 10–20 ng/mL (7, 34). This surge in cortisol, recognized for its immunosuppressive capabilities, notably impairs leukocyte proliferation and their critical functional roles, effectively obstructing the standard immunological processes essential for the identification and subsequent elimination of fetal tissues (7, 13).

Pre-parturition cortisol levels experience a marked increase, reaching their zenith during or shortly subsequent to the birth process. This elevation of cortisol plays a multifaceted role during parturition; it may exert a negative feedback mechanism on prostaglandin synthesis via the induction of lipocortin-1, a phospholipase inhibitor, or alternatively, it may contribute to the stress-induced labor process (35).

Normative plasma cortisol concentrations in cattle are delineated to range between 1.3 and 2.93 ng/mL (22). However, during the periparturient phase, a compromised immune system is observed, largely attributed to metabolic stress precipitated by hormonal and metabolic fluctuations, a negative energy balance, and deficiencies in proteins, minerals, and essential vitamins necessary to meet fetal demands and support the initiation of lactation (36). This metabolic stress is capable of activating the hypothalamic–pituitary-adrenocortical (HPA) axis, leading to an augmented secretion of plasma corticosteroids. As a result, there is a dramatic elevation in cortisol levels during the periparturient phase, notably on the day of calving. Cortisol, with its potent immunosuppressive properties, suppresses the proliferation and function of leukocytes during periods of stress, significantly reducing neutrophil phagocytosis, lymphocyte cytotoxic capacity, and cytokine activity. These reductions compromise the efficacy of immunological recognition and the expulsion of fetal membranes, thereby contributing to incidences of retained placenta (36). Cortisol levels 4 weeks prior to parturition in cows with RFM do not appear to be substantially higher than in cows with NP, according to our data. However, RFM cows presented increased cortisol levels 2 weeks prior to parturition. These modifications could indicate an increasing stress response or a

physiological preparation for the upcoming labor, which may be more pronounced in cows predisposed to RFM.

The literature suggests that the average insulin concentration during the periparturient period spans from 0.2 ng/mL to 1.6 ng/mL (37). Moreover, periparturient hypocalcemia is intricately linked to metabolic activities, where diminished calcium levels adversely affect insulin production, thereby reducing glucose delivery to various tissues (7, 14). This deficiency in glucose uptake triggers lipolysis, leading to a negative energy balance, metabolic stress, immunosuppression, and ketosis. The resultant hypotension or atony of the reproductive and digestive tract musculature, owing to reduced glucose and calcium levels within smooth muscle cells, heightens the risk of retained placenta (7, 32).

Comparative analyses reveal that insulin levels in bovines with normal calving are higher during the antepartum and calving phases in contrast to those with retained placenta, albeit lower across all sampling points than the literature average (37).

Furthermore, the mean concentration of insulin-like growth factor 1 (IGF-1) across various phases has been documented by Baldacim et al. (38), ranging from 8.67–11.62 ng/mL in the antepartum period to 2.50–4.50 ng/mL postpartum. Cows experiencing normal calving exhibit higher IGF-1 levels in the prepartum period as compared to those with retained placenta. Notably, during calving, the IGF-1 levels are comparable across both groups, with a subsequent increase observed in cows with normal calving relative to those with retained placenta.

Postpartum, a decrease in IGF-1 levels has been observed (39). Velazquez et al. (10) describe a pattern wherein IGF-I concentrations diminish in the final days of pregnancy, reach a low point in the initial weeks post-calving, and subsequently commence an upward trajectory.

The IGF-1 levels in cows undergoing normal calving remain within physiological parameters during both the antepartum and postpartum periods and exhibit a more rapid recovery. In contrast, cows with retained placenta showcase lower IGF-1 levels in the initial postpartum week than their healthy counterparts, falling beneath the concentration range specified in the literature (38). Nakada (12) associates lower IGF-I levels with retained placenta and endometritis, noting that IGF-I concentrations decline temporarily in cows suffering from postpartum reproductive disorders and seldom revert to baseline levels post-lactation cessation.

5 Conclusion

In conclusion, this clinical study reveals the multifaceted metabolic challenges faced by cows with retained fetal membranes (RFM) across various biochemical parameters during the periparturient period. Our findings elucidate the temporal complexity of metabolic alterations, including significant impacts of albumin, glucose, triglyceride, cholesterol levels, enzyme activities (AST, ALT), cortisol, insulin, and IGF-1 dynamics, highlighting the intricate interplay of metabolic stressors associated with RFM. Notably, the absence of significant prepartum differences in some parameters contrasts with marked postpartum fluctuations, indicating a critical period of metabolic adjustment and recovery following parturition. The significant prepartum and postpartum changes in these biochemical markers not only provide insights into the metabolic demands placed on cows by RFM but also offer potential diagnostic and management strategies to mitigate its impact. By closely monitoring these indicators, particularly during the critical weeks surrounding parturition, interventions can be targeted more effectively to support cow health, enhance recovery processes, and ultimately improve dairy herd productivity.

Data availability statement

The original contributions presented in the study are included in the article/supplementary material, further inquiries can be directed to the corresponding author.

Ethics statement

The animal study was approved by University of Agricultural Sciences and Veterinary Medicine Cluj-Napoca, Romania Bioethical Committee (256/21.04.2021) and the Regional Sanitary Veterinary and Food Safety Authority (no. 274/12.11.2021). The study was conducted in accordance with the local legislation and institutional requirements.

Author contributions

HR: Conceptualization, Investigation, Methodology, Software, Visualization, Writing – original draft. IO: Methodology, Resources, Writing – original draft. OC: Investigation, Methodology, Writing – original draft. AM: Investigation, Writing – original draft. DD: Investigation, Writing – original draft. CŞ: Investigation, Writing – original draft. DN: Investigation, Writing – original draft. AB: Investigation, Writing – original draft. SA: Conceptualization, Data curation, Resources, Supervision, Validation, Visualization, Writing – review & editing.

Funding

The author(s) declare that financial support was received for the research, authorship, and/or publication of this article. This work was supported by funds from the National Research Development Projects to finance excellence (PFE)-14 (ID 546) granted by the Romanian Ministry of Research, Innovation and Digitalization. This research was also funded by USAMV CN project 24905/08.11.2021.

Conflict of interest

The authors declare that the research was conducted in the absence of any commercial or financial relationships that could be construed as a potential conflict of interest.

Publisher's note

References

1. Bicalho MLS, Lima FS, Ganda EK, Foditsch C, Meira EBS Jr, Machado VS, et al. Effect of trace mineral supplementation on selected minerals, energy metabolites, oxidative stress, and immune parameters and its association with uterine diseases in dairy cattle. *J Dairy Sci*. (2014) 97:4281–95. doi: 10.3168/jds.2013-7832

2. Ocal H. Prolapsus uteri In: E Alaçam, editor. *Parturition and infertility in domestic animals*. Ankara: Medisan Publishing House (2002). 231–6.

3. Erisir M, Akar AR, Gurgoze SY, Yuksel M. Changes in plasma malondialdehyde concentration and some erythrocyte antioxidant enzymes in cows with prolapsus uteri, caesarean section, and retained placenta. *Revue Med Vet*. (2006) 157:80–3.

4. Kankofer M, Albera E, Feldman M, Gundling N, Hoedemaker M. Comparison of antioxidative/oxidative profiles in blood plasma of cows with and without retained fetal placental membranes. *Theriogenology*. (2010) 74:1385–95. doi: 10.1016/j.theriogenology.2010.06.009

5. Roche JR, Bell AW, Overton TR, Loor JJ. Nutritional management of the transition cow in the 21st century–a paradigm shift in thinking. *Anim Prod Sci*. (2013) 53:1000–23. doi: 10.1071/AN12293

6. Wathers DC. Interactions between energy balance, the immune system end the reproductive tract with influence on dairy cow fertility. *Cattle Pract*. (2010) 18:19–26.

7. Mordak R, Nicpoń J, Illek J. Metabolic and mineral conditions of retained placenta in highly productive dairy cows: pathogenesis, diagnostics and prevention–a review. *Acta Vet Brno*. (2017) 86:239–48. doi: 10.2754/avb201786030239

8. Sun Y, Wang B, Shu S, Zhang H, Xu C, Wu L, et al. Critical thresholds of liver function parameters for ketosis prediction in dairy cows using receiver operating characteristic (ROC) analysis. *Vet Q*. (2015) 35:159–64. doi: 10.1080/01652176.2015.1028657

9. Peter AT In: M Richard, editor. *Bovine reproduction, first edition*. Hoboken, New Jersey: Hopper John Wiley & Sons, Inc (2015), Chapter 49). 431–5.

10. Velazquez MA, Spicer LJ, Wathes DC. The role of endocrine insulin-like growth factor-I (IGF-I) in female bovine reproduction. *Domest Anim Endocrinol*. (2008) 35:325–42. doi: 10.1016/j.domaniend.2008.07.002

11. Wathes DC, Becker F, Buggiotti L, Crowe MA, Ferris C, Foldager L, et al. Associations between circulating IGF-1 concentrations, disease status and the leukocyte transcriptome in early lactation dairy cows. *Ruminants*. (2021) 1:147–77. doi: 10.3390/ruminants1020012

12. Nakada K. How to improve reproductive efficacy from now in Japan? Find out the factors of late lactation to predict postpartum reproductive diseases. *J Reprod Dev*. (2006) 52:177–83. doi: 10.1262/jrd.17090

13. Davies CJ, Hill JR, Edwards JL, Schrick FN, Fisher PJ, Eldridge JA, et al. Major histocompatibility antigen expression on the bovine placenta: its relationship to abnormal pregnancies and retained placenta. *Anim Reprod Sci*. (2004) 82-83:267–80. doi: 10.1016/j.anireprosci.2004.05.016

14. Lucy M. Mechanisms linking growth hormone, insulin and reproduction: lessons from postpartum dairy cow. *Cattle Pract*. (2006) 14:23–7.

15. Pelmus RS, Rotar MC, Lazăr C, Uță RA. Estimation the genetic parameters for milk yield in Romanian spotted, Simmental type cattle breed. *Archiva Zootechnica*. (2021) 24:105–21. doi: 10.2478/azibna-2021-0017

16. Ilie DE, Gavojdian D, Kusza S, Neamț RI, Mizeranschi AE, Mihali CV, et al. Kompetitive allele specific pcr genotyping of 89 SNPs in romanian spotted and romanian brown cattle breeds and their association with clinical mastitis. *Animals*. (2023) 13:1484. doi: 10.3390/ani13091484

17. Gradinaru AC, Petrescu-Mag IV, Oroian FC, Balint C, Oltean I. Milk protein polymorphism characterization: a modern tool for sustainable conservation of endangered Romanian cattle breeds in the context of traditional breeding. *Sustain For*. (2018) 10:534. doi: 10.3390/su10020534

18. Erina S, Cziszter LT, Acatincai S. *Livestock technologies – cattle*. Timisoara, Romania: Ed. Eurobit (2018). 98 p.

19. Cziszter LT, Ilie DE, Neamt RI, Neciu FC, Saplacan SI, Gavojdian D. Comparative study on production, reproduction and functional traits between Fleckvieh and Braunvieh cattle. *Asian Australas J Anim Sci*. (2017) 30:666–71. doi: 10.5713/ajas.16.0588

20. Farver TB, Werner P, Giger U, Haskins M, Kaneko JJ, Eckersall PD, et al. Proteins, proteomics, and the dysproteinemias In: JJ. Kaneko, JW. Harvey, ML. Bruss, editors. *Clinical biochemistry of domestic animals. 6th* ed. Amsterdam, Netherlands: Elsevier (2008). 117–48.

21. Weaver DM, Tyler JW, VanMetre DC, Hostetler DE, Barrington GM. Passive transfer of colostral immunoglobulins in calves. *J Vet Intern Med*. (2000) 14:569–77. doi: 10.1111/j.1939-1676.2000.tb02278.x

22. Farver TB, Werner P, Giger U, Haskins M, Kaneko JJ, Eckersall PD, et al. Apendix VII In: JJ. Kaneko, JW. Harvey, ML. Bruss, editors. *Clinical biochemistry of domestic animals. 6th* ed. Amsterdam, Netherlands: Elsevier (2008). 883–8.

23. Trevisi E, Ferrari AR, Bertoni G. Productive and metabolic consequences induced by the retained placenta in dairy cows. *Vet Res Commun*. (2008) 32:363–6. doi: 10.1007/s11259-008-9149-4

24. Semacan A, Sevinç M. Liver function in cows with retained placenta. *Turkish J Vet Anim Sci*. (2005) 29:775–8.

25. Seifi HA, Dalir-Naghadeh B, Farzaneh N, Mohri M, Gorji-Dooz M. Metabolic changes in cows with or without retained fetal membranes in transition period. *J Veterinary Med Ser A*. (2007) 54:92–7. doi: 10.1111/j.1439-0442.2007.00896.x

26. Trevisi ER, Amadori M, Cogrossi SI, Razzuoli E, Bertoni G. Metabolic stress and inflammatory response in high-yielding, periparturient dairy cows. *Res Vet Sci*. (2012) 93:695–704. doi: 10.1016/j.rvsc.2011.11.008

27. Hashem MA, Amer HA. Hormonal and biochemical anomalies in dairy cows affected by retained fetal membranes. *Int J Vet Med*. (2008) 185:1517–9.

28. Civelek T, Aydin I, Cingi CC, Yilmaz O, Kabu M. Serum non-esterified fatty acids and beta-hydroxybutyrate in dairy cows with retained placenta. *Pak Vet J*. (2011) 31:341–4.

29. Kumari S, Prasad S, Patbandha TK, Pathak R, Kumaresan A, Boro P, et al. Metabolic indicators for retention of fetal membranes in zebu and crossbred dairy cattle. *Anim Prod Sci*. (2015) 56:1113–20. doi: 10.1071/AN14941

30. Kaczmarowski M, Malinowski E, Markiewicz H. Some hormonal and biochemical blood indices in cows with retained placenta and puerperal metritis. *Bull Vet Inst Puławy*. (2006) 50:89–92.

31. Markiewicz H, Kuzma K, Malinowski E. Predisposing factors for puerperal metritis in cows. *Bull Vet Inst Puławy*. (2001) 45:281–8.

32. Kimura KA, Reinhardt TA, Goff JP. Parturition and hypocalcemia blunts calcium signals in immune cells of dairy cattle. *J Dairy Sci*. (2006) 89:2588–95. doi: 10.3168/jds.S0022-0302(06)72335-9

33. Farver TB, Werner P, Giger U, Haskins M, Kaneko JJ, Eckersall PD, et al. Hepatic function In: JJ. Kaneko, JW. Harvey, ML. Bruss, editors. *Clinical biochemistry of domestic animals. 6th* ed. Amsterdam, Netherlands: Elsevier (2008). 390.

34. Mormede P, Andanson S, Aupérin B, Beerda B, Guémené D, Malmkvist J, et al. Exploration of the hypothalamic–pituitary–adrenal function as a tool to evaluate animal welfare. *Physiol Behav*. (2007) 92:317–39. doi: 10.1016/j.physbeh.2006.12.003

35. Kindahl H, Kornmatitsuk B, Königsson K, Gustafsson H. Endocrine changes in late bovine pregnancy with special emphasis on fetal well-being. *Domest Anim Endocrinol*. (2002) 23:321–8. doi: 10.1016/S0739-7240(02)00167-4

36. Mordak R, Stewart PA. Periparturient stress and immune suppression as a potential cause of retained placenta in highly productive dairy cows: examples of prevention. *Acta Vet Scand*. (2015) 57:84. doi: 10.1186/s13028-015-0175-2

37. Zinicola M, Bicalho RC. Association of peripartum plasma insulin concentration with milk production, colostrum insulin levels, and plasma metabolites of Holstein cows. *J Dairy Sci*. (2019) 102:1473–82. doi: 10.3168/jds.2017-14029

38. Baldacim VA, Madureira KM, Ramos JS, Costa CP, Mori CS, Dias MRB, et al. Dynamic of metabolic indicators, insulin like-growth factor I (IGF-I) and cortisol in Holstein cows during the transition period. *Acta Sci Vet*. (2018) 46:8. doi: 10.22456/1679-9216.86674

39. Hammon HM, Stürmer G, Schneider F, Tuchscherer A, Blum H, Engelhard T, et al. Performance and metabolic and endocrine changes with emphasis on glucose metabolism in high-yielding dairy cows with high and low fat content in liver after calving. *J Dairy Sci*. (2009) 92:1554–66. doi: 10.3168/jds.2008-1634

frontiers | Frontiers in Veterinary Science

TYPE Original Research
PUBLISHED 30 May 2024
DOI 10.3389/fvets.2024.1410371

OPEN ACCESS

EDITED BY
Omer Ucar,
Muğla Sıtkı Koçman University, Türkiye

REVIEWED BY
Şükrü Güngör,
Mehmet Akif Ersoy University, Türkiye
Mihai Cenariu,
University of Agricultural Sciences and Veterinary Medicine of Cluj-Napoca, Romania

*CORRESPONDENCE
Zhili Chu
chuzhili@xxmu.edu.cn
Feng Ren
renfeng@xxmu.edu.cn
Xinglong Wu
wuxl32@hebau.edu.cn

RECEIVED 01 April 2024
ACCEPTED 29 April 2024
PUBLISHED 30 May 2024

CITATION
Jiao X, Chu Z, Li M, Wang J, Ren Z, Wang L, Lu C, Li X, Ren F and Wu X (2024) GnRH-mediated suppression of S100A4 expression inhibits endometrial epithelial cell proliferation in sheep via GNAI2/MAPK signaling.
Front. Vet. Sci. 11:1410371.
doi: 10.3389/fvets.2024.1410371

GnRH-mediated suppression of S100A4 expression inhibits endometrial epithelial cell proliferation in sheep via GNAI2/MAPK signaling

Xiyao Jiao[1], Zhili Chu[2,3]*, Meng Li[1], Jiurong Wang[2], Zilong Ren[2], Leyang Wang[2], Chengcheng Lu[2], Xiangyun Li[1], Feng Ren[2,3]* and Xinglong Wu[1]*

[1]College of Animal Science and Technology, Hebei Technology Innovation Center of Cattle and Sheep Embryo, Hebei Agricultural University, Baoding, China, [2]School of Basic Medical Sciences, Xinxiang Medical University, Xinxiang, China, [3]Henan International Joint Laboratory of Immunity and Targeted Therapy for Liver-Intestinal Tumors, Xinxiang Medical University, Xinxiang, China

Background: Gonadotrophin-releasing hormone (GnRH) administration significantly decreases the pregnancy rate of recipient ewes after embryo transfer, possibly because GnRH affects endometrial epithelial cell function. Therefore, this study investigated the effect of GnRH on endometrial epithelial cells.

Methods: Transcriptome sequencing was used to determine the regulatory effect of GnRH on the ewe endometrium, and the S100A4 gene, which showed altered transcription, was screened as a candidate regulator of this effect. Endometrial epithelial cells were further isolated, the S100A4 protein was immunoprecipitated, and host proteins that interacted with S100A4 were identified by mass spectrometry. We further verified the effects of S100A4 and GNAI2 on the proliferation of endometrial epithelial cells via overexpression/knockdown experiments and subsequent CCK-8 and EdU assays. The effect of S100A4 deletion in endometrial cells on reproduction was verified in mice with S100A4 knockout.

Results: Our results showed that S100A4 gene transcription in endometrial cells was significantly inhibited after GnRH administration. GNAI2 was identified as a downstream interacting protein of S100A4, and S100A4 was confirmed to activate the MAPK signaling pathway to promote cell proliferation by targeting GNAI2.

Conclusion: GnRH can suppress the expression of S100A4 in the endometrium, consequently inhibiting the proliferation of endometrial cells through the S100A4/GNAI2/MAPK signaling pathway. These findings suggest a potential explanation for the limited efficacy of GnRH in promoting embryo implantation.

KEYWORDS

sheep endometrial epithelial cells, GnRH, cell proliferation, S100A4, GNAI2, MAPK signaling pathway

1 Background

The application of assisted reproductive technology is important for increasing the pregnancy rate of sheep. Further research into the effects of different hormones on reproduction is therefore warranted. Gonadotrophin-releasing hormone (GnRH) plays a pivotal role in hormonal dynamics and reproductive efficiency in mammals. GnRH is a decapeptide hormone that is synthesized and secreted by specific hypothalamic neurons. This hormone is released into the pituitary portal system in a pulsed manner, binds to the GnRH receptor on the surface of the pituitary gland, regulates the hypothalamus-pituitary-gonadal (HPG) axis, stimulates the release of gonadotropins and steroid hormones, such as follicle stimulating hormone (FSH) and luteinizing hormone (LH) (1), and then regulates embryo implantation and placental formation, playing an essential role in maintaining the normal reproductive activities of animals (1–3). GnRH and GnRH receptors are found in the hypothalamus, pituitary glands, and various reproductive organ tissues, such as the ovaries, endometrium, and myometrium. GnRH mRNA is expressed in both epithelial and stromal cells of the human endometrium in a dynamic manner. In the early and middle secretory stages of the menstrual cycle, endometrial GnRH mRNA levels increase significantly, suggesting that GnRH may be involved in the embryo implantation process (4). GnRH receptors are expressed in human endometrial decidual stromal cells, and GnRH agonists can promote the release of enzymes that remodel the extracellular matrix and change cell movement (1, 5). GnRH agonists can inhibit the proliferation, migration, and differentiation of endometrial stem cells through the PI3K/Akt signaling pathway (6) and can also affect the receptivity of the endometrium by affecting the immune response and energy metabolism (7). GnRH and GnRH receptors are also expressed in the myometrium. GnRH agonists can inhibit DNA synthesis, TGF-β production in myometrial smooth muscle cells and proliferation of uterine fibroids (4, 8). In summary, GnRH participates in the embryo implantation process by mediating various functions of endometrial cells, and exogenous GnRH can affect uterine function. Therefore, GnRH is often used clinically to induce ovulation during superovulation (9–11) and to synchronize estrus (12, 13).

GnRH is widely used to increase pregnancy rates in sheep. GnRH agonists/antagonists were first used to control follicle development (9–11, 14) and to assess the efficacy of estrus induction during different periods (15). This molecule can also be used to induce estrus synchronization (12, 13, 16). However, we previously found that using GnRH in sheep fixed-time artificial insemination and embryo transfer programs does not increase the embryo and embryo transfer programs decreased the embryo implantation rate (17). Unfortunately, the mechanism of its negative effect is still unclear.

Physiological changes in endometrial cells are essential for cyclic changes in the uterus. In particular, the endometrium must respond to hormonal changes and proliferate to a state suitable for embryo implantation. Generally, endometrial cell proliferation is regulated by hormones such as estrogen, which acts as a transcription factor that directs target gene expression and exerts its effects through interactions with the membrane-bound estrogen receptor (ER). The ER utilizes intracellular signaling systems [such as mitogen-activated protein kinase (MAPK)/ERK, phosphoinositide 3-kinase (PI3K), and RAS signaling pathways] to participate in the regulation of gene expression (18). However, the molecular mechanism by which hormones activate endometrial cell proliferation after they act on endometrial cells is not fully understood. Studies have not shown whether GnRH treatment can affect endometrial cell proliferation.

The S100 protein family consists of 25 calcium-binding proteins with high sequence and structural similarities. S100A4 is a critical member expressed in various cell types, including lymphoid and myeloid cells such as macrophages, neutrophils, mast cells, and memory T cells. This molecule plays a crucial role in promoting cancer occurrence and metastasis. The S100A4 protein also regulates obesity (19), cell proliferation (20), migration (21, 22), inflammation, and cell death (23). Additionally, S100A4 is a key dynamic regulator of embryo implantation (24). In cases of inflammatory reactions in the bovine uterus, the expression level of S100A4 significantly decreases, suggesting its relevance to the pathogenesis of endometrial inflammation (25).

In the pathogenesis of uterine sarcoma, S100A4 also plays a crucial role in affecting epithelial–mesenchymal transition (26). Several studies have shown that S100A4 can promote the migration and metastasis of endometrial cancer cells (27). These findings collectively suggest that S100A4 plays an important regulatory role in uterine diseases.

However, the role of S100A4 in regulating endometrial cell proliferation remains to be explored. Transcriptome sequencing revealed that changes in S100A4 expression affect endometrial proliferation. Furthermore, the downstream interacting protein GNAI2 was identified through coimmunoprecipitation. These findings were validated through *in vitro* and *in vivo* experiments in mice with uterine-specific S100A4 knockout, confirming that S100A4 can regulate the MAPK signaling pathway to promote endometrial cell proliferation.

2 Materials and methods

2.1 Animal experiments

This experiment was conducted from November to December 2019 at a Kazakh sheep breeding farm in Liaoning Province, China (41°06′N 122°18′E). The 20 selected sheep had no reproductive disorders. The weight was 40–60 kg. The ewes selected for experiments were treated with an intravaginal vaginal sponge soaked with 45 mg of progesterone (Muqimuye Sci-Tech Co., Ltd., Shanghai, China) for 12 days. When the sponge was removed, 330 IU PMSG (Sansheng Biological Technology Co., Ltd., Ningbo, China) was injected intramuscularly. Ewes induced to undergo estrus were subjected to insemination 50 h after the sponge was removed. Laparoscopic uterine horn insemination was performed using an insemination device (Zhengmu Bio-Tech Co., Ltd., Baoding, China). Semen in 0.25 mL aliquots was thawed via conventional methods. The spermatozoa cell concentration was approximately 400×10^6 cells/mL. The experimental ewes were divided into two groups. The experimental group was administered 17 μg of A3 (a GnRH agonist triptorelin; Sansheng Biological Technology Co., Ltd., Ningbo, China) by intramuscular injection 12 h before insemination,

and the control group was administered 1 mL of sterile physiological saline solution via the same route. The endometrium was assessed 5 days after insemination. The Ethical Committee of Xinxiang Medical University approved this study.

2.2 Isolation and culture of sheep endometrial epithelial cells

Sheep uteri were collected at the slaughterhouse and immersed in physiological saline containing penicillin (100 IU/mL) and streptomycin (1 mg/mL). The uteri were then transported in an ice box to the laboratory. In a biosafety cabinet, the uteri were rinsed three times with PBS. During surgery, the uteri were cut into pieces, and efforts were made to remove nonendometrial tissue as thoroughly as possible. After the tissue was cut, the tissue homogenate was added to a cell culture dish, allowed to dry and fixed for 1 h. Cell culture medium containing 10% fetal bovine serum, penicillin, and streptomycin was added to the culture dish. The cells typically began to expand after approximately 7 days. When the cells reached approximately 70% confluence, they were harvested, digested, and frozen for future use. The Ethical Committee of Xinxiang Medical University approved this study.

2.3 Cell transfection with siRNA and plasmids

Plasmids for synthesizing siRNAs and overexpressing sheep S100A4 and GNAI2 were used. The target sequences are listed in Table 1. The cells were transferred to a 6-well cell culture plate one day in advance, with approximately 5×10^6 cells per well. During transfection, Lipofectamine 2000 was mixed with serum-free basic DMEM to create solution A, while plasmid/siRNA was mixed with serum-free high-glucose basic DMEM to create solution B. After 5 min, solutions A and B were combined, and the mixture was allowed to incubate at room temperature for 12 min. This mixture was subsequently added to the cell culture dish, and the culture medium was replaced with fresh medium after 6 h. Subsequent experiments were conducted 42 h after transfection.

2.4 Transcriptome sequencing

For processing of sheep tissue samples, the samples were ground and then lysed with TRIzol. For cell samples, the cell supernatant was discarded, and the cells were washed once with PBS and then lysed with TRIzol. RNA was subsequently extracted via the addition of chloroform and TRIzol at a 10% v/v ratio, followed by shaking, mixing, and centrifugation at 12,000 rpm for 10 min. The supernatant was transferred to a new centrifuge tube, and an equal volume of isopropanol was added. After inversion, mixing, and a 30-min incubation step, the mixture was centrifuged at 12,000 rpm for 10 min. The supernatant was gently discarded, and 1 mL of precooled 75% alcohol was added. The samples were centrifuged again at 12,000 rpm for 10 min, the supernatant was removed, and the pellet was allowed to dry in a fume hood. The RNA was subsequently dissolved in ddH2O for library construction.

Sheep uterine tissue sequencing and data analysis were performed by Beijing Geekgene Technology Co., Ltd. Sequencing following S100A4 knockdown was conducted by Suzhou GenePharma Co., Ltd. Transcriptome sequencing and analysis of GNAI2-overexpressing cells were performed by Beijing Novo Biotechnology Co., Ltd.

2.5 CCK-8 assays

Cells were seeded into a 96-well plate. After the corresponding treatment (as described in Materials and Methods 2), CCK-8 (C0005, Targetmol, United States) reagent was mixed with culture medium at a ratio of 1:9 in a centrifuge tube, and then, 100 μL of culture medium containing CCK-8 reagent was added to each well. The plate was placed in a cell culture incubator for further incubation. After 30 min, the OD450 was measured using a FlexStation 3 instrument.

2.6 EdU staining

After the cells were processed, EdU was dissolved in culture medium (10 μM), mixed evenly, and placed in a cell culture incubator for 30 min. Then, the culture medium in the original cell culture dish was discarded, and the above mixture was added. The cells were

TABLE 1 Primer sequences.

	Forward sequence	Reverse sequence
S100A4	TGAGCAACTTGGACAGCAACA	TTCCGGGGTTCCTTATCTGGG
GNAI2	GGTCGTCTACAGCAACACCA	GTCTTCACTCGAGTCCGCAG
C-fos	CCAGCCCTGACCTACAATGG	CTGCCTCCCGTCATGGTTT
c-JUN	CGACCTTCTACGACGATGCC	GGGGTTACTGTAGCCGTAGG
GAPDH	AGGTCGGTGTGAACGGATTTG	TGTAGACCATGTAGTTGAGGTCA
si-S100A4	GCAUCGCCAUGAUGUGCAATT	UUGCACAUCAUGGCGAUGCTT
si-NC	UUCUCCGAACGUGUCACGUTT	ACGUGACACGUUCGGAGAATT
si-GNAI2	GCACGAGAGCAUGAAGCUGUUTT	AACAGCUUCAUGCUCUCGUGCTT
Alb-cre-Primer 1	GAAGCAGAAGCTTAGGAAGATGG	TTGGCCCCTTACCATAACTG
Alb-cre-Primer 2	GGACAACTTATCCTTATCACAAGGG	TTGGCCCCTTACCATAACTG
koS100A4-LoxP	ACAATGAAGTTGACTTCCAGGAGTA	GCAAACTACACCCCAACACTTC

incubated for 1–3 h. Afterward, the culture medium containing EdU was discarded, and the cells were washed twice with PBS, fixed with 4% paraformaldehyde for 30 min, washed twice with PBS, and treated with a 0.3% Triton 100 solution for 15 min. The cells were stained according to the instructions of the working solution of the EdU kit and incubated for 30 min. After the staining solution was discarded, the cells were rinsed twice with PBS, PBS containing Hoechst 33342 was added, and images were captured using a fluorescence microscope (Ts2R-FL, Nikon, Japan).

2.7 Immunofluorescence and immunohistochemical staining

For immunofluorescence staining, tissue sections were subjected to conventional dewaxing, repaired with citric acid solution, and then washed with tap water to remove citric acid. Subsequently, the sections were blocked with 1% BSA for 30 min, and GnRHR (diluted with 1% BSA; 1:300; 19,950-1-AP; Proteintech, China) primary antibody or S100A4 primary antibody (1:100; sc-377059; Santa Cruz, United States) was added and incubated overnight at 4°C. After the primary antibody was removed by washing the next day, a fluorescent secondary antibody (1:200, AS037, Abclone, China) was applied, and the samples were incubated in the dark for 2 h. After the secondary antibodies were removed, the slides were covered with glycerol containing Hoechst 33342, and images were captured using a fluorescence microscope. For immunohistochemical staining of tissue sections, antigen retrieval solution was used to restore epitope–antibody binding. Endogenous peroxidase activity was blocked via the addition of a 3% hydrogen peroxide solution and incubation in the dark for 30 min at room temperature. Then, the tissue was blocked with 3% BSA for 30 min. The antibody was dissolved in PBS and placed in a humidified box overnight for 4 days. The next day, an HRP-labeled secondary antibody was added to the corresponding mixture, which was incubated at room temperature for 1 h. Subsequently, DAB chromogenic solution was used for color development, followed by hematoxylin counterstaining for 3 min and rinsing with tap water. The slides were dehydrated, mounted, and photographed using a microscope.

2.8 Mass spectrometry and coimmunoprecipitation (Co-IP)

For mass spectrometry, S100A4 (with an HA tag) was first overexpressed in endometrial epithelial cells. After 48 h, the cells were lysed with IP lysis buffer (Beyotime). Then, the cell lysates were incubated with precoated anti-HA primary antibody (CST) and Protein A/G. The cells were incubated for 12 h, followed by six rinses with NP-40 solution. Finally, the solution was discarded, and protein A/G beads were isolated for mass spectrometry analysis. Mass spectrometry-based detection and analysis were conducted by Jin Kairui Biotechnology, Ltd.

For Co-IP, 293 T cells were prepared and simultaneously transfected with the S100A4 and GNAI2 plasmids. After 48 h, the proteins were collected, and a portion of the total protein sample was stored for later use. The same procedures were followed as described above. After the proteins bound to the protein A/G beads were obtained, 50 μL of 1× loading buffer was added. The samples were heated in a 100°C metal bath for 5 min, after which electrophoresis was performed at 100 V constant voltage. A 300 mA constant current was used for 90 min for transfer. The PVDF membrane was blocked with 10% skim milk powder for 30 min, the corresponding primary antibody was added, and the membrane was incubated overnight at 4°C. The cells were rinsed with TBST for 3 × 10 min, incubated with the secondary antibody at room temperature for 2 h, and then rinsed with TBST for 3 × 10 min. Chemiluminescence solution (Bio-Rad, United States) was added, and images were captured.

2.9 Primer sequences and qPCR analysis

Total cellular RNA was extracted as described in (3). The RNA was reverse transcribed into cDNA using a reverse transcription kit (D7168M, Beyotime Biotechnology Co., Ltd.) and analyzed using a qPCR kit (A313-05, Beijing Kangrun Chengye Biotechnology Co., Ltd.). The components included 2 × qPCR Mix (10 μL), 1 μL each of Primer F and Primer R, 0.5 μL of cDNA, and 7.5 μL of H2O. The qPCR program involved denaturation at 94°C for 30 s, annealing at 60°C for 30 s, and replication at 72°C for 30 s; this process was repeated for 40 cycles. The primer sequences are listed in Table 1.

2.10 HE staining

The paraffin sections were dewaxed in water, stained with hematoxylin for 3–5 min, and then rinsed with tap water. The sections were counterstained with a bluing solution and then rinsed with running water. The sections were dehydrated in 85 and 95% gradient alcohol for 5 min each and subsequently immersed in an eosin staining solution for 5 min. Finally, the slices were placed in absolute ethanol solutions I, II, and III for 5 min each. The slides were cleared in xylene twice for 5 min each, sealed with neutral gum, allowed to dry, and imaged.

2.11 Animal breeding and analysis

Transgenic animals were purchased from Saiye Biotech and kept in specific pathogen-free (SPF) animal rooms with a 12 h/12 h dark/light cycle, after which the mice were allowed access to drinking water and food. A Mouse Direct PCR Kit (for genotyping) (B40013, Selleck) was used for mouse genotyping. The sequences of the primers used for genotype identification are shown in Table 1.

2.12 Statistical analysis

Statistical analysis was performed with GraphPad Prism 5 software (GraphPad Software, Inc., CA, United States). All values are expressed as the means ± SDs of three independent experiments. Student's t test and one-way ANOVA were used to evaluate the significance of differences; $p < 0.05$ was considered to indicate statistical significance (28).

3 Results

3.1 S100A4 expression in the sheep endometria decreased in response to GnRH treatment before insemination

We treated sheep with GnRH before insemination, but no satisfactory results were achieved. To investigate the reasons underlying embryo implantation failure in sheep treated with GnRH before insemination and explore the effects of GnRH on the endometrium, we divided the sheep into two groups: one group received 17 μg A3 (GnRH) before insemination, while the other group received 1 mL of sterile physiological saline solution as a control. Five days after insemination, we collected uterine tissue, scraped the endometrial tissue, and performed transcriptome sequencing. Analysis of the differentially expressed genes (DEGs) between samples from the control and treated sheep revealed substantial differences in the expression of S100A4 between the two groups of sheep (Figure 1A). S100A4 is known to regulate cell proliferation. Kyoto Encyclopedia of Genes and Genomes (KEGG) enrichment analysis revealed that GnRH affected the enrichment of cell proliferation-related signaling pathways, such as "growth" and "cell proliferation" (Figure 1B). We initially performed immunofluorescence analysis to assess the expression of the GnRH receptor protein (GnRHR) in the endometrium. The results revealed robust expression of the GnRH receptor protein in the endometrium, as indicated by green fluorescence (Figure 1C). To investigate the localization of the S100A4 protein in the sheep endometrium, we performed immunofluorescence staining. We found that S100A4 was expressed in the endometrium in a pattern similar to that of GnRHR (Figure 1C). These findings suggest that S100A4 may play a role in the effects of GnRH treatment on the endometrium, although the specific mechanism involved remains unclear.

3.2 S100A4 promotes sheep endometrial cell proliferation

To assess the effect of S100A4 expression on the sheep endometrium, we isolated endometrial epithelial cells and synthesized an siRNA targeting sheep S100A4 and a eukaryotic expression vector to overexpress sheep S100A4.

S100A4 was overexpressed in sheep cells, and one group of these cells was transfected with siRNA targeting S100A4 (siS100A4); then, the expression of HA-S100A4 was assessed through immunofluorescence. The results indicated that the anti-HA antibody could be used to identify HA-positive S100A4-overexpressing cells, and the fluorescence ratio decreased in the siS100A4-transfected group (Figure 2A). These findings suggested that both overexpression and knockdown of S100A4 can be achieved in endometrial epithelial cells.

Subsequently, we introduced siRNA into the cells, with the NC group serving as the control group. We then used a CCK-8 assay to assess changes in cell viability. The results revealed decreased cell viability after S100A4 knockdown (Figure 2B). Conversely, the S100A4-overexpressing group had a greater percentage of viable cells than did the empty vector group (Figure 2B).

To assess cell proliferation, we labeled endometrial epithelial cells with EdU for 2 h. A significantly greater proportion of cells with red fluorescence was found in the S100A4-overexpressing group than in the control group (Figures 2C,D). Conversely, the proportion of cells with red fluorescence decreased among the cells with S100A4 knockdown (Figures 2E,F). These findings suggest that S100A4 can indeed promote the proliferation of endometrial cells.

3.3 S100A4 knockdown affects cell proliferation-related signaling pathways in endometrial epithelial cells

To elucidate the mechanism by which S100A4 regulates endometrial cell proliferation, we conducted transcriptome sequencing on the NC and S100A4 knockdown groups. The volcano plot results showed that after S100A4 was knocked down, several genes, including S100A4 itself, were downregulated (Figure 3A). GO cluster analysis of these genes revealed that many of the DEGs were enriched in gene sets related to the regulation of "growth" and "cell proliferation" (Figure 3B). Furthermore, KEGG pathway enrichment analysis revealed that 52 of the DEGs were enriched in the MAPK signaling pathway (Figure 3C). These findings suggest that S100A4 may regulate cell proliferation through the MAPK signaling pathway.

To assess the effect of the MAPK signaling pathway on endometrial epithelial cell proliferation, we treated cells with the MAPK inhibitor U0126, which targets the key node protein ERK1/2. Endometrial epithelial cells were treated with various concentrations of the inhibitor for 12 h, followed by EdU labeling. Fluorescence staining revealed a significant reduction in the percentage of EdU-positive endometrial epithelial cells after MAPK pathway inhibition (Figures 3D,E), indicating that the MAPK signaling pathway indeed regulates the proliferation of these cells.

To determine whether S100A4 regulates cell proliferation via the MAPK signaling pathway, we added U0126 to cells overexpressing S100A4. EdU staining showed that, compared to that in the DMSO solvent group, the percentage of EdU-positive cells was significantly lower in the U0126 (50 nM) treatment group (Figures 3F,G). C-Jun and c-Fos are downstream target molecules of the MAPK signaling pathway and are known to be involved in regulating cell proliferation. qPCR analysis demonstrated that both the overexpression (Figure 3H) and knockdown (Figure 3I) of S100A4 affected the expression of C-Jun and c-Fos, and the expression of S100A4 was positively correlated with the expression of these two genes. These findings suggest that S100A4 may modulate sheep endometrial cell proliferation by regulating MAPK.

3.4 S100A4 promotes cell proliferation by interacting with the GNAI2 protein

To determine how S100A4 regulates cell proliferation, we employed mass spectrometry to identify proteins that interact with S100A4. First, we overexpressed S100A4, and after 48 h, the cells were lysed, and the total cellular protein was collected. Protein A/G beads coated with the HA tag antibody were then incubated with the harvested protein to allow binding to the S100A4-HA protein. After the samples were rinsed, we identified the proteins

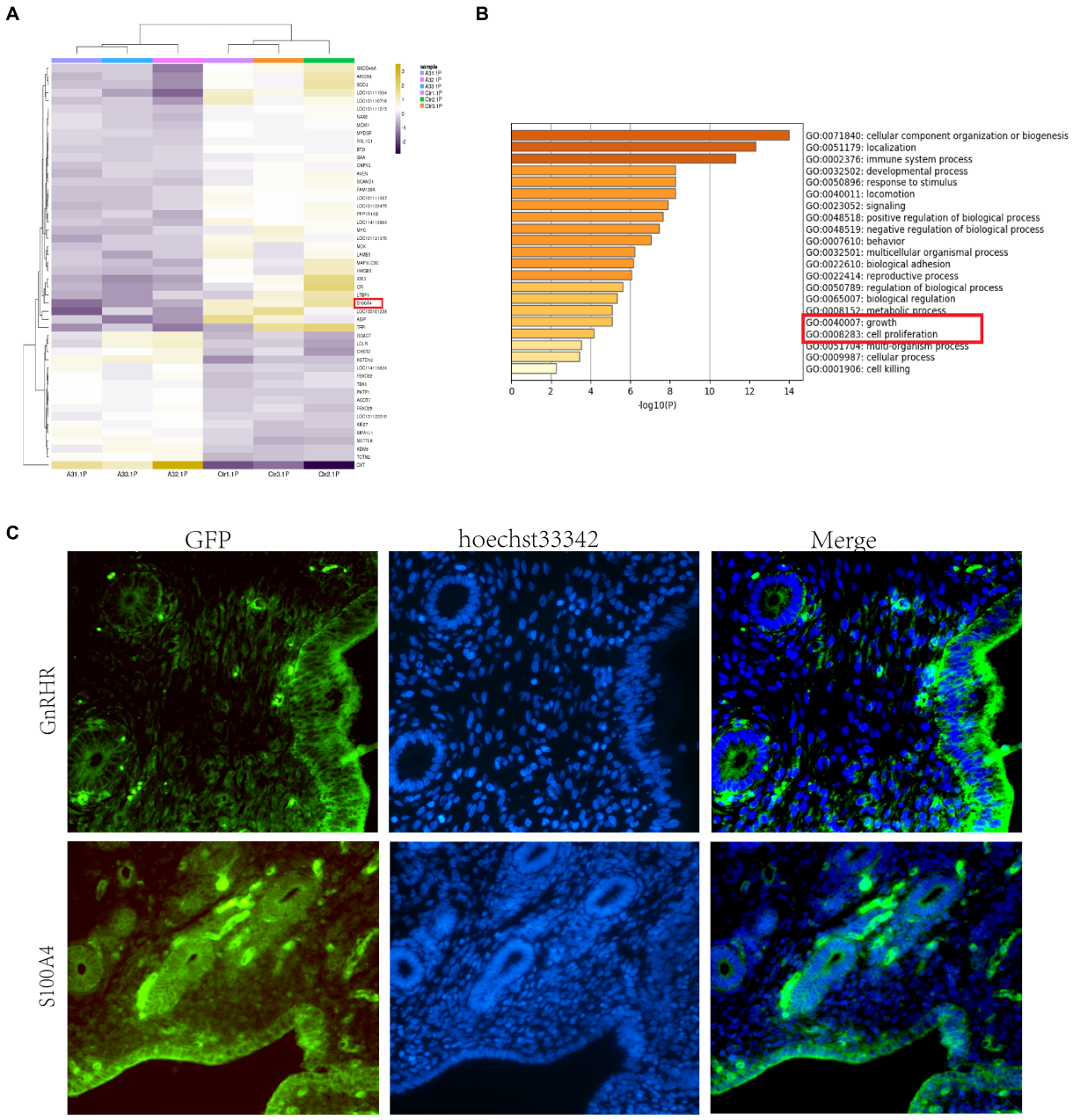

FIGURE 1
GnRH reduces the expression of S100A4 in the sheep endometrium. **(A)** Heatmap showing significant variation in the expression level of S100A4. **(B)** Transcriptome sequencing and GO analysis revealed that GnRH affects cell proliferation-related signaling pathways, such as "growth" and "cell proliferation," in treated sheep. **(C)** Expression of GnRHR and S100A4 in the sheep endometrium; the results show that the localization patterns of S100A4 and GnRHR are similar.

on the resin using mass spectrometry. The results revealed 35 proteins that specifically interact with S100A4 between the overexpression group and the empty vector group (Figure 4A, Supplementary Table S1). Cluster analysis of these proteins revealed that multiple differentially expressed proteins were involved in multiple physiological processes (Figure 4B) and enriched in the "cell growth and death" signaling pathway (Figure 4C), suggesting that interacting proteins downstream of S100A4 may play a role in regulating cell proliferation. We screened proteins that potentially regulate cell proliferation from a set of 35 S100A4-specific enriched proteins. Among them, GNAI2 has been reported to regulate cell proliferation. Therefore, we selected GNAI2 as a target for studying its role in regulating cell proliferation.

To further confirm the interaction between GNAI2 and S100A4, we cotransfected plasmids overexpressing S100A4 and GNAI2 into 293 T cells, with a control group with single plasmid transfection. We collected the protein 48 h after transfection, incubated most of the protein sample with Protein-A/G beads precoated with HA antibody, and used a rinse solution to remove unbound protein. Western blot analysis confirmed the presence of Flag-GNAI2 in the group cotransfected with GNAI2 and S100A4 constructs but not in the other

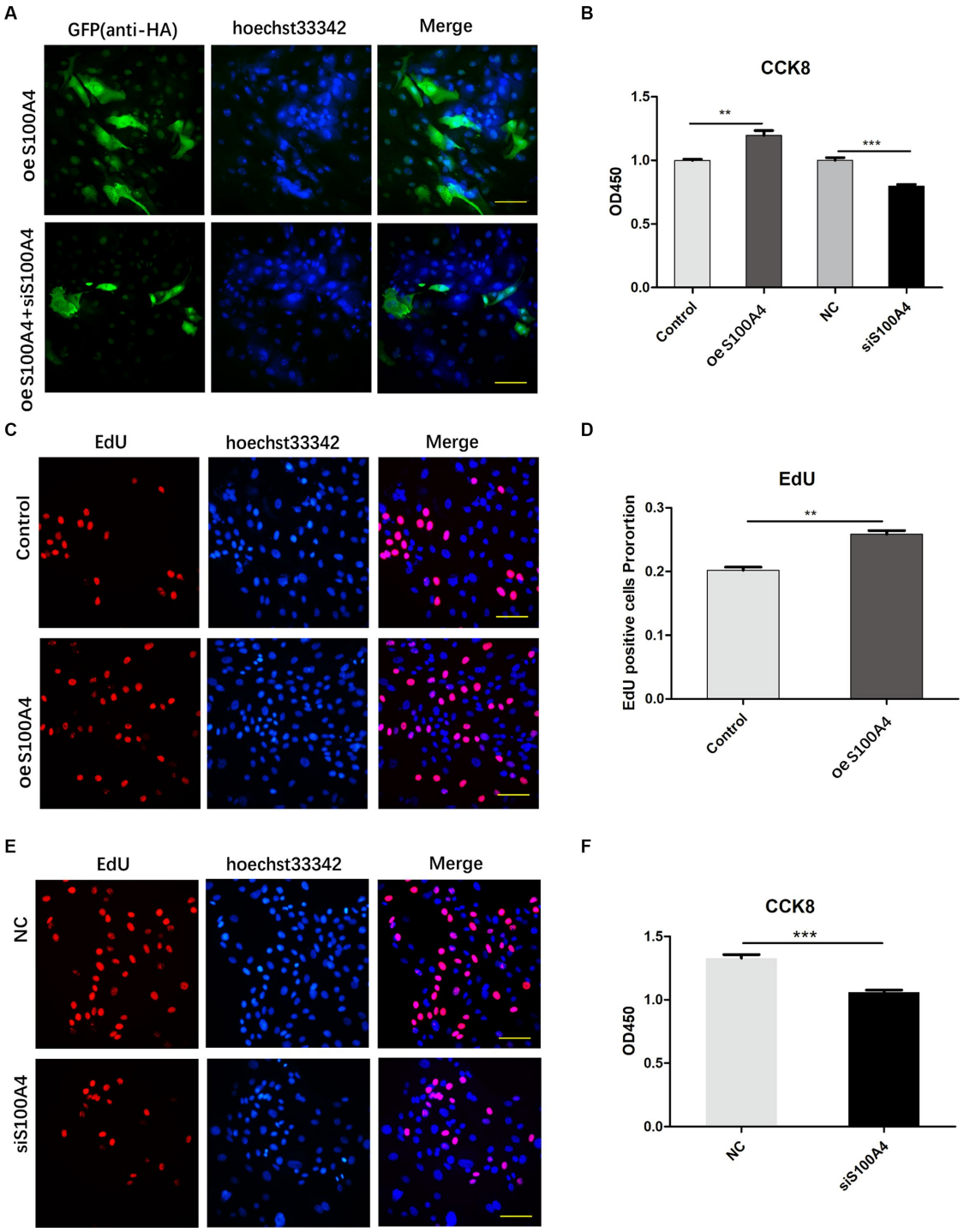

FIGURE 2
S100A4 overexpression promotes endometrial cell proliferation. **(A)** Confirmation of S100A4 overexpression and knockdown in endometrial epithelial cells through immunofluorescence. **(B)** CCK-8 analysis of the effects of S100A4 knockdown and overexpression on cell metabolism. **(C,D)** EdU staining-based determination of the effects of S100A4 overexpression on the proliferation of endometrial epithelial cells. **(E,F)** EdU staining-based determination of the effects of S100A4 knockdown on the proliferation of endometrial epithelial cells.

groups (Figure 4D), confirming the interaction between GNAI2 and S100A4.

We then cotransfected the lentiviral vector and viral packaging plasmid into 293 T cells to generate the lentivirus (Figure 4E). The cell supernatant containing the lentivirus was collected, and after endometrial epithelial cells were infected, we observed green fluorescence under a fluorescence microscope 48 h later (Figure 4F). EdU results further demonstrated an increase in cell proliferation after GNAI2 overexpression (Figures 4G,H). To further determine the effect of GNAI2 on cell proliferation, we synthesized a siRNA targeting GNAI2 and transfected the siRNA into endometrial epithelial cells for 24 h. EdU staining also revealed that cell proliferation was suppressed

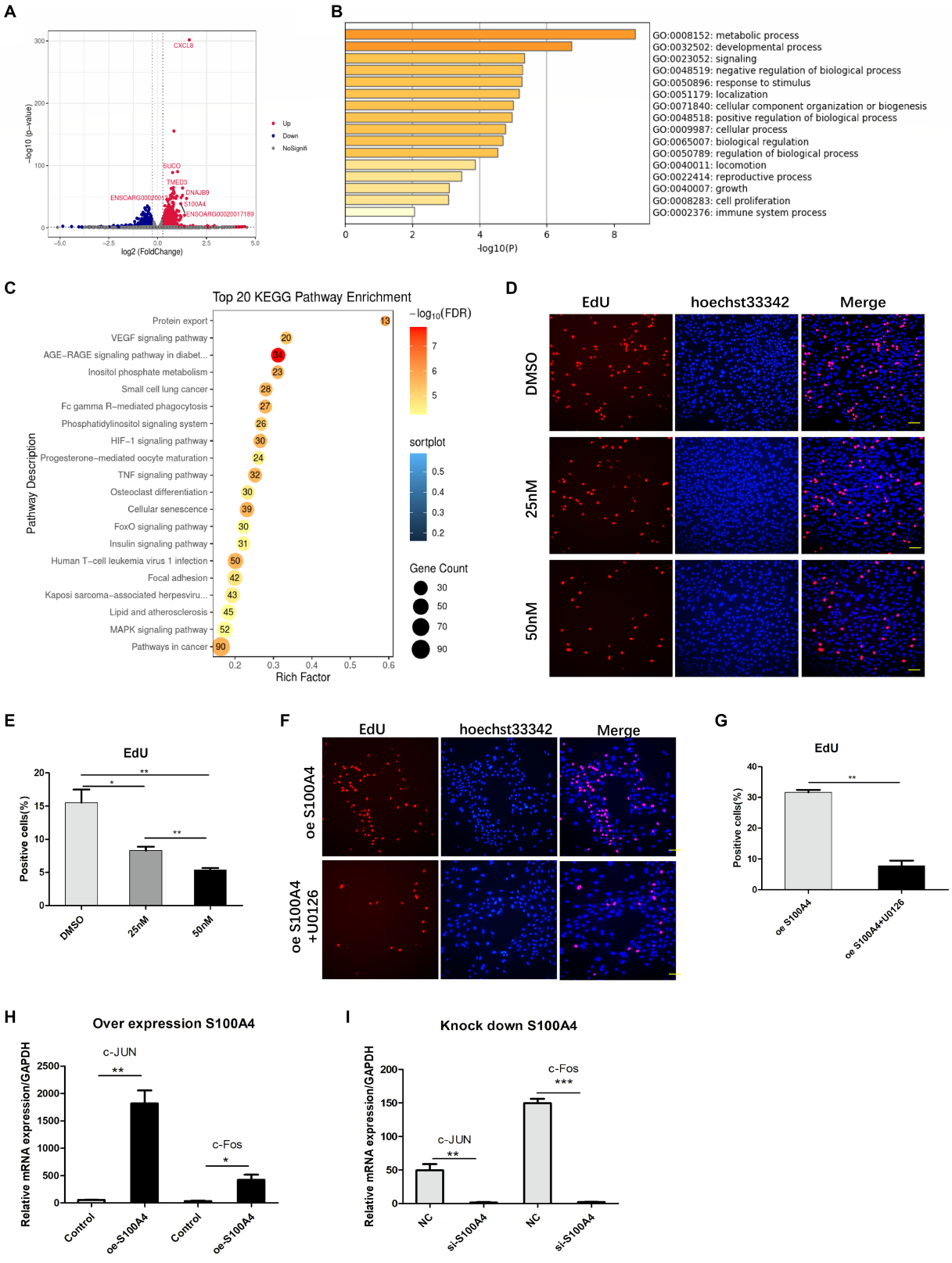

FIGURE 3
S100A4 regulates cell proliferation through the MAPK signaling pathway. **(A)** Volcano plot illustrating the impact of S100A4 knockdown on gene transcription in endometrial epithelial cells. **(B)** GO analysis indicating the effect of S100A4 knockdown on the expression of genes related to "growth" and "cell proliferation" in endometrial epithelial cells. **(C)** KEGG enrichment analysis revealing the enrichment of genes associated with the MAPK signaling pathway following S100A4 knockdown. **(D,E)** EdU staining-based analysis of endometrial epithelial cell proliferation after treatment with the MAPK inhibitor U0126. **(F,G)** EdU staining-based analysis of the effect of blocking the MAPK signaling pathway on cell proliferation after S100A4 overexpression. **(H)** qPCR analysis of the expression of the MAPK signaling pathway downstream genes C-Jun and c-Fos following S100A4 overexpression. **(I)** qPCR analysis of the expression of the MAPK signaling pathway downstream genes C-Jun and c-Fos following S100A4 knockdown.

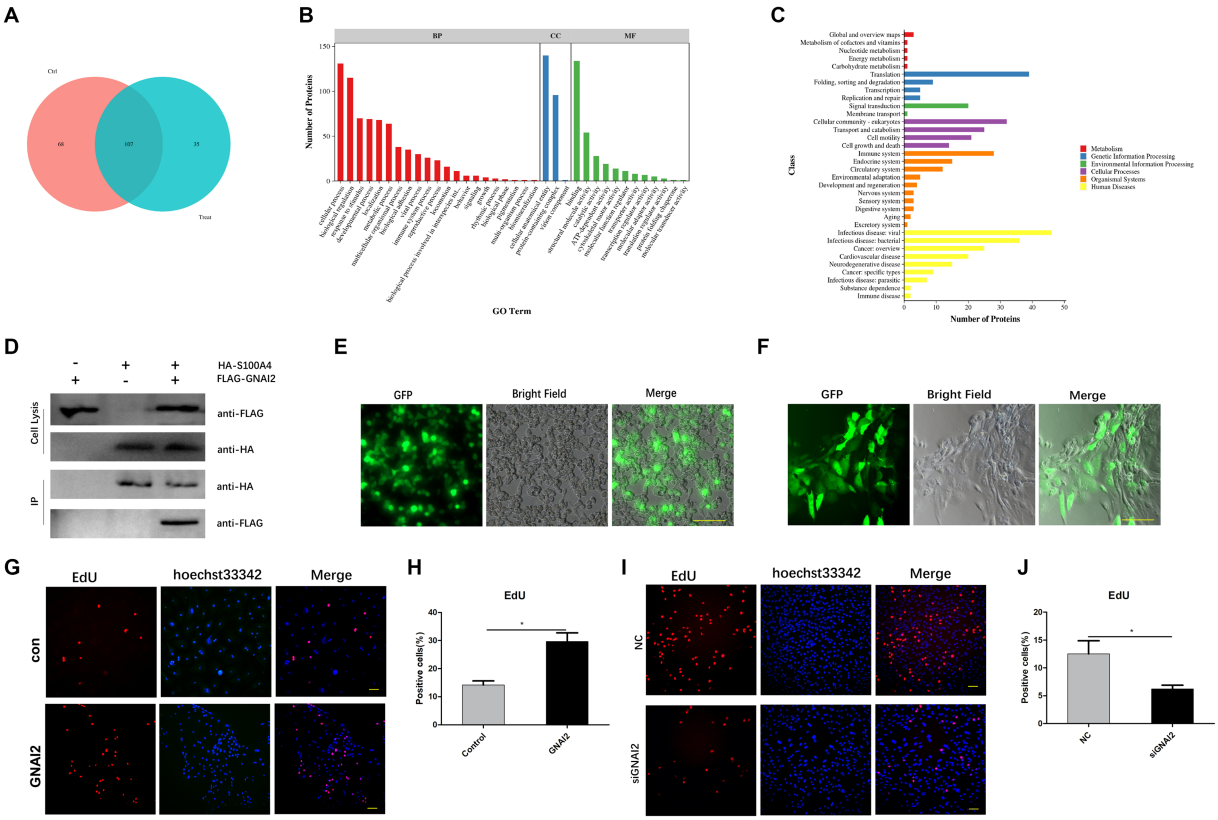

FIGURE 4
GNAI2 and S100A4 interact and promote cell proliferation. **(A)** Mass spectrometry was used to screen proteins that interact with S100A4. **(B)** GO analysis of proteins that interact with S100A4. **(C)** KEGG cluster analysis of proteins that interact with S100A4. **(D)** Co-IP analysis to verify the interaction between S100A4 and GNAI2. **(E)** Packaging of lentivirus overexpressing GNAI2. **(F)** Lentivirus transduction of GNAI2 into endometrial epithelial cells. **(G,H)** Proportion of EdU-positive cells in the GNAI2 overexpression group. **(I,J)** EdU staining-based analysis of the effect of GNAI2 knockdown on cell proliferation.

after GNAI2 was knocked down (Figures 4I,J). The above results suggest that GNAI2 can promote the proliferation of endometrial epithelial cells.

3.5 GNAI2 regulates the MAPK signaling pathway and interacts with S100A4 to promote cell proliferation

Given the interaction of GNAI2 with S100A4 and its ability to promote cell proliferation, we investigated whether GNAI2 regulates cell proliferation through a mechanism similar to that of S100A4. We conducted transcriptome sequencing to elucidate the mechanism through which GNAI2 promotes sheep endometrial cell proliferation. We established two groups of endometrial epithelial cells, the empty vector group and the GNAI2 overexpression group, each with three replicates. The results from the volcano plot revealed 1980 differentially expressed genes upon transcriptome sequencing. Among them, 1961 genes were upregulated, and 19 were downregulated following GNAI2 overexpression (Figure 5A). To assess the regulatory effect of S100A4 on GNAI2, we examined the expression level of GNAI2 after S100A4 overexpression using qPCR. The results indicated that overexpression of S100A4 significantly increased the transcription level of GNAI2 (Figure 5B). Cluster analysis of these DEGs revealed enrichment in the "MAPK signaling pathway" and "cell cycle" signaling pathways (Figure 5C), consistent with the findings of transcriptome sequencing analysis after S100A4 knockdown. Furthermore, to clarify whether GNAI2 is involved in the S100A4-mediated regulation of cell proliferation, we knocked down GNAI2 in the cells overexpressing S100A4 and performed EdU staining. The results revealed a notable reduction in the cell proliferation rate (Figures 5D,E). Moreover, to confirm whether GNAI2 regulates sheep endometrial cell proliferation through the MAPK signaling pathway, we treated the cells overexpressing GNAI2 with the MAPK inhibitor U0126 and conducted EdU staining. The results showed that the cell proliferation rate was significantly lower in the treated group than in the control group (Figures 5F,G). These findings suggest that GNAI2 might be a downstream factor in the S100A4-mediated regulation of endometrial epithelial cell proliferation via the MAPK signaling pathway.

3.6 Animal experiments verified the downstream regulation of cell proliferation by S100A4

We employed a crossbreeding approach in which the Pr-Cre enzyme–expressing mice were mated with the conditional S100A4 knockout mice to generate mice with uterine-specific S100A4

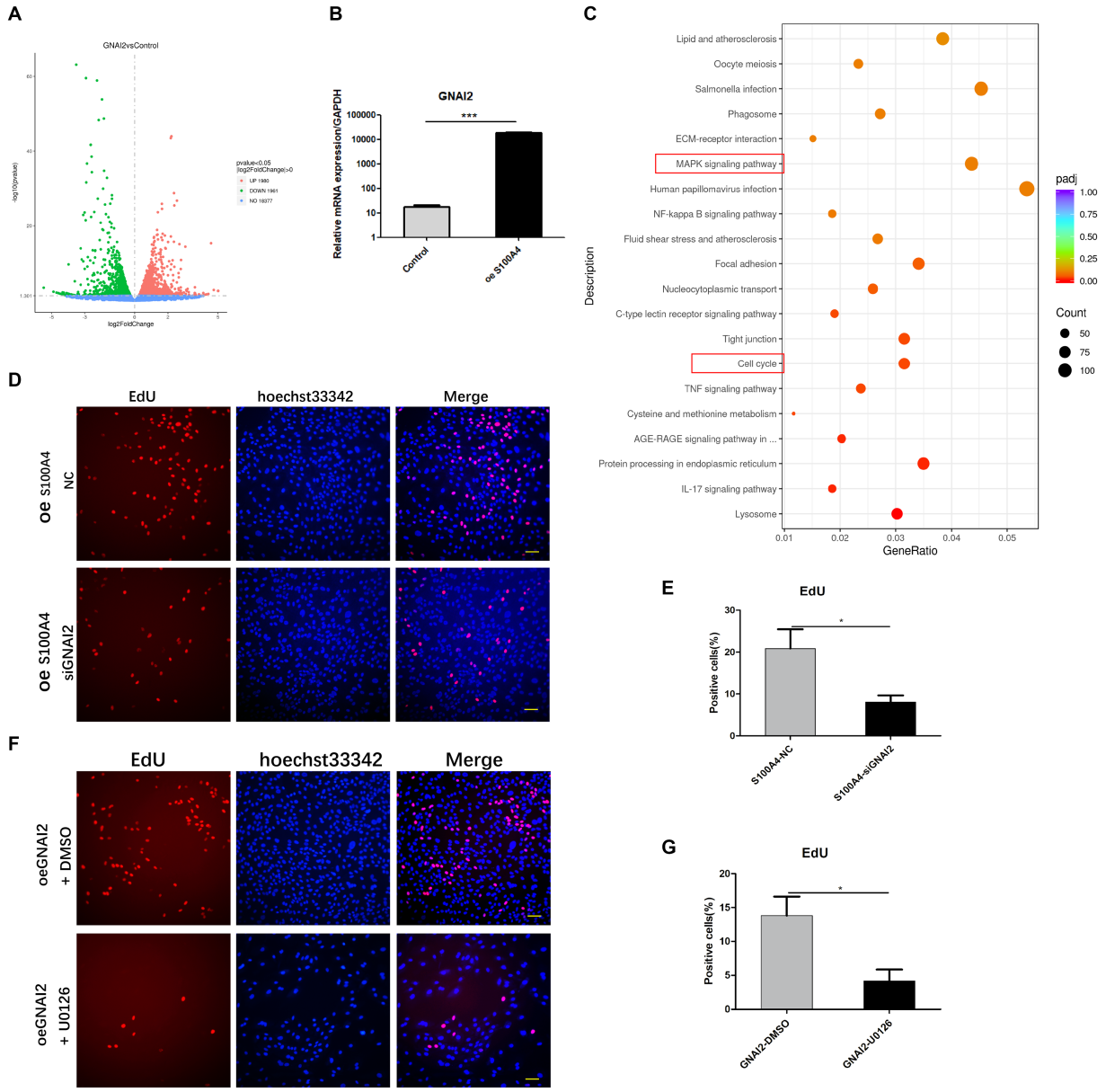

FIGURE 5
GNAI2 mediates the effects of S100A4 on the promotion of cell proliferation through the MAPK signaling pathway. **(A)** Volcano plot illustrating the transcriptome sequencing results following GNAI2 overexpression. **(B)** qPCR analysis of GNAI2 expression after S100A4 overexpression. **(C)** Cluster analysis of KEGG signaling pathways revealing enrichment of the "MAPK signaling pathway" and "cell cycle" signaling pathways. **(D,E)** EdU staining-based detection of the effect of GNAI2 knockdown on cell proliferation after S100A4 overexpression. **(F,G)** EdU staining-based analysis of the effect of blocking the MAPK signaling pathway on cell proliferation after GNAI2 overexpression.

deletion. Comparative analysis of the control mice and the mice with uterine-specific S100A4 deletion revealed no significant differences in the main organs. However, several differences in endometrial cell morphology and structure were observed (Figure 6A). In a comparison of the mice with uterine S100A4 deletion to heterozygous mice, one out of ten homozygous mice experienced sudden death before pregnancy but exhibited no other discernible abnormalities (surprisingly, death occurred only when homozygous mice were obtained by crossing heterozygous mice). However, during later rearing and breeding, no abnormal deaths occurred in the offspring of the homozygous mice. The reason is unclear). Another homozygous mouse died unexpectedly after two generations of reproduction, also without typical symptoms. The survival curve is shown in Figure 6B; these results suggest that uterine-specific S100A4 knockout can have systemic effects.

Regarding reproduction, we observed delayed implantation in the mice with uterine-specific deletion of S100A4, but there was no significant difference in the number of offspring per litter (Figure 6C). Preliminary sequencing results indicated that both S100A4 and GNAI2 can regulate downstream MAPK signaling pathways. The key protein node in the MAPK signaling pathway, ERK1/2, becomes phosphorylated (p-ERK1/2) upon pathway activation. Immunohistochemistry was used to determine the expression level of p-ERK1/2. The results demonstrated significantly lower p-ERK1/2 expression in the endometrium of the S100A4 knockout mice than in the endometrium of the control mice (Figure 6D).

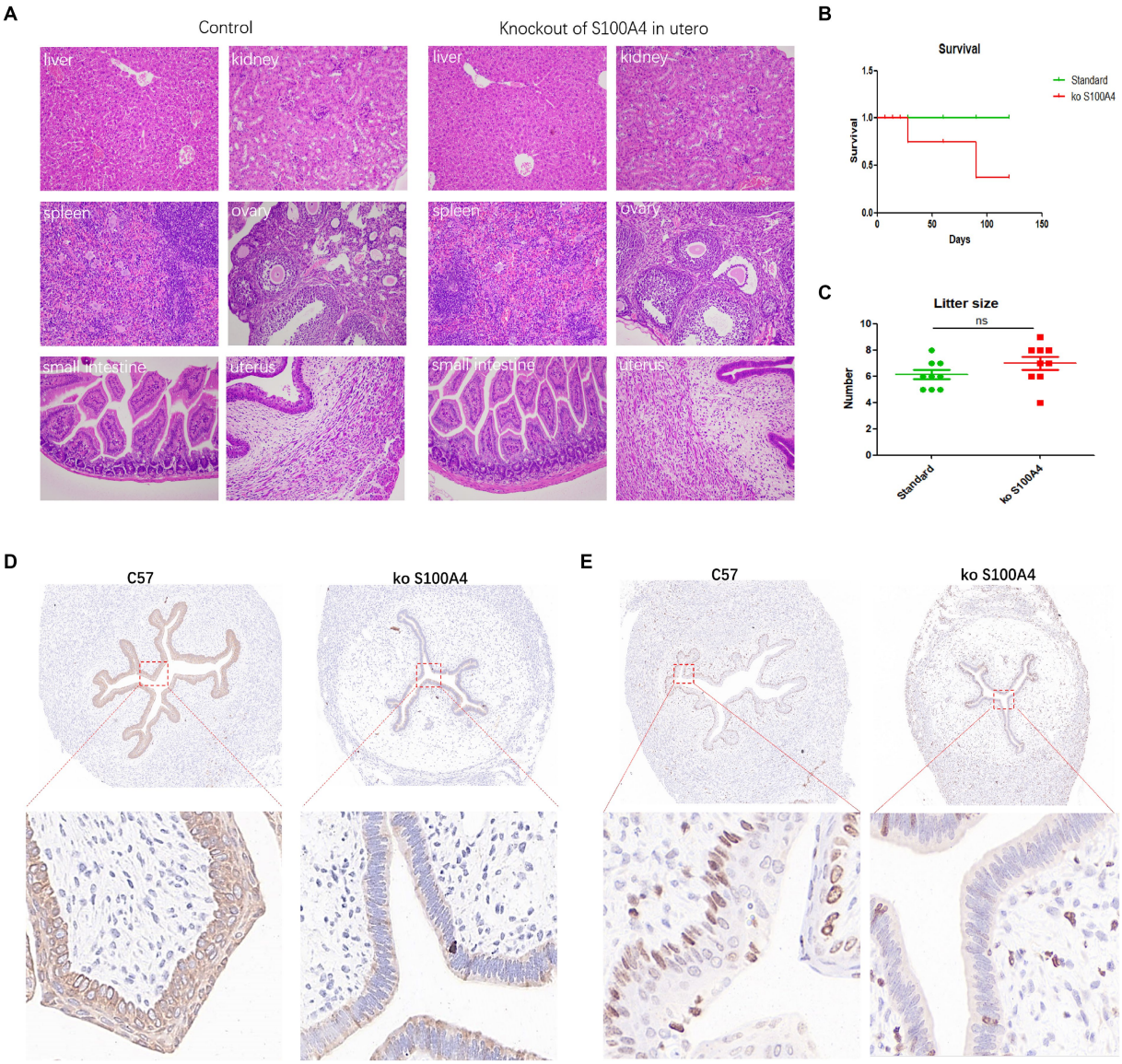

FIGURE 6
Animal experiments confirming the inhibition of endometrial cell proliferation by S100A4 knockout. **(A)** HE staining results of major organs in the control mice and uterine-specific S100A4 knockout mice. **(B)** Survival curve depicting the impact of S100A4 knockout. **(C)** Statistical analysis of the reproductive parameters. **(D)** Immunohistochemical analysis of p-ERK1/2 expression in the endometrium. **(E)** Immunohistochemical analysis of Ki67 expression in the endometrium.

To elucidate the impact of S100A4 on endometrial cell proliferation, we employed immunohistochemistry to assess Ki67 expression. The findings revealed a lower number of Ki67-positive cells in the S100A4 knockout group than in the control group (Figure 6E). These findings suggested that S100A4 knockout may inhibit endometrial cell proliferation by suppressing the MAPK signaling pathway.

4 Discussion

During embryo transfer, superovulation is often an important factor in regulating reproduction. The most commonly used superovulatory hormone in sheep is FSH (29, 30). The combined use of FSH and eCG can result in increased superovulation (31). GnRH is also widely used for superovulation, and experiments have shown that the combination of GnRH and other hormones has a good effect on superovulation (32). These results suggest that GnRH is effective in promoting superovulation in sheep. However, for embryo transfer in clinical practice, embryo implantation is another factor that affects reproduction. GnRH agonists and inhibitors are widely used in embryo implantation. For example, if a woman who has experienced embryo implantation failure undergoes human embryo transfer, pretreatment with GnRH agonists will increase the live birth rate. However, if women have not experienced embryo implantation failure, pretreatment with GnRH agonists does not increase the live birth rate (33). Similar results were found in patients with uterine fibroids, in which pretreatment with GnRH agonists before embryo transfer increased the live birth rate (34).

Conversely, if GnRH antagonists are used, only high doses will have adverse effects on embryo transfer (35). The effect on embryo implantation, especially at low concentrations, has not been proven. These results suggest that many unknown factors are involved in targeting GnRH to regulate embryo transfer.

In livestock, GnRH also plays a wide range of regulatory roles (36), but some factors are unknown. Five studies analyzed the use of a GnRH agonist versus a control. No significant benefit was demonstrated when GnRH agonists were used (37). Interestingly, these programs did not affect the time interval between calving and conception in dairy cows (38). Beckett and Lean reported that GnRH administration before 40 days after delivery may shorten the time to first estrus but was not associated with the final reproductive performance of the cow (39). A review described the current research on GnRH function in sheep reproduction and indicated that GnRH plays a role in many aspects of reproduction (36). However, there are no direct reports on whether GnRH can regulate embryo implantation or its mechanism. We previously found that treatment with GnRH did not increase the implantation rate of sheep after embryo transfer, but the underlying mechanism is still unclear. We studied the regulatory mechanism involved in endometrial cell proliferation to clarify whether GnRH facilitates sheep embryo transfer. Our results showed that GnRH may inhibit the expression of S100A4 in the endometrium; therefore, GnRH cannot be used during embryo transfer. Endometrial proliferation may also explain why the embryo implantation rate did not increase.

S100A4 has been shown to play an important regulatory role in various diseases and disease models, and its mechanisms of action are relatively diverse. Single-cell sequencing of human tissues revealed that S100A4 is a regulator of immunosuppressive T cells (40). Experiments in mice revealed that the S100A4-mediated increase in mitochondrial metabolism results in a decrease in acetyl-CoA levels, which impairs the transcription of effector genes, especially IFN-γ, facilitating cell survival, tolerance, and memory potential (41). Targeted blockade of S100A4 with an antibody suppressed epithelial-to-mesenchymal transition in asthmatic mice (42). Overexpression of S100A4 also inhibited endoplasmic reticulum stress and ameliorate ischemia–reperfusion injury (43). These findings suggest that S100A4 functions via multiple mechanisms.

The role of S100A4 in regulating proliferation may be most relevant for regulating endometrial receptivity after hormone treatment. Therefore, we performed experiments and found that S100A4 can promote the proliferation of endometrial epithelial cells. In a previous study, S100A4 protein was overexpressed in cultured cancer cells; the results showed that S100A4 protein overexpression did not significantly affect the proliferation of MCF-7 cells but inhibited the proliferation of MDA-MB-231 cells (44). Similarly, S100A4 was found to regulate cell migration but not cell proliferation in gastric adenocarcinoma (20). However, when S100A4 targets leukemia cells, it also promotes cell proliferation (45). In experiments on PC3 prostate cancer cells, intracellular S100A4 expression was found to be positively correlated with cell proliferation, revealing that S100A4 promotes cancer cell proliferation (46). The effect of S100A4 on cell proliferation may be affected by the cell type and the localization of S100A4.

We sequenced the transcriptome of endometrial epithelial cells with S100A4 knockdown, and subsequent Gene Ontology (GO) enrichment analysis of the DEGs revealed that S100A4 plays a role in cell proliferation-related mechanisms. KEGG enrichment analysis revealed enrichment of the MAPK signaling pathway. This pathway is important for regulating the proliferation of various cell types (47, 48). MAPK activation can promote cell proliferation. Sheep basic fibroblast growth factor (bFGF), epidermal growth factor (EGF), and vascular endothelial growth factor (VEGF) can quickly activate the MAPK signaling pathway to regulate cell proliferation (49). Several biologically active substances, such as osteocalcin (50), progesterone and FSH (51), and thyroid hormone (52), can target the MAPK signaling pathway to regulate cell proliferation. Similarly, GnRH can also regulate the MAPK signaling pathway to regulate cell proliferation (53). These findings suggested that S100A4 may regulate the proliferation of endometrial epithelial cells by activating the MAPK signaling pathway.

GNAI2, which belongs to the G protein family, is one of the key genes involved in melanogenesis (54). Studies have shown that GNAI2 can promote cell proliferation (54, 55). However, no studies have shown whether GNAI2 can promote cell proliferation, and its mechanism of action in endometrial cells is unclear. In our experiments, we found that S100A4 can interact with GNAI2 and that GNAI2 can promote endometrial cell proliferation, which expands the known list of targets of S100A4.

Various cells can secrete the S100A4 protein (56–58); this finding may also explain why mice can still reproduce normally after S100A4 is knocked out of the uterus. However, in the case of uterine-specific S100A4 knockout, some events require special consideration, such as the sudden death of mice, but the explanation is unclear. In addition, the proliferation of endometrial cells was significantly inhibited, and the expression of p-ERK1/2 was significantly reduced in the mice with uterine-specific S100A4 knockout. This result is similar to the results of previous cell experiments. We speculated that in animals, S100A4 can target the MAPK-ERK1/2 signaling pathway to regulate endometrial cell proliferation.

5 Conclusion

While GnRH is widely utilized in animal reproduction, particularly in practical operations such as embryo transfer to promote animal quality, our previous investigations have not conclusively demonstrated its efficacy in promoting embryo implantation. Furthermore, the underlying mechanism of action remains unclear. During our research, we discovered that the application of GnRH may actually impede the proliferation of endometrial cells through the S100A4-GNAI2-MAPK signaling pathway, which has adverse effects on embryo implantation. Our findings elucidated a previously unrecognized aspect of the mechanism by which GnRH regulates endometrial cell proliferation. These findings can potentially offer valuable guidance for optimizing hormone treatment in the context of animal reproduction.

Data availability statement

The original contributions presented in the study are publicly available. These data can be found in the NCBI BioProject repository: (1) https://www.ncbi.nlm.nih.gov/bioproject/PRJNA1090558. (2) https://www.ncbi.nlm.nih.gov/bioproject/PRJNA1090239.

Ethics statement

The animal studies were approved by the Ethical Committee of Xinxiang Medical University. The studies were conducted in accordance with the local legislation and institutional requirements. Written informed consent was obtained from the owners for the participation of their animals in this study.

Author contributions

XJ: Conceptualization, Data curation, Formal analysis, Investigation, Methodology, Software, Validation, Writing – original draft, Writing – review & editing. ZC: Conceptualization, Funding acquisition, Supervision, Visualization, Writing – original draft. ML: Data curation, Methodology, Writing – original draft. JW: Data curation, Methodology, Writing – original draft. ZR: Data curation, Methodology, Writing – original draft. LW: Data curation, Methodology, Writing – original draft. CL: Data curation, Methodology, Writing – original draft. XL: Writing – review & editing. FR: Funding acquisition, Writing – review & editing. XW: Conceptualization, Funding acquisition, Project administration, Resources, Supervision, Writing – review & editing.

Funding

The author(s) declare financial support was received for the research, authorship, and/or publication of this article. This work was supported by the Talents Special Fund of Hebei Agricultural University (Grant number: YJ201952), the Natural Science Foundation of Hebei Province (Grant number: C2021204039), the National Natural Science Foundation of China (Grant number: 82303770), and Key R&D Projects in Henan Province (project number: 231111311300).

Conflict of interest

The authors declare that the research was conducted in the absence of any commercial or financial relationships that could be construed as a potential conflict of interest.

Publisher's note

All claims expressed in this article are solely those of the authors and do not necessarily represent those of their affiliated organizations, or those of the publisher, the editors and the reviewers. Any product that may be evaluated in this article, or claim that may be made by its manufacturer, is not guaranteed or endorsed by the publisher.

Supplementary material

The Supplementary material for this article can be found online at: https://www.frontiersin.org/articles/10.3389/fvets.2024.1410371/full#supplementary-material

References

1. Wu H-M, Huang H-Y, Lee C-L, Soong Y-K, Leung PC, Wang HS. Gonadotropin-releasing hormone type II (GnRH-II) agonist regulates the motility of human decidual endometrial stromal cells: possible effect on embryo implantation and pregnancy *Biol Reprod.* (2015) 92:98. doi: 10.1095/biolreprod.114.127324

2. Maggi R, Cariboni AM, Marelli MM, Moretti RM, Andre V, Marzagalli M, et al. GnRH and GnRH receptors in the pathophysiology of the human female reproductive system *Hum Reprod Update*. (2016) 22:358–81. doi: 10.1093/humupd/dmv059

3. Li Z, Guo R, Gu Z, Wang X, Wang Y, Xu H, et al. Identification of a promoter element mediating kisspeptin-induced increases in GnRH gene expression in sheep *Gene*. (2019) 699:1–7. doi: 10.1016/j.gene.2019.03.006

4. Wu H-M, Chang H-M, Leung PC. Gonadotropin-releasing hormone analogs: mechanisms of action and clinical applications in female reproduction *Front Neuroendocrinol.* (2021) 60:100876. doi: 10.1016/j.yfrne.2020.100876

5. Abbara A, Jayasena CN, Christopoulos G, Narayanaswamy S, Izzi-Engbeaya C, Nijher GM, et al. Efficacy of kisspeptin-54 to trigger oocyte maturation in women at high risk of ovarian hyperstimulation syndrome (OHSS) during in vitro fertilization (IVF) therapy *J Clin Endocrinol Metab*. (2015) 100:3322–31. doi: 10.1210/jc.2015-2332

6. Park S-R, Cho A, Park ST, Park CH, Lim S, Jin M, et al. Double-edged sword of gonadotropin-releasing hormone (GnRH): A novel role of GnRH in the multiple beneficial functions of endometrial stem cells *Cell Death Dis.* (2018) 9:828. doi: 10.1038/s41419-018-0892-3

7. Chen Q, Yu F, Li Y, Zhang AJ, Zhu XB. Comparative proteomics reveal negative effects of gonadotropin-releasing hormone agonist and antagonist on human endometrium *Drug Des Devel Ther.* (2019) 13:1855–63. doi: 10.2147/DDDT.S201871

8. Chegini N, Rong H, Dou Q, Kipersztok S, Williams RS. Gonadotropin-releasing hormone (GnRH) and GnRH receptor gene expression in human myometrium and leiomyomata and the direct action of GnRH analogs on myometrial smooth muscle cells and interaction with ovarian steroids in vitro *J Clin Endocrinol Metab.* (1996) 81:3215–21. doi: 10.1210/jcem.81.9.8784072

9. Knox RV, Willenburg K, Rodriguez-Zas SL, Greger D, Hafs H, Swanson MJT. Synchronization of ovulation and fertility in weaned sows treated with intravaginal triptorelin is influenced by timing of administration and follicle size *Theriogenology*. (2011) 75:308–19. doi: 10.1016/j.theriogenology.2010.09.001

10. Lopes TP, Padilla L, Bolarin A, Rodriguez-Martinez H, Roca JJA. Weaned sows with small ovarian follicles respond poorly to the GnRH agonist buserelin *Animals*. (2020) 10:1979. doi: 10.3390/ANI10111979

11. Knox R, Stewart K, Flowers W, Swanson M, Webel S, Kraeling RJT. Design and biological effects of a vaginally administered gel containing the GnRH agonist, triptorelin, for synchronizing ovulation in swine *Theriogenology*. (2018) 112:44–52. doi: 10.1016/j.theriogenology.2017.08.021

12. Pursley J, Wiltbank M, Stevenson J, Ottobre J, Garverick H, Anderson LJ. Pregnancy rates per artificial insemination for cows and heifers inseminated at a synchronized ovulation or synchronized estrus *J Dairy Sci*. (1997) 80:295–300. doi: 10.3168/jds.S0022-0302(97)75937-X

13. Martinez M, Kastelic J, Adams G, Mapletoft RJ. The use of GnRH or estradiol to facilitate fixed-time insemination in an MGA-based synchronization regimen in beef cattle *Anim Reprod Sci.* (2001) 67:221–9. doi: 10.1016/S0378-4320(01)00128-2

14. Loi P, Ptak G, Dattena M, Ledda S, Naitana S, Cappai PJRND. Embryo transfer and related technologies in sheep reproduction *Reprod Nutr Dev.* (1998) 38:615–28. doi: 10.1051/rnd:19980604

15. Santos-Jimenez Z, Martinez-Herrero C, Encinas T, Martinez-Ros P, Gonzalez-Bulnes AJ. Comparative efficiency of oestrus synchronization in sheep with progesterone/eCG and progesterone/GnRH during breeding and non-breeding season *Reprod Domest Anim.* (2020) 55:882–4. doi: 10.1111/rda.13698

16. Titi H, Kridli R, Alnimer MA. Estrus synchronization in sheep and goats using combinations of GnRH, progestagen and prostaglandin F2α *Reprod Domest Anim.* (2010) 45:594–9. doi: 10.1111/j.1439-0531.2008.01309.x

17. Zhang J, Ma J, Aibibaimu, Wu XL, Liu YY, Li XY. Effects of exogenous GnRH administration on lambing performance of oestrus-synchronized Kazak ewes during the breeding season. *Reprod Domest Anim.* (2023) 58:465–9. doi: 10.1111/rda.14306

18. Hong K, Choi Y. Role of estrogen and RAS signaling in repeated implantation failure *BMB Rep.* (2018) 51:225–9. doi: 10.5483/bmbrep.2018.51.5.045

19. Xi P, Zhu W, Zhang Y, Wang M, Liang H, Wang H, et al. Upregulation of hypothalamic TRPV4 via S100a4/AMPKα signaling pathway promotes the development of diet-induced obesity *Biochim Biophys Acta Mol Basis Dis.* (2024) 1870:166883. doi: 10.1016/j.bbadis.2023.166883

20. Treese C, Hartl K, Pötzsch M, Dahlmann M, von Winterfeld M, Berg E, et al. S100A4 is a strong negative prognostic marker and potential therapeutic target in adenocarcinoma of the stomach and esophagus. *Cells*. (2022) 11:1056. doi: 10.3390/cells11061056

21. Ismail TM, Crick RG, Du M, Shivkumar U, Carnell A, Barraclough R, et al. Targeted Destruction of S100A4 Inhibits Metastasis of Triple Negative Breast Cancer Cells. *Biomolecules*. (2023) 13:1099. doi: 10.3390/biom13071099

22. Liu A, Li Y, Lu S, Cai C, Zou F, Meng XJCD, et al. Stanniocalcin 1 promotes lung metastasis of breast cancer by enhancing EGFR–ERK–S100A4 signaling *Cell Death Dis*. (2023) 14:395. doi: 10.1038/s41419-023-05911-z

23. Li M, Liu Y, Nie X, Ma B, Ma Y, Hou Y, et al. S100A4 promotes BCG-induced pyroptosis of macrophages by activating the NF-κB/NLRP3 inflammasome signaling pathway *Int J Mol Sci*. (2023) 24:12709. doi: 10.3390/ijms241612709

24. Rai A, Poh QH, Fatmous M, Fang H, Gurung S, Vollenhoven B, et al. Proteomic profiling of human uterine extracellular vesicles reveal dynamic regulation of key players of embryo implantation and fertility during menstrual cycle *Proteomics*. (2021) 21:e2000211. doi: 10.1002/pmic.202000211

25. Li Y, Wang D, Wu X, He B, Cheng Z, Szenci O, et al. Decreasing of S100A4 in bovine endometritis in vivo and in vitro *Theriogenology*. (2020) 153:68–73. doi: 10.1016/j.theriogenology.2020.05.015

26. Tochimoto M, Oguri Y, Hashimura M, Konno R, Matsumoto T, Yokoi A, et al. S100A4/non-muscle myosin II signaling regulates epithelial-mesenchymal transition and stemness in uterine carcinosarcoma *Lab Invest*. (2020) 100:682–95. doi: 10.1038/s41374-019-0359-x

27. Hua T, Wang X, Chi S, Liu Y, Feng D, Zhao Y, et al. Estrogen-related receptor γ promotes the migration and metastasis of endometrial cancer cells by targeting S100A4 *Oncol Rep*. (2018) 40:823–32. doi: 10.3892/or.2018.6471

28. Chu Z, Yang S, Li Q, Shang J, Ren Z, Ren F. The V protein in oncolytic Newcastle disease virus promotes HepG2 hepatoma cell proliferation at the single-cell level *BMC Cancer*. (2023) 23:346. doi: 10.1186/s12885-023-10815-4

29. Simonetti L, Forcada F, Rivera O, Carou N, Alberio R, Abecia J, et al. Simplified superovulatory treatments in Corriedale ewes *Anim Reprod Sci*. (2008) 104:227–37. doi: 10.1016/j.anireprosci.2007.01.020

30. Wang X, El-Gayar M, Knight P, Holtz WJT. The long-term effect of active immunization against inhibin in goats *Theriogenology*. (2009) 71:318–22. doi: 10.1016/j.theriogenology.2008.07.024

31. Blanco M, Simonetti L, Rivera OJSRR. Embryo production and progesterone profiles in ewes superovulated with different hormonal treatments *Small Ruminant Res*. (2003) 47:183–91. doi: 10.1016/S0921-4488(02)00245-6

32. Brasil O, Moreira N, Júnior GS, Silva B, Mariante A, Ramos AJSRR. Superovulatory and embryo yielding in sheep using increased exposure time to progesterone associated with a GnRH agonist *Small Ruminant Res*. (2016) 136:54–8. doi: 10.1016/j.smallrumres.2016.01.005

33. Xia L, Tian L, Zhang S, Huang J, Wu Q. Hormonal replacement treatment for frozen-thawed embryo transfer with or without GnRH agonist pretreatment: a retrospective cohort study stratified by times of embryo implantation failures *Front Endocrinol (Lausanne)*. (2022) 13:803471. doi: 10.3389/fendo.2022.803471

34. French HM, Zhang W, Movilla PR, Isaacson KB, Morris SN. Adenomyosis and fertility: does adenomyosis impact fertility and does treatment improve outcomes *Curr Opin Obstet Gynecol*. (2022) 34:227–36. doi: 10.1097/GCO.0000000000000789

35. Kol SJHR. Embryo implantation and GnRH antagonists: GnRH antagonists in ART: lower embryo implantation? *Hum Reprod*. (2000) 15:1881–2. doi: 10.1093/humrep/15.9.1881

36. Zhao W, Adjei M, Zhang Z, Yuan Z, Cisang Z, Song T. The role of GnRH in Tibetan male sheep and goat reproduction *Reprod Domest Anim*. (2023) 58:1179–87. doi: 10.1111/rda.14432

37. Glujovsky D, Pesce R, Sueldo C, Retamar AMQ, Hart RJ, Ciapponi A. Endometrial preparation for women undergoing embryo transfer with frozen embryos or embryos derived from donor oocytes *Cochrane Database Syst Rev*. (2007) 65:CD006359. doi: 10.1002/14651858.CD006359

38. Ball PJBVJ. Milk progesterone profiles in relation to dairy herd fertility *Br Vet J*. (1982) 138:546–51. doi: 10.1016/S0007-1935(17)30943-0

39. Beckett SD, Lean IJ. Gonadotrophin-releasing hormone in postpartum dairy cattle: a meta-analysis of effects on reproductive efficiency. *Anim Reprod Sci*. (1997) 48:93–112. doi: 10.1016/S0378-4320(97)00016-X

40. Abdelfattah N, Kumar P, Wang C, Leu JS, Flynn WF, Gao R, et al. Single-cell analysis of human glioma and immune cells identifies S100A4 as an immunotherapy target. *Nat Commun*. (2022) 13:767. doi: 10.1038/s41467-022-28372-y

41. Zhang H, Liu S, Li Y, Li J, Ni C, Yang M, et al. Dysfunction of S100A4(+) effector memory CD8(+) T cells aggravates asthma. *Eur J Immunol*. (2022) 52:978–93. doi: 10.1002/eji.202149572

42. Liu S, Liu M, Zhong J, Chen S, Wang Z, Gao X, et al. Anti-S100A4 antibody administration alleviates bronchial epithelial-mesenchymal transition in asthmatic mice. *Open Med (Wars)*. (2023) 18:20220622. doi: 10.1515/med-2022-0622

43. Yang J, Zhang X, Li Y, Yang N, Luo J, He T, et al. Inhibition of TLR4/NF-κB pathway and endoplasmic reticulum stress by overexpressed S100A4 ameliorates retinal ischemia-reperfusion injury of mice. *Mol Neurobiol*. (2023) 61:2228–40. doi: 10.1007/s12035-023-03709-w

44. Dukhanina EA, Portseva TN, Dukhanin AS, Georgieva SG. Triple-negative and triple-positive breast cancer cells reciprocally control their growth and migration via the S100A4 pathway. *Cell Adhes Migr*. (2022) 16:65–71. doi: 10.1080/19336918.2022.2072554

45. Lyu T, Wang Y, Li D, Yang H, Qin B, Zhang W, et al. Exosomes from BM-MSCs promote acute myeloid leukemia cell proliferation, invasion and chemoresistance via upregulation of S100A4. *Exp Hematol Oncol*. (2021) 10:24. doi: 10.1186/s40164-021-00220-7

46. Kim B, Jung S, Kim H, Kwon JO, Song MK, Kim MK, et al. The role of S100A4 for bone metastasis in prostate cancer cells. *BMC Cancer*. (2021) 21:137. doi: 10.1186/s12885-021-07850-4

47. Sun Y, Liu WZ, Liu T, Feng X, Yang N, Zhou HF. Signaling pathway of MAPK/ERK in cell proliferation, differentiation, migration, senescence and apoptosis. *J Recept Signal Transduct Res*. (2015) 35:600–4. doi: 10.3109/10799893.2015.1030412

48. Zhang W, Liu HT. MAPK signal pathways in the regulation of cell proliferation in mammalian cells. *Cell Res*. (2002) 12:9–18. doi: 10.1038/sj.cr.7290105

49. Zheng J, Bird IM, Melsaether AN, Magness RR. Activation of the mitogen-activated protein kinase cascade is necessary but not sufficient for basic fibroblast growth factor-and epidermal growth factor-stimulated expression of endothelial nitric oxide synthase in ovine fetoplacental artery endothelial cells. *Endocrinology*. (1999) 140:1399–407. doi: 10.1210/endo.140.3.6542

50. Liu S, Gao F, Wen L, Ouyang M, Wang Y, Wang Q, et al. Osteocalcin induces proliferation via positive activation of the PI3K/Akt, P38 MAPK pathways and promotes differentiation through activation of the GPRC6A-ERK1/2 pathway in C2C12 myoblast cells. *Cell Physiol Biochem*. (2017) 43:1100–12. doi: 10.1159/000481752

51. Long H, Yu W, Yu S, Yin M, Wu L, Chen Q, et al. Progesterone affects clinic oocyte yields by coordinating with follicle stimulating hormone via PI3K/AKT and MAPK pathways. *J Adv Res*. (2021) 33:189–99. doi: 10.1016/j.jare.2021.02.008

52. Davis PJ, Davis FB, Lin HY, Bergh JJ, Mousa S, Hercbergs A, et al. Cell-surface receptor for thyroid hormone and tumor cell proliferation. *Expert Rev Endocrinol Metab*. (2006) 1:753–61. doi: 10.1586/17446651.1.6.753

53. Harris D, Bonfil D, Chuderland D, Kraus S, Seger R, Naor Z. Activation of MAPK cascades by GnRH: ERK and Jun N-terminal kinase are involved in basal and GnRH-stimulated activity of the glycoprotein hormone LHbeta-subunit promoter. *Endocrinology*. (2002) 143:1018–25. doi: 10.1210/endo.143.3.8675

54. Hu S, Dai Y, Bai S, Zhao B, Wu X, Chen Y. GNAI2 promotes proliferation and decreases apoptosis in rabbit melanocytes. *Genes (Basel)*. (2021) 12:1130. doi: 10.3390/genes12081130

55. Ha JH, Jayaraman M, Yan M, Dhanasekaran P, Isidoro C, Song YS, et al. GNAi2/gip2-regulated transcriptome and its therapeutic significance in ovarian cancer. *Biomolecules*. (2021) 11:1211. doi: 10.3390/biom11081211

56. Li Z, Li Y, Liu S, Qin Z. Extracellular S100A4 as a key player in fibrotic diseases. *J Cell Mol Med*. (2020) 24:5973–83. doi: 10.1111/jcmm.15259

57. Sun H, Wang C, Hu B, Gao X, Zou T, Luo Q, et al. Exosomal S100A4 derived from highly metastatic hepatocellular carcinoma cells promotes metastasis by activating STAT3. *Signal Transduct Target Ther*. (2021) 6:187. doi: 10.1038/s41392-021-00579-3

58. Wang T. The function of S100A4 in pulmonary disease: A review. *Medicine (Baltimore)*. (2023) 102:e33466. doi: 10.1097/MD.0000000000033466

frontiers | Frontiers in Veterinary Science

TYPE Original Research
PUBLISHED 11 July 2024
DOI 10.3389/fvets.2024.1442931

OPEN ACCESS

EDITED BY
Stefan Gregore Ciornei,
Iasi University of Life Science (IULS), Romania

REVIEWED BY
Daniel Berean,
University of Agricultural Sciences and Veterinary Medicine of Cluj-Napoca, Romania
Laura Abril-Parreño,
University of Murcia, Spain

*CORRESPONDENCE
Xinglong Wu
✉ wuxl32@hebau.edu.cn
Xiangyun Li
✉ Lxyun@hebau.edu.cn

RECEIVED 03 June 2024
ACCEPTED 24 June 2024
PUBLISHED 11 July 2024

CITATION
Zhang J, Sun S, Bai X, Yang N, Liu Y, Wu X and Li X (2024) Metabolomics analysis of the effect of GnRH on the pregnancy rate of ewes with estrus synchronization scheme based on progesterone.
Front. Vet. Sci. 11:1442931.
doi: 10.3389/fvets.2024.1442931

Metabolomics analysis of the effect of GnRH on the pregnancy rate of ewes with estrus synchronization scheme based on progesterone

Jing Zhang[1], Shuyuan Sun[1], Xinyu Bai[2], Nana Yang[1], Yiyong Liu[3], Xinglong Wu[1]* and Xiangyun Li[1]*

[1]College of Animal Science and Technology, Hebei Technology Innovation Center of Cattle and Sheep Embryos, Hebei Agricultural University, Baoding, Hebei, China, [2]College of Animal Science, Tarim University, Alear, Xinjiang, China, [3]Institute of Xinjiang Yili Animal Science, Yining, Xinjiang, China

Introduction: Gonadotropin-releasing hormone (GnRH) is widely used in the timed artificial insemination protocol for sheep. However, there remains a debate regarding its impact on pregnancy rates during artificial insemination. This study aims to evaluate the effect of GnRH on the pregnancy rates in Huyang ewes, analyze the pre-implantation metabolite changes caused by GnRH using metabolomics, and elucidate the mechanism effect on pregnancy rates.

Methods: All ewes were administered a vaginal progesterone sponge containing 45 mg of flurogestone acetate for 12 days and received 330 units of equine chorionic gonadotropin (eCG) intramuscularly after sponge removal. The experimental group ($n = 69$) received an intramuscular treatment of 17 μg GnRH agonist triptorelin 48 h after sponge removal on Day 0, while the control group ($n = 41$) received 1 mL of sterile saline solution. All ewes underwent a single vaginal insemination 58 h after the withdrawal of the progesterone sponge. The difference in pregnancy rates between the two groups was calculated. Metabolomic analysis was performed on plasma samples collected on Day 7 after the treatment of GnRH agonist.

Results: Gonadotropin-releasing hormone (GnRH) treatment significantly reduced the pregnancy rate in the experimental group compared with the control group (72.2 vs. 82.9%, $p < 0.05$). Metabolomic analysis indicated that GnRH treatment affected metabolites involved in collagen synthesis and prostaglandin synthesis in the endometrial tissue, which includes a marked decrease in hydroxyproline amino acid content and a significant increase in corticosterone and prostaglandin D2 lipids and unsaturated fatty acids.

Conclusion: In summary, the injection of GnRH agonist Triptorelin 48 h after progesterone sponges removal reduces the pregnancy rate of Huyang ewe following artificial insemination. It also affects the metabolite levels related to endometrial collagen and prostaglandin synthesis, harming embryo implantation.

KEYWORDS

gonadotropin-releasing hormone, pregnancy rate, metabolomics, hydroxyproline, prostaglandin D2, corticosterone, ewes

1 Introduction

Promoting estrus synchronization and artificial insemination technology in the sheep industry can increase lamb production, improve reproductive efficiency, and enhance flock management and genetic improvement (1). Synchronized breeding results in synchronized lambing, simplifying centralized management and lamb sales (2). In production practice, a commonly used estrus synchronization program for ewes undergoing artificial insemination or serving as recipients in the Multiple Ovulation and Embryo Transfer (MOET) process involves the use of vaginal inserts or sponges containing fluorogestone acetate or medroxyprogesterone acetate and eCG (3, 4). Numerous studies have demonstrated the effectiveness of using gonadotropin-releasing hormone (GnRH) to synchronize and induce ovulation in farm animal reproduction (5–7). It has been demonstrated by Menchaca et al. (2) that administering a single dose of GnRH 24–36 h after removing the progesterone-releasing intravaginal device results in a luteinizing hormone peak approximately 40 h later. Additionally, 90% of ewes ovulate within 72 h after removing the device.

Although GnRH has been widely used in Fixed Time Artificial Insemination (FTAI) projects for sheep (8), resulting in a certain degree of economic benefit improvement in animal husbandry production (9), its effect on pregnancy rates is still debated (2). Some studies indicated that administering a single dose of GnRH after pessary removal increases pregnancy rates (10, 11), contrasting with findings of no effect (6, 12, 13) or a decrease in pregnancy rates in other studies (14). Similarly, in cows undergoing estrus synchronization, administering GnRH during insemination leads to the ovulation of physiologically immature follicles, impacting the pregnancy rate of cows and the fetal survival in later gestation (15). Pre-ovulatory follicle exposure to the gonadotropin surge triggered by exogenous GnRH may reduce oocyte quality, decreasing the pregnancy rate (16). Moreover, it has been inferred that GnRH might hinder embryo implantation, consequently affecting pregnancy rates in FTAI protocols (17).

Metabolomics is an important technology for studying the metabolic networks of biological systems. It involves quantitatively analyzing all metabolites in organisms and exploring the relative relationships between metabolites and physiopathological changes (18). This technique is extensively applied in plant research (19), drug development (20), and disease studies (21). Various studies have utilized metabolomics to detect sheep meat quality (22), feed and nutrition (23), and diseases (24). Relevant studies have also used metabolomics to analyze the composition of ewe cervical mucus and the negative impact of inflammatory responses on the transportation of semen in the cervix (25). However, research on the implantation environment during the peri-implantation period remains limited.

In the study, Huyang ewes were treated with estrus synchronization, GnRH agonist was injected 48 h after the withdrawal of progesterone sponges, and the difference in pregnancy rate was compared 40 days after insemination. Blood samples were collected on Day 7 post-GnRH treatment for metabolomics analysis to identify metabolic pathways and metabolites impacting pregnancy rates in Huyang ewes caused by GnRH. The objective of the present study was to evaluate the effect of GnRH treatment on pregnancy rates and pre-implantation metabolites in Huyang ewes.

2 Materials and methods

2.1 Animals and location

The study was conducted in January 2023 in Hulunbeir, Inner Mongolia. It is located at longitude 120°28′E and latitude 47°5′N. This region experiences a temperate continental climate and receives annual precipitation ranging from 300 to 500 mm. Winters are chilly and arid, while summers are hot and rainy, resulting in significant fluctuations in both annual and daily temperatures. The experiment selected 23 healthy and multiparous Huyang ewes (aged 1.5–4 years, weighing 40–45 kg, BSC ≥ 3, ranging from emaciation to obesity). All the ewes participating in the experiment possess healthy reproductive tracts and lactating abilities, with an average weaning period exceeding 3 months, thus qualifying them for estrus synchronization treatment. During the experimental period, the ewes were kept away from the rams to prevent voluntary mating. The ewes were kept indoors at night and allowed to graze at natural pastures on the farm throughout the day. When ewes were kept indoors, all ewes received TMR, including alfalfa hay, barley, and mixed concentrate according to NRC recommendation, and had free access to water and mineral block. This study was approved by the Animal Care and Use Committee of the Hebei Agricultural University, Baoding, China (Number: 2021011). All efforts were made to minimize animal suffering. The authors declare that all procedures in the experiment were conducted in ways consistent with the precepts of animal welfare, with personnel involved in the caring and handling of animals being licensed veterinarians.

2.2 Estrus synchronization and hormonal treatment

All experimental ewes comprised indigenous, multiparous Huyang ewes, which were synchronized using a progestogen-eCG combination protocol. Each ewe received a polyurethane intravaginal sponge impregnated with 45 mg flurogestone acetate (Muqimuye Sci-Tech Co., Ltd., Shanghai, China) for 12 days, followed by treatment with 330 IU of eCG i.m. (Sansheng Biological Technology Co., Ltd., Ningbo, China) at sponge removal. The experimental group (B, $n = 69$) was subjected to 48 h (Day 0) after sponge removal to intramuscular administration of 17 μg of the GnRH agonist triptorelin (Sansheng Biological Technology Co., Ltd., Ningbo, China), and the control group (Y, $n = 41$) with 1 mL of sterile physiological saline solution. All ewes underwent a single vaginal insemination 58 h after the withdrawal of progesterone sponges.

2.3 Fixed-time artificial insemination

Fresh sperm was collected from six healthy Huyang rams, and sperm motility and density were assessed using a hemocytometer and an optical microscope. The sperm (progressive motility more significant than 50% and density greater than 1×10^9 sperm/mL) was diluted using 5–7 times the volume of skim milk (Yili skimmed milk, Inner Mongolia Yili Industrial Group Limited by Share Ltd), ensuring that the motility of sperm after dilution remained above 0.5, and the density was adjusted to 4×10^8 sperm/mL. The diluted sperm was then

stored in a water bath kettle at 30°C. The experimental sheep were restrained upside down, and their vaginal mucus was cleaned with warm normal saline to ensure the hygiene of the vaginal environment, thereby reducing the impact on sperm viability. A vaginal speculum was inserted to open the vagina, and the cervical os was observed and located. A sheep-specific inseminator (produced by Baoding Zhengmu Biotechnology Co., Ltd.) was used to aspirate 0.3 mL of semen and inject it into the cervical os.

2.4 Blood sample collection

Ewes were randomly selected from the experimental group ($n = 13$) and the control group ($n = 10$). In the experimental group ($n = 13$) and the control group ($n = 10$), 5 mL of jugular venous blood was collected using vacuum blood collection tubes containing heparin sodium on Day 7 after the treatment of GnRH agonist. Afterward, the blood samples underwent centrifugation at 3,000 × *g* for 15 min at 4°C. The resulting supernatant plasma was carefully separated and transferred into enzyme-free 1.5 mL EP tubes using a precision pipette. The plasma samples were immediately stored at −80°C to preserve their integrity for subsequent metabolomics analysis.

2.5 Serum liquid chromatography–tandem mass spectrometry detection

Mix 100 µL of the sample with 400 µL of pre-cooled methanol, ensuring thorough mixing by vortexing. Incubate the mixture on ice for 5 min, centrifuge it at 15,000 × *g*, and 4°C for 20 min. Dilute a portion of the resulting supernatant with LC–MS grade water to achieve a final methanol concentration of 53%. Subsequently, transfer the diluted sample to a new centrifuge tube using a 0.22 µm filter and centrifuge it again at 15,000 × *g* and 4°C for 20 min. Finally, the filtered sample is injected into the LC–MS/MS system for analysis.

The LC–MS/MS analysis was conducted using the Vanquish UHPLC system (ThermoFisher, Germany) coupled with an Orbitrap Q ExactiveTMHF-X mass spectrometer (ThermoFisher, Germany). Samples were injected into a Hypersil Gold chromatographic column (100 mm × 2.1 mm, 1.9 µm) at a flow rate of 0.2 mL/min using a 17-min linear gradient. For the positive polarity mode, the mobile phases consisted of eluent A (0.1% Formic Acid in water) and eluent B (Methanol). For the negative polarity mode, the mobile phases were eluent A (5 mM ammonium acetate, pH 9.0) and eluent B (methanol). The solvent gradient was set as follows: 2%B, 1.5 min; 2–85%B, 3 min;85–100%B, 10 min; 100–2%B, 10.1 min; 2%B, 12 min. The Q ExactiveTMHF-X mass spectrometer was operated in both positive and negative modes with a spray voltage of 3.5 kV, a capillary temperature of 320°C, a sheath gas flow rate of 35 psi, and an auxiliary gas flow rate of 10 L/min, S-lens RF level of 60, Aux gas heater temperature of 350°C.

2.6 Pregnancy test

Forty days after insemination, a fixed technician used a B-ultrasound tester (DP-30Vet, Shenzhen Mindray Biomedical Electronics Co., Ltd.) to perform a pregnancy test on the inseminated ewes through the abdomen. The B-ultrasound screen showed a clear gestational sac, which was identified as pregnancy. The pregnancy rates were calculated as the percentage of pregnant ewes among the inseminated ewes.

2.7 Data analysis

Statistical analysis was carried out using GraphPad Prism 8.0 software. The pregnancy rates in the experimental and control groups were analyzed using a Chi-square Test. It was accepted as significant if the calculated p value <0.05. Use the Human Metabolome Database (HMDB, http://www.hmdb.ca/), Kyoto Encyclopedia of Genes and Genomes (KEGG, http://www.genome.jp/kegg/), and Lipidmaps (Lipid Metabolism Pathway Research Program, https://lipidmaps.org/) databases to annotate metabolites. Utilize metaX for Partial Least Squares Discriminant Analysis (PLS-DA) and employ univariate analysis (T-test) to calculate statistical significance (p value). PLS-DA was performed to compute Variable Importance in Projection (VIP) scores. Metabolites that fulfill the criteria of Variable Importance in Projection (VIP) > 1, p value <0.05, and either Fold Change (FC) > 1.2 or FC < 0.833 are deemed as differential metabolites. The functions of these metabolites and metabolic pathways were studied using the KEGG database. The metabolic pathways enrichment of differential metabolites was performed, and metabolic pathways were considered enrichment. When the p value of metabolic pathway <0.05, metabolic pathways were considered statistically significant enrichment.

3 Results

3.1 Effect of GnRH on pregnancy rates at 40 days after insemination

Pregnancy was detected by ultrasound 40 days after insemination, the result as shown in Table 1. The pregnancy rate of the experimental group was significantly lower than that of the control group (72.2 vs. 82.9%, $p < 0.05$). Results showed that GnRH treatment during artificial insemination decreased the pregnancy rates in Huyang ewes.

3.2 Classification of metabolites in ewes

To investigate the factors contributing to the reduced pregnancy rates following GnRH treatment in Huyang ewes, plasma samples from both experimental and control groups were collected 7 days after artificial insemination for metabolomics. All 23 samples identified 464 metabolites in positive ion mode (POS) and 376 in negative ion mode

TABLE 1 The effect of GnRH treatment on pregnancy rate in Huyang ewes.

Group	No. Inseminated ewes	No. Pregnant ewes	Pregnancy rate (%)
Experimental group	69	50	72.5*
Control group	41	34	82.9

The pregnancy rates were analyzed using a Chi-square Test. *$p < 0.05$.

(NEG). Positive ion mode analysis revealed a range of metabolites such as lipids and lipid-like molecules (57.38%), organic acids and derivatives (14.48%), organoheterocyclic compounds (10.86%), benzenoids (5.01%), phenylpropanoids and polyketides (3.90%), organic nitrogen compounds (3.34%), nucleosides, nucleotides, and analogs (2.79%), organic oxygen compounds (1.95%), and alkaloids and derivatives (0.28%) (Figure 1A). Negative ion mode analysis indicated the existence of lipids and lipid-like molecules (63.93%), organic acids and derivatives (13.44%), benzenoids (6.89%), organic oxygen compounds (4.26%), organoheterocyclic compounds (3.93%), phenylpropanoids and polyketides (3.93%), nucleosides, nucleotides, and analogs (2.95%), none (0.33%), and organic nitrogen compounds (0.33%) (Figure 1B).

In addition, the KEGG database was utilized for functional annotation of the identified metabolites to comprehend their functional traits and classifications (Figures 1C,D). In the positive and negative modes, the identified metabolites participate in pathway processes related to cellular processes, environmental information processing, genetic information processing, metabolism, and organic systems. Specifically, under the positive ion mode, metabolites primarily participate in biological processes such as cell growth and death, membrane transport, lipid metabolism, energy metabolism, and amino acid metabolism. In the negative ion mode, metabolites mainly involve biological processes, including cell growth and death, signaling molecules and interaction, lipid metabolism, amino acid metabolism, and the immune system.

3.3 Screening and analysis of differential metabolites

Partial Least Squares Discriminant Analysis established a relationship model between metabolite expression and sample category, facilitating sample category prediction. To discriminate the differential metabolites between the two groups, supervised PLS-DA was performed to find different metabolites. As shown in Figure 2, the prediction parameters of the PLS-DA evaluation model exhibit R2Y values of 0.84 and 0.78 in positive and negative ion modes (Figures 2A,B), with the Q2Y values of 0.09 and −0.03, respectively. The higher R2Y values compared to Q2Y in both modes indicate the reliability of the model used in this study.

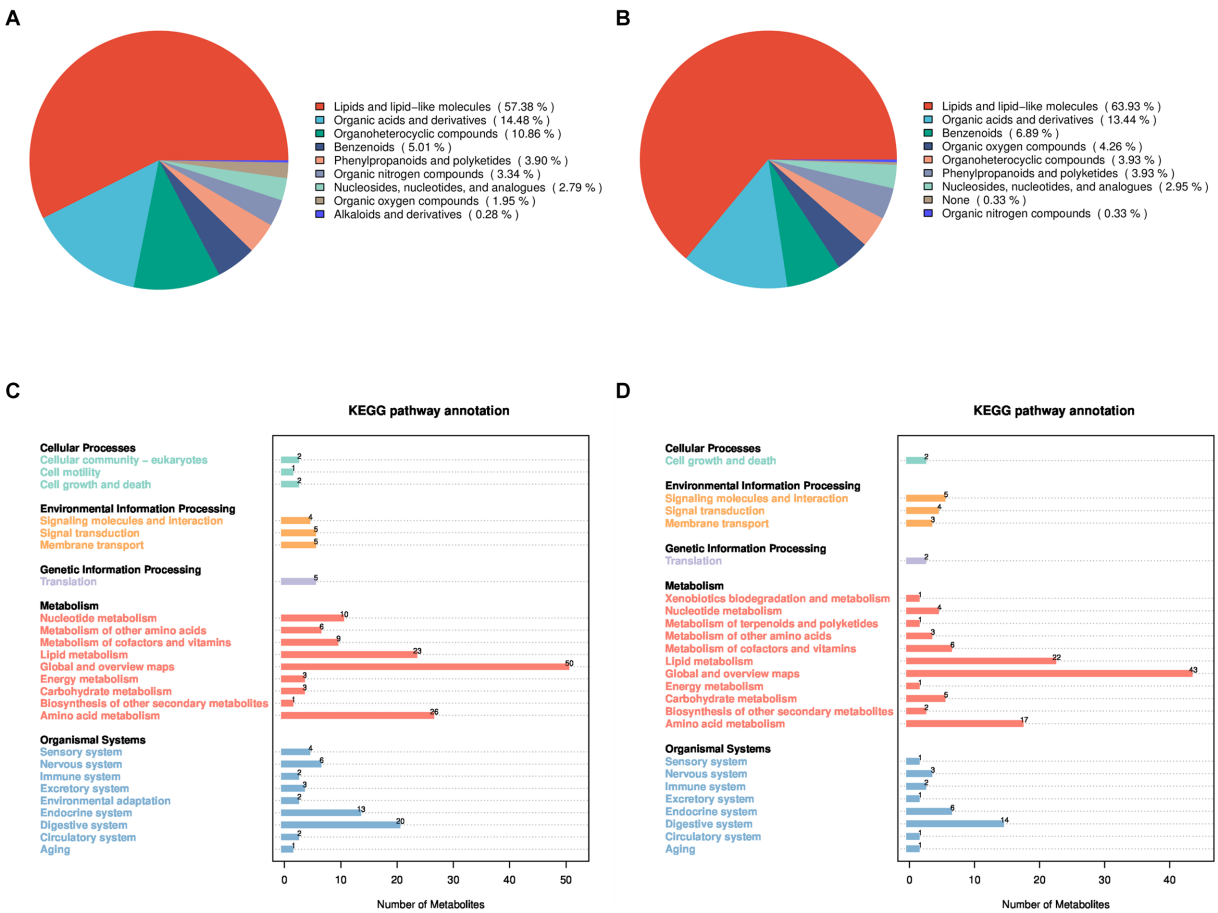

FIGURE 1
Identification and classification of all metabolites in Huyang ewe plasma samples. Chemical classification of all metabolites in the positive ion mode **(A)** and the negative ion mode **(B)**. On the left is a pie chart, and on the right is the proportion of metabolites. KEGG functional annotation of all metabolites in the positive ion mode **(C)** and the negative ion mode **(D)**, on the left is the metabolite-enriched pathway, and on the right is the number of metabolites in the pathway.

10.3389/fvets.2024.1442931

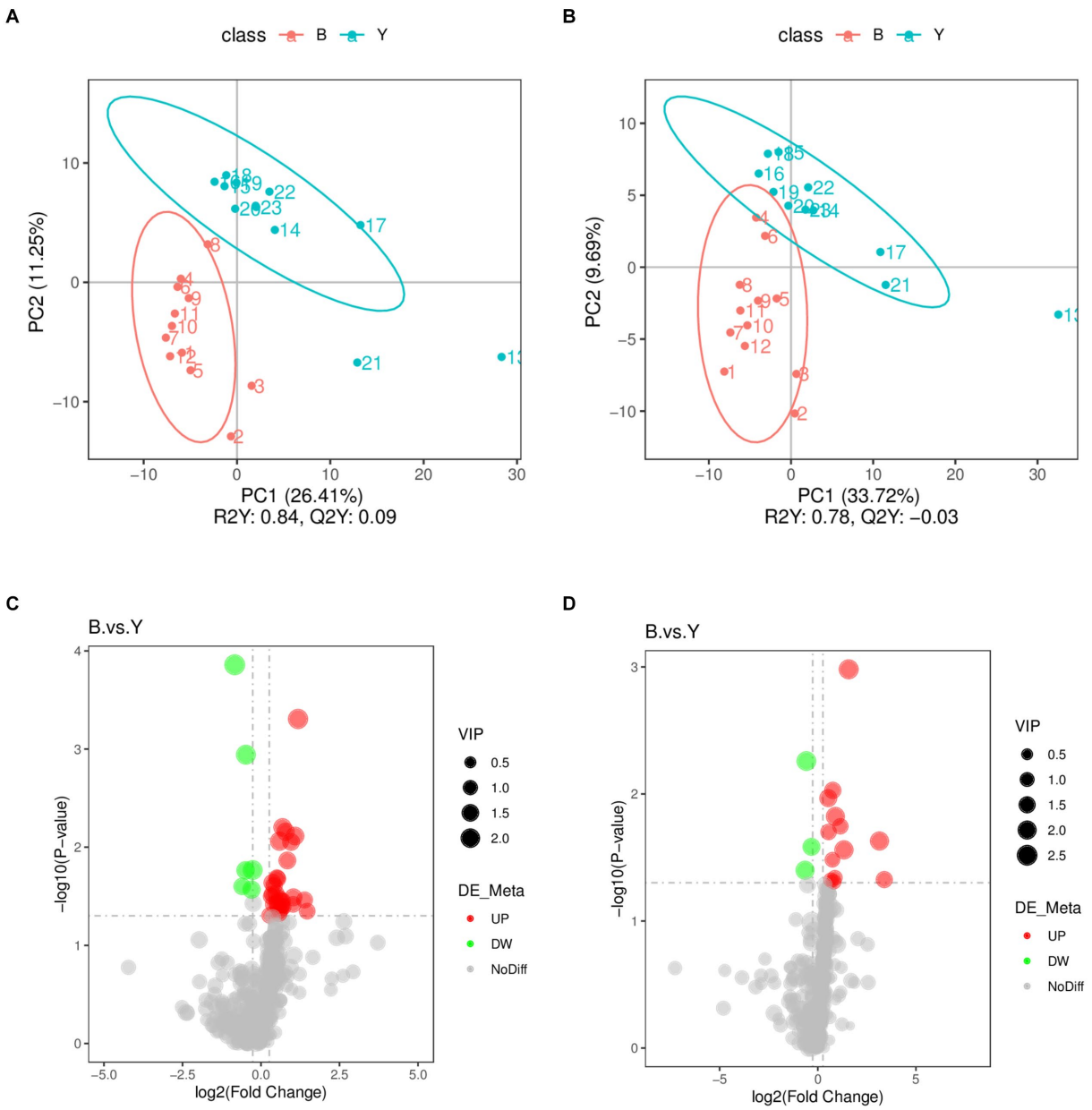

FIGURE 2
Screening of differential metabolites in Huyang ewe plasma samples. PLS-DA scatter plot of the experimental and control groups in positive ion modes **(A)** and negative ion modes **(B)**. The abscissa is the sample's score on the first principal component, and the ordinate is the sample's score on the second principal component. R2Y represents the interpretation rate of the model, Q2Y is used to evaluate the predictive ability of the PLS-DA model, and when R2Y is greater than Q2Y, the model is well established. Volcano plot of differential metabolites in positive ion mode **(C)** and the negative ion mode **(D)**. The gray plot shows there is no difference. The red plots show upregulated endogenous metabolites, while the green plots show downregulated endogenous metabolites. VIP value represents the important projection value of the metabolite obtained in the PLS-DA model compared to this group. B: experimental group; Y: control group.

Metabolomic data were analyzed using FC, *p* value, and VIP in univariate analysis. Differential metabolites were subsequently identified based on VIP > 1.0, FC > 1.2 or FC < 0.833, and $p < 0.05$. A total of 53 metabolites exhibiting significant differences were identified: 37 in positive ion mode, comprising 31 upregulated and six downregulated metabolites, and 16 in negative ion mode, with 13 upregulated and three downregulated (Table 2; Figures 2C,D). As shown in Figures 3A,B, the heat map showed all differential metabolites in positive and negative ion modes. The top 10 differential metabolites in positive ion mode are N,N′-di[4-(2,6-dimethylmorpholino)phenyl] thiourea, phosphatidylcholine (20:3e/19:2), 4-methoxycinnamic acid, phosphatidylcholine (18:1e/22:6), 2-arachidonyl glycerol ether, phosphatidylcholine (14:0e/3:0), tetranor-pgdm, cinchophen, phosphatidylcholine (15:0/16:1), and monoacylglycerol (18:2). The top 10 differential metabolites in negative ion mode are retinoic acid, methyltestosterone, corticosterone, (±) 18-hydroxyeicosa-5,8,11,14,16-pentaenoic acid (18-HEPE), prostaglandin D2, prostaglandin K1, lysophosphatidylcholine (LPC) 22:6, LPC 22:4, LPC 19:0, and

TABLE 2 Differential metabolites detected in Huyang ewe plasma samples under positive and negative ion modes.

Compared samples	No. Total Ident	No. Total Sig	No. Sig Up	No. Sig Down
B vs. Y_pos	464	37	31	6
B vs. Y_neg	376	16	13	3

B, Experimental group; Y, Control group. Compared samples: Compare the pairs of samples, for the former than the latter; No. Total Ident, Total metabolite identification results; No. Total Sig, The total number of metabolites with significant differences; No. Sig Up, The total number of significantly upregulated metabolites; and No. Sig Down, The total number of significantly downregulated metabolites.

DL-3,4-dihydroxyphenyl glycol. Among them, the metabolic levels of cortisone and hydroxyproline significantly decreased, and the pantothenic acid level significantly increased in the experimental group in positive ion mode. In negative ion mode, the metabolic levels of corticosterone and prostaglandin D2 of the experimental group significantly increased (Figure 3B). Correlation analysis of differential metabolites was performed using Pearson correlation analysis (Figures 3C,D). In positive ion mode, the metabolic levels of hydroxyproline had a significant positive correlation with cortisone and 5-nitrothiophene-3-carbaldehyde 3-(2-pyridyl) hydrazone (Figure 3C, $p < 0.05$). The metabolic levels of corticosterone and prostaglandin D2 were significantly positively correlated in negative ion mode (Figure 3D, $p < 0.05$).

3.4 The impact of GnRH on metabolic pathways

To explore the physiological functions of metabolites affected by GnRH treatment, KEGG pathway enrichment analysis was performed on 53 differential metabolites in positive and negative ion modes. KEGG pathway enrichment analysis revealed 22 significantly enriched pathways in positive and 19 in negative ion modes. These pathways belonged to five modules: metabolism, genetic information processing, cellular processes, environmental information processing, and organismal systems. The enriched pathways of differential metabolites in positive ion mode mainly included pantothenate and CoA biosynthesis, Foxo signaling pathway, mTOR signaling pathway, PI3K-Akt signaling pathway, cGMP-PKG signaling pathway, aldosterone-regulated sodium reabsorption, and cAMP signaling pathway (Figure 4A). Significantly downregulated hydroxyproline was enriched in the arginine and proline metabolism pathway (Figure 4B).

Conversely, in negative ion mode, differential metabolites were primarily enriched in aldosterone synthesis and secretion, arachidonic acid metabolism, neuroactive ligand-receptor interaction, steroid hormone biosynthesis, and Th17 cell differentiation, among other metabolic pathways (Figure 4C). Significantly upregulated corticosterone was primarily enriched in the aldosterone synthesis and secretion pathway and the steroid hormone biosynthesis pathway (Figure 4D). Additionally, there is a significant increase in the metabolic content of prostaglandin D2 in the arachidonic acid metabolism pathway and the interaction of neuroactive ligands with receptors (Figure 4D). Moreover, a KEGG regulatory network was constructed utilizing the differential metabolites (Figures 5A,B). The figure visually represents changes in metabolites such as hydroxyproline, corticosterone, and prostaglandin D2. It also displays the intersections and biological processes related to these metabolites and their corresponding pathways.

4 Discussion

Synchronization and artificial insemination techniques have been widely used in sheep reproduction, and GnRH treatment during insemination has become a relatively common practice in the sheep industry (26). However, the impact of GnRH on embryo development and implantation remains debated among various studies. Our study compared the 40-day pregnancy rates between GnRH-treated and control sheep. The results indicated that the pregnancy rate in the experimental group (72.5%, $n = 69$) was significantly lower than that in the control group (82.9%, $n = 41$) ($p < 0.05$).

The pregnancy results obtained in our control group are acceptable, which is consistent with the results of conventional progesterone + eCG synchronization treatment and artificial insemination (27). Previous studies have shown that treatment with GnRH 24–48 h after progesterone withdrawal in sheep does not enhance the pregnancy rate (11, 14). Corriedale sheep were treated with two prostaglandins to induce synchronization and FTAI with GnRH 24 h after the second prostaglandin used decreased the pregnancy rate following artificial insemination. However, treatment with GnRH 36 h later had no significant effect on the pregnancy rate (14). Additionally, administering GnRH simultaneously with single-timed insemination can potentially decrease the pregnancy rate (28). Similarly, GnRH treatment 36 h after progesterone withdrawal and performing insemination 48 h later did not lead to a significant improvement in the pregnancy rate in goats (6). In the MOET process, the receptors treated with GnRH analog Folligon also achieved a low pregnancy rate of 43.2% (29). These previous study results are consistent with the results in this study.

Moreover, metabolomics analysis was performed to investigate the potential reasons behind the lower pregnancy rate observed in GnRH-treated sheep. Metabolomics employs comprehensive analysis through positive and negative ion modes, aiming to capture the diverse metabolites within the organism. The positive ion mode tends to detect alkaline metabolites, while the negative ion mode focuses on acidic substances (30). This study conducted metabolite screening and discussion separately in two modes. Significantly, differential metabolites were screened, including hydroxyproline in positive ion mode and corticosterone and prostaglandin D2 in negative ion mode. Hydroxyproline, a distinctive amino acid found in collagen, is a marker for collagen degradation (31, 32). It comprises approximately 13% of collagen's total amino acid content, making it crucial for maintaining collagen's structure and function. During pregnancy, the uterine collagen content progressively rises, leading to a corresponding increase in hydroxyproline levels (33). Currently, the uterus and genital tract's extracellular matrix contain abundant collagen, essential for supporting the growing fetal load and maintaining gestation (34). Metabonomics results revealed that hydroxyproline metabolite was significantly downregulated in the arginine and proline metabolism pathway ($p < 0.05$) in Huyang ewes treated with GnRH during the peri-implantation period. This downregulation may decrease collagen synthesis, affecting endometrial tissue's stability and mechanical strength and potentially causing uterine tissue damage or dysfunction. Such conditions are unfavorable for establishing a suitable environment for embryo implantation. Furthermore, studies have demonstrated that collagen rapidly degrades after cows give birth, decreasing uterine size and weight as part of the uterine involution process (35). In conclusion, a significant reduction in hydroxyproline level during the

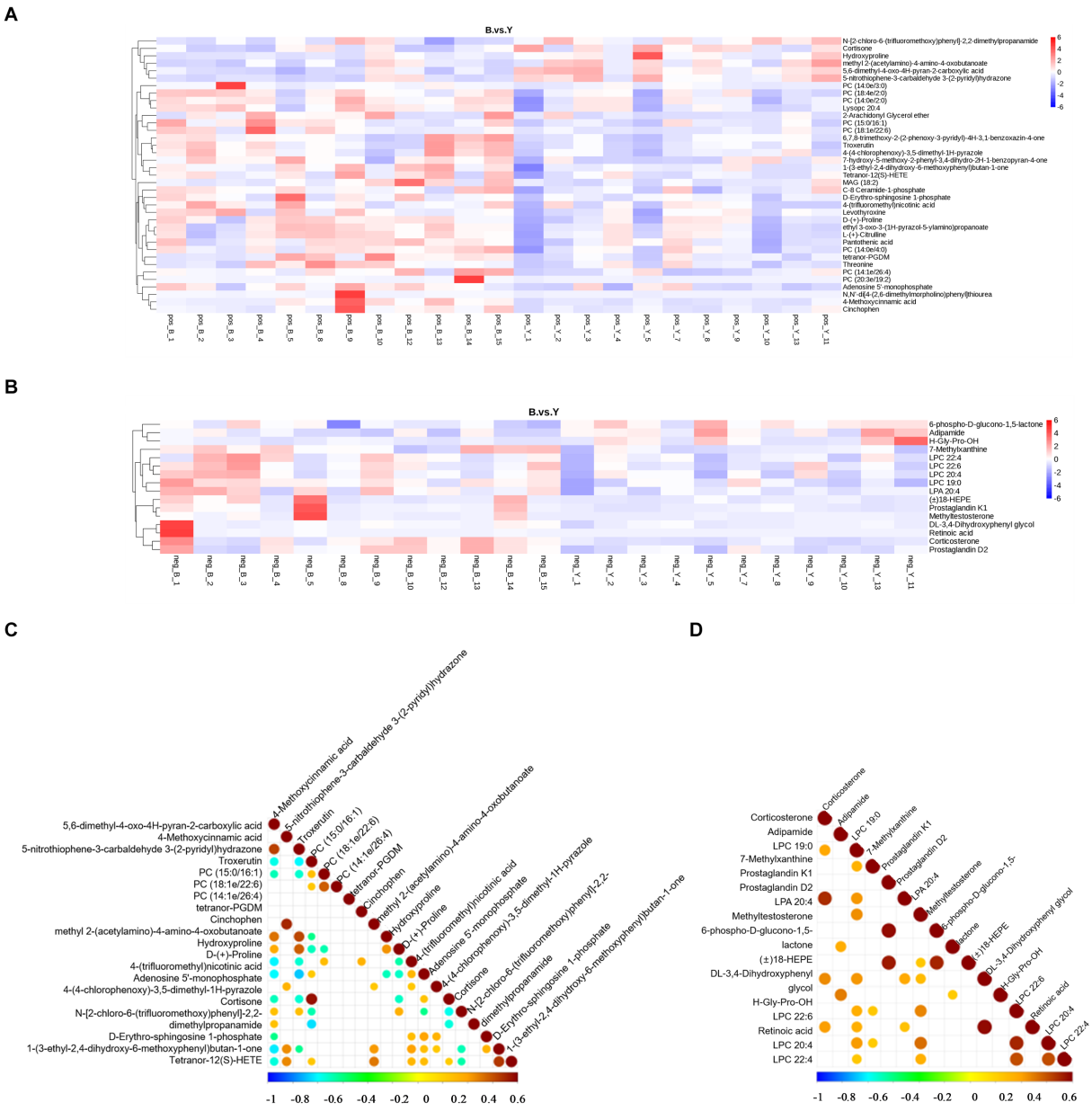

FIGURE 3
Analysis of differential metabolites in Huyang ewe plasma samples. Heat map of differential metabolite levels in positive ion mode **(A)** and the negative ion mode **(B)**. The vertical direction was the clustering of metabolites. The correlation diagram of differential metabolites in the positive ion model **(C)** and negative ion mode **(D)**. Pearson's correlation coefficient between all metabolites was calculated to analyze the correlation between each metabolite. When the linear relationship between the two metabolites is strengthened, the positive correlation tends to be 1, and the negative correlation tends to be −1. At the same time, the statistical test of significance was carried out on the correlation analysis of metabolites, and the threshold of significant correlation was selected as the significance level p value <0.05.

peri-implantation period is detrimental to embryo implantation in the uterus, ultimately decreasing the pregnancy rate in Huyang ewes.

The results of this study indicate that the metabolism of corticosterone in the aldosterone synthesis and secretion pathway significantly increased ($p = 0.01$) in Huyang ewes treated with GnRH. Corticosterone, produced primarily by the adrenal cortex, plays a crucial role in the stress response (36). Studies have shown that up-regulated corticosterone levels can inhibit embryonic development and decrease the number of inner cell mass cells, compromising embryo quality and affecting pregnancy rates (37). Zheng et al. continuously use exogenous corticosterone in mice during pregnancy days 1–4. Compared to the control group, using corticosterone resulted in a sharp decrease in phosphorylated Stat3, affecting endometrial receptivity and significantly reducing the number of implantation sites on day 5 (38). Similarly, studies on a mouse model of corticosterone excess have shown that elevated corticosterone levels affect female fertility by influencing the uterus rather than the oocytes (39). These findings are consistent with our results. So, we thought that treatment with GnRH during insemination significantly increases corticosterone levels in Huyang ewes before implantation, thereby affecting the uterine environment before implantation, disrupting endometrial receptivity, and ultimately decreasing the pregnancy rate.

Prostaglandin D2 (PGD2) belongs to the prostaglandin family and is synthesized from arachidonic acid (AA) via the action of

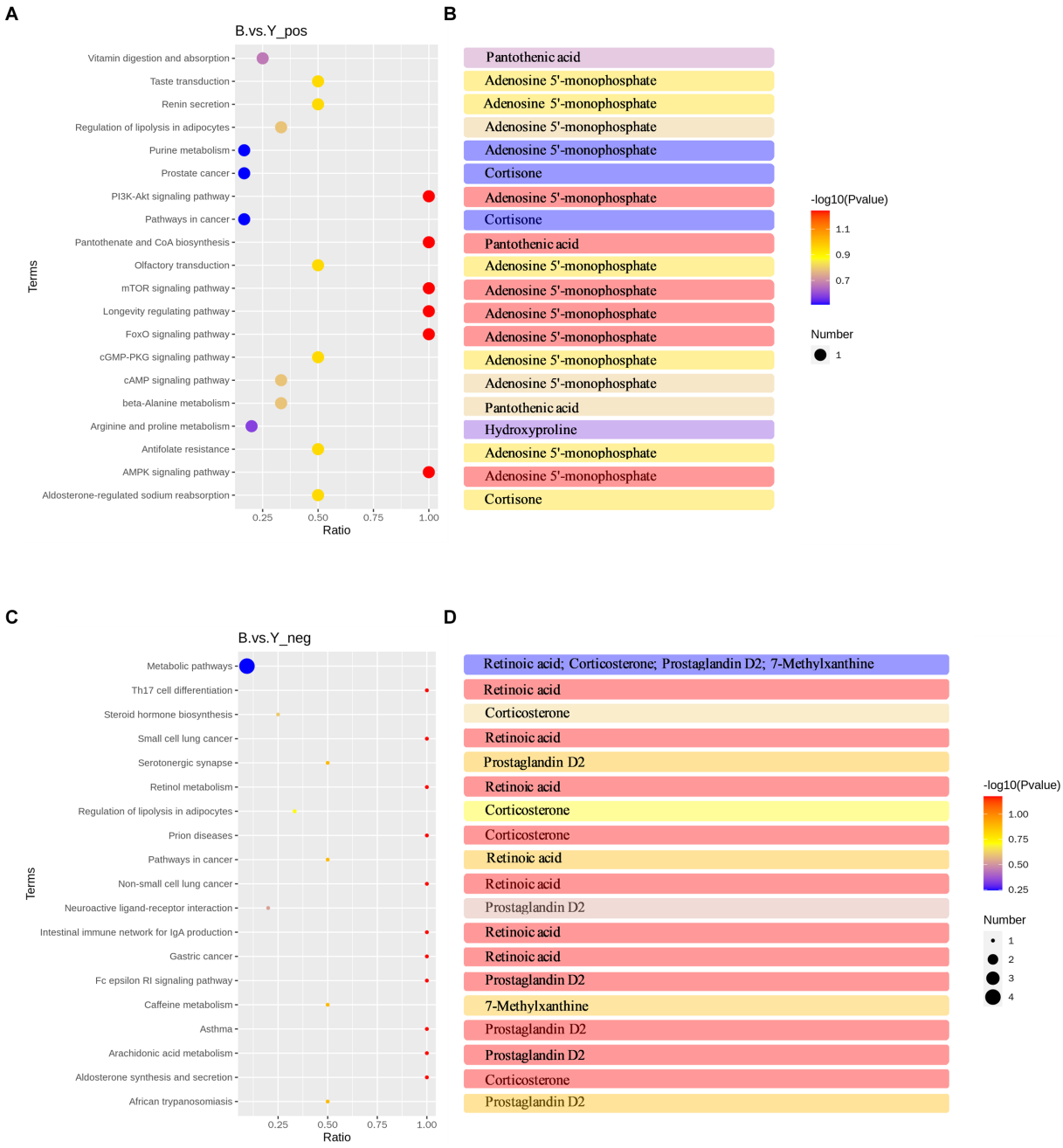

FIGURE 4
KEGG pathway analysis of differential metabolites in Huyang ewe plasma samples. **(A)** Top 20 KEGG enrichment pathways of differential metabolites in positive ion mode. **(B)** Metabolites have significant differences in each pathway in the positive ion mode. **(C)** Top 19 KEGG enrichment pathways of differential metabolites in the negative ion mode. **(D)** Metabolites have significant differences in each pathway in the negative ion mode. The horizontal coordinate is *x*/*y* (the number of differential metabolites in the corresponding metabolic pathway/the number of total metabolites identified in the pathway). The higher the value, the higher the enrichment degree of differential metabolites in the pathway. The color of the dot represents the *p* value of the hypergeometric test, and the smaller the value, the greater the reliability and statistical significance of the test. The size of the dot represents the number of differential metabolites in the corresponding pathway, and the larger the dot, the more differential metabolites in the pathway.

cyclooxygenase (COX) (40). Metabolomic analyses indicated a significant increase in prostaglandin D2 within the arachidonic acid metabolism pathway (p =0.017). Although PGD2 promotes luteal regression, its effect is less pronounced than that of Prostaglandin F2 alpha (PGF2α). Nonetheless, PGF2α and PGD2 exhibit synergistic effects in promoting luteal regression by effectively expanding blood vessels and increasing inflow to luteal tissue, which facilitates the influx of additional PGF2α synthesized in the endometrium and accelerates the luteal regression process (41). In addition, PGs serve as key mediators in the study of inflammation (42). Under inflammatory conditions or other stimuli, the expression of COX-2 is significantly upregulated, further promoting the synthesis of PGs to a notable degree (43). The induction of intrauterine inflammation can negatively impact the implantation and development of embryos within the uterus (44). Studies have revealed the presence of PGD2 in human endometrial and uterine smooth muscle tissues, where it stands out as the most potent substance within the PG

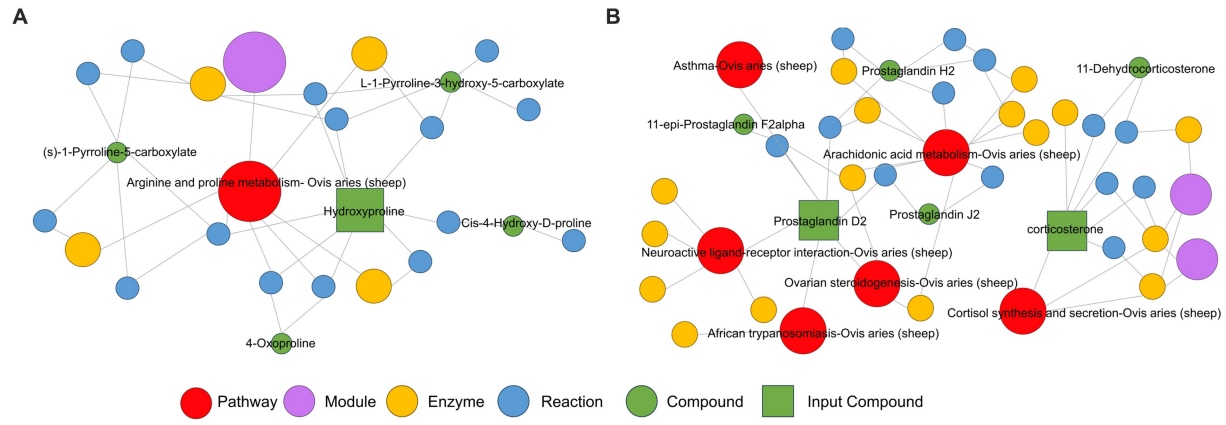

FIGURE 5
KEGG enrichment pathway network diagram of hydroxyproline, corticosterone, and prostaglandin D2 metabolites in the positive ion mode **(A)** and negative ion mode **(B)** of Huyang ewe plasma samples. In this network plot, the red dot represents a metabolic pathway, the yellow dot represents substance-related regulatory enzyme information, the green dot represents a background substance of a metabolic pathway, the purple dot represents a class of substance molecular module information, the blue dot represents a substance chemical interaction reaction, and the green square represents the difference substance obtained from this comparison.

family for augmenting blood flow to the endometrium and uterine muscles (45). The significant elevation of PGD2 can trigger and expedite uterine smooth muscle contraction frequency, ultimately decreasing embryo survival rate (46). Consequently, the imbalance of PGD2 levels in ewes adversely affects embryo implantation, resulting in a decreased pregnancy rate in the experimental group.

5 Conclusion

In summary, administering a single dose of the GnRH agonist triptorelin 48 h after sponge removal reduces the pregnancy rate in Huyang ewes after insemination. Metabolomic analysis revealed a significant decrease in hydroxyproline levels and a significant increase in corticosterone and prostaglandin D2 levels, which are linked to a decreased pregnancy rate in Huyang ewes.

Data availability statement

The data presented in the study are deposited in the MetaboLights repository, accession number MTBLS10318.

Ethics statement

The animal study was approved by Animal Care and Use Committee of the Hebei Agricultural University. The study was conducted in accordance with the local legislation and institutional requirements.

Author contributions

JZ: Data curation, Formal analysis, Investigation, Methodology, Project administration, Software, Validation, Writing – original draft, Writing – review & editing. SS: Data curation, Formal analysis, Investigation, Methodology, Resources, Writing – original draft. XB: Data curation, Formal analysis, Investigation, Methodology, Visualization, Writing – original draft. NY: Data curation, Methodology, Resources, Writing – review & editing. YL: Data curation, Methodology, Resources, Writing – review & editing. XW: Conceptualization, Formal analysis, Funding acquisition, Methodology, Supervision, Validation, Visualization, Writing – original draft, Writing – review & editing. XL: Conceptualization, Data curation, Funding acquisition, Methodology, Resources, Supervision, Validation, Visualization, Writing – original draft, Writing – review & editing.

Funding

The author(s) declare that financial support was received for the research, authorship, and/or publication of this article. This study was supported by the Key Research and Development Program of Ili Kazak Autonomous Prefecture (YZ2023A04) and Talents Special Fund of Hebei Agricultural University (YJ201952).

Acknowledgments

The authors are grateful to the Hulunbeir Longxingchuan Animal Husbandry Technology Co., Ltd. staff for assistance during this study. The authors thank Novogene (Novogene Co., Ltd., Beijing, China) for their metabolomics analysis services.

Conflict of interest

The authors declare that the research was conducted in the absence of any commercial or financial relationships that could be construed as a potential conflict of interest.

Publisher's note

References

1. Gibbons AE, Fernandez J, Bruno-Galarraga MM, Spinelli MV, Cueto MI. Technical recommendations for artificial insemination in sheep. *Anim Reprod*. (2019) 16:803–9. doi: 10.21451/1984-3143-AR2018-0129

2. Menchaca A, Rubianes E. New treatments associated with timed artificial insemination in small ruminants. *Reprod Fertil Dev*. (2004) 16:403–13. doi: 10.1071/RD04037

3. Titi HH, Kridli RT, Alnimer MA. Estrus synchronization in sheep and goats using combinations of GnRH, progestagen and prostaglandin F2alpha. *Reprod Domest Anim*. (2010) 45:594–9. doi: 10.1111/j.1439-0531.2008.01309.x

4. Ciornei ŞG, Drugociu D, Ciornei L, Roşca P. Ovarian response to P4-PGF-FSH treatment in Suffolk sheep and P4-PGF-PMSG synchronization in cross-bred ewes, for IVD and ET protocol. *Vet Med Sci*. (2022) 8:726–34. doi: 10.1002/vms3.705

5. Gonźalez-Bulnes A, Baird DT, Campbell BK, Cocero MJ, García-García RM, Inskeep EK, et al. Multiple factors affecting the efficiency of multiple ovulation and embryo transfer in sheep and goats. *Reprod Fertil Dev*. (2004) 16:421–35. doi: 10.1071/RD04033

6. Reyna J, Thomson PC, Evans G, Maxwell WM. Synchrony of ovulation and follicular dynamics in merino ewes treated with GnRH in the breeding and non-breeding seasons. *Reprod Domest Anim*. (2007) 42:410–7. doi: 10.1111/j.1439-0531.2006.00800.x

7. Balaro MF, Fonseca JF, Barbosa TG, Souza-Fabjan JM, Figueira LM, Teixeira TA, et al. Potential role for GnRH in the synchronization of follicular emergence before the superovulatory day 0 protocol. *Domest Anim Endocrinol*. (2016) 54:10–4. doi: 10.1016/j.domaniend.2015.07.002

8. Hameed N, Khan MI, Zubair M, Andrabi SMH. Approaches of estrous synchronization in sheep: developments during the last two decades: a review. *Trop Anim Health Prod*. (2021) 53:485. doi: 10.1007/s11250-021-02932-8

9. Berean D, Bogdan LM, Opris P, Cimpean R. Economical implications and the impact of gonadotropin-releasing hormone administration at the time of artificial insemination in cows raised in the extensive system in North Romania. *Front Vet Sci*. (2023) 10:1167387. doi: 10.3389/fvets.2023.1167387

10. Biehl MV, Ferraz Junior MVC, Ferreira EM, Polizel DM, Miszura AA, Barroso JPR, et al. Effect of reproductive methods and GnRH administration on long-term protocol in Santa Ines ewes. *Trop Anim Health Prod*. (2017) 49:1303–8. doi: 10.1007/s11250-017-1329-1

11. Kutlu M, Dinç DA. The effect of double-dose GnRH injections on reproductive performance parameters following short-term progestagen administration in lactated Awassi ewes during the non-breeding season. *Trop Anim Health Prod*. (2021) 53:277. doi: 10.1007/s11250-021-02735-x

12. Olivera-Muzante J, Fierro S, López V, Gil J. Comparison of prostaglandin- and progesterone-based protocols for timed artificial insemination in sheep. *Theriogenology*. (2011) 75:1232–8. doi: 10.1016/j.theriogenology.2010.11.036

13. Ayaseh M, Mirzaei A, Boostani A, Mehrvarz M. The effect of prostaglandin and gonadotrophins (GnRH and hCG) injection combined with the ram effect on progesterone concentrations and reproductive performance of karakul ewes during the non-breeding season. *Vet Med Sci*. (2021) 7:148–55. doi: 10.1002/vms3.353

14. Olivera-Muzante J, Gil J, Viñoles C, Fierro S. Reproductive outcome with GnRH inclusion at 24 or 36h following a prostaglandin F2α-based protocol for timed AI in ewes. *Anim Reprod Sci*. (2013) 138:175–9. doi: 10.1016/j.anireprosci.2013.02.013

15. Perry GA, Smith MF, Lucy MC, Green JA, Parks TE, MacNeil MD, et al. Relationship between follicle size at insemination and pregnancy success. *Proc Natl Acad Sci USA*. (2005) 102:5268–73. doi: 10.1073/pnas.0501700102

16. Moorey SE, Monnig JM, Smith MF, Ortega MS, Green JA, Pohler KG, et al. Differential transcript profiles in cumulus-oocyte complexes originating from pre-ovulatory follicles of varied physiological maturity in beef cows. *Genes (Basel)*. (2021) 12:893. doi: 10.3390/genes12060893

17. Fernandez J, Bruno-Galarraga MM, Soto AT, de la Sota RL, Cueto MI, Lacau-Mengido IM, et al. Effect of GnRH or hCG administration on day 4 post insemination on reproductive performance in merino sheep of North Patagonia. *Theriogenology*. (2019) 126:63–7. doi: 10.1016/j.theriogenology.2018.12.008

18. Fiehn O. Metabolomics--the link between genotypes and phenotypes. *Plant Mol Biol*. (2002) 48:155–71. doi: 10.1023/A:1013713905833

19. Hong J, Yang L, Zhang D, Shi J. Plant metabolomics: an indispensable system biology tool for plant science. *Int J Mol Sci*. (2016) 17:767. doi: 10.3390/ijms17060767

20. Wishart DS. Emerging applications of metabolomics in drug discovery and precision medicine. *Nat Rev Drug Discov*. (2016) 15:473–84. doi: 10.1038/nrd.2016.32

21. Johnson CH, Ivanisevic J, Siuzdak G. Metabolomics: beyond biomarkers and towards mechanisms. *Nat Rev Mol Cell Biol*. (2016) 17:451–9. doi: 10.1038/nrm.2016.25

22. Zhang X, Han L, Hou S, Raza SHA, Gui L, Sun S, et al. Metabolomics approach reveals high energy diet improves the quality and enhances the flavor of black Tibetan sheep meat by altering the composition of rumen microbiota. *Front Nutr*. (2022) 9:915558. doi: 10.3389/fnut.2022.915558

23. Zhang Z, Shahzad K, Shen S, Dai R, Lu Y, Lu Z, et al. Altering dietary soluble protein levels with decreasing crude protein may be a potential strategy to improve nitrogen efficiency in Hu sheep based on rumen microbiome and metabolomics. *Front Nutr*. (2022) 8:815358. doi: 10.3389/fnut.2021.815358

24. de Sousa EB, Dos Santos GC Jr, Duarte MEL, Moura VN, Aguiar DP. Metabolomics as a promising tool for early osteoarthritis diagnosis. *Braz J Med Biol Res*. (2017) 50:e6485. doi: 10.1590/1414-431x20176485

25. Abril-Parreño L, Krogenæs A, Fair S. Lipidomic profiling of cervical mucus reveals the potential role of pro-inflammatory derived metabolites on sperm transport across the ovine cervix. *Animal*. (2024) 18:101136. doi: 10.1016/j.animal.2024.101136

26. Türk G, Gür S, Sönmez M, Bozkurt T, Aksu EH, Aksoy H. Effect of exogenous GnRH at the time of artificial insemination on reproductive performance of Awassi ewes synchronized with progestagen-PMSG-PGF2alpha combination. *Reprod Domest Anim*. (2008) 43:308–13. doi: 10.1111/j.1439-0531.2007.00896.x

27. Berean D, Ergene O, Blaga-Petrean A, Bogdan I, Ciupe S, Cenariu M, et al. Comparative data about estrus induction and pregnancy rate on lacaune ewes in non-breeding season after melatonin implants and intravaginal progestagen. *Ind J Anim Res*. (2021) 55:517–21. doi: 10.18805/ijar.B-1282

28. Yilmazbas-Mecitoglu G, Karakaya E, Keskin A, Alkan A, Gumen A. Reducing the duration between gonadotropin-releasing hormone (GnRH) and prostaglandin $F_{2\alpha}$ treatment in the Ovsynch protocol to 6 days improved ovulation to second GnRH treatment, but inclined to reduce fertility. *J Dairy Sci*. (2013) 96:3817–24. doi: 10.3168/jds.2012-6496

29. Aybazov M, Selionova M, Trukhachev V, Malorodov V, Yuldashbayev Y, Easa AA. Embryo production and transplantation in non-breeding season of meat sheep breeds by stimulating superovulation with different follicle-stimulating hormone preparations. *Reprod Domest Anim*. (2023) 58:230–7. doi: 10.1111/rda.14279

30. Jeppesen MJ, Powers R. Multiplatform untargeted metabolomics. *Magn Reson Chem*. (2023) 61:628–53. doi: 10.1002/mrc.5350

31. Ghartey J, Anglim L, Romero J, Brown A, Elovitz MA. Women with symptomatic preterm birth have a distinct Cervicovaginal metabolome. *Am J Perinatol*. (2017) 34:1078–83. doi: 10.1055/s-0037-1603817

32. Woessner JF Jr. Catabolism of collagen and non-collagen protein in the rat uterus during post-partum involution. *Biochem J*. (1962) 83:304–14. doi: 10.1042/bj0830304

33. Shimizu K, Maekawa K. Collagen degradation in the mouse uterus during postpartum involution: extracellular pathway. *Acta Anat (Basel)*. (1983) 117:257–60. doi: 10.1159/000145795

34. Belstra BA, Flowers WL, Croom WJ, Degroot J, See MT. Urinary excretion of collagen degradation markers by sows during postpartum uterine involution. *Anim Reprod Sci*. (2005) 85:131–45. doi: 10.1016/j.anireprosci.2004.04.035

35. Rizzo A, Gazza C, Silvestre A, Maresca L, Sciorsci RL. Scopolamine for uterine involution of dairy cows. *Theriogenology*. (2018) 122:35–40. doi: 10.1016/j.theriogenology.2018.08.025

36. Austin SH, Harris RM, Booth AM, Lang AS, Farrar VS, Krause JS, et al. Isolating the role of corticosterone in the hypothalamic-pituitary-gonadal transcriptomic stress response. *Front Endocrinol*. (2021) 12:632060. doi: 10.3389/fendo.2021.632060

37. Zheng HT, Fu T, Zhang HY, Yang ZS, Zheng ZH, Yang ZM. Progesterone-regulated Hsd11b2 as a barrier to balance mouse uterine corticosterone. *J Endocrinol*. (2020) 244:177–87. doi: 10.1530/JOE-19-0349

38. Zheng HT, Zhang HY, Chen ST, Li MY, Fu T, Yang ZM. The detrimental effects of stress-induced glucocorticoid exposure on mouse uterine receptivity and decidualization. *FASEB J*. (2020) 34:14200–16. doi: 10.1096/fj.201902911RR

39. Diao H, Aplin JD, Xiao S, Chun J, Li Z, Chen S, et al. Altered spatiotemporal expression of collagen types I, III, IV, and VI in Lpar3-deficient peri-implantation mouse uterus. *Biol Reprod*. (2011) 84:255–65. doi: 10.1095/biolreprod.110.086942

40. Yue L, Durand M, Lebeau Jacob MC, Hogan P, McManus S, Roux S, et al. Prostaglandin D2 induces apoptosis of human osteoclasts by activating the CRTH2

receptor and the intrinsic apoptosis pathway. *Bone*. (2012) 51:338–46. doi: 10.1016/j.bone.2012.06.003

41. Mori A, Saito M, Sakamoto K, Nakahara T, Ishii K. Intravenously administered vasodilatory prostaglandins increase retinal and choroidal blood flow in rats. *J Pharmacol Sci*. (2007) 103:103–12. doi: 10.1254/jphs.FP0061061

42. Malhotra S, Deshmukh SS, Dastidar SG. COX inhibitors for airway inflammation. *Expert Opin Ther Targets*. (2012) 16:195–207. doi: 10.1517/14728222.2012.661416

43. Burdan F, Chałas A, Szumiło J. Cyklooksygenaza i prostanoidy--znaczenie biologiczne [Cyclooxygenase and prostanoids--biological implications]. *Postepy Hig Med Dosw*. (2006) 60:129–41.

44. Robertson SA, Care AS, Moldenhauer LM. Regulatory T cells in embryo implantation and the immune response to pregnancy. *J Clin Invest*. (2018) 128:4224–35. doi: 10.1172/JCI122182

45. Schramm W, Einer-Jensen N, Brown MB, McCracken JA. Effect of four primary prostaglandins and relaxin on blood flow in the ovine endometrium and myometrium. *Biol Reprod*. (1984) 30:523–31. doi: 10.1095/biolreprod30.3.523

46. Michimata T, Tsuda H, Sakai M, Fujimura M, Nagata K, Nakamura M, et al. Accumulation of CRTH2-positive T-helper 2 and T-cytotoxic 2 cells at implantation sites of human decidua in a prostaglandin D(2)-mediated manner. *Mol Hum Reprod*. (2002) 8:181–7. doi: 10.1093/molehr/8.2.181

frontiers | Frontiers in Veterinary Science

TYPE Original Research
PUBLISHED 19 July 2024
DOI 10.3389/fvets.2024.1434548

OPEN ACCESS

EDITED BY
Stefan Gregore Ciornei,
Iasi, University of Life Science (IULS), Romania

REVIEWED BY
Petru Rosca,
Ion Ionescu de la Brad University of Agricultural Sciences and Veterinary Medicine of Iași, Romania
Christian Hanzen,
University of Liège, Belgium

*CORRESPONDENCE
Shujuan Wang
✉ wangshujuan2012@hotmail.com

RECEIVED 18 May 2024
ACCEPTED 27 June 2024
PUBLISHED 19 July 2024

CITATION
Abulaiti A, Ahsan U, Naseer Z, Ahmed Z, Liu W, Ruan C, Pang X and Wang S (2024) Effect of dietary Chinese herbal preparation on dry matter intake, milk yield and milk composition, serum biochemistry, hematological profile, and reproductive efficiency of Holstein dairy cows in early postpartum period.
Front. Vet. Sci. 11:1434548.
doi: 10.3389/fvets.2024.1434548

Effect of dietary Chinese herbal preparation on dry matter intake, milk yield and milk composition, serum biochemistry, hematological profile, and reproductive efficiency of Holstein dairy cows in early postpartum period

Adili Abulaiti[1,2], Umair Ahsan[3,4], Zahid Naseer[5], Zulfiqar Ahmed[6], Wenju Liu[7], Chongmei Ruan[1], Xunsheng Pang[1] and Shujuan Wang[1,2]*

[1]College of Animal Science, Anhui Science and Technology University, Fengyang, Anhui, China, [2]Anhui Province Key Laboratory of Animal Nutritional Regulation and Health, Fengyang, Anhui, China, [3]Department of Plant and Animal Production, Burdur Vocational School of Food, Agriculture and Livestock, Burdur Mehmet Akif Ersoy University, İstiklal Yerleşkesi, Burdur, Türkiye, [4]Center for Agriculture, Livestock and Food Research, Burdur Mehmet Akif Ersoy University, İstiklal Yerleşkesi, Burdur, Türkiye, [5]Faculty of Veterinary and Animal Sciences, Pir Mehr Ali Shah Arid Agriculture University, Rawalpindi, Pakistan, [6]Faculty of Veterinary and Animal Sciences, University of Poonch, Rawalakot, Azad Jammu and Kashmir, Pakistan, [7]College of Life and Health Science, Anhui Science and Technology University, Fengyang, Anhui, China

The present study investigated the effects of various inclusion levels of dietary Chinese herbal medicine (CHM) preparation on feed consumption, milk yield and milk composition, serum biochemistry, hematological profile, and reproductive efficiency of Holstein dairy cows. A total of 117 lactating Holstein cows were randomly divided into four groups as control ($n = 27$; without CHM supplementation) and treatment groups CHM-0.5 ($n = 31$), CHM-0.75 ($n = 29$), and CHM-1 ($n = 30$) fed diet supplemented with 0.5, 0.75, and 1 kg/cow/d for 30 days, respectively. The study began at d 20 postpartum (d 0 of the study). At d 50 postpartum, the cows in all groups were subjected to estrus synchronization using a modified Ovsynch protocol (GPGMH) and observed for reproductive variables. Feed intake, milk yield and milk composition, serum biochemistry and hematological profile, and reproductive efficiency were measured. A significantly higher milk yield with improved milk lactose, milk protein and milk fat were found in the CHM-0.75 group compared to the other groups ($p < 0.05$). Besides, the estrus response, ovulation rate, ovulatory follicle diameter, and pregnancy rate increased in CHM-0.75 compared to CHM-0 or CHM-0.5 group ($p < 0.05$). The serum metabolites (glucose, AST, arginine, BUN, and NO) showed variations among the treatment groups at different time points (synchronization, AI, or post-AI). In conclusion, CHM supplementation improves the milk yield, milk composition, and serum metabolites in dairy cows. Daily supplementation of 0.75 kg CHM before the GPGMH protocol application enhances the reproductive traits in dairy cows under summer conditions.

KEYWORDS

Holstein cows, Chinese herbal medicine, modified GPGMH Ovsynch synchronization, milk production, reproductive performance

1 Introduction

In recent years, animal production in China has developed rapidly and it has become a key component of the agriculture sector. High-density large-scale commercial farming and intensive breeding paradigm lead to the deterioration of animal physiology. For efficient growth and maintenance of productivity, feed antibiotics were a common practice for the prevention and cure of animal diseases. The excessive use of antibiotics in livestock production amplified the antimicrobial resistance, high antibiotics residues in animal products and environmental contamination that negatively affected public health (1). Consequently, the use of in-feed antibiotics was banned in the European Union in 2006 followed by further ban in different countries across the globe. This attracted the development of alternatives for use in animal diets. In this scenario, Chinese herbal medicine (CHM) preparations have received considerable attention in recent years than synthetic feed additives. Due to the versatile composition of CHM preparations, several attempts have been made to replace antibiotics. The CHM preparations contain polysaccharides, vitamins, alkaloids, amino acids, saponins and act as immune enhancers, anti-stress agents, and hormone-like agents, insect repellents, galactagogues, and disease control agents (2). Previous studies have documented the beneficial effects of dietary CHM on growth, feed utilization, reproductive performance, and quality of animal products (3).

These preparations can boost anabolism and digestion by increasing the absorption of nutrients during the growth phase. Dietary supplementation of calf starter diet with CHM (four main Chinese herbs, i.e., *Leonurus cardiaca*, *Taraxacum officinale*, *Ligustrum lucidum*, and *Hordeum vulgare*) enhanced the rumen environment and improve the daily weight gains of calves (4). Similarly, piglets fed traditional CHM synergized with probiotics in grower-finisher ration had greater average daily gain (5). The CHM not only improve the growth but also enhance the reproductive efficiency of dairy cows (6) and sows (7). The use of other herbs, such as *Agaricus bisporus*, *Acorus tatarinowii*, *Wolfiporia extensa*, *Bupleurum falcatum*, *Crataegus monogyna Jacq.,* and *Agastache rugosa* also improved the feed intake in cows (8, 9). The ingestion of *Crataegus monogyna* and dried tangerine peel is greater in cows due to its attractive aroma. Additionally, the growth and development of mammary glands, increment in hormones levels, and improved lactation were significant outcomes of feeding CHM as supplements (10). A formulation with *Glycyrrhiza glabra, Astragalus L. (Fabaceae),* and *Gardenia jasminoides* successfully cured the subclinical mastitis in cows (11).

Keeping in view the beneficial effects of different CHM on cow health and production (12), we hypothesized that the inclusion of CHM in diets for dairy cows in early postpartum period might be useful to improve the growth, milk yield, and reproductive efficiency of dairy cows by improving the feed intake, digestibility, and nutrients absorption. Therefore, the present study was designed to evaluate the effects of a CHM preparation on the uterine involution rate, dry matter intake and blood metabolites, milk yield and composition, and reproductive performance of lactating Holstein cows in early postpartum period.

2 Materials and methods

Before execution of the study, an approval was obtained from the Animal Experimental Ethical Inspection of Laboratory Animal Centre, Huazhong Agricultural University, Wuhan (HZAUCA-2018-004). All the experimental protocols were performed according to the guidelines of the Committee of Animal Research Institute of the university.

2.1 Location and climatic conditions

The study was conducted during the summer season (July 12, 2022, to August 30, 2022) at Hebei JunYing dairy farm Co., Ltd. Hebei province (30°32′N, 111°5′E), China. The farm is geographically located in a subtropical monsoon region with average temperatures ranging from 1 to 5°C in winter and 27 to 35°C during summer (reaching up to 40°C sometimes in July and August months). During the study period, the average temperature was 36.5 ± 0.2°C, relative humidity 79.0 ± 1.1%, and temperature-humidity index (THI) was 91.0 ± 0.3. The observed THI level showed intense heat stress for dairy cows maintained in Hubei province.

2.2 Chinese herbal medicine

The CHM used in this study was based on Shi-Quan Da Bu Decoction procedures (13). The CHM contained the extracts of plants (*Eucommia ulmoides*, *A. L.* (Fabaceae), *Codonopsis pilosula*, *Angelica archangelica*, Atractylodes amurensis *G. glabra*, *Ligusticum striatum*, *W. extensa*, and *Pueraria montana*) extracted twice in the aqueous medium. The extracts were subjected to fermentation using *Lactobacillus acidophilus* (0.2×10^8 CFU/g), *Lactobacillus plantarum* (0.2×10^8 CFU/g), *Bacillus subtilis* (0.2×10^8 CFU/g), *Bacillus coagulans* (0.2×10^8 CFU/g), *Bacillus licheniformis* (0.2×10^8 CFU/g), *Enterococcus faecalis* (0.2×10^8 CFU/g), and *Saccharomyces cerevisiae* (0.2×10^8 CFU/g). All these ingredients were fermented (anaerobic) followed by cold granulation to prepare the fermented granules of CHM additive (Cat. C6H10N205, Longxi Huachuang Biotechnology Co. Ltd. Dingxi, Gansu province, China) used in the present study. The CHM preparation was characterized by total flavonoids, polyphenols, glycyrrhetinic acid, saponins, polysaccharides, and acids. Detailed nutritional composition and physicochemical properties of CHM have been presented in Table 1.

TABLE 1 Chemical composition and physicochemical properties of Chinese herbal medicine used in the study.

Item	Description	Item	Concentration
Color	Dark brown	Flavonoids, mg/kg	500
Odor	Medicinal aroma	Polyphenols, mg/kg	500
Total viable bacteria	5.4×10^8 cfu/g	Carotenoids, mg/kg	50
Aflatoxin B1	Not detected	Polysaccharides, g/kg	20
Escherichia coli	Not detected	Total acids, g/kg	38
Salmonella	Not detected	Saponins, g/kg	17
Lead	Not detected	Glycyrrhetinic acid, g/kg	2
Fluoride, mg/kg	12	Moisture, %	39.2
Arsenic, mg/kg	0.419	Ash, %	4.2
Mercury, mg/kg	0.036	Crude protein, %	8.6
Lactic acid bacteria, cfu/g	1.3×10^7	Crude fiber, %	25.9
Total mold count, cfu/g	1.8×10^3	Starch, %	2.18
		Crude fat, %	2.4

2.3 Study design

A total of one hundred and seventeen ($n = 117$) multiparous Holstein dairy cows in early postpartum period, aged between 4 and 7 years, were randomly divided into four experimental groups 20 days after parturition, i.e., control/CHM-0 ($n = 27$; without CHM supplementation), CHM-0.5 ($n = 31$; CHM 0.5 kg/cow/d), CHM-0.75 ($n = 29$; CHM 0.75 kg/cow/d), and CHM-1 ($n = 30$; CHM 1 kg/cow/d). Cows used in this study had moderate body condition score (3.4 ± 0.6) with average body weight of 578.1 ± 86.5 kg. The measured daily dose of CHM for each respective group was first sprinkled over concentrate, homogeneously mixed in total mixed ration (TMR) wagon with other ingredients and offered to the cows. Dietary supplementation of CHM was carried out twice a day. Measured daily dose of each group was divided into two and fed after mixing in morning and evening TMR meals. After each meal, it was ensured that each cow had consumed the approximate dose of CHM properly. The cows were supplemented with CHM for 30 days starting from d 20 of calving (d 0 of the study).

2.4 Management conditions

Cows were housed in a semi-intensive shed with cemented rooftop and the shed was fenced by galvanized wire mesh on two sides. Ventilation and cooling in the summer was provided by two exhaust fans and sprinklers installed inside the shed. Cows were fed a TMR twice a day (morning and evening) formulated according to the nutrient requirements of dairy cows (Table 2) recommended by NRC (2001) in an open feeding system. Cows had *ad libitum* access to fresh and clean water.

2.5 Dry matter intake

Dry matter intake (DMI) of cows was measured based on the feed consumption computed from the difference of amounts of daily feed offered and orts each day. Feed not consumed was weighed before the morning feeding. The DMI was calculated using the dry matter content of the diet and amount of feed consumed.

2.6 Fecal composition

At d 0, d 15, and d 30, cows ($n = 8$) were randomly selected from each group and feces were collected directly from the rectum of the cows and analyzed for dry matter (DM), crude protein (CP), acid detergent fiber (ADF), neutral detergent fiber (NDF), lignin, starch, total fatty acids (TFA), crude ash, Ca, P, Mg, and K using methods previously described in detail by Association of Official Analytical Chemists (14).

2.7 Milk yield and milk composition

Cows were milked thrice a day (at 06:00, 14:00, and 20:00) by machine milking throughout the supplementation period and the milk yield was recorded using carefully calibrated jars. Milk composition was analyzed on d 0, d 15 and d 30 of CHM supplementation using milk analyzer (MilkoScan Type 78,110; Foss A/S, Hillerød, Denmark).

2.8 Serum biochemistry, immunoglobulins, and hematological profile

Blood samples were randomly collected from the coccygeal veins of 5 cows in each group on d 0, d 15 and d 30 of CHM supplementation to evaluate the serum biochemistry (without anticoagulant) and hematologic profile (with anticoagulant) of dairy cows. Serum was separated by centrifugation after the clotting and subjected to analysis of alanine aminotransferase (ALT), aspartate aminotransferase (AST), total protein (TP), albumin (ALB), globulin (GLB), alkaline phosphatase (ALP), γ-glutamyl transpeptidase (GGT), lactate dehydrogenase (LDH), total bilirubin (TBIL), creatine kinase (CK), amylase, total bile acid (TBA), glucose (GLU), total cholesterol (CHOL), uric acid (UA), blood urea nitrogen (BUN), creatinine (CREA), triglyceride (TG), potassium (K), sodium (Na), chloride (Cl),

TABLE 2 Composition of basal total mixed ration fed to the Holstein dairy cows (as fed basis).

Item	%
Corn silage	48.02
Concentrate	24.98
Alfalfa	10.19
Corn, flaked	4.68
Oats, flaked	3.24
Whole cottonseed	3.60
Sugar beet pulp, pelleted	3.60
Soybean, puffed	0.96
Rumen bypass fat	0.36
Probiotics	0.19
Rumen protected glucose	0.12
Sodium bicarbonate	0.06
Nutritional composition (%, dry matter basis)	
Net energy for lactation, MJ/kg	7.21
Crude protein	13.81
Crude fat	4.49
Neutral detergent fiber	31.08
Phosphorus	0.31
Calcium	0.40

calcium (Ca), phosphorus (P), and magnesium (Mg) using commercial kits (Beijing Beijing Xinchuangyuan Biotechnology Co. Ltd., China) followed by reading in an automatic biochemical analyzer (TBA-120FR Auto Clinical Chemistry Analyzer, Toshiba Corporation, Tokyo, Japan).

Serum immunoglobulins A (IgA), G, (IgG), and M (IgM) were quantified by single radial immune diffusion method using commercially available kits for IgA, IgG, and IgM (Beijing North Biotechnology Research Institute Co., Ltd., Beijing, China).

Blood samples were subjected to automatic blood analyzer (Beckman Coulter Blood Routine Analyzer, Beckman Coulter Trading Co. Ltd. China) for hematological profile of dairy cows in terms of complete blood count.

2.9 Application of modified ovarian synchronization protocol

After 50 days of calving, a modified Ovsynch protocol (GPGMH) was used to synchronize the cows (15). Briefly, the first injection of gonadotropin-releasing hormone (GnRH 200 μg, Ningbo Sansheng Pharmaceutical Industry Co., Ltd., Ningbo, Zhejiang, China) was given to all the cows on day 0, an injection of PGF2α (0.5 mg, Ningbo Sansheng Pharmaceutical Industry Co., Ltd., Ningbo, Zhejiang, China) on day 7 of protocol and second dose of GnRH (200 μg) and mifepristone (0.4 mg/kg, IM, Hubei Yun Cheng Sai Technology, China) day 9 of protocol. The cows were inseminated artificially (AI) within 24 h of the 2nd GnRH dose. Moreover, the estrus signs (vaginal mucous discharge, bellowing, excitation, swollen vagina, and mounting behavior) were observed physically twice daily. An injection of human chorionic gonadotropin (hCG 2000 IU; Ningbo Sansheng Pharmaceutical Industry Co., Ltd., Ningbo, Zhejiang, China) was also administered to each cow on day 5 of AI (Figure 1).

Ultrasound scanner (WED-9618-v, Shenzhen Well.D Medical Electronics Co. Ltd., Guangdong, China) equipped with rectal probe (LV2-3/6.5 MHz) was used to monitor follicular dynamics twice daily (between 6 to 12th day of protocol). Ovulation was recorded by the sudden disappearance of dominant follicles between subsequent ultrasonographic examinations. Pregnancy diagnosis was made rectally by ultrasound scanner on the 35th day after AI, confirming fetal presence and viability.

2.10 Evaluation of uterine involution rate

Sixty-two postpartum cows (Among them, 12 cows were suffereing from uterine infections and 50 cows were uterine diseases) were monitored for uterine recovery during the CHM supplementation time. The rectal ultrasonography of the uterus was undertaken with a B-mode veterinary ultrasound scanner (LV2-2/6.5 MHZ, linear array transducer, Shenzhen, China). Photographs of the uterus were transferred to a computer workstation for analysis to assess the extent of uterine involution at different postpartum days according to the method established in our laboratory (16). Before the examination, the feces were gently removed from the rectum, the probe was inserted, and placed on the uterus. The same operator performed all ultrasound examinations to avoid system errors.

2.11 Statistical analysis

All the data were tested for normality using Shapiro–Wilk's test. Non-normalized variables were transformed by logarithmic or square-root transformation for normalization. The data related to DMI, fecal composition, body weight gain of calves, milk yield and milk composition, serum biochemistry, hematological profile, and reproductive traits were subjected to one-way analysis of variance (ANOVA) followed by Duncan's multiple range test as post-hoc test. Chi-square test was applied to analyze the data of estrus, ovulation, and pregnancy. Differences among the groups were assumed significant at 95% confidence interval ($p < 0.05$). All the statistical analyses were applied in a statistical package SPSS (version 24.0; IBM Corp., Armonk, NY, United States). Results were presented as mean ± standard deviation.

3 Results

3.1 Dry matter intake and fecal composition

The DMI of Holstein dairy cows fed different levels of dietary CHM has been shown in Table 3. The DMI was greater in CHM-0.5 and CHM-0.75 groups at d 0, CHM-0.75 at d 7, d 28, and d 36 compared to other dietary treatments ($p < 0.05$). In general, DMI increased in CHM-0.5 and CHM-0.75 groups whereas, no significant change in DMI was seen in other groups.

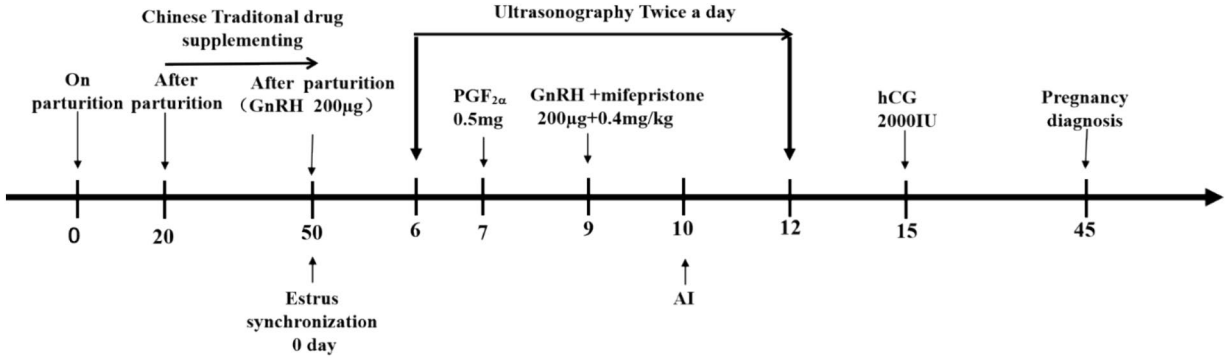

FIGURE 1
Timeline of the Chinese herbal medicine supplementation and the modified Ovsynch synchronization protocol.

TABLE 3 Dry matter intake (kg) of Holstein dairy cows fed different levels of dietary Chinese herbal medicine in early postpartum period.

Day	Control	CHM-0.5[1]	CHM-0.75[1]	CHM-1[1]
7	21.2 ± 0.7^{Bab}	19.8 ± 2.1^{Bb}	22.2 ± 0.9^{Ba}	21.5 ± 0.3^{ab}
14	21.8 ± 0.4^{B}	21.1 ± 1.9^{AB}	22.4 ± 0.5^{B}	21.9 ± 0.9
28	22.3 ± 0.4^{Aab}	21.4 ± 0.6^{ABb}	23.6 ± 1.0^{Aa}	21.8 ± 0.4^{b}
36	22.6 ± 0.3^{Ab}	22.2 ± 0.7^{Ab}	23.5 ± 0.2^{Aa}	22.1 ± 0.3^{b}

[a,b]Means with different superscripts in the same row are significantly different ($p < 0.05$). [A,B]Means with different superscripts in the same column against the same variable are significantly different ($p < 0.05$). [1]CHM-0.5 = 0.5 kg CHM; CHM-0.75 = 0.75 kg CHM; CHM-1 = 1 kg CHM.

Table 4 shows the fecal composition of dairy cows fed diets supplemented with different levels of dietary CHM. Fecal composition of Holstein dairy cows in early postpartum period remained unaffected across the groups except crude ash which was greater in CHM-0.75 group than CHM-1 group at d 15 ($p < 0.05$).

3.2 Milk yield and milk composition

Milk yield of Holstein dairy cows fed different supplemental levels of CHM in early postpartum period has been presented in Table 5. Dietary supplementation of different levels of CHM had no effect on the milk yield of dairy cows at d 0, d 5, d 15, d 20, and d 25 after parturition. However, CHM-0.75 group had greater milk yield than CHM-1 group at d 10 ($p = 0.001$) and control group at d 30 ($p = 0.040$) after parturition.

Milk composition of Holstein dairy cows fed different levels of dietary CHM in early postpartum period has been depicted in Table 6. Supplemental CHM had no effect on milk fat, milk protein, lactose, and somatic cell count. Total solids were greater in CHM-0.5 group compared to other groups at d 15 ($p < 0.05$) and compared to CHM-0.75 and CHM-1 groups at d 30 ($p < 0.05$). Supplemental CHM-0.5 increased the solids not fat compared to CHM-0.75 and CHM-1 groups at d 30 ($p < 0.05$). Milk urea nitrogen was greater in control group than CHM-0.5 group ($p < 0.05$).

3.3 Correlation analysis of treatment and parity effects on production performance

The correlation analysis results for the impact of group, parity, lactation days, and their interactions on milk production elucidate that the treatment and parity significantly influence milk production in Holstein dairy cows during the early postpartum period. The interaction effects of treatment*parity and DIM2*parity were not statistically significant (Table 7).

3.4 Serum biochemistry

Table 8 shows the serum biochemical indices of Holstein dairy cows fed different levels of dietary CHM in early postpartum period. Serum IgG was greater in CHM-0.75 supplemented group compared to the control group at d 15 ($p < 0.05$) while, IgA and IgM remained unaffected across the groups. Serum ALT, AST, ALB, ALP, LDH, TBA, uric acid, TG, and K were not different among the groups at any observation. Serum TP was lower in CHM-0.5 group than other groups at d 15 ($p < 0.05$) and compared to CHM-0.75 group at d 30 ($p < 0.05$). Cows in control and CHM-0.75 group had greater serum GLB than those in CHM-0.5 group at d 15 ($p < 0.05$) whereas, CHM-0.75 group had greater serum GLB in comparison with CHM-1 group at d 30 ($p < 0.05$). Serum TBIL was greatest ($p < 0.05$) in CHM-0.5 and CHM-1 groups at d 15 and d 30, respectively. At d 15 and d 30, serum GGT was lowest ($p < 0.05$) in CHM-0.5 and CHM-1 groups, respectively. Cows in CHM-0.5 group had greater serum CK than CHM-0.75 and CHM-1 groups at d 15 ($p < 0.05$), whereas no difference was seen among the groups at d 30. Supplemental CHM-0.5 lowered the serum amylase at d 30 compared to control group ($p < 0.05$). At d 30, supplemental CHM-1 lowered the BUN compared to the control group ($p < 0.05$). Serum CREA was greater in CHM-0.5 group at d 15 in comparison with other groups ($p < 0.05$). Supplemental CHM-0.5 lowered the serum CHOL at d 15 ($p < 0.05$) whereas, serum CHOL was greater in control and CHM-0.75 group than other groups at d 30 ($p < 0.05$). Cows fed CHM-0.5 diets had lower serum Na levels than other groups at d 15 ($p < 0.05$), however, it was lower in all groups at d 30 except CHM-0.75 group ($p < 0.05$). Serum Cl levels were greater in

10.3389/fvets.2024.1434548

TABLE 4 Fecal composition of Holstein dairy cows fed different levels of dietary Chinese herbal medicine in early postpartum period.

Item	Day	Control	CHM-0.5[1]	CHM-0.75[1]	CHM-1[1]
Moisture, %	0	82.1 ± 0.8	81.9 ± 0.5	84.9 ± 0.7	85.2 ± 1.6
	15	86.1 ± 0.9	83.9 ± 2.4	85.7 ± 1.8	86.2 ± 1.5
	30	85.3 ± 1.3	84.9 ± 2.1	85.4 ± 1.7	82.9 ± 4.7
Crude protein, g/kg	0	15.4 ± 2.6	15.1 ± 2.2	15.9 ± 1.2	14.75 ± 1.1
	15	17.7 ± 2.4	17.0 ± 1.9	17.3 ± 1.9	17.0 ± 1.1
	30	16.2 ± 1.8	16.5 ± 4.9	15.1 ± 1.7	16.3 ± 2.5
Acid detergent fiber, g/kg	0	38.9 ± 2.8	38.1 ± 3.3	39.1 ± 2.4	37.5 ± 4.1
	15	40.6 ± 2.5	41.4 ± 4.2	41.5 ± 3.8	38.9 ± 3.7
	30	39.9 ± 3.2	39.7 ± 6.7	40.4 ± 2.4	38.3 ± 5.0
Neutral detergent fiber, g/kg	0	55.4 ± 4.8	54.3 ± 4.6	53.9 ± 2.9	52.2 ± 4.5
	15	56.8 ± 4.1	56.2 ± 4.5	56.2 ± 5.6	56.0 ± 3.9
	30	56.9 ± 5.0	55.9 ± 10.1	57.6 ± 2.3	52.9 ± 5.2
Lignin, g/kg	0	9.1 ± 0.6	9.4 ± 1.1	9.9 ± 1.1	9.1 ± 1.5
	15	10.9 ± 0.6	10.6 ± 1.1	11.3 ± 1.3	10.3 ± 1.3
	30	9.9 ± 0.7	9.6 ± 1.9	9.8 ± 0.9	10.0 ± 1.1
NDF after 240 h, g/kg	0	47.5 ± 2.1	49.2 ± 4.9^{B}	47.2 ± 5.4	47.4 ± 5.9^{B}
	15	48.8 ± 2.3	50.9 ± 4.6^{B}	48.0 ± 5.0	45.8 ± 6.1^{B}
	30	51.4 ± 1.1	57.0 ± 7.7^{A}	51.9 ± 2.9	54.6 ± 6.4^{A}
Starch, g/kg	0	1.5 ± 0.6^{B}	2.5 ± 0.6	2.0 ± 1.2^{B}	1.6 ± 0.7^{B}
	15	1.6 ± 0.5^{B}	2.5 ± 0.5	1.9 ± 1.1^{B}	1.8 ± 0.7^{B}
	30	3.3 ± 1.9^{A}	2.8 ± 1.7	3.3 ± 0.6^{A}	4.5 ± 3.2^{A}
Total fatty acids, g/kg	0	2.1 ± 0.2	2.4 ± 0.8	2.3 ± 0.9	4.0 ± 3.2
	15	2.5 ± 0.6	2.5 ± 0.8	2.6 ± 1.1	4.1 ± 2.9
	30	2.2 ± 0.5	2.7 ± 0.7	2.5 ± 0.6	4.1 ± 3.1
Ash, g/kg	0	10.4 ± 1.5	11.2 ± 1.5	11.9 ± 1.2	8.8 ± 0.6^{B}
	15	10.6 ± 1.5^{ab}	11.4 ± 1.6^{ab}	12.2 ± 2.2^{a}	8.9 ± 0.6^{Bb}
	30	12.0 ± 0.5	13.1 ± 1.7	13.1 ± 1.4	13.7 ± 4.6^{A}
Ca, mg/kg	0	1.8 ± 0.1	1.7 ± 0.4	2.0 ± 0.2	2.1 ± 0.4
	15	2.1 ± 0.2	2.1 ± 0.4	2.1 ± 0.5	2.2 ± 0.4
	30	1.9 ± 0.2	1.9 ± 0.7	2.1 ± 0.2	2.4 ± 0.5
P, mg/kg	0	0.6 ± 0.2	0.6 ± 0.1	0.8 ± 0.1	0.7 ± 0.2
	15	0.8 ± 0.2	0.7 ± 0.2	0.9 ± 0.2	0.8 ± 0.1
	30	0.6 ± 0.1	0.7 ± 0.2	0.7 ± 0.1	0.8 ± 0.2
Mg, mg/kg	0	0.6 ± 0.1	0.7 ± 0.1	0.6 ± 0.2	0.6 ± 0.1
	15	0.7 ± 0.1	0.6 ± 0.1	0.6 ± 0.2	0.7 ± 0.2
	30	0.8 ± 0.1	0.6 ± 0.2	0.8 ± 0.1	0.8 ± 0.2
K, mg/kg	0	0.7 ± 0.1	0.8 ± 0.2	0.7 ± 0.1	0.7 ± 0.2
	15	0.7 ± 0.1	0.8 ± 0.1	0.8 ± 0.1	0.9 ± 0.1
	30	0.8 ± 0.2	0.9 ± 0.2	0.9 ± 0.1	0.8 ± 0.2

[a,b]Means with different superscripts in the same row are significantly different ($p < 0.05$). [A,B]Means with different superscripts in the same column against the same variable are significantly different ($p < 0.05$). [1]CHM-0.5 = 0.5 kg CHM; CHM-0.75 = 0.75 kg CHM; CHM-1 = 1 kg CHM.

CHM-0.75 group than CHM-0.5 group at d 30 ($p < 0.05$). At d 15, cows in CHM-0.5 group had lower serum Ca levels than those in other groups ($p < 0.05$) whereas, control and CHM-0.75 had greater serum Ca levels than CHM-0.5 and CHM-1 groups at d 30 ($p < 0.05$). Lower serum Mg levels were seen in CHM-1 group compared to control and CHM-0.75 groups at d 30 ($p < 0.05$). Cows in CHM-0.5 group had lowest serum P levels at d 15 in comparison with those in other groups ($p < 0.05$).

TABLE 5 Milk yield (kg) of Holstein dairy cows fed different levels of dietary Chinese herbal medicine in early postpartum period.

Day	Control	CHM-0.5[1]	CHM-0.75[1]	CHM-1[1]	*p*-value
0	24.6 ± 6.3	25.0 ± 7.9	23.5 ± 7.4	21.7 ± 7.3	0.181
5	22.5 ± 6.8	25.7 ± 6.8	24.3 ± 6.7	22.9 ± 7.9	0.216
10	23.4 ± 7.7^{ab}	26.0 ± 5.6^{ab}	28.1 ± 7.1^{a}	20.2 ± 6.6^{b}	0.001
15	23.1 ± 9.9	26.2 ± 10.5	24.1 ± 12.3	23.3 ± 11.0	0.809
20	22.9 ± 8.3	28.8 ± 8.8	24.7 ± 6.5	26.4 ± 8.5	0.203
25	22.5 ± 3.8	23.1 ± 6.5	26.1 ± 7.1	22.7 ± 6.3	0.243
30	24.4 ± 4.6^{b}	27.2 ± 5.3^{ab}	31.6 ± 6.1^{a}	28.5 ± 7.9^{ab}	0.040

^{a,b}Means with different superscripts in the same row are significantly different ($p < 0.05$). [1]CHM-0.5 = 0.5 kg CHM; CHM-0.75 = 0.75 kg CHM; CHM-1 = 1 kg CHM.

TABLE 6 Milk composition of Holstein dairy cows fed different levels of dietary Chinese herbal medicine in early postpartum period.

Item	Days	Control	CHM-0.5[1]	CHM-0.75[1]	CHM-1[1]
Milk fat, %	0	2.2 ± 0.2^{B}	4.1 ± 2.5^{B}	3.2 ± 1.4^{B}	2.0 ± 0.3^{B}
	15	2.1 ± 0.5^{B}	4.5 ± 3.3^{B}	3.2 ± 1.6^{B}	2.5 ± 0.6^{B}
	30	3.6 ± 1.4^{A}	4.6 ± 1.1^{A}	3.4 ± 1.9^{A}	3.5 ± 1.2^{A}
Milk protein, %	0	3.3 ± 0.3	4.5 ± 1.2	3.8 ± 0.4	3.6 ± 0.6
	15	3.6 ± 0.6	5.9 ± 3.3	3.6 ± 0.4	3.8 ± 0.5
	30	3.4 ± 0.4	4.2 ± 1.1	4.6 ± 3.1	3.5 ± 0.6
Lactose, %	0	4.3 ± 0.4	4.5 ± 0.7	4.8 ± 0.7	5.0 ± 0.2
	15	4.6 ± 0.6	4.2 ± 0.7	5.1 ± 0.5	4.9 ± 0.7
	30	4.5 ± 0.6	4.6 ± 0.3	5.0 ± 0.4	4.7 ± 0.3
Total solids, %	0	11.7 ± 0.5^{b}	15.1 ± 2.1^{a}	12.5 ± 1.6^{b}	11.5 ± 1.0^{b}
	15	11.9 ± 0.6^{b}	15.8 ± 3.4^{a}	12.1 ± 2.0^{b}	11.6 ± 0.9^{b}
	30	19.7 ± 4.1^{a}	19.7 ± 2.5^{a}	15.5 ± 2.9^{b}	16.6 ± 3.5^{b}
Solids not fat, %	0	9.1 ± 0.5	9.9 ± 1.1	9.3 ± 0.7	9.5 ± 0.6
	15	9.3 ± 0.5	11.2 ± 3.4	8.9 ± 0.8	9.4 ± 0.6
	30	10.2 ± 2.9^{ab}	10.1 ± 0.9^{a}	8.8 ± 0.7^{b}	9.0 ± 0.5^{b}
Milk urea nitrogen, mg/dL	0	16.1 ± 2.4^{B}	15.8 ± 1.6	17.3 ± 3.1^{B}	19.1 ± 3.3
	15	16.1 ± 3.1^{B}	18.5 ± 5.7	17.6 ± 3.2^{B}	18.4 ± 3.1
	30	26.9 ± 7.9^{Aa}	15.9 ± 6.2^{b}	21.9 ± 5.8^{Aab}	20.4 ± 5.4^{ab}
Somatic cell count, 10^3/mL	0	215.2 ± 35.7	190.4 ± 29.1	207.5 ± 25.6	201.8 ± 70.4
	15	210.4 ± 34.5	189.7 ± 29.1	202.8 ± 33.6	198.6 ± 27.1
	30	196.6 ± 34.7	178.2 ± 32.3	183.2 ± 18.7	173.8 ± 20.6

^{a,b}Means with different superscripts in the same row are significantly different ($p < 0.05$). ^{A,B}Means with different superscripts in the same column against the same variable are significantly different ($p < 0.05$). [1]CHM-0.5 = 0.5 kg CHM; CHM-0.75 = 0.75 kg CHM; CHM-1 = 1 kg CHM.

TABLE 7 Correlation analysis of group, parity, lactation days and interaction on milk production of Holstein dairy cows fed different levels of dietary Chinese herbal medicine in early postpartum period.

Main effects and interactions	χ^2-value	*F*-value	*p*-value
Treatment	10.64	3.55	0.014
Parity	7.96	3.98	0.019
Treatment*parity	2.67	0.53	0.750
DIM2	0.08	0.04	0.959
Treatment*DIM2	4.08	1.02	0.395
DIM2*parity	8.14	2.04	0.087
Treatment*DIM2*parity	0.19	0.10	0.908

10.3389/fvets.2024.1434548

TABLE 8 Serum biochemistry of Holstein dairy cows fed different levels of dietary Chinese herbal medicine in early postpartum period.

Item[1]	Day	Control	CHM-0.5[2]	CHM-0.75[2]	CHM-1[2]
Immune function tests					
IgG, g/L	0	8.6 ± 0.7^{b}	9.3 ± 1.4^{ab}	11.3 ± 0.5^{a}	10.1 ± 1.3^{ab}
	15	9.1 ± 3.0^{b}	9.9 ± 2.4^{ab}	11.3 ± 2.4^{a}	10.4 ± 0.6^{ab}
	30	9.8 ± 0.9^{b}	10.6 ± 1.5^{ab}	11.6 ± 0.7^{a}	10.9 ± 1.7^{ab}
IgA, g/L	0	0.6 ± 0.1	0.8 ± 0.1	0.7 ± 0.1	0.6 ± 0.2
	15	0.6 ± 0.3	0.7 ± 0.2	0.8 ± 0.3	0.7 ± 0.1
	30	0.7 ± 0.1	0.8 ± 0.2	0.8 ± 0.1	0.8 ± 0.1
IgM, g/L	0	2.3 ± 0.3	2.6 ± 0.5	2.6 ± 0.2	2.4 ± 0.3
	15	2.4 ± 0.6	2.6 ± 0.5	2.8 ± 0.5	2.5 ± 0.1
	30	2.5 ± 0.5	2.8 ± 0.6	2.8 ± 0.1	2.8 ± 0.5
Liver function tests					
ALT, U/L	0	13.4 ± 7.0^{B}	7.3 ± 1.7^{B}	17.9 ± 7.5^{B}	9.3 ± 2.1^{B}
	15	23.2 ± 3.1^{A}	22.4 ± 5.0^{A}	27.2 ± 4.8^{A}	22.4 ± 7.8^{A}
	30	14.4 ± 11.0^{B}	7.4 ± 2.7^{B}	18.4 ± 6.8^{B}	9.2 ± 2.2^{B}
AST, U/L	0	44.9 ± 36.1^{B}	45.8 ± 35.6^{B}	44.5 ± 26.8^{B}	53.5 ± 21.1^{B}
	15	83.6 ± 15.9^{A}	91.2 ± 17.8^{A}	81.0 ± 17.6^{A}	95.8 ± 31.9^{A}
	30	49.8 ± 32.1^{B}	51.8 ± 27.5^{B}	51.8 ± 24.5^{B}	62.4 ± 20.4^{A}
TP, g/L	0	40.6 ± 25.6^{B}	23.7 ± 5.6^{B}	51.5 ± 19.8^{B}	25.3 ± 5.2^{B}
	15	83.2 ± 10.8^{Aa}	60.1 ± 4.8^{Ab}	83.0 ± 12.1^{Aa}	77.1 ± 5.0^{Aa}
	30	43.7 ± 23.5^{Bab}	25.7 ± 7.9^{Bb}	54.4 ± 16.8^{Ba}	28.7 ± 4.7^{Bab}
ALB, g/L	0	18.6 ± 7.6^{B}	11.6 ± 4.2^{B}	23.4 ± 8.7^{B}	14.6 ± 3.3^{B}
	15	32.2 ± 3.0^{A}	34.7 ± 2.5^{A}	34.5 ± 3.2^{A}	35.9 ± 3.0^{A}
	30	19.6 ± 8.8^{B}	12.2 ± 3.9^{B}	24.4 ± 7.9^{B}	16.6 ± 2.9^{B}
GLB, g/L	0	23.5 ± 16.7^{B}	12.5 ± 7.3^{B}	28.95 ± 11.9^{B}	11.6 ± 2.1^{B}
	15	51.0 ± 10.2^{Aa}	25.4 ± 2.7^{Ab}	48.5 ± 13.7^{Aa}	41.1 ± 4.9^{Aab}
	30	24.0 ± 15.1^{Bab}	13.5 ± 4.4^{Bab}	30.0 ± 10.6^{Ba}	12.1 ± 2.2^{Bb}
ALB:GLB	0	0.8 ± 0.1	0.8 ± 0.1^{B}	0.8 ± 0.4	1.3 ± 0.2^{A}
	15	0.7 ± 0.1^{b}	1.4 ± 0.1^{Aa}	0.8 ± 0.3^{b}	0.9 ± 0.2^{Bb}
	30	0.9 ± 0.2^{b}	0.9 ± 0.2^{Bb}	0.9 ± 0.4^{b}	1.4 ± 0.2^{Aa}
TBIL, μmol/L	0	0.3 ± 0.1^{B}	0.3 ± 0.2^{B}	0.65 ± 0.4^{B}	3.4 ± 1.1^{A}
	15	1.1 ± 0.6^{Ab}	6.9 ± 5.4^{Aa}	1.1 ± 0.5^{Ab}	1.6 ± 1.1^{Bb}
	30	0.4 ± 0.2^{Bb}	0.4 ± 0.3^{Bb}	0.7 ± 0.5^{Bb}	3.5 ± 1.1^{Aa}
ALP, U/L	0	24.0 ± 21.0^{B}	18.8 ± 17.5^{B}	40.6 ± 43.1^{B}	22.8 ± 14.8^{B}
	15	65.4 ± 14.6^{A}	55.6 ± 10.4^{A}	58.0 ± 30.1^{A}	54.0 ± 5.1^{A}
	30	37.0 ± 19.0^{B}	20.8 ± 15.8^{B}	43.6 ± 31.1^{B}	25.8 ± 15.6^{B}
GGT, U/L	0	18.6 ± 7.6^{a}	16.7 ± 16.7^{a}	17.7 ± 8.4^{aB}	10.1 ± 2.8^{bB}
	15	32.6 ± 8.2^{Aa}	18.8 ± 5.6^{b}	30.6 ± 10.1^{Aa}	31.2 ± 9.9^{Aa}
	30	19.2 ± 4.6^{Ba}	17.6 ± 13.8^{a}	19.8 ± 8.4^{Ba}	9.8 ± 2.6^{Bb}
LDH, U/L	0	553.2 ± 26.2^{B}	479.9 ± 30.5^{B}	623.7 ± 28.1	514.1 ± 20.2^{B}
	15	992.2 ± 30.3^{A}	753.8 ± 51.8^{A}	746.0 ± 21.6	798.6 ± 68.3^{A}
	30	563.2 ± 26.6^{B}	498.9 ± 30.5^{B}	613.7 ± 27.1	501.8 ± 18.9^{B}
CK, U/L	0	130.0 ± 18.9	50.8 ± 14.2^{B}	124.0 ± 17.4	93.0 ± 20.8^{B}
	15	148.8 ± 40.1^{ab}	211.2 ± 48.3^{Aa}	123.6 ± 43.8^{b}	140.0 ± 49.0^{Ab}
	30	136.0 ± 10.9	54.8 ± 13.2^{B}	136.0 ± 16.4	105.8 ± 19.8^{B}

(Continued)

10.3389/fvets.2024.1434548

TABLE 8 (Continued)

Item[1]	Day	Control	CHM-0.5[2]	CHM-0.75[2]	CHM-1[2]
Pancrease function tests					
Amylase, U/L	0	26.6 ± 11.6^{B}	11.1 ± 5.3^{B}	22.6 ± 4.6^{B}	12.0 ± 2.1^{B}
	15	39.6 ± 17.6^{A}	42.8 ± 9.6^{A}	39.4 ± 8.2^{A}	40.8 ± 22.9^{A}
	30	27.6 ± 14.6^{Ba}	11.4 ± 7.8^{Bb}	23.8 ± 4.9^{Bab}	14.8 ± 4.4^{Bab}
TBA, μmol/L	0	10.3 ± 11.7	12.6 ± 4.3	9.3 ± 4.5	17.1 ± 5.3
	15	11.7 ± 4.9	20.7 ± 12.3	16.9 ± 6.7	22.1 ± 11.8
	30	13.7 ± 10.2	14.4 ± 5.3	11.1 ± 5.6	19.2 ± 5.2
GLU, μmol/L	0	2.8 ± 0.5	2.2 ± 0.4	3.3 ± 1.1	2.2 ± 0.2
	15	4.3 ± 0.2	3.8 ± 0.5	4.4 ± 0.3	4.7 ± 0.7
	30	2.9 ± 0.8	2.3 ± 0.5	3.5 ± 0.9	2.3 ± 0.3
Renal function tests					
BUN, μmol/L	0	4.1 ± 2.4	3.5 ± 1.1	4.3 ± 0.7	2.4 ± 0.5
	15	4.7 ± 0.5	3.6 ± 0.2	4.9 ± 0.5	4.7 ± 1.5
	30	4.9 ± 2.1^{a}	3.6 ± 0.9^{ab}	4.6 ± 0.6^{ab}	2.7 ± 0.5^{b}
UA μmol/L	0	29.6 ± 22.3	23.5 ± 4.5	28.6 ± 8.3	23.8 ± 0.9^{B}
	15	42.4 ± 8.6	32.0 ± 14.4	41.4 ± 7.3	49.2 ± 9.3^{A}
	30	32.8 ± 19.3	26.0 ± 8.6	30.6 ± 8.3	26.2 ± 3.3^{B}
CREA, μmol/L	0	32.3 ± 9.4	28.2 ± 6.7^{B}	35.5 ± 1.9	36.5 ± 3.7
	15	42.8 ± 3.3^{b}	68.2 ± 17.9^{Aa}	46.0 ± 7.4^{b}	47.4 ± 7.1^{b}
	30	34.2 ± 8.6	30.2 ± 5.8^{B}	36.6 ± 2.9	39.0 ± 4.6
Blood lipids profile					
CHOL, mmol/L	0	2.0 ± 0.7^{B}	0.7 ± 0.5	2.8 ± 1.3	0.5 ± 0.1^{B}
	15	4.5 ± 1.1^{Aa}	1.6 ± 0.3^{b}	4.8 ± 0.6^{a}	4.1 ± 2.2^{Aa}
	30	2.1 ± 0.8^{Ba}	0.8 ± 0.6^{b}	3.1 ± 1.3^{a}	0.6 ± 0.1^{Bb}
TG, mmol/L	0	0.2 ± 0.1	0.1 ± 0.01	0.1 ± 0.2	0.1 ± 0.02
	15	0.3 ± 0.03	0.3 ± 0.03	0.3 ± 0.02	0.3 ± 0.1
	30	0.2 ± 0.1	0.2 ± 0.01	0.2 ± 0.1	0.2 ± 0.02
Blood minerals profile					
K, mmol/L	0	4.5 ± 0.7^{B}	4.1 ± 0.3	4.5 ± 0.5	3.8 ± 0.3
	15	7.3 ± 2.5^{A}	4.4 ± 0.8	6.5 ± 2.4	4.6 ± 0.6
	30	4.4 ± 0.8^{B}	4.2 ± 0.4	4.7 ± 0.6	4.0 ± 0.3
Na, mmol/L	0	136.3 ± 6.4^{B}	128.3 ± 3.1	137.4 ± 6.7	124.4 ± 0.6^{B}
	15	151.0 ± 8.9^{Aa}	131.5 ± 1.5^{b}	152.5 ± 5.5^{a}	146.9 ± 10.8^{Aa}
	30	139.6 ± 5.7^{Bb}	132.3 ± 4.5^{b}	143.8 ± 8.7^{a}	128.4 ± 0.6^{Bb}
Cl, mmol/L	0	90.6 ± 2.2	87.2 ± 1.4	91.6 ± 1.6	93.1 ± 3.8
	15	93.6 ± 1.8	97.0 ± 9.1	94.9 ± 3.7	94.8 ± 4.1
	30	96.2 ± 2.4^{ab}	92.2 ± 2.4^{b}	97.5 ± 1.9^{a}	97.1 ± 3.8^{ab}
Ca, mmol/L	0	1.7 ± 0.3^{B}	1.3 ± 0.1^{B}	1.8 ± 0.2^{B}	1.3 ± 0.2^{B}
	15	2.3 ± 0.1^{Aa}	1.9 ± 0.4^{Ab}	2.2 ± 0.1^{Aa}	2.3 ± 0.1^{Aa}
	30	1.9 ± 0.4^{Bab}	1.4 ± 0.1^{Bb}	1.9 ± 0.3^{Ba}	1.4 ± 0.2^{Bb}
Mg, mmol/L	0	0.4 ± 0.2	0.3 ± 0.1	0.5 ± 0.2	0.1 ± 0.2^{B}
	15	0.6 ± 0.2	0.6 ± 0.3	0.7 ± 0.2	0.7 ± 0.2^{A}
	30	0.6 ± 0.3^{a}	0.4 ± 0.1^{ab}	0.6 ± 0.1^{a}	0.2 ± 0.2^{Bb}

(Continued)

TABLE 8 (Continued)

Item[1]	Day	Control	CHM-0.5[2]	CHM-0.75[2]	CHM-1[2]
P, mmol/L	0	1.2 ± 0.4	1.3 ± 0.3	1.2 ± 0.1	0.8 ± 0.2^{B}
	15	1.6 ± 0.2^{a}	0.9 ± 0.5^{b}	1.5 ± 0.1^{a}	1.8 ± 0.3^{Aa}
	30	1.4 ± 0.5	1.4 ± 0.4	1.3 ± 0.2	0.9 ± 0.2^{B}

^{a,b}Means with different superscripts in the same row are significantly different ($p < 0.05$). ^{A,B}Means with different superscripts in the same column against the same variable are significantly different ($p < 0.05$). [1]IgG, immunoglobulin G; IgA, immunoglobulin A; IgM, immunoglobulin M; ALT, alanine transaminase; AST, aspartate transaminase; TP, total protein; ALB, albumin; GLB, globulin; TBIL, total bilirubin; ALP, alkaline phosphatase; GGT, Gamma-glutamyl transferase; LDH, lactate dehydrogenase; CK, creatine kinase; TBA, total bile acids; GLU, glucose; BUN, blood urea nitrogen; UA, uric acid; CREA, creatinine; CHOL, total cholesterol; TG, triglycerides. [2]CHM-0.5 = 0.5 kg CHM; CHM-0.75 = 0.75 kg CHM; CHM-1 = 1 kg CHM.

3.5 Hematologic profile

Complete blood profile of Holstein dairy cows fed different levels of supplemental CHM are shown in Table 9. Results indicated that leukocytes (WBC), erythrocytes (RBC), hematocrit (HCT), mean corpuscular volume (MCV), mean corpuscular hemoglobin (MCH), mean corpuscular hemoglobin concentration (MCHC), erythrocyte distribution width – standard deviation (RDW-SD), erythrocyte distribution width – coefficient of variation (RDW-CV), mean platelet volume (MPV), platelet distribution width (PDW), and plateletcrit (PCT) values were not influenced by the dose of CHM. The lymphocytes range was within the range, however, their values increased in the CHM-0.5 group compared to the CHM-1 group at d 30 ($p < 0.05$). Higher granulocyte (%) values were observed in the CHM-1 group than in the CHM-0.5 group both at d 15 and d 30 ($p < 0.05$). The highest monocytes (%) level was recorded at d 30 in CHM-1 group compared to other groups ($p < 0.05$). The number of monocytes and granulocytes remained unaffected whereas, lymphocyte numbers were greater in control group than in CHM-1 group at d 15 and d 30 ($p < 0.05$). At d 30, lower hemoglobin levels were noted in the CHM-0.5 group compared to other groups ($p < 0.05$). Total platelet count increased in the CHM-1 group compared to the CHM-0.5 group at d 15 ($p < 0.05$) whereas, it was highest in control group than other groups at d 30 ($p < 0.05$). Cows in CHM-0.5 group had greater platelets than those in CHM-1 group at d 15 ($p < 0.05$), while CHM-0.75 group had greater number of platelets than CHM-0.5 and CHM-1 groups at d 30 ($p < 0.05$).

3.6 Reproductive performance

Reproductive performance of Holstein dairy cows fed different supplemental levels of CHM in early postpartum period has been presented in Table 10. Diameter of the first detecting follicle did not differ between the CHM-supplemented groups of cows. The CHM-0.75 group displayed a greater estrus response than a non-supplemented group of cows. Interval to estrus or ovulation after 2nd GnRH and estrus duration remained the same between the treatment groups. However, ovulation rate, follicle growth rate and ovulatory follicle diameter were significantly different in supplemented cows with a dose of 0.75 kg compared to control. Similarly, higher cows got pregnant in the CHM-0.75 group compared to the control and CHM-0.5 groups.

The results shown in Figure 2 indicate that 30 days of supplementation of CHM during the postpartum period. The involution period of the cervix, gravid and non-gravid horns in healthy crossbred cows were 33.6 ± 2.4, 36.8 ± 3.4, and 31.6 ± 1.8 days, respectively; however, postpartum uterine infected cows had comparatively extended uterine involution period of the cervix, gravid and non-gravid horns (43.1 ± 5.2, 45.6 ± 6.8, and 39.6 ± 5.7 days, respectively).

4 Discussion

Over the past decades, increasing number of studies involving the use of plant-based feed additives have reported alternative solutions to antibiotics and synthetic feed additives. The variety of herbs comprising of various bioactive molecules has increased the interest to include those substances in animal diets. It has prompted the mixing and blending of different components resulting in the availability of multi-herb preparations in the market. However, this has added to the difficulty of interpreting any result due to the differences in the mechanisms as well as possible interactions among the bioactive molecules from different sources. In the present study, supplemented CHM had a variety of herbs including *E. ulmoides, A. L. (Fabaceae), C. pilosula, A. archangelica, A. amurensis G. glabra, L. striatum, W. extensa,* and *P. montana* that provided various phytogenic bioactive molecules like saponins, glycyrrhizic acid, polyphenols, polysaccharides, phytosterols, flavonoids, and carotenoids. Generally, these bioactive molecules carry out numerous beneficial activities, therefore, the use of CHM is in practice as feed additives according to "China Veterinary Drug Specifications." Owing to the natural sources of CHM, these formulations are accepted by animals and humans with fewer drug residues and toxic/side effects. Amongst these, Eucommia, Astragalus, Codonopsis, Angelica, Atractylodes, and Liquorice nourish and strengthen the body by regulating the metabolism, and Chuanxiong promotes blood circulation, and nutrient digestion and absorption; Poria induce diuretic effects, and Pueraria act as heat dissipate and detoxifier, antibacterial and anti-inflammatory (17). Therefore, the present study was conducted to evaluate the effects of CHM on DMI, milk yield and milk composition, blood biochemistry, and reproductive performance of Holstein dairy cows in early postpartum period.

4.1 Dry matter intake and fecal composition

The DMI and subsequent nutrient digestibility are key components that drive the productive, reproductive, and health status of dairy cows. In this context, feed composition, minerals, and other

TABLE 9 Hematological profile of Holstein dairy cows fed different levels of dietary Chinese herbal medicine in early postpartum period.

Item[1]	Reference range	Days	Control	CHM-0.5[2]	CHM-0.75[2]	CHM-1[2]
Leukocytes, 10^9/L	5.0–16.0	0	12.9 ± 5.3	13.5 ± 4.3	12.8 ± 2.9	10.7 ± 3.1
		15	14.9 ± 7.1	15.8 ± 7.4	14.3 ± 3.9	11.7 ± 3.1
		30	19.4 ± 13.9	19.2 ± 7.3	16.8 ± 6.3	16.4 ± 11.4
Lymphocyte ratio, %	20.0–60.3	0	31.3 ± 18.1	32.2 ± 19.5^{B}	32.7 ± 15.7^{B}	27.2 ± 15.4
		15	36.3 ± 21.2	38.5 ± 23.2^{B}	33.3 ± 18.8^{B}	29.1 ± 18.3
		30	44.5 ± 31.4^{ab}	52.0 ± 27.1^{Aa}	45.5 ± 23.9^{Aab}	28.9 ± 21.4^{b}
Monocyte ratio, %	4.0–12.1	0	11.2 ± 6.6^{ab}	8.3 ± 4.3^{a}	11.0 ± 8.5^{ab}	14.4 ± 12.6^{a}
		15	10.2 ± 6.9^{ab}	7.4 ± 4.4^{b}	9.9 ± 7.6^{ab}	15.1 ± 11.6^{a}
		30	8.7 ± 8.1^{ab}	4.2 ± 2.4^{b}	6.1 ± 3.2^{ab}	10.8 ± 3.5^{a}
Granulocyte ratio, %	30.0–65.0	0	51.4 ± 14.3	51.2 ± 18.4	54.0 ± 17.0	53.5 ± 16.1
		15	53.4 ± 16.6	54.2 ± 20.2^{A}	56.9 ± 18.2	55.9 ± 17.1
		30	46.8 ± 26.2^{b}	43.8 ± 25.1^{Bb}	48.3 ± 21.1^{b}	60.3 ± 18.2^{a}
Lymphocytes, 10^9/L	1.5–9.0	0	4.7 ± 5.4^{B}	5.6 ± 2.1^{B}	4.3 ± 2.5	3.4 ± 2.6
		15	6.6 ± 6.9^{Ba}	7.2 ± 6.9^{ABab}	5.0 ± 3.7^{ab}	3.5 ± 2.4^{b}
		30	11.9 ± 8.6^{Aa}	10.9 ± 9.3^{Aab}	8.8 ± 8.2^{ab}	6.5 ± 7.4^{b}
Monocytes, 10^9/L	0.3–1.6	0	1.2 ± 0.4	0.5 ± 0.1	1.4 ± 1.4	1.6 ± 1.8
		15	1.2 ± 0.6	0.9 ± 0.3	1.4 ± 1.2	1.8 ± 1.7
		30	0.9 ± 0.4	0.7 ± 0.4	0.9 ± 0.4	1.5 ± 0.9
Granulocytes, 10^9/L	2.3–9.1	0	6.97 ± 1.1	7.5 ± 2.6	6.9 ± 1.7	5.6 ± 1.6
		15	6.9 ± 1.2	7.7 ± 3.4	7.8 ± 2.5	6.4 ± 2.5
		30	6.6 ± 3.0	7.6 ± 4.5	7.1 ± 1.9	8.4 ± 3.3
Erythrocytes, 10^{12}/L	5.00–10.10	0	5.6 ± 0.2	5.4 ± 0.7	5.8 ± 0.5	5.2 ± 0.3
		15	6.1 ± 0.6	5.7 ± 0.8	6.0 ± 0.6	5.6 ± 0.5
		30	66.0 ± 0.3	5.5 ± 0.6	6.3 ± 0.5	6.1 ± 0.4
Hemoglobin, g/L	90–130	0	106.7 ± 5.3	102.6 ± 13.1	105.1 ± 14.5^{B}	100.3 ± 15.2^{B}
		15	113.7 ± 5.6	106.6 ± 15.4	110 ± 15.6^{B}	102.3 ± 16.3^{B}
		30	113.6 ± 9.2^{a}	97.0 ± 19.4^{b}	121.8 ± 14.8^{Aa}	119 ± 11.5^{Aa}
Hematocrit, %	28.0–46.0	0	34.5 ± 1.6	32.9 ± 2.4	34.2 ± 5.0	32.5 ± 1.9
		15	36.7 ± 2.9	35.9 ± 4.8	36.6 ± 5.4	35.4 ± 2.7
		30	38.1 ± 3.0	32.4 ± 4.5	39.3 ± 5.4	38.7 ± 2.9
MCV, fL	38.0–53.0	0	56.7 ± 2.4	60.7 ± 2.1	53.6 ± 11.1	60.2 ± 3.5
		15	60.7 ± 3.4	62.7 ± 3.2	56.9 ± 12.1	62.3 ± 4.7
		30	62.5 ± 5.7	59.5 ± 4.4	62.7 ± 4.4	64.6 ± 3.6
MCH, pg	13.0–19.0	0	17.6 ± 1.5	14.5 ± 0.2	16.3 ± 0.7	17.1 ± 1.8
		15	18.8 ± 1.6	18.5 ± 0.6	18.1 ± 0.9	18.2 ± 1.6
		30	19.4 ± 0.7	17.5 ± 2.4	19.4 ± 0.9	18.9 ± 1.2
MCHC, g/L	300–370	0	308.3 ± 18.1	291.9 ± 6.4	278.6 ± 21.4	278.3 ± 31.3
		15	310.3 ± 21.1	295.9 ± 9.5	300.6 ± 18.4	287.3 ± 33.3
		30	312.0 ± 21.9	293.6 ± 26.7	310 ± 11.7	292.8 ± 9.8
RDW-SD, %	0.1–99.9	0	28.0 ± 3.2	29.7 ± 2.4	27.1 ± 7.2	33.7 ± 3.8
		15	31.0 ± 2.9	32.7 ± 3.9	30.1 ± 6.5	33.7 ± 3.8
		30	32.7 ± 4.1	29.7 ± 4.4	33.4 ± 3.9	34.2 ± 5.0

(Continued)

TABLE 9 (Continued)

Item[1]	Reference range	Days	Control	CHM-0.5[2]	CHM-0.75[2]	CHM-1[2]
RDW-CV, %	14.0–19.0	0	13.4 ± 1.0	16.1 ± 1.2	16.6 ± 1.2	15.4 ± 1.2
		15	16.7 ± 1.1	17.1 ± 1.4	16.9 ± 1.4	17.4 ± 1.2
		30	17.2 ± 1.1	16.3 ± 1.7	17.5 ± 1.2	17.4 ± 1.8
Platelets, g/L	120–820	0	308.1 ± 132.7^{Bb}	334.5 ± 140.2^{Aab}	370.4 ± 125.6^{Aa}	376.3 ± 199.1^{Ba}
		15	362.1 ± 188.7^{Bab}	344.5 ± 137.5^{Ab}	390.4 ± 130.9^{Aab}	407.3 ± 194.1^{Aa}
		30	400.2 ± 160.3^{Aa}	319.0 ± 143.7^{Bb}	305.2 ± 162.1^{Bb}	307.8 ± 159.8^{Bb}
MPV, %	3.8–7.0	0	7.7 ± 1.2	8.0 ± 1.1	7.3 ± 1.0	7.1 ± 0.2
		15	8.2 ± 1.4	8.1 ± 1.3	8.0 ± 1.0	7.3 ± 0.3
		30	8.8 ± 1.9	7.8 ± 1.4	9.4 ± 1.6	7.7 ± 1.6
PDW, %	0.1–30.0	0	8.3 ± 0.6	9.0 ± 1.2	8.3 ± 1.0	7.8 ± 0.5
		15	8.5 ± 0.8	9.2 ± 1.1	8.6 ± 0.9	8.9 ± 0.8
		30	8.4 ± 0.9	8.1 ± 0.4	8.9 ± 0.7	8.8 ± 0.9
Plateletcrit, %	0.01–9.99	0	0.1 ± 0.1	0.2 ± 0.1	0.3 ± 0.1	0.2 ± 0.1
		15	0.3 ± 0.2	0.3 ± 0.1	0.4 ± 0.2	0.3 ± 0.2
		30	0.4 ± 0.4	0.2 ± 0.1	0.3 ± 0.2	0.1 ± 0.1
Platelets ratio, %	0.1–99.9	0	2.1 ± 5.6^{B}	8.6 ± 2.3	6.5 ± 5.6^{B}	2.3 ± 2.1
		15	4.1 ± 9.6^{Bab}	8.9 ± 8.9^{a}	5.7 ± 8.7^{Bab}	2.5 ± 2.7^{b}
		30	10.1 ± 13.9^{Aab}	11.1 ± 9.2^{b}	14.9 ± 10.5^{Aa}	5.2 ± 6.9^{b}

[a,b]Means with different superscripts in the same row are significantly different ($p < 0.05$). [A,B]Means with different superscripts in the same column against the same variable are significantly different ($p < 0.05$). [1]MCV, mean corpuscular volume; MCH, mean corpuscular hemoglobin; mean corpuscular hemoglobin concentration; RDW-SD, erythrocyte distribution width – standard deviation; RDW-CV, erythrocyte distribution width – coefficient of variation; MPV, mean platelet volume; PDW, platelet distribution width. [2]CHM-0.5 = 0.5 kg CHM; CHM-0.75 = 0.75 kg CHM; CHM-1 = 1 kg CHM.

supplemental components influence the DMI by nutritive value and palatability factors. In our study, the supplementation of CHM promoted the DMI in supplemented groups except in high-dose groups. It has been noted that CHM have poor palatability due to the presence of essential oils or a combination of cinnamaldehyde and eugenol, and increased supplementation level of CHM made the feed unpalatable because of organoleptic effects of CHM components, hence feed intake did not change in the present study. According to the Dictionary of Chinese Medicine (Nanjing University of Chinese Medicine 2006), CHM energizes the stomach and the spleen for better digestion and appetite (18). In this study, improved feed intake by cows supplemented with low or medium-dose CHM can might be attributed to the above postulation.

Cows showed an increase in ash and starch digestibility in the control and high-dose CHM groups. In contrast, higher NDF digestibility was noted in the low-dose group. Such a change in digestibility indicates the digestion stimulating activity of CHM for cellulose-degrading/fibre-degrading bacteria and probiotic bacterial growth that, in turn, maintain the pH and digestive enzyme activity (19). Previously, inhibitory CHM affected the growth of protozoa and methane-producing bacteria in the rumen (20).

An improvement was observed in daily weight gain of calves fed supplemental CHM. The improvement in the growth of calves in this study is likely linked to better nutrient utilization and the antioxidant potential of the supplements offered. Such preparations increase energy, lipid and fat metabolism when offered even to calves. Previously, better growth rates were observed in growing calves in cattle and yak (12, 21) or lambs (22, 23). The use of CHM had stimulating effects on ruminal epithelium development and ruminal microbiota in early-weaned calves.

4.2 Milk yield and milk composition

It is well-known that milk yield and milk composition reflect the nutritional and metabolic status, udder condition, and overall health of dairy cows. In the present study, cows fed 0.75 kg CHM per day had greater milk yield than those in control group. The used combination of CHM is an optional supplement in lactating cows. Based on the theory of traditional Chinese medicine, the CHM formulation derived from herbs (Eucommia, Astragalus, Codonopsis, Angelica, Atractylodes, Liquorice, Chuanxiong, Poria, and Pueraria) has beneficial effects (24, 25). The formulation consists of synergistic detoxification effects and promotes blood circulation of internal organs by sharing the bioactive ingredients of flavonoids or polysaccharides. Previously, various formulations of CHM were offered to cows under normal (26, 27) and stressful conditions (28, 29) that showed varying effects on milk production performance of supplemented cows.

Improved milk fat, total solids, and milk urea nitrogen levels in CHM groups suggest that the supplemental CHM improved the ruminal fermentation by promoting the ruminal microbiota for better nutrient digestion and absorption. Efficient nutrient uptake in CHM-supplemented experimental cows directed the superfluous fatty acids, carbohydrates, and amino acids towards the mammary glands for milk fat, lactose, and protein (30). In addition, the galactagogue property of different herbs (31) could be a plausible reason for quality

TABLE 10 Reproductive performance of Holstein dairy cows fed different levels of dietary Chinese herbal medicine in early postpartum period.

Item	Control	CHM-0.5[1]	CHM-0.75[1]	CHM-1[1]
Diameter of first detecting follicle (mm)	9.9 ± 3.5	8.3 ± 3.3	8.4 ± 2.8	7.8 ± 1.4
Estrus response	17/27 (63.0%)[b]	24/31 (77.4%)[ab]	26/29 (89.7%)[a]	24/30 (80.0%)[ab]
Interval to estrus after 2nd GnRH (h)	8.5 ± 0.8[b]	10.3 ± 0.6[a]	9.6 ± 0.8[a]	8.3 ± 0.8[a]
Estrus duration (h)	15.4 ± 0.6	16.5 ± 0.4	16.3 ± 0.6	15.5 ± 0.5
Ovulation rate	15/27 (55.6%)[b]	22/31 (70.9%)[ab]	24/29 (82.8%)[a]	22/30 (73.3%)[ab]
Interval to ovulation after 2nd GnRH (h)	24.5 ± 0.9	25.5 ± 0.5	25.4 ± 0.8	24.8 ± 0.8
Follicle growth rate (mm/day)	0.01[b]	0.29[b]	0.68[a]	0.31[b]
Ovulatory follicle diameter (mm)	13.9 ± 2.4[b]	15.0 ± 3.8[ab]	16.7 ± 4.0[a]	14.7 ± 2.3[ab]
Pregnancy rate	9/27 (33.3%)[b]	16/31 (51.6%)[b]	21/29 (72.4%)[a]	17/30 (56.7%)[ab]

[a,b]Means with different superscripts in the same row are significantly different ($p < 0.05$). [1]CHM-0.5 = 0.5 kg CHM; CHM-0.75 = 0.75 kg CHM; CHM-1 = 1 kg CHM.

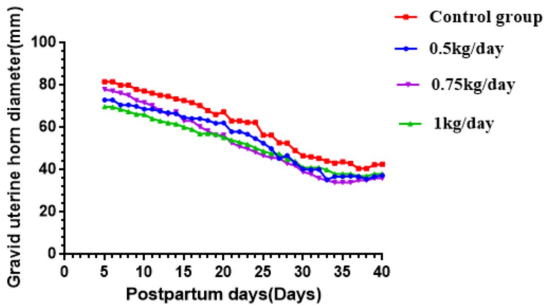

FIGURE 2
Uterine involution time and diameters of gravid uterine horn in Holstein dairy cows fed different levels of Chinese herbal medicine in early postpartum period.

milk production in the present study. Previously, there are variable findings in terms of milk fat, protein, lactose, milk urea nitrogen, and somatic cell count (32) that might have occurred due to the differences in experimental conditions, herb types, duration of supplementation, day in milk, and the bioavailability of active ingredients.

4.3 Serum biochemistry and hematological profile

Immunity-related indicators indicate the health status of animals. In the present study, the IgG levels rose in dairy cows after supplementation with a medium dose of CHM consistent with the previous studies in cows (33, 34). These studies report that CHM improved cell-mediated and humoral immunity by provoking nonspecific immunity factors via activation of the host immune cells.

Lower levels of ALT, protein, albumin, globulin, bilirubin, alkaline phosphatase, and gamma-glutamyl transpeptidase following supplementation or among the treatment groups describe the protective effects of CHM. These findings correspond to earlier documents where CHM were supplemented during stressful conditions of parturition and postpartum uterine infections (35). Beyond this, enormous fluctuations in protein and liver enzyme levels could indicate liver cell damage and increased liver cell membrane permeability, subsequently causing leakage of enzymes into the blood. Whereas the fluctuations in liver function tests are also linked to negative energy balance during the early postpartum time in cows due to excessive depletion of body fat to fulfill the energy for milk production (36). In the present study, no change was observed in total bile acids and glucose levels, which indicates that CHM provision did not influence insulin secretion Low amylase levels after CHM supplementation indicate the increased utilization of starch in the small intestine by amylase thereby reflecting the reduced amylase level. The CHM contributes the various nutritional factors, i.e., glucose, amino acids, fatty acids, and others that are used for synthesis and stimulating different enzymes, including amylase. In the present study, creatinine, urea and uric acid were within reference range after CHM supplementation suggesting the normal functioning of renal system. A decreasing trend was observed in renal function tests in CHM-supplemented groups but was not always significant. Similar findings were observed earlier in ruminants (34). Increased serum urea and creatinine levels reflect the protein intake and digestibility, fatty acids breakdown by the liver, muscular breakdown, and ruminal urea recycling (33). Serum lipids, total cholesterol, and triglycerides are the main lipids class particularly influenced by dietary factors. In the present study, supplemental CHM influenced the total cholesterol but not triglycerides. Reduced serum total cholesterol levels by CHM supplementation indicate the emulsifying effects (37) and fibrous nature (38). Such dietary properties regulate the ruminal microbiota, digestion, and absorption of nutrients.

The macro- and mirco-elements are essential in animals for normal physiological and biochemical processes and milk and meat production in ruminants. The mineral contents varied during the first and second observations after CHM provision might be related to the lactation stage of cows (39). Reported higher mineral levels by adding a CHM mixture to the diets of goats. They described that the CHM mixture remained unaffected by ruminal action and was transported

to the intestinal region, where it positively influenced the hindgut digestion of nutrients.

No earlier studies have reported the effect of supplemental CHM on the hematological profile of cows. In the present study, although there were variations in many hematological variables between the supplemented and control groups, they existed in normal ranges. Thus, CHM supplementation to cows at different levels had no negative effects on hematology. These findings are consistent with previous studies reporting the effects of different herbs on hematology (34, 40).

4.4 Reproductive performance

In order to avoid the prepartum and postpartum reproductive disorders, management of dairy cows may be subjected to nutritional and hormonal regimens before and after calving to support the early uterine involution and resumption of ovarian activity. Our study demonstrated that CHM supplementation can improve the estrus, ovulation, and conception rates in synchronized dairy cows in addition to expediting the uterine involution in early postpartum period. Consistent with our findings, previous studies have reported the earlier resumption of postpartum reproductive events in cows fed diets supplemented with CHM (32–34). In addition, improvements were witnessed in cows suffering from calving or postpartum reproductive disorders in response to dietary CHM supplementation (30, 33). The exact mechanism by which dietary CHM supplementation improved the reproductive performance of cows in early postpartum period is not yet known. It is speculated that the improvement in DMI providing superfluous energy might have supported the occurrence of these ovarian activities due to the potential antimicrobial, immunomodulatory, antioxidative, and energy and gut ecosystem enhancing properties of CHM. Increased permeability of blood vessels in addition to lowered blood triglycerides and cholesterol might have improved the uterine health in cows fed dietary CHM. Earlier studies have provided preliminary evidence regarding the positive effect of CHM on the fertility of cows in early postpartum period. It is, however, necessary to establish the efficacy, safety margins, and mechanisms of CHM in improving the fertility of cow using well-controlled experiments with larger sample size.

5 Conclusion

In conclusion, the CHM preparation had no adverse effects on the biochemical indicators for immunity, digestibility, metabolism, and production performance of cows. The estrus, ovulation, and pregnancy rates were improved by CHM supplementation prior to synchronization of dairy cows. No significant change in uterine involution was observed in uterine infected or healthy CHM-supplemented cows. However, there are certain limitations of the present study. The period of this study has focused on the early postpartum period (early lactation) that requires further evaluation of supplemental CHM in mid and late lactation. Moreover, this study lacks the investigation of mechanisms by which supplemental CHM exerted these effects on the studied biological indicators. Further studies are suggested to elucidate the mechanisms and pathways involved in the beneficial effects of CHM in dairy cows.

Data availability statement

The original contributions presented in the study are included in the article/supplementary material, further inquiries can be directed to the corresponding author.

Ethics statement

Before execution of the study, an approval was obtained from the Animal Experimental Ethical Inspection of Laboratory Animal Centre, Huazhong Agricultural University, Wuhan (HZAUCA-2018-004). All the experimental protocols were performed according to the guidelines of the Committee of Animal Research Institute of the university. The studies were conducted in accordance with the local legislation and institutional requirements. Written informed consent was obtained from the owners for the participation of their animals in this study.

Author contributions

AA: Conceptualization, Data curation, Formal analysis, Methodology, Resources, Software, Validation, Visualization, Writing – original draft, Writing – review & editing. UA: Conceptualization, Data curation, Formal analysis, Supervision, Writing – review & editing. ZN: Conceptualization, Data curation, Formal analysis, Methodology, Resources, Software, Validation, Writing – review & editing. ZA: Conceptualization, Data curation, Methodology, Project administration, Resources, Software, Writing – review & editing. WL: Conceptualization, Data curation, Formal analysis, Investigation, Project administration, Resources, Writing – review & editing. CR: Conceptualization, Formal analysis, Investigation, Methodology, Validation, Writing – review & editing. XP: Conceptualization, Data curation, Formal analysis, Funding acquisition, Investigation, Methodology, Resources, Software, Supervision, Visualization, Writing – review & editing. SW: Conceptualization, Formal analysis, Funding acquisition, Investigation, Methodology, Resources, Software, Supervision, Validation, Visualization, Writing – review & editing.

Funding

The author(s) declare financial support was received for the research, authorship, and/or publication of this article. This study was financially supported by the Natural Science Foundation of Anhui Province (2008085MC94), The National Natural Science Foundation (31301972) and Key Research and Development Project of Chuzhou (2018ZN014) and The Key Research and Development Program of Anhui Province (202004f06020048) Natural Science Research in Anhui Universities Key Projects (2023AH051839).

Conflict of interest

The authors declare that the research was conducted in the absence of any commercial or financial relationships that could be construed as a potential conflict of interest.

Publisher's note

References

1. Yunpeng W, Yue M. Use of antibiotics in aquaculture and their potential harm. *Chin J Anti*. (2008) 29:519–23. doi: 10.1016/S1872-2067(08)60048-0

2. Liu, H, Tong, J, Zhou, D. Utilization of Chinese herbal feed additives in animal production. *Agri Sci China*. (2002) 10:1262–72. doi: 10.1016/S1671-2927(11)60118-1

3. Abdallah, A, Zhang, P, Zhong, Q, Sun, Z. Application of traditional Chinese herbal medicine by-products as dietary feed supplements and antibiotic replacements in animal production. *Curr Drug Metab*. (2019) 20:54–64. doi: 10.2174/1389200219666180523102920

4. Manhong W. Effects of Chinese herbal feed additives on growth performance, apparent digestibility of nutrients and serum biochemical indexes of calves. *Feed Res*. (2022) 8:23–6. doi: 10.13557/j.cnki.issn1002-2813.2022.08.005

5. Genxin L, Lingqing Z, Cong W, Xinian W, Zhanhu W, Keyuan L. Effects of traditional Chinese medicine-probiotic preparations on growth performance, carcass performance and meat quality of growing-finishing pigs. *J Anim Hus Vet Med*. (2022) 41:71–4. Available at: https://chn.oversea.cnki.net/kcms/detail/detail.aspx?dbcode=CJFD&filename=XMSZ202203025&dbname=CJFDLAST2022

6. Huayan Z, Zecao Y, Hongliang Z, Jiaren A, Zhicai L, Shuilian W, et al. Effects of fermented Chinese herbal medicine complexes on antioxidant and reproductive performance of dairy cows. *J Hunan Agric Univ (Nat Sci Ed)*. (2021) 47:455–61. doi: 10.13331/j.cnki.jhau.2021.04.014

7. Guoliang, A. Study on improving sow reproductive performance by using Chinese herbal medicine feed additives. *J Hunan Agric Univ (Nat Sci Ed)*. (2007) 2:196–9. Available at: https://chn.oversea.cnki.net/kcms/detail/detail.aspx?dbcode=CJFD&filename=HNND200702018&dbname=CJFD2007

8. Qiyuan, F, Ting, X, Di, W, Hongbai, L. Effects of Chinese herbal medicine additives on some biochemical parameters and hormone levels of heat-stressed rainbow trout. *Chinese J Fish*. (2019) 32:6–13. Available at: https://chn.oversea.cnki.net/kcms/detail/detail.aspx?dbcode=CJFD&filename=SCXZ201902002&dbname=CJFDLAST2019

9. Dalu C, Sucai C, Weitao Z, Juanjuan Z, Aiyu L, Xiaoyu L, et al. Effects of Huopopuling powder on growth performance, digestibility and serum biochemical indexes in fattening lambs under heat stress. *Acta Vet Zootech Sin*. (2022) 53:1829–1840. doi: 10.11843/j.issn.0366-6964.2022.06.016

10. Jinghui L, Ying C, Wanying K, Hong Y, Hui L, Dezhi M, et al. Effects of Chinese herbal supplements on production performance, milk quality, somatic cell count, immune function and hormone levels of Holstein dairy cows during lactation. *Feed Res*. (2022) 45:22–6. doi: 10.13557/j.cnki.issn1002-2813.2022.07.005

11. Sashuang, W, Jiaping, W, Qian, L, Lianjie, W. Effects of fermented traditional Chinese medicine additives on the prevention of mastitis and milk production performance in dairy cows. *Feed Res*. (2019) 42:10–2. doi: 10.13557/j.cnki.issn1002-2813.2019.07.004

12. Wang, X, Xie, H, Liu, F, Wang, Y. Production performance, immunity, and heat stress resistance in Jersey cattle fed a concentrate fermented with probiotics in the presence of a Chinese herbal combination. *Anim Feed Sci Technol*. (2017) 228:59–65. doi: 10.1016/j.anifeedsci.2017.03.015

13. Zee-Cheng RK. A potent Chinese biological response modifier in cancer immunotherapy, potentiation and detoxification of anticancer drugs. *Methods Find Exp Clin Pharmacol*. (1992) 14:725–36.

14. AOAC. Official Methods of Analysis. *17th* ed. Gaithersburg, Maryland, United States: Association of Official Analytical Chemists (2000).

15. Abulaiti A, Naseer Z, Ahmed Z, Hua G, Yang L. Dietary provision of N-carbamoylglutamate to Holstein cows a strategy to enhance the productive and reproductive efficiency during summer. *Livestock Sci*. (2022) 258:104905 doi: 1016/j.livsci.2022.104905

16. Lin Y, Yang H, Ahmad MJ, Yang Y, Yang W, Riaz H, et al. Postpartum uterine involution and embryonic development pattern in Chinese Holstein dairy cows. *Front Vet Sci*. (2021) 7:604729. doi: 10.3389/fvets.2020.604729

17. Zimian D, Fengmin S. The current situation and prospect of Chinese herbal medicine feed additives. World science and technology - mode. *Trad Chinese Med*. (2013) 15:446–54.

18. Shan CH, Guo J, Sun X, Li N, Yang X, Gao Y, et al. Effects of fermented Chinese herbal medicines on milk performance and immune function in late-lactation cows under heat stress conditions. *J Anim Sci*. (2018) 96:4444–57. doi: 10.1093/jas/sky270

19. Zhihui Z, Wei L, Jinbo Z, Yongsheng H, Tongbao L. Effects of compound probiotics on serum biochemical indexes and immune performance of wagyu bulls. *Feed Res*. (2021) 44:7–11. doi: 10.13557/j.cnki.issn1002-2813.2021.02.002

20. Li XL, He WL, Wang ZB, Xu TS. Effects of Chinese herbal mixture on performance, egg quality and blood biochemical parameters of laying hens. *J Anim Physiol Anim Nutr*. (2016) 100:1041–9. doi: 10.1111/jpn.12473

21. Tiantian G, Fengmei C, Shilin H. Application of blood routine and blood biochemistry to evaluate the health status of lactating herds in large-scale dairy farms. *Shandong Anim Hus Vet Med*. (2019) 40:68–71. Available at: https://chn.oversea.cnki.net/kcms/detail/detail.aspx?dbcode=CJFD&filename=DCMY201912033&dbname=CJFDLAST2020

22. Qiyong, G, Xinhua, W, Jinzhong, T, Yansheng, G. Study on the changing rules of blood biochemical indexes in dairy cows after delivery. *Southwest China J Agric Sci*. (2021) 34:1810–14. doi: 10.16213/j.cnki.scjas.2021.8.032

23. Pingli H, Jinbo M. Effects of compound Chinese herbal medicine on lactation performance, milk quality and serum biochemical indexes of dairy cows[J/OL]. *Feed Res*. (2022) 10:14–7. doi: 10.13557/j.cnki.issn1002-2813.2022.10.004

24. Lee SH, Jaekal J, Bae CS, Chung BH, Yun SC, Gwak MJ, et al. Enzyme-linked immunosorbent assay, single radial immunodiffusion, and indirect methods for the detection of failure of transfer of passive immunity in dairy calves. *J Vet Int Med*. (2010) 22:212–8. doi: 10.1111/j.1939-1676.2007.0013.x

25. Jinmei M, Liang C, Ming Z, Huanqi L. Research progress on diagnostic technology of latent mastitis in dairy cows. China: Anim Health Inspection (2016). 33:71–4. Available at: https://chn.oversea.cnki.net/kcms/detail/detail.aspx?dbcode=CJFD&filename=ZGDW201611020&dbname=CJFDLAST2017

26. Changbin L, Xiaoling L, Lichao K, Zonggui T, Fengxia S, Chunxia L. Effects of compound Chinese herbal medicines on milk quality of dairy cows. *Jiangsu Agric Sci*. (2016) 44:239–42. doi: 10.15889/j.issn.1002-1302.2016.01.070

27. Jiaoqing, L, Meichen, L, Jiaqiao, Z, Shaofeng, Y, Zhuoxian, W, Weina, BL, et al. Dynamic effects of Chinese herbal medicine preparations on the development of chicken immune organs and the expression of immune factors in the spleen. *Chinese Poult*. (2020) 42:49–53. doi: 10.16372/j.issn.1004-6364.2020.03.010

28. Qingyang, M, Ruoxi, G, Yufei, C, Puyi, H, Li, H. Research progress on the inhibitory effect and mechanism of Chinese herbal medicine on Saprolegniasis pathogens. Heilongjiang Anim Hus *Vet Med*. (2022) 4:121–126 132. doi: 10.13881/j.cnki.hljxmsy.2021.03.0416

29. Qingchao M, Decui X, Bin Y, Shuzhi L, Hong T. Exploration and thinking on the application of Chinese herbal feed additives in pig production. *Modern Anim Hus Sci Tech*. (2020) 11:1–3+54. doi: 10.19369/j.cnki.2095-9737.2020.11.001

30. Defeng, W, Meihua, H, Mei, L, Jinming, L, Jianhui, H. Effects of anti-heat stress Chinese herbal medicine additives on milk yield and milk composition of dairy cows. *Adv Anim Med*. (2004) 3:66–70. doi: 10.16437/j.cnki.1007-5038.2004.03.022

31. Jun, W, Pingping, W, Erxue, X, Hongbing, Z. Effects of Chinese herbal feed additives on growth performance, disease resistance and meat quality of Wannan free-range chickens. *Feed Res*. (2022) 9:56–9. doi: 10.13557/j.cnki.issn1002-2813.2022.09.013

32. Tongtong Y, Ziwei C, Hailiang Z, Wang Ao H, Lirong WK, Hanpeng L, et al. Study on the effect of physiological stage on blood routine indexes of healthy Chinese Holstein lactating cows. *Heilongjiang Anim Hus Vet Med*. (2021) 23:18–24. doi: 10.13881/j.cnki.hljxmsy.2021.06.0224

33. Mengyou Y, Hui W, Siyuan M, Xueqin L, Wenlong L, Tang Yongjie H, et al. Effects of secondary teats on milk production performance and blood routine indexes of Chinese Holstein cattle. *Chin J Anim Hus*. (2022) 58:69–74. doi: 10.19556/j.0258-7033.20201216-01

34. Xianqin Z, Changrong G, Yunbo T, Jingxing Z, Qichao H. Effects of Chinese herbal medicine additives on carcass characteristics and meat quality of growing-finishing pigs. *J Yunnan Agric Univ*. (Nat Sci). (2002) 1:86–90. doi: 10.16211/j.issn.1004-390x(n).2002.01.020

35. Guoxi Z, Yue L, Han Y, Zhang Ning H, Xiaoyue FH, Xiao L, et al. Effects of Chinese herbal medicines on the development of small intestine and IL-2 mRNA expression in weaned rabbits. *Heilongjiang Anim Hus Vet Med*. (2021) 23:114–7. doi: 10.13881/j.cnki.hljxmsy.2021.05.0172

36. Linsen Zan. (2017). Cattle Production Science. *3rd* Beijing: China Agricultural Press. 249–250.

37. Zhang Chungang S, Xiaoshuang LG, Tianyou W, Jinshun Z, Guoqi Z. Effects of compound Chinese herbal medicine additives on immunity and lactation performance of Holstein dairy cows. *J Herbol*. (2017) 26:104–12.

38. Kong XF, Hu YL, Yin YL, Wu GY, Rui R, Wang DY, et al. Chinese herbal ingredients are effective immune stimulators for chickens infected with the Newcastle disease virus. *Poult Sci*. (2006) 85:2169–75. doi: 10.1093/ps/85.12.2169

39. Li Y, Sun T, Hong Y, Qiao T, Wang Y, Li W, et al. Mixture of five fermented herbs (Zhihuasi Tk) alters the intestinal microbiota and promotes the growth performance in piglets. *Front Microbiol*. (2021) 12:725196. doi: 10.3389/fmicb.2021.725196

40. Sammad A, Umer S, Shi R, Zhu H, Zhao X, Wang Y. Dairy cow reproduction under the influence of heat stress. *J Anim Physiol Anim Nutr (Berl)*. (2020) 104:978–86. doi: 10.1111/jpn.13257

frontiers | Frontiers in Veterinary Science

TYPE Original Research
PUBLISHED 03 September 2024
DOI 10.3389/fvets.2024.1456524

OPEN ACCESS

EDITED BY
Stefan Gregore Ciornei,
University of Life Science (IULS), Romania

REVIEWED BY
Carlos Eduardo Ambrósio,
University of São Paulo, Brazil
Mihaela Spataru,
Ion Ionescu de la Brad University of Agricultural Sciences and Veterinary Medicine of Iași, Romania

*CORRESPONDENCE
Nicola Bernabò
✉ nbernabo@unite.it

RECEIVED 28 June 2024
ACCEPTED 14 August 2024
PUBLISHED 03 September 2024

CITATION
Belda-Perez R, Cimini C, Valbonetti L, Orsini T, D'Elia A, Massari R, Di Carlo C, Paradiso A, Maqsood S, Scavizzi F, Raspa M, Bernabò N and Barboni B (2024) Exploring swine oviduct anatomy through micro-computed tomography: a 3D modeling perspective.
Front. Vet. Sci. 11:1456524.
doi: 10.3389/fvets.2024.1456524

Exploring swine oviduct anatomy through micro-computed tomography: a 3D modeling perspective

Ramses Belda-Perez[1,2], Costanza Cimini[1], Luca Valbonetti[1], Tiziana Orsini[3], Annunziata D'Elia[3], Roberto Massari[3], Carlo Di Carlo[1], Alessia Paradiso[1], Seerat Maqsood[1], Ferdinando Scavizzi[3], Marcello Raspa[3], Nicola Bernabò[1]* and Barbara Barboni[1]

[1]Department of Biosciences and Technology for Food, Agriculture and Environment, University of Teramo, Teramo, Italy, [2]Physiology of Reproduction Group, Department of Physiology, Faculty of Veterinary Medicine, International Excellence Campus for Higher Education and Research (Campus Mare Nostrum), University of Murcia, Murcia, Spain, [3]Institute of Biochemistry and Cell Biology (CNR-IBBC/EMMA/Infrafrontier/IMPC), National Research Council, Rome, Italy

The oviduct plays a crucial role in the reproductive process, serving as the stage for fertilization and the early stages of embryonic development. When the environment of this organ has been mimicked, it has been shown to enhance *in vitro* embryo epigenetic reprogramming and to improve the yield of the system. This study explores the anatomical intricacies of two oviduct regions, the uterotubal junction (UTJ) and the ampullary-isthmic junction (AIJ) by using micro-computed tomography (MicroCT). In this study, we have characterized and 3D-reconstructed the oviduct structure, by measuring height and width of the oviduct's folds, along with the assessments of fractal dimension, lacunarity and shape factor. Results indicate distinct structural features in UTJ and AIJ, with UTJ displaying small, uniformly distributed folds and high lacunarity, while AIJ shows larger folds with lower lacunarity. Fractal dimension analysis reveals values for UTJ within 1.189–1.1779, while AIJ values range from 1.559–1.770, indicating differences in structural complexity between these regions. Additionally, blind sacs or crypts are observed, akin to those found in various species, suggesting potential roles in sperm sequestration or reservoir formation. These morphological differences align with functional variations and are essential for developing an accurate 3D model. In conclusion, this research provides information about the oviduct anatomy, leveraging MicroCT technology for detailed 3D reconstructions, which can significantly contribute to the understanding of geometric-morphological characteristics influencing functional traits, providing a foundation for a biomimetic oviduct-on-a-chip.

KEYWORDS

oviduct, microCT, 3D-reconstruction, swine model, utero tubal junction, ampullary-isthmic junction

1 Introduction

The oviduct is the organ where the journey of life begins for all mammals. It is divided into 4 regions, the infundibulum, the ampulla, the isthmus, and the uterotubal junction. After ovulation, the infundibulum is responsible for collecting the cumulus-oocyte complex, and on the isthmus, the sperm will form the spermatic reservoir attaching to the epithelial cells, suffering changes in its membrane, and prolonging their viability. Before ovulation, spermatozoa will be released from the reservoir and they reach the ampulla, where fertilization takes place. On the other hand, the uterine-tubal junction could be considered one of the main selection barriers (1).

The epithelium of the oviduct is composed of two major types of cells: secretory and ciliated. The secretory cells are responsible for the formation of oviductal fluid (2), which plays an important role in creating an appropriate environment for the transport and nourishment of gametes, as well as in protecting the fertilized egg during its journey through the oviduct (3). Conversely, the ciliated cells possess carbohydrate residues that are recognized by lectin-like proteins on the head of spermatozoa, leading to their binding and the creation of the previously mentioned sperm reservoir (4). The oviduct offers a dynamic environment, since its cell proportion and functionality change in response to the hormonal swings that take place throughout the cycle (5, 6). For instance, during the follicular phase, ciliated cells prevail in the ampulla of the oviduct while during the luteal phase, secretory cells take the forefront in this region (7). By contrast, in other segments of the oviduct, like the isthmus, the proportion of these cell types remains relatively stable with minimal variations throughout the estrus cycle (7).

Due to the relevance of oviduct in fertilization, some authors have tried to mimic its effect in *in vitro* fertilization platforms used in artificial reproductive techniques (8, 9). Indeed, the addition to artificial environment designed to allow the fertilization could improve the system's out, mainly reducing the epigenetic differences between the *in vivo* derived and *in vitro* produced embryos.

In that context, for instance an oviduct-on-a-chip has been recently created (9). In one hand it represents a very interesting device, but in the other one hand it ignores the architectural features of the organ. Since it has been demonstrated that there is a correlation between oviduct architecture and function (10) here we carried out a set of measures to lay the foundation to a sort of reverse engineering work. In fact, in a recent work we identified, from a selection of 3D-printing-biocompatible materials previously used in cell cultures, the one suitable for construction the model of the oviduct, evaluating its toxic effects by mean of embryo development (11). Consequently, the present work emerges as a pilot study aimed at creating an anatomically accurate-3D model of the oviduct to furtherly design a biomimetic oviduct-on-a-chip. This approach will consider the organ's morphology, then we adopted an approach based on the use of microcomputed tomography (MicroCT) as a reliable tool for the anatomical study of oviduct: it is non-destructive technology characterized by high resolution and three-dimensional visualization capabilities, and it is able to allow sophisticated quantitative analysis and detailed 3D reconstructions.

2 Results

2.1 Utero tubal junction

In this segment of the oviduct, it is noteworthy that there are small folds present, and their dimensions typically fall within the range between 144–988 µm length and 70–366 µm width (Supplementary Table S1; Figure 1). These folds do not reach a great percentage of the lumen, an observation that is supported by the high lacunarity value (Supplementary Table S1).

On the contrary, the distribution of values for fractal dimension and lacunarity in UTJ is concentrated around a different subpopulation (Figure 2). The fractal dimension encompasses values within the range 1.189–1.1779, while the lacunarity values range within 0.901–2.701 (Supplementary Table S1). On the other hand, the shape factor values of the UTJ external and internal regions are provided (Table 1).

2.2 Ampullary-isthmic junction

In this section of the oviduct, we not only observe a higher prevalence of folds but also an increase in their individual sizes, ranging between 126–1,446 µm length (Supplementary Table S2) and 40–512 µm width (Supplementary Table S2), resulting in a more substantial occupancy within the lumen, reducing the lacunarity (Supplementary Table S2). In AIJ, distinct subpopulations of folds are discernible, with one set characterized by larger dimensions and another set exhibiting smaller dimensions. By contrast to the width measurements, where the data distribution is not centered around specific values, but rather displays a more homogeneous spread (Figure 3).

Similar to what we observed with the length of the folds, the fractal dimension and lacunarity are also divided into different subpopulation (Figure 4). The fractal dimension encompasses values within the range 1.559–1.770, while the lacunarity values ranges within 0.577–1.544 (Supplementary Table S2). On the other hand, the shape factor values of the AIJ external and internal region is provided (Table 2).

2.3 3-D reconstruction

In the 3D reconstruction, the tortuous structure of the oviduct is represented offering a detailed view of the high tortuosity it possesses (Supplementary Movie 1). The visualization highlights the spatial arrangement of the folds of the AIJ section and small blind-ended sacs (Figures 5A–D). On the other hand, in the UTJ of the oviduct, the lumen is narrower and exhibits a less tortuous structure compared to the other sections (Figures 5E–H).

3 Discussion

In this study, we have delved into the architectural examination of different segments of swine oviduct by using a medical imaging approach, reporting for the first-time parameters such as the shape factor, fractal dimension and lacunarity of the oviduct through microCT imaging. These parameters will be the basis for a more

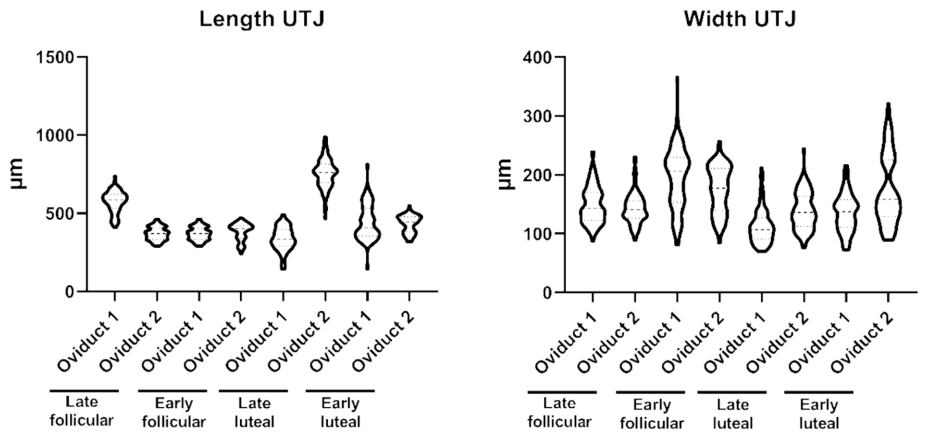

FIGURE 1
Violin plot representing the different measurement of length (left) and width (right) of the folds from the UTJ.

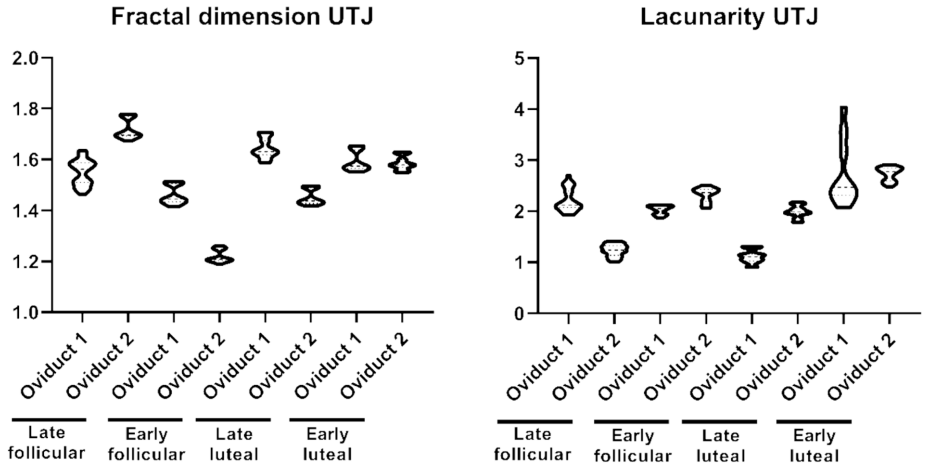

FIGURE 2
Violin plot representing the different measurement of fractal dimension (left) and lacunarity (right) of the folds from the UTJ.

accurate representation of reality in an oviduct-on-a-chip, enabling improved IVF and embryo culture performance, presumably enhancing epigenetic embryo reprogramming (9).

MicroCT has already been used to characterize the architecture of organs such as lungs (12), tendons or arteries (13), or even to recreate 3D images of breast cancer specimens (14). It generates 3D models that can then be converted into files suitable for 3D printing, thus enabling the creation of three-dimensional replicas of those organs (15). This technology has been used to create custom prostheses (16), and could be used to create models for surgeon planning (17) or for educational purposes (18). Recently, it has been used to create 3D bone phantoms through 3D printing, using CT generated images (19). In this context, this preliminary study means a progress into the creation of a novel oviduct 3D model considering the architecture of the organ, in the light to design a biomimetic 3D scaffold suitable for IVP.

The classical method for reconstructing the oviduct has traditionally involved using histology slides. However, it has been shown that this method may not be the most suitable, as it could result in gaps (20). Additionally, when using histology, it can be reconstruction inaccuracies ranging due to deformation of misalignment (21), due to the difficulty of managing three-dimensional orientation. Multiple manual artifacts affect the perfect alignment of the sample in all directions of space. In fact, the positioning procedures of the sample inside the embedding medium, the mounting of the histological specimen on the microtome, the simultaneous three-dimensional angulation of the specimen and the instrument are evident causes of problematic management of the spatial orientation of the specimens. This type of problem is partially overcome in the case of virtual histology that can be performed by microCT, which also becomes the basis of the three-dimensional model perfectly fitting the original sample. MicroCT technique has proven to be a valuable tool for studying mineralized biologic tissues (22), although its utility in the investigation of soft tissues has been somewhat constrained due to the limited contrast these tissues typically exhibit (23). Some tries have been made previously to study the internal structure of the oviduct through microCT (24). With the oviduct unmodified and without contrast, and other ones fill the oviduct with a strong contrast agent (24). The initial attempt proved

10.3389/fvets.2024.1456524

TABLE 1 Shape factor of the oviduct in UTJ region.

External shape factor								
	Late follicular		Early follicular		Late luteal		Early luteal	
	Oviduct 1	Oviduct 2	Oviduct 1	Oviduct 2	Oviduct 1	Oviduct 2	Oviduct 1	Oviduct 2
Volume (mm^3)	66.31	127.71	31.53	26.64	41.55	43.64	84.22	39.80
Surface (mm^2)	234.11	353.68	124.53	109.56	170.13	130.69	268.53	143.59
Height (mm)	4.46	4.46	4.46	4.46	4.46	4.46	4.46	4.46
Shape index	15.75	12.35	17.62	18.34	18.26	13.36	14.22	16.09
shape index (1/mm)	3.53	2.77	3.95	4.11	4.09	2.99	3.19	3.61
Internal shape factor								
Volume (mm^3)	3.95	3.2	0.52	0.80	1.66	1.58	7.78	2.87
Surface (mm^2)	77.88	50.2	13.83	16.31	30.20	23.92	106.27	30.19
Height (mm)	4.46	4.46	4.46	4.46	4.46	4.46	4.46	4.46
Shape index	87.94	69.97	118.62	90.93	81.14	67.52	60.92	46.92
shape index (1/mm)	19.72	15.69	26.60	20.39	18.19	15.14	13.66	10.52

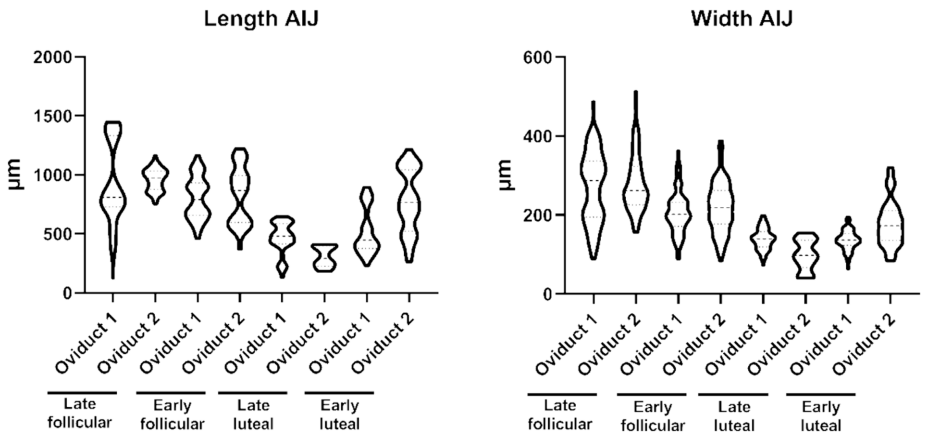

FIGURE 3
Violin plot representing the different measurement of length (left) and widths (right) of the folds from the AIJ.

to be unsuccessful as it yielded no discernible internal structures. In contrast, the subsequent approaches provided what could be likened to a photographic "negative" of the oviduct. This effect was achieved due to the significant disparity in clarity between the contrast agent and the surrounding tissue. However, when compared with histology slides, the structure observed was not very detailed. In our work, we employed the paraffin embedding method, a technique that enables us to visualize the high-resolution structure of the oviduct by leveraging its endogenous contrast, as previously described for murine embryos (25). Although in human the use of MicroCT to study the oviduct has been already achieved successfully (26), to our knowledge, those represent the first data obtained from swine oviducts through microCT.

Like what has been observed in humans (26, 27) or sheep (28), our results show throughout all phases of the cycle, at the UTJ level, mucosal folds are sparse and smaller in size, occupying limited space within the lumen. However, as we move away from the uterus and progress toward the oviduct until the ampulla, a significant increase in the size of these folds and the proportion of space they occupy within the lumen becomes evident. This increase in lumen occupancy is not only apparent from the measurements of the folds in the images but is also corroborated by the decrease in lacunarity. In addition, even

10.3389/fvets.2024.1456524

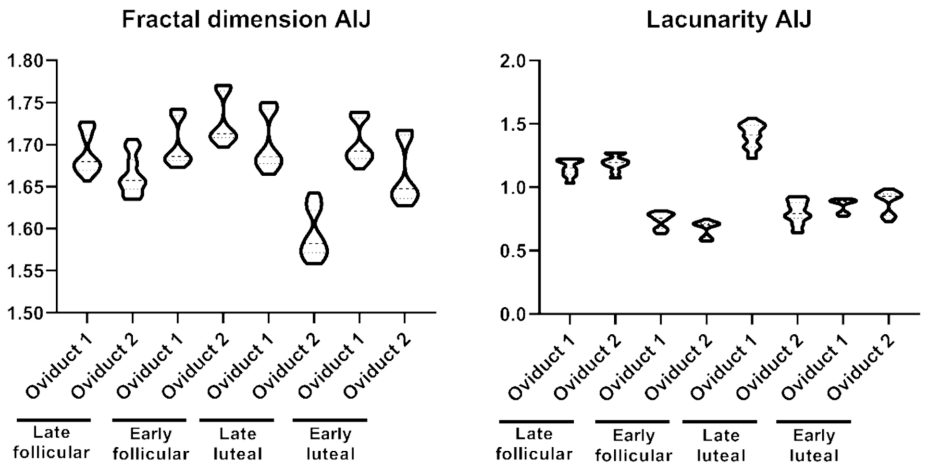

FIGURE 4
Violin plot representing the different measurement of fractal dimension (left) and lacunarity (right) of the folds from the UTJ.

TABLE 2 Shape factor of the oviduct in AIJ region.

External shape factor								
	Late follicular		Early follicular		Late luteal		Early luteal	
	Oviduct 1	Oviduct 2	Oviduct 1	Oviduct 2	Oviduct 1	Oviduct 2	Oviduct 1	Oviduct 2
Volume (mm^3)	40.79	44	23.6	26.51	29.83	23.79	35.10	48.41
Surface (mm^2)	226.97	225.73	234.99	286.61	155.14	84.67	166.89	323.40
Height (mm)	4.46	4.46	4.46	4.46	4.46	4.46	4.46	4.46
shape index	24.82	22.88	44.41	48.21	23.20	15.87	21.21	29.79
shape index (1/mm)	5.56	5.13	9.96	10.81	5.20	3.56	4.75	6.68
Shape factor								
Volume (mm^3)	4.87	4.32	6.36	5.88	1.99	0.40	0.81	8.34
Surface (mm^2)	66.76	73.22	103.86	141.18	41.52	8.96	18.91	195.45
Height (mm)	4.46	4.46	4.46	4.46	4.46	4.46	4.46	4.46
shape index	61.15	75.59	72.83	107.16	92.96	99.90	104.12	104.56
shape index (1/mm)	13.71	16.95	16.33	24.03	20.84	22.40	23.35	23.44

though our sample size is small, it is worth noting that the maximum fold amplitude is consistently observed during the follicular phase, as previously described using electronic microscopy (29). Cyclic variations during the estrous cycle have been even described in the serosal part of the oviduct where cells of the tubal epithelium are also present, being the ciliated cells predominant during the follicular phase and the secretory cells during the luteal phase (30). It has been suggested that the folds in the oviduct could play a crucial role in the transport of oocytes and embryos during the fertilization process. These oviductal epithelial folds serve to significantly increase the surface area of the epithelium, thereby enhancing the likelihood of contact between the oocyte/embryo and the ciliated cells within the oviduct (31). Moreover, the specific structure of these folds appears to play a key role in alleviating the pressure difference in the oviductal fluid before and after the passage of the oocyte/embryo (31). It has been observed that the Celsr1 gene controls the proper formation of these oviductal folds, and Celsr1-deficient mice present an altered ciliary beating coordination, and aberrant fold orientation distribution, even leading to infertility (32), presumably due to difficulties in the effective transport of oocytes and embryos through the oviduct.

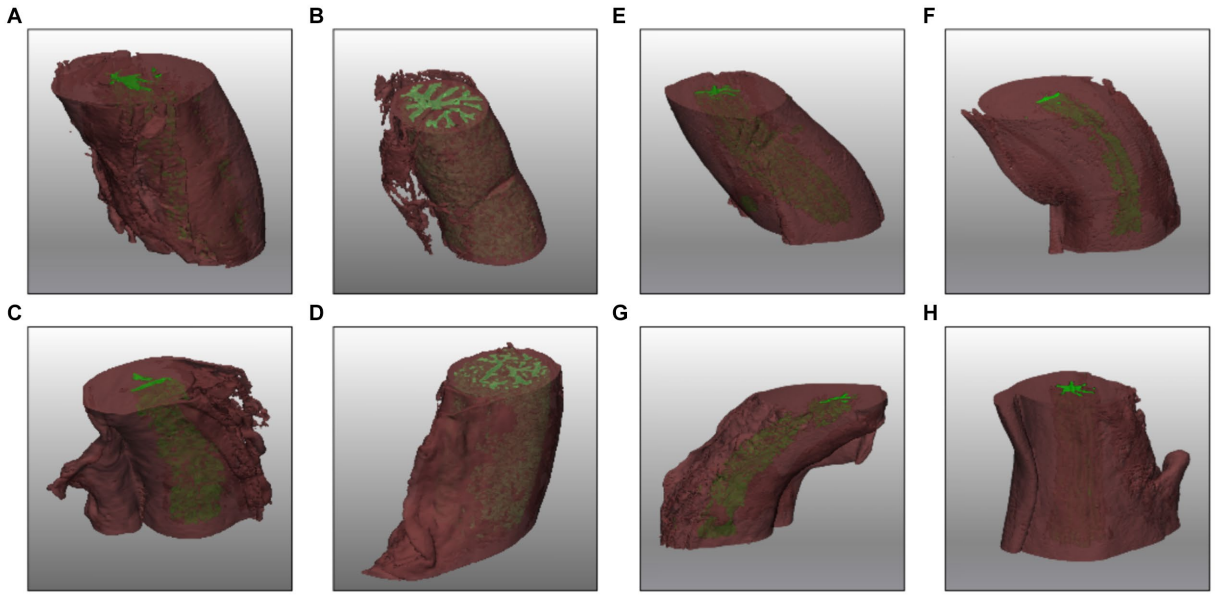

FIGURE 5
3D reconstruction of AIJ **(A–D)** and UTJ **(E–H)** regions in different phases of the cycle late follicular **(A,E)**, early follicular **(B,F)**, late luteal **(C,G)**, and early luteal **(D,H)**.

In the 3D reconstruction of the oviduct, we can observe numerous blind sacs or crypts, which are small, pouch-like structures within the oviduct. These anatomical features have been described in pigs (29) and in other animal species, including humans (26), ovine (28), marsupials (33, 34), hamster (35), bovine (6), and moles (36). In some animals, such as shrews, it has been suggested that the crypts in the oviduct mucosa may serve the function of "sequestering" sperm, thereby preventing polyspermy (37). Meanwhile, in other animals like cows (6) or sows (29), it has been proposed that these structures could also collaborate to form the sperm reservoir.

The data gleaned from this study possesses significant potential to lay the groundwork for the development of a sophisticated 3D model. Advanced printing techniques, including additive manufacturing processes, can then be employed to fabricate the physical device layer by layer, resulting in a tangible replica of the organ. This model would be meticulously crafted to encompass the intricate architecture of the oviduct. By meticulously incorporating the detailed structural nuances revealed by the microCT imaging, this 3D printing file would serve as a blueprint for creating a physical device that faithfully replicates the natural features of the organ. This innovative device, when combined with microfluidic systems, could have the potential to replicate the physiology of organs, offering a valuable tool for enhanced studies of organ function and disease (38). Notably, in recent years, research has shown that conducting *in vitro* fertilization processes within devices mimicking the oviduct can yield superior outcomes (9, 39). Considering this, the reconstructions obtained in this study hold the promise of serving as the blueprint for a 3D-printed device that accurately reflects this complex architecture. Thanks to its accuracy anatomy reconstruction, together with a microfluidic system, could even allow the study of the biophysics of the organ and a more reliable representation of the processes that's occurs in the oviduct, as sperm capacitation or the "taxis" (chemotaxis, thermotaxis and rheotaxis) that guides sperm cells within the oviduct (40).

In this work, we conducted a comprehensive assessment to determine the most suitable segmentation techniques for accurately representing the morphological traits of interest. This evaluation encompassed various segmentation methods, including automatic, interactive, and manual approaches. The challenge of segmentation in biomedical imaging, as highlighted in both the existing literature and this experimental investigation, predominantly arises from the lack of efficient automated tools.

In summary, the pursuit of optimal segmentation techniques in biomedical imaging is crucial for advancing both research and clinical practice. By addressing the challenges inherent in segmentation, such as automation and accuracy, researchers and clinicians can harness the full potential of biomedical imaging. Additionally, the integration of 3D printing technology further amplifies the impact of biomedical imaging by that facilitating the conversion of virtual models into physical prototypes capable of faithfully reproducing even the most intricate shapes and geometric features. For that reason and considering that our group have previously identified a suitable material together with the suitable appropriate 3D printing technology, the data presented in this work will allow the engineer of a new 3D scaffold as closely as possible to the oviduct in order to increase the quality of embryos produced with ARTs.

4 Materials and methods

4.1 Oviduct selection and collection

Genital tracts from sows and gilts were obtained at the local slaughterhouse and transported into the lab within 2 h of slaughter. Once in the lab, the cycle stage of the tracts was determined based on the ovarian morphology as described previously (41) and classified into early follicular ($n = 2$), late follicular ($n = 2$), early

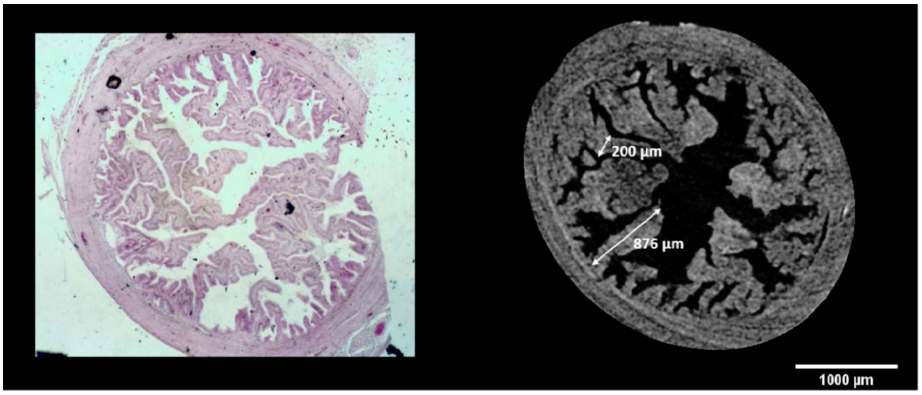

FIGURE 6
Comparison between virtual and histological oviduct sectioning, with a schematic representation of the measurement method performed.

luteal ($n = 2$), or late luteal phase ($n = 2$). Two oviduct from 4 animals were selected for each phase of the reproductive cycle, dissected and divided into segments. The portions corresponding to the isthmus and the uterine-tubal junction were washed in PBS and fixed in 4% paraformaldehyde for 1 h. Subsequently, the samples underwent dehydration through a series of alcoholic solutions (ranging from 50 to 100%) and soaked in xylene 3 times for 15 min each (45 min tot). An incubation step with xylene paraffin (1:1) was carried out for 45 min at 56°C before embedding in paraffin wax.

4.2 MicroCT and image acquisition

MicroCT datasets of swine oviducts at different stages of estrous cycle were acquired by using the high-resolution 3D-imaging system Skyscan 1172G (Bruker, Kontich – Belgium), using an L7901-20 Microfocus X-ray Source (Hamamatsu), with image pixel/size of 7.4 µm, camera binning 2×2, source voltage of 39 kV, source current of 240 µA, exposure time of 500 ms. The reconstructed tomographic volumes of the acquired images were performed using built-in NRecon Skyscan reconstruction software (Version: 1.6.6.0; Skyscan Bruker). 3D-images were generated using 3D-Visualization Software CTvox v. 2.5, while the volume rendering and virtual sectioning views using DataViewer v. 1.4.4 (Skyscan Bruker) and the analysis of the sample was performed using CT-Analyser software version 1.13.

4.3 Histology and light microscopy

Paraffin embedded oviducts were microtome-sectioned at 10 µm and stained with Hematoxylin (Sigma-Aldrich, cat. MHS16) – Eosin (Sigma-Aldrich, cat. 109,844) standard protocol to perform histological assay. Images were obtained with the stereomicroscope MZ12 (Leica) equipped with a color camera. The histological analysis highlighted the accuracy and fidelity of the two-dimensional and three-dimensional images obtained from microtomography, which has the further advantage of guaranteeing the structural integrity of the sample and avoiding distortions and artifacts resulting from the sectioning procedures (Figures 2, 5, 6).

4.4 Image analysis

Using microCT images, measurements of the length and width of the oviduct folds were conducted, as illustrated in Figure 6. The FIJI program (ImageJ 2.0.0-rc-43/1.50e) was employed for this purpose, utilizing its built-in measurement tool to ensure accuracy in anatomical dimensions. Similarly, to calculate the fractal dimension and lacunarity values, we applied the box-counting method using the FracLac plugin in Fiji.

4.5 Two-dimensional image processing

For the processing of two-dimensional images, the software Mimics from the Belgian company Materialise (Materialise, Leuven, Belgium) and 3Matic (Materialise, Leuven, Belgium) were used. Mimics is the primary software for processing biomedical images in the rapid prototyping sector. Initially, the DICOM files were loaded, and the correct orientation of the images (Top-Bottom, Anterior–Posterior, Right–Left) was set. Once the images were loaded, the software provided their visualization of the three anatomical planes: transverse/axial, coronal/frontal, and sagittal. It was decided to analyze, in particular, the series of images from the ampullary-isthmus junction (AIJ) and of the utero-tubal junction (UTJ). This approach ensured that images from all phases acquired were available, regardless of their original format. Each image series generated a project within Mimics, i.e., a file in .mcs format. At this point, an initial segmentation was performed on each of the four files by selecting the region of interest through the crop project operation. Specifically, various slices along all three directions (x, y, z) were excluded from the project, retaining only the structures of interest and reducing the number of slices to be analyzed. This helped eliminate the influence of regions not relevant to the study. To achieve this, the position and size of a rectangle were set in all three views (axial, coronal, and sagittal) to delimit the volume of interest in the resulting parallelepiped in the three-dimensional view. After a careful analysis of

the images from various contrast phases, the different anatomical structures that would be included in the overall three-dimensional virtual model have been segmented separately: both the external and internal structures of the reference tract (UTJ and AIJ). For each of these structures, it was assessed which image series was most suitable for their segmentation. This decision was based on the presence of enhanced visibility of the mentioned structures in those specific images. Regarding the improvement of image quality, especially in terms of contrast, a point-wise enhancement technique was employed. This involves applying a transformation that maps a small range of grey levels onto the entire possible range, aiming to achieve visual enhancement. Finally, it is specified that the term "mask" refers to a set of pixels that have been grouped together as a result of various operations performed on the three two-dimensional views. Each mask is associated with a specific color, a minimum HU value, and a maximum HU value.

4.6 Processing of the three-dimensional model

Once the segmentation of the different structures has been carried out, it is necessary to process the three-dimensional model by performing a smoothing operation with the appropriate number of iterations. This is done to achieve a virtual model suitable for both three-dimensional visualization and the subsequent potential 3D printing phase. The three-dimensional object calculated from the mask inevitably exhibits a step effect due to the spatial resolution of the images, which is evidently insufficient for our purposes. The edges of the three-dimensional object, reconstructed from the mask, tend to follow individual pixels that have dimensions of approximately 1 mm × 1 mm. This scaling effect can be observed both in the three-dimensional view and on the individual slices for each anatomical structure. The smoothing operation was performed in the Mimics software rather than the modelling software 3-Matic by Materialise, used in the later phase of processing the three-dimensional model and optimizing the mesh. This choice is because, once the smoothing operation with a certain number of iterations is completed in Mimics, it is possible to compare the result with CT images on individual sections (axial, coronal, and sagittal) by visualizing the contours of the obtained three-dimensional object. In general, smoothing operations contribute significantly to enhancing the surface quality of a model. Nevertheless, it is crucial to exercise caution, as an excessively high number of smoothing iterations can lead to alterations in the model, resulting in unexpected outcomes. It is important to keep in mind that real-life organs do not possess perfectly smooth surfaces. The complete virtual model obtained in this way enabled the three-dimensional visualization of various anatomical structures. In this visualization, appropriate degrees of transparency were set for different structures, allowing for the visualization of outer and inner structures as well.

4.7 Processing of the three-dimensional model

The calculation of the shape factor is a procedure used in various contexts, such as physics, engineering, or thermodynamics. The shape factor is a quantity that expresses the geometry of one body in relation to another, often concerning thermal radiation exchange or fluid dynamics. Its mathematical expression can vary depending on the specific context.

In general terms, the shape factor (F) that we used can be calculated using the following simplified formula:

$$F = \frac{S * h}{V}$$

where S and V are, respectively, the surfaces and volumes of the two bodies under consideration, the UTJ and AIJ, and h is the height of the traits. However, in more complex situations, such as radiation exchange between non-ideal surfaces, the formula can be more intricate and involve angles, distances, and emissivity properties of the surfaces.

Data availability statement

The original contributions presented in the study are included in the article/Supplementary material, further inquiries can be directed to the corresponding author.

Ethics statement

Ethical approval was not required for the study involving animals in accordance with the local legislation and institutional requirements because we collected samples at local slaughterhouse without any contact with live animals, and without interacting with them.

Author contributions

RB-P: Data curation, Formal analysis, Writing – original draft. CC: Data curation, Formal analysis, Writing – original draft, Writing – review & editing. LV: Conceptualization, Data curation, Formal analysis, Methodology, Visualization, Writing – original draft. TO: Data curation, Formal analysis, Writing – review & editing. AD'E: Data curation, Formal analysis, Methodology, Writing – review & editing. RM: Data curation, Formal analysis, Writing – review & editing. CDC: Data curation, Formal analysis, Writing – review & editing. AP: Data curation, Formal analysis, Writing – review & editing. SM: Data curation, Formal analysis, Writing – review & editing. FS: Data curation, Formal analysis, Writing – review & editing. MR: Data curation, Formal analysis, Writing – review & editing. NB: Conceptualization, Data curation, Formal analysis, Funding acquisition, Supervision, Validation, Writing – original draft, Writing – review & editing. BB: Data curation, Formal analysis, Funding acquisition, Supervision, Writing – review & editing.

Funding

The author(s) declare that financial support was received for the research, authorship, and/or publication of this article. This research was funded by the European Union-Next Generation EU. Project Code: 427 ECS00000041; Project CUP: C43C22000380007; Project Title: Innovation, digitalization and 428 sustainability for the diffused economy in Central Italy-VITALITY.

Conflict of interest

The authors declare that the research was conducted in the absence of any commercial or financial relationships that could be construed as a potential conflict of interest.

Publisher's note

All claims expressed in this article are solely those of the authors and do not necessarily represent those of their affiliated organizations, or those of the publisher, the editors and the reviewers. Any product that may be evaluated in this article, or claim that may be made by its manufacturer, is not guaranteed or endorsed by the publisher.

Supplementary material

The Supplementary material for this article can be found online at: https://www.frontiersin.org/articles/10.3389/fvets.2024.1456524/full#supplementary-material

References

1. Mahé C, Zlotkowska AM, Reynaud K, Tsikis G, Mermillod P, Druart X, et al. Sperm migration, selection, survival, and fertilizing ability in the mammalian oviduct†. *Biol Reprod*. (2021) 105:317–31. doi: 10.1093/biolre/ioab105

2. Hugentobler SA, Sreenan JM, Humpherson PG, Leese HJ, Diskin MG, Morris DG. Effects of changes in the concentration of systemic progesterone on ions, amino acids and energy substrates in cattle oviduct and uterine fluid and blood. *Reprod Fertil Dev*. (2010) 22:684–94. doi: 10.1071/RD09129

3. Ménézo Y, Guérin P, Elder K. The oviduct: a neglected organ due for re-assessment in IVF. *Reprod Biomed Online*. (2015) 30:233–40. doi: 10.1016/j.rbmo.2014.11.011

4. Talevi R, Gualtieri R. Molecules involved in sperm-oviduct adhesion and release. *Theriogenology*. (2010) 73:796–801. doi: 10.1016/j.theriogenology.2009.07.005

5. Steinhauer N, Boos A, Günzel-Apel AR. Morphological changes and proliferative activity in the oviductal epithelium during hormonally defined stages of the oestrous cycle in the bitch. *Reprod Domest Anim*. (2004) 39:110–9. doi: 10.1111/j.1439-0531.2004.00490.x

6. Yániz JL, Lopez-Gatius F, Santolaria P, Mullins AKJ. Study of the functional anatomy of bovine Oviductal mucosa. *Anat Rec*. (2000) 260:268–78. doi: 10.1002/1097-0185(20001101)260:3<268::AID-AR60>3.0.CO;2-L

7. Abe H. The mammalian oviductal epithelium: regional variations in cytological and functional aspects of the oviductal secretory cells. *Histol Histopathol*. (1996) 11:743–68.

8. Canovas S, Ivanova E, Romar R, García-Martínez S, Soriano-Úbeda C, García-Vázquez FA, et al. DNA methylation and gene expression changes derived from assisted reproductive technologies can be decreased by reproductive fluids. *eLife*. (2017) 6:23670. doi: 10.7554/eLife.23670

9. Ferraz MAMM, Rho HS, Hemerich D, Henning HHW, van Tol HTA, Hölker M, et al. An oviduct-on-a-chip provides an enhanced *in vitro* environment for zygote genome reprogramming. *Nat Commun*. (2018) 9:9. doi: 10.1038/s41467-018-07119-8

10. Michael J, Modell H, McFarland J, Cliff W. The "core principles" of physiology: what should students understand? *Adv Physiol Educ*. (2009) 33:10–6. doi: 10.1152/advan.90139.2008

11. Belda-Perez R, Heras S, Cimini C, Romero-Aguirregomezcorta J, Valbonetti L, Colosimo A, et al. Advancing bovine *in vitro* fertilization through 3D printing: the effect of the 3D printed materials. *Front Bioeng Biotechnol*. (2023) 11:1260886. doi: 10.3389/fbioe.2023.1260886

12. Scott AE, Vasilescu DM, Seal KAD, Keyes SD, Mavrogordato MN, Hogg JC, et al. Three dimensional imaging of paraffin embedded human lung tissue samples by micro-computed tomography. *PLoS One*. (2015) 10:e0126230. doi: 10.1371/journal.pone.0126230

13. Shearer T, Bradley RS, Hidalgo-Bastida LA, Sherratt MJ, Cartmell SH. Three-dimensional visualisation of soft biological structures by X-ray computed micro-tomography. *J Cell Sci*. (2016) 129:2483–92. doi: 10.1242/jcs.179077

14. DiCorpo D, Tiwari A, Tang R, Griffin M, Aftreth O, Bautista P, et al. The role of Micro-CT in imaging breast cancer specimens. *Breast Cancer Res Treat*. (2020) 180:343–57. doi: 10.1007/s10549-020-05547-z

15. Eltorai AEM, Nguyen E, Daniels AH. Three-dimensional printing in orthopedic surgery. *Orthopedics*. (2015) 38:684–7. doi: 10.3928/01477447-20151016-05

16. Dai KR, Yan MN, Zhu ZA, Sun YH. Computer-aided custom-made hemipelvic prosthesis used in extensive pelvic lesions. *J Arthroplast*. (2007) 22:981–6. doi: 10.1016/j.arth.2007.05.002

17. Starosolski ZA, Kan JH, Rosenfeld SD, Krishnamurthy R, Annapragada A. Application of 3-D printing (rapid prototyping) for creating physical models of pediatric orthopedic disorders. *Pediatr Radiol*. (2014) 44:216–21. doi: 10.1007/s00247-013-2788-9

18. Shelmerdine SC, Simcock IC, Hutchinson JC, Aughwane R, Melbourne A, Nikitichev DI, et al. 3D printing from microfocus computed tomography (micro-CT) in human specimens: education and future implications. *Br J Radiol*. (2018) 91:1–8. doi: 10.1259/BJR.20180306

19. Mei K, Pasyar P, Geagan M, Liu LP, Shapira N, Gang GJ, et al. Design and fabrication of 3D-printed patient-specific soft tissue and bone phantoms for CT imaging. *Res Sq*. (2023) 13:17495. doi: 10.1038/s41598-023-44602-9

20. Senter-Zapata M, Patel K, Bautista PA, Griffin M, Michaelson J, Yagi Y. The role of Micro-CT in 3D histology imaging. *Pathobiology*. (2016) 83:140–7. doi: 10.1159/000442387

21. Gibson E, Gaed M, Gómez JA, Moussa M, Romagnoli C, Pautler S, et al. 3D prostate histology reconstruction: an evaluation of image-based and fiducial-based algorithms. *Med Phys*. (2013) 40. doi: 10.1118/1.4816946

22. Neues F, Epple M. X-ray microcomputer tomography for the study of biomineralized endo- and exoskeletons of animals. *Chem Rev*. (2008) 108:4734–41. doi: 10.1021/cr078250m

23. Metscher BD. MicroCT for comparative morphology: simple staining methods allow high-contrast 3D imaging of diverse non-mineralized animal tissues. *BMC Physiol*. (2009) 9:11. doi: 10.1186/1472-6793-9-11

24. Burkitt M, Walker D, Romano DM, Fazeli A. Computational modelling of maternal interactions with spermatozoa: potentials and prospects. *Reprod Fertil Dev*. (2011) 23:976–89. doi: 10.1071/RD11032

25. Ermakova O, Orsini T, Gambadoro A, Chiani F, Tocchini-Valentini GP. Three-dimensional microCT imaging of murine embryonic development from immediate post-implantation to organogenesis: application for phenotyping analysis of early embryonic lethality in mutant animals. *Mamm Genome*. (2018) 29:245–59. doi: 10.1007/s00335-017-9723-6

26. Castro PT, Aranda OL, Matos APP, Marchiori E, de Araújo LFB, Alves HDL, et al. The human endosalpinx: anatomical three-dimensional study and reconstruction using confocal microtomography. *Pol J Radiol*. (2019) 84:e281–8. doi: 10.5114/pjr.2019.86824

27. Rocca M, El Habashy M, Nayel S, Madwar A. The intramural segment and the uterotubal junction: an anatomic and histologic study. *Int J Gynaecol Obstet*. (1989) 28:343–9. doi: 10.1016/0020-7292(89)90606-1

28. Yániz JL, Carretero T, Recreo P, Arceiz E, Santolaria P. Three-dimensional architecture of the ovine oviductal mucosa. *Anat Histol Embryol*. (2014) 43:331–40. doi: 10.1111/ahe.12078

29. Yaniz JL, Lopez-Gatius F, Hunter RHF. Scanning electron microscopic study of the functional anatomy of the porcine oviductal mucosa. *J. Vet. Med. Series C*. (2006) 35:28–34. doi: 10.1111/j.1439-0264.2005.00634.x

30. Yániz JL, Recreo P, Carretero T, Arceiz E, Hunter RHF, López-Gatius F. The peritoneal mesothelium covering the genital tract and its ligaments in the female pig shows signs of active function. *Anat Rec*. (2007) 290:831–7. doi: 10.1002/ar.20554

31. Koyama H, Shi D, Fujimori T. Biophysics in oviduct: planar cell polarity, cilia, epithelial fold and tube morphogenesis, egg dynamics. *Biophys Physicobiol*. (2019) 16:89–107. doi: 10.2142/biophysico.16.0_89

32. Shi D, Komatsu K, Hirao M, Toyooka Y, Koyama H, Tissir F, et al. Celsr1 is required for the generation of polarity at multiple levels of the mouse oviduct. *Development*. (2014) 141:4558–68. doi: 10.1242/dev.115659

33. Bedford JM, Breed WG. Regulated storage and subsequent transformation of spermatozoa in the fallopian tubes of an Australian marsupial, *Sminthopsis crassicaudata*. *Biol Reprod*. (1994) 50:845–54. doi: 10.1095/biolreprod50.4.845

34. Rodger JC, Bedford JM. Induction of oestrus, recovery of gametes, and the timing of fertilization events in the opossum, *Didelphis virginiana*. *J Reprod Fertil*. (1982) 64:159–69. doi: 10.1530/jrf.0.0640159

35. Smith TT, Koyanagi F, Yanagimachi R. Distribution and number of spermatozoa in the oviduct of the Golden Hamster after natural mating and artificial Inseminatio&. *Biol Reprod*. (1987) 37:5–234.

36. Bedford JM, Mock OB, Nagdas SK, Winfrey VP, Olson GE. Reproductive features of the eastern mole (*Scalopus aquaticus*) and star-nose mole (*Condylura cristata*). *J Reprod Fertil*. (1999) 117:345–53. doi: 10.1530/jrf.0.1170345

37. Bedford JM, Mock OB, Phillips DM. Unusual ampullary sperm crypts, and behavior and role of the cumulus oophorus, in the oviduct of the least shrew, *Cryptotis parva*. *Biol Reprod*. (1997) 56:1255–67. doi: 10.1095/biolreprod56.5.1255

38. Huh D, Hamilton GA, Ingber DE. From three-dimensional cell culture to organs-on-chips. *Trends Cell Biol*. (2011) 21:745–54. doi: 10.1016/j.tcb.2011.09.005

39. Ferraz MAMM, Henning HHW, Costa PF, Malda J, Melchels FP, Wubbolts R, et al. Improved bovine embryo production in an oviduct-on-a-chip system: prevention of poly-spermic fertilization and parthenogenic activation. *Lab Chip*. (2017) 17:905–16. doi: 10.1039/C6LC01566B

40. Monteiro Melo Ferraz M d A, Ferronato GDA. Opportunities involving microfluidics and 3D culture systems to the *in vitro* embryo production. *Anim Reprod*. (2023) 20:58. doi: 10.1590/1984-3143-ar2023-0058

41. Carrasco LC, Romar R, Avilés M, Gadea J, Coy P. Determination of glycosidase activity in porcine oviductal fluid at the different phases of the estrous cycle. *Reproduction*. (2008) 136: 833–842. doi: 10.1530/REP-08-0221

frontiers | Frontiers in Veterinary Science

TYPE Original Research
PUBLISHED 04 September 2024
DOI 10.3389/fvets.2024.1474386

OPEN ACCESS

EDITED BY
Mihai Cenariu,
University of Agricultural Sciences and Veterinary Medicine of Cluj-Napoca, Romania

REVIEWED BY
Gamal Mehaisen,
Cairo University, Egypt
Valeria Pasciu,
University of Sassari, Italy

*CORRESPONDENCE
Vibuntita Chankitisakul
✉ vibuch@kku.ac.th

RECEIVED 01 August 2024
ACCEPTED 23 August 2024
PUBLISHED 04 September 2024

CITATION
Koedkanmark T, Ratchamak R, Authaida S, Boonkum W, Semaming Y and Chankitisakul V (2024) Supplementation of sperm cooling medium with Eurycoma longifolia extract enhances native Thai chicken sperm quality and fertility potential. *Front. Vet. Sci.* 11:1474386. doi: 10.3389/fvets.2024.1474386

Supplementation of sperm cooling medium with Eurycoma longifolia extract enhances native Thai chicken sperm quality and fertility potential

Thirawat Koedkanmark[1], Ruthaiporn Ratchamak[2,3], Supakorn Authaida[1,2], Wuttigrai Boonkum[1,2], Yoswaris Semaming[4] and Vibuntita Chankitisakul[1,2]*

[1]Department of Animal Science, Faculty of Agricultural, Khon Kaen University, Khon Kaen, Thailand, [2]Network Center for Animal Breeding and Omics Research, Khon Kaen University, Khon Kaen, Thailand, [3]Major of Animal Science, Department of Agricultural Technology, Faculty of Technology, Mahasarakham University, Maha Sarakham, Thailand, [4]Program in Veterinary Technology, Faculty of Technology, Udon Thani Rajabhat University, Udon Thani, Thailand

Cooled semen storage methods result in oxidative stress generated by an imbalance between oxidation rates, specifically reactive oxygen species production, and sperm cell antioxidants, leading to degradation of semen quality. We aimed to investigate the impact of adding Eurycoma longifolia (EL) extract as an antioxidant supplement in semen storage medium (IGGKPh semen extender) on semen quality and fertility potential. EL extract at concentrations of 5, 10, 15, and 20mg/mL was assessed for its antioxidant capacity in IGGKPh semen extender. Our findings revealed that the total phenolic content in the EL extract did not vary significantly across the various concentrations and temperatures tested. However, incubation at 5°C was found to be the most effective temperature for increasing the EL extract antioxidant capacity as assessed via the 2,2-diphenyl-1-picrylhydrazyl inhibition assay in a dose-dependent manner. Supplementation of the IGGKPh semen extender with 15mg/mL EL extract was found to enhance semen quality during cold storage for up to 48h ($p<0.05$), as evidenced by decreased malondialdehyde levels in cooled semen ($p<0.05$). However, antioxidant enzyme activities showed no significant differences among the various experimental groups ($p>0.05$). The fertility test showed that the 15mg/mL EL extract group stored for 24h had a higher percentage than the control group ($p<0.05$). However, there was no significant difference in percentage between the two groups at 48h of storage ($p>0.05$). The hatchability showed no significant difference in both 24 and 48-h storage periods ($p>0.05$). Our results indicated that supplementing the IGGKPh semen extender with 15mg/mL EL extract may positively influence semen quality during storage, suggesting potential applications for enhancing semen quality.

KEYWORDS

cold semen preservation, antioxidant, Long Jack, rooster semen, lipid peroxidation

1 Introduction

Artificial insemination (AI) has become widely utilized in commercial turkey production due to their substantial body size (1), whereas its adoption in the broiler industry remains limited, primarily due to the labor-intensive breeding practices involved. However, in the context of native Thai chicken production, AI has gained popularity within battery cage systems for parent stocks. This method offers advantages such as enhanced ease of management and increased mating ratios (2). Implementation of AI in native Thai chicken has the potential to elevate the male-to-female ratio during natural mating from 1:10 to 1:25, resulting in economic benefits through reduced male requirements (3).

Semen viability is a critical concern for Thai farmers, as semen starts to lose fertility beyond 1-h post-collection due to dehydration (4). Rural farmers often utilize a saline (0.9% NaCl) solution as a short-term diluent in a 1:3 ratio to sustain sperm viability for immediate use. However, extended storage for 24 h at 25°C proves impractical with saline diluents (5). For optimal semen preservation over extended periods, dilution with suitable semen extenders, and storage at 2–5°C is necessary to minimize sperm metabolism (6). It has been reported that semen fertility decreases with semen stored for 24 h or longer (7), possibly due to oxidative stress incurred during storage (8, 9).

The oxidative stress attributed to semen storage significantly impacts sperm function, with an imbalance between antioxidants and free radicals exacerbating the decline in fertility parameters. The accumulation of malondialdehyde (MDA), an end product of lipid peroxidation, exhibits a marked increase after 24 h of semen storage at 4°C compared to MDA levels in fresh semen (10). Concurrently, antioxidant enzyme activity within semen diminishes progressively during the storage period (11). An increase in reactive oxygen species (ROS) levels in stored semen directly compromises sperm viability, acrosome integrity, mitochondrial potential, and DNA integrity, ultimately reducing semen fertility potential (12). Therefore, an antioxidant that would act as a scavenger of ROS is required to be added to the semen extender to improve sperm quality and fertility during semen storage and processing.

Plant extracts have emerged as natural sources of antioxidants and have shown promise in preserving and enhancing sperm function during semen storage. Eurycoma longifolia (EL), commonly known as 'Tongkat Ali' or 'Long Jack', is an herbal plant prevalent in Southeast Asia, and its root extract contains flavonoids, phenolic compounds, alkaloids, and antioxidants (13). EL extract shows a significant presence of superoxide dismutase (SOD) (14) that is pivotal for eliminating intracellular free radicals (15) and enhancing rooster sperm motility, viability, and structure preservation (16). Evidential studies in cattle species suggest that EL extract supplementation in cooled semen storage media can enhance sperm quality (17). However, its application in rooster semen preservation remains unexplored. As such, this study aimed to evaluate the antioxidant properties of the IGGKPh semen extender augmented with EL extract, assess the optimal concentration of EL extract for use as an antioxidant supplement in cooled semen storage, and determine its impact on semen quality. This involved measuring lipid peroxidation (as indicated by MDA levels) and antioxidant enzyme activities, ultimately assessing the potential effects on sperm fertility.

2 Methodology

2.1 Chemicals

The EL extract powder was obtained from Asian Bioplex Co. (Bangphra, Si-Racha, Chonburi, Thailand). It underwent a deionized water extraction process followed by spray drying. The powder exhibited a bulk density range of 0.20–0.50 g/mL, moisture content below 10%, and an active ingredient composition with a triterpenoid glycoside concentration exceeding 30%. Unless otherwise stated, all chemicals used in this study were acquired from Sigma-Aldrich (St. Louis, MO, USA).

2.2 Semen extender used

In this study, we used the IGGKPh semen extender for cooled semen storage experiments (18). Table 1 presents its chemical composition.

2.3 Quantitative determination of antioxidants

The impact of various extraction procedures, solvents, and temperatures on the degradation of endogenous plant compounds has been recognized in the scientific literature (19, 20). Therefore, we evaluated the antioxidant properties of the EL extract in the IGGKPh semen extender. The EL extract, in a powdered form, was added to the IGGKPh semen extender at different concentrations (5, 10, 15, and 20 mg/mL) and stirred continuously to ensure a uniform distribution. The samples were then incubated at different temperatures (5, 25, and 60°C) for 6 h. Afterward, the samples were filtered and stored frozen at −20°C until analysis to ascertain the antioxidant contents quantitatively. Three replicates were prepared for each concentration of EL extract and temperature condition.

The total phenolic content (TPC) was measured in milligrams of gallic acid equivalent per gram (mg GAE/g) of the dry extract, while the antioxidant capacity was assessed using 2,2-diphenyl-1-picrylhydrazyl (DPPH) percent inhibition assay.

2.3.1 Total phenolic content

Total phenolic content (TPC) is widely utilized as a crucial parameter for evaluating the overall antioxidant capacity of plants.

TABLE 1 Chemical composition of the IGGKPh semen extender.

Constituents	IGGKPh (g)
Potassium citrate monohydrate	0.70
Sodium glutamate	7.00
Sodium hydrogen phosphate	4.90
Sodium dihydrogen phosphate	1.05
Glucose	4.50
Inositol	4.50
mOsm	396
pH	6.9
Distilled water (mL)	500

TPC was quantified utilizing the Folin–Ciocalteu (F–C) assay (21), with gallic acid employed as a standard reference. Sample solutions for the assay were prepared at a concentration of 10 mg/mL. In parallel, calibration solutions of gallic acid were prepared at concentrations of 12.5, 25, 50, 100, 200, and 400 μg/mL in distilled water.

The reaction mixtures were then prepared by combining 50 μL of the sample solution with the F–C reagent in a 1:5 volume ratio. Subsequently, 100 μL of a 75% Na_2CO_3 solution was added to the mixtures and incubated at room temperature for 30 min. The absorbance of the reaction mixture was then measured at 765 nm utilizing a spectrophotometer (Microplate reader: TECAN, infinite 200 PRO, Switzerland). The inherent TPC value of samples was quantified by comparing the absorbance values to a blank. The TPC results were derived from a calibration curve constructed with gallic acid standards and were expressed in mg GAE/g of the dry EL extract.

2.3.2 DPPH radical scavenging activity of the EL extract

The radical scavenging activity of the EL extract was ascertained using the DPPH radical as previously described (22). Briefly, 100 μL of a 0.2 mM DPPH radical solution in ethanol was added to 100 μL of various concentrations of the EL extract. After incubation in the dark for 30 min at room temperature, the absorbance was measured at 517 nm using a spectrophotometer (Microplate reader: TECAN, infinite 200 PRO, Switzerland). Ascorbic acid served as a positive control, and all measurements were performed in triplicate. The concentration of the EL extract that yields 50% inhibition (IC50) was calculated by plotting inhibition percentages against various extract concentrations. The inhibition percentages were computed with the formula: Inhibition percentage (%) = $(A0 - A1)/A0 \times 100$, where A1 and A0 represent the absorbance of the DPPH radical solution after incubation with and without the EL extracts.

2.4 Animals and management

Twenty-five native Thai roosters (Pradu Hang Dum, 33 weeks of age) were kept in individual cages (48 × 45 × 45 cm) in an open-environment housing system. They were fed approximately 130 g of commercial feed (Balance 924, Betagro Company Limited, Thailand) that provided 17% protein, 3% fat, 6% fiber, and 13% moisture. Water was provided *ad libitum*. Semen was routinely collected weekly for AI.

Forty commercial laying hens (ISA-Brown breed, 34–40 weeks of age), with egg production >70%, were used for the fertility test. The hens were housed individually, fed approximately 120 g of the same commercial feed as the roosters, and provided with water *ad libitum*.

The Institutional Animal Care and Use Committee approved this study's experimental protocol based on the Ethics of Animal Experimentation of the National Research Council of Thailand [Record No. IACUC-KKU-13/67; Reference No. 660201.2.11/153 (15)].

2.5 Semen sample collection

Rooster semen samples were collected twice a week from individual roosters into 1.5 mL microtubes containing 100 μL of IGGKPh semen extender using the dorso-abdominal massage method. This dilution step was necessary to maintain sperm viability; otherwise, dehydration due to water evaporation from the seminal plasma could occur (23). The sperm concentration reported in subsequent analyses refers to the concentration after dilution.

Following semen collection, the samples were kept at a temperature between 22 and 25°C and transported to the laboratory within 20 min of collection. Individual semen samples were assessed for mass movement and scored on a scale of 0–5 (0 = no sperm movement; 5 = very rapid waves and whirlwinds visible, with more than 90% of sperm showing forward movement). A drop of 5–10 μL semen was placed on a slide without a coverslip and examined under a compound microscope (10× magnification; Olympus CH30, Tokyo, Japan). Only semen samples with a mass movement score > 3.5 were pooled for further experimentation.

2.6 Pooled semen evaluation

After pooling, the semen samples were evaluated for sperm concentration and viability. Sperm concentration was evaluated using a hemocytometer chamber. Initially, 999 μL of 4% sodium chloride solution was added to 1 μL of the semen sample. The diluted semen sample was placed in the hemocytometer and examined under a compound microscope (40× magnification). The sperm concentration was determined to be 1 billion (10^9) cells per mL. Sperm viability was determined using eosin-nigrosine staining. A 5 μL semen sample was mixed with 10 μL of eosin-nigrosine and smeared on the slide. After drying, 300 sperms were evaluated under a compound microscope (40× magnification). Sperm that appeared pink (stained with eosin) were regarded as dead, whereas sperm without any color (no penetration of eosin stain) were regarded as live. Only pooled samples meeting the following criteria were used in the experiments: sperm concentration $\geq 3 \times 10^9$ sperm/mL, and sperm viability ≥90%.

In the present study, the pooled semen quality regarding sperm concentration and viability was $4.46 \times 10^9 \pm 0.03$ sperm/mL and 94.95 ± 0.85%, respectively.

2.7 Experimental design

To determine the optimal concentration of EL extract to be used for supplementation of semen extender during semen storage at 5°C for up to 72 h, the pooled semen was divided into five aliquots and diluted with the IGGKPh extender (1:3 v/v) containing various concentrations of EL extract: 5, 10, 15, and 20 mg/mL. An IGGKPh extender sample without EL extract supplementation served as the control. Semen quality, including total motility (MOT), progressive motility (PMOT), and sperm viability, as well as lipid peroxidation (measured by MDA) and antioxidant enzyme activities (catalase [CAT] and superoxide dismutase [SOD]), was evaluated at 0, 24, 48, and 72 h after storage (T0, T24, T48, and T72, respectively). The experiment was repeated five times.

Fertility potential was examined using the treatment group that demonstrated the most favorable outcomes after 24 and 48 h of semen storage compared with the control group through AI conducted in hens once per week for a continuous period of 4 weeks. Fertility and hatchability rates were recorded.

2.8 Cooled semen processing

After fresh semen evaluation, semen samples were pooled and diluted (1:3 v/v) with the IGGKPh semen extender. The diluted semen was then cooled down to 5°C within 1 h and stored for 72 h, with the semen tubes being flipped every 6 h.

2.9 Evaluation of sperm quality

2.9.1 Sperm motility

MOT and PMOT were evaluated using a Computer-Assisted Sperm Analyser (CASA), HTM-IVOS Model 10.0 D (Hammilton-Thorne Bioscience, Beverly, MA, USA). This system was set up with the following parameters: frames per second, 60 Hz; minimum contrast, 25; minimum cell size, 10 µm. A sperm was defined as non-motile if the average path velocity was less than 5 µm/s, and sperm was considered progressively motile if the average path velocity was greater than 10 µm/s with a straightness index of 80. At least five fields of view were evaluated, with a minimum of 300 sperm per sample, to compute MOT and PMOT values.

2.9.2 Sperm viability

Sperm viability was analyzed using fluorescent staining to distinguish live sperm from dead sperm based on cell membrane integrity. Two dyes were used: SYBR-14 and propidium iodide (L7011; Invitrogen, Thermo Fisher Scientific, Waltham, MA, USA). For the test, 300 µL of semen was mixed with 5 µL of SYBR-14, incubated at ~25°C for 10 min, followed by the addition of 5 µL of propidium iodide and further incubation for 5 min. The sperm were then fixed with 10% formaldehyde, and at least 300 sperm cells were counted using an IX71 fluorescence microscope (40× magnification; Olympus, Tokyo, Japan). Sperm with an intact plasma membrane exhibited green fluorescence from SYBR-14, while sperm with damaged plasma membrane stained red with propidium iodide.

2.9.3 Lipid peroxidation

Lipid peroxidation was evaluated by determining the MDA concentration, the final product of lipid peroxidation, using the thiobarbituric acid reactive substances (TBARS) assay. This method involves a reaction between MDA and thiobarbituric acid (TBA), resulting in a pinkish-orange compound. In this study, the TBARS assay was performed on whole cells as described by (24). The procedure involves incubating semen with a sperm concentration of 250×10^6 or a semen volume of 250–300 µL with 0.25 mL of ferrous sulfate (0.2 mM) and 0.25 mL of sodium ascorbate (1 mM), incubated at 37°C for 1 h. Following incubation, 1 mL of 15% trichloroacetic acid and 1 mL 0.375% TBA (Sigma, T550-0) were added. The mixture was heated to 100°C and placed at 4°C before centrifugation at 5,000×*g* at 4°C for 10 min to obtain the supernatant. This was used to measure the MDA concentration using UV–visible spectrophotometry (Analytikjena Model Specord 250 plus) at a wavelength of 532 nm. MDA concentration was calculated using a standard curve generated from a known concentration of MDA (0, 0.83, 1.66, 2.40, 3.33, 4.16, 4.99, 5.83, and 6.66 µmol/mL), with results expressed in µmol/mL.

2.9.4 Antioxidant enzyme activity

The semen sample was centrifuged at a speed of 5,000×*g* at 4°C for 10 min to separate the sperm from seminal plasma. The seminal plasma was used to quantify the activity of two major antioxidant enzymes, namely SOD and CAT, as described previously (25).

2.9.4.1 SOD activity

SOD activity was measured using a spectrophotometric assay based on the inhibition of cytochrome c reduction by xanthine oxidase. Briefly, an aliquot of seminal plasma (10 µL) was mixed with a reaction mixture containing (1 mM), xanthine (50 mM), and 155 µL of xanthine oxidase, diluted in a buffer containing sodium and EDTA at concentrations of 50 mM and 100 mM, respectively. The decrease in absorbance at 550 nm was monitored over time, and the SOD activity was calculated based on the rate of cytochrome c reduction. One unit of SOD activity is defined as the amount of enzyme required to inhibit the rate of cytochrome c reduction by 50%. The SOD activity was expressed in units per milliliter (U/mL).

2.9.4.2 Catalase activity assay

Catalase activity was determined by measuring the rate of hydrogen peroxide (H_2O_2) decomposition using a spectrophotometer. A 10 µL sample of seminal plasma was mixed with a buffer solution containing 50 mM amino methane/EDTA and 250 mM Tris (hydroxymethyl) for a total volume of 90 µL. Then, 900 µL of 9.0 mM hydrogen peroxide (H_2O_2) was then added to initiate the reaction, which was incubated at pH 8.0 and 30°C for 8 min. The absorbance of the reaction mixture was measured every 5 s at 230 nm. The decrease in absorbance over time was used to calculate the rate of H_2O_2 decomposition, which was then expressed in units/mL (U/mL) to reflect catalase activity in the assessed seminal plasma sample.

2.9.5 Sperm fertility

The fertility rate of semen in semen extender supplemented with EL extract was evaluated by AI in ISA-Brown hens (10 hens per treatment group) as described previously (26). Using a tuberculin syringe (1 mL), 0.1 mL of cooled semen, with a concentration of approximately 100×10^6 sperm per insemination dose, was deposited into the cloaca, approximately 4 cm deep. AI was performed once per week and continued for 4 weeks. Fertility assessment was conducted by collecting eggs from Day 2 after the first insemination until Day 8 following the last insemination. Eggs were stored on paper trays at a controlled temperature (22–25°C) and incubated weekly to determine fertility status on Day 7 using candling. The fertility rate was calculated as the percentage of fertile eggs out of the total number of incubated eggs. Hatchability rate, defined as the percentage of hatched eggs from fertile.

2.10 Statistical analysis

To determine the optimal concentration of EL extract to be used for supplementation of semen extender during cooled semen storage at 5°C for up to 72 h, a split-plot design with five replicates was used with two factors (treatment and storage time). Five treatments were randomly arranged in the main plot, and storage

time at 5°C with four storage durations (0, 24, 48, and 72 h) were randomly distributed subplots.

The fertility potential was analyzed using a group t-test analysis, encompassing two treatments: a control group and EL extract supplementation in semen extender at a dose of 15 mg/mL.

All data underwent assessment for a normal distribution using univariate analysis and the Shapiro–Wilk test. Various parameters such as total motility, progressive motility, viability, mitochondrial potential, cell apoptosis, lipid peroxidation level, antioxidant enzyme activity, fertility, and hatchability were analyzed using analysis of variance via SAS software (SAS Institute, Inc., Cary, NC, USA). The mean values for each treatment group were compared using Tukey's test. Orthogonal polynomial contrasts were used to determine linear and quadratic responses to each treatment. Data were considered to be statistically significant at $p < 0.05$.

3 Results

3.1 Quantitative determination of antioxidants

Based on the data presented in Table 2, the TPC in semen extenders ranged from 4 to 7 mg GAE/g and did not exhibit variability based on the concentration of EL extract or the incubation temperatures. Conversely, the antioxidant capacity, as determined by DPPH inhibition, was found to be concentration-dependent and influenced by the temperature of incubation. Higher concentrations of the extract led to increased antioxidant capacity, as indicated by higher antioxidant capacity values at 20 mg/mL compared to those observed at lower concentrations of the extract at 5°C of incubation. Additionally, the temperature of incubation appeared to influence antioxidant capacity, with lower antioxidant capacity values observed at 25°C and 60°C compared with those seen at 5°C, and some values even display negative outcomes.

3.2 Effects of EL extract on cooled semen storage

3.2.1 Sperm quality parameters

The effects of the EL extract on semen quality after storage at 5°C for 72 h are presented in Table 3. The interaction effect between treatment and storage time was found to be significant for all sperm parameters ($p < 0.05$). Most sperm quality parameters continued to decrease as storage time increased ($p < 0.05$).

Our results showed significant differences in semen quality between the control and the groups supplemented with EL extract. At T0, the 10 mg/mL and 15 mg/mL EL extract groups displayed significantly higher PMOT and viability compared to the other EL extract groups and the control group ($p < 0.05$).

At T24, the 15 mg/mL group exhibited significantly higher MOT and PMOT than the 10 mg/mL group ($p < 0.05$), but no significant difference was observed in viability ($p > 0.05$). However, the viability of the 15 mg/mL group was higher than that of the 10 mg/mL group at T48 and T72 h ($p < 0.05$), while PMOT differed statistically between these groups only at T48 but not at T72.

The 5 mg/mL EL extract group did not exhibit significant differences in sperm parameters compared to the control group ($p > 0.05$). In contrast, the 20 mg/mL EL extract group exhibited a detrimental effect, with lower sperm motility at all storage times ($p < 0.05$).

Furthermore, orthogonal polynomial contrast analysis revealed a significant quadratic relationship ($p < 0.05$) between sperm quality parameters and KP extract concentration within each experimental period. This indicates that sperm quality increased with increasing EL extract concentrations, with the highest sperm quality observed at 15 mg/mL.

3.2.2 Lipid peroxidation and antioxidant enzyme activity

The results of lipid peroxidation, as indicated by MDA concentration, and the activities of the antioxidant enzymes SOD and CAT are presented in Table 4. At T0, MDA levels did not show

TABLE 2 Analysis of antioxidant properties of EL extract.

EL extract supplementation dosage in IGGKPh semen extender	Temperature of incubation (°C)		
	5	25	60
	Total phenolic content (mg GAE/g)		
5 mg/mL	5.87 ± 0.28	4.92 ± 0.21	4.70 ± 0.28
10 mg/mL	7.73 ± 0.74	6.05 ± 0.42	5.26 ± 0.49
15 mg/mL	6.50 ± 0.34	6.39 ± 0.46	5.00 ± 0.32
20 mg/mL	6.14 ± 0.17	5.20 ± 0.39	5.70 ± 0.24
	Antioxidant capacity DPPH (%) inhibition		
Ascorbic acid (control)	87.32 ± 1.26		
5 mg/mL	40.95 ± 1.59	6.25 ± 0.64	−46.03 ± 2.43
10 mg/mL	65.29 ± 0.64	19.29 ± 2.20	−20.34 ± 1.65
15 mg/mL	81.97 ± 0.49	27.88 ± 0.64	−43.32 ± 2.12
20 mg/mL	91.87 ± 0.50	−78.93 ± 0.96	−53.70 ± 2.67

DPPH, 2,2-diphenyl-1-picrylhydrazyl; GAE, gallic acid equivalent.

TABLE 3 Effects of EL extract treatments for various storage times (at 5°C for 0, 24, 48, and 72 h) on rooster semen quality (mean ± SEM).

Duration of storage (h)	EL extract treatment dosage					SEM	*p*-value				
	Control	5 mg/mL	10 mg/mL	15 mg/mL	20 mg/mL		Treatment	Time of storage	Interaction	Linear	Quadratic
MOT (%)											
T0	87.84^{aw}	87.66^{aw}	88.27^{aw}	88.16^{aw}	85.34^{bw}	1.89	<0.0001	<0.0001	0.0068	0.5484	<0.0001
T24	72.33^{cx}	72.54^{cx}	74.09^{bx}	76.90^{ax}	68.32^{dx}	1.50					
T48	67.50^{by}	67.62^{by}	71.36^{ay}	71.26^{ay}	65.80^{cy}	0.76					
T72	53.84^{dz}	55.19^{cz}	62.70^{bz}	65.77^{az}	50.92^{ez}	0.60					
PMOT (%)											
T0	81.81^{bw}	81.23^{bw}	84.03^{aw}	83.94^{aw}	81.44^{bw}	1.09	0.0003	<0.0001	0.0458	0.4870	0.0170
T24	64.45^{cx}	64.32^{cx}	67.03^{bx}	70.19^{ax}	62.19^{dx}	0.90					
T48	55.21^{cy}	54.71^{cy}	58.71^{by}	61.43^{ay}	54.42^{cy}	1.04					
T72	53.41^{az}	53.65^{az}	54.27^{az}	56.40^{az}	53.94^{az}	3.14					
Viability (%)											
T0	81.90^{bw}	81.33^{bw}	85.58^{aw}	86.42^{aw}	81.24^{bw}	2.83	<0.0001	<0.0001	<0.0001	0.0324	<0.0001
T24	74.42^{bx}	76.45^{bx}	81.63^{ax}	83.78^{ax}	75.69^{bx}	2.75					
T48	73.03^{cy}	73.72^{cy}	76.20^{by}	80.56^{ay}	73.95^{cy}	2.52					
T72	69.35^{cz}	70.90^{cz}	73.82^{bz}	75.81^{az}	68.68^{cz}	0.85					

Values within a row with different superscript letters $^{(a, b, c, d, e)}$ indicate significant differences between treatments; values within a column with different superscript letters $^{(w, x, y, z)}$ indicate significant differences between storage times. $p < 0.05$. MOT, total motility; PMOT, progressive motility. T0 = 0 h, T24 = 24 h, T48 = 48 h, T72 = 72 h after storage.

10.3389/fvets.2024.1474386

TABLE 4 Effects of EL extract treatments for various storage times (at 5°C for 0, 24, 48, and 72 h) on lipid peroxidation (malondialdehyde [MDA]), catalase (CAT), and superoxide dismutase (SOD) enzyme activities.

Duration of storage (h)	EL extract treatment dosage					SEM	*p*-value				
	Control	5 mg/mL	10 mg/mL	15 mg/mL	20 mg/mL		Treatment	Time of storage	Interaction	Linear	Quadratic
MDA (μmol/mL)											
T0	0.59^{aw}	0.72^{aw}	0.66^{aw}	0.59^{aw}	0.60^{aw}	0.11	<0.0001	0.0096	0.4970	0.0009	0.4725
T24	1.28^{ax}	1.31^{ax}	0.92^{bx}	0.60^{cx}	0.63^{cx}	0.05					
T48	2.40^{ay}	1.72^{by}	1.56^{by}	1.55^{by}	1.91^{by}	0.14					
T72	2.52^{az}	2.38^{az}	2.30^{az}	2.38^{az}	2.54^{az}	0.16					
SOD (U/mL)											
T0	4.07	3.91	4.07	4.11	3.96	0.08	0.3458	0.4934	0.8410	0.6963	0.1289
T24	4.03	4.00	4.14	4.09	3.98	0.08					
T48	3.97	4.08	3.97	4.02	3.90	0.11					
T72	3.96	3.96	4.25	4.11	4.13	0.08					
CAT (U/mL)											
T0	21.05	21.28	21.39	19.59	21.15	0.65	0.268	0.3189	0.7293	0.7297	0.7029
T24	20.17	20.10	20.65	20.07	21.28	0.58					
T48	21.58	21.05	22.06	19.80	21.35	0.59					
T72	19.53	21.22	20.90	19.95	21.35	0.23					

Values within a row with different superscript letters $^{(a, b, c, d, e)}$ indicate significant differences between treatments; values within a column with different superscript letters $^{(w, x, y, z)}$ indicate significant differences between storage times. $p < 0.05$. T0 = 0 h, T24 = 24 h, T48 = 48 h, T72 = 72 h after storage.

10.3389/fvets.2024.1474386

significant differences among treatments ($p > 0.05$). At T24, significantly lower MDA levels were observed in the groups supplemented with 15 mg/mL and 20 mg/mL of EL extract compared to the control group ($p < 0.05$). At T48, all EL extract groups (5 mg/mL, 15 mg/mL, and 20 mg/mL) showed significantly lower MDA levels compared to the control group ($p < 0.05$). MDA decreased linearly with increasing concentration levels of EL extract ($p < 0.05$). No significant differences were noted at T72 storage time ($p > 0.05$). In contrast, the SOD and CAT levels across the different groups did not exhibit significant differences at any of the storage times ($p > 0.05$).

3.2.3 Effects of EL extract on sperm fertility

Based on our sperm quality and lipid peroxidation results, supplementing the semen extender with 15 mg/mL of EL extract for a storage duration of 24–48 h was chosen as the treatment for further investigation into fertility.

The effects of the EL extract on fertility and hatchability values after storage at 5°C for 48 h are presented in Table 5. At a storage duration of 24 h (T24), the fertility rate in the EL extract group was higher than that of the control groups ($p < 0.05$) but was not significantly different between various treatment groups at T48 ($p > 0.05$). The hatchability values were not significantly different between groups at the same storage time ($p > 0.05$).

4 Discussion

Cooled rooster semen storage at 2–5°C is recommended to minimize sperm metabolism without inducing serious cold shock. However, it has been reported that the amount of ROS tends to increase gradually during cold storage (27). With the passage of semen storage time, this increase in ROS can lead to plasma membrane dysfunction, ultimately resulting in a reduced fertility potential when semen is stored for extended periods, such as 24 h or longer. In response to this challenge, supplementing the semen extender medium with EL extract at a concentration of 15 mg/mL has proven beneficial as an antioxidant substance. This supplementation has demonstrated the capacity to enhance semen quality during cooled storage for up to 48 h. Interestingly, a decrease in MDA levels, an indicator of lipid peroxidation, was noted in the EL extract treatment groups, even though antioxidant enzyme activities did not show significant differences among the groups. Our data revealed that the EL extract treatment groups exhibited increased sperm fertility rates for a cooled semen storage duration of 24 h. In addition, it is important to note that higher doses of EL extract supplementation have been observed to negatively affect sperm quality despite having greater antioxidant capacity (Table 2), indicating the need to establish an optimal EL extract dosage level to achieve the desired improvements in semen quality during cooled storage.

The extraction procedures, solvents, and temperatures utilized can significantly impact the degradation of endogenous plant compounds (19, 20). In the present study, we investigated the antioxidant properties of EL extract used to supplement the semen extender. While the levels of TPC (total phenolic content) in the various EL extract concentrations employed (between 5–20 mg/mL) and incubation temperatures used (5°C, 25°C, and 60°C) did not show a significant difference, ranging from 4.7 to 7.7 mg GAE/g, our findings suggest that TPC levels may not be markedly affected by EL extract dosage and incubation temperature. This observation is likely due to the limited solubility of phenolic compounds in water. The reported solubility of TPC in water from EL is 7.3229 mg GAE/g (28), which aligns with our findings (Table 2), showing consistent TPC levels in the EL extract within the semen extender despite variations in EL extract concentrations. The EL extract used in this study was prepared using a deionized water extraction method and incorporated into a distilled water base in the semen extender, reinforcing the idea that the solubility limitation of TPC in water is inherent to EL extract usage.

While previous studies have reported a decrease in phenolic and flavonoid contents in other plant extracts at elevated temperatures (29–33), our study did not observe a significant impact on total phenolic content at higher temperatures (up to 60°C). It's possible that elevated temperature affects certain phenolic compounds, as suggested by reports where exceeding 130°C during spinach extraction resulted in decreased flavonoid levels while the phenolic content remained unaffected (30). Similarly, extracting peach fruit at temperatures above 60°C caused a reduction in flavonoid levels while phenolic content remained stable (32). This suggests that EL extract might possess unique thermal stability (at temperatures below 60°C and incubation times less than 6 h, as used in this study) compared to other plant extracts.

However, despite this thermal stability, we found that temperature significantly affects the DPPH radical scavenging activity of EL extract. We demonstrated that incubation at 5°C was the most effective temperature for enhancing the antioxidant capacity, as indicated by increased percentages of DPPH inhibition in a dose-dependent manner. Conversely, as temperatures rose to 25°C and 60°C, the percentages of DPPH inhibition decreased markedly, with some reaching negative values, suggesting a loss of antioxidant properties and free radical scavenging activity. This discrepancy highlights the complexity of antioxidant activity and the need to

TABLE 5 Effects of EL extract treatment on fertility and hatchability rates after artificial insemination.

Parameters	Treatments					
	T24			T48		
	Control	15 mg/mL	*p*-value	Control	15 mg/mL	*p*-value
No. of eggs	239	218		200	196	
Fertility[1] (%)	73.59[a]	83.10[b]	0.0440	59.80	60.15	0.9325
Hatchability[2] (%)	73.03	73.27	0.9745	63.57	66.30	0.5675

[a,b]Different letters within a row of the same storage period indicate significant differences. $p < 0.05$. T24 = 24 h, T48 = 48 h after storage.
[1]Fertility rate was calculated as the percentage of fertile eggs out of the total number of incubated eggs.
[2]Hatchability rate was defined as the percentage of hatched eggs from fertile.

consider multiple factors beyond just TPC. It's possible that the temperature affects the reactivity of specific phenolic compounds within the extract or the presence of other antioxidants, leading to changes in DPPH scavenging activity. Further research is needed to fully understand the mechanisms by which temperature affects TPC and the temperature-dependent changes in DPPH inhibition and to determine the impact on the overall antioxidant profile of EL extract. This underscores the importance of considering the complex interplay of factors beyond TPC when assessing the antioxidant activity of plant extracts.

We found that the concentration of EL extract significantly influenced the duration of semen storage and the preservation of sperm motility, viability, and other important quality parameters. Notably, a concentration of 15 mg/mL exhibited the most favorable impact on semen quality, maintaining it for up to 48 h. This improvement in semen quality can be attributed to the phenolic compounds present in the EL extract that are known to stimulate mitochondrial function. This stimulation results in increased sperm motility by enhancing energy generation rates during cellular respiration processes (34). Furthermore, the antioxidant properties of the EL extract, particularly its ability to scavenge free radicals, are supported by the lower MDA levels observed in the semen supplemented with EL extract, particularly at 24 and 48 h of storage. This improvement in sperm quality is further supported by the lower MDA levels observed, suggesting that EL extract effectively scavenges free radicals and reduces oxidative stress damage during the early storage stages. However, after 72 h of storage, the antioxidant capacity of the EL extract may be depleted, as indicated by the less pronounced difference in MDA levels between the treatment groups. This suggests that while EL extract is effective in maintaining sperm quality for up to 48 h, its effectiveness may diminish over longer storage periods.

While previous studies highlight the crucial role of antioxidant enzymes like SOD, CAT, and glutathione peroxidase (GPx) in protecting semen from oxidative stress (35–37), our study did not detect significant differences in SOD and CAT activity across the different treatment groups (Table 4). This finding suggests that the primary role of SOD and CAT may be intracellular, protecting sperm cells from oxidative damage within their own environment. Previous research indicates SOD is pivotal in scavenging free radicals by converting O_2^- radicals into H_2O_2, while the subsequent transformation of H_2O_2 into water molecules is facilitated by CAT and GPx (35). GPx is reported as the dominant antioxidant enzyme in chicken semen (35, 37), potentially explaining why the observed lower levels of MDA, a marker of oxidative stress, were not accompanied by significant differences in SOD and CAT activities. Similar findings have been reported in previous studies (25, 38), where glutathione supplementation in chicken semen for cooled storage did not result in statistically significant differences in GPx and SOD activities in seminal plasma, while the total antioxidant capacity showed a significant difference ($p < 0.05$). Additionally, variations in MDA levels were observed between chicken semen with high and low motility, despite no differences in SOD and CAT activity (25). These findings suggest that while the presence of efficient antioxidant systems, including SOD and CAT, is important for protecting sperm cells from oxidative stress, other, potentially more dominant, antioxidant mechanisms might be at play. This emphasizes the complexity of antioxidant defense within semen and highlights the need for further investigation into the interplay of various antioxidant pathways, including both intracellular and extracellular mechanisms, to fully understand the impact of EL extract on semen quality during storage.

Besides their antioxidant properties, the EL extract possesses bactericidal properties attributed to its active components such as quassinoids and eurycomanone. These compounds induce membrane damage that leads to increased ion permeability, substance leakage, and disruption of bacterial enzymatic systems (39). These mechanisms may also affect sperm cell membranes, explaining why excessive supplementation of EL extract (20 mg/mL) may be detrimental. A study on *Rosmarinus officinalis* essential oil supplementation effects on rooster sperm motility at 4°C revealed that the highest level of supplementation (870 µg/mL) resulted in increased sperm cell death due to cell membrane destruction, highlighting the bactericidal properties of this plant extract as well (40). Additionally, elevated antioxidant concentrations have been reported to potentially dehydrate sperm cells within the solution, leading to hypertonic conditions (41, 42). High concentrations of phenolic compounds and flavonoids can negatively affect mitochondrial cellular respiration by directly reacting with mitochondrial membranes, and this impairs ATP production and the function of complex I and coenzyme Q-binding that is necessary for NADH electron transfer (43, 44). Excessive levels of quercetin, a flavonoid, can also inhibit sperm motility and viability by decreasing or halting Ca^{2+}-ATPase activity that is crucial for maintaining sperm cell motility (45).

The present study demonstrated that supplementation of semen extender with the EL extract at a concentration of 15 mg/mL significantly improved the fertility rate in native Thai rooster semen stored for 24 h. This enhancement in fertility can be attributed to the antioxidant properties of the EL root extract that positively affected sperm quality (13). Improved semen quality, particularly in terms of sperm motility and viability, likely contributed to the prolonged survival of sperm in the sperm storage tubules (SSTs) of hens and facilitated a higher rate of migration toward fertilization (46). However, the beneficial effects of EL extract supplementation on sperm fertility were not observed at a semen storage duration of 48 h, where no significant differences in fertility rates were found between the treated and control groups, even though the sperm quality in the treatment group was superior to that in the control group. There are two potential reasons for this outcome. First, while the viability of sperm after 48 h of storage in the treatment group remained high (approximately 80%), the PMOT was around 60%, which may be too low to allow successful migration to the SSTs (47). Second, the decline in antioxidant capacity after 48 h of semen storage could be insufficient to neutralize the increased levels of oxidative state associated with longer semen storage periods (10). Future research should explore strategies to extend the antioxidant efficacy of the EL extract and other potential supplements to improve semen quality over longer storage periods.

5 Conclusion

Supplementation of sperm cooling medium with EL extract at a concentration of 15 mg/mL enhanced semen quality during cold storage for up to 48 h, with a decrease in MDA levels in cooled semen. In addition, EL extract at a concentration of 15 mg/mL effectively

enhanced fertility rates of native Thai rooster semen when stored for up to 24 h.

Data availability statement

The original contributions presented in the study are included in the article/supplementary material, further inquiries can be directed to the corresponding author.

Ethics statement

The animal studies were approved by the Institutional Animal Care and Use Committee approved this study's experimental protocol based on the Ethics of Animal Experimentation of the National Research Council of Thailand. The studies were conducted in accordance with the local legislation and institutional requirements. Written informed consent was not obtained from the owners for the participation of their animals in this study because in this study, all experiments were conducted using animals belonging to the research unit under Khon Kaen University, Thailand. As these animals are owned and managed by the university's research facility, written informed consent from external owners was not necessary.

Author contributions

TK: Formal analysis, Methodology, Writing – original draft. RR: Methodology, Validation, Writing – original draft. SA: Methodology, Writing – original draft. WB: Data curation, Formal analysis, Resources, Writing – review & editing. YS: Data curation, Methodology, Writing – original draft. VC: Conceptualization, Data curation, Funding acquisition, Investigation, Project administration, Supervision, Validation, Writing – review & editing.

Funding

The author(s) declare that financial support was received for the research, authorship, and/or publication of this article. This research was funded by the Network Center for Animal Breeding and Omics Research, Khon Kaen University. The methodology of this study was supported by Mr. Khomsan Buathalad and Miss Jiraporn Juiputta.

Conflict of interest

The authors declare that the research was conducted in the absence of any commercial or financial relationships that could be construed as a potential conflict of interest.

Publisher's note

All claims expressed in this article are solely those of the authors and do not necessarily represent those of their affiliated organizations, or those of the publisher, the editors and the reviewers. Any product that may be evaluated in this article, or claim that may be made by its manufacturer, is not guaranteed or endorsed by the publisher.

References

1. Mohan J, Sharma SK, Kolluri G, Dhama K. History of artificial insemination in poultry, its components and significance. *Worlds Poult Sci J*. (2018) 74:475–88. doi: 10.1017/S0043933918000526

2. Pimprasert M, Kheawkanha T, Boonkum W, Chankitisakul V. Influence of semen collection frequency and seasonal variations on fresh and frozen semen quality in Thai native roosters. *Animals*. (2023) 13:573. doi: 10.3390/ani13040573

3. Kharayat N, Chaudhary GR, Katiyar RB, Balmurugan B, Patel M, Uniyal S, et al. Significance of Artificial insemination in poultry. *Res Rev J Vet Sci Technol*. (2016) 5:2319–3441. doi: 10.37591/rrjovst.v5i1.519

4. Vasicek J, Kuzelova L, Kulikova B, Chrenek P. Effect of diluent and storage time on sperm characteristics of rooster insemination doses. *Avian Biol Res*. (2015) 8:41–6. doi: 10.3184/175815515X14232453836759

5. Chankitisakul V, Boonkum W, Kaewkanha T, Pimprasert M, Ratchamak R, Authaida S, et al. Fertilizing ability and survivability of rooster sperm diluted with a novel semen extender supplemented with serine for practical use on smallholder farms. *Poult Sci*. (2022) 101:102188. doi: 10.1016/j.psj.2022.102188

6. Bustani GS, Baiee FH. Semen extenders: an evaluative overview of preservative mechanisms of semen and semen extenders. *Vet World*. (2021) 14:1220–33. doi: 10.14202/vetworld.2021.1220-1233

7. Kheawkanha T, Chankitisakul V, Thananurak P, Pimprasert M, Boonkum W, Vongpralub T. Solid storage supplemented with serine of rooster semen enhances higher sperm quality and fertility potential during storage at 5°C for up to 120 h. *Poult Sci*. (2023) 102:102648. doi: 10.1016/j.psj.2023.102648

8. Rehman ZU, Meng C, Sun Y, Safdar A, Pasha RH, Munir M, et al. Oxidative stress in poultry: lessons from the viral infections. *Oxidative Med Cell Longev*. (2018) 2018:5123147. doi: 10.1155/2018/5123147

9. Silvestre MA, Yániz JL, Peña FJ, Santolaria P, Castelló-Ruiz M. Role of antioxidants in cooled liquid storage of mammal spermatozoa. *Antioxidants*. (2021) 10:1096. doi: 10.3390/antiox10071096

10. Long JA, Kramer M. Effect of vitamin E on lipid peroxidation and fertility after artificial insemination with liquid-stored Turkey semen. *Poult Sci*. (2003) 82:1802–7. doi: 10.1093/ps/82.11.1802

11. Izanloo H, Soleimanzadeh A, Bucak MN, Imani M, Zhandi M. The effects of glutathione supplementation on post-thawed Turkey semen quality and oxidative stress parameters and fertilization, and hatching potential. *Theriogenology*. (2022) 179:32–8. doi: 10.1016/j.theriogenology.2021.11.010

12. Rui BR, Shibuya FY, Kawaoku AJT, Losano JDA, Angrimani DSR, Dalmazzo A, et al. Impact of induced levels of specific free radicals and malondialdehyde on chicken semen quality and fertility. *Theriogenology*. (2017) 90:11–9. doi: 10.1016/j.theriogenology.2016.11.001

13. Rehman SU, Choe K, Yoo HH. Review on a traditional herbal medicine, Eurycoma longifolia Jack (Tongkat Ali): its traditional uses, chemistry, evidence-based pharmacology and toxicology. *Molecules*. (2016) 21:331. doi: 10.3390/molecules21030331

14. Tambi MIBM, Imran MK. Eurycoma longifolia Jack in managing idiopathic male infertility. *Asian J Androl*. (2010) 12:376–80. doi: 10.1038/aja.2010.7

15. Triawanti , Sanyoto DD, Noor MS. The supplementation of pasak bumi (Eurycoma longifolia Jack.) in undernourished rats to increase spatial memory through antioxidant mechanism. *Clin Nutr Exp*. (2020) 33:49–59. doi: 10.1016/j.yclnex.2020.08.002

16. Partyka A, Niżański W, Bajzert J, Łukaszewicz E, Ochota M. The effect of cysteine and superoxide dismutase on the quality of post-thawed chicken sperm. *Cryobiology*. (2013) 67:132–6. doi: 10.1016/j.cryobiol.2013.06.002

17. Baiee FH, Wahid H, Rosnina Y, Ariff O, Yimer N, Jeber Z, et al. Impact of Eurycoma longifolia extract on DNA integrity, lipid peroxidation, and functional parameters in chilled and cryopreserved bull sperm. *Cryobiology*. (2018) 80:43–50. doi: 10.1016/j.cryobiol.2017.12.006

18. Surai PF, Wishart GJ. Poultry artificial insemination technology in the countries of the former USSR. *Worlds Poult Sci J*. (1996) 52:27–43. doi: 10.1079/WPS19960003

19. Siddhuraju P, Becker K. Antioxidant properties of various solvent extracts of total phenolic constituents from three different agroclimatic origins of drumstick tree (*Moringa oleifera* lam.) leaves. *J Agric Food Chem*. (2003) 51:2144–55. doi: 10.1021/jf026457x

20. Onyebuchi C, Kavaz D. Effect of extraction temperature and solvent type on the bioactive potential of *Ocimum gratissimum* L. extracts. *Sci Rep*. (2020) 10:21760. doi: 10.1038/s41598-020-78765-8

21. Adebiyi OE, Olayemi FO, Ning-Hua T, Guang-Zhi Z. In vitro antioxidant activity, total phenolic and flavonoid contents of ethanol extract of stem and leaf of Grewia carpinifolia. *Beni-Suef Univ J Basic Appl Sci*. (2017) 6:10–4. doi: 10.1016/j.bjbas.2016.12.003

22. Xiao X, Ren W, Zhang N, Bing T, Liu X, Zhao Z, et al. Comparative study of the chemical constituents and bioactivities of the extracts from fruits, leaves and root barks of *Lycium barbarum*. *Molecules*. (2019) 24:1585. doi: 10.3390/molecules24081585

23. Lake PE, Stewart JM. Artificial insemination in poultry. Bulletin 213. London, UK: Ministry of agriculture, Fisheries and Food, Her Majesty's Stationary Office (1978).

24. Chauychu-noo N, Thananurak P, Boonkum W, Vongpralub T, Chankitisakul V. Effect of organic selenium dietary supplementation on quality and fertility of cryopreserved chicken sperm. *Cryobiology*. (2021) 98:57–62. doi: 10.1016/j.cryobiol.2020.12.008

25. Mussa NJ, Ratchamak R, Ratsiri T, Chumchai R, Vongpralub T, Boonkum W, et al. Lipid peroxidation and antioxidant enzyme activity in fresh rooster semen with high and low sperm motility. *Cryobiology*. (2020) 97:144–52. doi: 10.1016/j.cryobiol.2020.09.002

26. Burrows WH, Quinn JP. The collection of spermatozoa from the domestic fowl and Turkey. *Poult Sci*. (1937) 16:19–24. doi: 10.3382/ps.0160019

27. Waberski D, Henning H, Petrunkina A. Assessment of storage effects in liquid preserved boar semen. *Reprod Domest Anim*. (2011) 46:45–8. doi: 10.1111/j.1439-0531.2011.01862.x

28. Mohamad M, Ismail Y. A study on antioxidant properties of *Eurycoma longifolia* (Tongkat Ali). *J Pharm Negat Results*. (2022) 13:146–9.

29. Larrauri JA, Rupérez P, Saura-Calixto F. Effect of drying temperature on the stability of polyphenols and antioxidant activity of red grape pomace peels. *J Agric Food Chem*. (1997) 45:1390–3. doi: 10.1021/jf9609405

30. Howard L, Pandjaitan N. Pressurized liquid extraction of flavonoids from spinach. *J Food Sci*. (2008) 73:C151–7. doi: 10.1111/j.1750-3841.2007.00658.x

31. Dorta E, Lobo MG, Gonzalez M. Reutilization of mango byproducts: study of the effect of extraction solvent and temperature on their antioxidant properties. *J Food Sci*. (2012) 77:C80–8. doi: 10.1111/j.1750-3841.2011.02444.x

32. Mokrani A, Madani K. Effect of solvent, time and temperature on the extraction of phenolic compounds and antioxidant capacity of peach (*Prunus persica* L.) fruit. *Sep Purif Technol*. (2016) 162:68–76. doi: 10.1016/j.seppur.2016.01.043

33. Silva EM, Souza JNS, Rogez H, Rees JF, Larondelle Y. Antioxidant activities and polyphenolic contents of fifteen selected plant species from the Amazonian region. *Food Chem*. (2007) 101:1012–8. doi: 10.1016/j.foodchem.2006.01.013

34. Olson KR, Briggs A, Devireddy M, Iovino NA, Skora NC, Whelan J, et al. Green tea polyphenolic antioxidants oxidize hydrogen sulfide to thiosulfate and polysulfides: a possible new mechanism underpinning their biological action. *Redox Biol*. (2020) 37:101731. doi: 10.1016/j.redox.2020.101731

35. Khan RU. Antioxidants and poultry semen quality. *Worlds Poult Sci J*. (2011) 67:297–308. doi: 10.1017/S0043933911000316

36. Partyka A, Łukaszewicz E, Niżański W. Effect of cryopreservation on sperm parameters, lipid peroxidation and antioxidant enzymes activity in fowl semen. *Theriogenology*. (2012) 77:1497–504. doi: 10.1016/j.theriogenology.2011.11.006

37. Surai P, Kostjuk I, Wishart G, Macpherson A, Speake B, Noble R, et al. Effect of vitamin E and selenium supplementation of cockerel diets on glutathione peroxidase activity and lipid peroxidation susceptibility in sperm, testes, and liver. *Biol Trace Elem Res*. (1998) 64:119–32. doi: 10.1007/BF02783329

38. Shamiah S, Abd El-Karim R, Eshera A. Antioxidant enzymes activity and its relation with sperm characteristics and fertility of local cocks as affected by glutathione levels and storage period. *J Sustain Agric Sci*. (2017) 43:129–40. doi: 10.21608/jsas.2017.1130.1009

39. Khanam Z, Wen CS, Bhat IUH. Phytochemical screening and antimicrobial activity of root and stem extracts of wild Eurycoma longifolia Jack (Tongkat Ali). *J King Saud Univ Sci*. (2015) 27:23–30. doi: 10.1016/j.jksus.2014.04.006

40. Touazi L, Aberkane B, Bellik Y, Moula N, Iguer-Ouada M. Effect of the essential oil of *Rosmarinus officinalis* (L.) on rooster sperm motility during 4°C short-term storage. *Vet. WORLD*. (2018) 11:590–7. doi: 10.14202/vetworld.2018.590-597

41. Bucak MN, Ateşşahin A, Varışlı Ö, Yüce A, Tekin N, Akçay A. The influence of trehalose, taurine, cysteamine and hyaluronan on ram semen: microscopic and oxidative stress parameters after freeze–thawing process. *Theriogenology*. (2007) 67:1060–7. doi: 10.1016/j.theriogenology.2006.12.004

42. Ratchamak R, Authaida S, Koedkanmark T, Boonkum W, Semaming Y, Chankitisakul V. Supplementation of freezing medium with ginseng improves rooster sperm quality and fertility relative to free radicals and antioxidant enzymes. *Animals*. (2023) 13:2660. doi: 10.3390/ani13162660

43. Sandoval-Acuña C, Lopez-Alarcón C, Aliaga ME, Speisky H. Inhibition of mitochondrial complex I by various non-steroidal anti-inflammatory drugs and its protection by quercetin via a coenzyme Q-like action. *Chem Biol Interact*. (2012) 199:18–28. doi: 10.1016/j.cbi.2012.06.006

44. Ferramosca A, Lorenzetti S, Di Giacomo M, Lunetti P, Murrieri F, Capobianco L, et al. Modulation of human sperm mitochondrial respiration efficiency by plant polyphenols. *Antioxidants*. (2021) 10:217. doi: 10.3390/antiox10020217

45. Khanduja KL, Verma A, Bhardwaj A. Impairment of human sperm motility and viability by quercetin is independent of lipid peroxidation. *Andrologia*. (2001) 33:277–81. doi: 10.1046/j.1439-0272.2001.00432.x

46. Sun Y, Xue F, Li Y, Fu L, Bai H, Ma H, et al. Differences in semen quality, testicular histomorphology, fertility, reproductive hormone levels, and expression of candidate genes according to sperm motility in Beijing-you chickens. *Poult Sci*. (2019) 98:4182–9. doi: 10.3382/ps/pez208

47. Donoghue AM, Wishart GJ. Storage of poultry semen. *Anim Reprod Sci*. (2000) 62:213–32. doi: 10.1016/S0378-4320(00)00160-3

frontiers | Frontiers in Veterinary Science

TYPE Original Research
PUBLISHED 13 September 2024
DOI 10.3389/fvets.2024.1452631

OPEN ACCESS

EDITED BY
Stefan Gregore Ciornei,
University of Life Science, Romania

REVIEWED BY
Emoke Pall,
University of Agricultural Sciences and Veterinary Medicine of Cluj-Napoca, Romania
Hiroyuki Imai,
Yamaguchi University, Japan

*CORRESPONDENCE
Ji-Su Kim
✉ kimjs@kribb.re.kr
Jungkee Kwon
✉ jkwon@jbnu.ac.kr

†These authors have contributed equally to this work and share first authorship

RECEIVED 21 June 2024
ACCEPTED 27 August 2024
PUBLISHED 13 September 2024

CITATION
Lee D-H, Yoon S-B, Jo Y-J, Mo JW, Kwon J, Lee SIl, Kwon J and Kim J-S (2024) Comparative analysis of superovulated versus uterine-embryo synchronized recipients for embryo transfer in cynomolgus monkeys (*Macaca fascicularis*). *Front. Vet. Sci.* 11:1452631. doi: 10.3389/fvets.2024.1452631

Comparative analysis of superovulated versus uterine-embryo synchronized recipients for embryo transfer in cynomolgus monkeys (*Macaca fascicularis*)

Dong-Ho Lee[1,2†], Seung-Bin Yoon[1†], Yu-Jin Jo[1], Jun Won Mo[1], Jeongwoo Kwon[1], Sang Il Lee[1], Jungkee Kwon[2*] and Ji-Su Kim[1*]

[1]Primate Resources Center, Korea Research Institute of Bioscience and Biotechnology, Jeongeup, Republic of Korea, [2]Department of Laboratory Animal Medicine, College of Veterinary Medicine, Jeonbuk National University, Iksan, Republic of Korea

Introduction: Assisted reproductive technologies (ARTs), such as intracytoplasmic sperm injection and embryo transfer, are essential for generating genetically edited monkeys. Despite their importance, ARTs face challenges in recipient selection in terms of time and the number of animals required. The potential of superovulated monkeys, commonly used as oocyte donors, to serve as surrogate mothers, remains underexplored. The study aimed to compare the efficacy of superovulated and uterine-embryo synchronized recipients of embryo transfer in cynomolgus monkeys (*Macaca fascicularis*).

Methods: This study involved 23 cynomolgus monkeys divided into two groups–12 superovulated recipients and 11 synchronized recipients. The evaluation criteria included measuring endometrial thickness on the day of embryo transfer and calculating pregnancy and implantation rates to compare outcomes between groups.

Results: The study found no statistically significant differences in endometrial thickness (superovulated: 4.48 ± 1.36 mm, synchronized: 5.15 ± 1.58 mm), pregnancy rates (superovulated: 30.8%, synchronized: 41.7%), and implantation rates (superovulated: 14.3%, synchronized: 21.9%) between the groups ($p > 0.05$).

Conclusion: The observations indicate that superovulated recipients are as effective as synchronized recipients for embryo transfer in cynomolgus monkeys. This suggests that superovulated recipients can serve as viable options, offering an efficient and practical approach to facilitate the generation of gene-edited models in this species.

KEYWORDS

assisted reproductive technologies, cynomolgus monkey, embryo transfer, pregnancy outcome, recipient

1 Introduction

Advanced gene-editing technologies such as CRISPR/Cas9 play a pivotal role in generating gene-edited animal models (1), enabling precise modifications in animal embryos. Traditionally, these models have been developed using mice, favoring genetic tractability and cost-effectiveness. However, nonhuman primates (NHPs), which closely mirror humans, offer a more accurate representation of human diseases (2). This feature has been underscored in several studies that have successfully developed gene-edited NHP models (3–6).

Assisted reproductive technologies (ARTs), initially devised to treat infertility in humans, have significantly broadened their applications to include the development of gene-edited animals. These technologies, including *in vitro* fertilization, intracytoplasmic sperm injection (ICSI), and embryo transfer, have been established in NHPs (7–10). However, the development of ARTs has been slow due to financial constraints, limited resources, and the complexity of the procedures.

Cynomolgus monkeys (*Macaca fascicularis*) are preferred for gene-edited NHP models due to their continuous breeding capability, suitable size, and similarities to humans in terms of their reproductive cycles and uterine structure (11). The successful generation of gene-edited cynomolgus monkeys conventionally requires superovulated females for oocyte donation and uterine-embryo synchronized recipients for embryo transfer. This approach can, however, pose challenges because synchronizing the embryo stage with the cycle phase of the recipient candidate is not always straightforward and often necessitates a larger number of female monkeys. Selecting female recipients using a more direct and efficient method for embryo transfer is, therefore, crucial. Very few reports have described the selection of recipients for embryo transfer during the generation of cynomolgus monkeys. Moreover, no previous studies have used donors as recipients for embryo transfer in this species. Research has only reported similar practices in other laboratory animals such as dogs and marmosets (12, 13).

This study, therefore, aimed to compare the efficacy of superovulated and uterine-embryo-synchronized recipients in cynomolgus monkeys for embryo transfer, an essential step in ARTs. By investigating the effects of superovulation on the condition of recipients and pregnancy outcomes, this study sought to enhance the efficiency of developing genetically edited animals using cynomolgus monkeys and contribute to advancing ARTs in this species.

2 Materials and methods

2.1 Animals

Sexually mature cynomolgus monkeys (88–116 months old) were imported from China by Biomedical Research and housed at the Primate Resources Center (Jeongeup, South Korea). They were individually caged in a room maintained at a temperature of 23 ± 3°C and a humidity of 55 ± 15%. The lighting was regulated on a 12-h light/12-h dark cycle. The monkeys had *ad libitum* access to water and were fed a primate-specific diet supplemented with multivitamins twice daily, with fruits or vegetables provided once daily. Qualified animal caretakers closely monitored all the animals at least twice daily for injuries and illnesses. Additionally, any abnormalities, including signs of pain and unusual behavior, were promptly reported to the veterinarians. Health and medical records were obtained for each animal. All the necessary steps were taken to ensure their well-being and minimize any potential stress or discomfort. All animal procedures performed in this research were in accordance with the ethical standards of the Institutional Animal Care and Use Committee of the Korea Research Institute of Bioscience and Biotechnology (approval numbers: KRIBB-AEC-21306, KRIBB-AEC-24098).

2.2 Ovarian stimulation and oocyte recovery

The ovarian stimulation protocol was adapted from previously published studies (14), as illustrated in Figures 1A,B. The regimen included the administration of a gonadotropin-releasing hormone (GnRH) antagonist, ganirelix (Orgalutran Inj, ORGANON, Seoul, Korea), at a dosage of 0.125 mg once daily, and recombinant human follicle-stimulating hormone (hFSH) (Gonal-F Pen, Merck, Serono, Italy) at 37.5 IU twice daily intramuscularly on days 1–6. Human menopausal gonadotropin (IVF-M HP, LG Chem, Cheongju, Korea) was administered at 37.5 IU twice daily intramuscularly on days 7–9. Human chorionic gonadotropin (hCG) (chorionic gonadotropin human, Sigma) was administered intramuscularly at a dose of 1,000 IU 36–38 h before oocyte recovery on day 9. Immediately before oocyte recovery, the developmental status of the follicles was confirmed via ultrasonography (USG), and females with a poor response to stimulation were excluded. During oocyte recovery, the monkeys were anesthetized with an intramuscular dose of 5 mg/kg Zoletil® 50 (Virbac, Carros, France). The ovaries were exposed through an incision in the middle of the lower abdomen, and cumulus-oocyte complexes (COCs) were aspirated using an 18-gage needle attached to a 10.0 mL syringe. The syringe was filled with Tyrode's albumin lactate pyruvate-4-(2-hydroxyethyl)-1-piperazineethanesulfonic acid (TALP-HEPES) medium, according to a method described by another study (15), supplemented with 4 mg/mL bovine serum albumin (A3311, Sigma, United States) and 5 IU/mL heparin (H3149-25KU, Sigma, USA).

2.3 Semen collection

Semen was obtained from male cynomolgus monkeys (71–110 months old) with proven fertility (16) via electrical stimulation and diluted in TALP-HEPES medium supplemented with 5 mg/mL bovine serum albumin. The sperm were then centrifuged at 2,000 rpm for 20 min using a PureSperm 90 gradient (PS90-100, Nidacon, Sweden) to separate the active sperm from the seminal plasma. The supernatant was discarded, and the sperm pellet was further washed by centrifugation at 2,000 rpm for 10 min in PureSperm Wash (PSW-100, Nidacon, Sweden). The top layer of the sperm was collected for use in ICSI.

2.4 Intracytoplasmic sperm injection and embryo culture

The COCs were initially rinsed with TALP-HEPES supplemented with 4 mg/mL bovine serum albumin, 5 IU/mL heparin, and 0.2% hyaluronidase (H4272, Sigma-Aldrich) to remove cumulus cells. Oocyte maturation was assessed under an inverted microscope (Leica DMI8; Leica Microsystems, Germany) at magnifications of ×100 or ×200 to

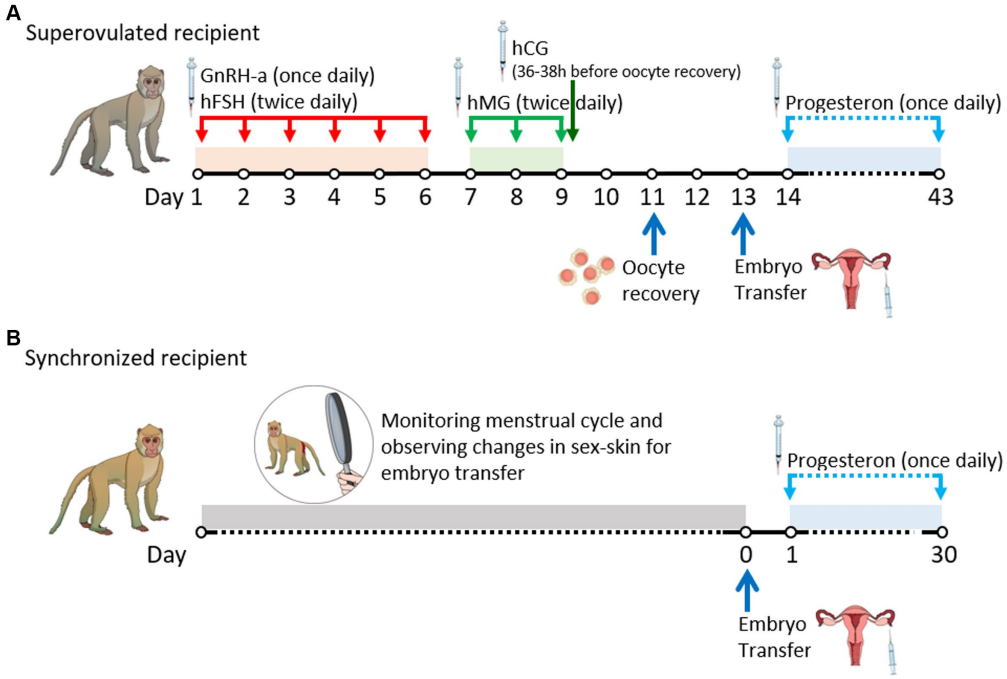

FIGURE 1
Timeline of experimental procedures by date. **(A)** Schedule of superovulated recipients. **(B)** Schedule of synchronized recipients. GnRH-a, gonadotrophin-releasing hormone antagonist; hCG, human chorionic gonadotrophin; hFSH, human follicle-stimulating hormone; hMG, human menopausal gonadotrophin.

identify the germinal vesicle (GV), metaphase I (MI), and metaphase II (MII) stages for analysis. Immature oocytes at the GV and MI stages were then cultured for up to 24 h until they reached the MII stage, in 50 µL drops of mCMRL-1066 medium (11,530,037, GIBCO, United States), supplemented with 10 mM sodium DL-lactate (L7900, Sigma, United States), 25 µg/mL 20% fetal bovine serum (16,000,044, Gibco, United States) and 5 µg/mL PMSG (Pregnant Mare Serum Gonadotropin, Prospec, Israel), 10 ug/ml hCG (CG10, Sigma, United States). The cultures were kept at 37°C in a 5% CO_2 and 6% O_2 atmosphere (Heracell 150i, Thermo Fisher Scientific, United States), under embryo-tested mineral oil (M3516, Sigma, United States). MII stage oocytes, either identified or derived from immature oocytes, were injected with monkey spermatozoa for genome editing according to a previously described method (17, 18). For the intracytoplasmic sperm injection (ICSI), spermatozoa were prepared in PureSperm Wash 10 min before the microinjection. A part of the suspended sperm was mixed with 10% polyvinylpyrrolidone. The zona pellucida of oocytes in injection media was covered with mineral oil and penetrated by several piezo pulses. The oolemma was punctured by the application of 1–2 piezo pulses, with the pipette tips reaching the opposite side of the oocyte cortex and the oolemma stretched without being broken. The sperm head was injected into the oocyte cytoplasm with a minimum amount of medium. Injected oocytes were incubated for at least 10 min in micromanipulation medium (TALP-HEPES) for stabilization. The oocytes were then transferred into mCMRL medium containing 0.4% BSA (A3311, Sigma, United States) and further cultured under embryo-tested mineral oil at 37°C in an atmosphere of 5% CO_2 and 6% O_2 for 48 h prior to embryo transfer.

2.5 Recipient selection

Oocyte donors also served as recipients in the superovulated group. In the synchronized group, recipient selection was based on monitoring the regular menstrual cycle and observing changes in sex-skin color and swelling (Supplementary Figure S1), which typically occur during ovulation between days 13 and 19 after menstruation. These observations established a 6–9 day window period for embryo transfer (19). Additionally, only those with a uterus presenting normal echo, as verified by USG before embryo transfer, were selected as embryo recipients in both groups.

2.6 Embryo transfer

Embryo transfer was performed 2 days after oocyte recovery, with the monkeys under anesthesia which was administered via an intramuscular dose of 5 mg/kg Zoletil® 50 (Virbac, Carros, France). Only the embryos that reached the four-cell stage were selected. Using a microglass capillary, 1 to 2 µL of BSA-free mCMRL medium containing the selected embryos were carefully picked up from the culture dishes. The embryos were surgically transferred to the oviduct via the infundibulum. In the standard procedure, two to three embryos were deposited in the oviduct. Luteal phase support was provided through daily intramuscular injections of progesterone (Taiyu Progesterone; Taiyu Chemical & Pharm, Taiwan) at a dosage of 3.5 mg, commencing the day after embryo transfer and continuing until ultrasonographic confirmation of pregnancy at 30 days.

2.7 Abdominal ultrasonography

USG was employed to assess ovarian conditions in oocyte donor monkeys before oocyte recovery and to evaluate uterine conditions in recipient monkeys before embryo transfer. Specifically, endometrial thickness in recipient monkeys was measured in the transverse plane at the point of the greatest uterine diameter. Pregnancy was diagnosed on day 30 following the transfer, confirming the presence of a yolk sac and embryonic cardiac motion using USG (20) (Supplementary Figure S2; Supplementary Video S1). The procedure was conducted under anesthesia induced by 10 mg/kg ketamine (Yuhan Ketamin 50 Inj., Yuhan Corporation, South Korea) by an experienced veterinarian using a high-resolution ultrasound device (LOGIQ e, GE Healthcare Technologies, Inc., Chicago, IL, United States) equipped with a 12.0 MHz probe.

2.8 Statistical analysis

All the data analyses were performed using the GraphPad Prism 8 software (GraphPad Software, LLC). Comparisons between groups for continuous variables were performed using the Student's t-test. Pregnancy and implantation rates were compared between groups using Fisher's exact test. The data were presented as mean ± standard deviation (SD). Differences were considered statistically significant at a p value of less than 0.05.

3 Results

3.1 Comparative characteristics of the superovulated vs. synchronized group

Table 1 provides a comparative overview of the characteristics of the superovulated and synchronized recipients in this study. The superovulated group had an average age of 98.4 ± 7.7 months, closely aligning with the average age of the synchronized group of 97.8 ± 9.0 months. The body weight for the superovulated group averaged 3.66 ± 0.45 kg, slightly less than the synchronized group at 3.92 ± 0.59 kg. There was no statistically significant difference in age and body weight between the two groups, as confirmed by the Student's t-test ($p > 0.05$).

The ovary size was measured before oocyte recovery and endometrial thickness was measured before embryo transfer using USG (Figures 2A,B). The ovary size in the superovulated group was measured before oocyte recovery, yielding dimensions of 19.62 ± 5.32 mm in length and 10.83 ± 2.73 mm in width. The ovary size in the synchronized group was not assessed. In terms of the endometrial thickness before embryo transfer, the superovulated group presented a slightly thinner endometrium at 4.48 ± 1.36 mm compared to 5.15 ± 1.58 mm in the synchronized group. However, these differences were not statistically significant, as determined by the Student's t-test ($p > 0.05$).

3.2 Pregnancy outcomes following embryo transfer in two groups

The data on pregnancy and implantation rates are summarized in Table 2. In the superovulated group, 35 embryos were transferred to 13 recipients, resulting in four pregnancies (30.8%), including one twin pregnancy. The remaining participants had singletons. In the synchronized group, 32 embryos were transferred to 12 recipients, leading to five pregnancies (41.7%), one of which was a triplet pregnancy. The implantation rates were 14.3% (five of 35 transferred embryos) in the superovulated group and 24.1% (seven of 32 transferred embryos) in the synchronized group. Although the pregnancy and implantation rates were higher in the synchronized group, these differences were not statistically significant ($p > 0.05$). Additionally, direct observations after embryo transfer revealed skin suture dehiscence in two cases, one in each group, which was attributed to the actions of the monkeys; however, no major infections, incision abnormalities, or other significant complications were observed.

4 Discussion

4.1 Principal findings of the study

The observations suggest that in embryo transfer, superovulated recipients are as effective as synchronized recipients and could be considered a preferable option because of their comparable pregnancy outcomes in cynomolgus monkeys.

4.2 Limitations of previous studies

The superovulated oocyte donor is commonly the recipient in human ARTs; however, its application is limited in NHPs. In NHPs,

TABLE 1 Comparative characteristics of superovulated vs. synchronized recipients.

	Superovulated group (n = 13)	Synchronized group (n = 12)
1. Age (month)	98.4 ± 7.7	97.8 ± 9.0
2. Body weight (kg)	3.66 ± 0.45	3.92 ± 0.59
3. *Ultrasonographic findings		
3.1 Ovary diameter (mm)		
3.1.1 Length	19.62 ± 5.32	Not applicable
3.1.2 Width	10.83 ± 2.73	Not applicable
3.2 Endometrial thickness (mm)	4.48 ± 1.36	5.15 ± 1.58

*Ovary size was measured before oocyte recovery and endometrial thickness was measured before embryo transfer. Data are presented as the means ± standard deviation. No significant differences were detected within rows using the Student's t-test ($p > 0.05$).

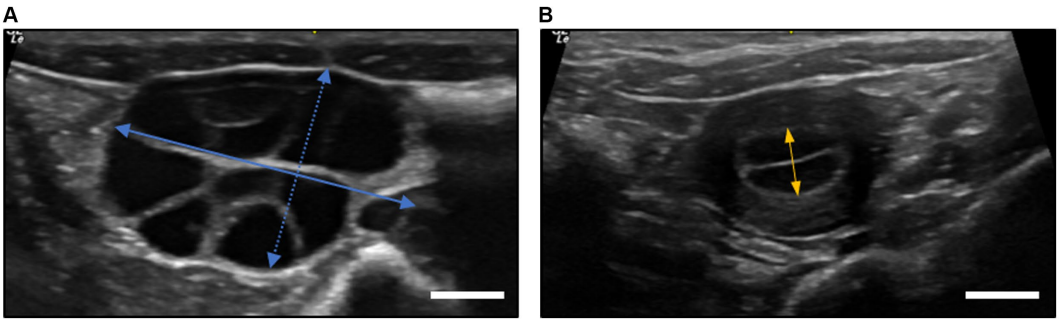

FIGURE 2
Ultrasonographic measurements of ovary diameter and endometrial thickness in cynomolgus monkeys. **(A)** Ovary diameter after superovulation procedures at oocyte recovery. The length of the ovary was defined as the longest axis (straight blue line), while the width was measured perpendicular to the length at its widest point (dotted blue line). **(B)** The endometrial thickness of recipients at embryo transfer. The measurement was taken at the thickest part of the endometrium, typically in the transverse plane of the uterus (straight orange line). All measurements were taken using a digital caliper in ultrasound device software with an accuracy of ±0.01 mm. The scale bar is 5.0 mm.

TABLE 2 **Pregnancy and implantation rates following embryo transfer in two groups.**

Group	Pregnancy rate	Implantation rate
Superovulated recipients	30.8% (4/13, 1 twin)	14.3% (5/35)
Synchronized recipients	41.7% (5/12, 1 triplet)	24.1% (7/32)

No significant differences were detected within the columns using the Fisher's exact test ($p > 0.05$).

surrogate recipients have primarily been used to increase the number of offspring produced for research purposes and avoid complications associated with transferring embryos back into the oocyte donor during the stimulation cycle. To date, numerous cynomolgus monkey offspring have been produced using ARTs with and without gene editing methods. To the best of our knowledge, no reports have documented the use of superovulated recipients; instead, most studies have employed embryo-uterus-synchronized recipients (Table 3). Research has predominantly focused on selecting the most suitable synchronized recipients because of the widely recognized importance of aligning the developmental stage of embryos with the uterine conditions of the recipients, which is essential for successful embryo transfer (8, 21).

4.3 Challenges in identifying uterine-embryo synchronized recipients

Identifying uterine embryo-synchronized recipients in cynomolgus monkeys can be challenging. In humans, oocyte donors often serve as recipients and synchronous embryo transfer has been associated with high pregnancy rates (22). Surrogates other than oocyte donors are usually employed in cynomolgus monkeys. The process of identifying a synchronized recipient typically involves confirming synchronization through various methods such as assessing estradiol levels, monitoring menses and sex-skin changes, and observing new stigma or new corpus luteum in the ovaries via USG or laparoscopy, either separately or in combination.

Hormone assays that detect serum estradiol levels are commonly used, with embryo transfer typically occurring 1–3 days after a peak in estradiol levels (8). However, this process requires daily blood collection over a long period to monitor estradiol levels, as the peak can occur anywhere from seven to 20 days after menstruation (19). This can cause stress in monkeys and complicate the synchronization of embryonic development with the recipient's uterine condition.

Predicting the ovulation date by monitoring the menstrual cycle and sex-skin changes may be straightforward. The menstrual cycle of cynomolgus monkeys is approximately 29 days, with ovulation occurring approximately 11–14 days after the onset of menstruation (23, 24). Sexual swelling and reddening are highly accurate indicators of ovulation timing (25). Nevertheless, monitoring a regular menstrual cycle is time-consuming, and not all female's exhibit changes in sex-skin (26).

The technique of detecting ovulation through the observation of a new stigma or corpus luteum using USG or laparoscopy is highly accurate for confirming synchronization. This method, however, requires specialized equipment and skilled personnel and may not always detect ovulation points during a normal menstrual cycle (19).

Selecting a synchronized recipient, therefore, requires significant time and resources as well as several female monkeys. This increases the complexity and ethical challenges involved in effective embryo transfer in NHP studies.

4.4 Analysis of endometrial thickness in superovulated and synchronized recipients

The endometrium of cynomolgus monkeys undergoes significant changes during the menstrual cycle, which are primarily driven by ovarian hormones and their receptors (26, 27).

The endometrium typically expands during the follicular phase and reaches its peak immediately after ovulation (28), and is considered a critical aspect of uterine receptivity. Uterine receptivity is crucial for embryo transfer, not only in humans but also in NHPs (29, 30).

In humans, studies on the effect of endometrial thickness have shown varied outcomes, with some studies suggesting a more favorable outcome for pregnancies with an endometrial thickness of

TABLE 3 Previous studies on recipient selection and pregnancy outcomes in cynomolgus monkeys through ARTs.

Previous studies	Year	ARTs	Gene-editing method	Recipient selection	Pregnancy rate (%)	Implantation rate (%)
Sun et al. (8)	2008	IVF, ICSI	None used	Synchronized recipients	27.6	13.6
Liu et al. (5)	2014	IVF	TALEN	Synchronized recipients	31.6	14.8
Niu et al. (3)	2014	ICSI	CRISPR/Cas9	Synchronized recipients	34.5	22.9
Wan et al. (4)	2015	ICSI	CRISPR/Cas9	Synchronized recipients	30.8	21.0
Seita et al. (47)	2016	ICSI	Lentivirus-mediated gene transfer	Not synchronized recipients	66.7	60.0
Ke et al. (48)	2016	ICSI	TALEN	N.A.	33.3	7.7
Zhao et al. (49)	2017	ICSI	CRISPR/Cas9	N.A.	8.1	2.6
Chen et al. (50)	2017	ICSI	TALEN	Synchronized recipients	34.1	13.0
Zhang et al. (51)	2018	ICSI	CRISPR/Cas9	Synchronized recipients	33.3	8.3
Cui et al. (52)	2018	ICSI	CRISPR/Cas9	Synchronized recipients	30.0	13.3
Zhou et al. (53)	2019	ICSI	CRISPR/Cas9	Synchronized recipients	46.2	18.0
Qiu et al. (54)	2019	ICSI	CRISPR/Cas9	Synchronized recipients	32.3	9.1
Tsukiyama et al. (55)	2019	ICSI	CRISPR/Cas9	Not synchronized recipients	33.7	N.A
Huang et al. (19)	2020	ICSI	None used	Synchronized recipients	25.0	27.3
Schmidt et al. (56)	2020	ICSI	CRISPR/Cas9	Synchronized or not synchronized recipients	0.0	0.0
Wang et al. (57)	2020	ICSI	CBE	Synchronized recipients	54.5	19.5
Chen et al. (58)	2021	ICSI	CRISPR/Cas9	Synchronized recipients	24.0	13.7
Li et al. (59)	2024	FPNT	None used	Synchronized recipients	20.0	11.4

Pregnancy rate = number of pregnant recipients/number of embryo-transferred recipients × 100; implantation rate = number of embryos implanted/number of embryos transferred × 100. CBE, cytosine base editing; CRISPR/Cas9, clustered regularly interspaced short palindromic repeats and CRISPR-associated protein 9; FPNT, female pronucleus transfer; ICSI, intracytoplasmic sperm injection; IVF, in vitro fertilization; N.A., not available; TALEN, transcription activator-like effector nuclease.

10.3389/fvets.2024.1452631

at least 10 mm and negative outcomes with thicknesses below 6 mm (31, 32) while others have reported successful pregnancies with thicknesses as low as 4 mm (33). Interestingly, additional research has indicated that endometrial thickness may not be directly related to pregnancy outcomes (34).

The comparison of endometrial thicknesses measured using ultrasound revealed no statistically significant differences between the superovulated and synchronized groups in this study. Furthermore, the observations presented no significant differences compared to those of a previous study, which reported an endometrial thickness of 5.7 mm (35). These findings suggest that the endometrial changes induced by superovulation are comparable to those occurring during the natural menstrual cycle and do not adversely affect the endometrial thickness, implying that superovulated recipients have a uterine receptivity similar to that of synchronized recipients.

For additional analysis, the results of this study were categorized into pregnant and non-pregnant recipients, with endometrial thicknesses measured at 4.89 ± 0.71 mm and 4.75 ± 1.79 mm, respectively. No significant differences were observed between the two groups ($p > 0.05$). The results suggest that endometrial thickness does not significantly affect pregnancy outcomes in cynomolgus monkeys, because endometrial thickness is often considered a factor in successful implantation and pregnancy.

4.5 The effect of superovulation on the pregnancy outcomes

In human ARTs, the impact of controlled ovarian hyperstimulation—the use of hormonal medications to stimulate the ovaries to produce multiple follicles, similar to superovulation in this study—on pregnancy and implantation rates has been extensively studied. Several studies have indicated that hyperstimulation does not negatively affect endometrial receptivity or pregnancy outcomes (36–39); however, others have highlighted the potential detrimental effects on the outcomes of assisted reproduction (40–43). Laboratory animal studies involving rats and mice have demonstrated mixed results in terms of the effects of ovarian hyperstimulation. Research on rats suggests that hyperstimulation can maintain normal uterine receptivity (44), while findings from mouse studies indicate potential negative impacts on implantation due to endometrial alterations (45). Despite this controversy, ovarian hyperstimulation is a critical component of fertility treatments and the generation of mutant animals, enhancing both the number of oocytes and the quality of embryos available for fertilization and subsequent development.

In the current study, no significant differences were observed in the pregnancy and implantation rates between the superovulated and synchronized recipient groups. It is believed that a superovulation protocol can effectively optimize the conditions for both follicular development and endometrial preparation by forcefully controlling the menstrual cycle. Furthermore, the administration of progesterone after embryo transfer, which is commonly used in human fertility treatments to aid embryo implantation and maintain pregnancy (46), is considered to have similar beneficial effects.

This study additionally achieved moderate success rates for pregnancy and implantation, comparable to those reported in other studies (Table 3). These findings support the effective use of superovulated recipients as synchronized recipients for embryo transfer in cynomolgus monkeys.

4.6 Strengths and weaknesses of the study

This innovative study confirmed that superovulated monkeys, traditionally used only as oocyte donors, can also serve as surrogate mothers. This finding is beneficial in terms of the time, cost, and reduction in the number of animals needed, as well as alleviating the cumbersome process associated with selecting surrogate recipients. The meticulous division and control of the two groups enhanced the reliability of the findings, suggesting that both methods were equally effective. Moreover, the study included measurements of endometrial thickness, which not only enhanced the understanding of the effects of superovulation but also enabled comparisons of endometrial thickness between pregnant and non-pregnant monkeys. This detail is particularly relevant as it may influence clinical approaches to reproductive technologies. This study, therefore, makes a practical contribution by identifying superovulated recipients as viable and efficient alternatives for generating genetically edited models and broadening the knowledge base of ARTs in cynomolgus monkeys.

This study was, however, limited by its small sample size, which may have restricted the generalizability of the results. The slightly higher pregnancy and implantation rates observed in the synchronized group suggest a trend that may become more apparent with larger sample sizes. Focusing predominantly on short-term outcomes additionally limits a comprehensive understanding of the long-term implications of these ART methods, such as complications of repeated surgery, pregnancy maintenance, and birth rates.

4.7 Unanswered questions and proposals for future studies

In future studies, it will be necessary to confirm these findings in superovulated recipients with larger sample sizes, slightly different superovulation protocols, and long-term outcomes to ensure the reliability and applicability of the results. Additionally, exploring biological mechanisms such as hormonal profiles, endometrial gene expression, and the uterine microenvironment in superovulated recipients will provide deeper insights into the underlying processes. Employing refined surgical methods such as laparoscopy can enhance animal welfare by reducing stress and increasing the safety of procedures. Ultimately, these studies will improve the overall efficacy and safety of ARTs for cynomolgus monkeys.

5 Conclusion

ARTs are vital for producing mutant monkeys; they, however, often encounter challenges in recipient selection. To the best of our knowledge, this is the first study to compare superovulated and uterine-embryo synchronized recipients in cynomolgus monkeys. The observations from this study highlighted that superovulated recipients, who are also oocyte donors, effectively serve as surrogates (Figure 3). This approach not only simplifies recipient selection and reduces the number of animals needed but also enhances the practical application of ARTs, facilitating the creation of gene-edited models in this species.

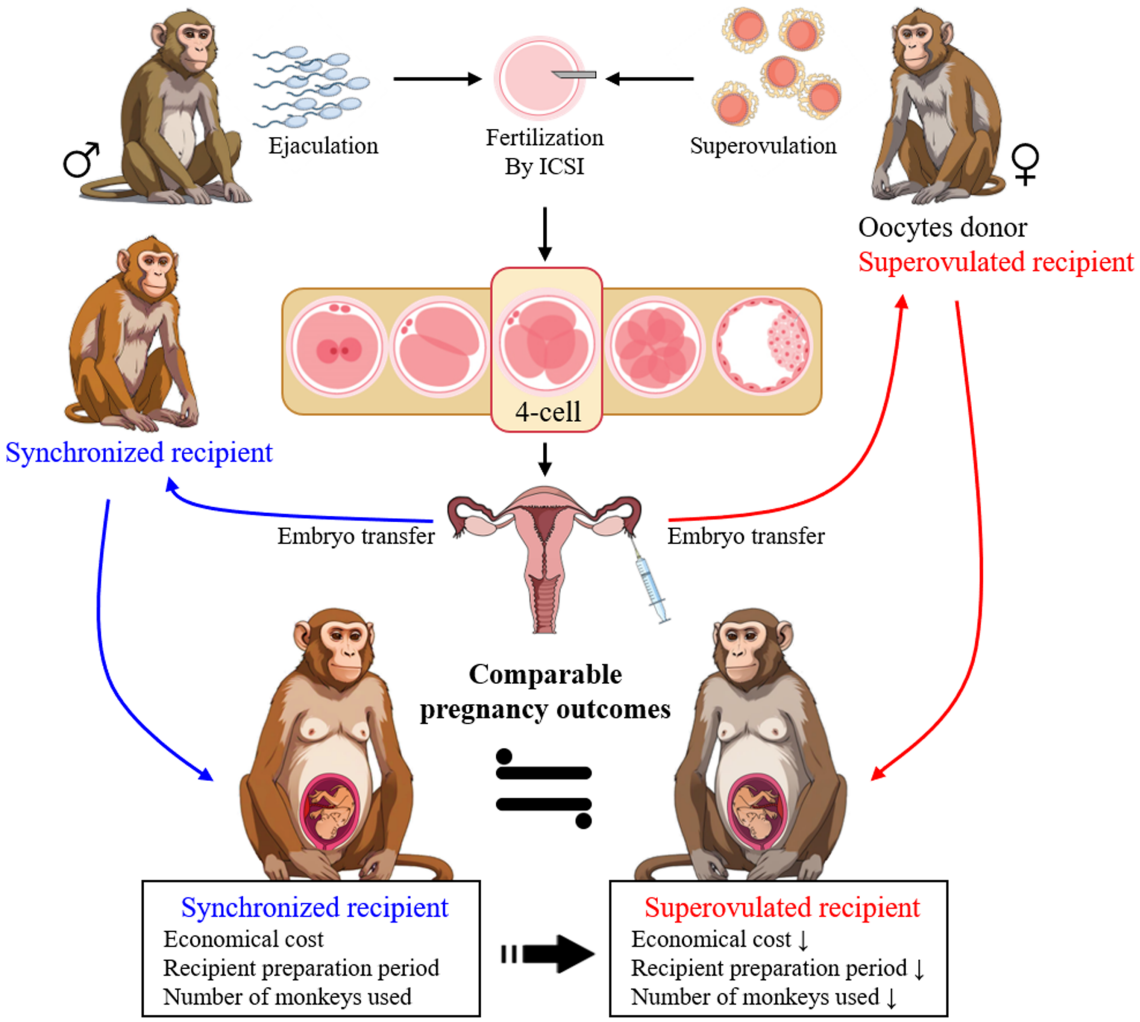

FIGURE 3
The highlight of superovulated recipients as effective surrogates compared to synchronized recipients in embryo transfer for generating gene-edited monkeys. The selection of superovulated recipients enhances efficiency and the practical application of ARTs in this species.

Data availability statement

The raw data supporting the conclusions of this article will be made available by the authors, without undue reservation.

Ethics statement

The animal study was approved by Institutional Animal Care and Use Committee of the Korea Research Institute of Bioscience and Biotechnology. The study was conducted in accordance with the local legislation and institutional requirements.

Author contributions

D-HL: Data curation, Formal analysis, Investigation, Resources, Visualization, Writing – original draft, Writing – review & editing. S-BY: Data curation, Investigation, Resources, Visualization, Writing – review & editing. Y-JJ: Data curation, Investigation, Resources, Writing – review & editing. JM: Data curation, Investigation, Resources, Writing – review & editing. JeK: Data curation, Investigation, Resources, Writing – review & editing. SL: Data curation, Investigation, Resources, Writing – review & editing. JuK: Conceptualization, Project administration, Supervision, Writing – review & editing. J-SK: Conceptualization, Funding acquisition, Methodology, Project administration, Supervision, Writing – review & editing.

Funding

The author(s) declare that financial support was received for the research, authorship, and/or publication of this article. This research was supported by a grant from the Korea Research Institute of Bioscience and Biotechnology (KRIBB) Research Initiative Program (KGM5162423).

Acknowledgments

We express our heartfelt thanks to the dedicated animal care staff at the Primate Resources Center for their exceptional care and support in ensuring the well-being of our research subjects.

Conflict of interest

The authors declare that the research was conducted in the absence of any commercial or financial relationships that could be construed as a potential conflict of interest.

Publisher's note

All claims expressed in this article are solely those of the authors and do not necessarily represent those of their affiliated organizations, or those of the publisher, the editors and the reviewers. Any product that may be evaluated in this article, or claim that may be made by its manufacturer, is not guaranteed or endorsed by the publisher.

Supplementary material

The Supplementary material for this article can be found online at: https://www.frontiersin.org/articles/10.3389/fvets.2024.1452631/full#supplementary-material

References

1. Faddy MJ, Gosden MD, Gosden RG. A demographic projection of the contribution of assisted reproductive technologies to world population growth. *Reprod Biomed Online*. (2018) 36:455–8. doi: 10.1016/j.rbmo.2018.01.006

2. Smith DG. Taxonomy of nonhuman primates used in biomedical research. Amsterdam, Netherlands: Nonhuman Primates in Biomedical Research, Elsevier, pp. 57–85 (2012).

3. Niu Y, Shen B, Cui Y, Chen Y, Wang J, Wang L, et al. Generation of gene-modified cynomolgus monkey via Cas9/RNA-mediated gene targeting in one-cell embryos. *Cell*. (2014) 156:836–43. doi: 10.1016/j.cell.2014.01.027

4. Wan H, Feng C, Teng F, Yang S, Hu B, Niu Y, et al. One-step generation of p53 gene biallelic mutant Cynomolgus monkey via the CRISPR/Cas system. *Cell Res*. (2015) 25:258–61. doi: 10.1038/cr.2014.158

5. Liu H, Chen Y, Niu Y, Zhang K, Kang Y, Ge W, et al. TALEN-mediated gene mutagenesis in rhesus and cynomolgus monkeys. *Cell Stem Cell*. (2014) 14:323–8. doi: 10.1016/j.stem.2014.01.018

6. Liu Z, Li X, Zhang J-T, Cai Y-J, Cheng T-L, Cheng C, et al. Autism-like behaviours and germline transmission in transgenic monkeys overexpressing MeCP2. *Nature*. (2016) 530:98–102. doi: 10.1038/nature16533

7. Bavister BD, Boatman DE, Collins K, Dierschke DJ, Eisele SG. Birth of rhesus monkey infant after in vitro fertilization and nonsurgical embryo transfer. *Proc Natl Acad Sci*. (1984) 81:2218–22.

8. Sun Q, Dong J, Yang W, Jin Y, Yang M, Wang Y, et al. Efficient reproduction of cynomolgus monkey using pronuclear embryo transfer technique. *Proc Natl Acad Sci*. (2008) 105:12956–60. doi: 10.1073/pnas.0805639105

9. Sasaki E, Suemizu H, Shimada A, Hanazawa K, Oiwa R, Kamioka M, et al. Generation of transgenic non-human primates with germline transmission. *Nature*. (2009) 459:523–7. doi: 10.1038/nature08090

10. Shimozawa N, Nakamura S, Takahashi I, Hatori M, Sankai T. Characterization of a novel embryonic stem cell line from an ICSI-derived blastocyst in the African green monkey. *Reproduction*. (2010) 139:565.

11. Yang S. Assisted reproductive technologies in nonhuman primates. *Reprod Technol Anim*. (2020) 1:181–91. doi: 10.1016/B978-0-12-817107-3.00012-6

12. Zou Q, Wang X, Liu Y, Ouyang Z, Long H, Wei S, et al. Generation of gene-target dogs using CRISPR/Cas9 system. *J Mol Cell Biol*. (2015) 7:580–3. doi: 10.1093/jmcb/mjv061

13. Abe Y, Nakao H, Goto M, Tamano M, Koebis M, Nakao K, et al. Efficient marmoset genome engineering by autologous embryo transfer and CRISPR/Cas9 technology. *Sci Rep*. (2021) 11:20234.

14. Kim J-S, Yoon S-B, Jeong K-J, Sim B-W, Choi S-A, Lee S-I, et al. Superovulatory responses in cynomolgus monkeys (*Macaca fascicularis*) depend on the interaction between donor status and superovulation method used. *J Reprod Dev*. (2017) 63:149–55. doi: 10.1262/jrd.2016-074

15. Ramsey C, Hanna C. In vitro culture of rhesus macaque (*Macaca mulatta*) embryos. *Comp Embryo Cult Methods Protoc*. (2019) 1:341–53. doi: 10.1007/978-1-4939-9566-0_23

16. American Association for Laboratory Animal Science. Association of Primate Veterinarians Guideline for semen collection in nonhuman Primates in biomedical research. *J Am Assoc Lab Anim Sci*. (2022) 61:223–5.

17. Meng Q, Li X, Wu T, Dinnyes A, Zhu S. Piezo-actuated zona-drilling improves the fertilisation of OPS vitrified mouse oocytes. *Acta Vet Hung*. (2007) 55:369–78.

18. Jo Y-J, Lee I-W, Jung S-M, Kwon J, Kim N-H, Namgoong S. Spire localization via zinc finger—containing domain is crucial for the asymmetric division of mouse oocyte. *FASEB J*. (2019) 33:4432–47. doi: 10.1096/fj.201801905R

19. Huang Z, Li Y, Jiang Q, Wang Y, Ma K, Li Q. Generation of cynomolgus monkey fetuses with intracytoplasmic sperm injection based on the MII-stage oocytes acquired by personalized superovulation protocol. *J Vet Sci*. (2020) 21:e48. doi: 10.4142/jvs.2020.21.e48

20. Chen Y, Niu Y, Yang S, He X, Ji S, Si W, et al. The available time window for embryo transfer in the Rhesus monkey (M acaca mulatta). *Am J Primatol*. (2012) 74:165–73. doi: 10.1002/ajp.21017

21. Santos MA, Kuijk EW, Macklon NS. The impact of ovarian stimulation for IVF on the developing embryo. *Reproduction*. (2010) 139:23–34.

22. Mandelbaum J, Junca AM, Plachot M, Alnot MO, Alvarez S, Debache C, et al. Human embryo cryopreservation, extrinsic and intrinsic parameters of success. *Hum Reprod*. (1987) 2:709–15. doi: 10.1093/oxfordjournals.humrep.a136619

23. Yoshida T, Nakajima M, Hiyaoka A, Suzuki MT, Cho F, Honjo S. Menstrual cycle lengths and the estimated time of ovulation in the cynomolgus monkey (*Macaca fascicularis*). *Jikken Dobutsu*. (1982) 31:165–74.

24. van Diepen HA, Pansier J, Oude Wesselink P, van Drie A, van Duin M, Mulders S. Non-invasive translational Cynomolgus model for studying folliculogenesis and ovulation using color Doppler ultrasonography. *J Med Primatol*. (2012) 41:18–23. doi: 10.1111/j.1600-0684.2011.00514.x

25. Tardif S, Carville A, Elmore D, Williams LE, Rice K. Reproduction and breeding of nonhuman primates. San Diego: Academic press, pp. 197–249. (2012).

26. Weinbauer GF, Niehoff M, Niehaus M, Srivastav S, Fuchs A, Van Esch E, et al. Physiology and endocrinology of the ovarian cycle in macaques. *Toxicol Pathol*. (2008) 36:7S–23S.

27. Brenner RM, Carlisle KS, Hess DL, Sandow BA, West NB. Morphology of the oviducts and endometria of cynomolgus macaques during the menstrual cycle. *Biol Reprod*. (1983) 29:1289–302.

28. Van Esch E, Cline JM, Buse E, Weinbauer GF. The macaque endometrium, with special reference to the cynomolgus monkey (*Macaca fascicularis*). *Toxicol Pathol*. (2008) 36:67S–100S. doi: 10.1177/0192623308326149

29. Revel A. Defective endometrial receptivity. *Fertil Steril*. (2012) 97:1028–32. doi: 10.1016/j.fertnstert.2012.03.039

30. Yoshinaga K. Uterine receptivity for blastocyst implantation. *Ann N Y Acad Sci*. (1988) 541:424–31.

31. Mahutte N, Hartman M, Meng L, Lanes A, Luo Z-C, Liu KE. Optimal endometrial thickness in fresh and frozen-thaw in vitro fertilization cycles: an analysis of live birth rates from 96,000 autologous embryo transfers. *Fertil Steril*. (2022) 117:792–800. doi: 10.1016/j.fertnstert.2021.12.025

32. Israel R, Isaacs JD Jr, Wells CS, Williams DB, Odem RR, Gast MJ, et al. Endometrial thickness is a valid monitoring parameter in cycles of ovulation induction with menotropins alone. *Fertil Steril*. (1996) 65:262–6. doi: 10.1016/S0015-0282(16)58082-0

33. Sundström P. Establishment of a successful pregnancy following in-vitro fertilization with an endometrial thickness of no more than 4 mm. *Hum Reprod*. (1998) 13:1550–2.

34. Ng EHY, Chan CCW, Tang OS, Yeung WSB, Ho PC. Factors affecting endometrial and subendometrial blood flow measured by three-dimensional power Doppler ultrasound during IVF treatment. *Hum Reprod*. (2006) 21:1062–9. doi: 10.1093/humrep/dei442

35. Maaskant A, Scarsi KK, Meijer L, Roubos S, Louwerse AL, Remarque EJ, et al. Long-acting reversible contraception with etonogestrel implants in female macaques (*Macaca mulatta* and *Macaca fascicularis*). *Front Vet Sci*. (2024) 10:1319862. doi: 10.3389/fvets.2023.1319862

36. Chemerinski A, Shen M, Valero-Pacheco N, Zhao Q, Murphy T, George L, et al. The impact of ovarian stimulation on the human endometrial microenvironment. *Hum Reprod*. (2024) 39:1023–41. doi: 10.1093/humrep/deae048

37. Levi AJ, Drews MR, Bergh PA, Miller BT, Scott RT Jr. Controlled ovarian hyperstimulation does not adversely affect endometrial receptivity in in vitro fertilization cycles. *Fertil Steril*. (2001) 76:670–4.

38. Sharara FI, McClamrock HD. High estradiol levels and high oocyte yield are not detrimental to in vitro fertilization outcome. *Fertil Steril*. (1999) 72:401–5. doi: 10.1016/S0015-0282(99)00293-9

39. Meldrum DR. Female reproductive aging—ovarian and uterine factors. *Fertil Steril*. (1993) 59:1–5. doi: 10.1016/S0015-0282(16)55608-8

40. Simon C, Cano F, Valbuena D, Remohi J, Pellicer A. Clinical evidence for a detrimental effect on uterine receptivity of high serum oestradiol concentrations in high and normal responder patients. *Hum Reprod*. (1995) 10:2432–7. doi: 10.1093/oxfordjournals.humrep.a136313

41. Yu Ng EH, Yeung WSB, Yee Lan Lau E, So WWK, Ho PC. High serum oestradiol concentrations in fresh IVF cycles do not impair implantation and pregnancy rates in subsequent frozen–thawed embryo transfer cycles. *Hum Reprod*. (2000) 15:250–5. doi: 10.1093/humrep/15.2.250

42. Shapiro BS, Daneshmand ST, Garner FC, Aguirre M, Hudson C, Thomas S. Evidence of impaired endometrial receptivity after ovarian stimulation for in vitro fertilization: a prospective randomized trial comparing fresh and frozen–thawed embryo transfer in normal responders. *Fertil Steril*. (2011) 96:344–8. doi: 10.1016/j.fertnstert.2011.05.050

43. Montoya-Botero P, Polyzos NP. The endometrium during and after ovarian hyperstimulation and the role of segmentation of infertility treatment. *Best Pract Res Clin Endocrinol Metab*. (2019) 33:61–75. doi: 10.1016/j.beem.2018.09.003

44. Xu C, Tang S. Alteration of endometrial receptivity in rats with ovarian hyperstimulation syndrome. *J Obstet Gynaecol*. (2014) 34:146–52. doi: 10.3109/01443615.2013.832735

45. Ertzeid G, Storeng R. The impact of ovarian stimulation on implantation and fetal development in mice. *Hum Reprod*. (2001) 16:221–5.

46. Labarta E, Rodríguez C. Progesterone use in assisted reproductive technology. *Best Pract Res Clin Obstet Gynaecol*. (2020) 69:74–84.

47. Seita Y, Tsukiyama T, Iwatani C, Tsuchiya H, Matsushita J, Azami T, et al. Generation of transgenic cynomolgus monkeys that express green fluorescent protein throughout the whole body. *Sci Rep*. (2016) 6:24868. doi: 10.1038/srep24868

48. Ke Q, Li W, Lai X, Chen H, Huang L, Kang Z, et al. TALEN-based generation of a cynomolgus monkey disease model for human microcephaly. *Cell Res*. (2016) 26:1048–61. doi: 10.1038/cr.2016.93

49. Zhao H, Tu Z, Xu H, Yan S, Yan H, Zheng Y, et al. Altered neurogenesis and disrupted expression of synaptic proteins in prefrontal cortex of SHANK3-deficient non-human primate. *Cell Res*. (2017) 27:1293–7. doi: 10.1038/cr.2017.95

50. Chen Y, Yu J, Niu Y, Qin D, Liu H, Li G, et al. Modeling Rett syndrome using TALEN-edited MECP2 mutant cynomolgus monkeys. *Cell*. (2017) 169:e10:945–55. doi: 10.1016/j.cell.2017.04.035

51. Zhang W, Wan H, Feng G, Qu J, Wang J, Jing Y, et al. SIRT6 deficiency results in developmental retardation in cynomolgus monkeys. *Nature*. (2018) 560:661–5. doi: 10.1038/s41586-018-0437-z

52. Cui Y, Niu Y, Zhou J, Chen Y, Cheng Y, Li S, et al. Generation of a precise Oct4-hrGFP knockin cynomolgus monkey model via CRISPR/Cas9-assisted homologous recombination. *Cell Res*. (2018) 28:383–6. doi: 10.1038/cr.2018.10

53. Zhou Y, Sharma J, Ke Q, Landman R, Yuan J, Chen H, et al. Atypical behaviour and connectivity in SHANK3-mutant macaques. *Nature*. (2019) 570:326–31. doi: 10.1038/s41586-019-1278-0

54. Qiu P, Jiang J, Liu Z, Cai Y, Huang T, Wang Y, et al. BMAL1 knockout macaque monkeys display reduced sleep and psychiatric disorders. *Natl Sci Rev*. (2019) 6:87–100. doi: 10.1093/nsr/nwz002

55. Tsukiyama T, Kobayashi K, Nakaya M, Iwatani C, Seita Y, Tsuchiya H, et al. Monkeys mutant for PKD1 recapitulate human autosomal dominant polycystic kidney disease. *Nat Commun*. (2019) 10:5517. doi: 10.1038/s41467-019-13398-6

56. Schmidt JK, Strelchenko N, Park MA, Kim YH, Mean KD, Schotzko ML, et al. Genome editing of CCR5 by CRISPR-Cas9 in Mauritian cynomolgus macaque embryos. *Sci Rep*. (2020) 10:18457. doi: 10.1038/s41598-020-75295-z

57. Wang F, Zhang W, Yang Q, Kang Y, Fan Y, Wei J, et al. Generation of a Hutchinson–Gilford progeria syndrome monkey model by base editing. *Protein Cell*. (2020) 11:809–24. doi: 10.1007/s13238-020-00740-8

58. Chen Z-Z, Wang J-Y, Kang Y, Yang Q-Y, Gu X-Y, Zhi D-L, et al. PINK1 gene mutation by pair truncated sgRNA/Cas9-D10A in cynomolgus monkeys. *Zool Res*. (2021) 42:469–77. doi: 10.24272/j.issn.2095-8137.2021.023

59. Li C-Y, Liu X-C, Li Y-Z, Wang Y, Nie Y-H, Xu Y-T, et al. Generation of mitochondrial replacement monkeys by female pronucleus transfer. *Zool Res*. (2024) 45:292–8. doi: 10.24272/j.issn.2095-8137.2023.287

frontiers | Frontiers in Veterinary Science

TYPE Original Research
PUBLISHED 13 September 2024
DOI 10.3389/fvets.2024.1444550

OPEN ACCESS

EDITED BY
Stefan Gregore Ciornei,
Iasi University of Life Science (IULS), Romania

REVIEWED BY
Jose Manuel Ortiz-Rodríguez,
University of Bologna, Italy
Bartłomiej M. Jaśkowski,
Wroclaw University of Environmental and Life Sciences, Poland

*CORRESPONDENCE
Jane M. Morrell
✉ jane.morrell@slu.se

†PRESENT ADDRESS
Anders Johannisson,
Department of Medical Sciences, Uppsala University, Uppsala, Sweden

RECEIVED 05 June 2024
ACCEPTED 09 August 2024
PUBLISHED 13 September 2024

CITATION
Hallberg I, Morrell JM, Malaluang P, Johannisson A, Sjunnesson Y and Laskowski D (2024) Sperm quality and *in vitro* fertilizing ability of boar spermatozoa stored at 4 °C versus conventional storage for 1 week. *Front. Vet. Sci.* 11:1444550. doi: 10.3389/fvets.2024.1444550

Sperm quality and *in vitro* fertilizing ability of boar spermatozoa stored at 4 °C versus conventional storage for 1 week

Ida Hallberg[1,2], Jane M. Morrell[1]*, Pack Malaluang[1], Anders Johannisson[1†], Ylva Sjunnesson[1] and Denise Laskowski[1]

[1]Department of Clinical Sciences, Centre for Reproductive Biology in Uppsala (CRU), Swedish University of Agricultural Sciences, Uppsala, Sweden, [2]Department of Animal Biosciences, Swedish University of Agricultural Sciences, Uppsala, Sweden

Introduction: Since boar spermatozoa show a marked deterioration in sperm quality when cooled, insemination doses are usually stored at 16–18 °C. However, maintaining this temperature during transport of semen doses is challenging, particularly during the summer months. An alternative could be to store the doses at 4 °C if cold-shock to the sperm could be prevented. The objective of this study was to evaluate boar sperm quality and fertility in *in vitro* fertilization after storage in AndroStar Premium at 4 °C for 1 week.

Methods: Insemination doses (n =9) in AndroStar Premium from a commercial boar semen collection station were transported to the laboratory at approximately 20 °C. At the laboratory, sperm quality evaluation and was preformed and each dose was split; half of each ejaculate was stored in a climate-controlled box at 16–18 °C, the other was slowly cooled to 4 °C. Both samples were stored for 1 week before further sperm quality evaluation and *in vitro* fertilization (IVF) were performed. Mean values were tested using generalized linear regression, with treatment and boar as fixed factors; $p \leq 0.05$ was considered significant.

Results: Sperm membrane integrity (mean±sem: 91±0.05 and 83±0.09% for 16 and 4 °C, respectively) and superoxide production (6.79±2.37 and 13.54±6.23% for 16 and 4 °C, respectively), were different between treatments. The DNA fragmentation index was lower in cold-stored samples than in conventionally stored samples (3.74±2.25 and 7.40±3.36% for 4 and 16 °C, respectively). The numbers of oocytes developing to blastocyst on Day 6 (mean±sd: 9.0±8.0 and 6.0±5.0%, for storage at 16 and 4 °C, respectively) were not different between treatments.

Discussion: Therefore, storage of boar semen doses in AndroStar Premium at 4 °C for up to 7days would be a viable alternative to current praxis.

KEYWORDS

porcine, *in vitro* embryo production, semen storage, artificial insemination, long term boar semen storage

1 Introduction

One of the major challenges in porcine reproductive biotechnologies lies in maintaining boar sperm quality in semen doses destined for artificial insemination (AI). This reproductive biotechnology is considered to be the most frequently used in pig breeding (1). Almost all pig

breeding involves AI (2), enabling better use of genetics, improved disease control and increased biosecurity than natural mating (3). Furthermore, AI improves the farm economy, being cheaper than natural mating while providing similar reproductive efficiency, and permitting access to a wider range of sires than is possible if farmers keep their own boars (4, 5).

In contrast to the situation in cattle AI, liquid semen, rather than frozen semen, is preferred for the vast majority of pig AIs (6), since there is considerable variation in the success of cryopreservation among boars and even among ejaculates from the same boar (7). The low ratio of cholesterol to phospholipid in the boar sperm membrane is believed to be one of the contributing factors in making boar sperm particularly susceptible to the adverse effects of cryopreservation (8). Boar spermatozoa are reported to be sensitive to cooling below 16 °C, with temperature-induced lipid phase changes to the sperm membranes that have a profound effect on sperm survival and functionality (9). However, results are conflicting: in one study, acceptable fertility rates could be achieved in Androhep extender under storage conditions as low as 12 °C for 48 h (10). In contrast, storage temperatures below 20 °C affected sperm motility and acrosome integrity in semen from Norwegian Landrace boars (11), although there was considerable variation among boars in sperm survival during storage at 10 °C.

Apart from the deleterious effects of low storage temperatures on boar spermatozoa, temperatures above 17 °C during transport are also deleterious to sperm quality, even when the sperm doses are placed in a sealed, insulated box. Sperm motility of semen doses was impaired during transport at a high ambient temperature of 37 °C and did not recover during subsequent storage at 17 °C (12). Release of heat shock proteins and increased apoptosis were observed, which the authors attributed to activation of adenosine monophosphate (AMP)-activated protein kinase.

Most boar semen for AI is currently stored at 16–18 °C and used within 3–5 days of collection (3). Due to the temperate climate in Sweden, boar semen doses are transported from the boar station to the pig farms at ambient temperature, and are subsequently stored at 16–18 °C. In other countries, where ambient temperatures can be considerably hotter than in Scandinavia, it is difficult to maintain sperm quality during transport. In any case, even when stored at 16–18 °C there is an increase in DNA fragmentation in boar semen after storage, either for approximately 48 h (13) or 72 h (14, 15); the underlying reason for this increase in DNA fragmentation is not known.

Adenosine triphosphate (ATP) production in boar sperm samples is reduced at temperatures below 17 °C, but not all spermatozoa are affected equally (16). This finding indicates that at least some spermatozoa could survive low-temperature storage. The manufacturers of boar semen extenders have developed formulations that they hope could be used to store boar semen at 4 °C. One such commercial extender is AndroStar Premium (Minitube International, Tiefenbach, Germany). Some preliminary studies investigated sperm quality and fertility of boar semen in these extenders [e.g., (17, 18)]. The manufacturer presents data on sperm motility after 9 days of storage in this new extender. If sperm fertility is not compromised by storage at 4 °C, the availability of this extender could be of considerable interest for pig producers.

The objective of this study was to investigate the *in vitro* fertility and sperm quality of boar spermatozoa stored at 4 °C for 1 week compared to conventional storage at 16–18 °C.

2 Materials and methods

2.1 Experimental design

Ejaculates from nine boars at a commercial boar station were split, with one portion being stored at 16–18 °C (conventional storage) and the other portion at 4 °C for 1 week. Sperm membrane integrity, chromatin integrity and reactive oxygen species production (ROS) were analysed immediately on arrival at the laboratory, and again after storage for 6 or 7 days, at which time the *in vitro* fertilizing capacity was also evaluated. Although the majority of the sperm samples were stored for 7 days, it was necessary to store some for only 6 days for practical reasons. Therefore, on a subsequent occasion, semen samples were used after both day 6 and day 7 of storage, for comparison.

2.2 Sperm samples

Ejaculates were collected from nine Hampshire boars at a commercial boar station (Köttforetagen, Hållsta, Sweden) using the gloved hand method and were extended in AndroStar Premium (kind gift of Minitube International GmbH, Tiefenbach, Germany) to give conventional semen doses of 2.4×10^9 spermatozoa in 80 mL. These doses were transported to the Swedish University of Agricultural Sciences in an insulated box at ambient temperature, arriving approximately 4 h after semen collection. After removing 1 mL of sample for sperm quality analyses, half of each sample was stored at 16–18 °C in a climate-controlled box (Unitron, Tørring, Denmark). The other half was slowly cooled to 4 °C, by placing a 50-mL tube containing half the insemination dose in an insulated box inside another insulated box in the cold room at 4 °C. The temperature of the semen doses reached 4 °C after approximately 6 h. Sperm quality was evaluated on arrival at the laboratory and again after 6 or 7 days, when the sperm samples were also used for *in vitro* fertilization (IVF) following standard protocols (19).

2.3 Sperm concentration

Sperm concentration was measured with a Nucleocounter SP-100 (Chemometec, Allerød, Denmark). Briefly, 50 µL of semen were mixed with 5 mL Reagent S100 (Chemometec, Allerød, Denmark) to break down cell membranes before loading a cassette containing propidium iodide (PI) with the sperm mixture. The cassette was then placed in the fluorescence reader and sperm concentration was displayed after approximately 30 s.

2.4 Flow cytometry

Analyses were performed using a FACSVerse flow cytometer (BDBiosciences; Franklin Lakes, NJ, United States) equipped with standard optics. Sperm samples were first diluted to 2×10^6

spermatozoa/mL with modified Beltsville Thawing Solution (BTS) (20), consisting of: glucose (3.7 g), tri-sodium citrate (0.6 g), sodium hydrogen carbonate (0.13 g), sodium EDTA (0.13 g) and potassium chloride (0.08 g) added to 100 mL distilled water, i.e., the modification was that no antibiotics were added to the mixture.

2.4.1 Membrane integrity

Membrane integrity was evaluated with SYBR-14 and propidium iodide (PI) (Live-Dead Sperm Viability Kit L-7011; Invitrogen, Eugene, OR, United States). The sperm samples, diluted to 2×10^6 spermatozoa/mL in BTS, were stained with 0.6 µL of SYBR-14 (1:50 in BTS; 40 nM) and 3 µL of PI (24 µM). The tubes were kept in the dark at 38 °C for 10 min. After excitation with a blue laser, green fluorescence (FL1) from SYBR-14 was detected with band-pass filter (527/32 nm), while red fluorescence (FL3) from PI was measured using a band-pass filter of 700/54 nm. From each sample, measurements from 50,000 events were collected and quantified as percentages. For the purposes of this experiment, spermatozoa were classified as having intact membranes (SYBR14+, PI−), or damaged membranes (either dead SYBR−, PI+ or SYBR14+, PI+).

2.4.2 Sperm chromatin structure assay

After mixing aliquots of sperm samples (50 µL) 1:1 with TNE buffer (Tris-sodium chloride-EDTA; 0.15 mol/L NaCl, 0.01 mol/L Tris–HCl, 1 mmol/L EDTA, pH 7.4), the samples were snap-frozen in liquid nitrogen and transferred to a − 80 °C freezer and stored until further analysis. The samples were thawed on crushed ice, aliquots (10 µL) were further diluted with TNE buffer (90 µL) and subjected to partial DNA denaturation *in situ* with a detergent solution (0.2 mL; 0.17% Triton X-100, 0.15 mol/L NaCl, and 0.08 mol/L HCl; pH 1.2). Then they were stained with acridine orange (0.6 mL; 6 µg/mL in 0.1 mol/L citric acid, 0.2 mol/L Na_2HPO_4, 1 mmol/L EDTA, 0.15 mol/L NaCl; pH 6.0). The samples were analysed using flow cytometry within 3–5 min. For each sample, at least 10,000 events were analyzed at a speed of 200 cells/s after excitation with a blue laser (488 nm). Both forward scatter (FSC) and side scatter (SSC) were collected. The FL1 (green fluorescence) was collected through a band-pass filter (527/32 nm); FL3 (red fluorescence) was collected using a band-pass filter for wavelengths 700/54 nm. After gating for spermatozoa in the FSC-SSC dot-plot, the DNA Fragmentation Index (%DFI, i.e., the ratio of cells with denatured, single-stranded DNA to total spermatozoa acquired) was calculated for each sample using flow cytometry standard (FCS) Express version 5 (*De Novo* Software, Pasadena, CA, United States). The proportion of high DNA staining samples (HDS) was also recorded.

2.4.3 Assessment of reactive oxygen species

Aliquots (300 µL) were stained with Hoechst 33258 at 0.4 µM (HO; Sigma, Stockholm), 0.4 µM hydroethidine (HE; Invitrogen Molecular Probes, Eugene, OR, United States) and 20 µM dichlorodihydro-fluorescein diacetate (DCFDA; Invitrogen Molecular Probes). The samples were incubated at 37 °C for 30 min before analyzing. Excitation was with a blue laser emitting at 488 nm and a violet laser emitting at 405 nm. Detection of green fluorescence from DCFDA (FL1) was via a band-pass filter (527/32 nm), red fluorescence from HE (FL3) was measured using a band-pass filter (700/54 nm), and blue/green fluorescence from Hoechst 33258 (FL5) was detected via a band-pass filter (528/45 nm). In total, 30,000 sperm-specific events were evaluated. After gating for spermatozoa in the FSC-SSC dotplot, they were classified as living or dead superoxide or H_2O_2 negative, and living or dead superoxide or H_2O_2 positive.

2.5 *In vitro* embryo production

Ovaries from gilts were collected at a local slaughterhouse and transported to the laboratory at the Swedish University of Agricultural Sciences where cumulus oocyte complexes (COCs) were harvested from the follicles and matured *in vitro* according to standardized procedures as previously described (19). In brief, the COCs were divided into two groups at random to minimize variation between treatments. For this study, in total 11 batches (replicates) were used, containing in total 874 oocytes leading to 64 developing to the blastocyst stage.

The procedure detailed in Leclercq et al. (19) was followed for IVF, using commercially available porcine oocyte maturation medium (POM), porcine fertilization medium (PFM), and porcine zygote medium (PZM) purchased from Research Institute for the Functional Peptides, FHK Fujihura Industry Co Ltd., Osaka, Japan. Wash media was used for handling oocytes and embryos outside the incubators and was produced on site (gentamicin sulfate 10 µg/mL, L-glutamine MW 146.14 1 mM, PVA 3 µg/mL in Hepes TCM 199; wash media for aspiration of COCs had, in addition, 20 U/mL heparin added). Media to be used in incubators were equilibrated for at least 2 h in 38.5 °C and 5.5% CO_2 before use.

The POM medium used for the first 22 h of maturation was enriched with follicle stimulating hormone (FSH) @ 0.05 IU/mL (FSH Porcine, OOPA00171, Insight Biotechnology, Middlesex, United Kingdom), luteinizing hormone (LH) @ 0.05 IU/mL (LH Protein, OOPA00173, Insight Biotechnology), and dibutyryl adenosine cyclic monophosphate (dbcAMP) @ 1 mM (dbcAMP, sodium salt, 1,698,950, Biogems, Westlake Village, United States). The following 23 h of maturation were carried out in the absence of LH, FSH or dbcAMP. *In vitro* maturation and *in vitro* fertilization were performed in an incubator with 5.5% CO_2 and 38.5 °C in maximum humidity; for *in vitro* culture, 5.5% O_2 was included in the gaseous mix. After maturation of the oocytes for 45 h in total, *in vitro* fertilization was carried out using sperm samples stored at 4 °C for one group of oocytes and those stored at 16–18 °C for the other group of oocytes. Semen preparation consisted of diluting 0.5 mL of each sperm sample in 4 mL of PFM. After mixing, 2 mL of the sperm dilution was placed on top of 4 mL of low density Porcicoll at room temperature (21). The preparations were then centrifuged for 20 min at 300 x g before removing the supernatant. The sperm pellets were diluted in PFM, the concentration was measured and the sperm concentration was adjusted to 0.6 $\times 10^6$/mL for IVF. The COCs were randomly distributed between the groups; the group sizes varied between 10 and 13 (50 µL drops under oil) and 35–50 (500 µL wells without oil). Ideally, only wells would have been used, but there was a concern that too few good quality oocytes would be available on any 1 day. Therefore, the alternative (culturing 10 oocytes in 50 µL drops of culture medium) was compared with our standard

TABLE 1 Effect of storage on membrane integrity, DNA fragmentation index and High DNA stainability in boar semen stored for 1 week at 4 °C or 16-18 °C ($n = 9$).

Parameter	Fresh	4 °C storage	*p*-value Fresh vs. 4 °C	16 °C storage	*p*-value Fresh vs. 16 °C	*p*-value 4 °C vs. 16-18 °C
Intact membranes (%)	89 ± 4%	83 ± 0.09%	0.10	91 ± 0.05%	NS	0.01
Damaged membranes (%)	0.12 ± 0.05%,	0.18 ± 0.10%	0.07	0.10 ± 0.05%	0.35	0.006
DNA fragmentation (%DFI)	3.58 ± 1.3	3.74 ± 2.25	0.87	7.40 ± 3.36	<0.001	0.0002
HDS (%)	0.27 ± 0.06	0.39 ± 0.18	0.14	0.40 ± 0.20	0.08	0.73

HDS, high DNA stainability.

practice (culturing 30–50 oocytes in 500 µL culture medium in wells). Since the results were consistent for both groups, we were able to use the drop method on days when there were insufficient oocytes for wells.

After 24 h in PFM, presumed zygotes were denuded by gentle pipetting, washed and cultured in PZM under oil for 6 days before fixation and staining. During the culture process, cleavage rate and cleavage rate above 2 cell stage were recorded 48 h post fertilization. Developing blastocysts were evaluated at day 5 post fertilization by light microscopy directly in the wells or drops. On day 6 post fertilization, all oocytes and embryos were collected, fixed in 2% paraformaldehyde and stained using 4′,6-diamidino-2-phenylindole (DAPI) to determine the number of spermatozoa still firmly attached to the zona pellucida. The number of blastocysts and developmental stages were documented. Note that the number of spermatozoa still attached to the zona pellucida at this stage might not correspond to the number that were attached in connection with fertilization, especially since the presumptive zygotes had been washed, but it still provides an indication of whether sperm function was affected by the storage temperature of the semen prior to its use in IVF.

2.6 Statistical analysis

The sperm parameters were log-transformed to estimate normal distribution. Generalized linear regression (package Lme4, R, 4.3.0) was used to test the effect of storage (4 °C or 16–18 °C) against the fresh semen sample, and the effect of storage temperature (4 °C or 16–18 °C) on semen quality parameters (damaged membranes, intact membranes, %DFI, HDS, Live superoxide +, Live superoxide −, Live H_2O_2+, Live H_2O_2−, Dead superoxide +, Dead H_2O_2+, Dead H_2O_2−). Treatment and days of storage (6 or 7 days) were included as fixed effects and Boar was included as a random effect to account for the individual variability among boars from which the sperm samples were collected. Model selection was based on Akaike Information Criterion (AIC) and likelihood ratio tests. Based on these criteria, storing the sample 6 or 7 days did not affect treatment outcome and therefore length of storage could be removed from the models. Therefore, the results from day 6 and 7 were combined and presented as one variable (day 7). Furthermore, the results from wells separately, and from wells and drops together were tested and yielded similar results. The results did not differ and therefore all replicates are included here.

The impact of treatment on oocyte developmental competence parameters (Proportion cleaved 48 h after fertilization, Proportion cleaved above 2 cell stage 48 h after fertilization, Proportion embryos day 5 and 6 days after fertilization) were assessed through mixed-effect logistic regression analysis (glmer from the MASS package in R). This analysis utilized a binary distribution, with replicate as a random factor and weighting for group size to determine the odds ratio. The odds ratio (OR) <1 indicates a negative effect of the treatment. To calculate the effect of treatment on the number of spermatozoa attached to the zona pellucida, non-parametric tests (Mann–Whitney) was used (wilcox.test model in R).

Raw *p*-values are presented (no adjustment for multiple testing was included); $p < 0.05$ was considered significant.

3 Results

The results for sperm membrane integrity and fragmented DNA are reported in Table 1. Membrane integrity in stored samples was similar to the fresh samples but was different between storage temperatures, being higher in the samples stored at 16 °C than at 4 °C (89 ± 4, 83 ± 0.09, and 91 ± 0.05%, for fresh samples and samples stored at 4 °C and 16 °C, respectively). There were more sperm with damaged membranes in the samples stored at 4 °C than at 16 °C (0.18 ± 0.10 and 0.10 ± 0.05%, respectively).

The %DFI was similar in fresh samples on Day 0 and in cold-stored samples on day 7 but was higher in samples stored at 16 °C (3.58 ± 1.30, 3.74 ± 2.25, and 7.40 ± 3.36% for fresh samples and samples stored at 4 °C and 16-18 °C, respectively; $p < 0.001$). The proportion of sperm with HDS was not different (0.27 ± 0.06, 0.39 ± 0.18, and 0.40 ± 0.02% for fresh samples and samples stored at 4 °C and 16-18 °C, respectively; $p > 0.05$).

The ROS status of the sperm samples is shown in Table 2. The proportion of live superoxide positive sperm was higher in cold-stored samples than in fresh samples ($p < 0.001$), but the proportion of spermatozoa in the other two categories for superoxide were not different. The proportion of live superoxide negative spermatozoa was higher in the fresh samples than for samples stored at 4 °C (82.04 ± 1.07 and 75.83 ± 2.49%, respectively; $p = 0.04$). In addition, although there was no difference between the proportions of live superoxide negative spermatozoa in fresh samples and in samples stored at 16-18 °C, there was a difference between samples stored at 4 °C and

TABLE 2 Effect of temperature of storage on reactive oxygen species in boar spermatozoa stored for 7 days at 4 °C or 16 °C ($n = 9$).

	Fresh	4 °C storage	*P*-value Fresh vs. 4 °C	16-18 °C storage	*p*-value Fresh vs. 16-18 °C	*P*-value 4 °C vs. 16-18 °C
Live superoxide positive (%)	5.38 ± 0.87	13.54 ± 6.23	<0.001	6.79 ± 2.37	0.35	<0.0001
Live superoxide negative (%)	82.04 ± 1.07	75.83 ± 2–49	0.04	83.44 ± 1.56	0.69	0.008
Dead superoxide positive (%)	12.04 ± 1.09	9.29 ± 0.80	0.27	9.11 ± 0.29	0.08	0.47
Live hydrogen peroxide positive (%)	0.20 ± 0.13	0.95 ± 1.44	<0.001	0.74 ± 0.43	0.001	0.61
Live hydrogen peroxide negative (%)	87.50 ± 1.12	89.37 ± 0.86	0.25	89.46 ± 1.56	0.23	0.97
Dead hydrogen peroxide positive (%)	0.025 ± 0.007	0.0527 ± 0.02	0.55	0.037 ± 0.008	0.69	0.28
Dead hydrogen peroxide negative (%)	12.27 ± 1.11	9.62 ± 0.76	0.06	9.83 ± 1.04	0.06	0.99

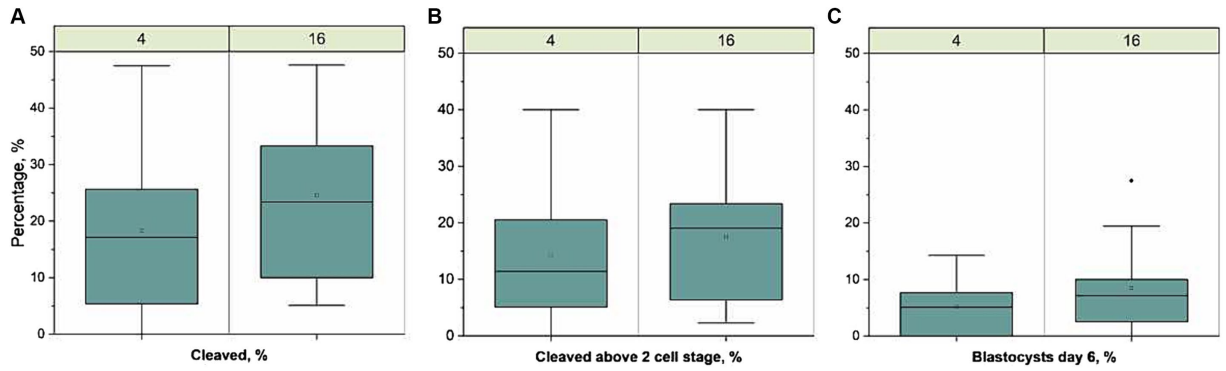

FIGURE 1
Developmental competence of oocytes fertilized with sperm samples stored for 1 week at 4 °C. ($n = 436$) or 16-18 °C ($n = 438$), run in 11 replicates. Boxplots present the proportion of **(A)** cleaved zygotes 44 h after fertilization from total matured oocytes, **(B)** cleaved above 2 cell stage 44 h after fertilization from total matured oocytes, and **(C)** blastocysts day 6 after fertilization from total matured oocytes,. The line represent the median of all replicates, the open circles represent the mean, the box the interquartile range (IQR), the whiskers length are 1.5 × IQR and filled dot represents outlier (>1.5 × IQR). There was a lower proportion of cleaved zygotes in the 4 °C group compared to the 16-18 °C group ($p = 0.04$) but there was no significant difference in the proportion of zygotes cleaved above the two cell stage or in blastocysts between the two groups.

16-18 °C (75.83 ± 2.49 and 83.44 ± 1.56%, respectively; $p < 0.008$). For hydrogen peroxide production, only the proportion of live hydrogen peroxide positive spermatozoa was different, being greater in the stored samples than in the fresh sperm samples ($p < 0.001$). There was no difference between samples stored at 4 °C and 16-18 °C.

An overview of the IVF results is presented in Figure 1. The total number of oocytes developing to blastocyst on Day 6 was 39 and 25 for sperm samples stored at 16-18 °C and 4 °C, respectively. The proportion of oocytes developing to blastocyst on Day 6 (mean ± sd) was 9.0 ± 8.0 and 6.0 ± 5.0%, for 16-18 °C and 4 °C, respectively, and was not different between treatments. The proportion cleaved 44 h after fertilization was 25 ± 16 and 20 ± 15% ($p = 0.04$), whereas the proportion cleaved above 2 cell stage was 19 ± 12 and 15 ± 13% for 16-18 °C and 4 °C, respectively. There was no difference between the proportions cleaved above 2 cell stage. The number of spermatozoa attached to the zona pellucida [median (min-max)] in the 16-18 °C group, i.e., 5 (0–55) was not different from the 4 °C group, i.e., 3 (0–13) ($p = 0.36$).

4 Discussion

The purpose of this experiment was to evaluate sperm quality and fertilizing capability of boar sperm samples after storage in AndroStar Premium for 6 or 7 days at 4 °C compared to conventional storage at 16–18 °C. The sperm samples were prepared for IVF using a low density colloid to separate the spermatozoa from extender and seminal plasma, i.e., to avoid selecting only the spermatozoa most capable of fertilization, which would have been the case if a high density colloid was used (22). Such selection would tend to negate temperature-induced differences in fertilizing capacity, since only a few spermatozoa are required to achieve fertilization. Thus, although it should be possible to detect differences in fertilizing capacity due to sperm storage, if they exist, no such differences were apparent here.

The results showed that most aspects of sperm quality were not different between the two storage temperatures, with the exception of %DFI, which was lower for the samples stored at 4 °C, and the proportion of live superoxide positive spermatozoa,

which was higher for samples stored at 4 °C. Although there was a small difference between the number of zygotes at the two cell stage, the number developing beyond this stage was not different between the two groups. These results are interesting since they indicate that boar spermatozoa can be cooled to 4 °C in AndroStar Premium, and stored at this temperature, without suffering from irreversible functional damage, i.e., cold-shock.

A previous report on cold-storage of boar semen in BTS showed that sperm cooled to 10 °C or 5 °C suffered from cold shock, with a loss of motility and viability, with a sub-lethal imbalance of ATP among the surviving sperm population if stored for more than 120 h (16). In contrast, in our study, not only was sperm viability (membrane integrity) retained in AndroStar Premium at 4 °C, but fertilizing ability in IVF was not different to the conventionally stored samples. Waberski et al. (18) reported that boar sperm viability was maintained in AndroStar® Premium at low temperatures, as opposed to Beltsville Thawing Solution, while Jäkel et al. (23) observed that there was no difference in pregnancy results following AI with semen samples stored at 5 °C compared to 17 °C. On the other hand, Menezes et al. (17) reported that although membrane integrity was maintained in boar semen stored at 5 °C, sperm motility was lower than in samples stored at 17 °C. These results are similar to those for membrane integrity in the present study. However, it is possible that spermatozoa stored at low temperatures require a longer incubation time prior to motility analysis to regain their full motility. This possibility was not examined here. According to the manufacturer, the extender contains membrane stabilizers and capacitation inhibitors, which help to maintain sperm quality long-term (24); it is possible that these inhibitors also reduce sperm motility.

Chromatin integrity was not analysed in the previous studies on cold storage of boar semen. This is surprising since the proportion of boar sperm with single-stranded DNA breaks was observed to rise after 2–3 days of storage at 16–18 °C (13–15), suggesting that this is a critical point for boar sperm storage. Since standard praxis is to store boar semen for up to 5 days before use, samples stored for more than 3 days may potentially have increased proportions of spermatozoa with fragmented chromatin. Spermatozoa with damaged chromatin are capable of fertilization, and the DNA-repair mechanisms of the oocyte can correct some damage (25). If the damage is too great, embryonic development is halted at some stage, potentially being seen as a reduction in litter size, or even a failed pregnancy if too few embryos survive to implant (26). Litter size was shown to be negatively correlated with DNA fragmentation, at least in Norwegian Landrace and Duroc breeds (27). In the present study, the %DFI was lower in the samples stored at 4 °C than in the samples stored at 16–18 °C, which is very promising for avoiding storage-induced DNA damage.

Reactive oxygen species, such as superoxide and hydrogen peroxide, are produced as byproducts of metabolism (28) during glycolysis or oxidative phosphorylation. Previously it was thought that different animal species tend to use mainly one or the other route for sperm ATP-production, but recently it was suggested that spermatozoa may be able to switch from one to the other according to their immediate environmental conditions (29). Regardless of how superoxide is produced, it is assumed that superoxide is converted to hydrogen peroxide by superoxide dismutase (30). Physiological concentrations of ROS are required for normal sperm capacitation (31) but excessive concentrations cause loss of sperm function. Lipid peroxidation and loss of motility were induced in boar spermatozoa by hydrogen peroxide (32), whereas acrosome exocytosis and glycolysis were observed to be caused by hydrogen peroxide (33). Our results showed that there were differences in ROS production in stored boar spermatozoa according to storage conditions, with more superoxide production in the samples stored at 4 °C than in conventionally stored samples. Moreover, more hydrogen peroxide was produced in the stored samples than in the fresh samples. Although membrane integrity was maintained better in the sperm samples stored at 16–18 °C than at 4 °C, DNA fragmentation was actually lower in the samples stored at 4 °C than at 16–18 °C. Thus, either the semen extender contained sufficient antioxidants to deactivate the ROS produced (34), or ROS were not responsible for membrane damage and DNA damage in boar sperm stored under the conditions of this study. These results are interesting and warrant further investigation. Previous studies with stallion sperm also revealed a situation in which increased superoxide production was not associated with declining sperm quality (35), and increased superoxide production was not linked to increased hydrogen peroxide production. Furthermore, another study revealed that hydrogen peroxide and superoxide are present in different compartments of stallion spermatozoa (36).

Our results show that boar semen can be stored refrigerated without losing its fertilizing capacity, at least in IVF, if it is extended in AndroStar Premium. However, the fertility of boar semen stored in this manner was not tested in an AI trial in this study. Previous studies have used cooled semen for AI after storage for 1 or 2 days, but to our knowledge, no studies have been done on fertility after 7 days of storage. Jäkel et al. (23) did not detect a difference in fertility when AI was performed with samples stored for 72 h at 5 °C and 17 °C.

The possibility of cooling boar semen for refrigerated storage and transport could help to avoid loss of quality during transport in the summer months. Although the infrastructure on pig farms is set up for storage of boar semen at 16–18 °C, it would not be too difficult to introduce refrigerated storage since most farms are already equipped with a refrigerator for storing medication and other perishable items. Furthermore, refrigerated transport is commonly used to transport food supplies all over the world. Therefore, refrigerated boar semen could offer considerable advantages over conventional storage temperatures for pig breeding, particularly in view of predicted climate changes.

5 Conclusion

The fertility of boar semen doses stored in AndroStar Premium at 16–18 °C or 4 °C for up to 7 days was not different in terms of number of blastocysts developing after *in vitro* fertilization. Sperm quality was affected slightly, in that membrane integrity was better in samples stored at 16–18 °C, but DNA fragmentation was less in the samples stored at 4 °C. Therefore, cold storage of boar semen is possible without a detrimental effect on fertility. It would be a viable alternative to current praxis for pig producers, allowing better control of semen doses during transport in the summer months.

Data availability statement

The original contributions presented in the study are included in the article/supplementary material, further inquiries can be directed to the corresponding author.

Ethics statement

Ethical approval was not required for the study involving animals in accordance with the local legislation and institutional requirements because semen collection from pigs is a recognized husbandry procedure and does not require ethical approval in Sweden. Oocytes were obtained from ovaries from the local slaughterhouse, which also does not require ethical approval.

Author contributions

IH: Formal analysis, Investigation, Visualization, Writing – review & editing. JM: Conceptualization, Funding acquisition, Methodology, Resources, Supervision, Writing – original draft. PM: Formal analysis, Investigation, Writing – review & editing. AJ: Formal analysis, Methodology, Writing – review & editing. YS: Investigation, Methodology, Writing – review & editing. DL: Formal analysis, Funding acquisition, Investigation, Methodology, Writing – review & editing.

Funding

The author(s) declare that financial support was received for the research, authorship, and/or publication of this article. This study was funded by the Sveriges Grisföretagares forskningsstiftelse, Västerås, Sweden (awarded to DL), by the Infrastructure Committee at SLU via the Cells for Life Platform (JM), and the Developmental Biology platform (YS).

Acknowledgments

We thank the personnel at Svenska Köttföretagen for supplying the boar semen for this project and Minitube International for providing the AndroStar Premium for this study.

Conflict of interest

The authors declare that the research was conducted in the absence of any commercial or financial relationships that could be construed as a potential conflict of interest.

Publisher's note

All claims expressed in this article are solely those of the authors and do not necessarily represent those of their affiliated organizations, or those of the publisher, the editors and the reviewers. Any product that may be evaluated in this article, or claim that may be made by its manufacturer, is not guaranteed or endorsed by the publisher.

References

1. Contreras MJ, Núñez-Montero K, Bruna P, García M, Leal K, Barrientos L, et al. Bacteria and boar semen storage: progress and challenges. *Antibiotics*. (2022) 11:1796. doi: 10.3390/antibiotics11121796

2. Maes D, Lopez Rodriguez A, Rijsselaere T, Vyt P, Van Soom A. Artificial insemination in pigs. Artificial insemination in farm animals. *INTECH*. (2011) 85:83–93. doi: 10.5772/16592

3. Knox RV. Artificial insemination in pigs today. *Theriogenology*. (2016) 85:83–93. doi: 10.1016/j.theriogenology.2015.07.009

4. Feitsma H. Artificial insemination in pigs, research and developments in the Netherlands, a review. *Acta Sci Vet*. (2009) 37:61–71.

5. Singh M, Mollier RT, Pongener N, Patton RN, Yadav R, Chaudhary JK, et al. Effect of artificial insemination in comparison to natural mating on the reproductive performance and profitability of smallholder pig production system in Indian Himalaya. *Front Sustain Food Syst*. (2022) 6:1067878. doi: 10.3389/fsufs.2022.1067878

6. Kajabova S, Silva H, Valadao L, Moreira da Silva F. Artificial insemination and cryopreservation of boar semen: current state and problematics. *Open Sci J*. (2020) 5:12. doi: 10.23954/osj.v5i2.2353

7. Roca J, Hernández M, Carvajal G, Vázquez JM, Martínez EA. Factors influencing boar sperm cryosurvival. *J Anim Sci*. (2006) 84:2692–9. doi: 10.2527/jas.2006-094

8. Bresciani C, Bianchera A, Bettini R, Buschini A, Marchi L, Cabassi CS, et al. Long-term liquid storage and reproductive evaluation of an innovative boar semen extender (Formula12®) containing a non-reducing disaccharide and an enzymatic agent. *Anim Reprod Sci*. (2017) 180:10–6. doi: 10.1016/j.anireprosci.2017.02.007

9. Drobnis EZ, Crowe LM, Berger T, Anchordoguy TJ, Overstreet JW, Crowe JH. Cold shock damage is due to lipid phase transitions in cell membranes: a demonstration using sperm as a model. *J Exp Zool*. (1993) 265:432–7. doi: 10.1002/jez.1402650413

10. Althouse GC, Wilson ME, Kuster C, Parsley M. Characterization of lower temperature storage limitations of fresh-extended porcine semen. *Theriogenology*. (1998) 50:535–43. doi: 10.1016/S0093-691X(98)00159-9

11. Paulenz H, Kommisrud E, Hofmo P. Effect of long-term storage at different temperatures on the quality of liquid boar semen. *Reprod Domest Anim*. (2000) 35:83–7. doi: 10.1046/j.1439-0531.2000.00207.x

12. Li J, Zhao W, Zhu J, Wang S, Ju H, Chen S, et al. Temperature elevation during semen delivery deteriorates boar sperm quality by promoting apoptosis. *Animals*. (2023) 13:3203–1. doi: 10.3390/ani13203203

13. Bielas W, Nižański W, Partyka A, Rząsa A, Mordak R. Effect of long-term storage in safe cell+ extender on boar sperm DNA integrity and other key sperm parameters. *Acta Vet Scand*. (2017) 59:58–69. doi: 10.1186/s13028-017-0325-9

14. Boe-Hansen GB, Ersbøll AK, Greve T, Christensen P. Increasing storage time of extended boar semen reduces sperm DNA integrity. *Theriogenology*. (2005) 63:2006–19. doi: 10.1016/j.theriogenology.2004.09.006

15. Khezri A, Narud B, Stenseth EB, Johannisson A, Myromslien FD, Gaustad AH, et al. DNA methylation patterns vary in boar sperm cells with different levels of DNA fragmentation. *BMC Genomics*. (2019) 20:897. doi: 10.1186/s12864-019-6307-8

16. Henning H, Nguyen QT, Wallner U, Waberski D. Temperature limits for storage of extended boar semen from the perspective of the sperm's energy status. *Front Vet Sci*. (2022) 9:953021. doi: 10.3389/fvets.2022.953021

17. de Alcantara Menezes T, Gonçalves Mellagi AP, da Silva Oliveira G, Bernardi ML, Wentz I, da Rosa Ulguim R, et al. Antibiotic-free extended boar semen preserved under low temperature maintains acceptable in-vitro sperm quality and reduces bacterial load. *Theriogenology*. (2020) 149:131–8. doi: 10.1016/j.theriogenology.2020.03.003

18. Waberski D, Luther AM, Grünther B, Jäkel H, Henning H, Vogel C, et al. Sperm function in vitro and fertility after antibiotic-free, hypothermic storage of liquid preserved boar semen. *Sci Rep O*. (2019) 9:14748. doi: 10.1038/s41598-019-51319-1

19. Leclercq A, Ranefall P, Sjunnesson YCB, Hallberg I. Occurrence of late-apoptotic symptoms in porcine preimplantation embryos upon exposure of oocytes to perfluoroalkyl substances (PFASs) under *in vitro* meiotic maturation. *PLoS One*. (2022) 17:e0279551. doi: 10.1371/journal.pone.0279551

20. Pursel VG, Johnson L. Freezing of boar spermatozoa. Fertilizing capacity with concentrated semen and a new thawing procedure. *J Anim Sci*. (1975) 40:99–102. doi: 10.2527/jas1975.40199x

21. Deori S, Johannisson A, Morrell JM. Single layer centrifugation with 20% or 30% Porcicoll separates the majority of spermatozoa from a sample without adversely affecting sperm quality. *Reprod Domest Anim*. (2020) 55:1337–42. doi: 10.1111/rda.13779

22. Sabes-Alsina M, Wallgren M, Sjunnesson YCB, Ntallaris T, Lundeheim N, López-Béjar M, et al. Effect of season on the in vitro fertilizing ability of frozen-thawed Spanish bovine spermatozoa. *J Dairy Sci*. (2020) 103:9525–33. doi: 10.3168/jds.2020-18472

23. Jäkel H, Scheinpflug K, Mühldorfer K, Gianluppi R, Lucca MS, Mellagi APG, et al. *In vitro* performance and *in vivo* fertility of antibiotic-free preserved boar

semen stored at 5 °C. *J Anim Sci Biotechnol*. (2021) 12:9. doi: 10.1186/s40104-020-00530-6

24. Wiebke M, Hensel B, Nitsche-Melkus E, Jung M, Schulze M. Cooled storage of semen from livestock animals (part I): boar, bull, and stallion. *Anim Reprod Sci*. (2022) 246:106822. doi: 10.1016/j.anireprosci.2021.106822

25. Fatehi AN, Bevers MM, Schoevers E, Roelen BAJ, Colenbrander B, Gadella BM. DNA damage in bovine sperm does not block fertilization and early embryonic development but induces apoptosis after the first cleavages. *J Androl*. (2006) 27:176–88. doi: 10.2164/jandrol.04152

26. Mateo-Otero Y, Llavanera M, Recuero S, Delgado-Bermúdez A, Barranco I, Ribas-Maynou J, et al. Sperm DNA damage compromises embryo development, but not oocyte fertilisation in pigs. *Biol Res*. (2022) 55:15. doi: 10.1186/s40659-022-00386-2

27. Myromslien FD, Tremoen NH, Andersen-Ranberg I, Fransplass R, Stenseth E-B, Zeremichael TT, et al. Sperm DNA integrity in landrace and Duroc boar semen and its relationship to litter size. *Reprod Dom Anim*. (2019) 54:160–6. doi: 10.1111/rda.13322

28. Aitken RJ, Buckingham D, West K, Wu FC, Zikopoulos K, Richardson DW. Differential contribution of leucocytes and spermatozoa to the high levels of reactive oxygen species recorded in the ejaculates of oligozoospermic patients. *J Reprod Fertil*. (1992) 94:451–62. doi: 10.1530/jrf.0.0940451

29. Amaral A. Energy metabolism in mammalian sperm motility. *WIREs Mech Dis*. (2022) 14:e1569. doi: 10.1002/wsbm.1569

30. Sakamoto T, Imai H. Hydrogen peroxide produced by superoxide dismutase SOD-2 activates sperm in *Caenorhabditis elegans*. *J Biol Chem*. (2017) 292:14804–13. doi: 10.1074/jbc.M117.788901

31. Aitken RJ. Reactive oxygen species as mediators of sperm capacitation and pathological damage. *Mol Reprod Dev*. (2017) 84:1039–52. doi: 10.1002/mrd.22871

32. Awda BJ, Mackenzie-Bell M, Buhr MM. Reactive oxygen species and boar sperm function. *Biol Reprod*. (2009) 81:553–61. doi: 10.1095/biolreprod.109.076471

33. Faggi M, Agustín Vanzetti A, Teijeiro JM. Effect of glucose and reactive oxygen species on boar sperm induced-acrosome exocytosis. *Res Vet Sci*. (2023) 164:105013. doi: 10.1016/j.rvsc.2023.105013

34. Bansal AK, Bilaspuri GS. Impacts of oxidative stress and antioxidants on semen functions. *Vet Med Int*. (2010) 2010:686137. doi: 10.4061/2011/686137

35. Morrell JM, Lagerquist A, Humblot P, Johannisson A. Effect of single layer centrifugation on reactive oxygen species and sperm mitochondrial membrane potential in cooled stallion semen. *Reprod Fertil Dev*. (2017) 29:1039–45. doi: 10.1071/RD15440

36. Macías-García B, González Fernández L, Gallardo Bolaños JM, Peña FJ, Johannisson A, Morrell JM. Androcoll-E-large selects a live subset of stallion sperm capable of producing ROS. *Anim Reprod Sci*. (2012) 132:74–82. doi: 10.1016/j.anireprosci.2012.03.017

frontiers | Frontiers in Veterinary Science

TYPE Original Research
PUBLISHED 04 October 2024
DOI 10.3389/fvets.2024.1439550

OPEN ACCESS

EDITED BY
Stefan Gregore Ciornei,
Iasi, University of Life Science, Romania

REVIEWED BY
Hossam El-Sheikh Ali,
University of Kentucky, United States
Tiberiu Nicolae Constantin,
University of Agronomic Sciences and Veterinary Medicine Bucharest, Romania

*CORRESPONDENCE
Aleona Swegen
✉ Aleona.Swegen@newcastle.edu.au

RECEIVED 28 May 2024
ACCEPTED 10 September 2024
PUBLISHED 04 October 2024

CITATION
Lawson EF, Pickford R, Aitken RJ, Gibb Z, Grupen CG and Swegen A (2024) Mapping the lipidomic secretome of the early equine embryo.
Front. Vet. Sci. 11:1439550.
doi: 10.3389/fvets.2024.1439550

Mapping the lipidomic secretome of the early equine embryo

Edwina F. Lawson[1], Russell Pickford[2], Robert John Aitken[1], Zamira Gibb[1], Christopher G. Grupen[3] and Aleona Swegen[1]*

[1]School of Environmental and Life Sciences, College of Engineering, Science and the Environment, University of Newcastle, Callaghan, NSW, Australia, [2]Bioanalytical Mass Spectrometry Facility, University of New South Wales, Sydney, NSW, Australia, [3]Sydney School of Veterinary Science, Faculty of Science, The University of Sydney, Camden, NSW, Australia

The lipidomic secretions of embryos provide a unique opportunity to examine the cellular processes of the early conceptus. In this study we profiled lipids released by the early equine conceptus, using high-resolution mass spectrometry to detect individual lipid species. This study examined the lipidomic profile in embryo-conditioned media from *in vivo*-produced, 8–9 day-old equine embryos ($n = 3$) cultured *in vitro* for 36 h, analyzed over 3 timepoints. A total of 1,077 lipid IDs were recorded across all samples, containing predominantly glycerolipids. Seventy-nine of these were significantly altered in embryo conditioned-media versus media only control ($p < 0.05$, fold-change >2 or < 0.5). Fifty-five lipids were found to be released into the embryo-conditioned media, of which 54.5% were triacylglycerols and 23.6% were ceramides. The sterol lipid, cholesterol, was also identified and secreted in significant amounts as embryos developed. Further, 24 lipids were found to be depleted from the media during culture, of which 70.8% were diacylglycerols, 16.7% were triacylglycerols and 12.5% were ceramides. As lipid-free media contained consistently detectable lipid peaks, a further profile analysis of the various components of non-embryo-conditioned media consistently showed the presence of 137 lipids. Lipid peaks in non-embryo-conditioned media increased in response to incubation under mineral oil, and contained ceramides, diacylglycerols and triacylglycerols. These results emphasize the importance of a defined embryo culture medium and a need to identify the lipid requirements of the embryo precisely. This study sheds light on early embryo lipid metabolism and the transfer of lipids during *in vitro* culture.

KEYWORDS

lipidomics, lipids, embryo, equine, pregnancy, *in vitro*

1 Introduction

Early pregnancy is one of the most challenging and enigmatic facets of mammalian reproduction. It comprises a precarious pre-implantation phase, in which the embryo is yet to develop placental attachments and the mother is yet to establish stable systemic support of the pregnant state. The early conceptus relies on localized embryo-maternal interactions for survival, including signaling its presence to the maternal environment and in turn receiving metabolic support through endometrial secretions. In women, pre-implantation embryo loss is estimated at 10–40% and overall pregnancy loss from fertilization to birth is approximately 40–60% (1). The equine pregnancy poses similar challenges with an estimated 20–30% of conceptions failing prior to implantation (2, 3). The role of embryo-maternal communications is particularly pertinent in the horse, as this species features a long period (40–45 days) before the development of definitive

placentation (4), while the signal that facilitates maternal recognition of pregnancy (MRP) remains undiscovered (5). Along with proteins and miRNA, lipids are anticipated to play a key role in both signaling between embryo and endometrium, as well as in nourishing and supporting the early embryo during this early period (6). While the abundance and function of some of these compounds in the embryo environment have begun to be investigated, the secreted lipids engaged in embryo-maternal signaling have yet to be profiled in any mammalian species.

For studying Assisted Reproductive Technology (ART), the horse is a fitting model for human clinical procedures. Women and mares are both mono-ovulatory, and have similar follicular dynamics and embryo developmental kinetics until the blastocyst stage (7). In addition, both species share infertility concerns due to obesity and aging (8–12), which are believed to influence the lipid composition of the oocyte. In comparison with many other species, the lipid content of equine oocytes and embryos is notably higher (13, 14). Embryonic cytoplasmic lipid droplets, in the form of triglycerides, represent the most abundant energy source and are accumulated during embryo development (15). In addition, the embryos of both equine and human species are particularly sensitive to both ambient and culture environments (16–18). In humans, it has been suggested that microtubule spindles are thermosensitive (19), and spindle integrity can be irreversibly altered by temperature (20). This sensitivity to the culture environment is particularly pertinent for the mare, where effective *in vitro* fertilization (IVF) has proven to be a major challenge and is not yet commercially available (21, 22). As such, intra-cytoplasmic sperm injection (ICSI) is currently the only commercial method for producing equine embryos *in vitro*. Reciprocal knowledge May be gained through the comparative study of equine and human ART and infertility treatments, helping to define the optimum *in vitro* requirements for oocyte maturation and embryo culture.

Lipids are expected to play roles in embryo maternal signaling. They regulate reproductive cyclicity and are intrinsically linked to pregnancy [reviewed in Lawson et al. (14)]. With the high metabolic rate of the early embryo, functionally, lipids serve as a primary energy source, but, they also serve as a molecular membrane scaffold that regulates cellular signaling (23). Acting primarily through their interactions with proteins, many of the pathways by which lipids modulate these proteins are not yet fully understood (24). Hence, understanding lipid biosynthesis and hormone structure will lay the groundwork for better understanding embryonic requirements and how this May influence maternal signaling. In equine embryos, researchers have previously identified proteins secreted by the early equine embryo (25–29), and attempted to identify a putative MRP factor secreted by the conceptus (30, 31). In a previous study of the protein component of the embryo secretome it was found that proteins involved in lipid-associated and lipoprotein function were consistently over-represented (29). Embryo-produced mediators, such as the phospholipid Platelet-activating factor (PAF) have been suggested to have an early stimulatory effect (32, 33) and precursors such as arachidonic acid and docosahexaenoic acid, which are essential constituents of membrane lipids in other species, have been postulated to play a crucial role in equine embryonic development (34). Such findings suggest lipids are potential regulators of the embryo-signaling response and, as such, warrant investigation into the lipidomic profile of equine embryos for investigations into MRP. This leads to the hypothesis that lipids themselves and the interactions between proteins and lipids have important roles in embryo-maternal signaling as well as equine embryo development.

Apart from maternal signaling, at the pre-implantation stage of development, embryos require the biosynthesis of lipids, particularly for energy metabolism, cell membrane construction and signaling events involved in gene activation (34). It is well established that until approximately day 22 after ovulation, the equine embryo is encased in a glycoprotein capsule (35), which covers the equine blastocyst after it loses its zona pellucida (36). The capsule is believed to play a protective role, and participate in fetal-maternal interface communication (37). Importantly for the study of lipids resent research suggests that exosomes and other extracellular vesicles secreted by the conceptus membranes May play important roles in equine embryo-maternal communication during this early period (38). However, despite this capsule embryos are able to produce and continue to secrete prostaglandin E2 and other prostaglandins, such as PGF2α and PGI_2 (39–41). More recently, prostaglandin synthesis enzymes were shown to be involved in embryo-driven forward motion motility, due to their location on the "peri-embryonic" pole (42). Prostaglandins are lipid autacoids derived from arachidonic acid by the cleavage action of phospholipase A2s (PLA2s). PLA2s are known to be functionally involved in diverse cellular events, including phospholipid metabolism, immune functions and signal transduction, and their actions generate bioactive lipid mediators (43). Such *de novo* biosynthesis of lipids indicates that equine embryos autotrophically produce their own lipid supply, contributing directly to the steroid environment of the intrauterine lumen (44). Such findings implicate the role of lipids and protein–lipid complexes in supporting the early equine embryo, particularly at the pre-implantation stage. As the lipidomic component of embryonic secretions have not been well described, defining what lipids are released by embryos will help delineate the signaling pathways important for a successful pregnancy. Therefore, this research sought to comprehensively describe the profile of lipids released by early equine embryos using high-resolution mass spectrometry.

Lipidomics is a systems-level analysis and characterization of lipids. Like other omics technologies, such as transcriptomics or proteomics, lipidomics is a global profiling of lipid species present in cells, tissues or extracted body fluids (45). The applications of lipidomics technology are rapidly evolving and currently it allows detection of a broad range of lipid classes, categories, and quantification of lipid species. The approach has also provided valuable information on biomarkers for disease pathophysiology, and shed light on the detailed biophysiological functions involved in reproductive biology (46). Currently, the LIPID MAPS® classification system organizes lipids into eight categories: fatty acyls, glycerolipids, glycerophospholipids, sphingolipids, sterol lipids, prenol lipids, saccharolipids and polyketides. Each category can be divided into numerous classes with individual lipid identities (47). Recent advances in mass spectrometry-based lipidomics technology have meaningfully improved the detection of a vast array of lipids (48). The technology allows for the detection of minute, yet biologically significant fluctuations in lipid levels. For example, it has recently been used to profile the fatty acid content of spermatozoa from different species (49). As such, the precision of lipidomic technology now offers opportunities to answer many of the remaining unanswered questions. Therefore, in this study we aim to profile the lipids secreted by the early equine embryo in an *in vitro* setting, and in addition, to examine the embryo culture model, by carrying out lipidomic profiling of embryo culture media.

2 Materials and methods

2.1 Artificial insemination

All procedures undertaken in this study were reviewed by the University of Newcastle Animal Ethics Committee and approved under the Australian code for the care and use of animals for scientific purposes (approval number A-2018-804). Standardbred mares ($n = 3$) were housed on pasture. Mares' reproductive cycles and ovulations were monitored by transrectal palpation and ultrasonography. Upon signs of impending ovulation, ovulation was induced with a synthetic analog of gonadotrophin-releasing hormone (GnRH), then inseminated with semen containing at least 5×10^8 motile spermatozoa, obtained from one of three fertile stallions, extended in SpermSafe (University of Newcastle, Callaghan, Australia), and stored for up to 3 days at 17°C. All mares received the same routine post-mating treatment consisting of an intrauterine infusion with 1 L of saline followed 8 h later by an intramuscular administration of oxytocin.

2.2 Embryo collection and culture

A visual summary of the experimental procedure, from embryo recovery to mass spectrometry lipid analysis, is presented in Figure 1. Embryos ($n = 3$) were obtained by transcervical uterine lavage 8–9 days after confirmed ovulation, from mares aged between 10 and 11 years, as per the method described by Swegen et al. (29). Briefly, this was done using a 34 French-gage silicone Foley catheter with a 100 cc balloon and Y-tube (MAI Animal Health, Elmwood, WI, United States). For the collection of embryos, warmed Emcare Complete Ultra flushing medium (1000–2000 mL per flush; ICPbio Reproduction, Auckland, New Zealand) was used and uterine fluidic content was collected through an Em-Con embryo filter (MAI Animal Health). Filter contents were transferred to search dishes, and embryos were recovered under a dissecting microscope before being transferred to transport media. This transport medium consisted of Hepes-buffered DMEM/F12 (11330–032; Gibco, Grand Island, NY, United States) supplemented with 0.5% w/v fatty acid-free bovine serum albumin (BSA; ICPbio), 10 units/mL penicillin-G and 10 µg/mL streptomycin sulphate. After transport (<30 min) to the laboratory, each embryo was assessed morphologically and rinsed by moving the embryo through dishes of BSA-containing culture medium (bicarbonate-buffered DMEM/F12 11320–033; Gibco) with 0.5% w/v BSA, 10 units/mL penicillin-G and 10 µg/mL streptomycin sulphate, deposited in a 50 µL droplet of BSA-containing culture medium under oil, and incubated for 2 to 3 h at 38.5°C in a humidified atmosphere of 5% O_2, 6% CO_2 and 89% N_2. Embryos were then washed twice in BSA-free culture medium (bicarbonate-buffered DMEM/F12 with 0.1% polyvinyl alcohol, 10 units/mL penicillin-G and 10 µg/mL streptomycin sulphate). Finally, embryos were transferred to a 50 µL droplet of BSA-free culture medium under oil and incubated at 38.5°C in a humidified atmosphere of 5% O_2, 6% CO_2 and 89% N_2. Following the initial incubation in protein-containing (BSA) medium, embryos were cultured for a total of 36 h in protein-free medium. Within this culture period, embryo-conditioned media were collected every 12 h. At each collection point embryos were imaged under a stereomicroscope (SMZ1500; Nikon Corporation, Kawasaki, Kanagawa, Japan) and their diameter measured to verify continued blastocyst development and expansion. Thereafter embryos washed and transferred to a droplet of fresh BSA-free culture medium before being measured. Embryo-conditioned medium was centrifuged at 14000 × g for 5 min to remove debris, and supernatants were transferred to cryovials, and immediately placed in liquid nitrogen, and stored at −80°C until further analysis. Medium-only controls were also collected at each timepoint.

2.3 Chemicals and materials

All solvents used were HPLC grade or higher. Glass pipettes and tubes were used wherever possible and the use of plasticware was minimized during lipid extraction to avoid contamination of samples. Glass tubes and glass transfer pipettes were purchased from Sigma and vWR. Lipid internal standards (ISTDs) were purchased from Avanti Polar Lipids Inc. (Alabaster, AL, United States). These include phosphatidylcholine (19:0_19:0), sphingomyelin (18:0_12:0), phosphatidylethanolamine (17:0_17:0), phosphatidylglycerol (17:0_17:0), phosphatidylserine (17:0_17:0), phosphatidic acid (17:0_17:0), ceramide (d18:1, 12:0), diglyceride (1,3 18:0 d5), cholesteryl ester (19:0), monoglyceride (17:0), triglyceride mix d5 (Avanti Code LM-6000), diglyceride mix d5 (Avanti Code LM-6001), phosphatidylinositol (17:0 14:1), C12 GluCer, C12 sulfatide, C17 ceramide, C17 sphingosine, C17 S1P, C12 C1P, D3 C20 fatty acid, and C12 LacCer. Lipid internal standards were prepared as a mixture at

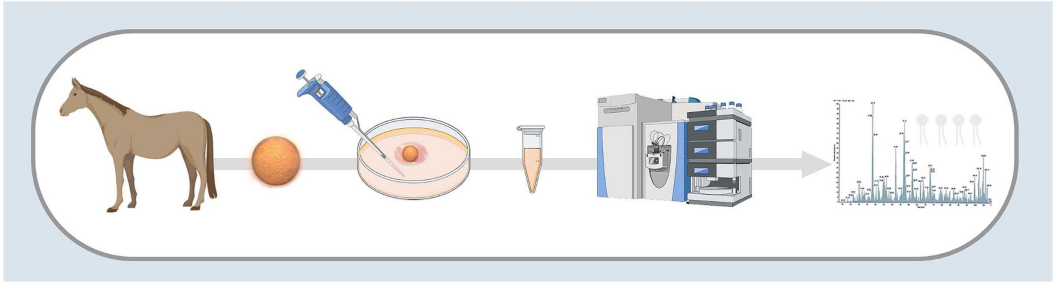

FIGURE 1
Visual summary of methods used to profile the lipids released and depleted by equine embryos. Image created with BioRender.

10 pmol/μl in methyl-tert butyl ether and methanol (MTBE:methanol, 1:1 v/v).

2.4 Lipid extraction

Lipids were extracted using chloroform, methanol, and isopropanol (Sigma Aldrich, St. Louis, MO, United States) and ultrapure water (Millipore). Medium lipid extraction was based on the Bligh and Dyer method; briefly, medium samples were thawed on ice and 80 μL aliquots were transferred into glass tubes. Methanol (600 μL), chloroform (1,000 μL) and ultrapure water (500 μL) were sequentially added with vortexing between each addition, followed by spiking with 10 μL of the aforementioned internal standards. Samples were then centrifuged at 300 x g for 10 min at room temperature. The lower solvent phase was collected and transferred to a new glass tube using a glass Pasteur pipette. Chloroform (600 μL) was added to the upper phase, vortexed and centrifuged at 900 x g for 10 min. The lower phase was collected and transferred into the same glass tube and dried under nitrogen gas. Dried lipid samples were reconstituted in 100 μL of isopropanol/methanol (1:1) and stored at −80°C in glass LC–MS vials.

2.5 Lipidomics mass spectrometry

Lipid extracts (10 μL) were analyzed using a Q-Exactive Plus Mass Spectrometer coupled to a U3000 UPLC system (ThermoFisher Scientific) according to the methods of Phan et al. and Castro-Perez et al. (50, 51). Chromatography was performed at 60°C on a Waters CSH C18 UHPLC column 2.1 × 100 mm, 1.8 μM with VanGuard guard column. Solvent A was 6:4 acetonitrile: water and Solvent B was 1:9 acetonitrile:isopropanol, both with 10 mM ammonium formate and 0.1% formic acid. Briefly, a 30 min gradient running from 30 to 100% of solvent B was performed, eluting lipids in order of hydrophobicity. Column eluate was directed into the electrospray ionization source of the mass spectrometer where a HESI probe was employed. Source parameters were broadly optimized on a range of lipid standards prior to the analysis. The mass spectrometer was run in data dependent acquisition mode. A survey scan over the mass range 200–1,200 at resolution 70 K was followed by 10 data dependent MS/MS scans on the most intense ions in the survey at 15 K resolution. Dynamic exclusion was used to improve the number of ions targeted. Cycle time was approximately 1 s. Samples were run in both positive and negative polarities. The samples were run in a random order (generated using Microsoft Excel) to avoid batch and replicate effects. Data were analyzed in LipidSearch sofware 4.1.16. Data were searched against the standard LipidSearch database with all common mammalian lipid classes included. The search results were then grouped according to sample type and aligned for differential analysis. Aligned data, containing lipid identity, retention time, peak area were exported to Excel software (Microsoft Corporation, WA, United States). Relative abundance of lipids was obtained from peak areas normalized to internal standards. LipidSearch-derived identities of fatty acid chain (fatty acid, FA1, FA2, FA3), CalcMz, IonFormula, retention time (RT) and peak intensity were additionally obtained in both embryo conditioned media (Supplementary Table S1) and in media only experiment (Supplementary Table S2).

2.6 Analysis

Identified intensity peaks were filtered with m-Score threshold (>5.0) and ID quality filter (A and B and C). Adducts included +H, $+NH_4$, +Na and + H-H_2O in positive mode, and-H, +HCOO, -2H and-CH3 in negative mode. Statistical analyses were performed using MetaboAnalyst software module[1] and Excel. For comparisons between time points and control groups, a two tailed students t-test was applied with statistical significance set at $p < 0.05$ in addition to fold changes between embryo-conditioned samples and media only control samples. Graphical representations of the data were generated using the MetaboAnalyst.

2.7 Media only samples

In further experiment, the various components of culture media were additionally examined. Different components of culture media were placed in a humidified atmosphere of 5% O_2, 6% CO_2 and 89% N_2 for 12 h at 37°C. Samples were incubated either under a mineral oil overlay or without a mineral oil overlay and included bicarbonate-buffered DMEM/F12 with and without 10 units/mL penicillin-G and 10 μg/mL streptomycin sulphate. Pure mineral oil was also incubated. Incubating media under oil was done to determine whether incubating under oil affected lipid quantification. Thus, a total of five media components/variations were assessed in addition to an ultrapure water (Millipore) in duplicate. Lipids extracted and intensity peaks were analyzed and as per the embryo conditioned media. For the media only samples, ion peaks were compared using one-way analyses to examine whether incubation under oil, DMEM/F12, or penicillin/streptomycin influenced the presence of each lipid in the media. The blocking function was used to account for possible interactions between influencing factors; i.e., analysis for the effect of incubation under oil was 'blocked' for presence of DMEM/F12, while analyses for effect of DMEM/F12 and penicillin/streptomycin were 'blocked' for incubation under oil to remove the effect of these parameters as confounding factors. Finally, lipid ion peaks in mineral oil were compared against those in all the aqueous media samples (blocking for incubation under oil as a possible confounding factor). These analyses were conducted in JMP (SAS Corp., NC) and p-value for all effects set at $p < 0.05$.

3 Results

3.1 Embryo experiment

Embryos ($n = 3$) were cultured *in vitro* in a protein-free medium over a period of 36 h, with each embryo expanding between 20 and

1 www.metaboanalyst.ca

30% in diameter during that time (30.17, 25.40, 20.42%). In the secreted media collected, a total of 1,077 lipids IDs were recorded across all samples, with 222 lipid IDs remaining after filtering for high confidence. Lipids which were both significantly different, in embryo conditioned media versus media only control samples ($p < 0.05$) for at-least one time point, and also had a fold change of greater than 2, were further examined for this study, which was a total of 79 individual lipid ions (Table 1). Of these, 55 individual lipids were detected to be more abundant in embryo-conditioned media (henceforth termed 'secreted' lipids), and 24 individual lipids were found to be depleted in embryo-conditioned media (henceforth termed 'depleted' lipids). The heatmaps depicted (Figure 2) show two distinct populations of lipids: those that were secreted into the media by the embryos during culture (Figure 2A), and those that were depleted from the media during culture (Figure 2B). Of the 55 lipid identities found elevated in the embryo conditioned media (Table 1), 30 were triacylglycerols (TGs) (54.5%), 13 were ceramides (23.6%), 4 were diacylglycerols (DGs) (7.3%) the sterol lipid cholesterol was also identified along with ubiquinone Co (Q9) and a single sphingomyelin. The 24 lipids found to be depleted from the embryo conditioned media comprised of 17 DGs (70.8%), 4 TGs (16.7%) and 3 ceramides (12.5%). Note that these are the numbers of individual lipid species identified and percentages do not represent quantities of lipid secreted or consumed by embryos.

In addition, a volcano plot analysis was carried out to pinpoint the differential change of individual lipids between the groups, with a cut-off for those lipids that had fold-change >2 and p-value <0.1. This was done for each individual time point, 12 h, 24 h and 36 h. In the embryo secreted group, ceramides and TGs were the predominant classes found to increase compared to the control. From the depleted lipid group, DGs were observed to be the dominant class (Figure 3). In total, the classes of lipids came from 5 lipid categories, including glycerolipids, sphingolipids, glycerophospholipids, sterol lipids and prenol lipids (Figure 4), with a greater diversity of classes observed in secreted lipids compared to depleted lipids. Comparisons of several individual relevant lipids, which were both significant and had a fold change >2 in the embryo conditioned media, are detailed in Figure 5.

3.2 Culture media only experiment

Lipid-free reagents had been used to prepare media for embryo lipidome experiments, so the detection of lipids depleted following embryo culture was unexpected. We therefore conducted a follow-up analysis several months later to validate the presence of lipids in non-conditioned (control) media and its individual components. For the media only experiment, a total of 137 lipid species were identified present across all 5 media samples (DMEM/F12 with and without 10 units/mL penicillin-G and 10 µg/mL streptomycin sulphate, both of these under a mineral oil overlay or without a mineral oil overlay and lastly pure mineral oil). These predominantly belong to the glycerolipid category. Of these, 109 lipid ions were significantly different between groups. Higher abundance of 18 lipids (15 TGs, 2 DGs, 1 PS) was associated with inclusion of DMEM/F12 in the formulation (predominantly glycerolipids; 94%). The inclusion of penicillin-G/streptomycin sulphate to DMEM/F12 medium had no influence on abundance of any of the lipids detected. Incubation under oil increased the abundance of 44 lipid species in media (90% were glycerolipids; 34 TGs and 5 DGs). In pure mineral oil, 47 lipid species were detected (i.e., showed $p < 0.05$ versus water only control). Of these, 91% were glycerolipids (28 TGs and 15 DGs), and 6% (3) were ceramides. Of the 24 DGs originally found to be depleted in embryo-conditioned media, promisingly only 5 indivuiduals were detected in the follow-up media analysis. Of these, two lipids were detected in mineral oil alone and were influenced by incubation under mineral oil [DG (18:0_17:0) + NH4 and DG(18:0_18:1) + NH4]; one lipid was detected in mineral oil but not affected by incubation under oil [DG(40:0) + NH4].

4 Discussion

This study used high-resolution mass spectrometry-based lipidomics to examine the changes in lipid profiles of media following culture of equine embryos. A total of 55 lipid species were found to be significantly increased in the embryo-conditioned media, compared to the control, and hence were presumed to be released or secreted by the embryo over time. In addition, 24 lipids were identified to be significantly decreased in the embryo-conditioned media following embryo incubation when compared to the embryo-free controls. These lipids were presumed to be taken up or depleted from the media by the embryos. After identifying this population of depleted lipids, a more comprehensive analysis was carried out of media without embryos. This was conducted to clarify which lipids or lipid categories were detectable in culture media, and in turn which components of the culture environment they were coming from. In this subsequent study we found that 109 lipids were contributed by the various media components, the majority of these being glycerolipids.

For those lipids found to be increased in the embryo-conditioned media, the dominant lipid categories identified were glycerolipids (66%) followed by sphingolipid (23%); the dominant lipid classes were TGs (56.6%) and ceramides (20.8%). Those depleted from the media in the presence of embryos again tended to be glycerolipids (88%), with the main class of these found to be DGs (70.8%). The depleted lipid groups May contribute to meeting the embryo's energy demands, whereas the secreted lipid groups are likely to either be involved in maternal signaling, or to be released in response to stress/increased bilayer fluidity. TGs are esters consisting of a glycerol backbone and three fatty acids; they represent the main form of lipid storage in adipose tissue and lipid droplets. TGs are synthesized in times of energy excess or hydrolyzed to DGs and fatty acids to be used for ATP generation in times of energy need. Thus, from a metabolic perspective, release of TGs by equine embryos indicates that energy stores May be adequate or excessive. Closer examination of the exact identities of TGs being secreted will be important in elucidating their potential roles in embryo-maternal signaling. Most of the secreted TGs that were identified contain medium-chain fatty acids. Medium chain fatty acids have been shown to enhance progesterone synthesis and improve embryo implantation in rats, albeit via a mechanism of dietary supplementation of fatty acids to the mother (52). It is worth investigating the direct effects of medium chain fatty acid TGs on the endometrium and whether their secretion by the embryo is able to influence pathways upstream of luteinisation and luteal maintenance, such as reduced PGF2a synthesis. The product of TG hydrolysis, DGs, consist of a glycerol covalently bonded to two fatty acid chains. They are typically found in both plant and animal fats, and are often used as emulsifiers (53). DGs are

TABLE 1 Individual lipid species secreted and depleted in embryo-conditioned media according to lipid category.

Result	Lipid species	Category	Percentage according to lipid category
Lipids increased in embryo conditioned media	Cer(d18:1_25:0)-H	Sphingolipids [SP]	25%
	Cer(d18:1_26:0) + H	Sphingolipids [SP]	
	Cer(d18:2_26:0) + H	Sphingolipids [SP]	
	Cer(d22:0_24:0) + H	Sphingolipids [SP]	
	Cer(d22:0_26:0) + H	Sphingolipids [SP]	
	Cer(d42:0 + O) + HCOO	Sphingolipids [SP]	
	Cer(t18:0_22:0 + O) + H	Sphingolipids [SP]	
	Cer(t18:0_26:0) + HCOO	Sphingolipids [SP]	
	Cer(t20:0_26:0) + H	Sphingolipids [SP]	
	Cer(t34:0) + H-H2O	Sphingolipids [SP]	
	Cer(t42:0 + O) + HCOO	Sphingolipids [SP]	
	SM(d34:1) + H	Sphingolipids [SP]	
	ChE() + H-H2O (cholesterol)	Sterol Lipids [ST]	
	Co(Q9) + NH4 (ubiquinone)	Prenol Lipids [PR]	
	DG(18:0_24:0) + NH4	Glycerolipids [GL]	2%
	DG(20:1e) + NH4	Glycerolipids [GL]	2%
	DG(25:0_18:0) + NH4	Glycerolipids [GL]	64%
	DG(26:0_18:0) + NH4	Glycerolipids [GL]	
	DG(39:1) + NH4	Glycerolipids [GL]	
	TG(12:0_12:0_12:0) + Na	Glycerolipids [GL]	
	TG(15:0_14:0_15:0) + NH4	Glycerolipids [GL]	
	TG(15:0_14:0_16:1) + NH4	Glycerolipids [GL]	
	TG(15:0_16:0_16:1) + NH4	Glycerolipids [GL]	
	TG(15:0_16:1_18:1) + NH4	Glycerolipids [GL]	
	TG(16:0_12:0_14:0) + NH4	Glycerolipids [GL]	
	TG(16:0_13:0_14:0) + NH4	Glycerolipids [GL]	
	TG(16:0_14:0_14:0) + Na	Glycerolipids [GL]	
	TG(16:0_14:0_14:0) + NH4	Glycerolipids [GL]	
	TG(16:0_14:0_16:1) + NH4	Glycerolipids [GL]	

(Continued)

10.3389/fvets.2024.1439550

TABLE 1 (Continued)

Result	Lipid species	Category	Percentage according to lipid category
	TG(16:0_18:2_18:3) + NH4	Glycerolipids [GL]	
	TG(16:0_18:2_20:4) + NH4	Glycerolipids [GL]	
	TG(16:0_8:0_18:1) + NH4	Glycerolipids [GL]	
	TG(16:1_14:0_14:0) + NH4	Glycerolipids [GL]	
	TG(16:1_14:0_16:1) + NH4	Glycerolipids [GL]	
	TG(16:1_14:0_18:1) + NH4	Glycerolipids [GL]	
	TG(16:1_16:1_17:1) + NH4	Glycerolipids [GL]	
	TG(16:1_16:1_18:1) + Na	Glycerolipids [GL]	
	TG(16:1_16:1_18:2) + Na	Glycerolipids [GL]	
	TG(16:1_17:1_18:2) + NH4	Glycerolipids [GL]	
	TG(16:1_18:2_18:2) + Na	Glycerolipids [GL]	
	TG(16:1_18:2_20:4) + NH4	Glycerolipids [GL]	
	TG(18:1_17:1_18:2) + Na	Glycerolipids [GL]	
	TG(18:1_18:2_18:3) + Na	Glycerolipids [GL]	
	TG(18:2_17:1_18:2) + NH4	Glycerolipids [GL]	
	TG(18:3_18:2_18:2) + Na	Glycerolipids [GL]	
	TG(20:3_18:2_18:2) + NH4	Glycerolipids [GL]	
	TG(20:5_20:5_20:5) + NH4	Glycerolipids [GL]	
	TG(4:0_16:0_16:0) + Na	Glycerolipids [GL]	
	TG(8:0_10:0_10:0) + Na	Glycerolipids [GL]	
	PC(16:0_18:1) + HCOO	Glycerophospholipids [GP]	
	PC(18:0_18:2) + HCOO	Glycerophospholipids [GP]	
	PC(34:2) + H	Glycerophospholipids [GP]	7%
	PC(36:1) + H	Glycerophospholipids [GP]	
	Cer(d18:1_19:0) + H	Sphingolipids [SP]	
	Cer(d19:2_23:0 + O) + H	Sphingolipids [SP]	

(Continued)

10.3389/fvets.2024.1439550

TABLE 1 (Continued)

Result	Lipid species	Category	Percentage according to lipid category
Lipids depleted in embryo conditioned media	Cer(d20:0_20:0) + H	Sphingolipids [SP]	13%
	DG(15:0_16:0) + NH4	Glycerolipids [GL]	
	DG(16:0_16:0) + H	Glycerolipids [GL]	
	DG(16:0_16:0) + NH4	Glycerolipids [GL]	88%
	DG(16:0_17:0) + NH4	Glycerolipids [GL]	
	DG(16:0_18:1) + NH4	Glycerolipids [GL]	
	DG(16:0_18:2) + NH4	Glycerolipids [GL]	
	DG(18:0_16:1) + NH4	Glycerolipids [GL]	
	DG(18:0_17:0) + NH4	Glycerolipids [GL]	
	DG(18:0_18:1) + H	Glycerolipids [GL]	
	DG(18:0_18:1) + NH4	Glycerolipids [GL]	
	DG(18:1_18:1) + NH4	Glycerolipids [GL]	
	DG(18:1_18:2) + NH4	Glycerolipids [GL]	
	DG(18:1e) + H	Glycerolipids [GL]	
	DG(18:1e) + NH4	Glycerolipids [GL]	
	DG(19:1_18:0) + NH4	Glycerolipids [GL]	
	DG(32:1) + NH4	Glycerolipids [GL]	
	DG(40:0) + NH4	Glycerolipids [GL]	
	TG(4:0_14:0_16:0) + NH4	Glycerolipids [GL]	
	TG(4:0_16:0_18:2) + NH4	Glycerolipids [GL]	
	TG(4:0_18:0_18:0) + NH4	Glycerolipids [GL]	
	TG(10:0_12:0_12:0) + NH4	Glycerolipids [GL]	
	TG(10:0_12:0_12:0) + NH4	Glycerolipids [GL]	
	TG(10:0_12:0_12:0) + NH4	Glycerolipids [GL]	

10.3389/fvets.2024.1439550

not only metabolic substrates but can activate certain lipid-sensitive receptors. Cellular DGs can bind to members of the protein kinase C (PKC) family, which leads to their activation and translocation to the plasma membrane and subsequent phosphorylation of interacting proteins (54). PKCs have been identified in developing embryos, and PKC inhibition halts embryo development beyond the eight to 16-cell stage in bovine embryos (55). Considering these observations, it is plausible that DGs in embryo culture media or mare uterine fluid have the capacity to support embryo development both as an energy source and as a messenger system that activates developmental processes via receptor activation. As DGs are metabolized by the lipase pathway for prostaglandin synthesis, while prostaglandins are suspected to stimulate the myometrial contractions that propel the conceptus throughout the uterine lumen during days 10–16 after ovulation (39, 56). If equine embryos do indeed actively deplete DGs from their direct environment, this May be related to their known ability to produce and continue to secrete prostaglandin E2 and other prostaglandins (39).

In this study most importantly, several individual lipids were both significantly increased and had a fold change of at least 2 in the embryo conditioned media (Figure 6). The sterol lipid cholesterol increased across all time points, including an approximate 8-fold increase at 12 h. In reproduction, the role of cholesterol is essential in early conceptus development as it maintains the integrity/fluidity of cell membranes and plays an important role in cell signaling (57). The lipid moderates important nuclear receptors, such as fetoprotein transcription factor, and is therefore involved in the most fundamental signaling pathways during embryonic development (58). Cholesterol is also the precursor of all steroid hormones (59) from which both progesterone and oestradiol are synthesized through the precursor steroid, pregnenolone. As such, the detection of cholesterol is particularly pertinent as oestradiol production by the early equine conceptus is considered very significant to the establishment of pregnancy (60) with substantial quantities of estrogens known to be produced by day 12 equine conceptus (61, 62). Another individual lipid, Ubiquinone Co(Q9), which is categorized as a prenol lipid (63)

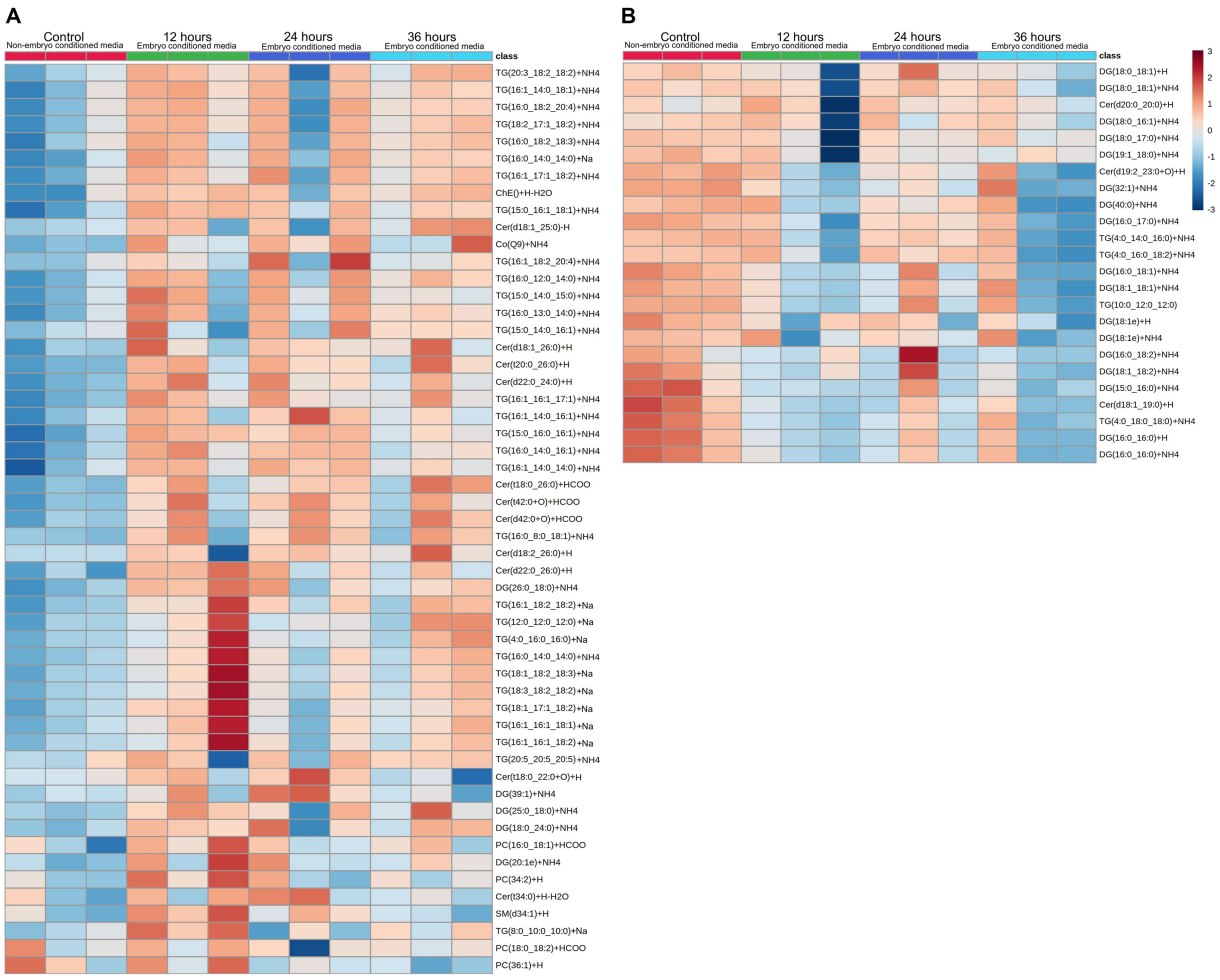

FIGURE 2
Heatmap visualization of identified lipid abundance (average peak intensity), representing lipid peaks identified. Those secreted **(A)** into embryo culture medium, and those which are depleted **(B)** from the medium. Each column represents the reading from one individual embryo, and each row depicts a different lipid identity. Medium were exchanged every 12 h and embryo-conditioned samples are compared against non-conditioned (embryo-free) control media. The heatmap color scale denotes the relative concentration of each lipid mass relative to the minimum and maximum of that lipid for all groups and is shown on the right-hand side of the figure. Values are measured by Euclidean distance with a Ward clustering algorithm ($n = 3$ per group). *$p < 0.05$ for each comparison with a fold change of greater than 2.

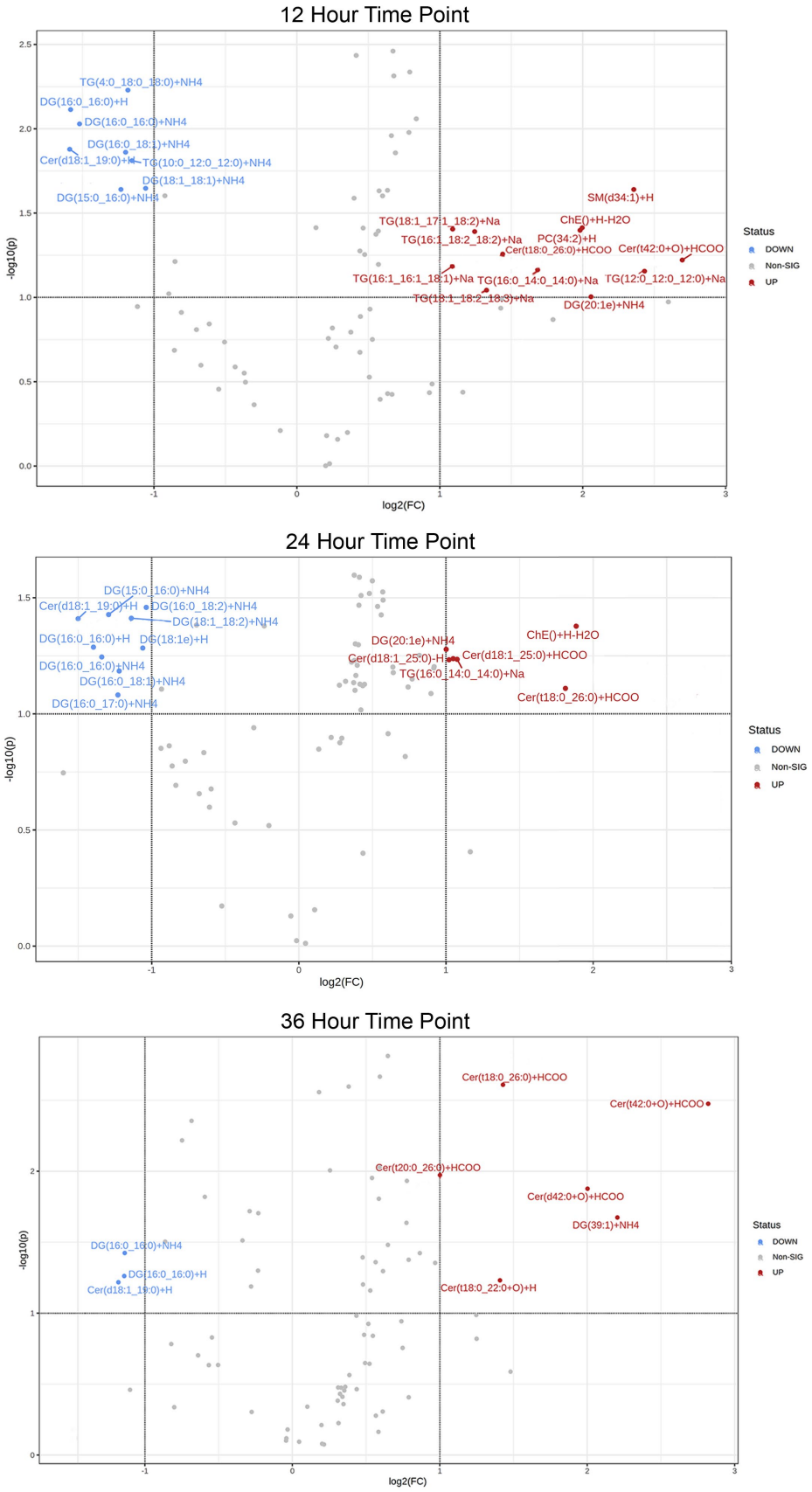

FIGURE 3
Volcano plot of lipid IDs from embryo secreted (red) and depleted (blue) medium. On the y-axis lipids with $p < 0.1$ are shown, with fold change (FC) >2 depicted on the x-axis and significance on y-axis.

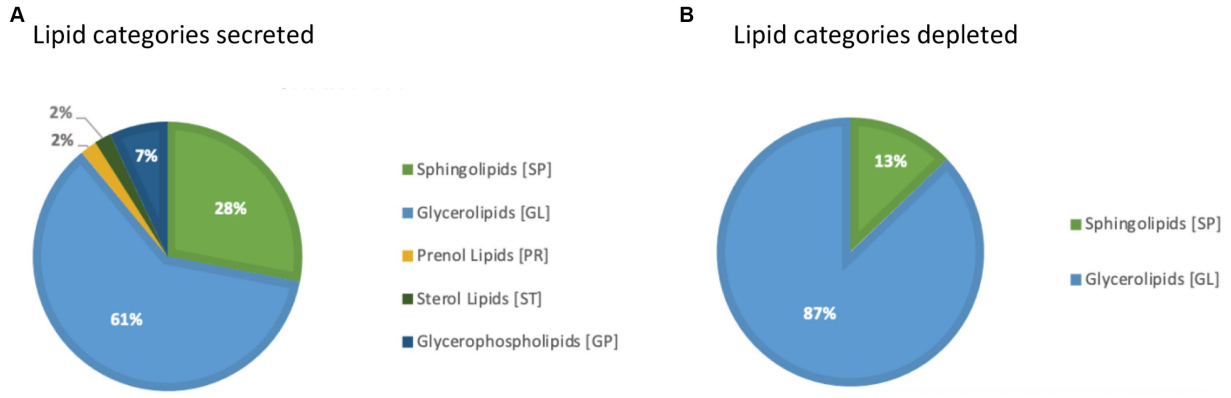

FIGURE 4
Pie graph of lipid categories secreted **(A)** and depleted **(B)** in embryo-conditioned media.

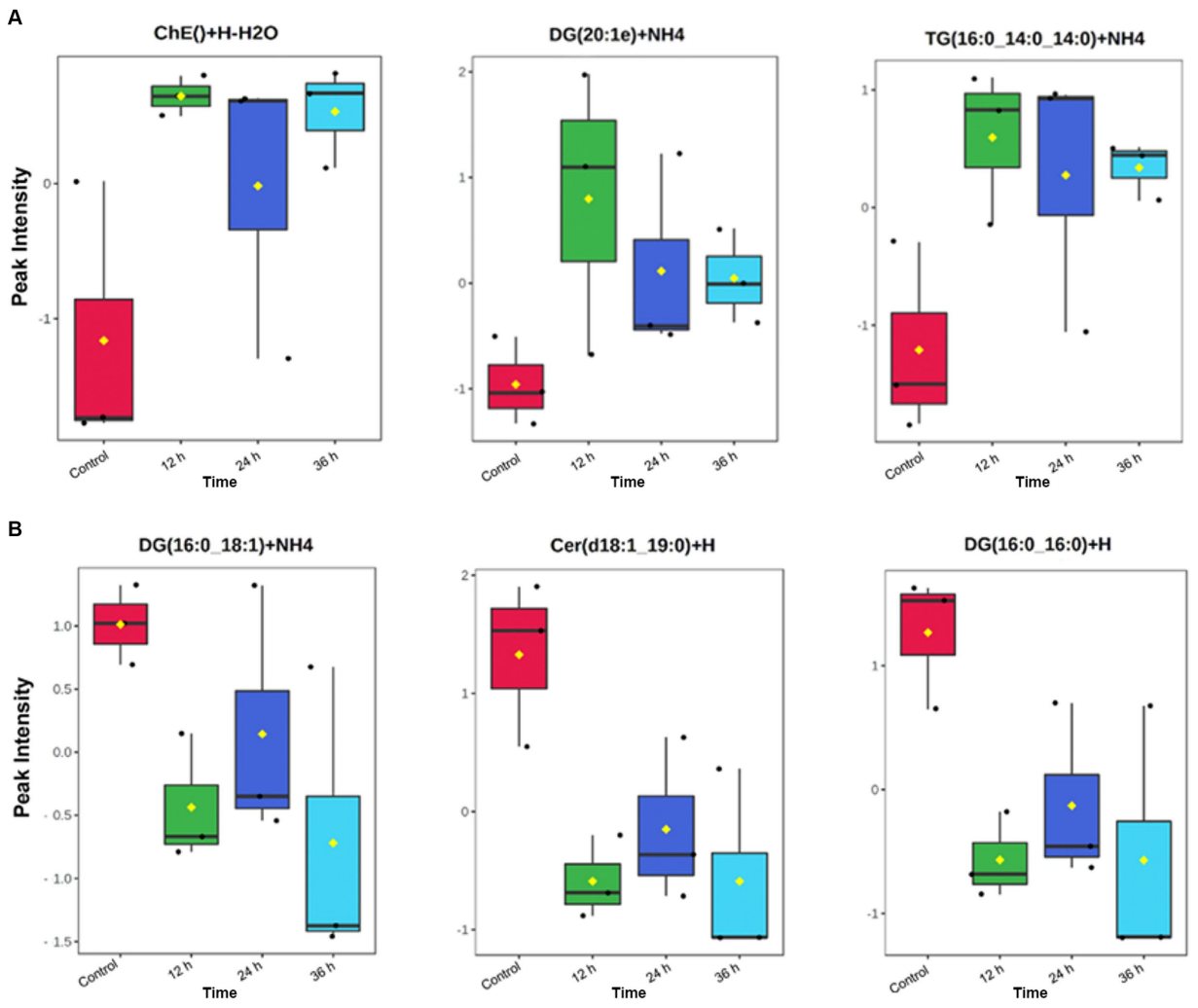

FIGURE 5
Individual identified lipids secreted **(A)** and depleted **(B)** in embryo-conditioned media. Representations of the intensity peaks for individual species with box and whisker plots. Each individual lipid is both significantly different between time points and has a fold has a fold change >2. Axis Y: Normalized peak intensities (areas) shown.

was significantly elevated in the media across all time points (Figure 6). Co(Q9) is an essential component of the mitochondrial electron transfer chain and thus is required for ATP synthesis. The presence of such lipids and their subsequent increase over time is encouraging, as they indicate embryos are producing a lipid profile that is bioactivity relevant. The cascade of events that occurs around the time of MRP indicates that lipids, such as Cholesterol, May play a more important role in the establishment of pregnancy both in terms of what the embryo is synthesizing and how the maternal endometrium is changing in response to such precursors.

For investigations into mare MRP, studies have examined the endometrial gene expression changes in response to the presence of a conceptus during MRP (64–68). Genes involved in lipid metabolism and those that serve a lipid biosynthetic process were found to be upregulated and overrepresented in the luminal epithelium of early pregnant mares (69). The prostaglandin transporter gene SLCO2A1, changes cyclically during the menstrual cycle in the human endometrium. In the bovine early embryo (70) and porcine early embryo (71, 72), its expression has been reported to increase. This gene was also found to be upregulated within the luminal epithelium of the pregnant mare (73), highlighting the importance of lipid-associated gene expression around the time of MRP. Interestingly, many of the genes upregulated in endometrial epithelium are involved in sphingolipid metabolism and signaling. The sphingolipid ceramide is known to be involved in regulation of proliferation via its signaling role (74), and thus embryo-secreted ceramides, such as those found in this study, could form part of the embryo-maternal signaling mechanism that stimulates or regulates proliferation of endometrial glands, which support the embryo's nutritional demands. Interestingly, ceramides can mimic the actions of progesterone in inducing maturation of amphibian oocytes *in vitro*, via the non-classical (membrane) progesterone receptor (75). Given the central role progesterone plays in supporting the early pregnancy, the influence of ceramides during *in vitro* culture requires further attention.

While we initially set out to profile the lipids increased in the media by the presence of equine embryos, the results of this study demonstrate that the "lipid-free" media contained consistently detectable amounts of lipids. The detection of MS peaks of residual lipids in the control media samples was an unexpected finding; some of these were significantly lower in the embryo-conditioned media than control media. The additional analysis of non-conditioned medium confirmed the presence of numerous glycerolipids in embryo-free culture media, the majority of which were DGs and TGs. Furthermore, lipid peaks in non-conditioned medium increased in response to culture under mineral oil, while mineral oil itself evidently contained ceramides, DGs and TGs, these were surprising findings. To our knowledge, the alteration of culture medium lipid composition by mineral oil overlay has not been described previously. Given the influence of lipids on preimplantation embryo development, the effect of culturing embryos in medium with and without an oil overlay warrants additional investigation. As this is the first lipidomic study of the

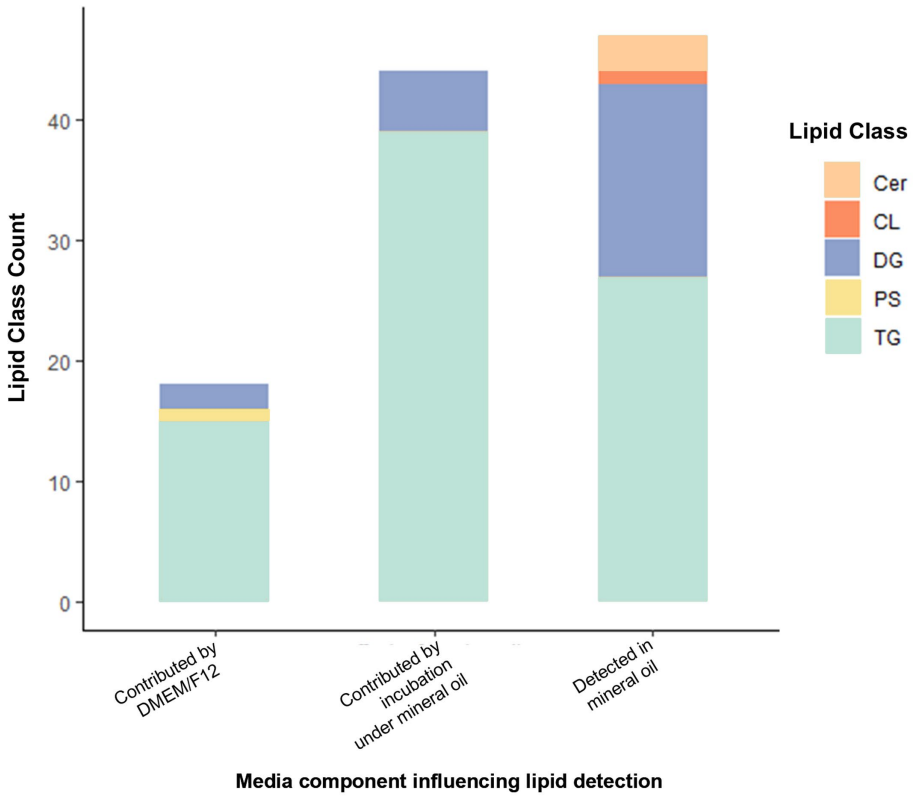

FIGURE 6
Lipid IDs whose detection was influenced by inclusion of DMEM/F12 or by incubation under mineral oil, and those detected in mineral oil. Cer, Ceramide; CL, Cardiolipin; DG, Diacylglycerol; PS, Phosphatidylserine; TG, Triacylglycerols. All lipids shown are those with $p < 0.05$ contribution from media components indicated (as determined by one-way analysis).

embryo secretome in mammals, the identification of potential glycerolipid uptake by embryos is of relevance to all mammalian embryos cultured *in vitro*. The definitive origin of these lipids remains uncertain but DMEM/F12 and mineral oil could not be ruled out as a potential source. Other possible origins include, but are not limited to, pipette tips, petri dishes, cryovials, streptomycin, or the ever-present possibility of sample contamination during handling. We propose that the predominant source of unknown lipids in our media was transfer from the fresh mineral oil. Furthermore, the identification of this lipid population highlights the capacity of the technology to detect and identify minute amounts of lipids in samples.

As reported in animal models, the lipid composition of culture medium can disturb embryo metabolism and gene expression and have consequences on preimplantation development and the health of resulting offspring following embryo transfer (76, 77). The presence and uptake of an unspecified population of lipids May indeed influence future development. As the embryo requirements for lipids during *in vitro* culture are not well understood, this area of enquiry has gained increasing attention over the past decade. Studies in which culture media were supplemented with different quantities and or different types of lipids have shown a range of effects on embryo development in various species (78). Notably the mare has recently gained traction as a particularly suitable model for investigations of human fertility and pregnancy, given it is a mono-ovulatory mammal with a gestation of a similar duration, as well as pertinent similarities in embryo development trajectory and mechanisms of pregnancy loss (7, 79, 80). In humans, different commercial embryo culture media have been reported to alter embryo quality and influence birthweight, with one study finding that supplementing embryo culture media with Human Serum Albumin (HSA) that contained high levels of residual lipids correlated with poorer pregnancy and fetal outcomes (81). The type of lipid is of great importance, as illustrated by supplementation of embryo culture media with saturated fatty acids, which was associated with metabolic stress, developmental delays, increased ROS production, and reduced implantation rates (81, 82). In addition, in the context of maternal communication, the ability for extracellular vesicles (EVs) to transfer molecular cargo, such as lipids, from one cell to another has generated a growing interest (83), and is relevant for our findings. Embryo-derived EVs have been pointed to as modulators of embryo communication *in vitro* (84), and embryos cultured *in vitro* have been confirmed to secrete EVs into their immediate environment (84, 85). Such research suggests that lipids and lipid-containing molecule, such as liposomes May also be secreted in the form of EVs by equine embryos, and hence the role of EVs and lipid transfer through media warrants further investigation.

In acknowledging the limitations of this study, the small sample size must be noted, along with the potential for the *in vitro* environment to induce a stress response. The *in vitro* culture conditions did support continued embryo growth and survival in this study, but it would still be prudent to assume that the change in environment elicited some stress in the embryos. Therefore, we do not know whether the ceramide secretion seen here is physiological or a response to the stress of *in vitro* culture. In liver, skeletal muscle, heart, kidney, and pancreatic β cells, elevated ceramide secretion has been observed in response to cellular stress and lipotoxicity, leading to apoptosis (86–88). Experiments examining the direct effects of ceramides on the endometrium will help to determine if these molecules play a role in embryo-maternal signaling. Lipotoxicity seems an unlikely cause for ceramide release in the present study, since the medium used for embryo culture was essentially lipid-free, even though residual levels of lipids were detected in the medium-only controls. Nevertheless, it must be considered that early embryos May be very sensitive to the lipid milieu and the precise requirements and sensitivities of the mammalian embryo need to be better understood, especially with regard to lipids in the immediate embryonic environment. Of note is that phytoceramides (tCer) are much less abundant in mammalian cells than in yeast (89) and are predominantly recovered in plants (90) a few of which were identified in the current data by LipidSearch, using diagnostic fragment ions (with all common mammalian lipid classes included). So, although mammalian cells do contain phytoceramides (91, 92), the subcellular localisation of their synthesis is still a matter of debate. As with any emerging technology, the field of lipidomics is still being refined. Further confirmatory work with targeted LC–MS analysis utilizing authentic standards, would be helpful to confirm whether these are secreted phytoceramides or mislabelled by the software. Thus, despite not being abundant in mammals, the identification of tCers warrants both inclusion in these findings, and future deeper investigation.

To summarize, this study presents the first high-resolution lipidomic profile of the pre-implantation embryo secretome in any mammalian species. Predominantly glycerolipids, and in particular triglycerides, were consistently released by early equine embryos into their culture environment. While the precise functions of defined lipids remain to be investigated, many of the lipids identified in this study have documented roles in cell signaling, metabolism and embryo development. Meanwhile, a cohort of lipids were depleted from media during culture, predominantly diglycerides. Since diglycerides have a documented capacity to regulate embryo developmental processes, these findings emphasize the importance of a defined embryo culture medium and a need to identify the lipid requirements of the embryo precisely. We also highlight that culture media formulated as "lipid-free" contains detectable amounts of a wide range of lipid species, many of which are absorbed by the early embryo. The profiles described contribute new knowledge about early embryo lipid metabolism and production during a critical period of pre-implantation development, which will contribute to our understanding of early equine pregnancy. Further investigation of the specific lipid ions identified in this study can clarify their functional roles in early equine pregnancy as well as the uptake of lipids present in the embryo culture environment.

Data availability statement

The original contributions presented in the study are included in the article/Supplementary material, further inquiries can be directed to the corresponding author/s.

Ethics statement

The animal study was approved by University of Newcastle Animal Ethics Committee. The study was conducted in accordance with the local legislation and institutional requirements.

Author contributions

EL: Conceptualization, Data curation, Formal analysis, Investigation, Methodology, Writing – original draft, Writing – review & editing. RP: Data curation, Formal analysis, Investigation, Methodology, Writing – original draft, Writing – review & editing. RA: Conceptualization, Supervision, Writing – original draft, Writing – review & editing. ZG: Conceptualization, Funding acquisition, Investigation, Methodology, Project administration, Supervision, Writing – original draft, Writing – review & editing. CG: Conceptualization, Investigation, Methodology, Writing – original draft, Writing – review & editing. AS: Conceptualization, Data curation, Funding acquisition, Investigation, Methodology, Project administration, Supervision, Writing – original draft, Writing – review & editing.

Funding

The author(s) declare that financial support was received for the research, authorship, and/or publication of this article. This work was supported by the Australian Research Council (LP160100824) and AgriFutures Australia Thoroughbred Horses Program (PRJ-011748). Swegen's salary was supported by Australian Research Council Discovery Early Career Researcher Award funding (DE220100121) and Gibb's salary was supported by Australian Research Council Future Fellowship funding (FT220100557).

Acknowledgments

The authors are grateful to José Cuenca for providing expert advice on statistical analysis of our datasets.

Conflict of interest

The authors declare that the research was conducted in the absence of any commercial or financial relationships that could be construed as a potential conflict of interest.

Publisher's note

Supplementary material

The Supplementary material for this article can be found online at: https://www.frontiersin.org/articles/10.3389/fvets.2024.1439550/full#supplementary-material

SUPPLEMENTARY TABLE S1
Full dataset of lipid ions detected in embryo-conditioned culture media.

SUPPLEMENTARY TABLE S2
Full dataset of lipid ions detected in 'media only' experiment.

References

1. Jarvis GE. Early embryo mortality in natural human reproduction: what the data say. *F1000Res*. (2016) 5:2765. doi: 10.12688/f1000research.8937.1

2. Satué K, Gardon JC. Pregnancy loss in mares In: MD Atef, editor. Genital infections and infertility. Rijeka: IntechOpen (2016)

3. Vanderwall DK. Early embryonic loss in the Mare. *J Equine Vet*. (2008) 28:691–702. doi: 10.1016/j.jevs.2008.10.001

4. Stout TA. Embryo-maternal communication during the first 4 weeks of equine pregnancy. *Theriogenology*. (2016) 86:349–54. doi: 10.1016/j.theriogenology.2016.04.048

5. Swegen A. Maternal recognition of pregnancy in the mare: does it exist and why do we care? *Reproduction*. (2021) 161:R139–r155. doi: 10.1530/REP-20-0437

6. Salamonsen LA, Evans J, Nguyen HP, Edgell TA. The microenvironment of human implantation: determinant of reproductive success. *Am J Reprod Immunol*. (2016) 75:218–25. doi: 10.1111/aji.12450

7. Benammar A, Derisoud E, Vialard F, Palmer E, Ayoubi JM, Poulain M, et al. The Mare: A pertinent model for human assisted reproductive technologies? *Animals (Basel)*. (2021) 11:2304. doi: 10.3390/ani11082304

8. Carnevale E, Ginther O. Relationships of age to uterine function and reproductive efficiency in mares. *Theriogenology*. (1992) 37:1101–15. doi: 10.1016/0093-691X(92)90108-4

9. Cuervo-Arango J, Claes AN, Stout TA. A retrospective comparison of the efficiency of different assisted reproductive techniques in the horse, emphasizing the impact of maternal age. *Theriogenology*. (2019) 132:36–44. doi: 10.1016/j.theriogenology.2019.04.010

10. Fretts RC, Schmittdiel J, Mclean FH, Usher RH, Goldman MB. Increased maternal age and the risk of fetal death. *N Engl J Med*. (1995) 333:953–7. doi: 10.1056/NEJM199510123331501

11. Gonzalez MB, Robker RL, Rose RD. Obesity and oocyte quality: significant implications for ART and emerging mechanistic insights. *Biol Reprod*. (2022) 106:338–50. doi: 10.1093/biolre/ioab228

12. Sessions-Bresnahan DR, Schauer KL, Heuberger AL, Carnevale EM. Effect of obesity on the Preovulatory follicle and lipid fingerprint of equine oocytes. *Biol Reprod*. (2016) 94:15. doi: 10.1095/biolreprod.115.130187

13. Catandi GD, Obeidat YM, Broeckling CD, Chen TW, Chicco AJ, Carnevale EM. Equine maternal aging affects oocyte lipid content, metabolic function and developmental potential. *Reproduction*. (2021) 161:399–409. doi: 10.1530/REP-20-0494

14. Lawson EF, Grupen CG, Baker MA, Aitken RJ, Swegen A, Pollard C-L, et al. Conception and early pregnancy in the mare: lipidomics the unexplored frontier. *Reprod Fertil*. (2022) 3:R1–R18. doi: 10.1530/RAF-21-0104

15. Abe H, Yamashita S, Satoh T, Hoshi H. Accumulation of cytoplasmic lipid droplets in bovine embryos and cryotolerance of embryos developed in different culture systems using serum-free or serum-containing media. *Mol Reprod Dev*. (2002) 61:57–66. doi: 10.1002/mrd.1131

16. Foss R, Ortis H, Hinrichs K. Effect of potential oocyte transport protocols on blastocyst rates after intracytoplasmic sperm injection in the horse. *Equine Vet J*. (2013) 45:39–43. doi: 10.1111/evj.12159

17. Wale PL, Gardner DK. The effects of chemical and physical factors on mammalian embryo culture and their importance for the practice of assisted human reproduction. *Hum Reprod Update*. (2016) 22:2–22. doi: 10.1093/humupd/dmv034

18. Yu K, Pfeiffer C, Burden C, Krekeler N, Marth C. High ambient temperature and humidity associated with early embryonic loss after embryo transfer in mares. *Theriogenology*. (2022) 188:37–42. doi: 10.1016/j.theriogenology.2022.05.014

19. Pickering SJ, Johnson MH, Braude PR, Houliston E. Cytoskeletal organization in fresh, aged and spontaneously activated human oocytes. *Hum Reprod*. (1988) 3:978–89. doi: 10.1093/oxfordjournals.humrep.a136828

20. Wang W-H, Sun Q-Y. Meiotic spindle, spindle checkpoint and embryonic aneuploidy. *Front Biosci*. (2006) 11:620–36. doi: 10.2741/1822

21. Felix MR, Turner RM, Dobbie T, Hinrichs K. Successful in vitro fertilization in the horse: production of blastocysts and birth of foals after prolonged sperm incubation for capacitation†. *Biol Reprod*. (2022) 107:1551–64. doi: 10.1093/biolre/ioac172

22. Leemans B, Gadella BM, Stout TA, De Schauwer C, Nelis H, Hoogewijs M, et al. Why doesn't conventional IVF work in the horse? The equine oviduct as a microenvironment for capacitation/fertilization. *Reproduction*. (2016) 152:R233–r245. doi: 10.1530/REP-16-0420

23. Gross RW, Han X. Lipidomics at the interface of structure and function in systems biology. *Chem Biol*. (2011) 18:284–91. doi: 10.1016/j.chembiol.2011.01.014

24. Saliba AE, Vonkova I, Gavin AC. The systematic analysis of protein-lipid interactions comes of age. *Nat Rev Mol Cell Biol*. (2015) 16:753–61. doi: 10.1038/nrm4080

25. Hatzel JN, Bouma GJ, Cleys ER, Bemis LT, Ehrhart EJ, Mccue PM. Identification of heat shock protein 10 within the equine embryo, endometrium, and maternal peripheral blood mononuclear cells. *Theriogenology*. (2015) 83:832–9. doi: 10.1016/j.theriogenology.2014.11.020

26. Lawson EF, Gibb Z, De Ruijter-Villani M, Smith ND, Stout TA, Clutton-Brock A, et al. Proteomic analysis of pregnant Mare uterine fluid. *J Equine Vet*. (2018) 66:171–2. doi: 10.1016/j.jevs.2018.05.064

27. Scholtz E, Ball B, Stanley S, Moeller B, Conley A. *Bioactivity of 5α-dihydroprogesterone in mares: endometrial response and maintenance of early pregnancy*. Proceedings of the 55th Annual Convention of the American Association of Equine Practitioners, Las Vegas, Nevada, USA, American Association of Equine Practitioners (AAEP), 262–263. (2009).

28. Smits K, Nelis H, Van Steendam K, Govaere J, Roels K, Ververs C, et al. Proteome of equine oviducal fluid: effects of ovulation and pregnancy. *Reprod Fertil Dev*. (2017) 29:1085–95. doi: 10.1071/RD15481

29. Swegen A, Grupen CG, Gibb Z, Baker MA, De Ruijter-Villani M, Smith ND, et al. From peptide masses to pregnancy maintenance: A comprehensive proteomic analysis of the early equine embryo Secretome, blastocoel fluid, and capsule. *Proteomics*. (2017) 17:1600433. doi: 10.1002/pmic.201600433

30. Klein C, Troedsson MH. Transcriptional profiling of equine conceptuses reveals new aspects of embryo-maternal communication in the horse. *Biol Reprod*. (2011) 84:872–85. doi: 10.1095/biolreprod.110.088732

31. Ohnuma K, Yokoo M, Ito K, Takahashi J, Nambo Y, Miyake YI, et al. Study of early pregnancy factor (EPF) in equine (*Equus caballus*). *Am J Reprod Immunol*. (2000) 43:174–9. doi: 10.1111/j.8755-8920.2000.430307.x

32. Lawson EF, Ghosh A, Grupen C, Netherton J, Aitken RJ, Smith ND, et al. Investigations into the role of platelet-activating factor in the peri-conception period of the mare. *Reproduction*. (2024) 168:e240049. doi: 10.1530/REP-24-0049

33. O'Neill C. The role of paf in embryo physiology. *Hum Reprod Update*. (2005) 11:215–28. doi: 10.1093/humupd/dmi003

34. Dutta-Roy AK. Fatty acid transport and metabolism in the feto-placental unit and the role of fatty acid-binding proteins. *J Nutr Biochem*. (1997) 8:548–57. doi: 10.1016/S0955-2863(97)00087-9

35. Stout TA, Meadows S, Allen WR. Stage-specific formation of the equine blastocyst capsule is instrumental to hatching and to embryonic survival in vivo. *Anim Reprod Sci*. (2005) 87:269–81. doi: 10.1016/j.anireprosci.2004.11.009

36. Oriol JG, Sharom FJ, Betteridge KJ. Developmentally regulated changes in the glycoproteins of the equine embryonic capsule. *J Reprod Fertil*. (1993) 99:653–64. doi: 10.1530/jrf.0.0990653

37. Flood PF, Betteridge KJ, Diocee MS. Transmission electron microscopy of horse embryos 3-16 days after ovulation. *J Reprod Fertil Suppl*. (1982) 32:319–27.

38. Gibson C, De Ruijter-Villani M, Rietveld J, Stout TAE. Expression of glucose transporters in the endometrium and early conceptus membranes of the horse. *Placenta*. (2018) 68:23–32. doi: 10.1016/j.placenta.2018.06.308

39. Stout TA, Allen WR. Prostaglandin E(2) and F(2 alpha) production by equine conceptuses and concentrations in conceptus fluids and uterine flushings recovered from early pregnant and dioestrous mares. *Reproduction*. (2002) 123:261–8. doi: 10.1530/rep.0.1230261

40. Weber J, Woods G, Freeman D, Vanderwall D. Prostaglandin E2-specific binding to the equine oviduct. *Prostaglandins*. (1992) 43:61–5. doi: 10.1016/0090-6980(92)90065-2

41. Weber JA, Freeman DA, Vanderwall DK, Woods GL. Prostaglandin E2 secretion by oviductal transport-stage equine embryos. *Biol Reprod*. (1991) 45:540–3. doi: 10.1095/biolreprod45.4.540

42. Budik S, Walter I, Leitner MC, Ertl R, Aurich C. Expression of enzymes associated with prostaglandin synthesis in equine conceptuses. *Animals (Basel)*. (2021) 11:1180. doi: 10.3390/ani11041180

43. Wang H, Dey SK. Lipid signaling in embryo implantation. *Prostaglandins Other Lipid Mediat*. (2005) 77:84–102. doi: 10.1016/j.prostaglandins.2004.09.013

44. Sharp DC. The early fetal life of the equine conceptus. *Anim Reprod Sci*. (2000) 60-61:679–89. doi: 10.1016/S0378-4320(00)00138-X

45. Dennis EA. Lipidomics joins the omics evolution. *Proc Natl Acad Sci*. (2009) 106:2089–90. doi: 10.1073/pnas.0812636106

46. Wenk MR. The emerging field of lipidomics. *Nat Rev Drug Discov*. (2005) 4:594–610. doi: 10.1038/nrd1776

47. Fahy E, Subramaniam S, Murphy RC, Nishijima M, Raetz CRH, Shimizu T, et al. Update of the LIPID MAPS comprehensive classification system for lipids. *J Lipid Res*. (2009) 50:S9–S14. doi: 10.1194/jlr.R800095-JLR200

48. Xu T, Hu C, Xuan Q, Xu G. Recent advances in analytical strategies for mass spectrometry-based lipidomics. *Anal Chim Acta*. (2020) 1137:156–69. doi: 10.1016/j.aca.2020.09.060

49. Evans HC, Dinh TTN, Hardcastle ML, Gilmore AA, Ugur MR, Hitit M, et al. Advancing semen evaluation using Lipidomics. Frontiers in veterinary. *Science*. (2021) 8:601794. doi: 10.3389/fvets.2021.601794

50. Castro-Perez JM, Kamphorst J, Degroot J, Lafeber F, Goshawk J, YU K, et al. Comprehensive LC-MS E lipidomic analysis using a shotgun approach and its application to biomarker detection and identification in osteoarthritis patients. *J Proteome Res*. (2010) 9:2377–89. doi: 10.1021/pr901094j

51. Phan K, He Y, Pickford R, Bhatia S, Katzeff JS, Hodges JR. Uncovering pathophysiological changes in frontotemporal dementia using serum lipids. *Sci Rep*. (2020) 10:3640. doi: 10.1038/s41598-020-60457-w

52. Ye Q, Cai S, Wang S, Zeng X, Ye C, Chen M, et al. Maternal short and medium chain fatty acids supply during early pregnancy improves embryo survival through enhancing progesterone synthesis in rats. *J Nutr Biochem*. (2019) 69:98–107. doi: 10.1016/j.jnutbio.2019.03.015

53. Suematsu R, Miyamoto T, Saijo S, Yamasaki S, Tada Y, Yoshida H, et al. Identification of lipophilic ligands of Siglec5 and-14 that modulate innate immune responses. *J Biol Chem*. (2019) 294:16776–88. doi: 10.1074/jbc.RA119.009835

54. Lim PS, Sutton CR, Rao S. Protein kinase C in the immune system: from signalling to chromatin regulation. *Immunology*. (2015) 146:508–22. doi: 10.1111/imm.12510

55. Yang QE, Ozawa M, Zhang K, Johnson SE, Ealy AD. The requirement for protein kinase C delta (PRKCD) during preimplantation bovine embryo development. *Reprod Fertil Dev*. (2016) 28:482–90.

56. Gastal MO, Gastal EL, Torres CA, Ginther OJ. Effect of PGE2 on uterine contractility and tone in mares. *Theriogenology*. (1998) 50:989–99.

57. Baardman ME, Kerstjens-Frederikse WS, Berger RMF, Bakker MK, Hofstra RMW, Plösch T. The role of maternal-fetal cholesterol transport in early fetal life: current Insights1. *Biol Reprod*. (2013) 88:24. doi: 10.1095/biolreprod.112.102442

58. Paré JF, Malenfant D, Courtemanche C, Jacob-Wagner M, Roy S, Allard D, et al. The fetoprotein transcription factor (FTF) gene is essential to embryogenesis and cholesterol homeostasis and is regulated by a DR4 element. *J Biol Chem*. (2004) 279:21206–16. doi: 10.1074/jbc.M401523200

59. Roy R, Belanger A. Elevated levels of endogenous pregnenolone fatty acid esters in follicular fluid high density lipoproteins support progesterone synthesis in porcine granulosa cells. *Endocrinology*. (1992) 131:1390–6. doi: 10.1210/endo.131.3.1505469

60. Raeside J, Christie H, Renaud R, Waelchli R, Betteridge K. Estrogen metabolism in the equine conceptus and endometrium during early pregnancy in relation to estrogen concentrations in yolk-sac fluid. *Biol Reprod*. (2004) 71:1120–7. doi: 10.1095/biolreprod.104.028712

61. Choi SJ, Anderson GB, Roser JF. Production of free estrogens and estrogen conjugates by the preimplantation equine embryo. *Theriogenology*. (1997) 47:457–66. doi: 10.1016/S0093-691X(97)00004-6

62. Zavy MT, Vernon MW, Sharp DC, Bazer FW. Endocrine aspects of early pregnancy in pony mares: a comparison of uterine luminal and peripheral plasma levels of steroids during the estrous cycle and early pregnancy. *Endocrinology*. (1984) 115:214–9. doi: 10.1210/endo-115-1-214

63. Quehenberger O, Armando AM, Brown AH, Milne SB, Myers DS, Merrill AH. Lipidomics reveals a remarkable diversity of lipids in human plasma 1. *J Lipid Res*. (2010) 51:3299–305. doi: 10.1194/jlr.M009449

64. Klein C, Scoggin KE, Ealy AD, Troedsson MH. Transcriptional profiling of equine endometrium during the time of maternal recognition of pregnancy. *Biol Reprod*. (2010) 83:102–13. doi: 10.1095/biolreprod.109.081612

65. Klohonatz KM, Coleman SJ, Islas-Trejo AD, Medrano JF, Hess AM, Kalbfleisch T, et al. Coding RNA sequencing of equine endometrium during maternal recognition of pregnancy. *Genes (Basel)*. (2019) 10:749. doi: 10.3390/genes10100749

66. Klohonatz KM, Hess AM, Hansen TR, Squires EL, Bouma GJ, Bruemmer JE. Equine endometrial gene expression changes during and after maternal recognition of pregnancy1. *J Anim Sci*. (2015) 93:3364–76. doi: 10.2527/jas.2014-8826

67. Merkl M, Ulbrich SE, Otzdorff C, Herbach N, Wanke R, Wolf E, et al. Microarray analysis of equine endometrium at days 8 and 12 of pregnancy. *Biol Reprod*. (2010) 83:874–86. doi: 10.1095/biolreprod.110.085233

68. Smits K, Gansemans Y, Tilleman L, Van Nieuwerburgh F, Van De Velde M, Gerits I. Maternal recognition of pregnancy in the horse: are MicroRNAs the secret messengers? *Int J Mol Sci*. (2020) 21:419. doi: 10.3390/ijms21020419

69. Rudolf Vegas A, Podico G, Canisso IF, Bollwein H, Almiñana C, Bauerssachs S. Spatiotemporal endometrial transcriptome analysis revealed the luminal epithelium as key player during initial maternal recognition of pregnancy in the mare. *Sci Rep*. (2021) 11:22293. doi: 10.1038/s41598-021-01785-3

70. Ribeiro E, Greco L, Bisinotto R, Lima F, Thatcher W, Santos J. Biology of preimplantation conceptus at the onset of elongation in dairy cows. *Biol Reprod*. (2016) 94:97. doi: 10.1095/biolreprod.115.134908

71. Seo H, Choi Y, Shim J, Yoo I, Ka H. Prostaglandin transporters ABCC4 and SLCO2A1 in the uterine endometrium and conceptus during pregnancy in pigs. *Biol Reprod*. (2014) 90:1–10. doi: 10.1095/biolreprod.113.114934

72. Zeng S, Bick J, Kradolfer D, Knubben J, Flöter VL, Bauersachs S, et al. Differential transcriptome dynamics during the onset of conceptus elongation and between female and male porcine embryos. *BMC Genomics*. (2019) 20:679. doi: 10.1186/s12864-019-6044-z

73. Ribeiro ES, Santos JEP, Thatcher WW. Role of lipids on elongation of the preimplantation conceptus in ruminants. *Reproduction*. (2016) 152:R115–26. doi: 10.1530/REP-16-0104

74. Sharma K, Shi Y. The yins and yangs of ceramide. *Cell Res*. (1999) 9:1–10. doi: 10.1038/sj.cr.7290001

75. Moussatche P, Lyons TJ. Non-genomic progesterone signalling and its non-canonical receptor. *Biochem Soc Trans*. (2012) 40:200–4. doi: 10.1042/BST20110638

76. Ménézo Y, Lichtblau I, Elder K. New insights into human pre-implantation metabolism in vivo and in vitro. *J Assist Reprod Genet*. (2013) 30:293–303. doi: 10.1007/s10815-013-9953-9

77. Pawlak P, Malyszka N, Szczerbal I, Kolodziejski P. Fatty acid induced lipolysis influences embryo development, gene expression and lipid droplet formation in the porcine cumulus cells†. *Biol Reprod*. (2020) 103:36–48. doi: 10.1093/biolre/ioaa045

78. Chronopoulou E, Harper JC. IVF culture media: past, present and future. *Hum Reprod Update*. (2015) 21:39–55. doi: 10.1093/humupd/dmu040

79. Carnevale EM. The mare model for follicular maturation and reproductive aging in the woman. *Theriogenology*. (2008) 69:23–30. doi: 10.1016/j.theriogenology.2007.09.011

80. Lawson JM, Salem SE, Miller D, Kahler A, Van Den Boer WJ, Shilton CA, et al. Naturally occurring horse model of miscarriage reveals temporal relationship between chromosomal aberration type and point of lethality. *Proc Natl Acad Sci USA*. (2024) 121:e2405636121. doi: 10.1073/pnas.2405636121

81. Zander-Fox D, Villarosa L, Mcpherson NO. Albumin used in human IVF contain different levels of lipids and modify embryo and fetal growth in a mouse model. *J Assist Reprod Genet*. (2021) 38:2371–81. doi: 10.1007/s10815-021-02255-5

82. Desmet KLJ, Van Hoeck V, Gagné D, Fournier E, Thakur A, O'Doherty AM, et al. Exposure of bovine oocytes and embryos to elevated non-esterified fatty acid concentrations: integration of epigenetic and transcriptomic signatures in resultant blastocysts. *BMC Genomics*. (2016) 17:1004. doi: 10.1186/s12864-016-3366-y

83. Almiñana C, Bauersachs S. Extracellular vesicles: multi-signal messengers in the gametes/embryo-oviduct cross-talk. *Theriogenology*. (2020) 150:59–69. doi: 10.1016/j.theriogenology.2020.01.077

84. Saadeldin IM, Kim SJ, Choi YB, Lee BC. Improvement of cloned embryos development by co-culturing with parthenotes: a possible role of exosomes/microvesicles for embryos paracrine communication. *Cell Reprogram*. (2014) 16:223–34. doi: 10.1089/cell.2014.0003

85. Rosenbluth EM, Shelton DN, Wells LM, Sparks AET, Van Voorhis BJ. Human embryos secrete microRNAs into culture media—a potential biomarker for implantation. *Fertil Steril*. (2014) 101:1493–500. doi: 10.1016/j.fertnstert.2014.01.058

86. Konstantynowicz-Nowicka K, Harasim E, Baranowski M, Chabowski A. New evidence for the role of ceramide in the development of hepatic insulin resistance. *PLoS One*. (2015) 10:e0116858. doi: 10.1371/journal.pone.0116858

87. Schaffer JE. Lipotoxicity: when tissues overeat. *Curr Opin Lipidol*. (2003) 14:281–7. doi: 10.1097/00041433-200306000-00008

88. Watt MJ, Barnett AC, Bruce CR, Schenk S, Horowitz JF, Hoy AJ. Regulation of plasma ceramide levels with fatty acid oversupply: evidence that the liver detects and secretes de novo synthesised ceramide. *Diabetologia*. (2012) 55:2741–6. doi: 10.1007/s00125-012-2649-3

89. Rego A, Trindade D, Chaves SR, Manon S, Costa V, Sousa MJ, et al. The yeast model system as a tool towards the understanding of apoptosis regulation by sphingolipids. *FEMS Yeast Res*. (2014) 14:160–78. doi: 10.1111/1567-1364.12096

90. Abbas HK, Tanaka T, Duke SO, Porter JK, Wray EM, Hodges L, et al. Fumonisin- and AAL-toxin-induced disruption of sphingolipid metabolism with accumulation of free sphingoid bases. *Plant Physiol*. (1994) 106:1085–93. doi: 10.1104/pp.106.3.1085

91. Crossman MW, Hirschberg CB. Biosynthesis of phytosphingosine by the rat. *J Biol Chem*. (1977) 252:5815–9. doi: 10.1016/S0021-9258(17)40095-0

92. Madison KC, Swartzendruber DC, Wertz PW, Downing DT. Sphingolipid metabolism in organotypic mouse keratinocyte cultures. *J Invest Dermatol*. (1990) 95:657–64. doi: 10.1111/1523-1747.ep12514333

frontiers | Frontiers in Veterinary Science

TYPE Original Research
PUBLISHED 07 October 2024
DOI 10.3389/fvets.2024.1481248

OPEN ACCESS

EDITED BY
Stefan Gregore Ciornei,
Iasi, University of Life Science (IULS), Romania

REVIEWED BY
Gabriele Brecchia,
University of Milan, Italy
Mohammed Ahmed Elmetwally,
Mansoura University, Egypt
Abdallah Mohamed,
Fort Valley State University, United States

*CORRESPONDENCE
Nicolae Tiberiu Constantin
✉ tiberiu.constantin@fmvb.usamv.ro

RECEIVED 15 August 2024
ACCEPTED 24 September 2024
PUBLISHED 07 October 2024

CITATION
Posastiuc FP, Rizzoto G, Constantin NT, Nicolae G, Chiers K, Diaconescu AI, Șerban AI, Van Soom A and Codreanu MD (2024) Anti-Müllerian hormone as a diagnostic marker for testicular degeneration in dogs: insights from cryptorchid models. *Front. Vet. Sci.* 11:1481248. doi: 10.3389/fvets.2024.1481248

Anti-Müllerian hormone as a diagnostic marker for testicular degeneration in dogs: insights from cryptorchid models

Florin Petrișor Posastiuc[1,2], Guilherme Rizzoto[1], Nicolae Tiberiu Constantin[2]*, George Nicolae[3], Koen Chiers[4], Alexandru Ilie Diaconescu[2], Andreea Iren Șerban[5,6], Ann Van Soom[1] and Mario Darius Codreanu[2]

[1]Department of Internal Medicine, Reproduction and Population Medicine, Faculty of Veterinary Medicine, Ghent University, Merelbeke, Belgium, [2]Department of Clinical Sciences II, Faculty of Veterinary Medicine, University of Agronomic Sciences and Veterinary Medicine of Bucharest, Bucharest, Romania, [3]Department of Paraclinical Sciences, Faculty of Veterinary Medicine, University of Agronomic Sciences and Veterinary Medicine of Bucharest, Bucharest, Romania, [4]Department of Pathobiology, Pharmacology and Zoological Medicine, Faculty of Veterinary Medicine, Ghent University, Merelbeke, Belgium, [5]Department of Preclinical Science, Faculty of Veterinary Medicine, University of Agronomic Sciences and Veterinary Medicine of Bucharest, Bucharest, Romania, [6]Department of Biochemistry and Molecular Biology, Faculty of Biology, University of Bucharest, Bucharest, Romania

Introduction: The increasing prevalence of infertility in male dogs in clinical practice mirrors current trends seen in human medicine. Acquired infertility is notably more common in dogs compared to congenital causes, with conditions such as testicular degeneration leading to irreversible loss of fertility. Current diagnostic methods for testicular degeneration, such as histopathological and cytological examinations, rely on testicular biopsy or fine needle aspiration, making them less feasible for routine use. Anti-Müllerian hormone (AMH), produced by Sertoli cells, has emerged as a potential alternative biomarker for testicular health, which can be measured in serum. This study evaluates AMH as a potential marker for testicular degeneration, using cryptorchid dogs as models for impaired fertility and altered testicular histology.

Methods: The relationship between serum AMH levels and AMH tissue expression with impaired spermatogenesis and altered histology was investigated. Serum AMH levels were determined in intact, cryptorchid, and castrated individuals using an immuno-enzymatic ELISA kit and compared between subgroups based on testicular location. Tissue AMH immuno-expression was differentially quantified in two regions of interest (ROIs), the interstitial space and the seminiferous tubule, in both descended and retained gonads. Furthermore, testicles were analyzed using histomorphometric analysis in seminiferous tubules, while spermatogenesis was evaluated using the Johnsen score.

Results: Serum AMH levels were positively correlated with AMH expression assessed in both interstitial space ($\rho = 0.494$, $p \leq 0.01$) and seminiferous tubules ($\rho = 0.610$, $p \leq 0.001$). Conversely, serum AMH levels showed a negative correlation with the seminiferous tubule area ($\rho = -0.435$, $p \leq 0.05$). Smaller seminiferous tubule areas were linked to increased AMH reactivity in both seminiferous tubules ($\rho = -0.774$, $p \leq 0.001$) and interstitial space ($\rho = -0.725$, $p \leq 0.001$). Additionally, lower Johnsen scores were associated with higher serum AMH levels ($\rho = -0.537$, $p \leq 0.01$) and elevated AMH expression in both

seminiferous tubules ($\rho = -0.756$, $p \leq 0.001$) and interstitial space ($\rho = -0.679$, $p \leq 0.001$).

Discussion: Our results suggest that higher serum levels and tissue expression of AMH are linked to smaller seminiferous tubules and poorer Johnsen scores, reflecting degenerative changes and Sertoli cell dysfunction in retained testicles. Given the similarities in the mechanisms that increase AMH levels in both cryptorchid and non-cryptorchid testicles affected by testicular degeneration, this study recommends using AMH as a marker for diagnosing testicular degeneration in dogs.

KEYWORDS

anti-Müllerian hormone, testicular degeneration, cryptorchidism, spermatogenesis, canine infertility

1 Introduction

Infertility in male dogs is defined as either the inability to mate or the failure to fertilize multiple fertile bitches despite optimal breeding timing (1). This issue is becoming increasingly significant in clinical practice, mirroring the trends seen in human medicine (2, 3). Consequently, there is a growing focus on developing objective predictors for fertility and testicular health in male dogs. Such advancements could facilitate early detection of declining fertility, which would enable timely intervention. Infertility in male dogs is described as either congenital or acquired, with the latter being the more frequently observed cause of reproductive failure (4). Acquired infertility, linked to factors such as hormonal disturbances, infectious diseases, stress, hyperthermia, nutritional deficiencies, toxins, and autoimmune disorders (5, 6), has been notably attributed to testicular degeneration in dogs, with a reported prevalence of up to 57.6% (1, 3, 7). When some of these factors come into play, they can cause significant alterations in testicular structure, potentially leading to irreversible consequences for fertility. Testicular degeneration directly impacts the quality of the ejaculate, progressively impairing both sperm morphology and motility parameters (8). Therefore, current clinical approaches involve assessing the reproductive function of male dogs through sequential sperm analyses. When a decline in fertility is detected and treatment is initiated, reevaluation of the ejaculate after one full spermatogenic cycle is usually recommended. However, spermatogenesis in dogs spans approximately 62 days, with an additional 14 days for epididymal transit (9). Given the extended duration of this process, waiting for sperm production to improve may not be effective. Issues during this period can lead to a complete cessation of spermatogenesis (10). Therefore, timely intervention is crucial to avoid missing treatment opportunities. More objective assessments of testicular health can be achieved through diagnostic techniques such as histopathological and cytological examinations, following testicular biopsies and fine needle aspirations, respectively (11). However, due to their invasive nature and potential complications, both methods are rarely employed.

As an alternative, determining the concentration of anti-Müllerian hormone (AMH) in serum or plasma has recently emerged as a promising tool for the assessment of testicular function and integrity. Research conducted on mice has demonstrated that AMH is a reliable biomarker for detecting testicular damage secondary to aggressive chemotherapy (12, 13). Similarly, monitoring serum AMH levels has been recommended as a useful method for the early detection of testicular degeneration caused by toxic insults in stallions (14). AMH is a glycoprotein produced by Sertoli cells (15, 16). Therefore, the levels of AMH should be linked to Sertoli cell functionality, as it was scrutinized in bulls with heat-induced testicular degeneration (17). In dogs, results suggest that AMH secretion is increased not only in immature or tumorous Sertoli cells but also in degenerative Sertoli cells (18). Moreover, Sertoli cell degeneration may lead to decreased spermatogenic output, which is also marked by increased AMH production (19). Another study suggested that higher serum AMH concentrations were correlated with a lower percentage of morphologically normal spermatozoa (20).

Cryptorchidism is characterized by the failure of one or both testicles to descend into the scrotum (21). This condition results in the testicles being exposed to a different thermal environment compared to their normal scrotal location (8), which can lead to structural and functional changes (22–24) similar to those observed in non-cryptorchid individuals experiencing testicular degeneration and subsequent fertility drops (3).

In this study, cryptorchid dogs were used as models for impaired fertility and altered testicular histology. The aim was to assess the potential of AMH as a marker for testicular degeneration and impaired spermatogenesis. To achieve this, we investigated serum AMH levels in cryptorchid, intact, and castrated dogs, and analyzed AMH expression in both retained testicles and descended gonads. Finally, we examined the relationship between AMH levels, altered testicular histology, and impaired spermatogenesis.

2 Materials and methods

2.1 Sample collection

A total of 50 client-owned male dogs of various ages and breeds were recruited for the study. Twenty dogs with at least one retained testicle were classified into the CRYPTO group. Another 20 intact males with both testicles located inside the scrotum were assigned to the INTACT group. Additionally, 10 bilaterally gonadectomized dogs were included as negative controls, forming the CASTRATED group. All dogs underwent clinical examination, and no concerns were noted

regarding their general or reproductive health. The cryptorchid patients were subjected to ultrasound examinations to confirm the position of the retained testicle prior to any proposed surgical intervention.

The composition of the three groups in terms of age, breed, unilateral or bilateral cryptorchid status, and the location of the retained testicle is detailed in Supplementary Table 1.

Blood samples were collected from all dogs participating in the serological study. The samples were drawn from the cephalic vein and stored in plain red-top collection tubes without additives (BD Vacutainer, Plymouth, UK). For CRYPTO and INTACT dogs, samples were taken before undergoing orchiectomy, and for dogs in the CASTRATED group, samples were collected at least 6 months post-castration. After allowing the blood to clot for 5 min at room temperature, the samples were centrifuged at 2,500×*g* for 10 min. The resulting serum was then stored at −80°C until further processing.

Ten dogs from each of the CRYPTO and INTACT groups underwent gonadectomy with owner consent. Both gonads were fixed in 10% neutral buffered formalin and subsequently embedded in paraffin blocks. For the unilateral cryptorchids, the contralateral descended gonad was available for analysis, with one exception. One unilateral cryptorchid had only the retained testicle available, as the scrotal one had been previously removed through surgery.

All sampling protocols underwent review and approval by the Ethical Committee of the Faculty of Veterinary Medicine, Bucharest (Approval Number: EA nr. 34-03/2024).

2.2 Evaluation of serum AMH levels

AMH serum levels were quantified using a validated three-step sandwich type immunoassay kit kit (Canine/Feline AL-116 ELISA, Ansh Labs, Webster, TX, USA), which has been previously used in dog-based studies (25, 26). Each coated well of the microplate was initially treated with 75 µL of Canine AMH Assay Buffer, in accordance with the manufacturer's recommendations. Subsequently, after adding a volume of 25 µL of calibrators, controls, and serum samples, the plate underwent a 60-min incubation at room temperature on an orbital microplate shaker at 600 rpm. Following incubation, the wells were thoroughly washed, and 100 µL of Antibody-Biotin Conjugate was added to each well, followed by another incubation under the same conditions as per the manufacturer's protocol. After additional washing steps, the wells were treated with Streptavidin-HRP conjugated enzyme for 30 min. The reaction was developed with a 10-min incubation using 100 µL of TMB chromogen solution and stopped with 100 µL of stopping solution. The plate absorbance was read at 450 nm, with background wavelength correction at 630 nm, using a PR 4100 Absorbance Microplate Reader (Bio-Rad Laboratories, Hercules, CA, USA). The intra-assay coefficient of variation was below 10%. Since all samples were processed simultaneously in a single batch, no inter-assay coefficient of variation was calculated. The detection limit of the kit was 0.015 ng/mL.

2.3 Tissue sample preparation

The previously stored paraffin blocks were sectioned repeatedly at 4 µm in order to create two different batches. The first one was stained with hematoxylin and eosin (HE) and directed to conventional microscopical evaluation, followed by histomorphometrical analysis and spermatogenesis assessment. The second batch was reserved for the immunohistochemical assessment.

Randomized sections from both descended (DES) gonads of the INTACT group were analyzed. All retained (RET) testicles from the admitted cryptorchid individuals were also analyzed. When available, the contralateral testicle (CONTRA) of unilateral cryptorchids was evaluated. A detailed description of sample availability for the histological and immunohistochemical assessments is presented in Table 1.

2.3.1 Immunohistochemical staining

The dedicated tissue sections were mounted on 3-aminopropyltriethoxysilane-coated slides. These slides were subjected to deparaffinization with xylene, followed by rehydration in decreasing concentrations of ethanol (100, 96, 50%) and 100% H_2O. For antigen retrieval, the slides were placed in a box filled with distilled water and citrate buffer (pH 6.0), which was then placed inside a pressure cooker containing 600 mL of distilled water. The system (cooker + slides) was microwaved at 850 W for 12 min and then at 300 W for 10 min. After retrieval, the box containing the slides was cooled to room temperature for 20 min.

After a 5-min wash with PBS, 200 µL of H_2O_2 was added to each section for 5 min. The slides were then washed twice with PBS. The primary antibody used was anti-AMH C-terminal (anti-rabbit, Abcam, Cambridge, UK) at a 1:400 dilution (antibody diluent with background reduction, DAKO Agilent – S3022832, Santa Clara, CA, USA). The slides were incubated with the diluted primary antibody for 30 min, washed twice with PBS, and then exposed to 200 µL/slide of Envision Link rabbit (DAKO Agilent – K400311-2) for 30 min.

After this incubation, the slides were washed twice in PBS for 5 min and then treated with 200 µL/slide of 3,3-diaminobenzidine solution (DAB, DAKO Agilent – K346811-2) for a final 30-min incubation. Ultimately, the slides were washed in PBS again for 5 min, counterstained with hematoxylin, dehydrated, mounted with coverslips, and stored for further analysis.

2.4 Tissue sample analysis

Slides were assessed in a blinded manner, by one trained operator, using a Leica DM5500 B microscope (Leica Microsystems CMS GmbH, Wetzlar, Germany). Further image acquisition, digital processing and pixel analysis were performed using Leica Application Suite (LAS version 4.13, Wetzlar, Germany).

2.4.1 General histology, spermatogenesis and histomorphometrical evaluation

Using the HE-stained slides, 20 sections of seminiferous tubules and the neighboring interstitial compartment were analyzed per sample. General histological traits specific to testicular degeneration were assessed, such as reduced seminiferous tubule diameter, decreased numbers of germinal cells, and interstitial fibrosis (27). For spermatogenesis evaluation, the presence of different cell types within the seminiferous tubules—spermatogonia, spermatocytes, spermatids, spermatozoa, and Sertoli cells—was assessed. Based on this assessment, a score from 1 to 10 was assigned to each of the 20 sections, following the Johnsen scale criteria adapted for use in dogs (28).

TABLE 1 Sample availability for histological and immunohistochemical assessments.

No	Breed	Age (months)	Left testicle		Right testicle	
			Location	Availability	Location	Availability
1	Mixed breed	48	Inguinal	Yes	Scrotal	Yes
2	Mixed breed	18	Scrotal	Yes	Inguinal	Yes
3	Mixed breed	24	Scrotal	No	Abdominal	Yes
4	Cocker Spagnel	14	Abdominal	Yes	Scrotal	Yes
5	Mixed breed	13	Inguinal	Yes	Scrotal	Yes
6	Mixed breed	14	Abdominal	Yes	Abdominal	Yes
7	Maltese	24	Abdominal	Yes	Abdominal	Yes
8	Pekingnese	18	Scrotal	Yes	Abdominal	Yes
9	Husky	12	Inguinal	Yes	Scrotal	Yes
10	Chihuahua	34	Inguinal	Yes	Scrotal	Yes
11	Mixed breed	26	Scrotal	Yes	Scrotal	Yes
12	Mixed breed	12	Scrotal	Yes	Scrotal	Yes
13	French Bulldog	12	Scrotal	Yes	Scrotal	Yes
14	Mixed breed	25	Scrotal	Yes	Scrotal	Yes
15	Mixed breed	12	Scrotal	Yes	Scrotal	Yes
16	German Shepherd	24	Scrotal	Yes	Scrotal	Yes
17	Mixed breed	12	Scrotal	Yes	Scrotal	Yes
18	Swiss Shepherd	26	Scrotal	Yes	Scrotal	Yes
19	Mixed breed	14	Scrotal	Yes	Scrotal	Yes
20	Mixed breed	12	Scrotal	Yes	Scrotal	Yes

Moreover, the area of seminiferous tubules was determined using a methodology similar to the one previously used in stallions (29). Specifically, five round or nearly round tubules from the previously examined 20 sections were visualized at 400× magnification and measured across their major and minor axes. The seminiferous tubule area was calculated using the formula:

$$\text{Seminiferous tubule area} = \pi \times \frac{\text{major axis}}{2} \times \frac{\text{minor axis}}{2}$$

2.4.2 Tissue AMH expression quantification

Immunostaining quantification was performed through pixel analysis on five different randomly obtained images per sample, employing standardized color correction via white balance and a standardized threshold. The results were expressed as percentages of reactive areas relative to the total surface of two predefined Regions of Interest (ROIs). The ROIs were defined as follows: ROI[1]—the seminiferous tubule, including the entire intratubular area; and ROI[2]—the interstitial space between a minimum of two neighboring tubules. For both ROIs, the area was determined by tracking predefined margins and using the automated measuring tool specific to the LAS software.

2.5 Statistical analysis

The data were processed and subjected to statistical analysis using IBM SPSS version 18.0 for Windows (IBM Corp., Armonk, NY, USA). The normality of the variables was assessed using the Shapiro–Wilk test, with a significance level set at $\alpha = 0.05$. Results were presented as median and interquartile range (IQR), outliers being identified and removed based on the IQR method. For comparisons across multiple groups, the Kruskal-Wallis test was applied to determine differences in the distribution of non-normally distributed data, followed by pairwise comparisons with significance values adjusted using the Bonferroni correction. For paired data without grouping variables, differences were evaluated using the Wilcoxon signed-rank test. Spearman's rank correlation coefficient was employed to investigate potential associations within the dataset. Statistical significance was determined by considering *p*-values less than 0.05. The relation between the age and AMH variables was computed in all individuals included in the serological study and with the exclusion of the CASTRATED subjects. Afterwards, the remaining individuals were also split into young (age range 0–24 months) and adult (≥25 months).

The experimental design is illustrated in Figure 1.

3 Results

3.1 AMH serum levels and age

An outlier was identified in the CRYPTO group secondary to IQR calculations. The value of 10 ng/mL fell below the lower bound (15.65 ng/mL) and was therefore excluded from further analysis. Remaining data on serum AMH levels showed significant differences among specific groups (Figure 2). The CRYPTO group had significantly higher AMH levels ($n = 19$; median 27.4 ng/mL,

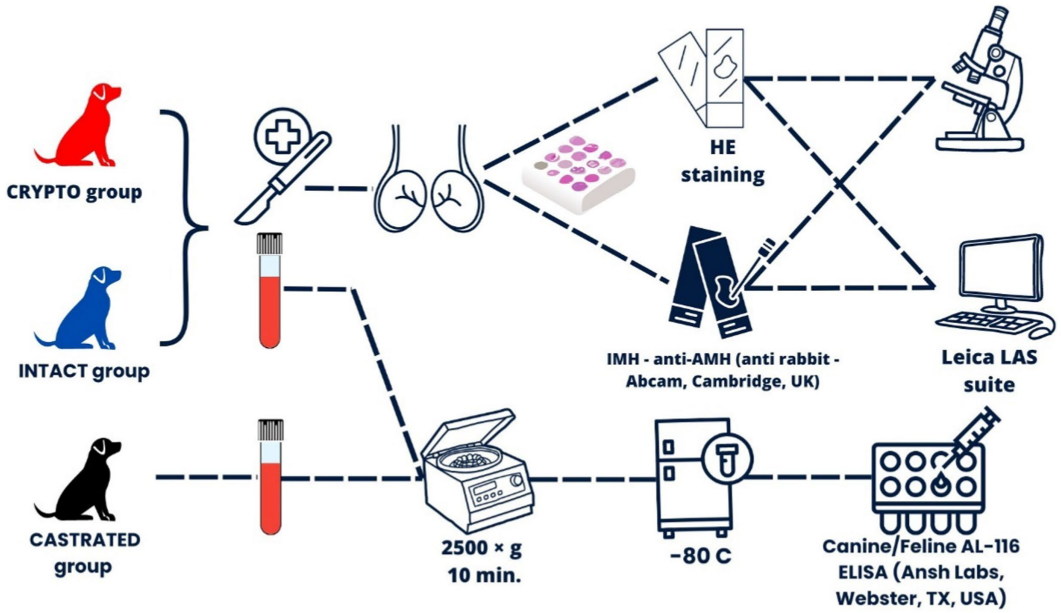

FIGURE 1
Experimental design overview illustrating the overall workflow, including the recruitment and classification of subjects into three main groups: CRYPTO (dogs with at least one retained testicle), INTACT (dogs with both testicles in the scrotum), and CASTRATED (dogs that had been castrated for more than 6 months prior to the study).

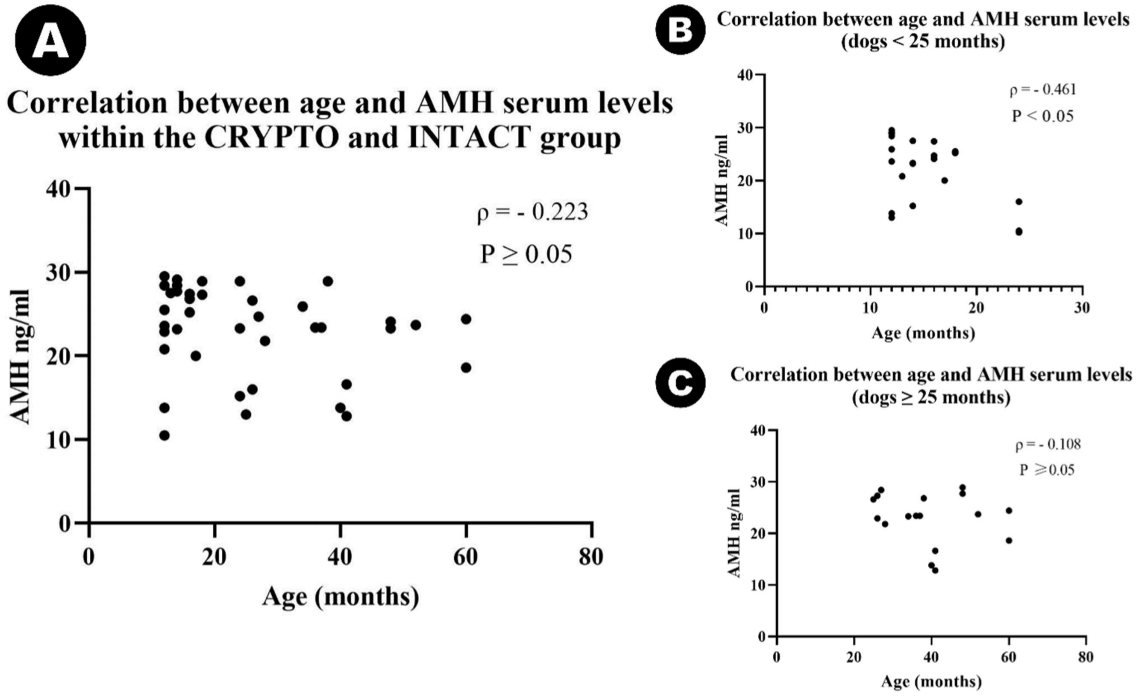

FIGURE 2
Violin plot representing median AMH serum concentrations among cryptorchid dogs (CRYPTO), intact males with both testicles in the scrotum (INTACT), and castrated males (CASTRATED) (A). Subcategories within the CRYPTO group (unilateral, bilateral, abdominal, and inguinal cryptorchids) are also depicted (B,C). Data are presented as median and quartiles (25th and 75th percentiles). The violin shapes illustrate the distribution of the data, the dashed lines indicate the medians, and the dotted lines represent the quartiles. Significance levels are indicated as $p \leq 0.05$ (*), $p \leq 0.01$ (**) and $p \leq 0.001$ (***).

IQR = 3.7) compared to both the INTACT ($n = 20$; median 20.4, IQR 9.25, $p \leq 0.01$) and CASTRATED groups ($n = 10$; 0.01 ± 0.01 ng/mL $p \leq 0.001$) (Figure 2A). The subjects from the CASTRATED group ($n = 20$) exhibited only serum AMH values below the described detection limit of the kit leading to a significant difference when compared to the INTACT AMH serum levels as well. However, no

significant differences were detected between unilateral and bilateral cryptorchids ($p = 1.000$) (Figure 2B), nor between abdominal and inguinal cryptorchids ($p = 1.000$) (Figure 2C). After excluding the outlier in AMH values, the median age across all groups was 24 months ($n = 49$, IQR = 27). No statistically significant differences were observed in the age distribution among the CRYPTO, CASTRATED, and INTACT groups $p \geq 0.05$. Notably, a negative correlation between age and AMH levels was detected across all groups ($\rho = -0.415$, $p \leq 0.01$). However, when computing the analysis excluding the CASTRATED individuals—who typically have low AMH levels irrespective of age—the correlation between age and AMH values remained negative ($\rho = -0.223$) but was no longer statistically significant ($p \geq 0.05$) (Figure 3A). Moreover, when the relationship between age and AMH serum levels was investigated within the separated age groups, a negative correlation was identified between the two variables in dogs younger than 24 months ($\rho = -0.461$, $p < 0.05$) (Figure 3B). Conversely, this correlation was not significant in the adult category (≥25 months) ($\rho = -0.108$, $p \geq 0.05$) (Figure 3C).

3.2 Tissue analysis

3.2.1 General histology

The analyzed samples from the RET category exhibited seminiferous tubules with few germ cells, with 76.7% of the evaluated tubule sections being classified as Sertoli-cell-only tubules. Additionally, a marked reduction or absence of the lumen was noted (Figure 4A). Furthermore, seminiferous tubule degeneration was evident, characterized by a general loss of cellular detail. The basement membrane surrounding the tubules appeared thickened compared to samples from the CONTRA and DES groups. Moreover, in the interstitial space of the RET testicles, an increase in Leydig cell numbers was subjectively observed, accompanied by an increased amount of connective tissue (Figure 4A), when compared to the DES samples (Figure 4B).

3.2.2 Seminiferous tubule areas

Significantly lower tubule areas were found in the RET group (median 13,027.40 μm^2, IQR = 3,764.41) when compared to the CONTRA (median 31,908.82 μm^2, IQR = 7,061.17, $p \leq 0.05$) and DES (median 38,339.93 μm^2, IQR = 9,898.29, $p \leq 0.001$) (Figure 5A). However, there was no significant difference in seminiferous tubule areas between the CONTRA and DES testicles ($p = 1.000$) (Figure 5A), nor when the distribution of the values was compared between the inguinally retained gonads and the abdominally located ones ($p = 1.000$). Interestingly, lower AMH serum values were specific to higher seminiferous tubule areas ($\rho = -0.435$, $p \leq 0.05$).

3.2.3 Johnsen score

All values of the Johnsen scale score have been assigned to the sections in the three categories except for scores 1 and 6 (Figure 6). The Johnsen score for the RET category (median 2, IQR = 0.5) was significantly lower than both the CONTRA (median 9.2, IQR = 0.8,

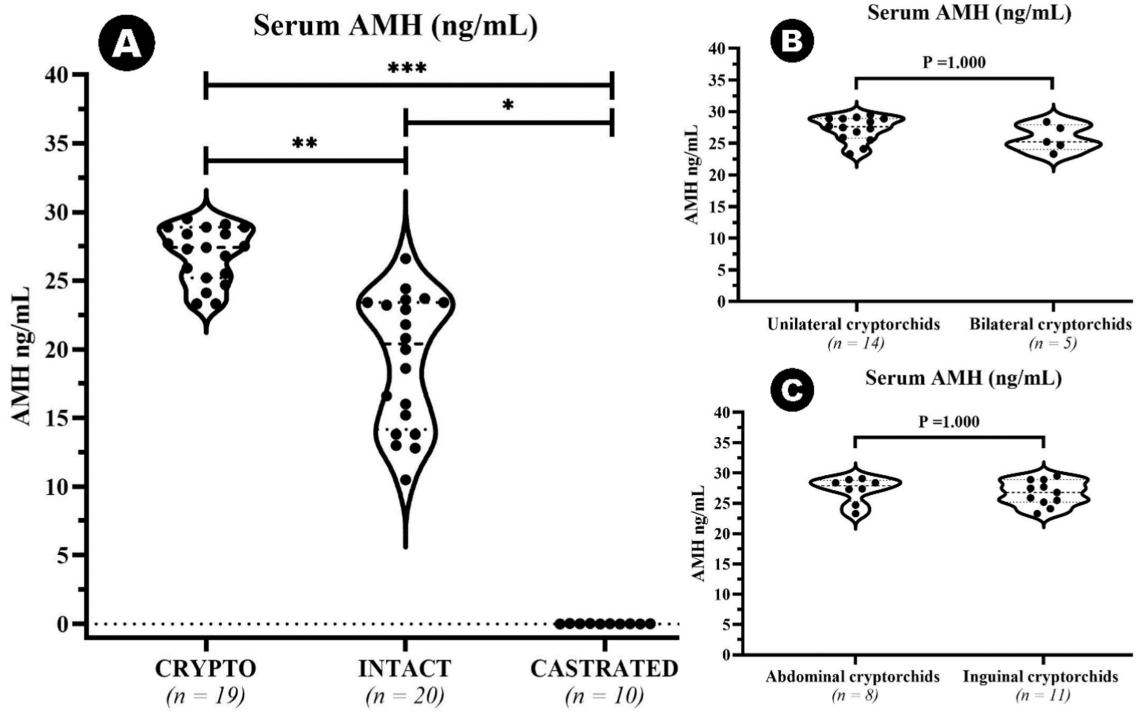

FIGURE 3
Scatter plots illustrating the correlation between age and AMH serum levels in different subgroups: (A) Scatter plot showing the correlation between age and serum AMH levels in cryptorchid dogs (CRYPTO) and intact males with both testicles in the scrotum (INTACT). (B) Scatter plot representing the correlation between age and AMH levels in CRYPTO and INTACT dogs aged 0–24 months. (C) Scatter plot representing the correlation between age and AMH levels in CRYPTO and INTACT dogs aged ≥25 months.

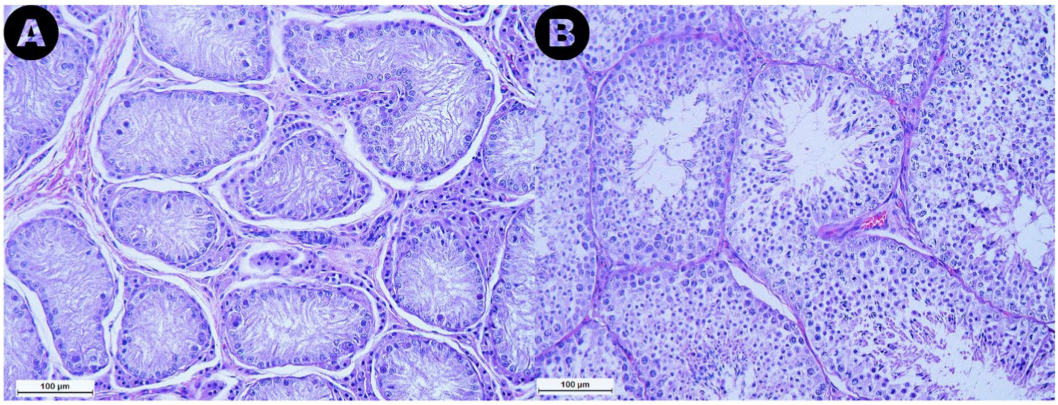

FIGURE 4
Microphotographs obtained from the retained (A) and the descended (B) testicles at a 200× magnification after Hematoxylin and Eosin staining. Note the marked reduction in size of the seminiferous tubules in the retained testicle compared to the descended one, along with the reduction or absence of the lumen observed in the retained gonad. Additionally, an increase in Leydig cell numbers and connective tissue in the interstitial space of the retained testicle can be noted.

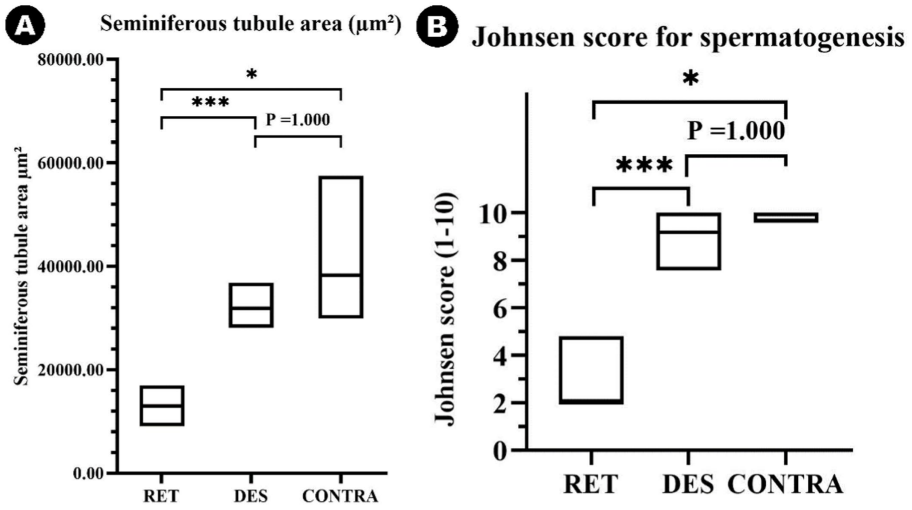

FIGURE 5
Floating bar graph depicting the seminiferous tubule areas (µm²) (A) and Johnsen score values (1–10) (B) across the retained testicles (RET), descended testicle samples from previously intact males with both testicles located in the scrotum (DES), and contralateral testicles from unilateral cryptorchids (CONTRA). Data is presented as floating bars (minimum to maximum). The line is equivalent to the median value of each group. Significance levels are indicated as $p \leq 0.05$ (*) and $p \leq 0.001$ (***).

$p \leq 0.05$) and DES groups (median 9.7, IQR = 0.4, $p \leq 0.001$) (Figure 5B). Additionally, higher scores were associated with lower AMH serum levels ($\rho = -0.537$, $p \leq 0.01$) and bigger seminiferous tubules ($\rho = 0.828$, $p \leq 0.001$). Similar to the seminiferous tubule areas, the comparison between the distribution of Johnsen scores assigned to the inguinally retained and abdominally retained gonads did not show significant differences ($p = 1.000$).

3.2.4 Tissue AMH expression quantification

The AMH expression was revealed as brown staining in both ROIs (Figure 7). Higher AMH expression was observed in the Sertoli cells of retained testicles, resulting in significantly higher expression levels in the seminiferous tubules of the RET group (median 32.42%, IQR = 15.11) compared to the CONTRA group (median 9.25%, IQR = 5.55, $p \leq 0.05$) and the DES group (median 4.63%, IQR = 1.43, $p \leq 0.001$). However, the difference in AMH expression between the CONTRA and DES groups was not significant ($p = 0.444$). The reactivity in the interstitial space ROI was lower than the intratubular expression across all samples ($Z = -4.703$, $p < 0.001$). Group-based comparisons showed that interstitial space reactivity values within the DES samples (median 0.05%, IQR = 0.08) was lower compared to the RET samples (median 2.36%, IQR = 3.24, $p \leq 0.001$), but did not significantly differ from the CONTRA samples (median 0.12%, IQR = 0.15, $p = 1.000$). Moreover, intratubular and interstitial AMH expression levels did not substantially vary between inguinally retained testicles ($p = 1.000$) and abdominally retained gonads ($p = 1.000$).

Interestingly, serum AMH values were positively correlated with the tissue AMH expression in both the interstitial space ($\rho = 0.494$,

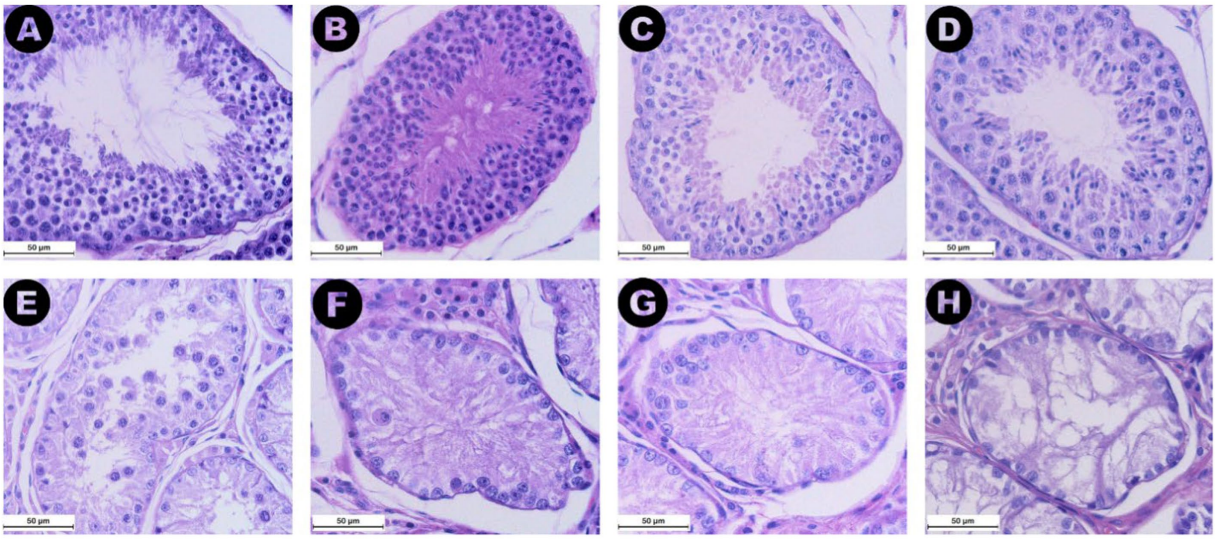

FIGURE 6
Images from (A) to (H) display 400× magnified microphotographs HE staining of seminiferous tubules graded according to the Johnsen score criteria defined by Merz et al. (28), with each image representing a different level of spermatogenic activity. (A) (Score 10) shows complete spermatogenesis with numerous spermatozoa. (B) (Score 9) depicts many spermatozoa (>10) but with disorganized epithelium and an obliterated lumen. (C) (Score 8) illustrates a low number of spermatozoa (<10). (D) (Score 7) features numerous spermatids (>10) but no spermatozoa. (E) (Score 5) displays several spermatocytes (>10) but no spermatozoa or spermatids. (F) (Score 4) shows a low number of spermatocytes (<5) without any spermatids or spermatozoa. (G) (Score 3) depicts seminiferous tubules with only spermatogonia present. (H) (Score 2) features tubules with only Sertoli cells and no germ cells. No images corresponding to scores of 6 or 1 were identified in the present groups.

$p \leq 0.01$) and the seminiferous tubules ($\rho = 0.610$, $p \leq 0.001$). Conversely, smaller seminiferous tubules were associated with higher AMH reactivity in both ROIs (seminiferous tubule: $\rho = -0.774$, $p \leq 0.001$; interstitial space: $\rho = -0.725$, $p \leq 0.001$). Similarly, Johnsen scores decreased as tissue AMH expression increased in the two analyzed compartments (seminiferous tubule: $\rho = -0.756$, $p \leq 0.001$; interstitial space: $\rho = -0.679$, $p \leq 0.001$). All correlations between the analyzed variables are briefly presented in Table 2.

4 Discussion

In this study, the potential of AMH as a biomarker for testicular degeneration and impaired spermatogenesis was assessed. Serum AMH levels and tissue AMH expression were evaluated in relation to histological findings specific to the degenerative processes and spermatogenic arrest identified in selected cryptorchid dogs.

Similar to other studies (26, 30), our results demonstrated the ability of serum AMH to identify the presence of functional testicular tissue, as evidenced by the significant differences observed between castrated and intact males. Moreover, the assay successfully differentiated cryptorchid individuals from those with scrotal-located gonads, which aligns with previous studies (30–32). However, in our study, it was unable to distinguish between unilateral and bilateral cryptorchidism or determine the location of the retained testicle. These findings suggest that AMH levels may be more closely related to the intensity of the degenerative processes than to whether one or both gonads are altered. This is further supported by the observation that, regardless of the location or the bilateral or unilateral cryptorchid state, AMH levels were higher in individuals with smaller seminiferous tubules and lower Johnsen scores.

Multiple human-based studies have consistently demonstrated a negative correlation between age and serum AMH levels, indicating a decline in AMH as age increases (33, 34). One particular study also reported variability in the rate of this decline among individuals, which was attributed to differences in the preservation of Sertoli cell output during aging (34). In our study, when castrated individuals were excluded from the analysis, this correlation between age and AMH levels was no longer supported. The relationship between these variables was evident only when the results were stratified by age group, suggesting that this association might be more relevant to younger individuals. Nevertheless, due to the limited sample size and uneven age distribution in the study, these findings should be interpreted with caution in dog populations, as they do not establish a definitive trend.

Interestingly, two studies in dogs revealed a correlation between increased AMH levels and a decline in sperm quality (19, 20). However, a relationship between age and AMH levels was observed in only one of these studies (19). This indicates that aging alone may not fully account for variations in AMH levels, and that these changes could be more closely related to structural and functional alterations in the testes that occur secondary to aging (28). Nonetheless, the relationship between age, AMH, and testicular degeneration remains unclear, as neither study (19, 20) explored the potential connection between degenerative changes in the testes and AMH levels within the context of sperm quality assessments.

Structural degenerative changes in canine cryptorchid testicles have been already described, including the reduction of seminiferous epithelium and tubule size along with cellular degeneration leading to

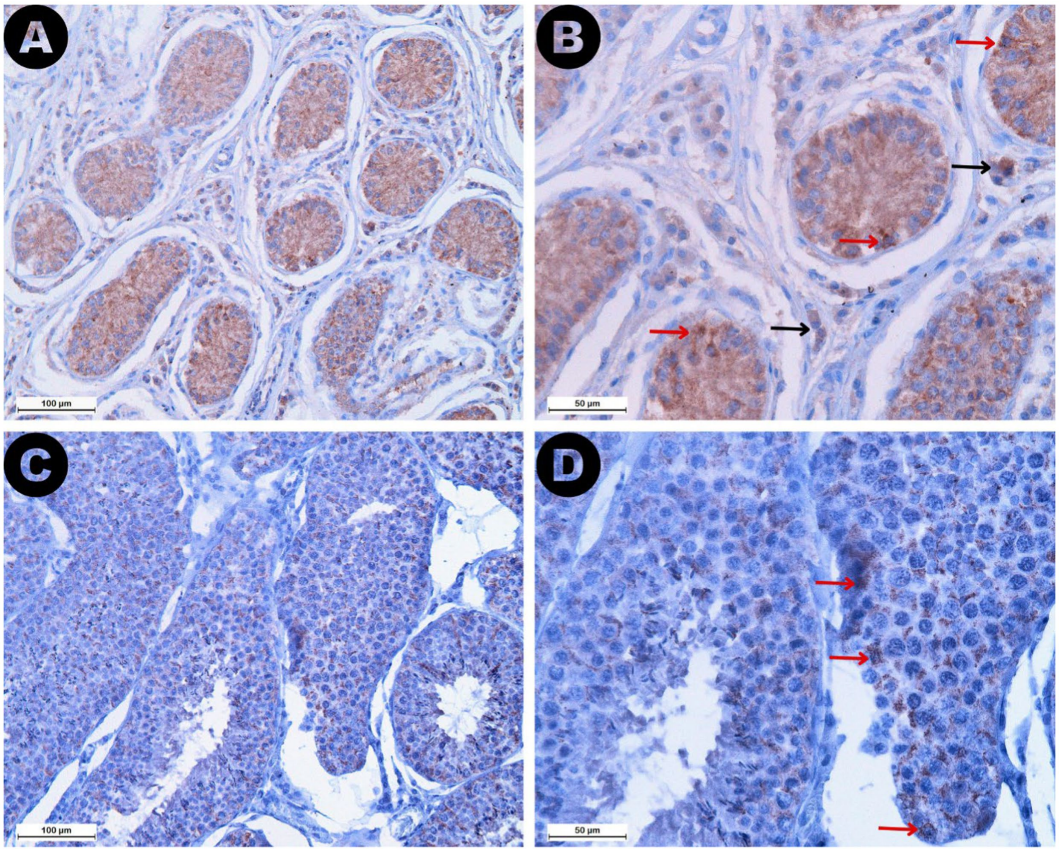

FIGURE 7
AMH immunostaining in both retained (A,B) and descended testicles (C,D) is depicted at different magnifications: 200× (A,C) and 400× (B,D). Note the higher AMH expression identified in the seminiferous tubules of the retained testicles compared to the descended gonads. Red arrows mark reactive Sertoli cells identified in both sample types, but lower intensity staining and fewer reactive cells were specific to the descended testicle samples. Black arrows show reactive Leydig cells identified exclusively in the interstitial space of the retained testicles.

arrested spermatogenesis (35, 36). Furthermore, these alterations were investigated together with AMH levels in cryptorchid stallions, revealing that smaller seminiferous tubules and lower Johnsen scores are associated with higher AMH serum levels (29), similar to our results. In cryptorchid patients, these structural and functional disruptions are explained by the effects of heat stress resulting from the different temperature regime to which the retained testicle is subjected. Heat stress may exert its effects by downregulating specific binding proteins, thereby interfering with the spermatogenetic process (37, 38). Moreover, elevated temperatures can lead to oxidative stress, which consequently results in germ cell degeneration and may impair Sertoli cell function (35, 39–41). The impact of heat stress on Sertoli cells has also been demonstrated in non-cryptorchid patients (17). A study involving bulls subjected to scrotal insulation revealed that heat-induced Sertoli cell dysfunction can lead to alterations in AMH levels, even in the absence of a cryptorchid state (17). This effect was explained by the capacity of heat stress to induce the reversion of Sertoli cells to an immature prepubertal phenotype (42), similar to cryptorchid testicles (43). In fact, this dematuration of Sertoli cells was considered the main reason for serum AMH increase when other factors were responsible for inducing acute testicular degeneration in stallions (14). The same approach was taken in mice and humans exposed to gonadotoxic treatments (12). The administration of doxorubicin and busulfan resulted in elevated serum AMH levels, which correlated with a significant reduction in seminiferous tubule size and a marked loss of meiotic germ cells, including spermatocytes, spermatids, and spermatozoa (12), in line with our findings in cryptorchids.

According to our results, AMH expression was higher in the seminiferous tubules of the retained testicles compared to the descended gonads, due to the more reactive Sertoli cells of the cryptorchid testicles. In other words, the tissue AMH expression intensified in the compressed tubules showing either few germ cells or Sertoli cells-only. These findings align with published data on cryptorchid stallions and tomcats in which AMH staining was negatively correlated with seminiferous tubule areas and Johnsen scores (29, 44). In dogs, higher AMH immunostaining in retained testicles was also explained by the presence of fewer germ cells in the seminiferous tubules, when compared to scrotal gonads (31). Therefore, AMH tissue expression appears to increase due to structural or functional changes within the testicle, associated with Sertoli cell dedifferentiation or dematuration, leading to elevated AMH serum levels (14, 45). Severely damaged mouse testicles showed increased AMH staining intensity, primarily identifying reactive Sertoli cells, and correlating with a higher degree of apoptosis (12). In testicles of infertile men, tubular atrophy was marked by the co-expression of AMH and CK-18 in the Sertoli cells (45). This expression pattern was specific for the tubules showing spermatogenic

TABLE 2 Spearman's rank correlation matrix of the analyzed variables.

		Serum AMH	Seminiferous tubule area	AMH reactivity in ROI[1a]	AMH reactivity in ROI[2b]	Johnsen score
Serum AMH	Correlation coefficient	1.000	−0.435*	0.610**	0.494**	−0.537**
	p-value	–	0.018	<0.001	0.006	0.003
Seminiferous tubule area	Correlation coefficient	−0.435*	1.000	−0.774**	−0.725**	0.828**
	p-value	0.018	–	<0.001	<0.001	<0.001
AMH reactivity in ROI[1a]	Correlation coefficient	0.610**	−0.774**	1.000	0.831**	−0.756**
	p-value	<0.001	<0.001	–	<0.001	<0.001
AMH reactivity in ROI[2b]	Correlation coefficient	0.494**	−0.725**	0.831**	1.000	−0.679**
	p-value	0.006	<0.001	<0.001	–	<0.001
Johnsen score	Correlation coefficient	−0.537**	0.828**	−0.756**	−0.679**	1.000
	p-value	0.003	<0.001	<0.001	<0.001	–

This table displays the Spearman's rank correlation coefficients and associated two-tailed *p*-values, highlighting the relationships among serum anti-Müllerian hormone (AMH) levels, seminiferous tubule areas, AMH reactivity in two defined regions of interest (ROIs), namely ROI[1] and ROI[2], and the Johnsen scores within the study cohort.
[a]ROI[1] = region of interest defined as the area within the seminiferous tubule.
[b]ROI[2] = region of interest defined as a limited area within the interstitial space between a minimum of two neighboring tubules.
*Correlation is significant at the 0.05 level (2-tailed).
**Correlation is significant at the 0.05 level (2-tailed).

arrest at the spermatogonia stage, as well as in tubules displaying Sertoli cells only (45), similar our Johnsen score 2 and 3 tubules.

The AMH receptor was initially thought to be located exclusively on the membrane of Sertoli cells, but subsequent research has also identified its presence on Leydig cells (46). Moreover, the interaction between AMH and the receptors located on Leydig cells may have the potential to inhibit testosterone production (46). Interestingly, in retained testicle samples a higher reactivity was noted in the interstitial space in comparison to the same compartment of the descended gonads, suggesting a higher interaction between the above-mentioned receptors and the AMH. Therefore, we may consider that AMH could also reflect the steroidogenic capacity of testicular tissue, which may be altered by degenerative insults such as those seen in stallions with thermally induced testicular degeneration (47).

The contralateral descended testicles of unilateral cryptorchids did not significantly differ from the descended testicles of intact individuals in any of the analyzed aspects. These findings are consistent with previous observations in dogs, where similar comparisons were made across three different age categories, examining various developmental stages of cryptorchids (35). In this light and considering that serum AMH was unable to differentiate between unilateral and bilateral cryptorchids, we can hypothesize that AMH might not be effective in indicating whether one or both testicles are undergoing testicular degeneration. However, it could still be a valuable marker for raising awareness when structural changes begin to develop in at least one of the gonads.

In spite of the valuable aspects of this study, there are some limitations to consider. One limitation is the lack of ejaculate collection from the dogs prior to castration, which would have provided important insights into sperm functionality and morphology at the time of blood sampling. Another limitation is the use of cryptorchid dogs as models for testicular degeneration, along with healthy controls that lacked a complete reproductive history. Future studies could focus on dogs suffering from various degrees of degeneration due to other causes, such as mechanical insults or neoplasia, to deepen the understanding of testicular degeneration mechanisms. Additionally, including only dogs with proven fertility as healthy controls could offer more robust insights for future research.

In conclusion, this study supports the use of AMH as a biomarker for testicular degeneration, as demonstrated in cryptorchid dogs. This condition exhibits structural and functional changes similar to those seen in descended testicles affected by agents such as heat stress or gonadotoxic compounds, which also induce testicular degeneration. Elevated serum AMH levels and increased AMH tissue expression in retained testicles were closely correlated with structural damage and impaired spermatogenesis, indicating that AMH reflects significant alterations within testicular tissue. While serum AMH proves to be a promising minim-invasive tool for the early detection of testicular dysfunction, its current limitations in assessing the severity of degeneration highlight the need for further research and complementary diagnostic methods to enhance the evaluation of testicular health and fertility in male dogs.

Data availability statement

The original contributions presented in the study are included in the article/Supplementary material, further inquiries can be directed to the corresponding author.

Ethics statement

The animal studies were approved by the Ethical Committee of the Faculty of Veterinary Medicine, Bucharest (Approval Number: EA nr. 34-03/2024). The studies were conducted in accordance with the local legislation and institutional requirements. Written informed consent was obtained from the owners for the participation of their animals in this study.

Author contributions

FP: Conceptualization, Data curation, Formal analysis, Investigation, Methodology, Visualization, Writing – original draft. GR: Resources, Writing – review & editing. NC: Investigation, Writing – review & editing. GN: Investigation, Writing – original draft. KC: Investigation, Writing – original draft. AD: Investigation, Writing – review & editing. AŞ: Investigation, Writing – review & editing. AV: Resources, Supervision, Writing – review & editing. MC: Supervision, Writing – review & editing.

Funding

The author(s) declare that financial support was received for the research, authorship, and/or publication of this article.

Acknowledgments

The authors gratefully acknowledge the staff of the Veterinary Pathology Laboratory from Ghent University for their assistance with sample preparation and thank Sarah Loomans for excellent technical assistance. The collaboration between the authors in this study was supported by the Romanian Ministry of Education through the Agency for Student Loans and Grants, under the mobility grant HG 118/2023-2024, contract No. 3323/23.01.2024.

Conflict of interest

The authors declare that the research was conducted in the absence of any commercial or financial relationships that could be construed as a potential conflict of interest.

Publisher's note

All claims expressed in this article are solely those of the authors and do not necessarily represent those of their affiliated organizations, or those of the publisher, the editors and the reviewers. Any product that may be evaluated in this article, or claim that may be made by its manufacturer, is not guaranteed or endorsed by the publisher.

Supplementary material

The Supplementary material for this article can be found online at: https://www.frontiersin.org/articles/10.3389/fvets.2024.1481248/full#supplementary-material

References

1. Domosławska A, Zdunczyk S. Clinical and spermatological findings in male dogs with acquired infertility: a retrospective analysis. *Andrologia*. (2020) 52:1–8. doi: 10.1111/and.13802

2. Aitken RJ. The changing tide of human fertility. *Hum Reprod*. (2022) 37:629–38. doi: 10.1093/humrep/deac011

3. Câmara LBRM, Câmara DR, Maiorino FC, Júnior VAS, Guerra MMP. Canine testicular disorders and their influence on sperm morphology. *Anim Reprod*. (2014) 11:32–6.

4. Zdunczyk S, Domoslawska A. Effect of drugs on fertility in male dogs: a review. *Reprod Domest Anim*. (2022) 57:949–56. doi: 10.1111/rda.14173

5. Fontbonne A. Infertility in male dogs: recent advances. *Rev Bras Reprod Anim*. (2011) 35:266–73.

6. Gobello C, Corrada Y. Acquired infertility in male dogs with normal libido. *Compend Contin Educ Pract Vet*. (2004) 26:18–28.

7. Ortega-Pacheco A, Rodríguez-Buenfil J, Segura-Correa J, Bolio-Gonzalez M, Jiménez-Coello M, Linde FC. Pathological conditions of the reproductive organs of male stray dogs in the tropics: prevalence, risk factors, morphological findings and testosterone concentrations. *Reprod Domest Anim*. (2006) 41:429–37. doi: 10.1111/j.1439-0531.2006.00688.x

8. Robinson BR, Netherton JK, Ogle RA, Baker MA. Testicular heat stress, a historical perspective and two postulates for why male germ cells are heat sensitive. *Biol Rev*. (2023) 98:603–22. doi: 10.1111/brv.12921

9. Ibach B, Weissbach L, Hilscher B. Stages of the cycle of the seminiferous epithelium in the dog. *Andrologia*. (2009) 8:297–307. doi: 10.1111/j.1439-0272.1976.tb01659.x

10. Mason SJ. An update on male canine infertility. *Vet Clin N Am Small Anim Pract*. (2023) 53:1063–81. doi: 10.1016/j.cvsm.2023.04.006

11. Gouletsou PG, Galatos AD, Leontides LS, Sideri AI. Impact of fine or large needle aspiration on the dog's testis: in vitro ultrasonographic, bacteriological, gross anatomy and histological assessment. *Theriogenology*. (2010) 74:1604–14. doi: 10.1016/j.theriogenology.2010.06.032

12. Levi M, Hasky N, Stemmer SM, Shalgi R, Ben-Aharon I. Anti-Müllerian hormone is a marker for chemotherapy-induced testicular toxicity. *Endocrinology*. (2015) 156:3818–27. doi: 10.1210/en.2015-1310

13. Levi M, Popovtzer A, Tzabari M, Mizrachi A, Savion N, Stemmer SM, et al. Cetuximab intensifies cisplatin-induced testicular toxicity. *Reprod Biomed Online*. (2016) 33:102–10. doi: 10.1016/j.rbmo.2016.04.004

14. Pozor M, Conley AJ, Roser JF, Nolin M, Zambrano GL, Runyon SP, et al. Anti-Müllerian hormone as a biomarker for acute testicular degeneration caused by toxic insults to stallion testes. *Theriogenology*. (2018) 116:95–102. doi: 10.1016/j.theriogenology.2018.05.009

15. Walter B. Anti-Müllerian hormone in dogs and cats reproduction. *Reprod Domest Anim*. (2020) 55:26–31. doi: 10.1111/rda.13603

16. Posastiuc FP, Diaconescu AI, Constantin NT, Micşa C, Codreanu DM. Potential biomarkers for testicular cancer in dogs-groundwork for innovative screening programs: a review. *Sci Works Ser C Vet Med*. (2022) 67:100–7.

17. Ferrer MS, Palomares RA, Hurley DJ, Norton N, Bullington AC, Hoyos-Jaramillo A, et al. Changes in serum testosterone and anti-Müllerian hormone concentration in bulls undergoing scrotal insulation. *Domest Anim Endocrinol*. (2022) 78:106685. doi: 10.1016/j.domaniend.2021.106685

18. Walter B, Fischer S, Otzdorff C. Anti-Mullerian hormone concentrations in dogs with testicular atrophy. In: 1st European symposium on animal reproduction. Nantes, France: Reproduction in Domestic Animals. (2023). 191.

19. Hallberg I, Olsson H, Lau A, Wallander S, Snell A, Bergman D, et al. Endocrine and dog factors associated with semen quality. *Sci Rep*. (2024) 14:1–11. doi: 10.1038/s41598-024-51242-0

20. Domain G, Buczkowska J, Kalak P, Wydooghe E, Banchi P, Pascottini OB, et al. Serum anti-Müllerian hormone: a potential semen quality biomarker in stud dogs? *Animals*. (2022) 12:323. doi: 10.3390/ani12030323

21. Johnston S. D., Root Kustritz M. V., Schultz Olson P. Canine and feline theriogenology. Philadelphia: WB Saunders Company. (2001). 341–343.

22. Pecile A, Groppetti D, Pizzi G, Banco B, Bronzo V, Giudice C, et al. Immunohistochemical insights into a hidden pathology: canine cryptorchidism. *Theriogenology*. (2021) 176:43–53. doi: 10.1016/j.theriogenology.2021.09.011

23. Moon JH, Yoo DY, Jo YK, Kim GA, Jung HY, Choi JH, et al. Unilateral chryptochidism induces morphological changes of testes and hyperplasia of Sertoli cells in a dog. *Lab Anim Res*. (2014) 30:185–9. doi: 10.5625/lar.2014.30.4.185

24. Kawakami E, Tsutsui T, Yamada Y, Yamauchi M. Cryptorchidism in the dog: occurrence of cryptorchidism and semen quality in the cryptorchid dog. *Japanese J Vet Sci*. (1984) 46:303–8. doi: 10.1292/jvms1939.46.303

25. Hollinshead F, Walker C, Hanlon D. Determination of the normal reference interval for anti-Müllerian hormone (AMH) in bitches and use of AMH as a potential predictor of litter size. *Reprod Domest Anim*. (2017) 52:35–40. doi: 10.1111/rda.12822

26. Themmen APN, Kalra B, Visser JA, Kumar A, Savjani G, de Gier J, et al. The use of anti-Müllerian hormone as diagnostic for gonadectomy status in dogs. *Theriogenology*. (2016) 86:1467–74. doi: 10.1016/j.theriogenology.2016.05.004

27. Foster RA. Male reproductive system In: FJ Zachary, editor. Pathologic basis of veterinary disease. *6th* ed. St. Louis, Missouri: Elsevier (2017). 1194–222.

28. Merz SE, Klopfleisch R, Breithaupt A, Gruber AD. Aging and senescence in canine testes. *Vet Pathol*. (2019) 56:715–24. doi: 10.1177/0300985819843683

29. Tsogtgerel M, Komyo N, Murase H, Hannan MA, Watanabe K, Ohtaki T, et al. Serum concentrations and testicular expressions of insulin-like peptide 3 and anti-Müllerian hormone in normal and cryptorchid male horses. *Theriogenology*. (2020) 154:135–42. doi: 10.1016/j.theriogenology.2020.05.026

30. Horňáková L, Vrbovská T, Pavľak M, Valenčáková-Agyagosová A, Halo M, Hajurka J. The evaluation of blood concentrations of testosterone, 17β-oestradiol and anti-Müllerian hormone in dogs with cryptorchidism and testicular tumours. *Pol J Vet Sci*. (2017) 20:677–85. doi: 10.1515/pjvs-2017-0085

31. Prapaiwan N, Manee-in S, Thanawongnuwech R, Srisuwatanasagul S. Anti-Müllerian hormone levels in serum and testes of male dogs: relations with neuter status and bilateral abdominal cryptorchidism. *Theriogenology*. (2023) 208:171–7. doi: 10.1016/j.theriogenology.2023.06.015

32. Claes A, Ball BA, Almeida J, Corbin CJ, Conley AJ. Serum anti-Müllerian hormone concentrations in stallions: developmental changes, seasonal variation, and differences between intact stallions, cryptorchid stallions, and geldings. *Theriogenology*. (2013) 79:1229–35. doi: 10.1016/j.theriogenology.2013.03.019

33. Ramezani Tehrani F, Mansournia MA, Solaymani-Dodaran M, Minooee S, Azizi F. Serum variations of anti-Mullerian hormone and total testosterone with aging in healthy adult Iranian men: a population-based study. *PLoS One*. (2017) 12:e0179634. doi: 10.1371/journal.pone.0179634

34. Chong YH, Dennis NA, Connolly MJ, Teh R, Jones GT, van Rij AM, et al. Elderly men have low levels of anti-Müllerian hormone and inhibin b, but with high interpersonal variation: a cross-sectional study of the sertoli cell hormones in 615 community-dwelling men. *PLoS One*. (2013) 8:e70967. doi: 10.1371/journal.pone.0070967

35. Hernández-Jardón N, Rojas-Castañeda JC, Landero-Huerta D, Reyes-Cruz E, Reynoso-Robles R, Juárez-Mosqueda M d L, et al. Cryptorchidism: the dog as a study model. *Front Vet Sci*. (2022) 13:9. doi: 10.3389/fvets.2022.935307

36. Posastiuc F, Constantin T, Micșa C, Nicolae G, Sprinţu I, Andrei C, et al. Is serum anti-Mullerian hormone a useful biomarker for testicular atrophy in dogs? In: 1st European symposium on animal reproduction. Nantes: Reproduction in Domestic Animals, (2023); 58: 261.

37. Cai H, Ren Y, Li XX, Yang JL, Zhang CP, Chen M, et al. Scrotal heat stress causes a transient alteration in tight junctions and induction of TGF-β expression. *Int J Androl*. (2011) 34:352–62. doi: 10.1111/j.1365-2605.2010.01089.x

38. Yang WR, Li BB, Hu Y, Zhang L, Wang XZ. Oxidative stress mediates heat-induced changes of tight junction proteins in porcine sertoli cells via inhibiting CaMKKβ-AMPK pathway. *Theriogenology*. (2020) 142:104–13. doi: 10.1016/j.theriogenology.2019.09.031

39. Ishii T, Matsuki S, Iuchi Y, Okada F, Toyosaki S, Tomita Y, et al. Accelerated impairment of spermatogenic cells in sod 1-knockout mice under heat stress. *Free Radic Res*. (2005) 39:697–705. doi: 10.1080/10715760500130517

40. Ikeda M, Kodama H, Fukuda J, Shimizu Y, Murata M, Kumagai J, et al. Role of radical oxygen species in rat testicular germ cell apoptosis induced by heat stress. *Biol Reprod*. (1999) 61:393–9. doi: 10.1095/biolreprod61.2.393

41. Vigueras-Villaseñor RM, Ojeda I, Gutierrez-Pérez O, Chavez-Saldaña M, Cuevas O, Maria DS, et al. Protective effect of α-tocopherol on damage to rat testes by experimental cryptorchidism. *Int J Exp Pathol*. (2011) 92:131–9. doi: 10.1111/j.1365-2613.2010.00757.x

42. Aldahhan RA, Stanton PG, Ludlow H, de Kretser DM, Hedger MP. Acute heat-treatment disrupts inhibin-related protein production and gene expression in the adult rat testis. *Mol Cell Endocrinol*. (2019) 498:110546. doi: 10.1016/j.mce.2019.110546

43. Sharpe RM, McKinnell C, Kivlin C, Fisher JS. Proliferation and functional maturation of Sertoli cells, and their relevance to disorders of testis function in adulthood. *Reproduction*. (2003) 125:769–84. doi: 10.1530/rep.0.1250769

44. Posastiuc FP, Rizzoto G, Constantin NT, Nicolae G, Chiers K, Diaconescu AI, et al. Anti-Müllerian hormone in feline cryptorchidism: serum levels, tissue expression, and implications for testicular health. *Theriogenology*. (2024) 230:54–60. doi: 10.1016/j.theriogenology.2024.09.002

45. Steger K, Rey R, Louis F, Kliesch S, Behre HM, Nieschlag E, et al. Reversion of the differentiated phenotype and maturation block in Sertoli cells in pathological human testis. *Hum Reprod*. (1999) 14:136–43. doi: 10.1093/humrep/14.1.136

46. Racine C, Rey R, Forest MG, Louis F, Ferré A, Huhtaniemi I, et al. Receptors for anti-Müllerian hormone on Leydig cells are responsible for its effects on steroidogenesis and cell differentiation. *Proc Natl Acad Sci*. (1998) 95:594–9. doi: 10.1073/pnas.95.2.594

47. Blanchard T, Varner D, Johndon L, Roser JF, Hill J, Miller C. Testicular and hormonal changes in stallions with thermally induced testicular degeneration. *J Reprod Fertil*. (2000) 1:51–9.

frontiers | Frontiers in Veterinary Science

TYPE Original Research
PUBLISHED 22 October 2024
DOI 10.3389/fvets.2024.1494065

OPEN ACCESS

EDITED BY
Stefan Gregore Ciornei,
Iasi, University of Life Science (IULS), Romania

REVIEWED BY
Christian Hanzen,
University of Liège, Belgium
Umut Cagin ARI,
Kafkas University, Türkiye

*CORRESPONDENCE
Brijesh Kumar
✉ drbrijeshvet02@gmail.com

RECEIVED 10 September 2024
ACCEPTED 07 October 2024
PUBLISHED 22 October 2024

CITATION
Gawai M, Kumar B, Mehrotra S, Chandra P, Kohli K, Donadkar M, Yadav V, Yadav BK, Warghat C, Kharayat N, Yadav D, Singhal S, Chouhan V, Singh S and Khan M (2024) Impact of antral follicle count on follicular–luteal characteristics, superovulatory response, and embryo quality in Sahiwal cows.
Front. Vet. Sci. 11:1494065.
doi: 10.3389/fvets.2024.1494065

Impact of antral follicle count on follicular–luteal characteristics, superovulatory response, and embryo quality in Sahiwal cows

Mohan Gawai[1], Brijesh Kumar[1]*, S. Mehrotra[1], Pradeep Chandra[1], Kalpendra Kohli[1], Manoj Donadkar[1], Vandana Yadav[2], Brijesh Kumar Yadav[3], Chinmay Warghat[1], Nitish Kharayat[4], Dushyant Yadav[5], Sumit Singhal[5], V.S. Chouhan[6], S.K. Singh[1] and M.H. Khan[1]

[1]Animal Reproduction Division, ICAR-Indian Veterinary Research Institute (ICAR-IVRI), Bareilly, India, [2]Livestock Production and Management Section, ICAR-IVRI, Bareilly, India, [3]Department of Teaching Veterinary Clinical Complex, DUVASU, Mathura, India, [4]Temperate Animal Husbandry Division, ICAR-IVRI, Mukteswar Campus, Bareilly, India, [5]Department of Veterinary Gynaecology and Obstetrics, BASU, Patna, India, [6]Department of Veterinary Physiology and Climatology, ICAR- IVRI, Bareilly, India

The study aimed to evaluate the effect of antral follicle count (AFC) on follicular and luteal development during the estrous cycle and superovulatory period, as well as on superovulatory response and *in vivo* embryo quality within the MOET program. A total of 48 estrus-induced (500 μg PGF2α, Single dose, IM) Sahiwal cows (*Bos indicus*) with a BCS between 3.5 and 4.0 were selected for the study. On the day of wave emergence, the animals were divided into two groups based on the AFC, i.e., low AFC (≤18) and high AFC (>18). Both the groups were monitored daily using B-mode ultrasonography (USG) for one cycle, and the superovulation protocol was initiated on the 9th day of the subsequent estrous cycle. A total of 240 μg of FSH in eight divided doses were given in a tapering sequence for 4 days and simultaneous administration of 500 μg PGF2α, along with the fifth dose of FSH. Donors were inseminated at superovulatory estrus using double straws of high-quality frozen semen thrice at 12-h intervals, and non-surgical flushing was performed on day 7 of the superovulatory estrus followed by embryo searching and evaluation under a stereo zoom microscope. Ovulatory waves of the high-AFC Sahiwal cows have significantly ($p \leq 0.05$) larger sizes of preovulatory follicles (POF) (12.06 ± 0.19 mm *vs* 11.56 ± 0.16 mm) and corpus luteum (CL) (19.57 ± 0.28 mm *vs* 18.26 ± 0.35 mm), as compared to low AFC. The ovarian size was significantly ($p < 0.0001$) larger in cows with high AFC during the superovulatory protocol. The number of large, medium, and small follicles was significantly ($p < 0.0001$) high on the day of superovulatory estrus (SOE), PGF2α administration, and initiation of superovulatory protocol, respectively, in high AFC. Donors with high AFC had a notably greater ($p < 0.0001$) count of CL and embryos retrieved per flushing, including excellent and fair-quality embryos. A strong association ($p < 0.0001$) between high AFC and ovarian size ($r = 0.9136$), superovulatory response ($r = 0.9350$), and embryo quality ($x^2 = 8.788$; $p = 0.032$) and number ($r = 0.9858$) were also recorded. Based on these results, AFC is considered a dependable indicator for forecasting reproductive capacity. *Bos indicus* donors with an average AFC of 30 or higher are recommended.

KEYWORDS

antral follicle counts, superovulatory follicular development, embryo quality, Sahiwal cattle, luteal development

1 Introduction

Reproductive biotechnologies, such as embryo production, play a crucial role in enhancing the reproductive efficiency of cattle over a short period. While the utilization of *in vitro* embryo production (IVEP) has grown significantly over the past decade, embryo production through multiple ovulation and embryo transfer (MOET—*in vivo* method) programs remains a substantial portion of global cattle embryo production (1). To harvest the maximum potential of assisted reproductive techniques (ART), it is crucial to have dependable biomarkers that demonstrate strong consistency and heritability and are linked to the reproductive performance of cows (2, 3). Intrinsic and extrinsic factors govern the success of a MOET program, including season, genetics, age, nutrition, management, stress, type of gonadotropins used, and treatment protocols adopted (4). Despite improved control over external factors, the inconsistency in the ovarian response indicates that intrinsic factors are primarily responsible for this variability (5).

In this context, the antral follicle count (AFC), which reflects the population of antral follicles present in an ovary, has been indicated as an important phenotypic characteristic related to female fertility and positively correlated with the superovulatory response and performance of *in vivo* and *in vitro* embryo production (IVEP) (6, 7). Over time, there has been a growing understanding of pharmacological strategies to manage the estrous cycle, the physiological processes of ovarian superstimulation using hormonal protocols (8), and various factors influencing embryo production (9), allowing a choice of strategies and the early control of factors that can improve embryo yield [Bo (10)]. Among the various factors influencing the *in vivo* production of bovine embryos (9, 10), the antral follicle count (AFC) stands out as one of the most significant and is closely related to donor selection (7). Once a female's high genetic potential is confirmed (11), AFC can serve as a criterion for selecting donors with a high AFC (6, 12). A significant correlation ($r = 0.88$) has been discovered between anti-Müllerian hormone (AMH) and AFC, with both being regarded as markers of ovarian response (13–15).

AFC and serum AMH levels are reproductive parameters that exhibit significant variability among females but demonstrate high consistency within the same animal (16, 17). Additionally, while AMH measurement requires laboratory analysis, the AFC can be assessed via a single ultrasound examination of both ovaries by a trained operator at any time in the cycle to classify females based on the AFC numbers (16). *Bos indicus* and *Bos taurus* cattle appear to have different fertility responses based on their AFC category. Moreover, females with high AFC showed a greater number of embryos produced by the donors in *Bos taurus* (18), crossbred *indicus-taurus* (17), and *Bos indicus* (19). Additionally, cows with high AFC had higher conception rates than those with low AFC (20, 21).

Considering the application of AFC as a valuable tool to assist cattle performance and reproductive biotechnology, thus the aim of this study was to determine follicular and luteal development in relation to AFC and its association with ovarian size, superovulatory response, and embryo quality and number in Sahiwal donor (*Bos indicus*) subjected to a MOET program.

2 Materials and methods

2.1 Location, animals, and management

A total of 48 Sahiwal cows (*Bos indicus*) of 1–4 parity, minimum 60 days postpartum, with a body condition score (BCS) between 3.5 and 4.0 on a scale of 1–5 (22) with a mean live weight 345 ± 6 kg (minimum 290, maximum 410 kg) acted as embryo donor. These cows were maintained at Cattle and Buffalo Farm, ICAR-IVRI, Izatnagar, located at an altitude of 564 meters above mean sea level, at latitude and longitude of 28° N and 79°E, respectively.

The total experiment was conducted during the winter months (November to March). All cows were fed 3.5–4.5 kg of concentrate feed per day, containing 20% digestible crude protein (DCP) and 70% total digestible nutrients (TDN), had *ad libitum* access to fresh drinking water, and wheat straw, and were provided green fodder twice a day. All the animals were maintained under hygienic and optimal management conditions in a semi-intensive system with access to a large, open paddock for free movement. Heat detection in the herd was carried out twice daily at 07:00 and 16:00 using a vasectomized bull (teaser) accompanied by skilled herdsmen. Health and vaccination protocols were followed as per the standard schedule of farm management.

2.2 Experimental design

A total of 48 estrus-induced (500 µg PGF2α, Estrumate™, MSD animal health, India, Single dose, IM) Sahiwal cows (*Bos indicus*) with a BCS between 3.5 and 4.0 were selected for the study from the herd. Both the right and left ovaries (the pair) were scanned ultrasonographically with a 7.5-MHz transducer (Exago ECM, France), and on the day of wave emergence, antral follicles (all follicles >2 mm) were counted to determine the total number of antral follicles as previously described by Morotti et al. (16).

Donors were categorized into two groups based on their AFC results. 48 donors were chosen from the herd, with 24 having a consistently low AFC (≤ 18 follicles; mean = 13.21 ± 0.90 follicles; range = 8–18 follicles) and the other 24 having a consistently high AFC (> 18 follicles; mean = 30.08 ± 1.64 follicles; range = 19–46 follicles). Both groups were monitored daily using a B-mode ultrasonography (USG) for one cycle to record follicular and luteal development. The superovulation protocol was initiated on the ninth day of the following estrous cycle.

Intramuscular injections of STIMUFOL® (Reprobiol SPRL, Belgium), of a total dose of 240 µg in eight fragmented doses (45,45; 35,35; 25,25; 15,15 µg morning and evening) were given in tapering sequence for 4 days and simultaneous administration of 500 µg PGF2α, along with the 5th dose of FSH. Donors were inseminated during superovulatory estrus using double straws of high-quality frozen semen, thrice at 12 h. intervals. Non-surgical flushing of both horns was carried out on the 7th day of the superovulatory estrus (Figure 1) using a Woerlein catheter (IMV Technology, India), followed by embryo searching and evaluation under a stereo zoom microscope (SMZ 1000, Nikon, Japan). The embryo quality has been determined in accordance with the International Embryo Technology Society (IETS) standards.

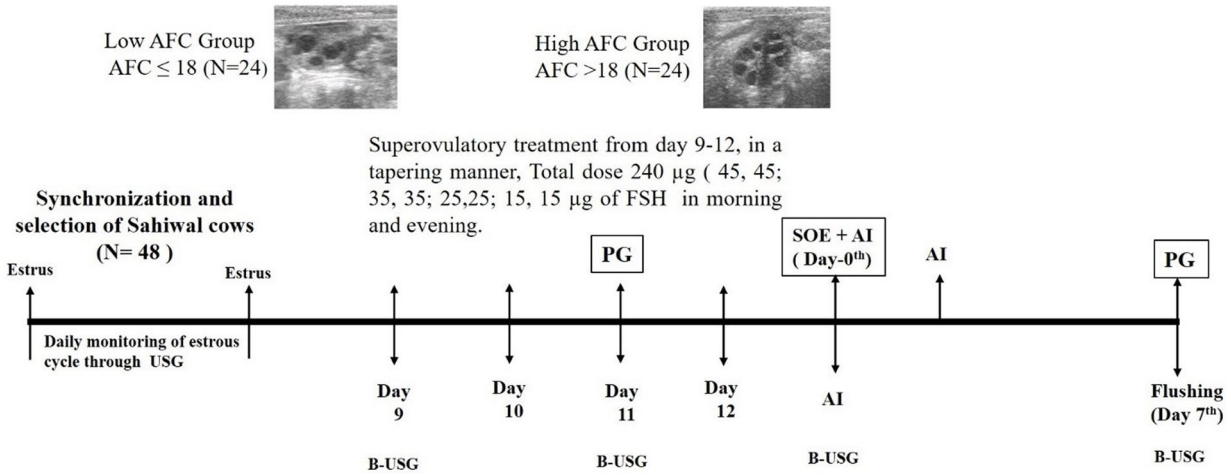

FIGURE 1
Experimental design, B-mode ultrasound monitoring of follicular and luteal development in high- and low-AFC Sahiwal cows (*Bos indicus*). Evaluations were performed at the same time, and ovulation was determined by the disappearance of POF in the ultrasound images. Superovulatory protocol was started on day 9 of the subsequent estrus. Non-surgical flushing was performed on day 7 post-superovulatory AI. AFC, Antral follicle count; USG, ultrasonography; PG, prostaglandin F2 alpha; SOE, superovulatory estrus; AI, artificial insemination.

2.3 Statistical analysis

All data from the high- and low-AFC groups were analyzed for mean and standard error (SE) using the GraphPad Prism 8.0.1 software module. The different follicular and luteal developmental attributes in both groups were analyzed using an unpaired *t*-test. The significance among different groups or days was assessed through *post-hoc* Tukey's testing. For descriptive analysis, the data were presented as the mean and standard (M ± SE). Pearson's correlation analysis was applied to explore the potential relationship of AFC with ovarian size, superovulatory response, and embryo production. The significance level for rejecting H0 (the null hypothesis) was 5%; therefore, a significance level of $p \leq 0.05$ was considered to indicate an effect of the categorical variables and their interaction, whereas a significance level of $p > 0.05$ indicated a lack of statistical significance.

3 Results

3.1 Follicular characteristics in non-ovulatory and ovulatory waves

The wave emergence in high-AFC Sahiwal cows was significantly ($p = 0.04$) earlier however, deviating late ($p = 0.03$) with a larger size of the dominant follicle in the non-ovulatory wave (Table 1). The follicular attributes of subordinate follicles of non-ovulatory waves of high- and low-AFC Sahiwal cattle did not vary significantly ($p > 0.05$) (Table 2). Similarly, ovulatory waves of high-AFC Sahiwal cows have significantly ($p = 0.04$) larger sizes of preovulatory follicles as compared to low-AFC Sahiwal cows (Table 3). Furthermore, the inter estrus period, inter ovulatory interval (Table 3), and various attributes of the subordinate follicle of ovulatory wave did not significantly differ ($p > 0.05$) between high- and low-AFC Sahiwal cows (Table 4).

TABLE 1 Follicular characteristics (Mean ± SEM) of non-ovulatory wave of high- and low-AFC Sahiwal cows.

Follicular characteristics	High AFC (*N* = 24)	Low AFC (*N* = 24)	*p*-value
Day of wave emergence	0.13 ± 0.15	0.67 ± 0.21	0.04
No. of follicles at wave emergence	29.5 ± 1.55	14.25 ± 0.73	0.00
Day of deviation	4.0 ± 0.30	3.29 ± 0.19	0.04
Diameter at deviation (mm)	8.39 ± 0.21	8.02 ± 0.18	0.18
Dominant follicle maximum diameter (mm)	11.95 ± 0.24	10.83 ± 0.16	0.03
Day of maximum diameter	6.83 ± 0.37	7.38 ± 0.42	0.34
Growth rate (mm/day)	1.07 ± 0.07	0.98 ± 0.03	0.28
Growth period (days)	5.54 ± 0.35	6.25 ± 0.33	0.15
Onset of regression (day)	8.00 ± 0.36	8.54 ± 0.38	0.31
Regression rate (mm/day)	0.89 ± 0.05	0.91 ± 0.06	0.77
Regression period (days)	6.21 ± 0.32	6.17 ± 0.42	0.94
Duration of wave (days)	12.50 ± 0.60	13.92 ± 0.60	0.10

N, Number of Sahiwal cows; AFC, antral follicle count; SEM, standard error of the mean.

3.2 Luteal characteristics of high- and low-AFC donors

The day of CL detection was significantly ($p = 0.03$) late with a larger ($p = 0.001$) diameter at detection as well as the maximum diameter ($p = 0.01$) of CL was reported in the high-AFC group (Table 5).

TABLE 2 Follicular characteristics (mean ± SEM) subordinate follicles of non-ovulatory wave of high- and low-AFC Sahiwal cows.

Follicular characteristics	High AFC (*N* = 24)	Low AFC (*N* = 24)	*P*-value
Subordinate follicle maximum diameter (mm)	7.16 ± 0.13	7.16 ± 0.16	0.97
Growth rate (mm/day)	0.78 ± 0.05	0.73 ± 0.03	0.51
Growth period (days)	3.00 ± 0.16	3.38 ± 0.25	0.21
Regression rate (mm/day)	0.83 ± 0.05	0.81 ± 0.04	0.81
Regression period (days)	2.88 ± 0.16	3.17 ± 0.12	0.15

N, Number of Sahiwal cows; AFC, antral follicle count; SEM, standard error of the mean.

TABLE 3 Follicular characteristics (mean ± SEM) of ovulatory wave of high- and low-AFC Sahiwal cows.

Follicular characteristics	High AFC (*N* = 24)	Low AFC (*N* = 24)	*P*-value
Day of wave emergence	10.96 ± 0.33	10.25 ± 0.31	0.13
No. of follicles at wave emergence	30.08 ± 1.64	13.21 ± 0.90	<0.0001
Day of deviation	14.75 ± 0.41	13.88 ± 0.32	0.10
Diameter at deviation (mm)	7.98 ± 0.20	8.03 ± 0.14	0.84
Growth rate (mm/day)	1.09 ± 0.06	0.95 ± 0.48	0.11
Duration of wave (days)	11.25 ± 0.49	11.92 ± 0.52	0.36
Size of preovulatory follicle (mm)	12.06 ± 0.19	11.56 ± 0.16	0.04
Day of maximum diameter of POF	20.21 ± 0.38	19.79 ± 0.59	0.56
Inter estrus period (days)	20.33 ± 0.21	19.71 ± 0.35	0.13
Inter-ovulatory interval (days)	21.38 ± 0.27	20.67 ± 0.40	0.15

N, Number of Sahiwal cows; AFC, antral follicle count; SEM, standard error of the mean.

TABLE 4 Follicular characteristics (mean ± SEM) subordinate follicles of ovulatory wave of high- and low-AFC Sahiwal cows.

Follicular characteristics	High AFC (*N* = 24)	Low AFC (*N* = 24)	*P*-value
Subordinate follicle maximum diameter (mm)	7.29 ± 0.10	7.1 ± 0.14	0.27
Growth rate (mm/day)	0.97 ± 0.06	0.81 ± 0.06	0.34
Growth period (days)	3.20 ± 0.22	3.29 ± 0.22	0.90
Regression rate (mm/day)	0.74 ± 0.04	0.78 ± 0.03	0.40
Regression period (days)	2.67 ± 0.13	2.58 ± 0.15	0.67

N, Number of Sahiwal cows; AFC, antral follicle count; SEM, standard error of the mean.

3.3 Ovarian size of high- and low-AFC donors

The ovarian size (diameter) of high-AFC Sahiwal donors showed significantly ($p < 0.0001$) larger measurements than low AFC on the day of estrus, during the superovulatory protocol, and on the day of flushing (Table 6).

3.4 Follicular development during the superovulatory period

Large, medium, and small follicles were significantly ($p < 0.0001$) higher on the day of superovulatory estrus (SOE), the day of PGF2α injection, and the day of initiation of superovulatory treatment, respectively, in high-AFC cattle than low-AFC cattle (Table 7). The low-AFC cattle attained significantly ($p = 0.03$) larger POF size at SOE than high AFC, and no significant ($p > 0.05$) differences were observed in medium-size follicles between the groups (Table 8).

3.5 Superovulatory response

The total number of CL was significantly ($p < 0.0001$) higher in high-AFC cattle; however, there was no significant ($p > 0.05$) difference in the diameter of CL between the groups on the day of flushing (Table 9).

3.6 Embryo production and quality

The number of embryos recovered per flushing with excellent and fair-quality embryos (Transferable) was significantly ($p \leq 0.05$) higher in high-AFC Sahiwal donors (Tables 10, 11). AFC was positively correlated to the ovarian size ($r = 0.9136$ $p < 0.0001$), superovulatory response ($r = 0.9350$ $p < 0.0001$), and embryo production ($r = 0.9858$ $p < 0.0001$) (Table 12).

4 Discussion

The present study reveals cows with high AFC showed larger POF, and follicles with large diameters before ovulation are associated with better reproductive performance in bovine females (23). According to USG studies, a high AFC may be related to superior reproductive performance, such as increased fertility, shorter open period, and higher reactivity to superovulation treatment in cows (21, 24, 25). In this regard, an increase in the number of 3–8-mm-sized antral follicles is expected to reflect the size of the ovaries. High AFC is related to several characteristics such as larger ovaries with higher possibilities of pregnancy toward the end of breeding seasons (21).

The number of follicles at wave emergence in both non-ovulatory and ovulatory waves of high-AFC cattle was comparable to the findings of Morotti et al. (11) and de Lima et al. (26) in Nelore cows and higher than in Holstein cows (27, 28). Furthermore, Ireland et al. (24) also recorded similar results in beef heifers and stated that the number of total follicles during the non-ovulatory and ovulatory waves were 2-fold higher in the high-AFC group than in the low-AFC group. A high degree of variability in AFC is evident and can be attributed to multiple factors such as the day of the estrous cycle (18), age (29), and the body condition of the animal (30, 31), genetics (32), maternal

TABLE 5 Luteal characteristics (Mean ± SEM) during estrous cycle of high- and low-AFC Sahiwal cows.

Luteal characteristics	High AFC (*N* = 24)	Low AFC (*N* = 24)	*P*-value
Day of detection of CL	3.13 ± 0.20	2.42 ± 0.24	0.03
Diameter at detection (mm)	10.04 ± 0.37	9.12 ± 0.19	0.001
Day of maximum diameter of CL	12.42 ± 0.44	12.13 ± 0.68	0.72
Maximum diameter of CL (mm)	19.57 ± 0.28	18.26 ± 0.35	0.01
CL growth rate (mm/day)	1.09 ± 0.09	0.97 ± 0.08	0.34
Growth period (day)	9.33 ± 0.46	10.58 ± 0.52	0.08
Regression rate (mm/day)	0.93 ± 0.04	1.38 ± 0.07	<0.0001
Regression period (day)	6.50 ± 0.41	5.75 ± 0.30	0.15
Lifespan of CL (day)	18.00 ± 0.39	18.71 ± 0.50	0.27

N, Number of Sahiwal cows; AFC, antral follicle count; SEM, standard error of the mean.

TABLE 6 Effect of AFC on ovarian size (mm) during superovulatory protocol (mean ± SE) in Sahiwal cows.

Different days of super ovulatory protocol	High AFC (N = 24)	Low AFC (N = 24)	*P*-value
D-estrus	22.49 ± 0.32	20.78 ± 0.20	<0.0001
D1-FSH	23.42 ± 0.27	21.12 ± 0.24	<0.0001
D-PG	26.81 ± 0.41	24.27 ± 0.35	<0.0001
D-SOE	33.33 ± 0.37	27.81 ± 0.34	<0.0001
D-flushing	41.95 ± 0.75	32.61 ± 0.58	<0.0001

D-estrus, Day of estrus; D1-FSH, day of initiation of superovulatory treatment; D-PG, day of prostaglandin injection; D-SOE, day of superovulatory estrus; N, number of Sahiwal cows; AFC, antral follicle count; SEM, standard error of the mean.

TABLE 7 Various types of follicles (mean ± SEM) at different days of superovulatory protocol in high- and low-AFC Sahiwal cows.

Different days of superovulatory protocol	High AFC (*N* = 24)	Low AFC (*N* = 24)	*P*-value
Large-size follicle			
D1-FSH	0.71 ± 0.09	0.67 ± 0.13	0.80
D-PG	2.46 ± 0.26	1.71 ± 0.16	0.02
D-SOE	15.83 ± 1.04	8.92 ± 0.68	<0.0001
Medium-size follicle			
D1-FSH	2.29 ± 0.37	1.29 ± 0.11	0.02
D-PG	17.25 ± 1.17	9.08 ± 0.57	<0.0001
D-SOE	3.21 ± 0.23	2.79 ± 0.17	0.16
Small-size follicle			
D1-FSH	24.42 ± 1.32	12.75 ± 0.63	<0.0001
D-PG	3.46 ± 0.52	3.12 ± 0.22	0.56

D1-FSH, Day of initiation of superovulatory treatment; D-PG, day of prostaglandin injection; D-SOE, day of superovulatory estrus; N, number of Sahiwal cows; AFC, antral follicle count; SEM, standard error of the mean.

environment, and health (13, 20, 33). In the present study, cattle with high AFC exhibited a larger size of the dominant follicle, which is contradictory to the findings of Santos et al. (19) in Indicus-taurus cows; Morotti et al. (11) and de Lima et al. (26) in Nelore cows; and Bonato et al. (27) in Holstein cows noticed that cows with low AFC exhibited larger preovulatory follicles than high-AFC cows. Larger POF diameter in low-AFC cattle has been attributed to fewer follicles receiving gonadotropin stimulation, it is possible to expect that each follicle would obtain a larger amount of FSH at the emergence of the follicular wave. Conversely, those females with a high AFC would have more follicles to share the same amount of gonadotropins (14, 26). Larger size preovulatory follicles in the high-AFC group of the present study might be due to the large number of granulosa cells and higher concentration of estradiol (28). Scheetz et al. (34) reported that the cultured granulosa cells derived from the low-AFC cows showed lower secretion of estradiol, which is essential for granulosa cell proliferation. Angiogenic factors, such as endothelial nitric oxide synthase (eNOS), are expressed in ovarian follicles and involved in folliculogenesis, steroidogenesis, oocyte maturation, ovulation, and ultimately embryo development through the production of a free radical gas, nitric oxide (NO) (35–38). No significant difference in the diameter of subordinate follicles between the groups is in agreement with Burns et al. (29) and Ireland et al. (24) in beef heifers. In the present study, significant differences in the day and diameter of CL at detection with early detection in the low-AFC group were recorded. The maximum diameter of CL differed significantly between the groups with greater diameter in the high-AFC group that exhibited a larger diameter of POF. Similar findings were reported by Vasconcelos et al. (39) and Baruselli et al. (40) that ovulation of smaller size preovulatory follicles results in smaller CL that secrete less progesterone compared to larger CL. The difference in the diameter of CL may be due to the difference in the size of the preovulatory follicle. In contrast to the present study, Bonato et al. (27) in Holstein cows and Lima et al. (26) in *Bos indicus* found that cows with low AFC displayed larger preovulatory follicles and CL in comparison with the high-AFC group. The larger diameter and relatively faster growth rate of CL in the high-AFC group are probably due to the high vascularity of granulosa cells with increased angiogenic and growth factors in developing CL.

The number of medium and large follicles on the day of PGF2α injection and SOE were significantly high in the high-AFC group as compared to the low-AFC group, respectively. Corresponding to the present findings, Singh et al. (41) reported a positive correlation between the numbers of follicles measuring 5–7 mm and > 8 mm or larger at the end of the ovarian superstimulation process in the high-AFC crossbred Hereford cows than the low AFC. The larger size of medium and large follicles on the day of SOE corresponds to the findings of Tessaro et al. (42) reported that the greater size of large and medium follicles may be attributed to increased blood flow rates in developing follicles of high-AFC animals.

We recorded a significant difference in the total number of CL on the day of flushing and the mean value was greater in the high-AFC group than the low-AFC group, which aligned with the results of Ireland et al. (24) who documented that following ovarian stimulation the taurus donors with a high AFC had a greater number of CL than those with a low AFC on the day of flushing. Similar results were

TABLE 8 Size of various types of follicles (mean ± SEM) at different days of superovulatory protocol in high- and low-AFC Sahiwal cows.

Different days of superovulatory protocol	High AFC (*N* = 24)	Low AFC (*N* = 24)	*P*-value
Large-size follicle (mm)			
D1-FSH	9.07 ± 0.93(n = 20)	9.21 ± 0.97(n = 19)	0.35
D-PG	9.48 ± 0.43	9.72 ± 0.16	0.61
D-SOE	10.34 ± 0.10	10.70 ± 0.12	0.03
Medium-size follicle (mm)			
D1-FSH	6.63 ± 0.53	7.07 ± 0.33	0.51
D-PG	7.34 ± 0.09	7.25 ± 0.09	0.53
D-SOE	7.56 ± 0.18	7.37 ± 0.45	0.47

D1-FSH, Day of initiation of superovulatory treatment; D-PG, day of prostaglandin injection; D-SOE, day of superovulatory estrus; N, number of Sahiwal cows; AFC, antral follicle count; SEM, standard error of the mean.

TABLE 9 Effect of AFC on superovulatory response (mean ± SEM) in Sahiwal cows.

Parameters (on the day of flushing)	High AFC (*N* = 24)	Low AFC (*N* = 24)	*P*-value
Number of CL	11.25 ± 0.69	6.04 ± 0.46	<0.0001
Mean diameter of CL (mm)	12.88 ± 0.25	12.24 ± 0.25	0.08

N, Number of Sahiwal cows; AFC, antral follicle count; SEM, standard error of the mean; CL, corpus luteum.

TABLE 10 Effect of AFC on embryo recovered per flushing and its quality (mean ± SE) in Sahiwal cows.

Parameters	High AFC (N = 15)	Low AFC (*N* = 17)	*P*-value
Embryo recovered per flushing	7.46 ± 1.12	3.88 ± 0.42	0.0039
Embryo quality			
Excellent or good	4.4 ± 0.67	2.29 ± 0.50	0.0161
Fair	1.6 ± 0.34	0.71 ± 0.21	0.0191
Poor	0.66 ± 0.12	0.81 ± 0.18	0.529
Dead and degenerated	0.33 ± 0.12	0.35 ± 0.11	0.9109

N, Number of Sahiwal cows flushed; AFC, antral follicle count; SEM, standard error of the mean.

TABLE 11 Effect of AFC on total recovered embryo and its quality in Sahiwal cows.

Parameters	High AFC (*N* = 15)	Low AFC (*N* = 17)	*P*-value
Total no. of embryos recovered	112	66	$X^{2(df,1)} = 8.788^{a}$
Embryo quality			*P* = 0.032 Likelihood ratio = 0.036 Linear-by-Linear Association = 0.005
Excellent or good	63.39% (71/112)	48.4% (32/66)	
Fair	25% (28/112)	22.7% (15/66)	
Poor	8.9% (10/112)	19.6% (13/66)	
Dead and degenerated	4.4% (3/112)	9.09% (6/66)	

N, Number of Sahiwal cows flushed; AFC, antral follicle count; SEM, standard error of the mean.

TABLE 12 Pearson's correlation (r) for the association of AFC with ovarian size, superovulatory response, and embryo production and the significance score for each variable.

Variable	Ovarian size		Superovulatory response		Embryo production	
	r	*p*	*r*	*p*	*r*	*p*
High AFC	0.9136	<0.0001	0.9350	<0.0001	0.9858	<0.0001
Low AFC	0.9011	<0.0001	0.9304	<0.0001	0.9589	<0.0001

reported in Sahiwal (43) and in Nelore donors (7). Center et al. (44) recorded that the high-AFC cows expressed greater superovulatory response and produced a higher number of embryos as compared to low-AFC cows.

Ovarian follicular population or reserve is directly associated with superovulatory response. The AFC at the time of the start of FSH administration had a positive and significant correlation with the superovulatory response, indicating that cows having higher AFC at the start of FSH, developed more CL (18, 19). The growth of small antral follicles and their maturation and ovulation is supported by exogenous FSH and PMSG causing multiple ovulations therefore the population of small antral follicles at the beginning of stimulation is positively correlated with superovulatory response (19).

The ovarian size (diameter) of high-AFC Sahiwal donors showed significantly larger measurements than low AFC on the day of estrus, during the superovulatory protocol, and on the day of flushing. This is in accordance with the findings of Ireland et al. (18), who reported that animals with a consistently low AFC had significantly smaller wet weights of ovaries as well as smaller ovarian heights and lengths than those with a high AFC during follicular waves in Hereford x Angus x Charolais crossbred beef heifers. Morotti et al. (16) observed similar results in *Bos indicus* cattle, finding that cows with a high AFC had a larger diameter and ovarian area than those with a low AFC. Martinez et al. (45) found a similar correlation between AFC and ovarian area in *Bos taurus* cattle.

The high-AFC group yielded a greater number of total embryos, embryos recovered per flushing, excellent, and fair-quality (transferable) embryos, and a smaller proportion of poor and dead or degenerated embryos as compared to low-AFC Sahiwal donors. This is in agreement with a previous study by Morotti et al. (14). They pointed out that the early embryos retrieved on day 7 were greater in number and their quality was significantly better in donors belonging to the high-AFC group than those in the low-AFC group.

A positive and significant correlation of AFC with ovarian size, superovulatory response, and total embryo production with a higher number of transferable embryos was recorded in the Sahiwal donor of the present study. Morotti et al. (46) observed comparable results in Indicus-Taurus animals, where they found that donors with high AFC had a notably greater number of embryos per collection (6.9 ± 5.3) in

contrast to those with lower AFC (1.9 ± 2.1). Silva-Santos et al. (17) also reported comparable results in Braford donors. On the other hand, Lollato et al. (7) reported contradictory findings regarding embryo production and quality. They noted that Nelore donors with either low or high AFC showed comparable outcomes regarding the total counts of viable and freezable embryos, along with the incidence of degenerated embryos.

A positive but non-significant result between the AFC group and the total number of recovered and transferable embryos was reported by Imtiyaz et al. (43). Similar findings have been noted in *in vitro* embryo production (IVEP), where donors with a high AFC demonstrated significantly higher production of oocytes and embryos via ovum pick up (OPU) in both *Bos taurus* and *Bos indicus* cattle (12, 17, 19, 47). This observation could be explained by the higher proportion of mature oocytes in the high-AFC group, which exhibited increased mitochondrial activity prior to maturation. This led to enhanced ova viability and higher rates of cleavage and blastocyst development (6, 48). Another possible reason for the superior embryo quality in high-AFC donors could be linked to changes in lipid composition. Rosa et al. (49) found that embryos retrieved from high-AFC Nelore donors exhibited increased triglyceride levels and decreased concentrations of cholesterol and diacylglycerol compared to embryos from low-AFC cows. Similarly, Idrissi et al. (50) observed analogous results, noting increased triglyceride levels and decreased diacylglycerol concentrations in grade 1 bovine embryos.

5 Conclusion

The result of this study demonstrates that high-AFC Sahiwal cows have a larger diameter of preovulatory follicles and greater corpus luteum size. The antral follicle population showed a strong positive correlation with ovarian size, superovulatory response, and embryo production with more transferable embryos. Based on these findings, AFC is concluded to be a reliable phenotypic marker to predict the reproductive potential of Sahiwal donors. This is a crucial factor to take into account in commercial programs aiming for *in vivo* embryo production.

Data availability statement

The original contributions presented in the study are included in the article/supplementary material, further inquiries can be directed to the corresponding author.

Ethics statement

All experimental procedures were conducted following the Institute Animal Ethics Committee of ICAR-Indian Veterinary Research Institute, Izatnagar (ICAR-IVRI), U.P. India (26–3/2020-21/JD(R)/IAEC). The study was conducted in accordance with the local legislation and institutional requirements.

Author contributions

MG: Conceptualization, Data curation, Investigation, Methodology, Supervision, Writing – review & editing. BK: Conceptualization, Investigation, Software, Writing – original draft. SM: Conceptualization, Data curation, Investigation, Supervision, Writing – original draft. PC: Conceptualization, Formal analysis, Investigation, Methodology, Validation, Writing – review & editing. KK: Data curation, Formal analysis, Investigation, Methodology, Writing – original draft. MD: Conceptualization, Data curation, Methodology, Validation, Writing – review & editing. VY: Conceptualization, Data curation, Methodology, Validation, Writing – original draft. BY: Data curation, Investigation, Supervision, Validation, Writing – review & editing. CW: Data curation, Formal analysis, Investigation, Writing – review & editing. NK: Conceptualization, Investigation, Methodology, Project administration, Visualization, Writing – review & editing. DY: Conceptualization, Data curation, Supervision, Visualization, Writing – review & editing. SS: Investigation, Methodology, Project administration, Software, Validation, Writing – review & editing. VC: Conceptualization, Investigation, Methodology, Validation, Writing – review & editing. SKS: Investigation, Project administration, Resources, Software, Supervision, Visualization, Writing – review & editing. MK: Project administration, Resources, Supervision, Validation, Writing – review & editing.

Funding

The author(s) declare that no financial support was received for the research, authorship, and/or publication of this article.

Acknowledgments

The authors would like to thank the Director and In-charge of Cattle and Buffalo Farm, ICAR-IVRI, Izatnagar, India, for facilitating the study.

Conflict of interest

The authors declare that the research was conducted in the absence of any commercial or financial relationships that could be construed as a potential conflict of interest.

Publisher's note

References

1. Viana J. Statistics of embryo production and transfer in domestic farm animals. *Embryo Technol Newsl*. (2019) 36:17.

2. Gobikrushanth M, Purfield DC, Colazo MG, Butler ST, Wang Z, Ambrose DJ. The relationship between serum anti-Müllerian hormone concentrations and fertility, and genome-wide associations for anti-Müllerian hormone in Holstein cows. *J Dairy Sci*. (2018) 101:7563–74. doi: 10.3168/jds.2017-13940

3. Nawaz MY, Jimenez-Krassel F, Steibel JP, Lu Y, Baktula A, Vukasinovic N, et al. Genomic heritability and genome-wide association analysis of anti-Müllerian hormone in Holstein dairy heifers. *J Dairy Sci*. (2018) 101:8063–75. doi: 10.3168/jds.2018-14798

4. González-Bulnes A, Baird DT, Campbell BK, Cocero MJ, García-García RM, Inskeep EK, et al. Multiple factors affecting the efficiency of multiple ovulation and embryo transfer in sheep and goats. *Reprod Fertil Dev*. (2004) 16:421–35. doi: 10.1071/RD04033

5. Bartlewski PM, Seaton P, Franco Oliveira ME, Kridli RT, Murawski M, Schwarz T. Intrinsic determinants and predictors of superovulatory yields in sheep: circulating concentrations of reproductive hormones, ovarian status, and antral follicular blood flow. *Theriogenology*. (2016) 86:130–43. doi: 10.1016/j.theriogenology.2016.04.024

6. Alward KJ, Cockrum RR, Ealy AD. Associations of antral follicle count with fertility in cattle. *J Dairy Sci Commun*. (2023) 4:132–7. doi: 10.3168/jdsc.2022-0283

7. Lollato JPM, Souza ACC, Silva RCP, Marques MO, Crozara AS, Gonçalves RL, et al. In vivo embryo production in bovine donors with low and high antral follicle counts superovulated with low and high FSH doses. *Livest Sci*. (2022) 262:104985. doi: 10.1016/j.livsci.2022.104985

8. Baruselli P, Ferreira R, Sales J, Gimenes L, Sá Filho MF, Martins CM, et al. Timed embryo transfer programs for management of donor and recipient cattle. *Theriogenology*. (2011) 76:1583–93. doi: 10.1016/j.theriogenology.2011.06.006

9. Mikkola M, Hasler JF, Taponen J. Factors affecting embryo production in superovulated *Bos taurus* cattle. *Reprod Fertil Dev*. (2020) 32:104–24. doi: 10.1071/RD19279

10. Bó GA, Mapletoft RJ. Superstimulation of ovarian follicles in cattle: gonadotropin treatment protocols and FSH profiles. *Theriogenology*. (2020) 150:353–9. doi: 10.1016/j.theriogenology.2020.02.001

11. Morotti F, Santos GMG, Koetz Júnior C, Silva-Santos KC, Roso VM, Seneda MM. Correlation between phenotype, genotype and antral follicle population in beef heifers. *Theriogenology*. (2017a) 91:21–6. doi: 10.1016/j.theriogenology.2016.12.025

12. Garcia SM, Morotti F, Cavalieri FLB, Lunardelli PA, de Oliveira Santos A, Membrive CMB, et al. Synchronization of stage of follicle development before OPU improves embryo production in cows with large antral follicle counts. *Anim Reprod Sci*. (2020) 221:106601. doi: 10.1016/j.anireprosci.2020.106601

13. Ireland JJ, Smith GW, Scheetz D, Jimenez-Krassel F, Folger JK, Ireland JLH, et al. Does size matter in females? An overview of the impact of the high variation in the ovarian reserve on ovarian function and fertility, utility of anti-Müllerian hormone as a diagnostic marker for fertility and causes of variation in the ovarian reserve in cattle. *Reprod Fertil Dev*. (2010) 23:1–14. doi: 10.1071/RD10226

14. Morotti F, Zangirolamo AF, da Silva NC, da Silva CB, Rosa CO, Seneda MM. Antral follicle count in cattle: advantages, challenges, and controversy. *Anim Reprod*. (2017b) 14:514–20. doi: 10.21451/1984-3143-AR994

15. Zangirolamo AF, Morotti F, da Silva NC, Sanches TK, Seneda MM. Ovarian antral follicle populations and embryo production in cattle. *Anim Reprod*. (2018) 15:310–5. doi: 10.21451/1984-3143-AR2018-0072

16. Morotti F, Moretti R, Dos Santos GMG, Silva-Santos KC, Cerqueira PHR, Seneda MM. Ovarian follicular dynamics and conception rate in *Bos indicus* cows with different antral follicle counts subjected to timed artificial insemination. *Anim Reprod Sci*. (2018) 188:170–7. doi: 10.1016/j.anireprosci.2017.12.001

17. Silva-Santos KC, Santos GM, Koetz Junior C, Morotti F, Siloto LS, Marcantonio TN, et al. Antral follicle populations and embryo production in vitro and in vivo of *Bos indicus* taurus donors from weaning to yearling ages. *Reprod Domest Anim*. (2014) 49:228–32. doi: 10.1111/rda.12255

18. Ireland JLH, Scheetz D, Jimenez-Krassel F, Themmen APN, Ward F, Lonergan P, et al. Antral follicle count reliably predicts number of morphologically healthy oocytes and follicles in ovaries of young adult cattle. *Biol Reprod*. (2008) 79:1219–25. doi: 10.1095/biolreprod.108.071670

19. Santos-Dos GMG, Silva-Santos KC, Barreiros TRR, Morotti F, Sanches BV, de Moraes FLZ, et al. High numbers of antral follicles are positively associated with in vitro embryo production but not the conception rate for FTAI in Nelore cattle. *Anim Reprod Sci*. (2016) 165:17–21. doi: 10.1016/j.anireprosci.2015.11.024

20. Evans ACO, Mossa F, Walsh SW, Scheetz D, Jimenez-Krassel F, Ireland JLH, et al. Effects of maternal environment during gestation on ovarian folliculogenesis and consequences for fertility in bovine offspring. *Reprod Domest Anim*. (2012) 47:31–7. doi: 10.1111/j.1439-0531.2012.02052.x

21. Mossa F, Walsh SW, Butler ST, Berry DP, Carter F, Lonergan P, et al. Low numbers of ovarian follicles ≥ 3 mm in diameter are associated with low fertility in dairy cows. *J Dairy Sci*. (2012) 95:2355–61. doi: 10.3168/jds.2011-4325

22. Broster WH, Broster VJ. Body score of dairy cows. *J Dairy Res*. (1998) 65:155–73. doi: 10.1017/S0022029997002550

23. Pfeifer LFM, Leal SCBS, Schneider A, Schmitt E, Corrêa MN. Effect of the ovulatory follicle diameter and progesterone concentration on the pregnancy rate of fixed-time inseminated lactating beef cows. *Rev Bras de Zootec*. (2012) 41:1004–8. doi: 10.1590/S1516-35982012000400024

24. Ireland JJ, Ward F, Jimenez-Krassel F, Ireland JL, Smith GW, Lonergan P, et al. Follicle numbers are highly repeatable within individual animals but are inversely correlated with FSH concentrations and the proportion of good quality embryos after ovarian stimulation in cattle. *Hum Reprod*. (2007) 22:1687–95. doi: 10.1093/humrep/dem071

25. Sakaguchi K, Yanagawa Y, Yoshioka K, Suda T, Katagiri S, Nagano M. Relationships between the antral follicle count, steroidogenesis, and secretion of follicle-stimulating hormone and anti-Müllerian hormone during follicular growth in cattle. *Reprod Biol Endocrinol*. (2019) 17:88–13. doi: 10.1186/s12958-019-0534-3

26. de Lima MA, Morotti F, Bayeux BM, de Rezende RG, Botigelli RC, de Bem THC, et al. Ovarian follicular dynamics, progesterone concentrations, pregnancy rates and transcriptional patterns in *Bos indicus* females with a high or low antral follicle count. *Sci Rep*. (2020) 10:19557. doi: 10.1038/s41598-020-76601-5

27. Bonato DV, Ferreira EB, Gomes DN, Bonato FGC, Droher RG, Morotti F, et al. Follicular dynamics, luteal characteristics, and progesterone concentrations in synchronized lactating Holstein cows with high and low antral follicle counts. *Theriogenology*. (2022) 179:223–9. doi: 10.1016/j.theriogenology.2021.12.006

28. Nagai K, Yanagawa Y, Katagiri S, Nagano M. The relationship between antral follicle count in a bovine ovary and developmental competence of in vitro-grown oocytes derived from early antral follicles. *Biomed Res J*. (2016) 37:63–71. doi: 10.2220/biomedres.37.63

29. Burns DS, Jimenez-Krassel F, Ireland JL, Knight PG, Ireland JJ. Numbers of antral follicles during follicular waves in cattle: evidence for high variation among animals, very high repeatability in individuals, and an inverse association with serum follicle-stimulating hormone concentrations. *Biol Reprod*. (2005) 73:54–62. doi: 10.1095/biolreprod.104.036277

30. Cushman RA, McNeel AK, Freetly HC. The impact of cow nutrient status during the second and third trimesters on age at puberty, antral follicle count, and fertility of daughters. *Livest Sci*. (2014) 162:252–8. doi: 10.1016/j.livsci.2014.01.033

31. de Moraes FLZ, Morotti F, Costa CB, Lunardelli PA, Seneda MM. Relationships between antral follicle count, body condition, and pregnancy rates after timed-AI in *Bos indicus* cattle. *Theriogenology*. (2019) 136:10–4. doi: 10.1016/j.theriogenology.2019.06.024

32. Walsh SW, Mossa F, Butler ST, Berry DP, Scheetz D, Jimenez-Krassel F, et al. Heritability and impact of environmental effects during pregnancy on antral follicle count in cattle. *J Dairy Sci*. (2014) 97:4503–11. doi: 10.3168/jds.2013-7758

33. Pancarci SM, Arı UÇ, Atakişi O, Güngör Ö, Çiğremiş Y, Bollwein H. Nitric oxide concentrations, estradiol-17 beta progesterone ratio in follicular fluid, and COC quality with respect to perifollicular blood flow in cows. *Anim Reprod Sci*. (2012) 130:9–15. doi: 10.1016/j.anireprosci.2011.12.013

34. Scheetz D, Folger JK, Smith GW, Ireland JJ. Granulosa cells are refractory to FSH action in individuals with a low antral follicle count. *Reprod Fertil Dev*. (2012) 24:327–36. doi: 10.1071/RD11020

35. Grazul-Bilska AT, Navanukraw C, Johnson ML, Arnold DA, Reynolds LP, Redmer DA. Expression of endothelial nitric oxide synthase in the ovine ovary throughout the estrous cycle. *Reproduction*. (2006) 132:579–87. doi: 10.1530/REP-06-0009

36. Pancarci ŞM, Güngör Ö, Atakişi O, Çiğremiş Y, Arı UÇ, Bollwein H. Changes in follicular blood flow and nitric oxide levels in follicular fluid during follicular deviation in cows. *Anim Reprod Sci*. (2011) 123:149–56. doi: 10.1016/j.anireprosci.2011.01.001

37. Rosselli M, Keller PJ, Dubey RK. Role of nitric oxide in the biology, physiology and pathophysiology of reproduction. *Hum Reprod*. (1998) 4:3–24. doi: 10.1093/humupd/4.1.3

38. Thaler CD, Epel D. Nitric oxide in oocyte maturation, ovulation, fertilization, cleavage and implantation: a little dab'll do ya. *Curr Pharm Des*. (2003) 9:399–409. doi: 10.2174/1381612033391748

39. Vasconcelos JLM, Sartori R, Oliveira HN, Guenther JG, Wiltbank MC. Reduction in size of the ovulatory follicle reduces subsequent luteal size and pregnancy rate. *Theriogenology*. (2001) 56:307–14. doi: 10.1016/S0093-691X(01)00565-9

40. Baruselli PS, Sales JNS, Sala RV, Vieira LM, Sá Filho MFD. History, evolution and perspectives of timed artificial insemination programs in Brazil. *Anim Reprod*. (2012) 9:139–52.

41. Singh J, Domínguez M, Jaiswal R, Adams GP. A simple ultrasound test to predict the superstimulatory response in cattle. *Theriogenology*. (2004) 62:227–43. doi: 10.1016/j.theriogenology.2003.09.020

42. Tessaro I, Luciano AM, Franciosi F, Lodde V, Corbani D, Modina SC. The endothelial nitric oxide synthase/nitric oxide system is involved in the defective quality of bovine oocytes from low mid-antral follicle count ovaries. *J Anim Sci*. (2011) 89:2389–96. doi: 10.2527/jas.2010-3714

43. Imtiyaz N, Brar PS, Singh N, Singh H, Singhal S, Malik VS. Relationship of antral follicle count, plasma Estradiol and progesterone levels with super ovulatory response and embryo production in Sahiwal cows. *Int J Curr Microbiol App Sci*. (2020) 9:352–9. doi: 10.20546/ijcmas.2020.906.046

44. Center K, Dixon D, Looney C, Rorie R. Anti-Mullerian hormone and follicle counts as predictors of superovulatory response and embryo production in beef cattle. *Adv Reprod Sci*. (2018) 6:22–33. doi: 10.4236/arsci.2018.61003

45. Martinez MF, Sanderson N, Quirke LD, Lawrence SB, Juengel JL. Association between antral follicle count and reproductive measures in New Zealand lactating dairy cows maintained in a pasture-based production system. *Theriogenology*. (2016) 85:466–75. doi: 10.1016/j.theriogenology.2015.09.026

46. Morotti F, Barreiros TRR, Machado FZ, González SM, Marinho LSR, Seneda MM. Is the number of antral follicles an interesting selection criterium for fertility in cattle? *Anim Reprod Sci*. (2015) 12:479–86.

47. Pontes JHF, Nonato-Junior I, Sanches BV, Ereno-Junior JC, Uvo S, Barreiros TRR, et al. Comparison of embryo yield and pregnancy rate between in vivo and in vitro methods in the same Nelore (*Bos indicus*) donor cows. *Theriogenology*. (2009) 71:690–7. doi: 10.1016/j.theriogenology.2008.09.031

48. Faria ACF, de Moraes GF, Pereira LS, Cunha RR, dos Santos RM. Influence of antral follicle count on in vitro embryo production, sexual precocity and conception rate of Senepol cattle. *Anim Prod Sci*. (2021) 61:1418–24. doi: 10.1071/AN20355

49. Rosa CO, Costa CB, de Lima CB, da Silva CB, Zangirolamo AF, Ferreira CR, et al. Lipid profile of in vitro embryos produced from *Bos indicus* cows with low and high antral follicle counts. *Livest Sci*. (2021) 250:104586. doi: 10.1016/j.livsci.2021.104586

50. Idrissi- Janati S, Le Bourhis D, Lefevre A, Emond P, Le Berre L, Desnoës O, et al. Lipid profile of bovine grade-1 blastocysts produced either in vivo or in vitro before and after slow freezing process. *Sci Rep*. (2021) 11:11618. doi: 10.1038/s41598-021-90870-8

frontiers | Frontiers in Veterinary Science

TYPE Original Research
PUBLISHED 13 November 2024
DOI 10.3389/fvets.2024.1499266

OPEN ACCESS

EDITED BY
Graça Lopes,
University of Porto, Portugal

REVIEWED BY
Viola Zappone,
University of Messina, Italy
Luisa Mateus,
University of Lisbon, Portugal

*CORRESPONDENCE
Guillaume Domain
guillaume.domain@ugent.be

RECEIVED 20 September 2024
ACCEPTED 28 October 2024
PUBLISHED 13 November 2024

CITATION
Domain G, Kappen M, Van Mil A, De Beijer I, Van Puyvelde M, Van Leeuwenberg R, Spanoghe L, Posastiuc F and Van Soom A (2024) Rising trends in the use of frozen dog sperm: a retrospective study in Belgium and the Netherlands. *Front. Vet. Sci.* 11:1499266. doi: 10.3389/fvets.2024.1499266

Rising trends in the use of frozen dog sperm: a retrospective study in Belgium and the Netherlands

Guillaume Domain[1]*, Maarten Kappen[2], Amber Van Mil[2], Ilse De Beijer[2], Matthieu Van Puyvelde[1], Robby Van Leeuwenberg[1], Lotte Spanoghe[1], Florin Posastiuc[1] and Ann Van Soom[1]

[1]Department of Internal Medicine, Reproduction and Population Medicine, Faculty of Veterinary Medicine, Ghent University, Merelbeke, Belgium, [2]Cryolab Eersel B.V., Eersel, Netherlands

Introduction: Sperm cryopreservation is a valuable technique for storing valuable canine genetics. However, little is known concerning the fate of frozen sperm stored in a sperm bank. This study aimed to characterize dogs presented for sperm cryopreservation and describe the use and popularity of frozen sperm in the Netherlands and Belgium over recent years.

Methods: Medical records from dogs presented for sperm cryopreservation between January 1, 2014 and December 31, 2022 at two different freezing centers were reviewed retrospectively. Imported frozen sperm was excluded due to lack of usage information. Each sperm cryopreservation was considered a single event, and data were collected separately for each cryopreserved sample.

Results: A total of 3,090 ejaculates from 1,040 males of 157 different breeds were included and investigated using exploratory data analysis. The findings showed a steady rise in the popularity of sperm cryopreservation, with annual growth rates ranging from 8.4 to 41.9%. The majority of dogs (88.5%) were between 1 and 9 years old at the time of sperm cryopreservation, with nearly one-third aged 2–4 years. Most dogs were collected for sperm cryopreservation once (62.8%) or twice (21.6%). Sperm banks were used for both short- and long-term storage needs, and 6.83% of ejaculates were eventually discarded. The primary use of froze sperm was for international shipment, while 21.8% was used locally for artificial insemination. Depending on the year of cryopreservation, between 44.1 and 79.6% of frozen ejaculates remained unused or only partially used at the time of data collection.

Discussion: The results of this study provides the first comprehensive analysis of the use and popularity of frozen sperm among dog breeders in Belgium and the Netherlands and suggest a change in breeding practices in recent years. The percentage of breeders resorting to sperm cryopreservation and the extent of frozen sperm use in current breeding strategies remain to be defined in future studies.

KEYWORDS

sperm, cryopreservation, dog, storage, sperm bank

1 Introduction

Sperm cryopreservation offers the opportunity to preserve the gametes of dogs with high genetic or sentimental value and to overcome the temporal and geographical limits of traditional dog breeding (1–3). With advancements in insemination techniques and satisfactory pregnancy rates—approaching 80% following insemination with frozen-thawed sperm (4)—sperm cryopreservation has become increasingly

appealing to breeders, providing access to international markets and facilitating strategic breeding decisions, particularly in managing valuable bloodlines (5, 6).

Frozen sperm offers greater flexibility in breeding, allowing its use even after the dog has experienced age-related decline of fertility, sterility—whether pathological or elective—or even death (1, 7). It also enables the preservation of genetics from disease-free donors with valuable traits, making it possible to establish open access to these genetics when the owner does not wish to breed their dog (8). Transporting frozen sperm instead of live animals reduces stress, minimizes sanitary restrictions, and circumvents potential quarantine requirements associated with live animals transport (2, 7). Additionally, cryopreservation maximizes the return on an ejaculate, as it may be divided into insemination doses and used for different inseminations, sometimes several years apart. However, the efficiency of sperm cryopreservation depends on the quantity and quality of sperm before and after cryopreservation, which can vary significantly between dogs and individual ejaculates (9, 10).

The storage of frozen sperm in liquid nitrogen tanks has led to the development of dedicated facilities known as sperm banks. Initially established at universities, sperm banks have expanded to private companies that offer breeding services and manage the daily international trade of frozen sperm (11). Today, they play a crucial role in enhancing genetic diversity in dogs, particularly important among rare breeds and working dogs that are represented by a limited number of individuals, often geographically distant from one another (12). Dog breeders utilize sperm banks for both personal and commercial purposes, selling sperm to other breeders as opportunities arise. Recently, several assistance dog organizations have integrated sperm cryopreservation into their breeding strategies, freezing sperm from young male dogs before castration to preserve valuable genetics. Similarly, pet owners may seek sperm freezing services for their aging dogs when they wish to preserve the option of having a future litter but lack an immediate breeding opportunity, though sperm quality in elderly dogs is often insufficient for freezing (9, 10, 13).

While several studies have documented the satisfactory fertility results following artificial insemination with frozen-thawed sperm, the specific use and management of frozen dog sperm stored in a sperm bank remain to be described (5, 6, 14–16). This study aimed to characterize dogs presented for sperm cryopreservation and describe the use and popularity of frozen sperm in the Netherlands and Belgium over recent years.

2 Materials and methods

2.1 Patients and inclusion criteria

Medical records from two sperm freezing centers, Cryolab Eersel in the Netherlands and Ghent University in Belgium, were retrospectively reviewed in July 2023 to identify sperm freezing procedures conducted between January 1, 2014, and December 31, 2022. The start date was decided upon the availability of computerized medical records for all cryopreservation procedures, while the end date ensured adequate follow-up time for the use of frozen sperm. Exclusion criteria included imported frozen sperm due to incomplete data on the utilization of the entire ejaculate. Each sperm cryopreservation event was considered distinct, and data were recorded separately. In total, 3,090 ejaculates (2,957 from Cryolab and 133 from Ghent University) from 1,440 males of 157 different breeds recognized—either definitively or provisionally—by the Fédération Cynologique Internationale were included in the study. The most representative breeds were Belgian Shepherd Dogs—Malinois ($n = 215$), Golden Retriever ($n = 59$), Labrador Retriever ($n = 58$), German Shepherd ($n = 51$), Dutch Shepherd ($n = 42$), Border Collie ($n = 41$), Bullmastiff ($n = 39$), Belgian Shepherd Dogs—Tervueren ($n = 38$), French Bulldog ($n = 33$), and Rottweiler ($n = 31$). Detailed information on the number of dogs for each breed can be found in Supplementary Table 1.

2.2 Data collection

Data collected for each cryopreservation procedure included: the date of sperm collection, the birth date of the dog, breed, the number of straws frozen, detailed utilization of the frozen straws, and the number of remaining straws. From these data, additional data were calculated: the age of the dog at sperm collection, the number of freezing procedures per individual, the storage period before the first use, and the storage period before the last use if no straws remained.

If straws were discarded, the disposal date, number of discarded straws, and the reason for disposal were recorded. Subsequently, the storage period before disposal was calculated.

2.3 Statistical analysis

Data from the computerized record systems of both freezing centers were exported to a Microsoft Excel spreadsheet (Microsoft Corporation, Redmond, USA). Missing data ranged between 0 and 2.1% depending on the variable, and ejaculates with missing data were excluded from the analysis of the corresponding variable. Exploratory data analyses were performed using the Base and rstatix packages for descriptive statistics, while visualizations (histograms, box plots, and Q-Q plots) were created using ggplot2 (17). Results are presented as median and interquartile range (IQR). To examine trends in the number of cryopreserved ejaculates over time, a linear regression analysis was performed, with statistical significance set at $P < 0.05$.

3 Results

3.1 Popularity of sperm cryopreservation

Since 2014, the number of cryopreservations has increased steadily each year, with annual growth rates ranging from 8.5 to 41.9%. By 2019, the number of ejaculates cryopreserved was 2.4 times higher than in 2014. A sharp rise occurred between 2019 and 2021, nearly doubling (1.8×) within 2 years. However, in 2022, the number of freezing procedures decreased by 28.8% compared to 2021 (Figure 1; Supplementary Table 2). Despite the decline in 2022, linear regression analysis over the 9-year study confirmed a significant positive trend in cryopreserved ejaculates ($P < 0.001$), with an average annual increase of 52.32 ejaculates.

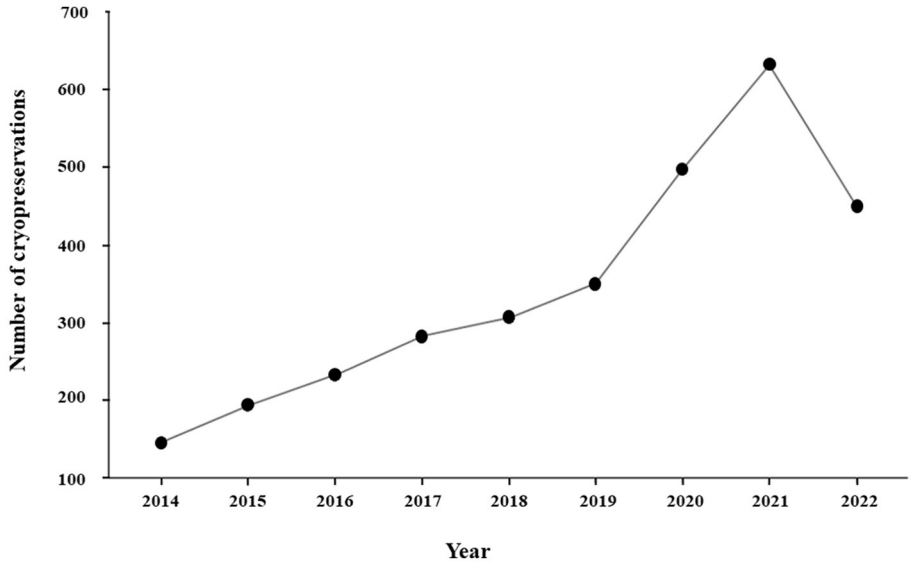

FIGURE 1
Evolution of the number of cryopreservations between 2014 and 2022.

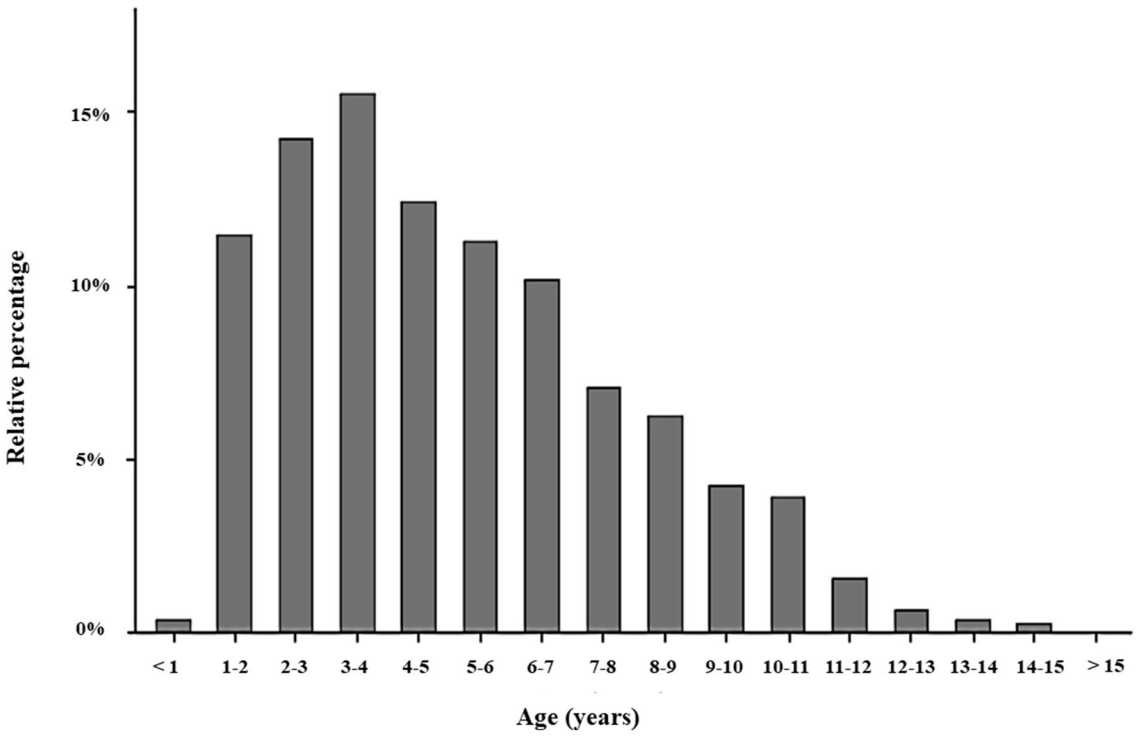

FIGURE 2
Bar plot representing the proportion of dogs, in %, for each age range at the time of sperm cryopreservation.

3.2 Age at collection

Dogs were collected for sperm cryopreservation at a median age of 55 months (IQR: 34–83 months), with ages ranging from 8 to 181 months. The majority of dogs (88.5%) were collected between 1 and 9 years of age, with a notable peak (15.6%) observed between 3 and 4 years. Nearly one-third of the dogs were collected between 2 and 4 years of age. A small proportion of dogs were collected before 1 year of age (0.4%) or after 11 years of age (2.9%) (Figure 2; Table 1).

TABLE 1 Frequency, relative percentage, and cumulative relative percentage of dogs for each age range at the time of sperm cryopreservation.

Age at collection (years)	Number of dogs	Relative percentage (%)	Cumulative relative percentage (%)
<1	12	0.40	0.40
1–2	347	11.46	11.86
2–3	431	14.24	26.10
3–4	471	15.56	41.66
4–5	376	12.42	54.08
5–6	342	11.30	65.38
6–7	308	10.18	75.55
7–8	214	7.07	82.62
8–9	190	6.28	88.90
9–10	129	4.26	93.16
10–11	119	3.93	97.09
11–12	48	1.59	98.68
12–13	20	0.66	99.34
13–14	11	0.36	99.70
14–15	8	0.26	99.97
15–16	1	0.03	100.00

3.3 Frequency of cryopreservation

The median number of cryopreservations per dog was 1 (IQR:1–2), ranging from 1 to 66. Most dogs had their sperm cryopreserved once (62.8%) or twice (21.6%), while only a small percentage (1.9%) had their sperm cryopreserved more than six times.

3.4 Use of frozen sperm

At the time of data analysis, 1,074 of the 3,090 frozen ejaculates (34.8%) were fully used, 626 (20.3%) were partially used, and 1,390 (45.0%) remained unused in the sperm banks. A total of 2,197 unique uses were recorded, comprising 1,605 international shipments (73.0%), 480 artificial inseminations (21.8%), and 112 national ownership transfers (5.1%).

When frozen ejaculates were exported, 59.7% were shipped as whole ejaculates (all the straws obtained from the ejaculate) after a median storage time of 60 days (IQR: 12–168) in the sperm bank. The most frequent destinations for international shipments were countries outside the European Union (EU) (Figure 3). When ejaculates were used at the freezing center, artificial inseminations were performed after a median storage period of 342 days (IQR: 114–1,084).

Over the 9-year study period, 211 ejaculates (6.8%) were discarded, primarily due to poor sperm quality after thawing. Other reasons included increased storage fee, identification of a (presumed) inherited condition in the male dog or previous litters, lack of need following a successful pregnancy or natural breeding availability, shifts in breeding strategies involving frozen sperm, or owner dissatisfaction with fertility results after artificial insemination. Discards occurred after a median storage time of 803 days (IQR: 403.5–1,273.5), mostly as whole ejaculates (69.2%).

The relative percentage of remaining ejaculates varied between 44.1 and 79.6% depending on the year of cryopreservation, with lower percentages observed for longer storage durations (Figure 4). Detailed year-by-year percentages of remaining frozen ejaculates are provided in Supplementary Table 2.

4 Discussion

The present study characterizes the population of dogs presented for sperm cryopreservation and highlights the growing popularity of this reproductive technology among breeders in the Netherlands and Belgium over the past 9 years. The consistent annual increase in sperm cryopreservation suggests a rising interest among dog breeders in enhancing their breeding program by incorporating genetic material from diverse and geographically distant bloodlines. This trend aligns with previous findings that reported increased gene flow between countries based on pedigree database analyses (18). However, it is important to consider that a potential increasing reputation of the freezing centers examined in this study may have also contributed to this upward trend.

The significant difference in the number of ejaculates collected by Cryolab (2,957) and Ghent University (133) could be attributed to several factors, including Belgium's smaller demographic size and the presence of multiple freezing centers, which likely diffuse the caseload. In contrast, Cryolab is the only dedicated freezing center in the Netherlands and a private veterinary practice with a strong focus on sperm freezing and international export, which likely attracts a higher volume of clients.

The breeds most represented in this study—Belgian Shepherd Dogs, Dutch Shepherds, and German Shepherds—are primarily working dog breeds known for their roles in police, military, and security services. Popular pet breeds, such as Golden Retrievers and Labrador Retrievers, were also well-represented. This breed distribution suggests that cryopreservation is gaining traction not only among working dog breeders but also among those of popular family pets.

The significant spike in sperm cryopreservations observed in 2020 and 2021 was likely influenced by the global COVID-19 pandemic, which caused a marked increase in the demand for puppies (19). At the same time, restrictions on physical contact and border closures between countries limited direct interactions between breeders. Consequently, sperm cryopreservation and international shipments became an effective alternative to maintain breeding schedules and genetic exchange during this period. Although cryopreservation numbers declined in 2022, this decrease does not overshadow the overall trend of steady growth, supported by an average annual increase of 52.32 cryopreserved ejaculates. The drop in 2022 likely reflects a return to pre-pandemic norms rather than a reversal in the growing use of frozen sperm.

Most sperm cryopreservation were from dogs aged 1–9 years, with nearly a third (29.8%) between 2 and 4 years old. This

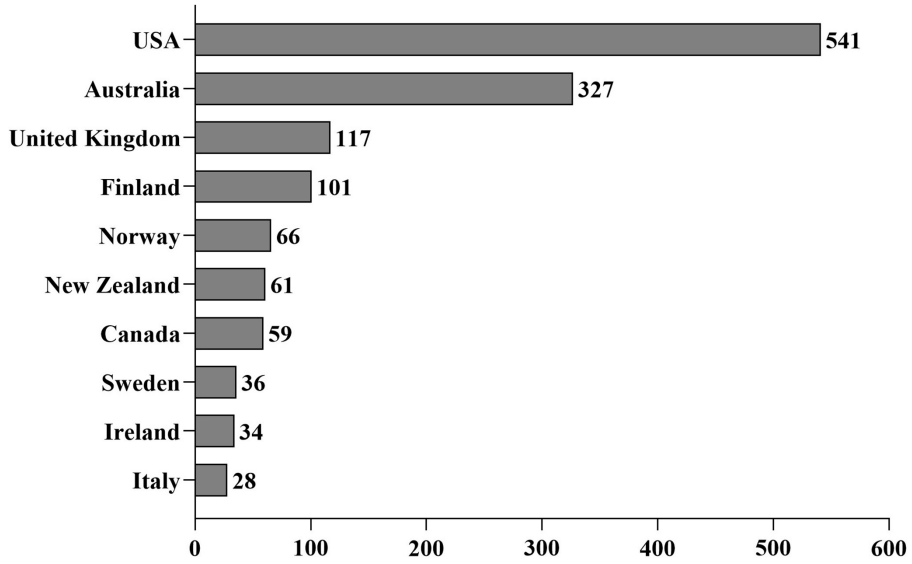

FIGURE 3
The number of international shipments of frozen sperm to the ten most popular destinations.

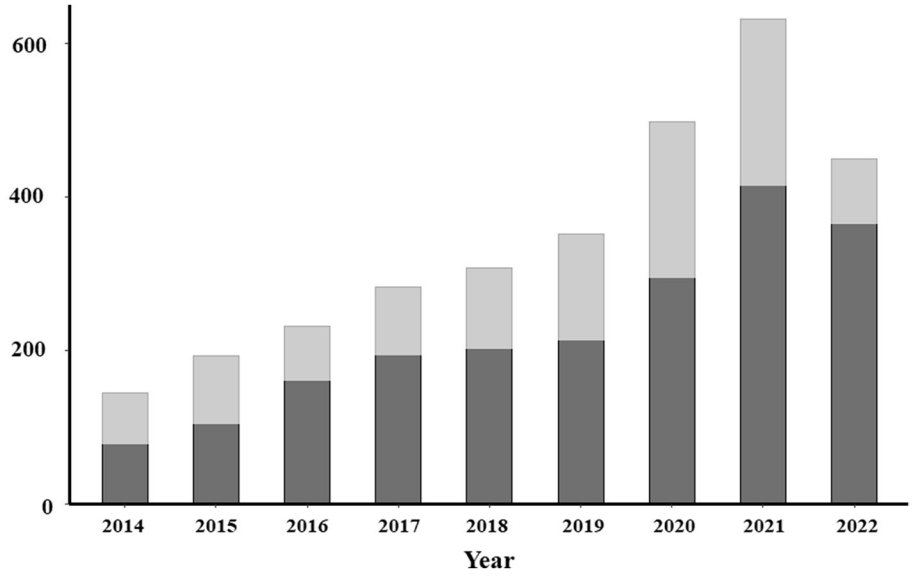

FIGURE 4
Bar plot representing the number of cryopreservations between 2014 and 2022. The dark gray represents the proportion of remaining frozen ejaculates from each year in the sperm banks.

age distribution likely reflects the inclusion of young, recently certified breeding males that have proven their worth in shows or working competitions (20). In contrast, fewer than 10% of the dogs were 10 years or older, aligning with evidence that sperm quality generally declines with age (10, 13, 21–24). However, the age distribution may be skewed toward younger dogs, as it excluded those initially presented for cryopreservation but deemed unsuitable due to poor semen quality. In some cases, some owners may choose to freeze sperm from older dogs despite reduced semen quality, driven by emotional attachment or unique breed traits. Nonetheless, achieving pregnancy in such cases is unlikely without advanced reproductive technologies, like *in vitro* fertilization, and the advanced age of the dog may further impair sperm fertility (24–26). Additionally, surgical artificial insemination is illegal in several European countries, including the United Kingdom, Norway, Sweden, and the Netherlands (27).

Most dogs were presented only once or twice for sperm cryopreservation. However, the case of one dog presented 66 times highlights the intense use of certain sires by some breeders. Such practices are not recommended, as they pose

significant risks to genetic diversity and can facilitate the spread of inherited disorders within a breed (12, 28). Fortunately, these extreme cases were rare, with only 1.9% of dogs being presented more than six times. To mitigate these issues, some national breeding organizations have implemented restrictions on the use of specific sires or the total number of breedings allowed per male (29).

Frozen sperm was primarily used for international shipments, after a median storage time of 60 days. This relatively short storage duration indicates that many breeders use sperm banks as temporary storage facilities, awaiting the accumulation of sufficient straws or the finalization of logistical arrangements for shipment. This finding supports our assumption that a 6-month period between the last cryopreservation and data collection was adequate for assessing the use of frozen sperm by dog breeders. This timeframe provided ample time for sperm utilization, while minimizing the risk of missing late usage cases. However, it remains unknown whether the exported frozen sperm is used shortly after arrival or stored for a longer period in another sperm bank. In most cases (59.7%), all straws from a single ejaculate were shipped, which contrasts with practices in other species, such as stallions and bulls, where dividing ejaculates into multiple insemination doses is common practice (30, 31). This difference likely arises from the lower total sperm count in dogs and the relatively high recommended sperm concentration per insemination dose, i.e., 100 million progressively motile and normal spermatozoa (5, 16).

The most popular destinations for international shipment were typically countries with extended transit times (16, 32). International shipment to EU member countries, such as Finland, Sweden, Ireland, and Italy, may reflect a growing popularity of frozen dog sperm in these regions or logistical choices favoring frozen transport due to geographical distances from the investigated sperm banks. In addition to international shipments, artificial inseminations performed at the freezing centers accounted for 21.8% of frozen sperm use. Many owners of frozen sperm likely prefer insemination at the sperm bank to avoid the additional costs and risks associated with shipping, although this option is limited by the location of the bitch. Lastly, 6.8% of the frozen ejaculates were discarded, indicating that a small but notable proportion of breeders ultimately decided to discontinue sperm storage for various reasons.

A significant portion of frozen ejaculates (44.1–79.6%) remained unused or only partially used at the time of data collection. Although this percentage decreased over time, it remained considerable even 9 years after cryopreservation. This finding supports the long-term storage of frozen sperm and highlights the need for continuous expansion of semen banks as the number of remaining frozen straws increases. This expansion requires not only increasing the number of storage containers but also enhancing administrative and logistical support for organizing international shipments and artificial inseminations, while maintaining robust safety protocols and high-quality service.

Overall, this study provides valuable insights into the use of frozen dog sperm by breeders in Belgium and the Netherlands. Although the findings may not be fully generalizable to other regions, the increasing popularity of sperm cryopreservation reflects the evolving landscape of canine reproductive management. Further studies should aim to quantify the proportion of breeders resorting to sperm cryopreservation and the extent of frozen sperm usage in breeding programs.

Data availability statement

The raw data supporting the conclusions of this article will be made available by the authors, without undue reservation.

Author contributions

GD: Conceptualization, Data curation, Formal analysis, Funding acquisition, Investigation, Methodology, Visualization, Writing – original draft, Writing – review & editing. MK: Resources, Writing – review & editing. AVM: Investigation, Writing – review & editing. ID: Investigation, Writing – review & editing. MV: Investigation, Writing – review & editing. RV: Investigation, Writing – review & editing. LS: Investigation, Writing – review & editing. FP: Visualization, Writing – review & editing. AVS: Resources, Supervision, Writing – review & editing.

Funding

The author(s) declare financial support was received for the research, authorship, and/or publication of this article. This study was supported by the Research Foundation—Flanders (FWO) for strategic basic research (SB) under grant number 1S78222N.

Conflict of interest

MK, AVM, and ID were employed by Cryolab Eersel B.V.

The remaining authors declare that the research was conducted without any commercial or financial relationships that could be perceived as a conflict of interest.

Publisher's note

Supplementary material

The Supplementary Material for this article can be found online at: https://www.frontiersin.org/articles/10.3389/fvets.2024.1499266/full#supplementary-material

References

1. Yanez-Ortiz I, Catalan J, Rodriguez-Gil JE, Miro J, Yeste M. Advances in sperm cryopreservation in farm animals: cattle, horse, pig and sheep. *Anim Reprod Sci.* (2022) 246:106904. doi: 10.1016/j.anireprosci.2021.106904

2. Suzuki H, Watanabe H, Abe Y. Assisted reproductive techniques for canines: preservation of genetic material in domestic dogs. *J Reprod Dev.* (2022) 68:1–11. doi: 10.1262/jrd.2021-111

3. Kim SH Yu DH, Kim YJ. Effects of cryopreservation on phosphatidylserine translocation, intracellular hydrogen peroxide, and DNA integrity in canine sperm. *Theriogenology.* (2010) 73:282–92. doi: 10.1016/j.theriogenology.2009.09.011

4. Mason SJ. A retrospective clinical study of endoscopic-assisted transcervical insemination in the bitch with frozen-thawed dog semen. *Reprod Domest Anim.* (2017) 2:275–80. doi: 10.1111/rda.12864

5. Mason SJ. Current review of artificial insemination in dogs. *Vet Clin N Am Small Anim Pract.* (2018) 48:567–80. doi: 10.1016/j.cvsm.2018.02.005

6. Thomassen R, Sanson G, Krogenaes A, Fougner JA, Berg KA, Farstad W. Artificial insemination with frozen semen in dogs: a retrospective study of 10 years using a non-surgical approach. *Theriogenology.* (2006) 66:1645–50. doi: 10.1016/j.theriogenology.2006.01.022

7. Thomassen R, Farstad W. Artificial insemination in canids: a useful tool in breeding and conservation. *Theriogenology.* (2009) 71:190–9. doi: 10.1016/j.theriogenology.2008.09.007

8. Domain G, Wydooghe E, Broeckx BJG, Hoogewijs M, Van Soom A. Semen donation and establishment of an open canine semen bank: a novel tool to prevent inbreeding in pedigree dogs. *Vlaams Diergen Tijds.* (2019) 88:55–61. doi: 10.21825/vdt.v88i1.16045

9. Farstad W. Cryopreservation of canine semen - new challenges. *Reprod Domest Anim.* (2009) 2:336–41. doi: 10.1111/j.1439-0531.2009.01418.x

10. Lechner D, Aurich J, Schafer-Somi S, Aurich C. Effects of age, size and season on cryotolerance of dog semen - a retrospective analysis. *Anim Reprod Sci.* (2022) 236:106912. doi: 10.1016/j.anireprosci.2021.106912

11. Farstad W. Semen cryopreservation in dogs and foxes. *Anim Reprod Sci.* (1996) 42:251–60. doi: 10.1016/0378-4320(96)01483-2

12. Lampi S, Donner J, Anderson H, Pohjoismaki J. Variation in breeding practices and geographic isolation drive subpopulation differentiation, contributing to the loss of genetic diversity within dog breed lineages. *Canine Med Genet.* (2020) 7:1–10. doi: 10.1186/s40575-020-00085-9

13. Rijsselaere T, Maes D, Hoflack G, de Kruif A, Van Soom A. Effect of body weight, age and breeding history on canine sperm quality parameters measured by the Hamilton-Thorne analyser. *Reprod Domest Anim.* (2007) 42:143–8. doi: 10.1111/j.1439-0531.2006.00743.x

14. Linde-Forsberg C. Artificial insemination with fresh, chilled extended, and frozen-thawed semen in the dog. *Semin Vet Med Surg.* (1995) 10:48–58.

15. Nizanski W. Intravaginal insemination of bitches with fresh and frozen-thawed semen with addition of prostatic fluid: use of an infusion pipette and the Osiris catheter. *Theriogenology.* (2006) 66:470–83. doi: 10.1016/j.theriogenology.2006.01.001

16. Linde-Forsberg C. Regulations and recommendations for international shipment of chilled and frozen canine semen. *Recent Adv. Small Anim. Reprod.* (2019). Available at: https://www.ivis.org/library/recent-advances-small-animal-reproduction/regulations-and-recommendations-for-international (accessed September 12, 2024).

17. Wickham H. ggplot2. *Wiley Interdiscipl Rev.* (2011) 3:180–5. doi: 10.1002/wics.147

18. Wang S, Leroy G, Malm S, Lewis T, Strandberg E, Fikse WF. Merging pedigree databases to describe and compare mating practices and gene flow between pedigree dogs in France, Sweden and the UK. *J Anim Breed Genet.* (2017) 134:152–61. doi: 10.1111/jbg.12242

19. Packer RMA, Brand CL, Belshaw Z, Pegram CL, Stevens KB, O'Neill DG. Pandemic puppies: characterising motivations and behaviours of UK owners who purchased puppies during the 2020 COVID-19 pandemic. *Animals.* (2021) 11:2500. doi: 10.3390/ani11092500

20. Farrell LL, Schoenebeck JJ, Wiener P, Clements DN, Summers KM. The challenges of pedigree dog health: approaches to combating inherited disease. *Canine Genet Epidemiol.* (2015) 2:1–14. doi: 10.1186/s40575-015-0014-9

21. Hesser A, Darr C, Gonzales K, Power H, Scanlan T, Thompson J, et al. Semen evaluation and fertility assessment in a purebred dog breeding facility. *Theriogenology.* (2017) 87:115–23. doi: 10.1016/j.theriogenology.2016.08.012

22. Brito MM, Angrimani DSR, Lucio CF, Vannucchi CI. A case trial study of the effect of ageing on fresh and post-thaw sperm in dogs. *Andrologia.* (2018) 50:e13123. doi: 10.1111/and.13123

23. Tesi M, Sabatini C, Vannozzi I, Di Petta G, Panzani D, Camillo F, et al. Variables affecting semen quality and its relation to fertility in the dog: a retrospective study. *Theriogenology.* (2018) 118:34–9. doi: 10.1016/j.theriogenology.2018.05.018

24. Abah KO, Fontbonne A, Partyka A, Nizanski W. Effect of male age on semen quality in domestic animals: potential for advanced functional and translational research? *Vet Res Commun.* (2023) 47:1125–37. doi: 10.1007/s11259-023-10159-1

25. Colombo M, Alkali IM, Prochowska S, Luvoni GC. Fighting like cats and dogs: challenges in domestic carnivore oocyte development and promises of innovative culture systems. *Animals.* (2021) 11:2135. doi: 10.3390/ani11072135

26. Kim HJ, Oh HJ, Jang G, Kim MK. Birth of puppies after intrauterine and intratubal insemination with frozen-thawed canine semen. *J Vet Sci.* (2007) 8:75–80. doi: 10.4142/jvs.2007.8.1.75

27. Standards & Advice Update (2019). Available at: https://www.rcvs.org.uk/news-and-views/features/standards-and-advice-update-january-2019/?&&type=rfst&set=true#cookie-widget (accessed September 12, 2024).

28. Leroy G, Baumung R. Mating practices and the dissemination of genetic disorders in domestic animals, based on the example of dog breeding. *Anim Genet.* (2011) 42:66–74. doi: 10.1111/j.1365-2052.2010.02079.x

29. Fokreglement ESSCN (2021). Available at: https://www.esscn.nl/pup-en-fokkersinfo/fokreglement-esscn (accessed September 12, 2024).

30. Aurich J, Kuhl J, Tichy A, Aurich C. Efficiency of semen cryopreservation in stallions. *Animals.* (2020) 10:1033. doi: 10.3390/ani10061033

31. Ugur MR, Saber Abdelrahman A, Evans HC, Gilmore AA, Hitit M, Arifiantini RI, et al. Advances in cryopreservation of bull sperm. *Front Vet Sci.* (2019) 6:268. doi: 10.3389/fvets.2019.00268

32. Rijsselaere T, Maes D, Van den Berghe F, Van Soom A. Preservation and shipment of chilled and cryopreserved dog semen. *Vlaams Diergen Tijds.* (2011) 80:248–53. doi: 10.21825/vdt.87276

frontiers | Frontiers in Veterinary Science

TYPE Original Research
PUBLISHED 27 November 2024
DOI 10.3389/fvets.2024.1466482

OPEN ACCESS

EDITED BY
Stefan Gregore Ciornei,
Iasi University of Life Sciences, Romania

REVIEWED BY
Singh Rajender,
Central Drug Research Institute (CSIR), India
Andreea Iren Serban,
University of Agronomic Sciences and Veterinary Medicine, Romania

*CORRESPONDENCE
Xiangyun Li
lxyun@hebau.edu.cn
Zhili Chu
chuzhili@xxmu.edu.cn
Xinglong Wu
wuxl32@hebau.edu.cn

†These authors have contributed equally to this work and share first authorship

RECEIVED 18 July 2024
ACCEPTED 06 November 2024
PUBLISHED 27 November 2024

CITATION
Jiao X, Jiao Y, Cui J, Zhang H, Li X, Chu Z and Wu X (2024) S100A4 targets PPP1CA/IL-17 to inhibit the senescence of sheep endometrial epithelial cells.
Front. Vet. Sci. 11:1466482.
doi: 10.3389/fvets.2024.1466482

S100A4 targets PPP1CA/IL-17 to inhibit the senescence of sheep endometrial epithelial cells

Xiyao Jiao[1†], Yaoxuan Jiao[1†], Jingwen Cui[2], Haorui Zhang[2], Xiangyun Li[1*], Zhili Chu[2,3*] and Xinglong Wu[1*]

[1]College of Animal Science and Technology, Hebei Technology Innovation Center of Cattle and Sheep Embryo, Hebei Agricultural University, Baoding, China, [2]School of Basic Medical Sciences, Xinxiang Medical University, Xinxiang, China, [3]Henan International Joint Laboratory of Immunity and Targeted Therapy for Liver-Intestinal Tumors, Xinxiang Medical University, Xinxiang, China

Background: Gonadotropin-releasing hormone (GnRH) is commonly used in animal reproduction and production, but it was previously reported that GnRH decreases the embryo implantation rate during artificial insemination or embryo transfer in sheep. In addition to the finding that GnRH can target S100A4 to inhibit endometrial epithelial cells proliferation, it was also found that endometrial cells were in poor condition and experienced cell death in S100A4 knockout mice, but the mechanism is unclear.

Methods: The protein PPP1CA, which interacts with S100A4, was detected by immunoprecipitation-mass spectrometry of overexpression and knockdown of S100A4 and PPP1CA. The effect of S100A4 and PPP1CA on cell senescence was detected by Galactosidase staining. To further reveal the mechanism effect of S100A4 and PPP1CA on cell senescence, transcriptome sequencing was conducted. Additionally, *in vivo* experiments were performed to assess PPP1CA protein expression in the endometrial tissue of S100A4 knockout mice.

Results: S100A4 inhibited cell senescence by activating PPP1CA, while PPP1CA overexpression suppressed the activation of the IL-17 signaling pathway. Inhibition of the IL-17 signaling pathway inhibited the senescence of endometrial cells.

Conclusion: S100A4 can target the PPP1CA/IL-17 signaling pathway and inhibit endometrial epithelial cell senescence.

KEYWORDS

Cell senescence, endometrial epithelial cells, S100A4, PPP1CA, IL-17

1 Introduction

Sheep are important livestock species worldwide that provide humans with meat, leather, and wool. Despite high breeding numbers, many traditional local breeds may not meet the efficiency demands for growth rates and meat yields. Therefore, breeding activities to improve quality are crucial for sheep farming, with artificial insemination and embryo transfer representing technologies for rapid breeding improvement. GnRH is associated with the dual activity of FSH and LH; it can promote ovulation and is widely used in assisted reproductive technology in sheep, cattle, and humans. However, previous studies have shown that GnRH administration at the time of insemination reduced pregnancy rates in Kazak ewes (1). Similarly, GNRH administration to recipient ewes also reduced the embryo transfer success rate (2). In human-assisted reproductive technology, two main protocols for the use of GnRH are the gonadotrophin-releasing hormone agonist (GnRH-a) protocol and the gonadotrophin-releasing hormone antagonist (GnRH-ant) protocol. GnRH can effectively promote ovulation,

but it has not been shown to significantly improve the outcome of fresh embryo transfers (3). Neither protocol has achieved perfect results in promoting embryo implantation (4). For example, GnRH-a pretreatment seems to improve frozen–thawed embryo transfer outcomes but is associated with a higher preterm birth rate (5).

Many factors can influence embryo implantation, including the proliferative capacity of endometrial cells, cell apoptosis (6), and cell senescence (7), all of which can affect the uterine environment and further impact embryo implantation. Our previous results indicated that GnRH can reduce the expression level of S100A4 in the endometrium and suppress endometrial cell proliferation (8). However, we also found that mice with endometrial S100A4 knockout tended toward a thinner endometrium and increased endometrial cell apoptosis, suggesting that GnRH treatment might also accelerate endometrial cell aging and death. Protein phosphatase 1 catalytic subunit alpha (PPP1CA) is an alpha subunit of the PP1 complex that is known to be involved in the regulation of various cellular processes (9). Evidence suggests that PPP1CA can inhibit cell senescence (10).

This study identified PPP1CA as an interacting protein downstream of S100A4. *In vitro* experiments verified the effect of PPP1CA on the senescence of sheep endometrial cells, and *in vivo* experiments using S100A4 knockout mice revealed that the absence of S100A4 could decrease PPP1CA protein levels. Further transcriptome sequencing revealed that IL-17 is downstream of S100A4 and PPP1CA, suggesting that inhibiting IL-17 can suppress the senescence of sheep endometrial cells. These findings provide a theoretical basis for the use of GnRH in sheep embryo transfer.

2 Materials and methods

2.1 Isolation and culture of endometrial epithelial cells from sheep

The methods used to isolate and culture the cells were described in our previous study (8). Briefly, freshly excised uteri were soaked in PBS containing penicillin (100 IU/mL) and streptomycin (0.1 mg/mL) and transported to the laboratory. The uteri were washed three times with PBS containing antibiotics. Under a microscope, the endometrium was peeled off, cut into 1–2 mm^3 pieces, and evenly spread on a cell culture dish. The dish was incubated at 37°C for 1 h to allow the tissue fragments to adhere to the dish. Then, DMEM (Cytiva) containing antibiotics and 10% FBS (fetal bovine serum, PAN-Biotech) was added. The culture mixture was returned to the incubator and maintained for 7–10 days to allow cells to migrate from the tissue edges. After this incubation period, the cells were digested and passaged for use in subsequent experiments.

2.2 β-galactosidase staining

A β-galactosidase staining kit was purchased from Beyotime Biotechnology. The staining procedure was performed according to the manufacturer's instructions. The main steps involved fixing the cells with a fixative solution for 15 min, preparing the staining solution, adding it to the cell dishes, and incubating the cells in a cell culture incubator for 1 h. After removing the staining solution, the cells were washed once with PBS, and fresh PBS was added for imaging (Ts2R-FL, Nikon, Japan).

2.3 Y-320 treatment

Y-320 was dissolved in DMSO to prepare a concentrated solution (5 mg/mL). To prepare the working solution, 50 μL of the concentrated solution was added to a 20% SBE-*β*-CD in saline solution. The mixture was gently shaken and left to stand for a few minutes until clear. Y-320 was added to sheep endometrial cells at a dilution of 1:10,000 in the cell culture medium, resulting in a final concentration of 0.05 μg/mL (approximately 99 nM). After culturing for 48 h, *β*-galactosidase staining was performed.

2.4 siRNA transfection and lentiviral packaging

siRNAs were purchased from GENEWIZ Biotechnology Co., Ltd., and their sequence information is provided in Table 1. Before transfecting siRNA, sheep endometrial cells were seeded into 6-well culture plates at a density of 5 × 10^4 cells per well. The next day, non-adherent cells were discarded and fresh medium was added. To transfect the cells, 50 pmol of siRNA was mixed with 200 μL of Opti-MEM™ I Reduced Serum Medium (Cat. No. 31985070, Gibco). Separately, 5 μL of RNAiMAX (Lipofectamine™ RNAiMAX, Cat. No. 13778-075, Invitrogen) was also mixed with 200 μL of Opti-MEM. After incubating each mixture for 5 min, the solutions were combined and allowed to stand at room temperature for 15 min. The siRNA complex was then added to the cells and incubated at 37°C. The medium was not changed until the cells were harvested for further analysis. As a control, NC (Negative Control siRNA) transfections were performed in parallel.

TABLE 1 siRNA and primers sequences.

Name	Sense (5′-3′)	Antisense (5′-3′)
siPPP1CA-1	GAAGCUCAACCUGGACUCUAUTT	AUAGAGUCCAGGUUGAGCUUCTT
siPPP1CA-2	GCAAGAGACGCUACAACAUCATT	UGAUGUUGUAGCGUCUCUUGCTT
siPPP1CA-3	GCUGGCCUAUAAGAUCAAGUATT	UACUUGAUCUUAUAGGCCAGCTT
siNC	UUCUCCGAACGUGUCACGUTT	ACGUGACACGUUCGGAGAATT
GAPDH	AGGTCGGTGTGAACGGATTTG	TGTAGACCATGTAGTTGAGGTCA
IL-17	TAGCGGTAAAGACGGTGGAG	TTTACCCTTGCTGGTGCAGT

Lentiviruses overexpressing S100A4 and PPP1CA were synthesized by GeneChem Co., Ltd., with the synthesis report provided in Supplementary materials 2, 3. During lentiviral packaging, the backbone vector, along with the auxiliary vectors VSVG and PAX2, were transfected into 293 T cells at a 2: 1:1 ratio. Forty-eight hours after transfection, the cell supernatant was collected and used to infect sheep cells. The sheep cells were seeded in a 60 mm dish. Once the cells reached 60% confluency, the culture medium was discarded, and 6 mL of the lentiviral supernatant was added, along with Polybrene at a final concentration of 5 μg/mL. After 6 h of incubation, the viral medium was replaced with fresh culture medium, and the cells were further cultured. After 48–72 h, once most of the sheep cells expressed GFP, they were ready for subsequent experiments.

2.5 EdU staining

An EdU staining kit was purchased from Beyotime Biotechnology. The main steps of the staining protocol were as follows: EdU was diluted in cell culture medium to a final concentration of 10 μM. The original culture medium was discarded and replaced with EdU-containing medium. The cells were incubated in a cell culture incubator for 3–4 h, fixed with 4% paraformaldehyde for 15 min, and permeabilized with 0.25% Triton X-100 for 12 min. The Click reaction mixture was then prepared according to the manufacturer's instructions and added to the cells. The cells were incubated at room temperature in the dark for 1 h, after which the reaction mixture was discarded. The cells were washed once with PBS, fresh PBS containing hoechst33342 was added, and the cells were imaged after 5 min of incubation at room temperature.

2.6 Transcriptome sequencing and analysis

RNA samples from sheep endometrial cells with S100A4 knockdown were obtained by transfecting siRNA targeting S100A4, following the same procedure as described in Section 2.3. After 24 and 48 h post-transfection, the medium was discarded, and the cells were washed twice with PBS. Each well of a 6-well plate was lysed using 1 mL of RNAiso Plus (Cat. No. 9109, TAKARA), and three wells of similarly treated cells were pooled into one sample.

For generating samples overexpressing PPP1CA, lentiviral vectors overexpressing PPP1CA were packaged in 293T cells, following the method described in Section 2.3. The harvested lentiviral supernatant was centrifuged, and the cells were seeded in a 60 mm dish. Once the cells reached 60% confluency, the culture medium was discarded, and 6 mL of the lentiviral supernatant was added, along with Polybrene at a final concentration of 5 μg/mL. After 6 h of incubation, the viral medium was replaced with fresh culture medium, and the cells were further cultured. Sequencing and analysis were performed by Beijing Novo Biotechnology Co., Ltd. Transcriptome sequencing was performed by Suzhou Jinweizhi Biotechnology Co., Ltd.

Differential gene expression was analyzed using the DESeq2 package, and a volcano plot was generated with log10 fold-change values on the y-axis. GO and KEGG enrichment analyses were conducted using the clusterProfiler program, while Pearson correlation heatmaps were generated using Pheatmap.

For samples with S100A4 knockdown, NC1, NC2, and NC3 represent Negative Control Sample1, Negative Control Sample2 Negative, and Control Sample3, respectively, and KD1, KD2, and KD3 represent Knock down Sample 1, Knock down Sample 2, and Knock down Sample 3, respectively. For samples overexpressing PPP1CA, Control represents the control group with empty vector, and PPP1CA represents the experimental group with overexpression.

2.7 Mass spectrometry and co-immunoprecipitation (Western blot)

In sheep endometrial cells overexpressing HA-tagged S100A4 (HA is the tag added when constructing the vector), 48 h after transfection, cells were washed twice with PBS. The cells were then lysed using NP-40 lysis buffer containing a protease inhibitor and incubated on ice for 30 min. The lysate was collected into a centrifuge tube and spun at 12,000 rpm for 10 min at 4°C. The supernatant was incubated with Protein A/G resin pretreated with an HA primary antibody (anti-HA, Cat. No. AE105, Abclone) at room temperature for 2 h. The resin was then washed six times with NP-40 buffer, and the supernatant was discarded after each wash by centrifuging at 500 rpm for 5 min. As a control, Protein A/G resin without the HA primary antibody was also used. The bound protein was eluted with protein loading buffer, heated at 100°C for 10 min, then cooled to room temperature. Protein samples were run SDS-PAGE on electrophoresis at 110 V for 1 h, and the gel was sent to Jin Kairui Biotechnology, Ltd. for mass spectrometry-based detection and analysis. GO enrichment analysis of the identified proteins was performed using the clusterProfiler program.

For Co-immunoprecipitation, HA-S100A4 and Flag-PPP1CA proteins were overexpressed in 293 T cells. When protein samples were collected 48 h after transfection, a small amount of the cell lysate was taken in advance for verification. Western blot analysis was performed with 12% polyacrylamide gel electrophoresis for both the co-precipitated and whole-cell proteins. Thirty micrograms of protein were loaded into each well, and the maximum volume of immunoprecipitated protein was used. Electrophoresis was carried out at 110 V for 1.5 h, followed by protein transfer onto a PVDF membrane at 300 mA on ice for 1.5 h. The membrane was blocked with 10% skimmed milk for 30 min, then rinsed with TBST for 10 min. The corresponding primary antibodies (anti-HA, Cat. No. AE105, ABclonal; anti-Flag, Cat. No. AE092, ABclonal) were added, and the membrane was incubated overnight at 4°C. The next day, the membrane was washed three times with TBST, followed by incubation with HRP-conjugated secondary antibody (HRP Conjugated AffiniPure Goat Anti-rabbit IgG (H + L), Cat. No. BA1055, Boster) at room temperature for 1 h. After washing three more times with TBST, Clarity Western ECL Substrate (Bio-Rad) was added to the membrane. The PVDF membrane was then placed in a chemiluminescence analyzer (MiniChemi® 610, SINSAGE) for imaging.

2.8 Immunofluorescence staining

Cells were fixed with 4% paraformaldehyde for 15 min and permeabilized with 0.25% Triton X-100 for 12 min, followed by three washes in PBS for 5 min each. The cells were blocked with 1% BSA for

30 min and then incubated overnight at 4°C with primary antibodies diluted in 1% BSA (S100A4 antibody, 1:100, sc-377059, Santa Cruz, USA; PPP1CA, A24288, Abclone, China). After three washes in PBS, the cells were incubated with fluorescent secondary antibodies (DyLight 594-conjugated AffiniPure goat anti-mouse IgG (H + L) (1:100, BA1141, Boster, China) and ABflo® 488-conjugated goat anti-rabbit IgG (H + L) (1:100, AS053, Abclone, China)) for 1 h at room temperature in the dark. After three washes in PBS, the cells were stained with PBS containing Hoechst 33342 and imaged with a confocal laser scanning microscope.

2.9 HE staining and immunohistochemistry

HE staining was performed as described previously (8). For immunohistochemistry, paraffin sections were deparaffinized, repaired, blocked, and then incubated overnight with a PPP1CA antibody (1:100, A24288, Abclone, China). After the samples were reacted with an HRP-conjugated goat anti-rabbit secondary antibody, color development was performed using a DAB staining kit (G1212-200 T, Servicebio, China). The sections were counterstained with hematoxylin, rinsed with tap water, mounted, and imaged under a microscope.

2.10 Animal breeding and analysis

To generate uterine-specific S100A4 knockout mice, C57BL/6J-S100A4em1 (flox) Cya mice (strain number CKOCMP-20198-S100a4-B6J-VA, Cyagen Biosciences, Inc.) were crossed with PR-Cre transgenic mice (model number C001035, Cyagen Biosciences, Inc.). Homozygous flox mice positive for the PR-Cre genotype were used as experimental subjects, while wild-type and heterozygous mice served as controls. Transgenic mice were kept in specific pathogen-free (SPF) animal rooms with a 12 h/12 h dark/light cycle. The mice were allowed access to drinking water and food. A Mouse Direct PCR Kit (for genotyping) (B40013, Selleck) was used for genotyping.

Female mice, aged 8 weeks, were euthanized by CO_2 asphyxiation. Uterine tissues were excised, fixed in formalin overnight, embedded in paraffin, and sectioned for hematoxylin and eosin (HE) staining and immunohistochemistry.

2.11 Data analysis

Statistical analysis was performed with GraphPad Prism 5 software (GraphPad Software, Inc., CA, United States). Student's t-test and one-way ANOVA were used to evaluate the significance of differences; $p < 0.05$ indicated statistical significance (8).

3 Results

3.1 S100A4 inhibits cell senescence

Previous experiments have shown that S100A4 can promote cell proliferation (8). Considering the cyclical metabolism of endometrial cells and that cell proliferation and senescence are generally opposing processes, we hypothesized that S100A4 might influence the senescence of endometrial cells. Senescence-associated β-galactosidase staining can be used to detect cellular senescence. We performed β-galactosidase staining on endometrial cells overexpressing S100A4 for 48 h and on control cells. The results revealed that blue staining was relatively weak in cells overexpressing S100A4, and the proportion of stained cells decreased (Figure 1A). After the cells were transfected with a siRNA targeting S100A4 and stained for β-galactosidase after 48 h, the results revealed that, compared with the NC (negative control) group, the S100A4-knockdown group presented an increased number of β-galactosidase-positive cells (Figure 1B). Given that S100A4 promotes cell proliferation, we extended the S100A4 treatment time. After S100A4 was overexpressed or knocked down for 48 h, we performed EdU labeling to detect cell proliferation. The results revealed that the percentage of EdU-positive cells was significantly greater in the S100A4-overexpressing group than in the control group (Figure 1C), whereas the percentage of EdU-positive cells was significantly lower in the S100A4-knockdown group than in the NC group (Figure 1D). These results further indicate that overexpressing S100A4 inhibits cell senescence.

3.2 S100A4 inhibits activation of the IL-17 signaling pathway

We previously performed transcriptome sequencing 24 h after S100A4 was knocked down and reported that S100A4 can promote cell proliferation by targeting GNAI2–MAPK (8). Because the cell senescence process is relatively slow, we performed transcriptome sequencing 48 h after S100A4 was knocked down to determine how S100A4 regulates cell senescence. Compared with those at 24 h, there were significant changes in cell transcription at 48 h, indicating the formation of a distinct subgroup of cells (Figure 2A). A heatmap generated from the gene transcription data also revealed changes in the expression levels of many genes between 24 and 48 h after S100A4 knockdown (Figure 2B). It is approximately 2000 gene transcripts showed up-regulation and down-regulation respectively (Figure 2C). GO enrichment analysis of the differentially expressed genes revealed enrichment in cellular physiological responses related to senescence, such as the "ubiquitin-dependent ERAD pathway," "response to unfolded protein," and "response to endoplasmic reticulum stress" (Figure 2D). These results indicate that the cells initiated the senescence process at the transcriptional level 48 h after S100A4 knockdown. Furthermore, KEGG enrichment analysis revealed significant signaling pathway changes 48 h after S100A4 knockdown compared with 24 h, particularly activation of the IL-17 signaling pathway (Figure 2E). Given that the IL-17 signaling pathway can regulate cell senescence, these results suggest that activating the IL-17 signaling pathway may promote cell senescence following S100A4 knockdown.

3.3 S100A4 targets and regulates PPP1CA

Previous immunoprecipitation–mass spectrometry studies identified proteins that interact with S100A4 (8). The cluster of orthologous groups (COG) classification of these proteins revealed

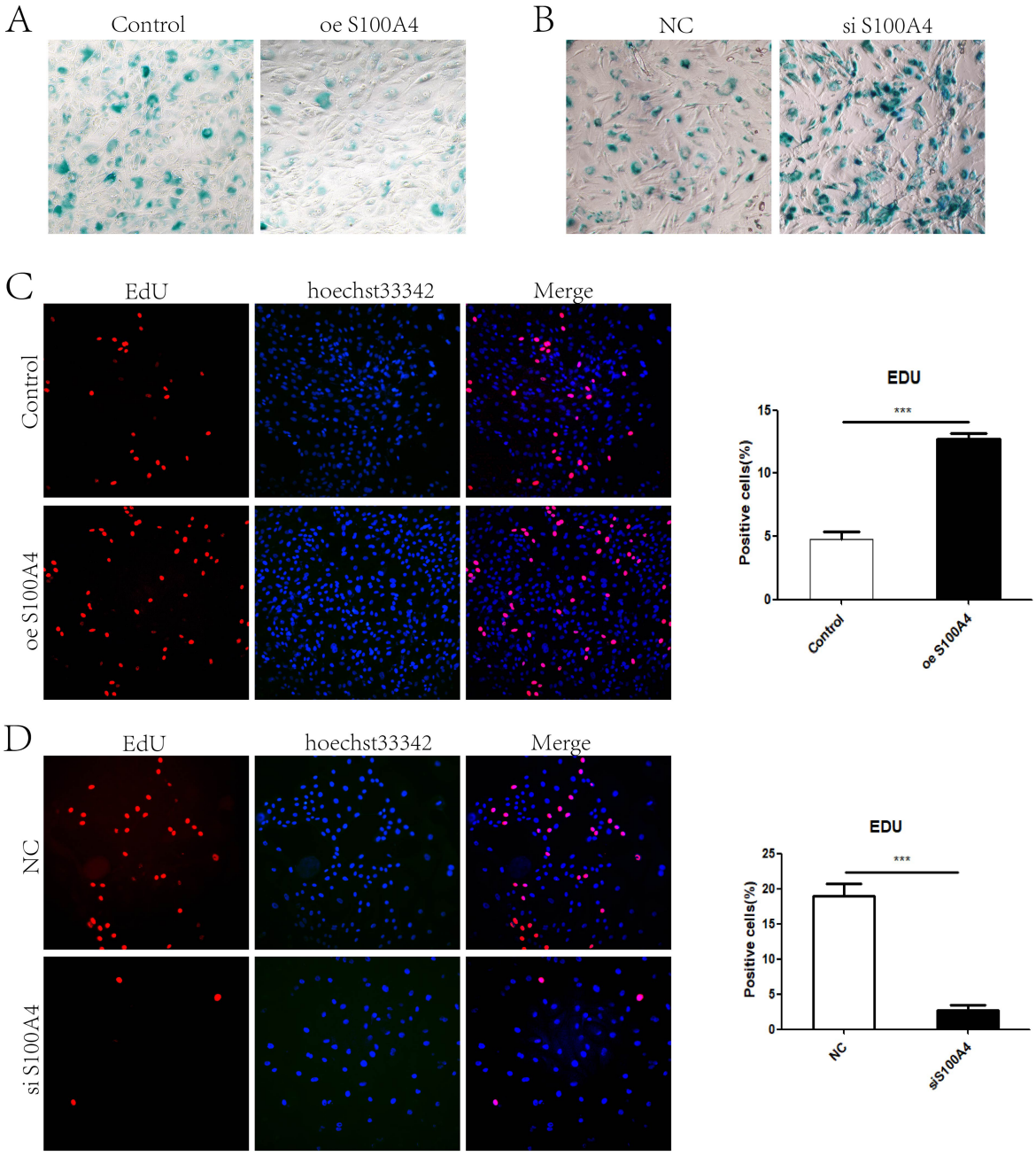

FIGURE 1
S100A4 inhibits the senescence of sheep endometrial epithelial cells **(A)** Galactosidase staining after S100A4 overexpression. **(B)** Galactosidase staining after S100A4 knockdown. **(C)** EdU staining to detect cell proliferation after S100A4 overexpression. **(D)** EdU staining to detect cell proliferation after S100A4 knockdown.

enrichment in functions related to cell senescence, such as "replication, recombination and repair" and "cell cycle control, cell division, chromosome partitioning" (Figure 3A). Among these proteins, PPP1CA is related to cell senescence. Immunoprecipitation experiments confirmed the interaction between S100A4 and PPP1CA (Figure 3B). Immunofluorescence staining and confocal microscopy revealed that S100A4 (RFP) interacted with PPP1CA (GFP), with the interaction occurring in the cell nucleus (Figure 3C). These results suggest that S100A4 may regulate cell senescence by interacting with PPP1CA.

3.4 PPP1CA inhibits cell senescence

To verify whether PPP1CA regulates cell senescence, we constructed a lentiviral vector overexpressing PPP1CA. First, the lentivirus was packaged in 293 T cells (Figure 4A) and then transduced into sheep endometrial cells to overexpress PPP1CA (Figure 4B). β-Galactosidase staining 48 h after transduction revealed a reduction in the proportion of positive cells (Figure 4C). PPP1CA overexpression promotes cell proliferation, as demonstrated by EdU staining (Figure 4D). These results suggest that overexpressing PPP1CA can inhibit cell senescence.

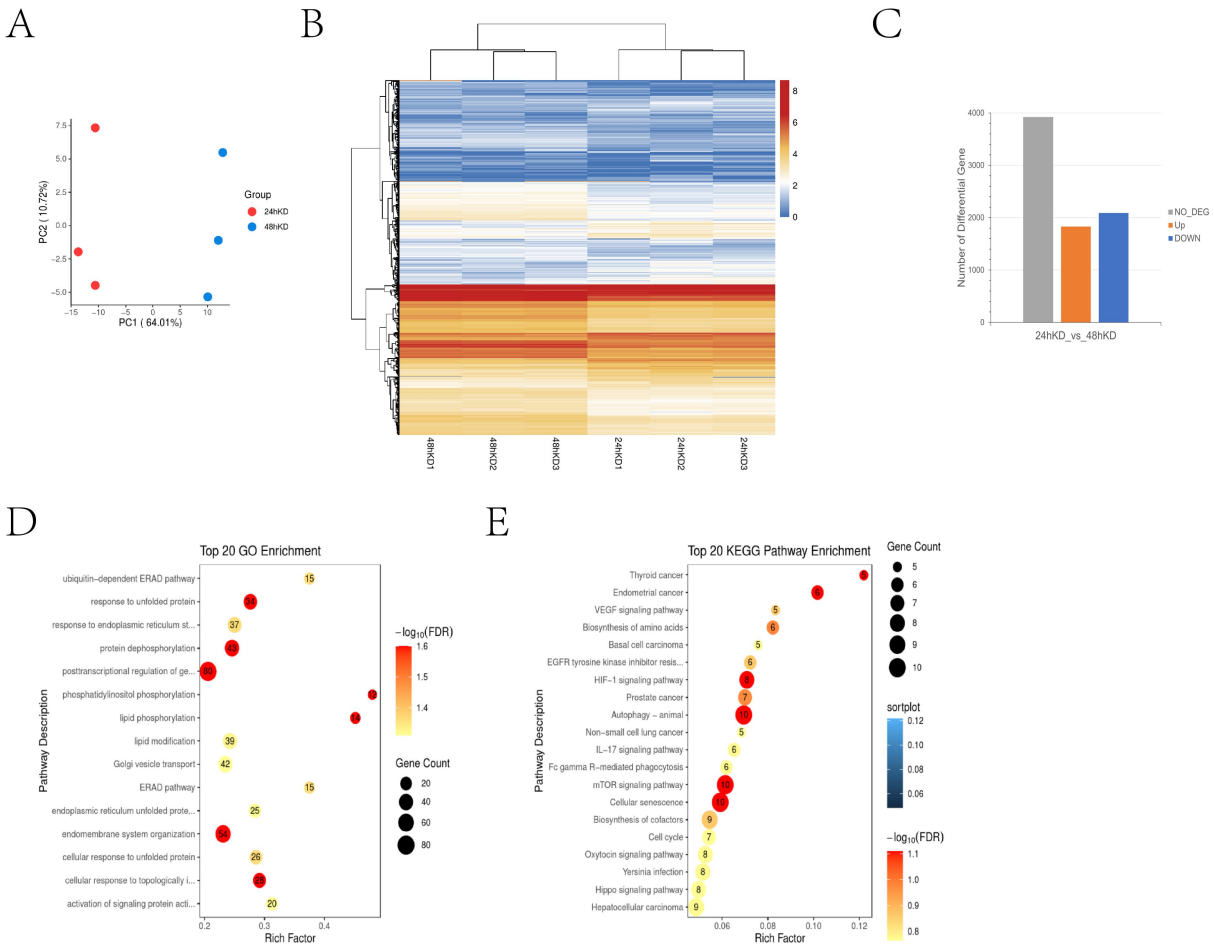

FIGURE 2
Transcriptome sequencing revealed that S100A4 knockdown can activate the IL-17 signaling pathway **(A)** Principal Component Analysis (PCA) results show significant spatial separation between samples, indicating distinct gene expression profiles after different treatments. For PCA, the first two or three principal components (PC1, PC2) were used to represent the largest variances in gene expression, which allows for clearer differentiation between sample groups. **(B)** Heatmap analysis of gene transcription differences at 24 and 48 h after S100A4 knockdown. The heatmap colors range from blue to red, with blue representing lower expression (log2 fold change) and red representing higher expression. **(C)** Differential gene expression statistics indicate that the number of up-and down-regulated genes (~2,000 each) occurred 24 and 48 h post-S100A4 knockdown. **(D)** GO enrichment analysis highlights key functions, such as post-transcriptional regulation and endomembrane system organization. **(E)** KEGG pathway enrichment identifies IL-17 signaling and pathways related to autophagy and cellular senescence. -log10 (FDR) was used to illustrate the FDR value, with larger values indicating greater statistical significance.

However, the mechanism by which PPP1CA inhibits the senescence of sheep endometrial cells requires further exploration.

3.5 PPP1CA inhibits activation of the IL-17 signaling pathway

To explore the mechanism by which PPP1CA regulates cell senescence in sheep endometrial cells, we performed transcriptome sequencing on cells overexpressing PPP1CA and control cells. Pearson correlation analysis revealed that the expression profiles of the three PPP1CA-overexpressing groups were all close to 1, indicating stable transcriptional states and reliable sequencing results (Figure 5A). The sequencing results revealed that overexpressing PPP1CA increased the transcription levels of 2,661 genes and decreased the transcription levels of 2,709 genes (Figure 5B). Additionally, 545 genes were newly activated, and 484 genes were silenced upon PPP1CA overexpression (Figure 5C). KEGG enrichment analysis of the downregulated genes revealed pathways such as "protein processing in the endoplasmic reticulum," "IL-17 signaling pathway," and "cell cycle" (Figure 5D). Although these pathways are related to cell senescence, they are also associated with cell proliferation. Previous results indicated that GNAI2 could regulate "cell cycle"-related pathways (7). To further identify PPP1CA-specific signaling pathways, we performed differential analysis between genes regulated by GNAI2 and those regulated by PPP1CA (Figure 5E). KEGG clustering analysis revealed enrichment of the IL-17 signaling pathway, suggesting that it may be a key downstream regulatory pathway of PPP1CA.

3.6 Inhibition of the IL-17 signaling pathway suppresses cell senescence

There is currently no evidence that IL-17 can regulate the proliferation of sheep endometrial cells. To verify whether blocking the IL-17 signaling pathway can inhibit cell senescence, we treated cells with the IL-17 antagonist Y-320 for 48 h. β-Galactosidase staining

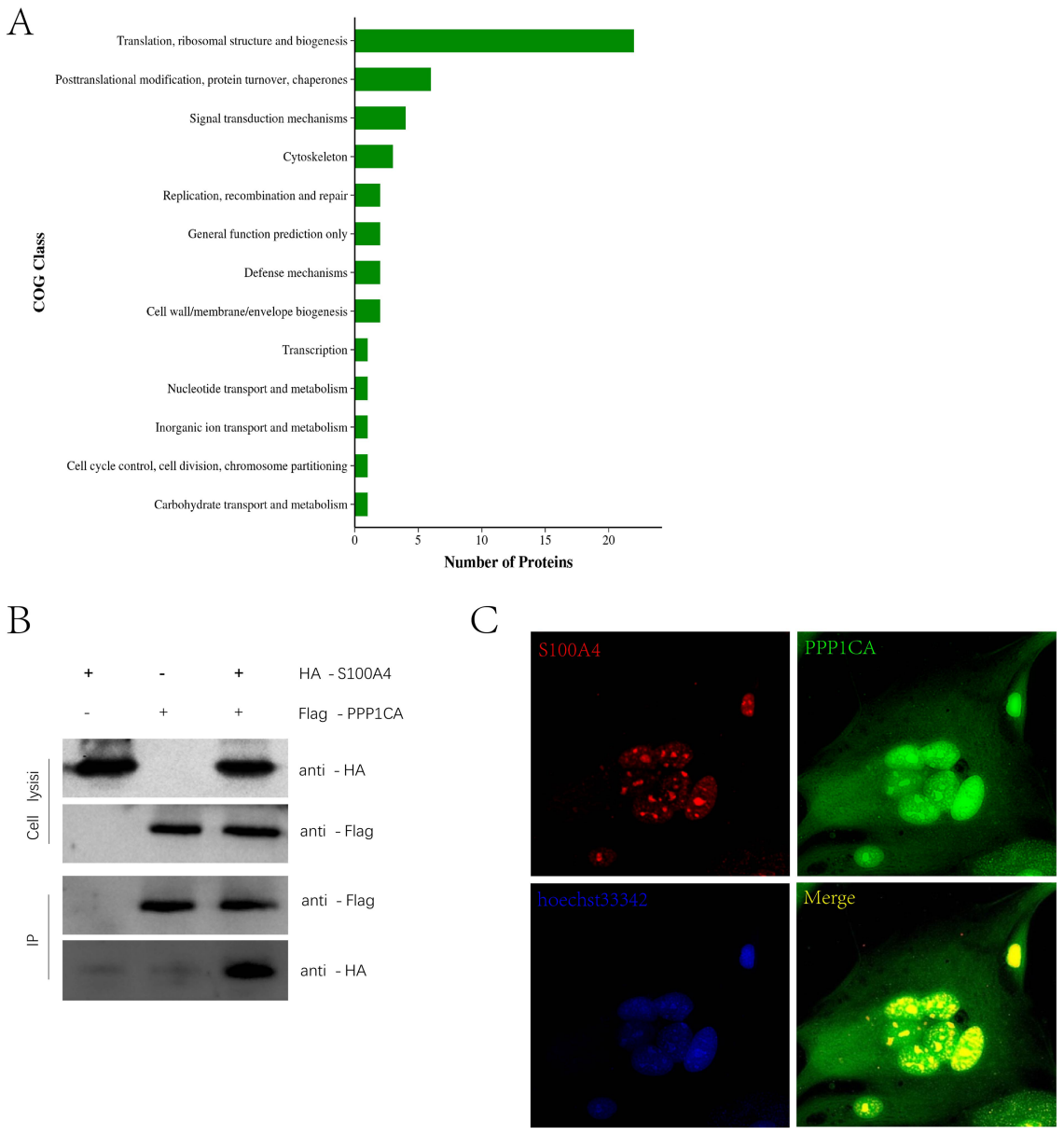

FIGURE 3
Interaction of S100A4 and PPP1CA **(A)** COG analysis of interacting proteins detected by mass spectrometry after immunoprecipitation of S100A4. **(B)** Immunoprecipitation detection of the interaction between S100A4 and PPP1CA. **(C)** Laser confocal detection of the interaction between S100A4 and PPP1CA.

revealed that Y-320 treatment significantly reduced the number of positive cells (Figure 6). In addition, after overexpression of S100A4 and PPP1CA in sheep endometrial cells, decreased IL-17 gene transcription levels were detected (Supplementary Figure 1). These results suggest that the inhibition of the IL-17 signaling pathway resulting from S100A4 and PPP1CA overexpression might be responsible for the reduced senescence of sheep endometrial cells.

3.7 *In vivo* experiments show that uterine endometrial cells lacking S100A4 promote senescence

To determine whether S100A4 can regulate PPP1CA *in vivo*, we generated S100A4-deficient mice through breeding (8). HE staining of the endometrium revealed that the epithelial cells in the S100A4-deficient mice were mostly single-layer columnar cells, whereas those in the control group were multilayer epithelial cells. Additionally, the endometrial thickness was uneven and relatively thin in the S100A4-deficient group. Furthermore, nuclear fragmentation and cell death in the epithelial cells of the endometrium in the S100A4-deficient group (Figure 7A) indicate that S100A4 deficiency altered the normal state of endometrial epithelial cells. Immunohistochemical staining revealed reduced PPP1CA expression levels in the endometrial cells of S100A4-deficient mice (Figure 7B). These results suggest that knocking out S100A4 *in vivo* can reduce PPP1CA protein levels lead to endometrial cell damage. Based on these results, it can be speculated that S100A4 and PPP1CA inhibit the senescence of sheep endometrial cells, possibly by inhibiting the activation of the IL-17 signaling pathway (Figure 7C).

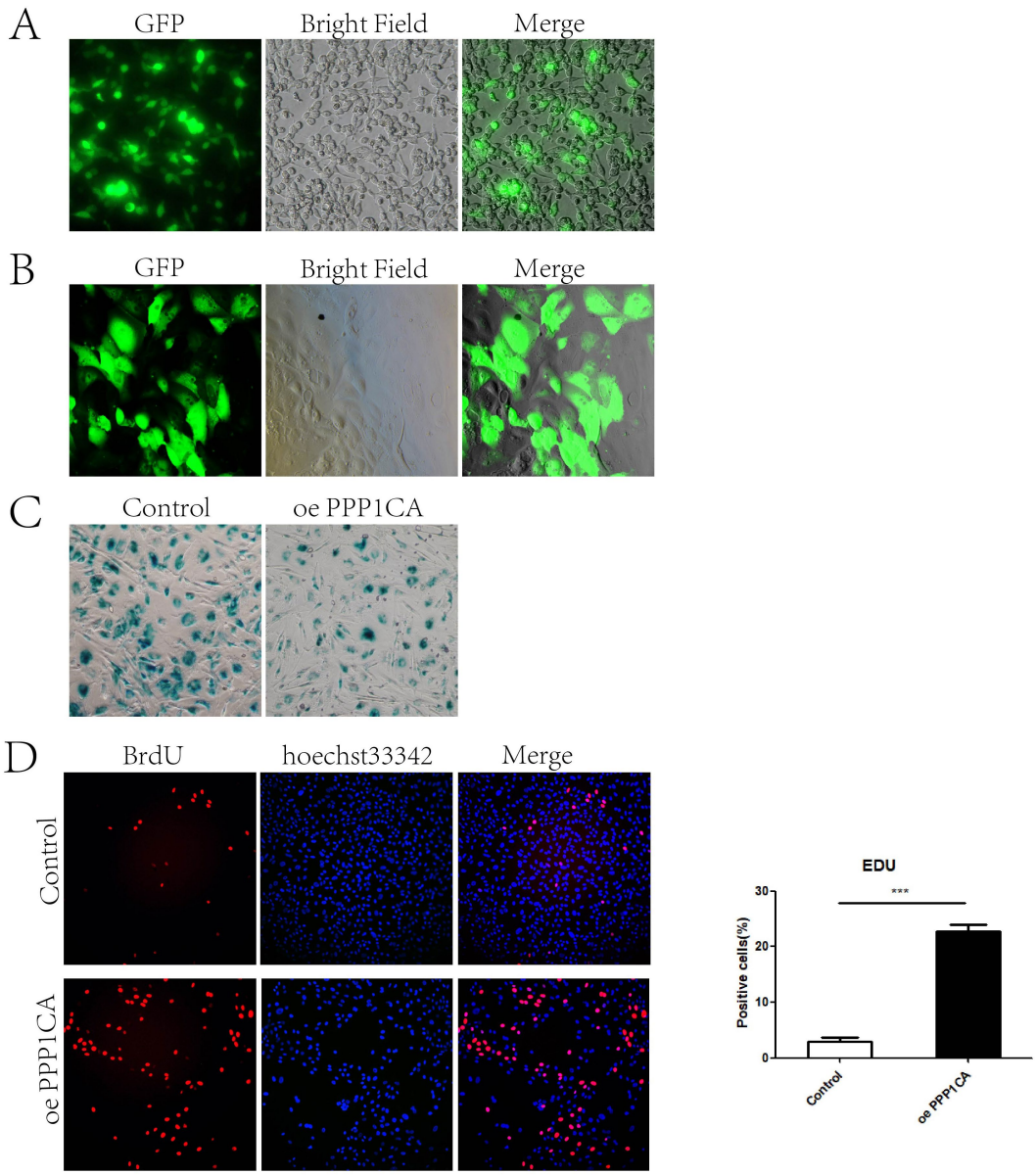

FIGURE 4
PPP1CA inhibits cell senescence **(A)** 293T cells packaged with lentivirus. **(B)** Lentivirus transduction into sheep endometrial epithelial cells. **(C)** Galactosidase staining after PPP1CA overexpression. **(D)** EdU staining to detect cell proliferation. ***$p < 0.001$.

4 Discussion

In human clinical studies, compared with GnRH agonist protocols, GnRH antagonist protocols for *in vitro* fertilization (IVF) typically result in lower pregnancy rates, with decreased S100P expression, while apoptosis is increased following GnRH antagonist treatment (11). However, the use of GnRH agonists in human EC cell lines reduces cell proliferation (12), a phenomenon that has been confirmed in various cell types (13). During sheep embryo transplantation, GnRH agonists do not facilitate embryo implantation; instead, they inhibit the expression of S100A4, which promotes the proliferation of endometrial epithelial cells (8). In addition to affecting the proliferation of sheep endometrial epithelial cells, GnRH also reduces the number of endometrial cells and induces apoptosis. The final outcome for cells that stop proliferating is often cellular senescence (14). In this study, we found that S100A4 knockdown promotes endometrial epithelial cell senescence, revealing a new mechanism for S100A4's role in endometrial cell regulation.

The activation of the IL-17 signaling pathway is a major cause of cellular senescence in various cell types. Skin aging is associated with signs of chronic inflammation, and single-cell sequencing has revealed that IL-17 produced by lymphocytes is a cause of skin aging (15). In arthritis, Th17 cells induce fibroblast senescence, and injecting IL-17-neutralizing antibodies into the joints of patients reduces the expression levels of senescence markers (16). Additionally, in degenerative arthritis, the senescence of chondrocytes is significantly linked to IL-17 expression (17). In studies of vascular endothelial dysfunction, IL-17 has been shown to induce endothelial cell senescence (18, 19). This study revealed changes in the IL-17 signaling pathway in S100A4-and PPP1CA-induced

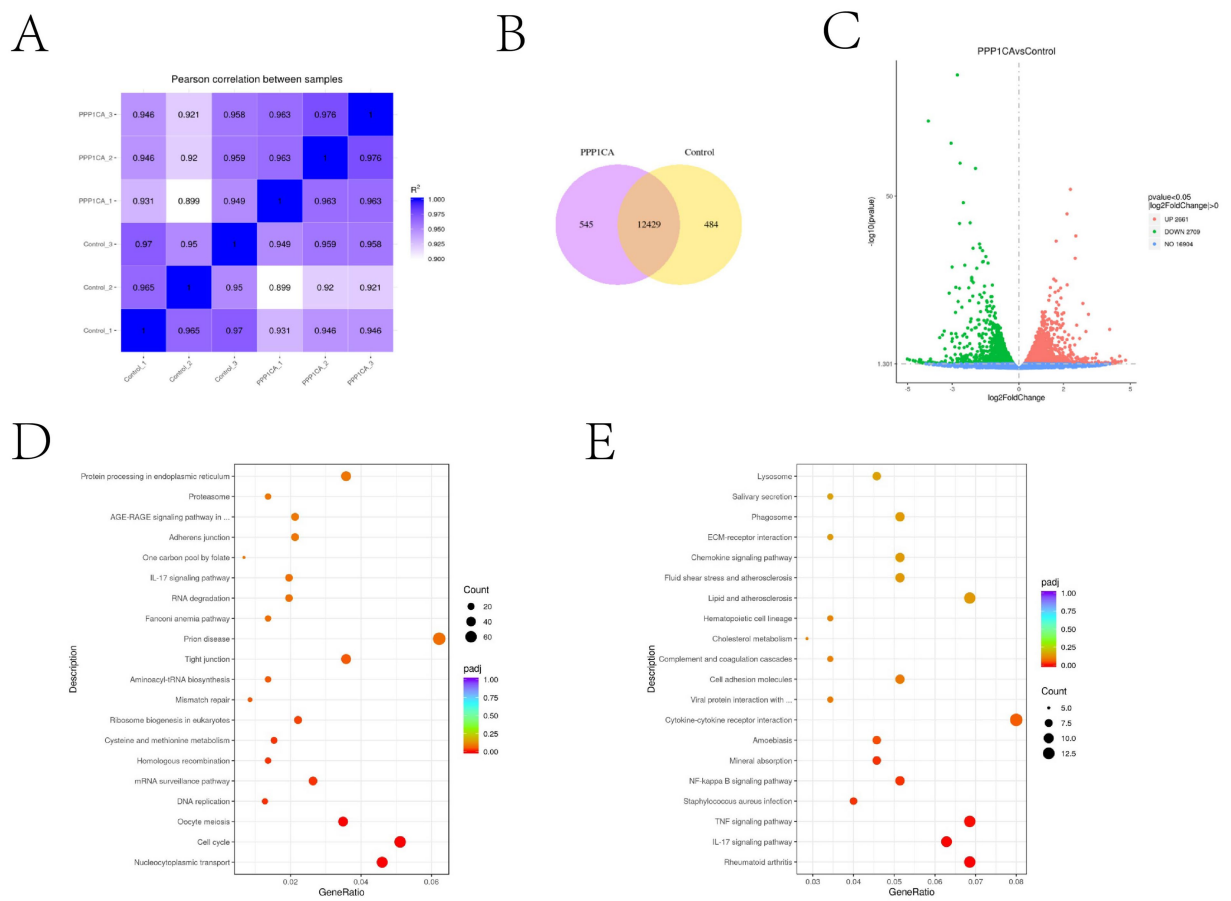

FIGURE 5
Transcriptome sequencing revealed that PPP1CA can inhibit the IL-17 signaling pathway **(A)** Pearson correlation between samples. **(B)** Changes in the expression levels of specific genes after PPP1CA overexpression. **(C)** Volcano plot showing genes with transcriptional changes after PPP1CA overexpression. -log10 (Pvalue) was used to measure the expression level. The larger the value, the greater the difference in gene expression. **(D)** KEGG enrichment of signaling pathways downregulated after PPP1CA overexpression. **(E)** KEGG enrichment showing differences in signaling pathways after GNAI2 and PPP1CA overexpression. padj (adjusted *p*-value) is a *p*-value that has been corrected to account for the fact that you are performing statistical tests, lower padj values (closer to zero) typically indicate more statistically significant results.

senescence, suggesting that IL-17 pathway activation is a significant cause of endometrial cell senescence.

We identified the regulatory molecules S100A4 and PPP1CA, which modulate the IL-17 signaling pathway in endometrial cells. S100A4 expression is significantly decreased in sheep endometrial tissue after GnRH agonist treatment (8). Further *in vitro* experiments revealed that S100A4 knockdown activated the IL-17 pathway. Although no previous reports have linked S100A4 to aging, S100A4 has been extensively studied for its role in promoting the proliferation of breast cancer cells (20, 21), liver cancer cells (22), lung cancer cells (23), prostate cells (24), and endometrial cancer cells (25). In addition to regulating cell proliferation, S100A4 influences immune cell proliferation and mast cell recruitment (26). Single-cell sequencing analysis identified S100A4 as an important immune-suppressing T-cell regulator in glioma (27). S100A4 activates the NF-κB/NLRP3 inflammasome signaling pathway to promote macrophage pyroptosis induced by *Mycobacterium tuberculosis* infection (28). It is also a marker of microglial reactivity, suggesting its role in neuroinflammation (29). These findings imply that S100A4 can regulate cell fate and immune responses. The activation of the IL-17 pathway, which is based on immune response-regulated cellular senescence, indicates that S100A4 has the potential to regulate cellular senescence. Indeed, our experiments confirmed that knocking out S100A4 promotes the senescence of sheep endometrial cells, increasing our understanding of the functional mechanisms of S100A4.

PPP1CA can regulate immune responses, affecting immune cell infiltration and breast cancer tumor cell proliferation (30). In glioma cells, PPP1CA collaborates with KIF18A to regulate cancer cell proliferation (31). In MIO-M1 cells, PPP1CA promotes YAP phosphorylation to regulate cell proliferation (32). In studies of intervertebral disc degeneration, PPP1CA was shown to mediate nucleus pulposus cell senescence (10). Our work revealed the interaction between PPP1CA and S100A4 and verified the role of PPP1CA in sheep endometrial cell senescence. These findings expand the scope of PPP1CA regulation of cellular senescence and elucidate the mechanisms through which PPP1CA is regulated.

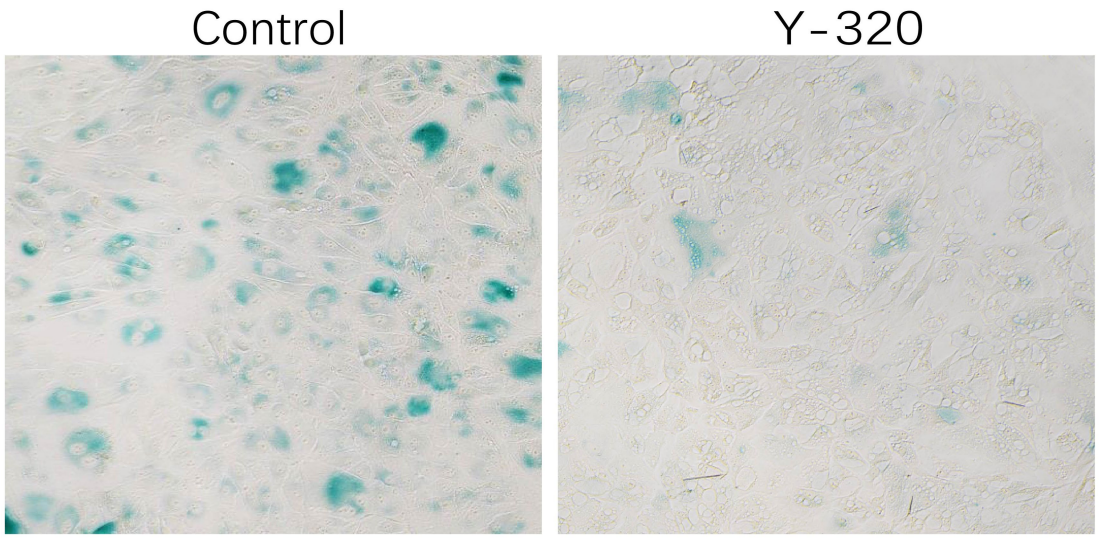

FIGURE 6
Cell senescence is reduced after treatment with an IL-17 inhibitor.

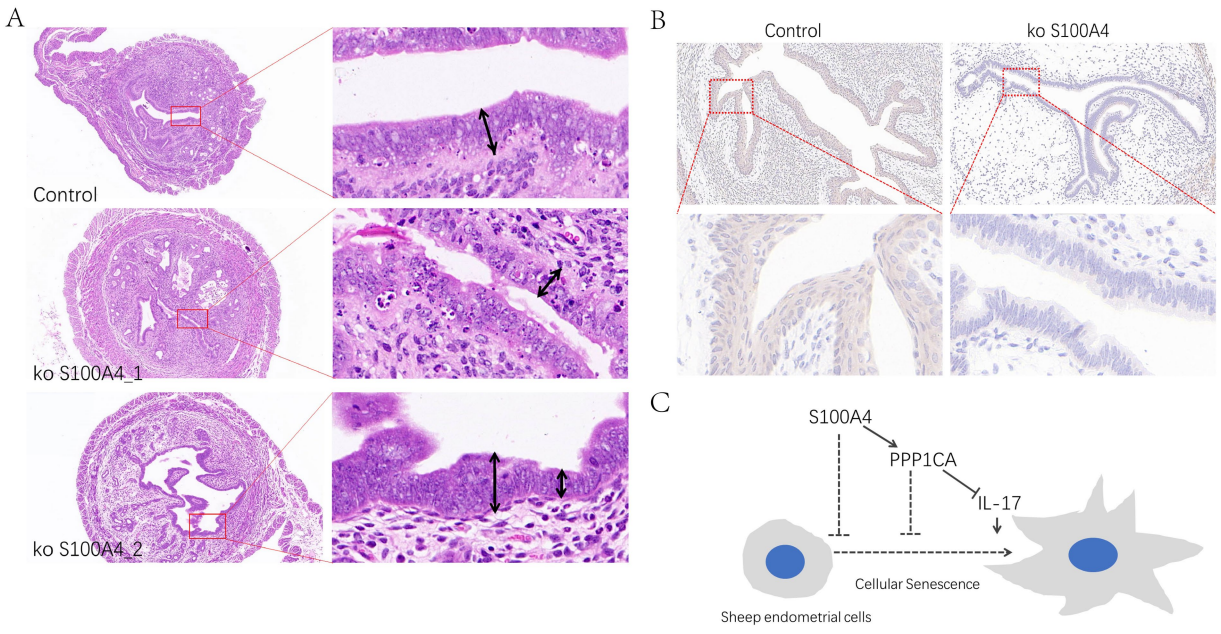

FIGURE 7
Effects of S100A4 knockout on the mouse endometrial epithelium (A) Effects of HE staining of tissue sections of the endometrium. (B) Immunohistochemical staining of PPP1CA expression in the mouse endometrium. (C) Mechanistic diagram of signaling pathway.

5 Conclusion

This study revealed that GnRH can regulate endometrial cell senescence, identified the interaction between S100A4 and PPP1CA and described its role in regulating cellular senescence, and revealed the regulatory role of the S100A4/PPP1CA/IL-17 signaling pathway in sheep endometrial cell senescence. These findings provide theoretical guidance for hormone selection during sheep embryo tansfer in clinical settings. Future research on the interaction between different cell types and their impact on sheep endometrial cell senescence will increase the understanding of these mechanisms and aid in identifying regulatory targets to enhance sheep embryo implantation.

Data availability statement

The datasets presented in this study can be found in online repositories. The names of the repository/repositories and accession number(s) can be found at: https://www.ncbi.nlm.nih.gov/, PRJNA1090558; https://www.ncbi.nlm.nih.gov/, PRJNA1090239.

Ethics statement

The animal study was approved by the Ethical Committee of Xinxiang Medical University. The study was conducted in accordance with the local legislation and institutional requirements.

Author contributions

XJ: Conceptualization, Data curation, Formal analysis, Investigation, Methodology, Software, Validation, Writing – original draft, Writing – review & editing. YJ: Formal analysis, Investigation, Methodology, Software, Validation, Writing – original draft. JC: Data curation, Methodology, Writing – original draft. HZ: Data curation, Methodology, Writing – original draft. XL: Writing – review & editing. ZC: Conceptualization, Funding acquisition, Supervision, Visualization, Writing – original draft. XW: Conceptualization, Funding acquisition, Project administration, Supervision, Writing – review & editing.

Funding

The author(s) declare financial support was received for the research, authorship, and/or publication of this article. Talents Special Fund of Hebei Agricultural University (Fund No: YJ201952 to XW); Natural Science Foundation of Hebei Province (Fund No.: C2021204039 to XW); National Natural Science Foundation of China (Fund No.:82303770 to ZC).

Conflict of interest

The authors declare that the research was conducted in the absence of any commercial or financial relationships that could be construed as a potential conflict of interest.

Publisher's note

All claims expressed in this article are solely those of the authors and do not necessarily represent those of their affiliated organizations, or those of the publisher, the editors and the reviewers. Any product that may be evaluated in this article, or claim that may be made by its manufacturer, is not guaranteed or endorsed by the publisher.

Supplementary material

The Supplementary material for this article can be found online at: https://www.frontiersin.org/articles/10.3389/fvets.2024.1466482/full#supplementary-material

References

1. Zhang J, Ma J, Aibibaimu WX, Liu Y, Li X. Effects of exogenous GnRH administration on lambing performance of oestrus-synchronized Kazak ewes during the breeding season. *Reprod Domest Anim*. (2023) 58:465–9. doi: 10.1111/rda.14306

2. Zhang J, Wu X, Li X. GnRH administration after estrus induction protocol decreases the pregnancy rate of recipient ewes following transfer of frozen-thawed embryos. *Small Rumin Res*. (2022) 217:106849. doi: 10.1016/j.smallrumres.2022.106849

3. Zhou C, Yang X, Wang Y, Xi J, Pan H, Wang M, et al. Ovulation triggering with hCG alone, GnRH agonist alone or in combination? A randomized controlled trial in advanced-age women undergoing IVF/ICSI cycles. *Hum Reprod*. (2022) 37:1795–805. doi: 10.1093/humrep/deac114

4. Liu C, Tian T, Lou Y, Li J, Liu P, Li R, et al. Live birth rate of gonadotropin-releasing hormone antagonist versus luteal phase gonadotropin-releasing hormone agonist protocol in IVF/ICSI: a systematic review and meta-analysis. *Expert Rev Mol Med*. (2023) 26:e2:1–30. doi: 10.1017/erm.2023.25

5. Li X, Lin J, Zhang L, Liu Y. Effects of gonadotropin-releasing hormone agonist pretreatment on frozen embryo transfer outcomes in artificial cycles: a meta-analysis. *Arch Gynecol Obstet*. (2023) 308:675–83. doi: 10.1007/s00404-022-06823-7

6. Li X, Yao X, Xie H, Zhang G, Deng M, Deng K, et al. PPP2R2A affects embryonic implantation by regulating the proliferation and apoptosis of Hu sheep endometrial stromal cells. *Theriogenology*. (2021) 176:149–62. doi: 10.1016/j.theriogenology.2021.09.026

7. Cui L, Xu F, Jiang Z, Wang S, Li X, Ding Y, et al. Melatonin regulates proliferation and apoptosis of endometrial stromal cells via MT1. *Acta Biochim Biophys Sin Shanghai*. (2021) 53:1333–41. doi: 10.1093/abbs/gmab108

8. Jiao X, Chu Z, Li M, Wang J, Ren Z, Wang L, et al. GnRH-mediated suppression of S100A4 expression inhibits endometrial epithelial cell proliferation in sheep via GNAI2/MAPK signaling. *Front Vet Sci*. (2024) 11:1410371. doi: 10.3389/fvets.2024.1410371

9. Wang X, Sun J, Fu C, Liu C. Generation of a PPP1CA knockout human pluripotent stem cell line via CRISPR/Cas 9. *Stem Cell Res*. (2023) 69:103077. doi: 10.1016/j.scr.2023.103077

10. Liang H, Luo R, Li G, Zhang W, Zhu D, Wu D, et al. Lysine methylation of PPP1CA by the methyltransferase SUV39H2 disrupts TFEB-dependent autophagy and promotes intervertebral disc degeneration. *Cell Death Differ*. (2023) 30:2135–50. doi: 10.1038/s41418-023-01210-4

11. Zhang D, Han M, Zhou M, Liu M, Li Y, Xu B, et al. Down-regulation of S100P induces apoptosis in endometrial epithelial cell during GnRH antagonist protocol. *Reprod Biol Endocrinol*. (2021) 19:99. doi: 10.1186/s12958-021-00787-0

12. Emons G, Gründker C. The role of gonadotropin-releasing hormone (GnRH) in endometrial Cancer. *Cells*. (2021) 10:292. doi: 10.3390/cells10020292

13. Ohta H, Sakamoto H, Satoh K. In vitro effects of gonadotropin-releasing hormone (GnRH) analogue on cancer cell sensitivity to cis-platinum. *Cancer Lett*. (1998) 134:111–8. doi: 10.1016/s0304-3835(98)00270-5

14. Hsu CH, Altschuler SJ, Wu LF. Patterns of early p21 dynamics determine proliferation-senescence cell fate after chemotherapy. *Cell*. (2019) 178:361–373.e12. doi: 10.1016/j.cell.2019.05.041

15. Solá P, Mereu E, Bonjoch J, Casado-Peláez M, Prats N, Aguilera M, et al. Targeting lymphoid-derived IL-17 signaling to delay skin aging. *Nat Aging*. (2023) 3:688–704. doi: 10.1038/s43587-023-00431-z

16. Faust HJ, Zhang H, Han J, Wolf MT, Jeon OH, Sadtler K, et al. IL-17 and immunologically induced senescence regulate response to injury in osteoarthritis. *J Clin Invest*. (2020) 130:5493–507. doi: 10.1172/JCI134091

17. Wang B, Sun W, Bi K, Li Y, Li F. Apremilast prevents IL-17-induced cellular senescence in ATDC5 chondrocytes mediated by SIRT1. *Int J Mol Med*. (2021) 47:12. doi: 10.3892/ijmm.2021.4845

18. Zhang L, Liu M, Liu W, Hu C, Li H, Deng J, et al. Th17/IL-17 induces endothelial cell senescence via activation of NF-κB/p53/Rb signaling pathway. *Lab Investig*. (2021) 101:1418–26. doi: 10.1038/s41374-021-00629-y

19. Li N, Luo R, Zhang W, Wu Y, Hu C, Liu M, et al. IL-17A promotes endothelial cell senescence by up-regulating the expression of FTO through activating JNK signal pathway. *Biogerontology*. (2023) 24:99–110. doi: 10.1007/s10522-022-09999-2

20. Dukhanina EA, Portseva TN, Dukhanin AS, Georgieva SG. Triple-negative and triple-positive breast cancer cells reciprocally control their growth and migration via the S100A4 pathway. *Cell Adhes Migr*. (2022) 16:65–71. doi: 10.1080/19336918.2022.2072554

21. Katte RH, Chou RH, Yu C. Pentamidine inhibit S100A4- p53 interaction and decreases cell proliferation activity. *Arch Biochem Biophys*. (2020) 691:108442. doi: 10.1016/j.abb.2020.108442

22. Zhu K, Huang W, Wang W, Liao L, Li S, Yang S, et al. Up-regulation of S100A4 expression by HBx protein promotes proliferation of hepatocellular carcinoma cells and its correlation with clinical survival. *Gene*. (2020) 749:144679. doi: 10.1016/j.gene.2020.144679

23. Wu X, Zhang H, Jiang G, Peng M, Li C, Lu J, et al. Exosome-transmitted S100A4 induces immunosuppression and non-small cell lung cancer development by activating STAT3. *Clin Exp Immunol*. (2022) 210:309–20. doi: 10.1093/cei/uxac102

24. Yang L, Liu J, Yin J, Li Y, Liu J, Liu D, et al. S100A4 modulates cell proliferation, apoptosis and fibrosis in the hyperplastic prostate. *Int J Biochem Cell Biol*. (2024) 169:106551. doi: 10.1016/j.biocel.2024.106551

25. Ren W, Chi YB, Sun JL. Effect of shRNA-mediated regulation of S100A4 gene expression on proliferation and apoptosis of KLE endometrial cancer cells. *Clin Transl Oncol*. (2021) 23:148–54. doi: 10.1007/s12094-020-02406-7

26. Wu T, Ma L, Jin X, He J, Chen K, Zhang D, et al. S100A4 is critical for a mouse model of allergic asthma by impacting mast cell activation. *Front Immunol*. (2021) 12:692733. doi: 10.3389/fimmu.2021.692733

27. Liu S, Zhang H, Li Y, Zhang Y, Bian Y, Zeng Y, et al. S100A4 enhances protumor macrophage polarization by control of PPAR-γ-dependent induction of fatty acid oxidation. *J Immunother Cancer*. (2021) 9:e002548. doi: 10.1136/jitc-2021-002548

28. Li M, Liu Y, Nie X, Ma B, Ma Y, Hou Y, et al. S100A4 promotes BCG-induced pyroptosis of macrophages by activating the NF-κB/NLRP3 inflammasome signaling pathway. *Int J Mol Sci*. (2023) 24:12709. doi: 10.3390/ijms241612709

29. Serrano A, Apolloni S, Rossi S, Lattante S, Sabatelli M, Peric M, et al. The S100A4 transcriptional inhibitor niclosamide reduces pro-inflammatory and migratory phenotypes of microglia: implications for amyotrophic lateral sclerosis. *Cells*. (2019) 8:1261. doi: 10.3390/cells8101261

30. Xie W, Sun Y, Zeng Y, Hu L, Zhi J, Ling H, et al. Comprehensive analysis of PPPCs family reveals the clinical significance of PPP1CA and PPP4C in breast cancer. *Bioengineered*. (2022) 13:190–205. doi: 10.1080/21655979.2021.2012316

31. Yang J, Zhang Q, Yang Z, Shu J, Zhang L, Yao Y, et al. KIF18A interacts with PPP1CA to promote the malignant development of glioblastoma. *Exp Ther Med*. (2023) 25:154. doi: 10.3892/etm.2023.11853

32. Guo Y, Cang X, Zhu L, Zhu M, Li A, Wang Z, et al. PPP1CA/YAP/GS/Gln/mTORC1 pathway activates retinal Müller cells during diabetic retinopathy. *Exp Eye Res*. (2021) 210:108703. doi: 10.1016/j.exer.2021.108703

frontiers | Frontiers in Veterinary Science

TYPE Brief Research Report
PUBLISHED 11 December 2024
DOI 10.3389/fvets.2024.1456324

OPEN ACCESS

EDITED BY
Regiane R. Santos,
Schothorst Feed Research, Netherlands

REVIEWED BY
Emoke Pall,
University of Agricultural Sciences and Veterinary Medicine of Cluj-Napoca, Romania
Christian Hanzen,
University of Liège, Belgium

*CORRESPONDENCE
Petru Roșca
✉ petru.rosca@iuls.ro
Florin Nechifor
✉ florin.nechifour@iuls.ro
Ștefan Gregore Ciornei
✉ ștefan.ciornei@iuls.ro

RECEIVED 28 June 2024
ACCEPTED 28 November 2024
PUBLISHED 11 December 2024

CITATION
Nechifor F, Ciornei ȘG and Roșca P (2024) Bacteriological load in Holstein Friesian cows with dystocia.
Front. Vet. Sci. 11:1456324.
doi: 10.3389/fvets.2024.1456324

Bacteriological load in Holstein Friesian cows with dystocia

Florin Nechifor*, Ștefan Gregore Ciornei* and Petru Roșca*

Department Clinics, Reproduction, Faculty of Veterinary Medicine, University of Life Sciences (IULS), Iași, Romania

The research took place on a farm in North-Eastern Romania with Holstein Friesian cows aged between 3 and 9 years. Bacteriological investigations were carried out throughout the year 2023, on a total of 35 cows, including 25 multiparous cows and 10 primiparous cows, 23 cows had eutocic parturitions and 12 cows had dystocic parturitions, during the first 3 weeks postpartum. In the case of dystocic parturition, biological samples yielded isolates including 9.3% strains classified as *Staphylococcus*, 8.1% strains of *Escherichia coli*, 4.1% strains of *Arcanobacterium*, and 2.3% strains of *Klebsiella*. Other bacterial types were identified in lesser proportions. In the case of eutocic parturition, *Escherichia coli* was most frequently isolated: 18.6% of the isolated bacterial strains, followed by 5.8% *Pseudomonas* spp., 4.6% *Enterococcus* spp., 4.6% *Streptococcus* species, 3.5% *Staphylococcus* spp., and *Corynebacterium* spp., and 2.3% *Arcanobacterium* spp. It is noted that on the 7th day of puerperium, the mean value of colony-forming units per milliliter (CFU/mL) was 74×10^4 CFU/mL in normal calving cows compared to 29×10^6 CFU/mL in cows with dystocia. The total number of recorded germs increases significantly during the first 14 days postpartum in all cases, higher levels being shown in cows with dystocic calving. For statistical analysis, the independent t-test ($p < 0.05$) was made by using the SPSS 16 software. The object of the research is the bacteriological load in Holstein Friesian cows depending on the type of eutocic parturition/dystocia.

KEYWORDS

cow, dystocia, eutocic, bacteria, puerperium, fertility

1 Introduction

Puerperal infections of the reproductive tract in dairy cows can lead to fertility problems and represent a relevant economic problem due to their frequency. Uterine disorders lead to the reduction in cow welfare due to inflammation of the genital tract and they should not be underestimated (1, 2).

Understanding the morpho-functional activities of the genital apparatus is an essential condition for specialists who prevent and treat disorders that may occur at this level (3).

The general understanding is that the reproductive ability of animals, expressed by the term fertility, is based on two anatomo-physiological coordinates of the genital apparatus: the structural component and the dynamic component, represented by the peculiarities of reproductive function (4, 5). These two values are integrated into a morphophysiological complex that constitutes the entire animal organism (6, 7).

Through gynecological examinations and by clinical and laboratory research, the causal agents of reproductive disorders have been highlighted. These agents can lead to various lesion and functional changes of the genital apparatus (8, 11).

The postpartum period is predominantly included in the complex of conditions affecting sexual activity (9, 10, 12).

The puerperal period is conditioned and influenced by several factors: the physical and health status of the female, the course of parturition, the quality of parturition assistance,

nutrition, milk production, environmental conditions, or stress factors (13, 16, 17).

Under these conditions, this period is characterized by: postpartum uterine involution, lochia elimination, postpartum ovarian activity resumption and postpartum uterine bacteriology (14, 18).

The various obstetric disorders that can occur during this period cause serious disturbances in the course of the puerperium, negatively influencing the main reproductive parameters, including fecundity and female fertility (7, 15).

However, bacterial contamination of the uterus in postpartum cows is common and the development of uterine inflammation depends on local immunity and the intensity of contamination (6).

Obstetric disorders that may occur during this period can cause serious disturbances in the course of the puerperium.

Infections in the puerperal period may lead to puerperal metritis or clinical endometritis. Thus, uterine bacterial infections have been shown to adversely affect uterine and ovarian function and fertility (13). These conditions can be so severe that they can permanently compromise reproductive function (17).

In addition to understanding the physiological phenomena that occur during the puerperal period, it is recognized that within the reproductive cyclogram, in case of disturbances that may occur, some modifications in the female's subsequent fertility are observed (9, 15).

The numerous functional transformations that take place during the postpartum period, recorded at the cellular level up to the level of organs and systems, can have different effects negatively influencing the body's recovery and delaying or blocking the resumption of sexual function (18).

Under the influence of these factors and in the conditions of the great lability of postpartum body recovery processes, the pathology of the puerperal period is diverse and complex, being directly related to the pathology of parturition and the periparturient period (16).

Monitoring the puerperal period involves coordinating the factors that determine the smooth running of sexual processes, with an important component being the optimal resumption of physiological and morphofunctional parameters close to the ante-partum period (14).

The object of the research is to determine the bacteriological load in Holstein Friesian cows depending on the type of eutocic parturition/dystocia.

2 Materials and methods

Bacteriological investigations were carried out throughout the year 2023, on a total of 35 cows, including 25 multiparous cows and 10 primiparous cows, 23 cows had eutocic parturitions and 12 cows had dystocic parturitions, during the first 3 weeks postpartum. The research took place in North-eastern Romania on Holstein Friesian cows aged between 3 and 9 years.

Sampling was performed with an exudate swab made in the laboratory. For this, 40 cm metal rods were used, the ends of which were protected with cotton wool. One of them was inserted into a 30 cm test tube and finally they were distributed individually in bags to be sterilized by autoclaving. Sterilization was carried out at 121°C for 60 min. In this way, a proper sterilization and a suitable size for this type of harvest was ensured.

For the isolation and identification of potentially pathogenic bacterial agents, both standard culture media and differential and selective media were used.

Differential media contain substrates for specific bacterial enzymes or cytotoxins and an indicator that confirms the reactivity on this substrate. This category also includes blood agar, which differentiates between hemolytic and non-hemolytic bacteria, or lactose media with various pH indicators. Selective culture media for bacteria contain specific indicators that confirm certain characteristics of bacteria, such as their ability to use certain substrates, to produce certain enzymes, or to resist certain antimicrobial agents.

The selective and differential media used were: EMB Agar (Oxoid); Mac Conkey Agar (Merck); Chapman Agar (Oxoid); Columbia Agar (Oxoid); Infusion Brain Heart Agar (Oxoid); Agar-bile-esculin-sodiumazide; Brucella Agar (Oxoid); CCDAgar (Charcoal Cefoperozone Deoxycholate agar, Oxoid); SPS Agar (Sulphite Polymyxin Sulfadiazine, Oxoid); TSI (triple sugar iron agar, Oxoid); MIU (motility, indole, urease, Oxoid); MILF (motility, indole, lysinedecarboxylase, phenylalaninedeaminase, Oxoid); Simmons Agar (Oxoid) and oxidase test.

Pathological materials were subjected to laboratory investigations according to the general guidelines of bacteriological diagnosis.

The culture media used are produced by: Oxoid (UK) and Merg (Germany).

Selective media contain substances that inhibit the growth of contaminating bacteria, possibly collected during sampling. All special culture media, used for bacterial isolation, contain, according to the technical file, different substances that can inhibit or favor the multiplication of certain species of microorganisms. Depending on their recommendation, their composition is different.

For identification of bacterial strains Api galleries were used.

Api systems allow easy and rapid identification of 20–30 biochemical tests of aerobic and anaerobic bacteria.

The API tests were selected according to the results obtained following the examination of the tinctorial, morphological and cultural characters of the isolated strains.

API 20 A galleries were used to test anaerobic bacteria.

The evaluation methodology is a classic one in microbiology. After the isolation of the strains in pure culture, the bacteria were subjected to specific work steps for biochemical testing using the API galleries. The protocol is extensive and we are not allowed to describe the work steps, but summarizing we can mention: isolation in pure culture on the solid medium; obtaining a bacterial suspension equivalent to 0.5 Mc Farland (1.5×10^8 CFU), adding it to the wells of the API galleries. Incubation at 37°C for 24–48 h under aerobic or anaerobic conditions, checking each test based on color change by automatic reading with the help of the API reading system.

Determinations were made using the API LAB Plus.

The complex biochemical identification systems used were: mini API galleries for API 20 NE, API 20 E, API 32 GN. ID32GN is used for the identification of Gram-negative species, but we used API 32 E, which also allowed the identification of other non-Enterobacteriaceae species. The galleries used are produced by Biomerieux. To reconstitute the substrate, the galleries were inoculated with a bacterial suspension made from the studied colony. Bacterial suspensions were made from the 24-h strains brought to a bacterial density equivalent to the 0.5 Mc Farland standard (1.5×10^8 cfu).

When the results were inconclusive after the first reading, the galleries were further incubated for another 24 h. After reading, additional agents were introduced, which differ from one identification system to another: Api 20E (TDA, IND). Sometimes, the substrates in the wells of the API galleries are not conclusive enough in terms of color shift and the reading can give errors. In this case, it is useful and in practice it is recommended that the API galleries be maintained for another 24 h in the thermostat and only then the final reading is done.

The bacteriological examination protocol requires isolating bacteria from pathological materials on culture media and identifying the cultures.

Inoculation was performed directly onto culture media without prior processing. The inoculum was spread using an exudate swab or an inoculation loop onto agar medium. Inoculum spreading was performed using the quadrant streaking technique to obtain isolated colonies.

Inoculation on liquid media was carried out using a Pasteur pipette, transferring the biological sample from the transport tube into the appropriate growth medium.

Following inoculation, culture media were incubated in a thermostat at 37°C under aerobic and anaerobic conditions.

The pathological material taken from the patient was discharged into one milliliter of sterile physiological serum, from which decimal dilutions were then carried out up to dilution 10^8. From each dilution, 1 mL was taken and distributed in two sterile Petri dishes, over which the Mueller Hinton Agar medium was added, melted and cooled to 45°C so as not to influence cell viability in the suspension, and the dishes were incubation at 37°C. After 24 h, bacterial colonies were counted from the last plates, where the density of the colonies allowed them to be counted. The results obtained on the two dilution plates were averaged and multiplied by the dilution factor, thus obtaining the total number of germs per 1 mL of biological sample suspension. The results were reported in CFU/mL.

The results of the bacterioscopic examination conducted on the collected pathological materials revealed bacterial morphologies and different staining affinities, depending on the sampling area and the evolution of the infectious site. The purpose of the bacterioscopic examination was to guide bacteriological investigations to obtain relevant results.

Microscopic examination of Gram-stained smears identified fields with: coccal forms of 1 μm, arranged in shorter or longer chains, or grouped in clusters, stained Gram-positive; bacilli with club-shaped or rounded ends and deformed bacterial bodies with endospores, Gram-positive, of various sizes, some unbranched, non-sporulated, grouped in palisades, Chinese letter shapes, or short chains, with or without metachromatic granules; branched, filamentous filaments, long bacilli, some fusiform, Gram-positive or Gram-negative, some arranged radially; kidney-shaped cocci, arranged in diplo or tetrads, stained Gram-negative; cocobacilli or Gram-negative bacilli, with or without bipolar staining, sporulated or non-sporulated.

2.1 Statistical analysis

For statistical analysis, the independent *t*-test ($p < 0.05$) was made by using the SPSS 16 software.

3 Results

3.1 Bacteriological examination from a quantitative point of view

It is observed that, in the 7th day of puerperium the average value of colony-forming units per milliliter (CFU/mL) was 74×10^4 CFU/mL in cows with normal parturition compared with 29×10^6 CFU/mL in cows with dystocia. In this situation, the differences in the bacterial load are obvious (Figure 1A).

For $p < 0.05$ (independent student t-test), the difference between average CFU/mL of 7th day samples from cows with normal parturition and average CFU/mL of 7th day samples from cows with dystocia is statistically significant.

At 14th day of puerperium the average value for cows with normal parturition was 52×10^6 CFU/mL and for those with dystocia the average grew up until 19×10^7 CFU/mL (Figure 1B).

For $p < 0.05$ (independent student t-test), the difference between average CFU/mL of 14th day samples from cows with normal parturition and average CFU/mL of 7th day samples from cows with dystocia is not statistically significant.

At 21st day of puerperium, the average CFU/mL for cows with normal parturition was 27×10 CFU/mL, while for those with dystocia the average was 27×10^6 CFU/mL (Figure 1C).

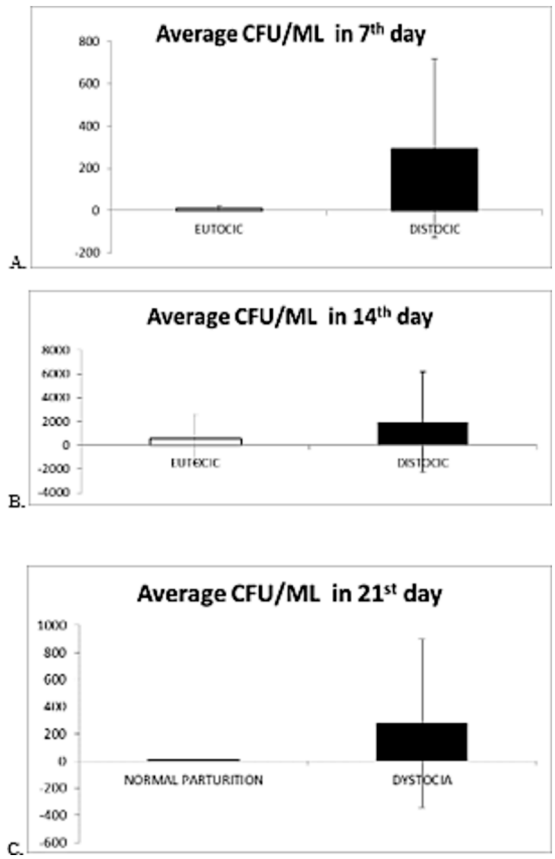

FIGURE 1
Graphical representation of the average value and standard deviation of evolution of the microbial load from cows in 7th day **(A)**, 14th **(B)**, 21st day **(C)** of puerperium with normal parturition/dystocia.

For $p < 0.05$ (independent student t-test), the difference between average CFU/mL of 14th day samples from cows with normal parturition and average CFU/mL of 7th day samples from cows with dystocia is statistically significant.

The results obtained from the quantitative evaluation of biological samples do not indicate significant differences in cows with eutocic calving concerning CFU/mL, which are consistent with those mentioned in specialized literature. For most cows with eutocic calving, the microbial load varied at 7 days between 10^3–10^7, at 14 days between 10^5–10^6, and at 21 days between 10^4–10^5. Similarly, there are no major differences between the compared results obtained in the study for cows with dystocic calving, except for one case, where the bacterial load varied within wider limits. Thus, in cow with identification number 4092, with dystocic calving, the total number of germs varied from 25×10^5 at 7 days postpartum, to 11×10^8 at 14 days, and slightly decreased to 16×10^7 at 21 days. Bacteriological examination of vaginal and cervical biological samples from cows in the postpartum period led to the isolation of numerous bacterial strains.

The primary analysis of these data shows that, from these biological samples, 9 (5.24%) bacterial strains were isolated in pure cultures and 163 (94.76%) mixed bacterial strains (Table 1).

The classification of the isolated microorganisms according to respiratory type revealed the predominant presence of 163 aerobic bacterial strains, of which 71 were Gram-positive and 92 Gram-negative. Anaerobic bacteria were present in small numbers, with 9 (5.24%) strains, of which 4 Gram-positive and 5 Gram-negative strains.

By correlating cultural, morphological, and biochemical characteristics, the majority of isolated bacterial strains were classified up to the level of bacterial species.

Microbiological investigations revealed that *Escherichia coli* was the most frequently isolated bacterium from vaginal and cervical samples, with 46 (26.7%) strains, followed by *Staphylococcus* spp. with 22 (12.8%) strains and *Arcanobacterium pyogenes* with 11 (6.4%) strains (Table 2).

From the data obtained in the bacteriological examination, it arises that, based on the course of parturition, out of the 35 cows, 23 experienced eutocic calving from which 110 bacterial strains were isolated, while dystocic calving was observed in 12 cows from which 62 bacterial strains were isolated. Additionally, it is noted that *E. coli* was predominantly isolated from the biological samples, both in the case of eutocic calving (19.14%) and dystocic calving (9.21%).

In the case of dystocic birth, 9.3% of the strains were classified in the *Staphylococcus* genus, 8.1% *E. coli* strains, 4.1% *Arcanobacterium* strains, and 2.3% *Klebsiella* strains isolated from the biological samples. In the case of eutocic calving, *E. coli* was the most frequently isolated: 18.6% of the bacterial strains isolated, followed by 5.8% *Pseudomonas* spp.

3.2 Bacteriological examination from a qualitative point of view

The results of the bacterioscopic examination, performed on the pathologic specimens, revealed different bacterial morphologies and dye affinity, depending on the area of sampling and the evolution of the infectious outbreak. The aim of the bacterioscopic examination was to guide the bacteriologic investigations in order to obtain appropriate results.

Microscopic examination of Gram-stained smears identified fields with:

TABLE 2 Classification of bacterial strains according to the type of parturition.

Bacterian strains			Eutocic parturition		Distocic parturition	
			Nr.	%	Nr.	%
Gram +	*aerob*	*Staphylococcus*	6	3.5	16	9.3
	aerob	*Streptococcus*	8	4.6	-	
	aerob	*Enterococcus*	8	4.6	-	
	aerob	*Micrococcus*	7	4.1	-	
	aerob	*Corynebacterium*	6	3.5	3	1.7
	aerob	*Arcanobacterium*	4	2.3	7	4.1
	aerob	*Listeria*	1	0.5	2	1.1
	anaerob	*Clostridium*	5	2.9	2	1.1
Gram –	*aerob*	*Escherichia coli*	32	18.6	14	8.1
	aerob	*Citrobacter*	2	1.1	3	1.7
	aerob	*Pseudomonas*	10	5.8	-	-
	aerob	*Klebsiella*	4	2.3	4	2.3
	aerob	*Proteus*	4	2.3	2	1.1
	aerob	*Pasteurella*	3	1.7	-	-
	aerob	*Actinomyces*	3	1.7	1	0.5
	aerob	*Enterobacter*	2	1.1	3	1.7
	aerob	*Serratia*	-	-	1	0.5
	anaerob	*Bacteroides*	-	-	1	0.5
	aerob	*Neisseria*	7	4.1	-	-
	aerob	*Actinobacillus*	-	-	1	0.5

TABLE 1 Classification of bacterial strains according to respiratory type and tinctorial affinity.

Species		Total number of bacterial strains	Respiratory type	Strains		Gram +		Gram –	
				Nr.	%	Nr.	%	Nr.	%
Cows		172	Aerob bacteria	163	94.76	71	41.2	92	53.4
Parturition Eutocic 23 (65.7%)	Parturition Distocic 12 (34.3)		Anaerob bacteria	9	5.24	4	0.23	5	0.29
Total				172	100%	75	43.6	97	56.4

- 1 μm cocoid forms, arranged in shorter, longer chains or grouped in clusters, Gram stained Gram positive;
- Rod-shaped or rounded bacilli with deformed bacterial bodies of endospores, Gram-positive, of various sizes, some unamamified, unsporulated, grouped in palisades, Chinese idiograms or short chains, with or without metachromatic granulation;
- Branched filaments, filamentous, long bacilli, some fusiform, Gram-positive or Gram-negative, some radially arranged;
- Coci reniform, arranged in tetrads, Gram-negative stained;
- Cocobacilli or Gram-negative bacilli, polymorphous, with or without bipolar coloration, sporulating or non-sporulating (Figure 2).

4 Discussion

Sampling is an important step for bacteriological examination. For the bacteriological examination, sterile genital secretions were collected from the cervix and vagina.

The direct bacterioscopic examination often does not provide accurate identification of the bacteria. Therefore, the working protocol of the bacteriological examination involves isolating bacteria from pathological materials on culture media and identifying the cultures themselves.

To achieve this, pathological materials were inoculated onto both regular aerobic, anaerobic culture media, as well as special and selective media. Most samples were investigated within 30 min of collection.

Puerperal infections of the genital tract in cows can lead to a series of fertility problems and due to their incidence, they are still an essential problem from an economic point of view (5, 20). Also, postpartum hygiene of cows has a major influence on the course of puerperal inflammation and recovery of sick cows (18).

Ante- and post-partum hygiene has a major influence on the development of puerperal disorders (16).

According to the authors, this bacterial contamination is not specific, but includes a large number of different bacteria. Sheldon et al. (10), attempted to classify bacteria isolated from the postpartum uterus based on their pathogenic potential and assigned high pathogenicity to *Trueperella pyogenes*, *Prevotella* spp., *E. coli* and *Fusobacterium* spp.

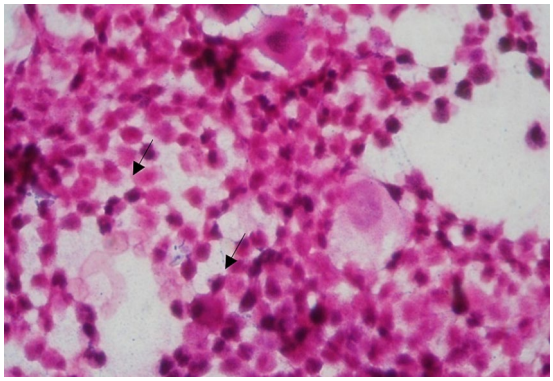

FIGURE 2
The microscopic aspect of the cow's genital secretion 21 days post-partum. Microscopic field with different bacteria types. Direct smear, Gram coloration, 20×100.

The biological barriers are broken and thus the bacteria ascend to the vagina and uterus. This is an inevitable consequence, but it seems that some cattle face more challenges in controlling this bacterial contamination than other cows (1, 18).

According to the specialized authors, this bacterial contamination in this species is not specific, but includes an extremely large number of different bacteria. Thus, there is a risk that the bacterial contamination becomes bacterial infections, because the cow's defense mechanisms do not cope (1). Sheldon et al. (10), states that in the first 14 days post-partum, a wide variety of bacteria can be detected in about 90% of cattle.

According data, Williams et al. (7), reached conclusion; *E. coli* and *Fusobacterium necrophorum* were associated with endometrial inflammation, while the presence of gram-negative staphylococci and streptococci seemed to exert a protective effect against the condition after postpartum calving.

This was true for *bacteroides* spp. *Escherichia coli*, for example. These bacteria were also detected significantly more often in the sick animals compared to the healthy ones (6, 21).

Moore et al. (17), also reported that coagulase negative Staphylococci were more prevalent in animals that did not show uterine infections and reduced the risk of abnormal vaginal discharge.

The genus *Actinobacillus* spp. was isolated from the postpartum uterus of dairy cows, but has not been associated with positive or negative effects on uterine health, only with epididymitis in rams (12).

Acinetobacter spp. is described by Sheldon et al. (4) as a potential pathogen of uterine infections.

Staphylococcus spp. in our research and the increased occurrence of potential pathogens genera, as seen with *Clostridium* spp. in cows with dystocic parturitions versus those with eutocic parturitions.

Uterine bacteriology and defense capacity are important in the evolution of the puerperal period, various studies report that the bacteria most commonly associated with uterine infections include *E. coli, Corynebacterium, Actinomyces, Arcanobacterium pyogenes*, and anaerobic bacteria such as *Fusobacterium necrophorum, F. nucleatum and Bacteroides* spp. (18, 19), compared to similar results obtained by us.

Other recent research shows that *E. coli* and *Staphylococcus* spp. were the most frequently isolated bacteria, a total of 52 bacterial isolates (20).

Even in the case of subclinical endometritis reported by Sikra et al. (21), uterine bacteriology shows an included Gram-positive bacteria in percentage of 62.5 and 37.5% Gram-negative bacteria. The highest incidence was reported for *Escherichia coli* (16.66%), vancomycin-resistant *Enterococcus* spp. (16.66%), *Staphylococcus* spp. (14.58%) and *Streptococcus agalactiae* (12.5%).

5 Conclusion

Postpartum bacterial load in the uterus first increased and then decreased in cows with dystocic parturition; bacterial diversity in the uterus of cows with eutocic parturitions was lower. Characteristic changes in the relative abundance of uterine bacteria in cows with dystocia included increased *Staphylococcus* and *Corynebacterium*, decreased *Actinomyces* and *Bacteroides*.

Data availability statement

The raw data supporting the conclusions of this article will be made available by the authors, without undue reservation.

Ethics statement

The animal studies were approved by Ethics committee of Iasi, Faculty of Veterinary Medicine. The studies were conducted in accordance with the local legislation and institutional requirements. Written informed consent was obtained from the owners for the participation of their animals in this study.

Author contributions

FN: Writing – original draft, Writing – review & editing. ŞGC: Investigation, Supervision, Writing – review & editing. PR: Formal analysis, Supervision, Validation, Writing – review & editing.

Funding

The author(s) declare that financial support was received for the research, authorship, and/or publication of this article. The article is funded by IULS project, Economic Agent no: 12599/19.07.2024.

Conflict of interest

The authors declare that the research was conducted in the absence of any commercial or financial relationships that could be construed as a potential conflict of interest.

Publisher's note

All claims expressed in this article are solely those of the authors and do not necessarily represent those of their affiliated organizations, or those of the publisher, the editors and the reviewers. Any product that may be evaluated in this article, or claim that may be made by its manufacturer, is not guaranteed or endorsed by the publisher.

References

1. Miranda-CasoLuengo R, Lu J, Williams EJ, Miranda-CasoLuengo AA, Carrington SD, Evans ACO, et al. Delayed differentiation of vaginal and uterine microbiomes in dairy cows developing postpartum endometritis. *PLoS One*. (2019) 14:e0200974. doi: 10.1371/journal.pone.0200974

2. Hopper RM. Postpartum uterine infection Diplomate–Bovine reproduction. Hoboken, NJ: John Wiley and Sons, Inc. (2014) pp. 440–448.

3. Neubrand L, Wagener K, Drillich M. Bovine uterine diseases: aspects of microbiology, molecular biology, and immunology. *Tierarztl Praxis Ausg G Grosstiere/Nutztiere*. (2020) 48:253–61. doi: 10.1055/a-1197-5720

4. Sheldon IM, Lewis GS, LeBlanc S, Gilbert RO. Defining postpartum uterine disease in cattle. *Theriogenology*. (2006) 65:1516–30. doi: 10.1016/j.theriogenology.2005.08.021

5. Sheldon IM, Williams EJ, Miller AN, Nash DM, Herath S. Uterine diseases in cattle after parturition. *Vet J*. (2008) 176:115–21. doi: 10.1016/j.tvjl.2007.12.031

6. Dubuc J, Duffield TF, Leslie KE, Walton JS, LeBlanc SJ. Risk factors for postpartum uterine diseases in dairy cows. *J Dairy Sci*. (2010) 93:5764–71. doi: 10.3168/jds.2010-3429

7. Williams EJ, Fischer DP, Pfeiffer DU, England GC, Noakes DE, Dobson H, et al. Clinical evaluation of postpartum vaginal mucus reflects uterine bacterial infection and the immune response in cattle. *Theriogenology*. (2005) 63:102–17. doi: 10.1016/j.theriogenology.2004.03.017

8. Gilbert RO, Santos NR. Dynamics of postpartum endometrial cytology and bacteriology and their relationship to fertility in dairy cows. *Theriogenology*. (2016) 85:1367–74. doi: 10.1016/j.theriogenology.2015.10.045

9. Piersanti RL, Bromfield JJ. The consequence of postpartum uterine disease on dairy cow fertility. *EDIS*. (2019) 2019:1–4.

10. Sheldon IM, Cronin J, Goetze L, Donofrio G, Schuberth HJ. Defining postpartum uterine disease and the mechanisms of infection and immunity in the female reproductive tract in cattle. *Biol Reprod*. (2009) 81:1025–32. doi: 10.1095/biolreprod.109.077370

11. Foldi J, Kulcsar M, Pecsi A, Huyghe B, de Sa C, Lohuis JA, et al. Bacterial complications of postpartum uterine involution in cattle. *Anim Reprod Sci*. (2006) 96:265–81. doi: 10.1016/j.anireprosci.2006.08.006

12. Ciornei SG, Roșca P. Upgrading the fixed-time artificial insemination (FTAI) protocol in Romanian buffaloes. *Front Vet Sci*. (2023) 10:1265060. doi: 10.3389/fvets.2023.1265060

13. Gilbert RO. Management of Reproductive Disease in dairy cows. *Vet Clin N Am Food Anim Pract*. (2016) 32:387–410. doi: 10.1016/j.cvfa.2016.01.009

14. Sharma A, Singh M, Kumar P, Sharma A, Neelam AMJ, Sharma P. Postpartum uterine infections in cows and factors affecting it–a review. *Int J Curr Microbiol App Sci*. (2017) 6:1020–8. doi: 10.20546/ijcmas.2017.609.123

15. Nechifor F, Drugociu D, Solcan C, Ciornei Ş, Roșca P. Morphostructural role of rete ovarii in adult cows. *Anatomia Histologia Embryologia*. (2014):66. doi: 10.1111/ahe.12127/abstract

16. Nechifor F, Drugociu D, Ciornei SG, Bădioi DP, Roșca P. 2023 - research on the development and therapy of persistent corpus luteum in cows. *Scientific Papers J Vet Series*. (2023) 66:64–9. doi: 10.61900/SPJVS.2023.01.13

17. Moore SG, Ericsson AC, Behura SK, Lamberson WR, Evans TJ, McCabe MS, et al. Concurrent and long-term associations between the endometrial microbiota and endometrial transcriptome in postpartum dairy cows. *BMC Genomics*. (2019) 20:405. doi: 10.1186/s12864-019-5797-8

18. Drillich M, Beetz O, Pfützner A, Sabin M, Sabin HJ, Kutzer P, et al. Evaluation of a systemic antibiotic treatment of toxic puerperal metritis in dairy cows. *J Dairy Sci*. (2001) 84:2010–7. doi: 10.3168/jds.S0022-0302(01)74644-9

19. Sheldon IM, Noakes DE, Rycroft AN, Pfeiffer DU, Dobson H. Influence of uterine bacterial contamination after parturition on ovarian dominant follicle selection and follicle growth and function in cattle. *Reproduction*. (2002) 123:837–45.

20. Alemu M, Aragaw K, Sheferaw D, Sibhat B, Abebe R, Abera M, et al. Incidence of puerperal metritis and associated risk factors in dairy cows in Hawassa, southern Ethiopia. *Res Vet Sci*. (2024) 181:105447. doi: 10.1016/j.rvsc.2024.105447

21. Sikra AA, Popovici I, Borș SI, Rîmbu CM, Horhogea C, Pavel G, et al. Bacteriological and cytological findings in postpartum dairy cows with subclinical endometritis. *Revista Romana De Medicina Veterinara*. (2023) 33:17–25.

frontiers | Frontiers in Veterinary Science

TYPE Original Research
PUBLISHED 13 December 2024
DOI 10.3389/fvets.2024.1475329

OPEN ACCESS

EDITED BY
Graça Lopes,
University of Porto, Portugal

REVIEWED BY
Pablo Daniel Cetica,
Universidad de Buenos Aires, Argentina
Rosa Pereira,
National Institute for Agricultural and Veterinary Research (INIAV), Portugal

*CORRESPONDENCE
Joohyeong Lee
durubit@gmail.com
Sang-Hwan Hyun
shhyun@cbu.ac.kr

RECEIVED 03 August 2024
ACCEPTED 21 November 2024
PUBLISHED 13 December 2024

CITATION
Jawad A, Oh D, Choi H, Kim M, Ham J, Oh BC, Lee J and Hyun S-H (2024) Myo-inositol improves developmental competence and reduces oxidative stress in porcine parthenogenetic embryos. *Front. Vet. Sci.* 11:1475329. doi: 10.3389/fvets.2024.1475329

Myo-inositol improves developmental competence and reduces oxidative stress in porcine parthenogenetic embryos

Ali Jawad[1,2], Dongjin Oh[1,2], Hyerin Choi[1,2], Mirae Kim[1,2], Jaehyung Ham[1,2], Byoung Chol Oh[3], Joohyeong Lee[4]* and Sang-Hwan Hyun[1,2,5,6]*

[1]Veterinary Medical Center and College of Veterinary Medicine, Laboratory of Veterinary Embryology and Biotechnology (VETEMBIO), Chungbuk National University, Cheongju, Republic of Korea, [2]Institute of Stem Cell and Regenerative Medicine (ISCRM), Chungbuk National University, Cheongju, Republic of Korea, [3]Department of Plastic and Reconstructive Surgery, Johns Hopkins University School of Medicine, Baltimore, MD, United States, [4]Department of Companion Animal Industry, College of Healthcare and Biotechnology, Semyung University, Jecheon, Republic of Korea, [5]Vet-ICT Convergence Education and Research Center (VICERC), Chungbuk National University, Cheongju, Republic of Korea, [6]Chungbuk National University Hospital, Cheongju, Republic of Korea

Objective: Myo-inositol (Myo-Ins), the most abundant form of inositol, is an antioxidant and plays a crucial role in the development and reproduction of mammals and humans. However, information elucidating the role of Myo-Ins in porcine embryonic development after parthenogenetic activation (PA) is still lacking. Therefore, we investigated the effect of Myo-Ins on porcine embryos and its underlying mechanisms.

Methods: In this study, various concentrations of Myo-Ins (0, 5, 10, and 20 mM) were added to the porcine zygotic medium (PZM3) during the *in vitro* culture (IVC) of porcine embryos. Several characteristics were evaluated, including cleavage rate, blastocyst formation rate, intracellular glutathione (GSH) and reactive oxygen species (ROS) levels in 4–5 cell stage embryos, total cell number, apoptotic rate in blastocysts, mitochondrial membrane potential (MMP), mitochondrial quantity, mitochondrial stress in the blastocysts, and gene expression for antioxidant and mitochondrial function markers. Additionally, the immunofluorescence of *HO-1* was assessed.

Results: The results showed that Myo-Ins at concentrations of 10 and 20 mM significantly increased the blastocyst formation rate compared to the control group. Embryos supplemented with 20 mM Myo-Ins exhibited higher GSH levels and lower ROS levels than those in the control group. Myo-Ins supplementation also decreased the rate of apoptosis and the apoptotic index in the treatment groups. Additionally, embryos supplemented with 20 mM Myo-Ins showed increased mitochondrial membrane potential (MMP), greater mitochondrial quantity, and reduced oxidative stress in the mitochondria. Interestingly, the expression levels of genes related to mitochondrial function and the nuclear erythroid factor 2-related factor (*NRF2*) pathway were elevated in the Myo-Ins treated groups. Furthermore, immunofluorescence results indicated that 20 mM Myo-Ins significantly increased *HO-1* expression in blastocysts compared to the control group.

Conclusion: In conclusion, 20 mM Myo-Ins supplementation enhanced blastocyst development and improved mitochondrial function by regulating apoptosis, reducing oxidative stress, and activating the *NRF2* pathway.

KEYWORDS
myo-inositol, embryos, mitochondria, parthenogenesis, oxidative stress

1 Introduction

In vitro embryo production (IVP) is an essential technique for early-stage porcine embryos that provides sufficient embryos for biomedical technology uses, such as genetic modification and cloning, compared to *in vivo* embryos. Consequently, the creation of porcine models for biomedical research is an important step in the IVP embryos with high implantation potential (1, 2). The quality of embryos during IVP directly affects the subsequent implantation of embryos and the early development of the fetus. In IVP, the easiest method to evaluate pre-implantation embryos is the blastocyst formation rate; nonetheless, this technique has not significantly improved during the past 20 years. The *in vitro* culture (IVC) system's inability to accurately mimic the natural *in vivo* microenvironment of embryo development is an obstacle to making significant advancements in the assessment of blastocyst formation rate, particularly in porcine embryos. This is mainly because pig embryos are extremely susceptible to reactive oxygen species (ROS) impeding their growth (3, 4). Thus, it is crucial to optimize embryo culture systems to improve the competency and quality of early embryonic development.

Excessive ROS levels result in oxidative stress, which ultimately affects embryonic development (5). ROS can result from the surrounding culture environment or the embryo's metabolism, and cause protein denaturation (6), lipid peroxidation (7), DNA damage (8), and mitochondrial damage (9), which, in turn, results in the inhibition of embryo development (10). Enhancing the efficiency and quality of porcine embryo production is a viable strategy for impeding the generation of excessive ROS. Previous studies have demonstrated that the addition of antioxidants, such as melatonin (11), cysteine (12), linoleic acid (13), laminarin (14), and resveratrol (15), diminishes the oxidative stress of embryos. Nevertheless, the existing IVC conditions fail to mimic the *in vivo* environment. Consequently, understanding the mechanisms of antioxidative damage and investigating potent antioxidant substances for incorporation into culture media are effective approaches for enhancing the *in vitro* developmental capabilities of embryos (10).

Inositol is a crucial component of structural lipids. Phosphatidylinositol, a key element in cellular membranes, especially mitochondrial membranes, plays a pivotal role in the maintenance and function of mitochondria (16). Myo-inositol (Myo-Ins), the predominant form of inositol in nature, actively participates in cytogenesis, cell morphogenesis, lipid synthesis, cell membrane formation, and cell growth. Myo-Ins is recognized as a precursor of secondary messengers in cell signaling systems and is therefore involved in the regulation of intracellular calcium concentrations (17, 18). Consequently, it plays a crucial role in regulating cardiac function, increasing insulin sensitivity, influencing metabolic changes, and remarkably impacting reproductive processes (19–22). Myo-Ins present in body fluids, particularly the follicular fluid, plays a crucial role in generating essential intracellular signals. Additionally, it is vital for follicle maturation of follicles and serves as an indicator of high oocyte quality (23–25).

Research on farming animals has indicated that Myo-Ins plays a role in mammalian preimplantation development, as the supplementation of culture media with Myo-Ins increases blastocysts formation, expansion, and hatching in rabbits and bovines (26, 27), ultimately supporting the development of healthy animals (26). In addition, it has been shown that Myo-Ins exhibits antioxidant properties and mitigates oxidative stress (28, 29). Previous studies have reported that Myo-Ins plays a protective role against oxidative stress by activating the *NRF2/KEAP1* signaling pathway (30, 31). However, there is a lack of evidence elucidating the association between Myo-Ins and the *NRF2/KEAP1* signaling pathway, specifically in porcine *in vitro* embryonic development. Therefore, the objective of this study was to explore porcine *in vitro* embryonic development and elucidate the underlying mechanisms by incorporating optimal concentrations of Myo-Ins into the IVC medium. This involved the assessment of blastocyst quality, monitoring of intracellular levels of ROS and glutathione (GSH), and evaluation of mitochondrial quantity and membrane potential. Furthermore, we aimed to determine the correlation between Myo-Ins and the *NRF2/KEAP1* signaling pathway during porcine early embryogenesis.

2 Materials and methods

2.1 Chemical and reagents

All the chemicals and reagents were purchased from Sigma-Aldrich (St.Louis, MO, United States). MitoSOX Red mitochondrial superoxide indicator and JC-1 were obtained from Invitrogen by Thermo Fisher Scientific (Carlsbad, CA, United States). *HO-1/HMOX-1* primary antibody was purchased from Proteintech (10701-1-AP, Proteintech, Illinois, USA).

2.2 Oocyte collection and *in vitro* maturation (IVM)

Porcine ovaries were procured from a local abattoir and promptly transported to the laboratory within 3 h in a 0.9% (v/v) NaCl solution maintained at 37–39°C. Upon arrival, the ovaries were subjected to two washes with a 0.9% (v/v) NaCl solution. Medium-sized follicles (3–7 mm in diameter) were selected for the retrieval of cumulus-oocyte complexes (COCs) using an 18G needle and a 10 mL disposable syringe (32). Subsequently, the collected complexes were transferred to 15 mL conical tubes. COCs exhibiting evenly granulated cytoplasm and compact cumulus cell layers were selected, and 50–60 COCs were cultured in each well of a four-well dish (Nunc, Roskilde, Denmark) containing 500 μL of IVM medium and not covered with mineral oil. The IVM medium consisted of TCM199 (Invitrogen Corporation, Carlsbad, CA, United States) supplemented with 0.91 mM sodium pyruvate, 0.6 mM cysteine, 75 ug/mL kanamycin, 10 ng/mL epidermal growth factor, 10% (v/v) porcine follicular fluid, and 1 μg/mL insulin. During the initial 22 h of IVM, the COCs were incubated with 10 IU/mL equine chorionic gonadotropin (eCG) and

10 IU/mL human chorionic gonadotropin (hCG), followed by a subsequent 20 h incubation without these hormones. All IVM procedures were conducted in a humidified incubator (Astec, Fukuoka, Japan) maintained at 39°C with a 5% CO_2 atmosphere.

2.3 Parthenogenetic activation (PA) and *in vitro* culture (IVC) of porcine embryos

PA was conducted in accordance with a previously published protocol (33). Initially, metaphase II stage (MII) oocytes were collected following IVM and treated with 0.1% hyaluronidase for 1 min to facilitate the removal of cumulus cells through gentle mechanical pipetting. Subsequently, the MII oocytes were rinsed twice with an activation solution comprising 280 mM mannitol, 0.01 mM $CaCl_2$ and 0.05 mM $MgCl_2$ before undergoing activation in 2 mL of the same solution. Activation was achieved through the administration of two direct electrical pulses at 120 V/mm for 60 μs, delivered via a cell fusion generator (LF101; NepaGene, Chiba, Japan). Subsequently, the activated oocytes were cultured in PZM3 containing cytochalasin B within a humidified environment of 5% CO_2, 5% O_2, and 95% N_2 for 4 h (34). All embryos were subjected to electrical activation and underwent three washes with IVC medium droplets (containing 10 oocytes per 30 μL) fully covered with mineral oil. PA was initiated on day 0, with embryo transferring to fresh droplets on days 2 (48 h) and 4 (96 h) of development. The cleavage rates of the embryos were analyzed on the second day and categorized into five groups based on the number of cells: 1, 2–3, 4–5, 6–8 cells, and fragmented embryos. On the seventh day, embryonic development was quantitatively assessed by determining blastocyst formation rates across three groups categorized by blastocyst morphology: early, expanded, and hatched. To quantify cell numbers in blastocysts, all blastocysts displaying a blastocoel were stained with 10 μg/mL Hoescht-33342 for 10 min. Following staining, each blastocyst was mounted on a glass slide in a drop of 100% and examined under an epifluorescence microscope (TE 300; Nikon, Tokyo, Japan) at 200 x magnification. The cell numbers were manually counted, and blastocysts with a blastocoel and at least 20 cells were classified as blastocysts (34–36). Myo-Ins supplementation was introduced into the IVC media at concentrations of 0 (control), 5, 10, and 20 mM, without any prior research on its use. The optimal concentration for Myo-Ins supplementation was determined through analysis, as depicted in Supplementary Figure S1 and Supplementary Table S1.

2.4 Measurement of intracellular GSH and ROS levels

As previously described (37) intracellular GSH and ROS levels were assessed following established procedures. Embryos at the 4–5 cell stage were selected from each experimental group on day 2 for analysis. Intracellular GSH (indicated by blue fluorescence) and ROS (indicated by green fluorescence) levels within the embryo cytoplasm were quantified utilizing CellTracker Blue CMF_2HC (Invitrogen) and H_2DCFDA (Invitrogen), respectively. The embryos were stained by incubating them in a solution of TLH-PVA medium containing either 10 μM CMF_2HC or H_2DCFDA for 30 and 10 min, respectively. Following this, the samples were washed three times with TLH-PVA before being transferred to 8 μL droplets of TLH-PVA. The levels of glutathione (GSH) and ROS were quantified using a fluorescence microscope (TE300; Nikon, Tokyo, Japan) equipped with ultraviolet filters (370 nm for GSH and 460 nm for ROS). The fluorescence intensity of each embryo was then assessed using Image J software and normalized against that of the control group.

2.5 Terminal deoxynucleotidyl transferase-mediated dUTP nick end labeling assay (TUNEL assay)

The number of apoptotic cells in the blastocysts stained with TUNEL was determined using an *in-situ* cell death detection kit as previously described (38). On the seventh day, Myo-Ins-treated and control group blastocysts were washed three times in 0.1% PBS-PVA (PVS). The blastocysts were then fixed in 4% paraformaldehyde (PFA) in PBS at 25°C (room temperature (RT)) for 30 min. In the subsequent stage, the blastocysts underwent two washes in a solution containing 0.1% PVS, in conjunction with 0.1% Tween 20 and 0.01% Triton X-100 (v/v). Subsequently, the blastocysts were treated with 0.3% Triton X-100 in PBS for 1 h at 37°C in order to facilitate permeabilization. Subsequently, the TUNEL assay was conducted utilizing fluorescein-conjugated deoxy uridine triphosphate (dUTP) and terminal deoxynucleotidyl transferase (obtained from Roche, Mannheim, Germany) for 90 min at 37°C. Subsequently, the blastocysts were subjected to two further washes in 0.1% PVS, after which they were counterstained with 5 μg/mL Hoechst-33342 for 10 min at RT in order to visualize the nuclei.

2.6 Assay of mitochondrial membrane potential ($\Delta\Psi m$)

Blastocysts on day 7 were cultured in PZM 3 supplemented with 2.5 μM 5,5′,6,6′-tetrachloro-1,1′,3,3′-tetraethyl-imidacarbocyanine iodide (JC-1) (Cat # T3168, Invitrogen, Eugene, OR, USA) for 30 min at 38.5°C in 5% CO_2. Membrane potential was determined by calculating the ratio of red fluorescence, which corresponds to activated mitochondria (J-aggregates), to green fluorescence, which corresponds to less activated mitochondria (J-monomers) (39). Images were captured using an epifluorescence microscope (TE300; Nikon, Tokyo, Japan), and Image J software was used to quantify the relative fluorescence intensities.

2.7 Colocalization assay of the mitochondria and mitochondrial ROS

To examine the colocalization of the mitochondria and mitochondrial ROS, blastocysts were incubated with 500 nM MitoTracker Red CMXRos (Cat #M7512, Invitrogen, Eugene, OR, USA) and 0.4 μM MitoSOX red (Cat # 2201584, Invitrogen, Oregon, USA) at 38.5°C for 30 min (39, 40). The fluorescence signals were visualized using an epifluorescence microscopy (TE300; Nikon, Tokyo, Japan) and the relative fluorescence intensities were quantified using the Image J software.

2.8 Quantitative reverse transcription-polymerase chain reaction

Blastocysts (n = 20/group) were collected from the control and Myo-Ins treated groups and washed with DPBS before being stored in 1.5 mL microcentrifuge tubes (SPL Life Sciences, Co., Ltd., Pocheon, Gyeonggi-do, Republic of Korea) and placed at −80°C until analysis. For the extraction of total RNA, TRIzol reagent (TaKaRa Bio, Inc., Otsu, Shiga, Japan) was used. Following the manufacturer's protocol, cDNA was synthesized using a 5× reverse transcription master mix (Elpis Bio, Inc., Chungcheongnam-do, Daejeon, Republic of Korea). For qRT-PCR, the synthesized cDNA (0.5 μg/μL) was mixed with 2× SYBR Premix Ex Taq (TaKaRa Bio Inc.) and 10 pmol of specific primers (Macrogen, Inc., Seoul, Republic of Korea). The primers used in this study are listed in Supplementary Table S2. A CFX96 Touch real-time PCR detection system (Bio-Rad, Hercules, CA, United States) was used for the qRT-PCR analysis. The reactions were initiated by pre-denaturation at 95°C for 5 min, followed by 40 cycles of denaturation at 95°C for 15 s, annealing at 57°C for 15 s, and extension at 72°C for 30 s. Data were collected during the extension phase of each cycle, and the relative quantification (R) value was calculated using the following equation: $R = 2^{-[\Delta Ctsample - \Delta Ctcontrol]}$ (41). The expression levels of genes were normalized to *RN18S* as a control.

2.9 Immunofluorescence assay

The immunofluorescence technique was employed in accordance with the methodology described by Yoon et al. (42) with certain modifications. In brief, 4% PFA in PBS was employed to fix the blastocysts for 30 min at RT. Subsequently, the blastocysts were permeabilized in 0.5% Triton X-100 at RT for 1 h, after which they were washed twice with 0.1% PVS. The Image-iT™ FX Signal Enhancer (Invitrogen, Carlsbad, CA, United States) was employed to treat the blastocysts for a period of 30 min at RT. Subsequently, they were incubated in PBS containing 3% BSA and 0.05% Tween 20 for 1 h and 30 min at RT. The blastocysts were incubated overnight at 4°C with a rabbit anti-*HO-1/HMOX-1* primary antibody (10701-1-AP, 1:100 dilution in blocking buffer, Proteintech, Illinois, USA). On the following day, the blastocysts were washed three times with 0.1% Tween 20 and 0.01% Triton X-100 in 0.1% PVS (TTVS) at RT for 5 min. They were then incubated with the appropriate secondary antibody, goat anti-rabbit IgG (H + L) Alexa Fluor 488 (A11029, 1:200; Invitrogen Corporation, Carlsbad, CA, USA), for 2 h at RT. Following three washes in TTVS, the blastocysts were counterstained with Hoechst-33342 for 10 min and mounted on glass slides in an anti-fade mounting medium (Molecular Probes, Inc., Eugene, OR, USA). The stained blastocysts were analyzed using an epifluorescence microscope (TE 300; Nikon) equipped with UV filters. The ImageJ software was employed to quantify the fluorescence intensity of the stained blastocysts.

2.10 Experimental design

In experiment 1, a total of 954 embryos were used across three replicates to assess the effects of different concentrations of Myo-Ins (0, 5, 10, 20, 40, and 80 mM) on the *in vitro* development of porcine PA embryos. The embryos were cultured in IVC medium supplemented with the specified concentrations of Myo-Ins throughout the entire IVC period. Developmental competence was evaluated by measuring cleavage rate, blastocyst formation rate, and total cell number in blastocysts. Based on the results, high concentrations of Myo-Ins (40 and 80 mM) decreased the blastocyst formation rate, suggesting that these levels may negatively impact embryo development. Therefore, lower concentrations (0, 5, 10, and 20 mM) were selected for further experiments to optimize the *in vitro* development of porcine PA embryos. In experiment 2, 352 total embryos were used in three biological replicates to assess various concentrations of Myo-Ins (0, 5, 10, and 20 mM). We aimed to investigate whether Myo-Ins can reduce oxidative stress in early 4-cell staged PA embryos by monitoring intracellular GSH and ROS levels. In experiment 3, a total of 168 blastocysts were used across three independent replicates to evaluate the effect of different concentrations of Myo-Ins (0, 5, 10, and 20 mM) on apoptosis. The number of TUNEL-positive cells and cell number were measured to assess apoptosis levels in the blastocysts. In experiment 4, a total of 280 blastocysts were used in at least three replicates to investigate mRNA expression levels of antioxidant and mitochondrial related genes in porcine PA blastocysts. In experiment 5, a total of 281 blastocysts were used across three biological replicates to evaluate the ($\Delta\Psi$m) in porcine blastocysts after PA with different concentrations of Myo-Ins (0, 5, 10, and 20 mM). In experiment 6, a total of 144 blastocysts were used across three biological replicates to assess mitochondrial distribution in porcine blastocysts after PA with different concentrations of Myo-Ins (0, 5, 10, and 20 mM). In experiment 7, a total of 167 blastocysts were used across three replicates to assess mitochondrial reactive oxygen species (ROS) levels in porcine blastocysts after PA with different concentrations of Myo-Ins (0, 5, 10, and 20 mM). In experiment 8, a total of 140 blastocysts were used across three replicates to investigate the effect of various concentrations of Myo-Ins (0, 5, 10, and 20 mM) on HO-1 protein levels after immunofluorescence assay.

2.11 Statistical analysis

Statistical analysis was performed using SPSS (version 12.0; SPSS, IBM, Armonk, NY, United States) and GraphPad Prism (GraphPad Software, San Diego, CA, United States). All the experiments were performed at least three times unless stated otherwise. Data were presented as the mean ± SEM. Percentage data (cleavage and blastocysts formation rates) and average data (intracellular GSH and ROS in 4–5 cell stage embryos, TUNEL assay in blastocysts, mitochondrial membrane potential, Mito tracker, MitoSoX, and relative gene expression levels) were analyzed using one-way analysis of variance. Statistical significance was set at $p < 0.05$.

3 Results

3.1 Myo-ins enhances development of porcine PA embryos

The optimal concentration of Myo-Ins was investigated by adding different concentrations (0, 5, 10, 20, 40, and 80 mM) during IVC for

porcine embryonic development following PA, as shown in Supplementary Figure S1 and Supplementary Table S1. Considering these findings, we selected the 5, 10 and 20 mM Myo-Ins treatment groups for this experiment. On day 2, the embryonic cleavage rate was evaluated in all the Myo-Ins treatment groups (82.7% ± 4.7, 82.0% ± 3.6, 85.0% ± 4.8%) compared with the control group (77.5% ± 3.1%) (Table 1) (Figures 1A,B). Myo-Ins treatment did not show any differences in the cleavage rate when compared with the control group. The blastocyst formation rates were found to be significantly increased ($p < 0.05$) in the 10 (50.9% ± 2.5%) and 20 mM (61.9% ± 6.7%) Myo-Ins treated groups compared to the control group (36.7% ± 1.7%) (Figures 1A,C). The supplementation of Myo-Ins at concentrations of 5-(37.0% ± 0.7%), 10-(38.7% ± 2.6%) and 20-(40.2% ± 3.2%) did not result in a significant increase in the average total cell number of blastocysts in comparison to the control group (40.5% ± 2.2%) (Table 1).

3.2 Myo-ins modulates intracellular GSH and ROS levels in PA cleaved embryos

To investigate the antioxidative effect of Myo-Ins, we analyzed the intracellular GSH and ROS levels in 4–5 cell stage embryos cultured with Myo-Ins-supplemented medium on day 2 after PA (Figure 2). The 20 mM Myo-Ins group showed significantly higher ($p < 0.05$) intracellular GSH levels than those in the control group. Furthermore, embryos in the 10 and 20 mM treated groups displayed significantly lower ($p < 0.05$) intracellular ROS levels compared to than those in the control group.

3.3 Myo-ins regulates apoptosis in porcine PA embryos

To evaluate the quality of porcine PA blastocyst, the incidence of apoptosis and total nuclei were counted. Myo-Ins supplementation during IVC did not affect the total number of nuclei compared to the control group (Figures 3A,B). Nonetheless, the number of apoptotic nuclei and the apoptotic index significantly decreased ($p < 0.05$) in the Myo-Ins-treated groups compared to those in the control group (Figures 3A,C,D).

3.4 Myo-ins modifies gene expression in porcine PA embryos

To investigate whether Myo-Ins supplementation during IVC after PA affects the expression levels of mitochondrial function-related genes and antioxidant pathway genes such as *NRF2/HO-1*, blastocysts from each group were analyzed (Figure 4). Myo-Ins significantly increased ($p < 0.05$) the expression of mitochondrial function-related genes, such as solute carrier family 2 member 1 (*SLC2A1*) and ATP synthase (*ATP5F1A*), in the 10 and 20 mM groups compared to the control group (Figure 4). Additionally, the mRNA transcript levels of *NRF2*, *HO-1*, and *GCLC* were significantly higher ($p < 0.05$) in the 20 mM Myo-Ins group than in the control group. *SOD1* transcript levels were significantly higher in the 10 mM Myo-Ins-treated group than in the control group. However, no significant differences were observed in the other mitochondrial-related genes or antioxidant genes when compared to the control group (Figure 4).

3.5 Myo-ins improves mitochondrial function in porcine PA embryos

Mitochondria are the main organelles responsible for ROS production, and any malfunction regarding them may compromise embryonic development (43, 44). Therefore, Myo-Ins supplementation in the IVC medium was assessed in three ways: mitochondrial membrane potential (MMP), mitochondrial distribution (Mitotracker), and mitochondrial ROS (MitoSox). Myo-Ins at 20 mM significantly improved ($p < 0.05$) mitochondrial dysfunction by enhancing MMP (Figures 5A,B). Moreover, the mitochondrial quantity also significantly increased ($p < 0.05$) in the 20 mM Myo-Ins-treated group compared to that in the control group (Figures 6A,B). In addition, mitochondrial oxidative stress was reduced ($p < 0.05$) in the Myo-Ins-treated groups compared to that in the control group (Figures 7A,B).

3.6 Myo-ins activates *HO-1* expression in porcine PA embryos

Previous study reported the antioxidant role of Myo-Ins against oxidative stress in boar sperm in which *NRF2* gene expression was significantly increased compared to that in the control group. However, downstream genes of the *NRF2* pathway have not been discussed before in porcine IVC (30). Therefore, to investigate whether Myo-Ins supplementation during IVC stimulates the *NRF2/HO-1* pathway at the porcine blastocyst stage, we analyzed the expression of the *HO-1* protein using immunofluorescence. The blastocysts treated with 20 mM Myo-Ins showed a significant increase ($p < 0.05$) in the level of *HO-1* protein compared to that in the control group (Figures 8A,B).

TABLE 1 Effect of Myo-Ins treatment during *in vitro* culture (IVC) for 7 days on embryonic development after parthenogenetic activation (PA).

Myo-Ins concentration (mM)	No. of embryos cultured, N	No. (%) of embryos developed to		Total cell number in blastocysts
		≥ 2-cell	Blastocyst	
0	114	88 (77.5 ± 3.1)	42 (36.7 ± 1.7) [a]	40.5 ± 2.2
5	115	95 (82.7 ± 4.7)	57 (49.1 ± 3.5) [a,b]	37.0 ± 0.7
10	106	87 (82.0 ± 3.6)	54 (50.9 ± 2.5) [b]	38.7 ± 2.6
20	118	100 (85.0 ± 4.8)	72 (61.9 ± 6.7) [b]	40.2 ± 3.2

N: Three times replicated. [a,b] Values with different superscripts within a column differ significantly ($p < 0.05$).

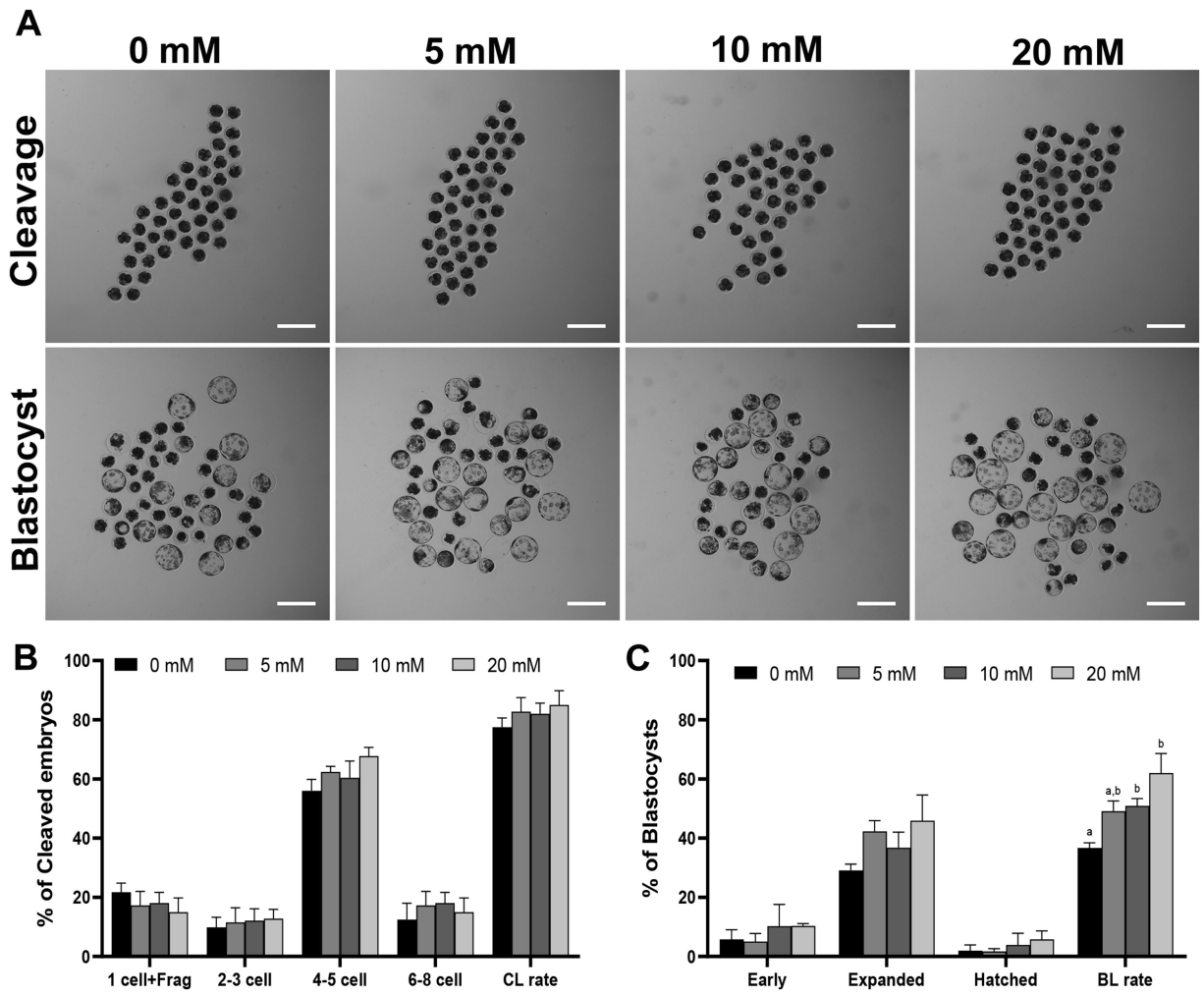

FIGURE 1
(A) Effect of Myo-Ins treatment on the blastocysts formation patterns of PA embryos. Scale bar = 300 μm. The cleavage pattern **(B)** and blastocyst formation **(C)** rate of PA embryos. Within each endpoint, the bars with different letters (a, b) indicate significant differences ($p < 0.05$) at various Myo-Ins concentrations. Frag, fragmentation; CL, cleavage; BL, blastocyst. The cleavage and blastocyst formation rates were evaluated on Day 2 and 7 after PA, respectively. For all the graphs, the values represent the mean ± SEM. The experiment was replicated at least three times.

4 Discussion

This study aimed to examine the effects of Myo-Ins supplementation on porcine PA embryos during IVC. During IVC, embryos are more susceptible to oxidative stress because of the differences between the *in vivo* and *in vitro* environments. Oxidative stress induced by ROS can cause various impairments in developmental parameters, such as decreased blastocyst formation rate and cell number (45). Antioxidant supplementation can improve embryonic developmental competence by preventing the excessive accumulation of ROS. Therefore, the effect of Myo-Ins on porcine parthenogenetic preimplantation embryos was investigated. We also investigated the optimal concentration of Myo-Ins in porcine parthenogenetic embryos during IVC. The addition of Myo-Ins significantly increased the blastocyst formation rate and GSH levels, and decreased the ROS levels in 4–5 cell stage embryos. Additionally, apoptosis in blastocysts was downregulated by the inclusion of Myo-Ins. Moreover, Myo-Ins supplementation improves mitochondrial dysfunction in blastocysts by reducing oxidative stress and increasing mitochondrial distribution, resulting in increased MMP levels. In addition, supplementation with Myo-Ins significantly increased the expression of genes related to the *NRF2/HO-1* pathway, mitochondrial function markers, and *HO-1* proteins in the blastocysts.

Enhancing embryo quality is crucial for developing effective animal models for biomedical research. Nevertheless, unlike the controlled environment of the oviduct, the *in vitro* setting exposes embryos to various stress-inducing factors, leading to an uneven distribution of antioxidants and free radicals in the cytoplasm (46). Thus, minimizing oxidative stress is important to improve the developmental competence and quality of *in vitro*-produced porcine embryos. In the present study, we confirmed that supplementation with Myo-Ins during IVC enhanced the developmental competence of porcine parthenogenetic (PA-derived) embryos. Of the various concentrations (0, 5, 10, and 20 mM) of Myo-Ins added, only the inclusion of 10 and 20 mM Myo-Ins in the IVC medium significantly increased the blastocyst formation rate. Therefore, the optimal Myo-Ins concentration for porcine IVC was identified as 20 mM which is similar to previous study in which the addition of 20 mM

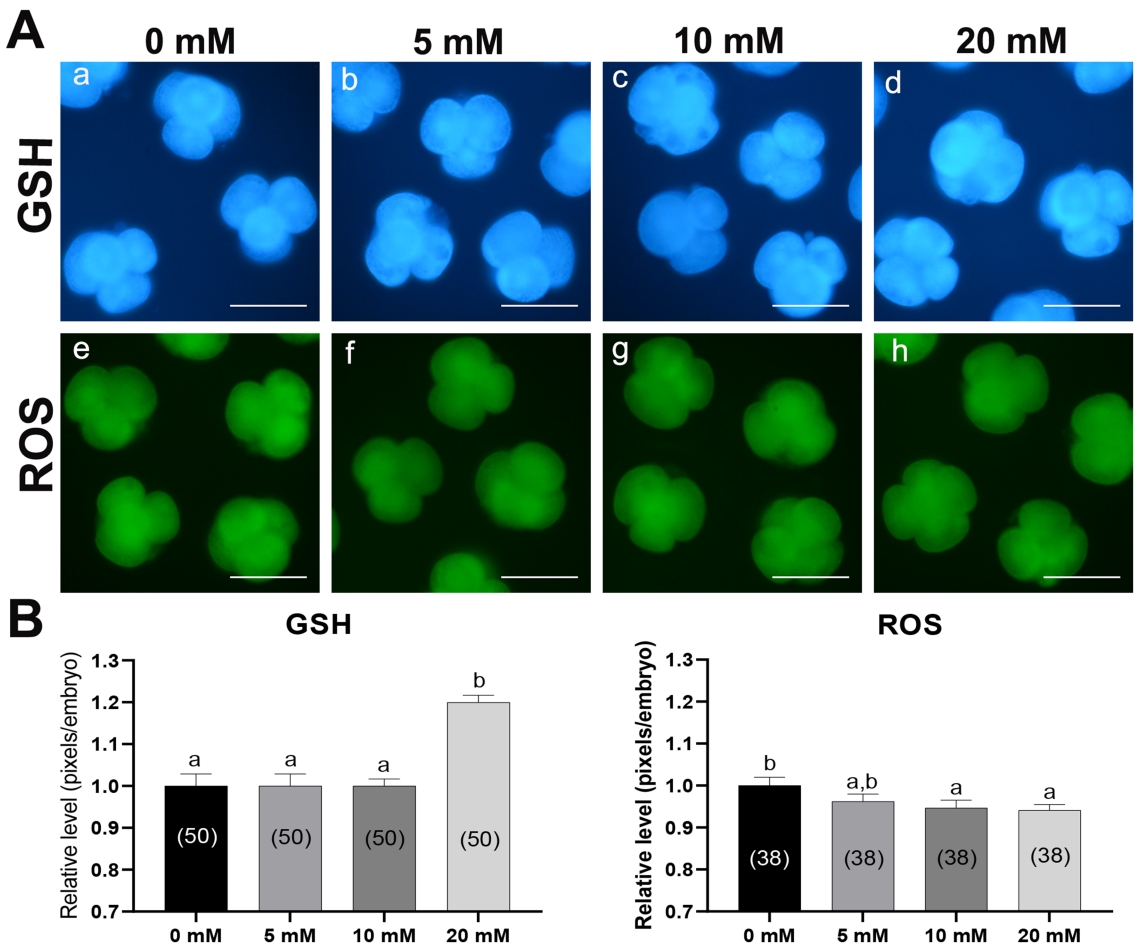

FIGURE 2
Epifluorescence photomicrographs and quantitative analysis of PA-derived 4-cell embryos with Myo-Ins supplementation during IVC for 2 days. **(A)** Representative epifluorescence photomicrographs of embryos stained with Cell Tracker Blue (a–d) and H_2DCFDA (e–h), used to detect intracellular levels of glutathione (GSH) and reactive oxygen species (ROS), respectively. Scale bar = 100 μm. **(B)** The relative levels of intracellular GSH and ROS levels within the *in vitro* cultured porcine embryos treated with Myo-Ins during IVC. The number of embryos examined in each experimental group is indicated in parentheses. Bars with different letters (a, b) within each endpoint represent significant differences between groups ($p < 0.05$). Data are presented as mean ± SEM. The experiment was replicated three times. Scale bar = 100 μm.

Myo-Ins increased the developmental competence of mouse oocytes (47).

The idea that a regulated redox system is crucial for normal embryonic development is supported by the observation that dysregulation of redox equilibrium severely affects normal embryonic development (48). During IVC, the embryos are prone to damage caused by ROS-induced oxidative stress. These ROS function as secondary messengers and regulate essential transcription factors associated with oxidative processes (49). Moreover, GSH levels are crucial during the oxidative stress process in porcine or rodent embryos, as GSH plays a vital role in scavenging ROS in damaged cells and is associated with cell proliferation events during embryonic development (50–52). A previous study has revealed the antioxidant properties of Myo-Ins in murine MII oocytes. It effectively reduced ROS levels and increased GSH levels after a preincubation period of 4 h (47). In this study, the elevated intracellular GSH levels and reduced ROS levels in the embryos treated with Myo-Ins on day 2 indicate that the *in vitro* system's uncontrolled balance between pro-oxidative and antioxidative stresses, which can inhibit embryonic development, might be able to be regulated by Myo-Ins supplementation.

Apoptosis is a programmed cell death process that occurs regularly to maintain a balance between cell formation and cell death. It is essential for homeostasis and regulates numerous genes. However, excessive apoptosis can lead to the oocyte degeneration and early embryo death and can also disrupt normal blastocyst formation (53). In this study, apoptosis and the apoptotic index were significantly downregulated in the Myo-Ins treated groups compared to those in the control group. In contrast, an increase in apoptosis can indicate inadequate *in vitro* conditions for oocytes (54). Therefore, Myo-Ins inclusion prevented apoptosis in the blastocysts; however, further research is needed to investigate the mechanisms of action of Myo-Ins against apoptosis in porcine blastocysts.

Mitochondria are vital organelles that play a crucial role in embryonic development and with excessive ROS levels disrupt mitochondrial function (43, 44). Disruption of mitochondrial function impairs embryonic development and causes abnormal autophagy and apoptosis, leading to death (55, 56). MMP is a

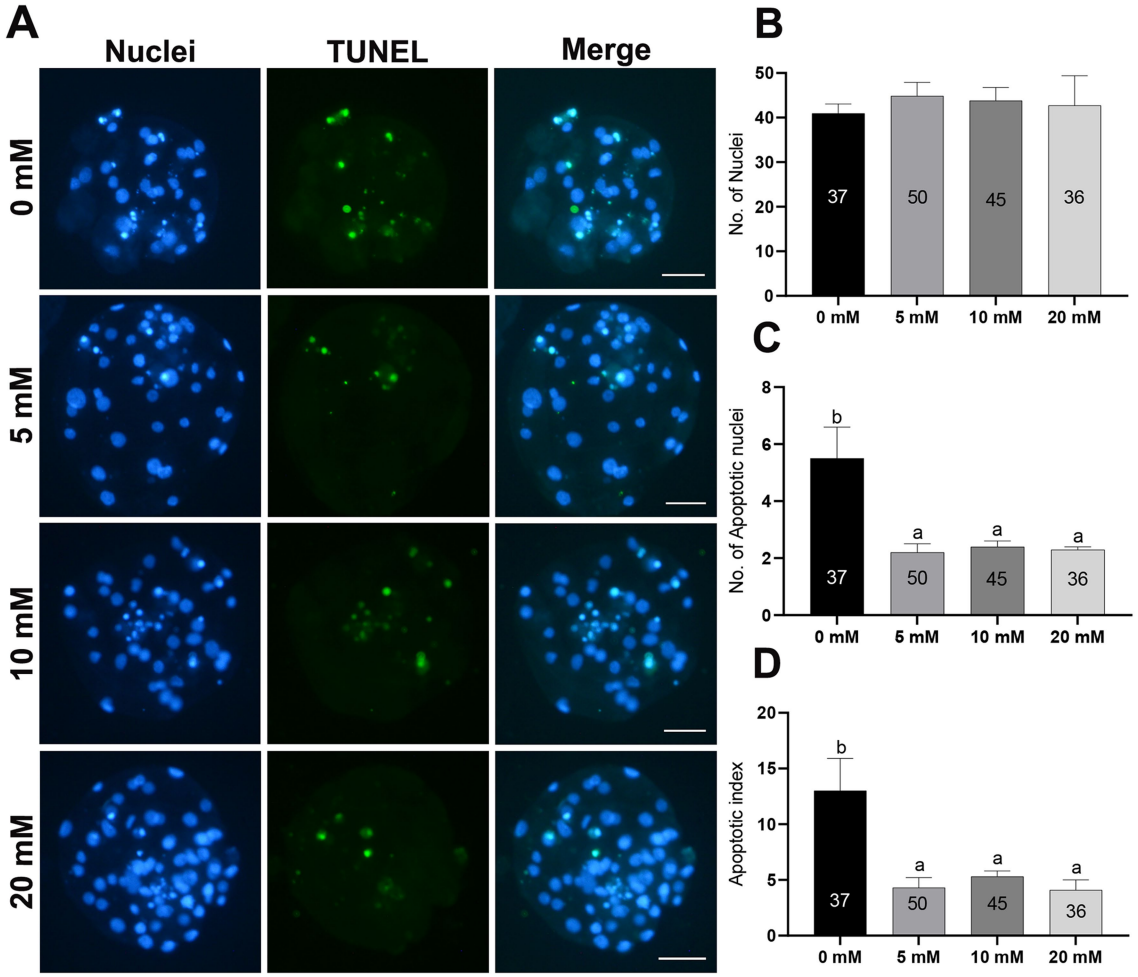

FIGURE 3
Total cell number and apoptotic nuclei in PA-derived blastocysts treated with different concentrations of Myo-Ins during IVC for 7 days. **(A)** TUNEL assay of porcine PA blastocysts in the control and Myo-Ins treated groups. The blastocysts were stained green for TUNEL and the nuclei were stained blue with Hoechst (33342). Scale bar = 50 μm. **(B–D)** Quantification of the total and apoptotic cell numbers, and apoptotic index in the indicated groups. The number of embryos examined in each experimental group is shown in parentheses. Within each endpoint, the bars with different letters (a,b) indicate significant differences ($p < 0.05$) for each group. For all the graphs, the values represent the mean ± SEM. The experiment was replicated at least three times.

commonly used indicator of mitochondrial function. However, excessive ROS accumulation can hinder mitochondrial biogenesis, which involves the synthesis of new mtDNA, mitochondrial division, and membrane formation (57). A study conducted on mouse oocytes found that preincubation with 20 mM Myo-Ins for 4 h and 8 h improved MMP (47). In the present study, mitochondrial dysfunction was improved by the enhancement of MMP and the distribution of mitochondrial quantity within Myo-Ins-treated blastocysts. Furthermore, Myo-Ins treatment decreased the mitochondrial ROS levels, specifically superoxide levels, in porcine blastocysts. These results are consistent with those of a previous study conducted in mice, in which pre-incubation with 20 mM Myo-Ins improved MMP and mitochondrial distribution in their oocytes (47). However, previous research was only conducted on mouse oocytes, and this is the first report of Myo-Ins supplementation in porcine blastocysts during IVC, in which mitochondrial function improved. Based on these results, we speculated that Myo-Ins enhances mitochondrial function in porcine blastocysts by regulating oxidative stress.

A previous study revealed that Myo-Ins supplementation during the liquid preservation of boar sperm improved oxidative stress, increased the activity of the nuclear factor (erythroid-derived 2) like 2 (*NRF2*)-regulated antioxidant pathway and acted as a ROS scavenger (30). *NRF2* is a well-known transcription factor involved in antioxidant protein expression (58). Under normal conditions, *NRF2* remains inactive because it is tethered to its negative regulator, Kelch-like associated protein 1 (*KEAP1*), which is located in the cytoplasm. However, during oxidative stress, it detaches from *KEAP1* and translocates to the nucleus, where it binds to ARE (antioxidant response elements) (59). Subsequently, genes are activated by the expression of antioxidant enzymes such as *HO-1*and *SOD*, as well as enzymes responsible for the formation of GSH, are expressed (59). In this study, 20 mM Myo-Ins treatment significantly upregulated *NRF2* gene expression and the expression of downstream genes such as

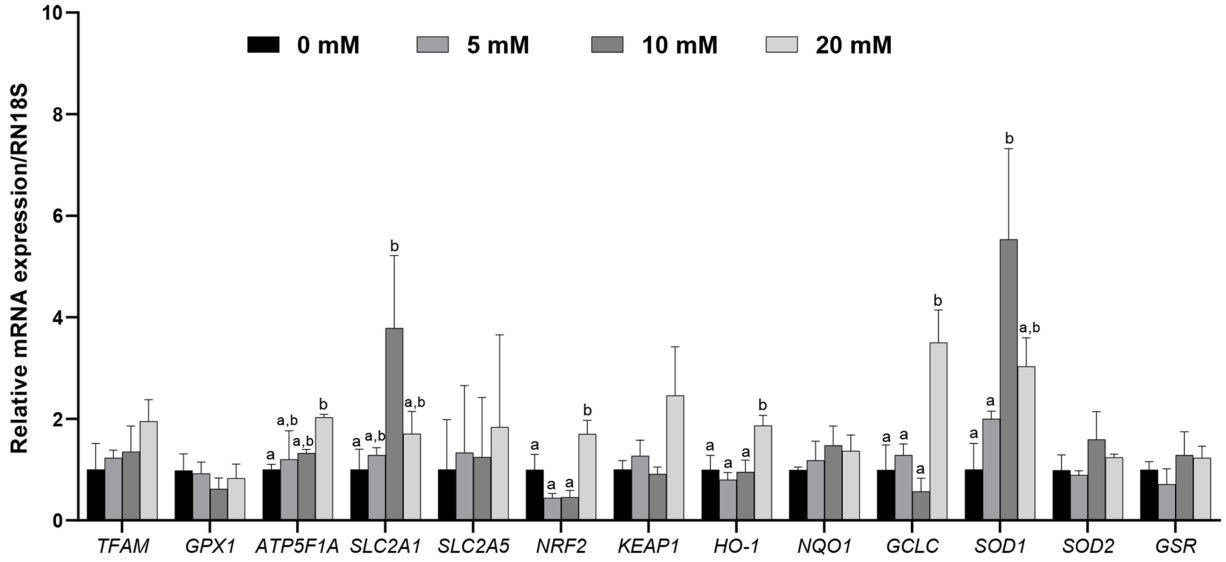

FIGURE 4
Relative mRNA expression levels of genes associated with mitochondria, including mitochondrial transcription factor A (*TFAM*), glutathione peroxidase 1 (*GPX1*), ATP synthase (*ATP5F1A*), solute carrier family 2 member 1 (*SLC2A1*), and solute carrier family 2 member 5 (*SLC2A5*), along with genes associated with antioxidant signaling, including nuclear erythroid factor 2 related genes (*NRF2*), Kelch like associated protein (*KEAP1*), Heme oxygenase 1 (*HO-1*), quinine oxidoreductase 1 (*NQO1*), glutamate-cysteine ligase catalytic subunit (*GCLC*), superoxide dismutase 1, 2 (*SOD1, SOD2*), and glutathione-disulfide reductase (*GSR*), were analyzed in porcine blastocysts treated with Myo-Ins at concentrations of 5, 10, and 20 mM, with data normalized to the *RN18S* gene and different letters (a, b) indicating significant differences between the groups, and all values representing mean ± SEM from experiments replicated three or four times.

HO-1 and *GCLC*. However, *SOD1* upregulation was observed with 10 mM the Myo-Ins, illustrating the antioxidative role of Myo-Ins via the *NRF2/HO-1* pathway in porcine blastocysts. These results were further verified by immunofluorescence staining of the *HO-1* protein in blastocysts; 20 mM significantly increased *HO-1* expression in the blastocysts. Further studies are required to investigate the mechanisms underlying the antioxidant role of Myo-Ins in blastocysts via the *NRF2/HO-1* pathway.

The mitochondria are of significant importance in the generation of ATP during oocyte and embryonic development (60). This study found that blastocysts supplemented with Myo-Ins had higher mtDNA copy numbers and different mRNA expression levels of mitochondrial transcription factor A (*TFAM*) than the control group. May-Panloup et al. reported that mtDNA copy number may increase due to the elevated levels of *TFAM* transcripts, which rise simultaneously with mtDNA replication during bovine embryogenesis (61). However, this study illustrates that higher mtDNA copy numbers in porcine Myo-Ins-supplemented blastocysts may improve blastocyst quality with elevated mRNA expression levels of *TFAM* which is similar to the results of a previous study in bovines (61). Furthermore, in the blastocysts treated with Myo-Ins, there was a change in energy production via glucose metabolism, which is crucial for adequate mitochondrial function. Blastocysts supplemented with Myo-Ins showed elevated expression levels of *SLC2A1* and *SLC2A5*. These genes are responsible for active glucose and fructose transport across the plasma membrane, indicating the redirection of energy substrates towards anaerobic glycolysis (62). In oocytes, mitochondria play a crucial role in fertilization and embryonic developmental competence. They produce ATP through the expression of ATP synthase (*ATP5A1*) and regulate ROS via the oxidative stress marker glutathione peroxidase (*GPX1*), which is mediated by ROS (62). In this study, *ATP5F1A* was upregulated in the 20 mM Myo-Ins group compared to that in the control group, which showed high ATP production in the blastocysts. Moreover, the oxidative stress marker *GPX1* expression was slightly reduced with 10 and 20 mM Myo-Ins and significantly decreased in the 5 mM Myo-Ins treated group, indicating that a low concentration of Myo-Ins may be beneficial in lowering *GPX1* in porcine blastocysts. These results suggest that Myo-Ins may improve mitochondrial functions. However, further studies are required to assess these mitochondrial functional marker genes in porcine blastocysts to understand the underlying mechanisms.

5 Conclusion

In conclusion, the results of this study indicated that Myo-Ins supplementation in porcine PA embryos during IVC was highly efficient, highlighting the role of Myo-Ins in enhancing blastocyst formation rate and, decreasing apoptosis, and oxidative stress in 4–5 cell stage embryos. Moreover, Myo-Ins supplementation regulated mitochondrial dysfunction by increasing the mitochondrial distribution and MMP and reducing mitochondrial ROS. Furthermore, Myo-Ins also upregulated the *NRF2/HO-1* related pathway genes and mitochondrial function marker genes. *HO-1* protein expression was upregulated in blastocysts, highlighting the defense mechanism of Myo-Ins against oxidative stress. To the best of our knowledge, this was the first study to investigate the role of Myo-Ins in oxidative stress and mitochondrial dysfunction in porcine PA embryos. Overall, these findings

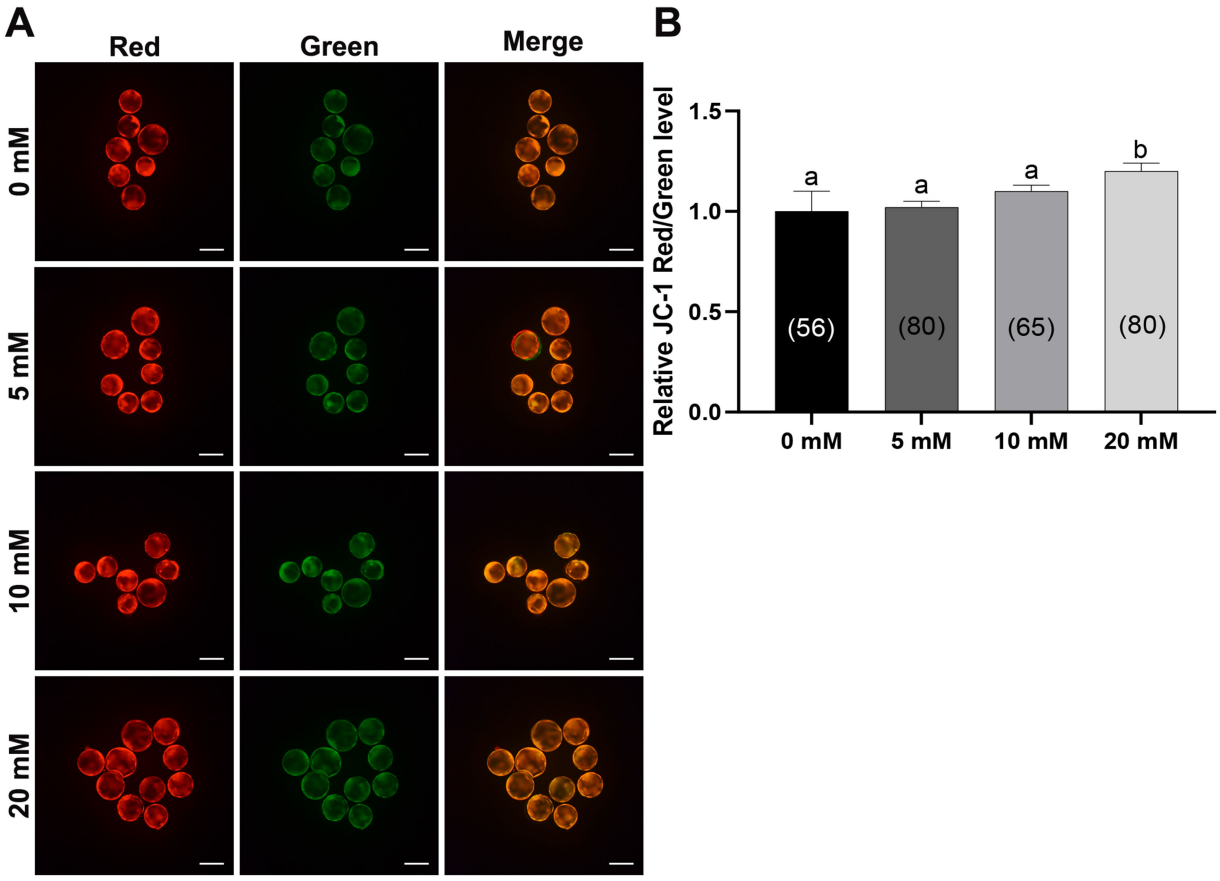

FIGURE 5
Myo-Ins prevented mitochondrial dysfunction in porcine blastocysts. **(A)** Representative fluorescence images of JC-1 staining in blastocysts. Scale bar = 200 μm. **(B)** Quantification of the ratio of fluorescence intensity (red/green) of JC-1 in blastocysts. The number of the blastocysts is shown in parentheses. Data are expressed as the mean ± SEM. Within each endpoint, bars with different letters (a, b) indicate significant differences ($p < 0.05$). The experiment was replicated at least four times.

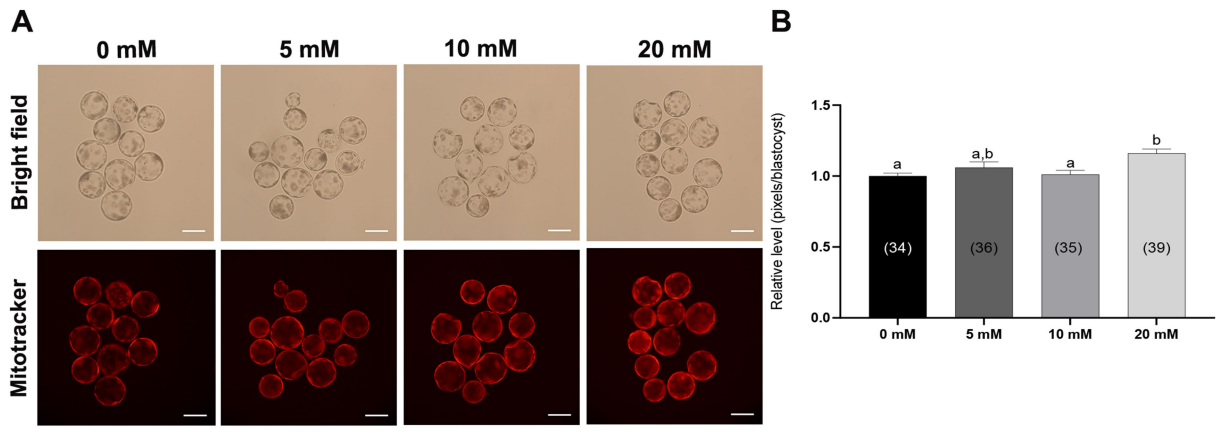

FIGURE 6
Effect of Myo-Ins on mitochondrial function in porcine PA embryos. **(A)** Representative fluorescent images of MitoTracker Deep Red staining of the Myo-Ins treated groups (5, 10, and 20 mM) and control group. Scale bar = 100 μm. **(B)** Relative MitoTracker fluorescence intensities in the blastocysts of the Myo-Ins treated groups and control group. The number of blastocysts is indicated in parentheses. Within each endpoint, bars with different letters (a, b) indicate significant differences ($p < 0.05$) at various Myo-Ins concentrations. For all the graphs, the values represent the mean ± SEM. The experiment was replicated three times.

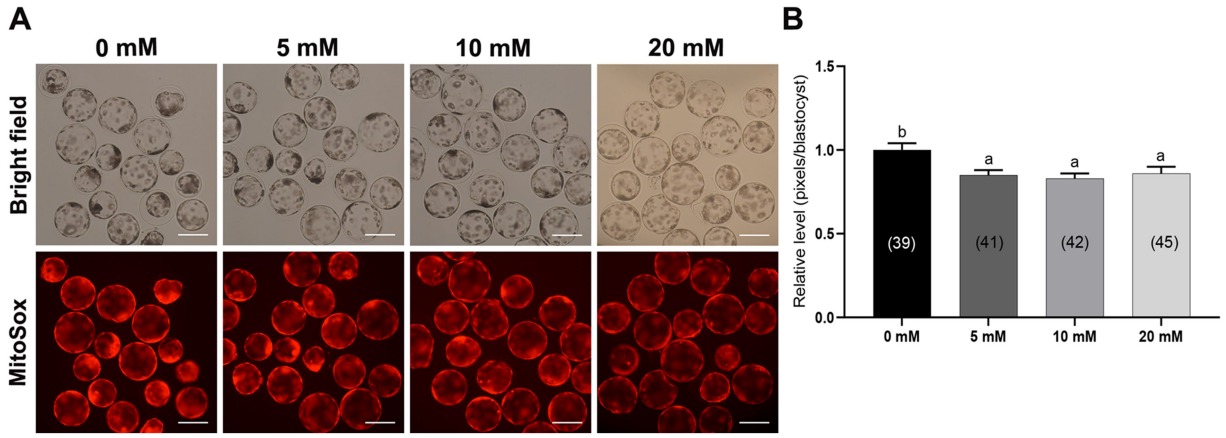

FIGURE 7
Effect of Myo-Ins on mitochondrial ROS in porcine PA embryos. **(A)** Representative fluorescent images of MitoSox staining of the Myo-Ins treated groups (5, 10, and 20 mM) and control group. Scale bar = 200 μm. **(B)** Relative MitoSox fluorescence intensities in the blastocysts of the Myo-Ins treated groups and control group. The number of blastocysts is indicated in parentheses. Within each endpoint, bars with different letters (a, b) indicate significant differences ($p < 0.05$) at various Myo-Ins concentrations. For all the graphs, the values represent the mean ± SEM. The experiment was replicated three times.

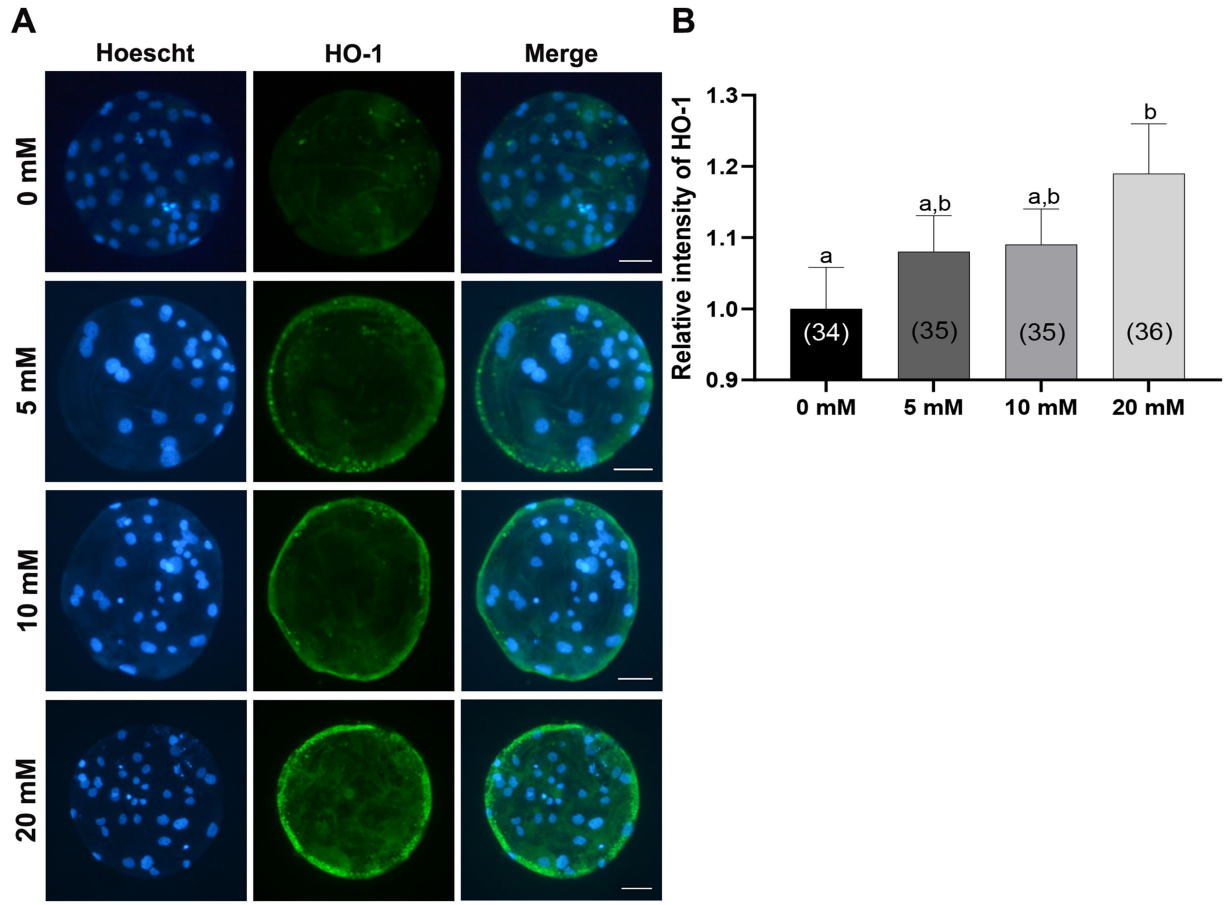

FIGURE 8
Effects of Myo-Ins treatment during *in vitro* culture (IVC) for 7 days on the heme oxygenase-1 (*HO-1*) expression of parthenote embryos. **(A)** Immunofluorescence images (200x) of porcine parthenote blastocysts labeled with *HO-1* (green) and Hoechst 33342 (total nuclei, blue) following *in vitro* culture (IVC) for 7 days. Scale bar = 50 μm. **(B)** The relative intensity of *HO-1* was quantified in both the control and Myo-Ins treatment groups. The number of embryos analyzed in each experimental group is indicated in brackets. Within each endpoint, bars with different letters (a, b) indicate significant differences ($p < 0.05$) at different concentrations of Myo-Ins. The graph displays the mean ± SEM values. The experiment was replicated three times.

offerred detailed and novel insights into the antioxidative, and anti-apoptotic protection provided by Myo-Ins in *in vitro* models.

Data availability statement

The datasets presented in this study can be found in online repositories. The names of the repository/repositories and accession number(s) can be found in the article/Supplementary material.

Ethics statement

Ethical approval was not required for the study involving animals in accordance with the local legislation and institutional requirements because Since pig ovaries, a by-product discarded by a local abattoir were obtained, only the oocytes were collected and used for further experiments.

Author contributions

AJ: Conceptualization, Formal analysis, Investigation, Methodology, Validation, Writing – original draft, Writing – review & editing. DO: Formal analysis, Investigation, Methodology, Writing – review & editing. HC: Formal analysis, Investigation, Methodology, Writing – review & editing. MK: Formal analysis, Investigation, Methodology, Writing – review & editing. JH: Formal analysis, Investigation, Writing – review & editing. BO: Writing – review & editing, Conceptualization, Data curation, Formal analysis, Validation, Investigation. JL: Funding acquisition, Writing – review & editing, Formal analysis, Investigation, Methodology. S-HH: Conceptualization, Funding acquisition, Supervision, Validation, Writing – original draft, Writing – review & editing.

Funding

The author(s) declare that financial support was received for the research, authorship, and/or publication of this article. This work was supported, in part, by a grant from the "National Research Foundation of Korea Grant funded by the Korean Government (2020R1A2C2008276, 2021R1C1C2013954). Technology Innovation Program (20023068) funded by the Ministry of Trade, Industry & Energy (MOTIE, Korea) and Korea Institute of Planning and Evaluation for Technology in Food, Agriculture, Forestry and Fisheries (IPET) through Agriculture and Food Convergence Technologies Program for Research Manpower development funded by Ministry of Agriculture, Food and Rural Affairs (MAFRA) (grant number: RS-2024-00398561).

Acknowledgments

The authors are grateful to Miss. Eun Jeong Kim for her technical support including the ovaries collection from the slaughterhouse. We would like to thank editage korea (www.editage.co.kr) for its linguistic assistance during the preparation of this manuscript.

Conflict of interest

The authors declare that the research was performed without the aid of any commercial or financial relationships that could be construed as a potential conflict of interest.

Publisher's note

Supplementary material

The Supplementary material for this article can be found online at: https://www.frontiersin.org/articles/10.3389/fvets.2024.1475329/full#supplementary-material

SUPPLEMENTARY FIGURE S1
Effect of various concentrations of Myo-Ins supplementation during in vitro culture (IVC) on embryonic development after parthenogenetic activation (PA). **(A)** Representative morphologies of porcine blastocysts from each group 7 days after PA. Scale bar = 300 μm. **(B)** Effect of Myo-Ins supplementation during IVC on the cleavage pattern of PA embryos at day 2. **(C)** Effect of Myo-Ins supplementation during IVC on the percentage of PA embryos that developed to the blastocyst stage at day 7. For all graphs, the value represents the mean ± SEM. Within each end point, bars with different letters (a and b) are significantly ($p < 0.05$) different. Statistical significance was determined by one-way ANOVA. 1 cell + fragmentation embryos; 2-3 cells; 4-5 cells; 6-8 cells; CL, cleavage; BL, blastocyst. The experiment was replicated three times.

SUPPLEMENTARY TABLE S1
Effect of Myo-Ins treatment during in vitro culture (IVC) for seven days on embryonic development after parthenogenetic activation (PA).

References

1. Zhao J, Ross JW, Hao Y, Spate LD, Walters EM, Samuel MS, et al. Significant improvement in cloning efficiency of an inbred miniature pig by histone deacetylase inhibitor treatment after somatic cell nuclear Transfer1. *Biol Reprod*. (2009) 81:525–30. doi: 10.1095/biolreprod.109.077016

2. Ren J, Yu D, Wang J, Xu K, Xu Y, Sun R, et al. Generation of immunodeficient pig with hereditary tyrosinemia type 1 and their preliminary application for humanized liver. *Cell Biosci*. (2022) 12:26. doi: 10.1186/s13578-022-00760-3

3. Booth PJ, Holm P, Callesen H. The effect of oxygen tension on porcine embryonic development is dependent on embryo type. *Theriogenology*. (2005) 63:2040–52. doi: 10.1016/j.theriogenology.2004.10.001

4. Shahbazi MN, Jedrusik A, Vuoristo S, Recher G, Hupalowska A, Bolton V, et al. Self-organization of the human embryo in the absence of maternal tissues. *Nat Cell Biol*. (2016) 18:700–8. doi: 10.1038/ncb3347

5. Takahashi M. Oxidative stress and redox regulation on in vitro development of mammalian embryos. *J Reprod Dev*. (2012) 58:1–9. doi: 10.1262/jrd.11-138N

6. Ezraty B, Gennaris A, Barras F, Collet JF. Oxidative stress, protein damage and repair in bacteria. *Nat Rev Microbiol*. (2017) 15:385–96. doi: 10.1038/nrmicro.2017.26

7. Muralikrishna Adibhatla R, Hatcher JF. Phospholipase A2, reactive oxygen species, and lipid peroxidation in cerebral ischemia. *Free Radic Biol Med*. (2006) 40:376–87. doi: 10.1016/j.freeradbiomed.2005.08.044

8. Storr SJ, Woolston CM, Zhang Y, Martin SG. Redox environment, free radical, and oxidative DNA damage. *Antioxid Redox Signal*. (2013) 18:2399–408. doi: 10.1089/ars.2012.4920

9. Slimen IB, Najar T, Ghram A, Dabbebi H, Ben Mrad M, Abdrabbah M. Reactive oxygen species, heat stress and oxidative-induced mitochondrial damage. A review. *Int J Hyperthermia*. (2014) 30:513–23. doi: 10.3109/02656736.2014.971446

10. Guérin P, El Mouatassim S, Ménézo Y. Oxidative stress and protection against reactive oxygen species in the pre-implantation embryo and its surroundings. *Hum Reprod Update*. (2001) 7:175–89. doi: 10.1093/humupd/7.2.175

11. Rodriguez-Osorio N, Kim IJ, Wang H, Kaya A, Memili E. Melatonin increases cleavage rate of porcine preimplantation embryos in vitro. *J Pineal Res*. (2007) 43:283–8. doi: 10.1111/j.1600-079X.2007.00475.x

12. Li XX, Lee KB, Lee JH, Kim KJ, Kim EY, Han KW, et al. Glutathione and cysteine enhance porcine preimplantation embryo development in vitro after intracytoplasmic sperm injection. *Theriogenology*. (2014) 81:309–14. doi: 10.1016/j.theriogenology.2013.09.030

13. Khalil WA, Marei WF, Khalid M. Protective effects of antioxidants on linoleic acid-treated bovine oocytes during maturation and subsequent embryo development. *Theriogenology*. (2013) 80:161–8. doi: 10.1016/j.theriogenology.2013.04.008

14. Jiang H, Liang S, Yao XR, Jin YX, Shen XH, Yuan B, et al. Laminarin improves developmental competence of porcine early stage embryos by inhibiting oxidative stress. *Theriogenology*. (2018) 115:38–44. doi: 10.1016/j.theriogenology.2018.04.019

15. Lee K, Wang C, Chaille JM, Machaty Z. Effect of resveratrol on the development of porcine embryos produced in vitro. *J Reprod Dev*. (2010) 56:330–5. doi: 10.1262/jrd.09-174K

16. Gohil VM, Greenberg ML. Mitochondrial membrane biogenesis: phospholipids and proteins go hand in hand. *J Cell Biol*. (2009) 184:469–72. doi: 10.1083/jcb.200901127

17. Marat AL, Haucke V. Phosphatidylinositol 3-phosphates-at the interface between cell signalling and membrane traffic. *EMBO J*. (2016) 35:561–79. doi: 10.15252/embj.201593564

18. Foskett JK. Inositol trisphosphate receptor Ca2+ release channels in neurological diseases. *Eur J Physiol*. (2010) 460:481–94. doi: 10.1007/s00424-010-0826-0

19. Oudit GY, Penninger JM. Cardiac regulation by phosphoinositide 3-kinases and PTEN. *Cardiovasc Res*. (2009) 82:250–60. doi: 10.1093/cvr/cvp014

20. Santamaria A, Di Benedetto A, Petrella E, Pintaudi B, Corrado F, D'Anna R, et al. Myo-inositol may prevent gestational diabetes onset in overweight women: a randomized, controlled trial. *J Mater Fetal Neonatal Med*. (2016) 29:3234–7. doi: 10.3109/14767058.2015.1121478

21. Santamaria A, Giordano D, Corrado F, Pintaudi B, Interdonato ML, Vieste GD, et al. One-year effects of myo-inositol supplementation in postmenopausal women with metabolic syndrome. *Climacteric*. (2012) 15:490–5. doi: 10.3109/13697137.2011.631063

22. Iuorno MJ, Jakubowicz DJ, Baillargeon JP, Dillon P, Gunn RD, Allan G, et al. Effects of d-chiro-inositol in lean women with the polycystic ovary syndrome. *Endocrine Pract*. (2002) 8:417–23. doi: 10.4158/EP.8.6.417

23. Lewin LM, Szeinberg A, Lepkifker E. Gas chromatography measurement of myo-inositol in human blood, cerebrospinal fluid and seminal fluid. *Clinic Chim Acta*. (1973) 45:361–8. doi: 10.1016/0009-8981(73)90036-3

24. Fujiwara T, Nakada K, Shirakawa H, Miyazaki S. Development of inositol trisphosphate-induced calcium release mechanism during maturation of hamster oocytes. *Dev Biol*. (1993) 156:69–79. doi: 10.1006/dbio.1993.1059

25. Chiu TT, Rogers MS, Law EL, Briton-Jones CM, Cheung LP, Haines CJ. Follicular fluid and serum concentrations of myo-inositol in patients undergoing IVF: relationship with oocyte quality. *Hum Reprod*. (2002) 17:1591–6. doi: 10.1093/humrep/17.6.1591

26. Holm P, Booth PJ, Schmidt MH, Greve T, Callesen H. High bovine blastocyst development in a static in vitro production system using SOFa a medium supplemented with sodium citrate and myo-inositol with or without serum-proteins. *Theriogenology*. (1999) 52:683–700. doi: 10.1016/S0093-691X(99)00162-4

27. Warner SM, Conlon FV, Kane MT. Inositol transport in preimplantation rabbit embryos: effects of embryo stage, sodium, osmolality and metabolic inhibitors. *Reproduction*. (2003) 125:479–93. doi: 10.1530/rep.0.1250479

28. Jiang WD, Kuang SY, Liu Y, Jiang J, Hu K, Li SH, et al. Effects ofmyo-inositol on proliferation, differentiation, oxidative status and antioxidant capacity of carp enterocytes in primary culture. *Aquac Nutr*. (2013) 19:45–53. doi: 10.1111/j.1365-2095.2011.00934.x

29. Mohammadi F, Varanloo N, Heydari Nasrabadi M, Vatannejad A, Amjadi FS, Javedani Masroor M, et al. Supplementation of sperm freezing medium with myoinositol improve human sperm parameters and protects it against DNA fragmentation and apoptosis. *Cell Tissue Bank*. (2019) 20:77–86. doi: 10.1007/s10561-018-9731-0

30. Jawad A, Oh D, Choi H, Kim M, Cai L, Lee J, et al. Myo-inositol improves the viability of boar sperm during liquid storage. *Front Vet Sci*. (2023) 10:1150984. doi: 10.3389/fvets.2023.1150984

31. Jiang WD, Hu K, Liu Y, Jiang J, Wu P, Zhao J, et al. Dietary myo-inositol modulates immunity through antioxidant activity and the Nrf2 and E2F4/cyclin signalling factors in the head kidney and spleen following infection of juvenile fish with *Aeromonas hydrophila*. *Fish Shellfish Immunol*. (2016) 49:374–86. doi: 10.1016/j.fsi.2015.12.017

32. Kwak S-S, Yoon JD, Cheong S-A, Jeon Y, Lee E, Hyun S-H. The new system of shorter porcine oocyte in vitro maturation (18 hours) using ≥8 mm follicles derived from cumulus-oocyte complexes. *Theriogenology*. (2014) 81:291–301. doi: 10.1016/j.theriogenology.2013.09.028

33. Kim M, Hwang SU, Yoon JD, Lee J, Kim E, Cai L, et al. Beneficial effects of Neurotrophin-4 supplementation during in vitro maturation of porcine cumulus-oocyte complexes and subsequent embryonic development after parthenogenetic activation. *Front Vet Sci*. (2021) 8:779298. doi: 10.3389/fvets.2021.779298

34. Kim M, Lee J, Cai L, Choi H, Oh D, Jawad A, et al. Neurotrophin-4 promotes the specification of trophectoderm lineage after parthenogenetic activation and enhances porcine early embryonic development. . *Front Cell Dev Biol*. (2023) 11:1194596. doi: 10.3389/fcell.2023.1194596

35. Dinnyés A, Hirao Y, Nagai T. Parthenogenetic activation of porcine oocytes by electric pulse and/or butyrolactone I treatment. *Cloning*. (1999) 1:209–16. doi: 10.1089/15204559950019843

36. Do SQ, Nguyen HT, Wakai T, Funahashi H. Exogenous expression of PGC-1α during in vitro maturation impairs the developmental competence of porcine oocytes. *Theriogenology*. (2024) 228:30–6. doi: 10.1016/j.theriogenology.2024.07.021

37. Choi H, Lee J, Yoon JD, Hwang SU, Cai L, Kim M, et al. The effect of copper supplementation on in vitro maturation of porcine cumulus-oocyte complexes and subsequent developmental competence after parthenogenetic activation. *Theriogenology*. (2021) 164:84–92. doi: 10.1016/j.theriogenology.2021.01.009

38. Cai L, Jeong YW, Jin YX, Lee JY, Jeong YI, Hwang KC, et al. Effects of human recombinant granulocyte-colony stimulating factor treatment during in vitro culture on porcine pre-implantation embryos. *PLoS One*. (2020) 15:e0230247. doi: 10.1371/journal.pone.0230247

39. Niu YJ, Zhou W, Guo J, Nie ZW, Shin KT, Kim NH, et al. C-Phycocyanin protects against mitochondrial dysfunction and oxidative stress in parthenogenetic porcine embryos. *Sci Rep*. (2017) 7:16992. doi: 10.1038/s41598-017-17287-0

40. Yang S-G, Park H-J, Kim J-W, Jung J-M, Kim M-J, Jegal H-G, et al. Mito-TEMPO improves development competence by reducing superoxide in preimplantation porcine embryos. *Sci Rep*. (2018) 8:10130. doi: 10.1038/s41598-018-28497-5

41. Oh D, Choi H, Kim M, Cai L, Lee J, Jawad A, et al. Interleukin-7 enhances in vitro development and blastocyst quality in porcine parthenogenetic embryos. *Front Vet Sci*. (2022) 9:1052856. doi: 10.3389/fvets.2022.1052856

42. Yoon JD, Hwang SU, Kim M, Lee G, Jeon Y, Hyun SH. GDF8 enhances SOX2 expression and blastocyst total cell number in porcine IVF embryo development. *Theriogenology*. (2019) 129:70–6. doi: 10.1016/j.theriogenology.2019.02.007

43. Scherz-Shouval R, Elazar Z. ROS, mitochondria and the regulation of autophagy. *Trends Cell Biol*. (2007) 17:422–7. doi: 10.1016/j.tcb.2007.07.009

44. Harvey AJ. Mitochondria in early development: linking the microenvironment, metabolism and the epigenome. *Reproduction*. (2019) 157:R159–79. doi: 10.1530/REP-18-0431

45. Joo YE, Jeong P-S, Lee S, Jeon S-B, Gwon M-A, Kim MJ, et al. Anethole improves the developmental competence of porcine embryos by reducing oxidative stress via the sonic hedgehog signaling pathway. *J Anim Sci Biotechnol*. (2023) 14:32. doi: 10.1186/s40104-022-00824-x

46. Cagnone G, Sirard MA. The embryonic stress response to in vitro culture: insight from genomic analysis. *Reproduction*. (2016) 152:R247–61. doi: 10.1530/REP-16-0391

47. Mohammadi F, Ashrafi M, Zandieh Z, Najafi M, Niknafs B, Amjadi FS, et al. The effect of Preincubation time and Myo-inositol supplementation on the quality of mouse MII oocytes. *J Reprod Infertility*. (2020) 21:259–68. doi: 10.18502/jri.v21i4.4330

48. Ufer C, Wang CC, Borchert A, Heydeck D, Kuhn H. Redox control in mammalian embryo development. *Antioxid Redox Signal*. (2010) 13:833–75. doi: 10.1089/ars.2009.3044

49. Agarwal A, Gupta S, Sharma RK. Role of oxidative stress in female reproduction. *Reprod Biol Endocrinol*. (2005) 3:28. doi: 10.1186/1477-7827-3-28

50. Gardiner CS, Reed DJ. Status of glutathione during oxidant-induced oxidative stress in the preimplantation mouse embryo. *Biol Reprod*. (1994) 51:1307–14. doi: 10.1095/biolreprod51.6.1307

51. Ishibashi M, Akazawa S, Sakamaki H, Matsumoto K, Yamasaki H, Yamaguchi Y, et al. Oxygen-induced embryopathy and the significance of glutathione-dependent antioxidant system in the rat embryo during early organogenesis. *Free Radic Biol Med*. (1997) 22:447–54. doi: 10.1016/S0891-5849(96)00338-3

52. Ozawa M, Nagai T, Fahrudin M, Karja NW, Kaneko H, Noguchi J, et al. Addition of glutathione or thioredoxin to culture medium reduces intracellular redox status of porcine IVM/IVF embryos, resulting in improved development to the blastocyst stage. *Mol Reprod Dev*. (2006) 73:998–1007. doi: 10.1002/mrd.20533

53. Chen HL, Cheng JY, Yang YF, Li Y, Jiang XH, Yang L, et al. Phospholipase C inhibits apoptosis of porcine oocytes cultured in vitro. *J Cell Biochem*. (2020) 121:3547–59. doi: 10.1002/jcb.29636

54. Kim JS, Cho YS, Song BS, Wee G, Park JS, Choo YK, et al. Exogenous dibutyryl cAMP affects meiotic maturation via protein kinase a activation; it stimulates further embryonic development including blastocyst quality in pigs. *Theriogenology*. (2008) 69:290–301. doi: 10.1016/j.theriogenology.2007.09.024

55. Lee J, Giordano S, Zhang J. Autophagy, mitochondria and oxidative stress: cross-talk and redox signalling. *Biochem J*. (2012) 441:523–40. doi: 10.1042/BJ20111451

56. Czarny P, Pawlowska E, Bialkowska-Warzecha J, Kaarniranta K, Blasiak J. Autophagy in DNA damage response. *Int J Mol Sci*. (2015) 16:2641–62. doi: 10.3390/ijms16022641

57. Bhatti JS, Bhatti GK, Reddy PH. Mitochondrial dysfunction and oxidative stress in metabolic disorders - a step towards mitochondria based therapeutic strategies. *Biochim Biophys Acta Mol Basis Dis*. (2017) 1863:1066–77. doi: 10.1016/j.bbadis.2016.11.010

58. Shu K, Zhang Y. Protodioscin protects PC12 cells against oxygen and glucose deprivation-induced injury through miR-124/AKT/Nrf2 pathway. *Cell Stress Chaperones*. (2019) 24:1091–9. doi: 10.1007/s12192-019-01031-w

59. Francisqueti-Ferron FV, Ferron AJT, Garcia JL, Silva C, Costa MR, Gregolin CS, et al. Basic concepts on the role of nuclear factor erythroid-derived 2-like 2 (Nrf2) in age-related diseases. *Int J Mol Sci*. (2019) 20:208. doi: 10.3390/ijms20133208

60. Dadarwal D, Adams GP, Hyttel P, Brogliatti GM, Caldwell S, Singh J. Organelle reorganization in bovine oocytes during dominant follicle growth and regression. *Reprod Biol Endocrinol*. (2015) 13:124. doi: 10.1186/s12958-015-0122-0

61. May-Panloup P, Vignon X, Chrétien M-F, Heyman Y, Tamassia M, Malthièry Y, et al. Increase of mitochondrial DNA content and transcripts in early bovine embryogenesis associated with upregulation of mtTFA and NRF1 transcription factors. *Reprod Biol Endocrinol*. (2005) 3:65. doi: 10.1186/1477-7827-3-65

62. Traut M, Kowalczyk-Zieba I, Boruszewska D, Jaworska J, Lukaszuk K, Woclawek-Potocka I. Mitochondrial DNA content and developmental competence of blastocysts derived from pre-pubertal heifer oocytes. *Theriogenology*. (2022) 191:207–20. doi: 10.1016/j.theriogenology.2022.07.017

Frontiers in Veterinary Science

Transforms how we investigate and improve animal health

The third most-cited veterinary science journal, bridging animal and human health with a comparative approach to medical challenges. It explores innovative biotechnology and therapy for improved health outcomes.

Discover the latest Research Topics

See more →

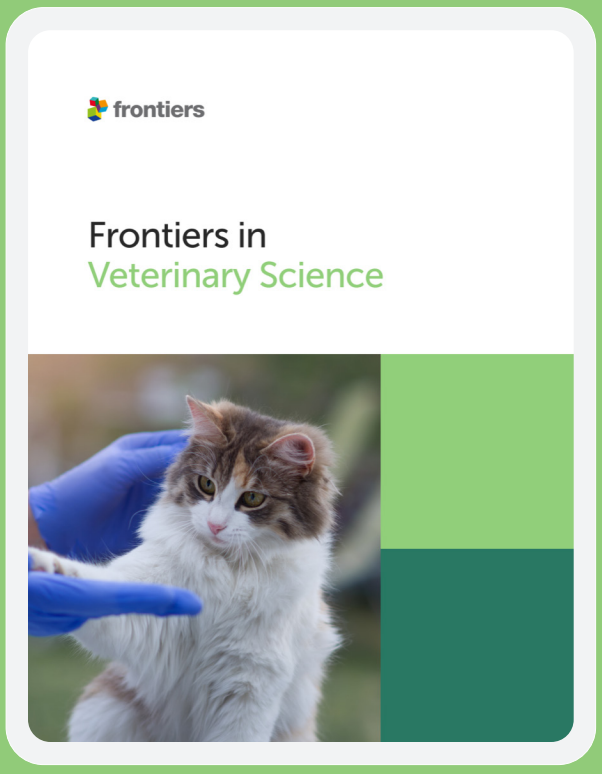

Frontiers

Avenue du Tribunal-Fédéral 34
1005 Lausanne, Switzerland
frontiersin.org

Contact us

+41 (0)21 510 17 00
frontiersin.org/about/contact